



PHOTONICS ASIA.

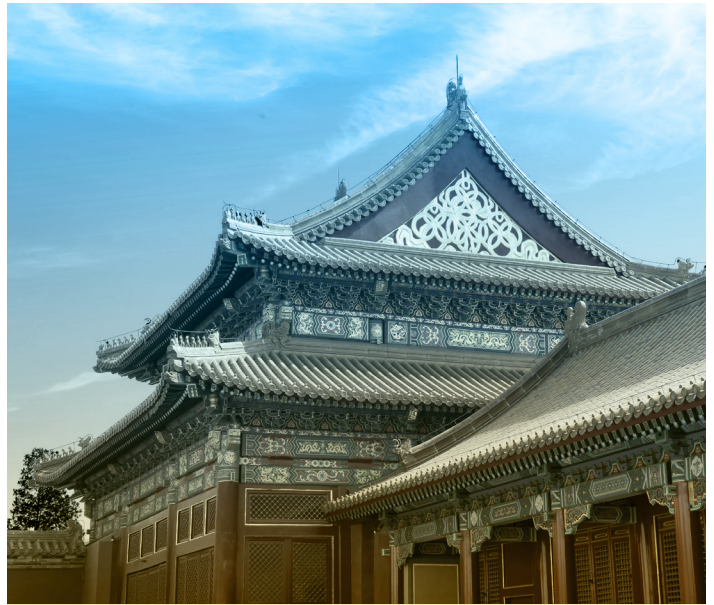
**TECHNICAL
SUMMARIES**

Beijing International Convention Center
Beijing, China

WWW.SPIE.ORG/PA

Conference: 9-11 October 2014

SPIE. | PHOTONICS COS ASIA



GENERAL CHAIRS:



H. Philip Stahl
SPIE President
NASA Marshall
Space Flight
Center (USA)



Bingkun Zhou
COS President
Tsinghua
University
(China)

SPONSORED BY:

SPIE.



COOPERATING ORGANIZATIONS:

Tsinghua University	Changchun Institute of Optics, Fine Mechanics and Physics, CAS
Peking University	Institute of Semiconductors, CAS
University of Science and Technology of China	Institute of Optics and Electronics, CAS
Zhejiang University	Institute of Physics, CAS
Tianjin University	Shanghai Institute of Technical Physics, CAS
Beijing Institute of Technology	China Instrument and Control Society
Beijing University of Posts and Telecommunications	Optoelectronics Technology Committee, COS
Nankai University	SPIE-China Committee
Changchun University of Science and Technology	Japan Optical Society
University of Shanghai for Science and Technology	Korea Optical Society
Capital Normal University	Australia Optical Society
Huazhong University of Science and Technology	Singapore Optical Society
Beijing Jiaotong University	European Optical Society
Shanghai Institute of Optics and Fine Mechanics, CAS	

SUPPORTED BY:

China Association for Science and Technology (CAST)
Department of Information of National Nature Science Foundation, China (NSFC)

CONTENTS:

9266: High-Power Lasers and Applications VII	3
9267: Semiconductor Lasers and Applications VI	19
9268: Optics in Health Care and Biomedical Optics VI	30
9269: Quantum and Nonlinear Optics III	56
9270: Optoelectronic Devices and Integration V	71
9271: Holography, Diffractive Optics, and Applications VI	89
9272: Optical Design and Testing VI	111
9273: Optoelectronic Imaging and Multimedia Technology III	129
9274: Advanced Sensor Systems and Applications VI	161
9275: Infrared, Millimeter-Wave, and Terahertz Technologies III	180
9276: Optical Metrology and Inspection for Industrial Applications III	196
9277: Nanophotonics and Micro/Nano Optics II	215
<hr/>	
NEW	
9278: Plasmonics	232
9279: Real-time Photonic Measurements, Data Management, and Processing	244

Conference 9266: High-Power Lasers and Applications VII

Thursday - Saturday 9 -11 October 2014

Part of Proceedings of SPIE Vol. 9266 High-Power Lasers and Applications VII

9266-1, Session 1

High-energy hundred-picosecond laser pulse generation based on stimulated Brillouin scattering with a non-focusing scheme (*Invited Paper*)

Yulei Wang, Harbin Engineering Univ. (China); Xuehua Zhu, Henan Polytechnic Univ. (China); Zhiwei Lu, Harbin Institute of Technology (China)

In this paper, a high energy sub-400ps laser pulse generation technology with high temporal stability is presented. Our experiment was carried out with a non-focusing scheme for energy extending. A frequency-doubled high power Nd:glass laser system with the wavelength of 527nm is used as the pump source, the beam diameter is 20mm (scaled down from 60mm), the laser pulses are nearly super-Gaussian shaped with pulse-width of 3ns, and the highest single pulse energy is above 10J. The Heavy fluorocarbon liquid material FC-40 is selected as the nonlinear medium, and the medium cell length is 60cm. According to Fourier theory, there are some sideband in the frequency domain of the flat top laser pulses. When the collimated laser pulses irradiated onto the surface of the rear cell window, a small percent of the pulse is reflected to transmit in the opposite direction. The Stokes component within the weak feedback pulse, whose frequency difference with the main frequency of the pump pulse equals to Brillouin shift of the nonlinear medium, can be amplified by the forward pump laser and leads to the pulse compression. The experimental results show that 350ps compressed pulse with the energy of 1.67J was obtained while the pump energy is 4.16J, and the energy conversion efficiency is 40%. In addition, the time jitter of the compressed pulses is much smaller than that generated from the focusing geometry owing to the weak feedback characteristic of our non-focusing scheme. This pulse compression technique is simple to operate and is scalable to much higher energy lasers.

9266-2, Session 1

Noise filtering in parametric amplification by dressing the seed beam with spatial chirp

Jing Wang, Shanghai Jiao Tong Univ. (China); Jingui Ma, Fudan Univ. (China) and Shanghai Jiao Tong Univ. (China); Yongzhi Wang, Fudan Univ. (China); Peng Yuan, Guoqiang Xie, Shanghai Jiao Tong Univ. (China); Liejia Qian, Fudan Univ. (China)

Pulse contrast is a crucial parameter in high-intensity laser-matter interaction experiments. To date, contrast enhancement techniques for optical parametric chirped-pulse amplification (OPCPA) systems are limited to cleaning seed pulse with saturable absorber or other nonlinear temporal filtering schemes. Active solutions for the contrast degradation in subsequent amplification stages are almost blank. There are mainly three kinds of noises produced in parametric amplifiers including parametric super-fluorescence, pump-distortion-induced noise and surface-reflection-initiated prepulses. To separate out the noise from the signal is inherently difficult, as they overlap each other in all the spatial, temporal and spectral domains. Here we present a novel and promising method valid for filtering out all the three noises. Noise filtering is realized via dressing the seed beam with a small amount of spatial chirp. Due to the simultaneous spatial and temporal chirp, the seed acquires a

strong spatiotemporal coupling in the intensity distribution. This coupling is then passed on to the noise field during dechirping the amplified signal. Hence, the noises become highly distinguishable from the signal in both time and space at the compressor output. Effective and expedient noise filtering can thus be implemented using a simple near-field slit. Numerical simulations have shown that this proposed method is capable of reducing the noises produced in parametric amplifiers by an order of magnitude and enhancing the temporal contrast by several orders of magnitude. The results suggest that spatial chirp can be regarded as an enabling tool in noise filtering for high-intensity ultra-short laser pulses.

9266-3, Session 1

Temporal pulse cleaning by a self-diffraction process for ultrashort laser pulses

Na Xie, Xiaodong Wang, Li Sun, Kainan Zhou, Yi Guo, Qing Li, Jingqin Su, China Academy of Engineering Physics (China)

Applying the self-diffraction process to clean ultrashort laser pulses temporally is a recently developed effective way to temporal contrast enhancement. Temporal contrast can be improved by large orders of magnitude with the method since the self-diffraction process is a third-order nonlinear process and the generated self-diffraction pulses are spatially separated from incident pulses, avoiding the usage of polarization discrimination device. In this study, we attempt to clean ultrashort laser pulses temporally by the self-diffraction process. Experiments were carried out to study the conversion efficiency of the generated self-diffraction pulses and the temporal contrast improvement in the front end system of an ultraintense and ultrashort laser facility, i.e. the super intense laser for experiment on the extremes (SILEX-I), with a wavelength of 800 nm. The pulse duration from a preamplifier was compressed to ~100 fs for the experiments. The results show that the conversion efficiency of the first-order self-diffraction pulses is greater than 10%. The temporal contrast is improved by two orders of magnitude, i.e. to 10^3 , for a 2.4 ns prepulse with an initial contrast of ~ 10 . There is a cubic relationship between the temporal contrast of the first-order self-diffraction pulses and the initial temporal contrast. The result is in good agreement with the theoretical prediction. For a 5.4 ns prepulse with an initial contrast of 2×10^3 , the temporal contrast is improved by more than three orders of magnitude, which is beyond the maximum range of the measurement system, i.e. 3×10^6 .

9266-4, Session 1

An experimental method for pulse-width measurement in partial positions of an ultrashort-pulsed beam

Chao Tan, Xiquan Fu, Hunan Univ. (China)

We experimentally show a method for pulse-width measurement. Pulse widths at different partial positions of an ultrashort-pulsed beam are measured, results show that pulse widths in the center of the beam are less than that of in the edge because of the existence of residual spatial chirp. We also investigate the temporal evolution at a strongest spatial modulation position of the beam during small-scale self-focusing, it finds that its pulse width decreases as power increases due to a spatiotemporal

coupling effect. We find that this method not only can be used to accurately measure the pulse width at any one spatial position of the beam, but also be useful for real-time monitoring of spatial-temporal evolution.

9266-5, Session 1

Analysis of temporal contrast degradation due to wave front deviation in large aperture ultra-short pulse focusing system

Ping Zhu, Shanghai Institute of Optics and Fine Mechanics (China) and Univ. of Chinese Academy of Sciences (China); Xinglong Xie, Jianqiang Zhu, Qingwei Yang, Haidong Zhu, Jun Kang, Ailin Guo, Qi Gao, Shanghai Institute of Optics and Fine Mechanics (China)

In extremely intense laser system used for plasma physics experiments, temporal contrast is an important property of the ultra-short pulse. In this paper, we theoretically study the temporal contrast degradation due to wave front deviation in large aperture ultra-short pulse focusing system. Two-step focusing fast Fourier transform (FFT) algorithm with the coordinate transform based on Fresnel approximation in space domain and Fourier integral transform method in time domain were used to simulate the focusing process spatially and temporally, in which the spatial distribution of ultra-short pulse temporal contrast characteristics at the focal spot is related to the wave front in large aperture off-axis parabolic mirror focusing optical system. Firstly, temporal contrast degradation due to wave front noise with higher spatial frequency is analyzed and appropriate evaluation parameters for large aperture ultra-short pulse focusing system is put forward from the perspective of temporal contrast. Secondly, the influence of wave front distortion with lower spatial frequency on temporal contrast is revealed comparing different degradation characteristics of various aberrations. At last, a method by controlling and optimizing the wave front to improve temporal contrast of large aperture ultra-short laser system is proposed, which is of great significance for high temporal contrast petawatt laser facilities.

9266-6, Session 2

Research and construction progress of SG-III laser facility (*Invited Paper*)

Xuwei Deng, China Academy of Engineering Physics (China)

The under-construction SG-III laser facility is a huge high power solid laser driver, which contains 48 beams and is designed to deliver 180kJ energy at 3ns pulse duration. Till the end of 2013, 4 bundle lasers finished their construction and adjusting, and 2 round of physics experiments have already been carried. The great progresses in the laser performance and the physics experiment have already demonstrated that the facility is in excellent accordance with the designs, which establish a solid foundation for completing all the construction goals.

The SG-III laser facility will be used to investigate and grasp target physics for both direct-drive and indirect-drive ICF except for ignition physics, and to scale up to ignition parameters in China in the future. According to the engineering design, the SG-III facility possesses 48 laser beams, which are divided into 6 bundles with 4?2 arrangement. The designed output energy of blue light (351nm), i.e. the tripled frequency 3λ , is 180kJ/3ns, an order of magnitude larger than the 24kJ of upgraded SG-II facility, providing an environment much more approaching ignition conditions for target physics research.

The infrastructure construction of the laboratory building was

started in 2007, three years before optical device entered. Till now, 4 bundle lasers have finished their construction and adjusting, which can provide main shots for the physics experiment. The main engineering construction is expected to end this year. The aim of the SG-III laser facility then is to provide main shots with full capability in the end of 2014.

9266-7, Session 2

Analysis of influence factors on laser induced static deformation of deformable mirrors

Binbin Wei, Wenguang Liu, Kun Xie, Zongfu Jiang, Qiong Zhou, National Univ. of Defense Technology (China)

Laser-induced static surface shape changes of deformable mirrors will cause difficulties for beam control of the laser system. The overall peak and valley (PV) value of the deformable mirror will reach the scale of micrometer when irradiated by high power lasers. We have investigated the changes in the static surface shape of a 37-element deformable mirror caused by laser-induced thermoelastic deformation. It is found that the laser-induced profile change of the mirror depends highly on the particular arrangement of actuators, the thickness of the mirror and material properties of the deformable mirror.

In this paper, the finite element method is used to analyze the surface shape of the deformable mirror when it is irradiated by high power laser and its dependence on the arrangement of actuators, the thickness of the mirror and material properties. The surface shape is fitted using the Zernike polynomial and the simulation results show that the lower-order aberrations can be corrected by the deformable mirror itself at the cost of a reduced ability of aberration correction, as the available amount of stroke will decrease. The simulation results are verified through experiments.

Thus, when designing a deformable mirror, the material and parameters of it should be chosen carefully in order to reduce the laser-induced surface shape change. Based on this, some design considerations which could reduce the effect of laser-induced thermoelastic deformation are proposed.

9266-8, Session 2

Ray-tracing method to analyze and quantify the light enhancement around subsurface defects in transparent materials

Rong Wu, Dongfeng Zhao, Lei Zhang, Ping Shao, Neng Hua, Zunqi Lin, Shanghai Institute of Optics and Fine Mechanics (China)

Laser-induced damage (LID) to optical glass has become a growing problem in high-power laser systems. It is well known that the main reason of glass being damaged is due to defects and impurities in the material. Damage caused by subsurface defects (SSDs) is especially common in actual system running. Accordingly, in the presence of SSDs, a simple and alternative calculation method is developed to evaluate the enhancement of light field around the incident and exit surface. This ray tracing approach, based on the classical optics theory, is very direct and clear to show the optical phenomena of light intensity enhancement. Some basic SSD shapes have been studied and investigated here, which reveals the importance and boundary condition of controlling the size and density of SSDs in grinding and polishing process. Finally, to achieve optimal breadth depth ratio, the least etching amounts by hydrofluoric (HF) acid is investigated. The theoretical analysis and simulation results

provide an appropriate range of removal amounts, which is very important in the HF etching process.

9266-9, Session 2

Analysis of nonlinear self-focusing phenomenon in high-power laser system based on ray-tracing

Weiwei Wang, Zhaofeng Cen, Xiaotong Li, Luwei Zhang, Zhejiang Univ. (China)

In high power laser systems, third-order nonlinear effect is the main reason for beam wavefront aberration, nonlinear self-focusing and even "Hot Spot" effects. How to reduce the impact of nonlinear effect, which can improve beam quality and the performance of high power laser systems, has always been one of the top concerns of researchers. Based on the accomplished hybrid ray-tracing method in linear and nonlinear media, this paper focuses on the impact of third-order nonlinear effect of Kerr medium on beam propagation and beam quality.

Considering the complexity of high power laser systems, traditional modeling methods based on surfaces are no longer convenient when it comes to tilted and decentered surfaces. A new modeling method based on elements and components instead of surfaces which is convenient for designers is presented in this paper.

Start with an example of a focus system with KDP crystal as nonlinear media, this paper introduces a result of simulation of the influence of nonlinear effect on beam quality with different laser power densities. In order to make a compensation of nonlinear effect, a optimization method in which component intervals, instead of the positions of focal plane are variable.

Since paraxial approximation is not a part of the ray-tracing method in this paper, the influence of system aberrations can be considered well in the simulation of propagation. Additionally, the effect of component surface errors is also able to be considered in the process. Hopefully, the simulation results can be taken as reference in future designs of high power laser systems.

9266-10, Session 2

Design and comparison of laser windows for high-power solid-state lasers

Yanxiong Niu Sr., Wenwen Liu, Haixia Liu, Caili Wang, Haisha Niu, Da Man, BeiHang Univ. (China)

High-power laser systems are getting more and more widely used in industry and military affairs. It is necessary to develop a high-power laser system which can operate over long periods of time without appreciable degradation in performance. When a high-energy laser beam transmits through a laser window, it is possible that the permanent damage be caused to the window because of the energy absorption by window materials. So, when we design a high-power laser system, a suitable laser window material must be selected and the laser damage threshold of the window must be known.

In this paper, a thermal analysis model of high-power laser window is established, and the relationship between the laser intensity and the thermal-stress field distribution is studied by deducing the formulas through utilizing the integral-transform method. The influence of window radius, thickness and laser intensity on the temperature and stress field distributions is analyzed. Then, the performance of K9 glass and the fused silica glass is compared, and the laser-induced damage mechanism is analyzed. Finally, the damage thresholds of laser windows are calculated. The results show that compared with K9 glass, the fused silica glass has a higher damage threshold due to its good

thermodynamic properties. The presented theoretical analysis and simulation results are helpful for the design and selection of high-power laser windows.

9266-11, Session 2

Precise measurement of transmittance and reflectance for large-aperture optics

Jie Miao, Dean Liu, Pengqian Yang, Hongchao Hui, Lin Yang, Jie Zhang, Baoqiang Zhu, Jianqiang Zhu, Shanghai Institute of Optics and Fine Mechanics (China)

The large optics for high power laser facilities create not only a number of logistical and technological challenges for optics themselves, but also for their measurement. And the uniformity measurement, transmittance and reflectance of the optics in other words, is one of the essential specifications. Both high reproducibility for large-size and precision with wide dynamic range make such testing a real challenge to take.

In order to measure the spectral characteristics, custom laser-based measuring systems have been constructed with laser lines at 1053, 532, and 351 nm. Both transmission and reflection are simultaneously measured. A 350mmx350mm mirror is scanned past a 2-mm laser beam, and the repetitive rate results about 0.05% and 0.1% for transmittance and reflectance respectively.

Furthermore, a balanced heterodyne detection technique is proposed to promote accuracy and SNR, especially for a weak signal in case those with high transmittance or reflectance coatings. Kinds of noise can be effectively suppressed with such optical modulation method by principle of balanced heterodyne detection. In consequence, high accuracy over an unprecedented dynamic range can be realized. A demonstrative experiment of transmittance detection by balanced heterodyne is performed, and it results that it is valid compared with conventional direct detection.

9266-12, Session 3

Optical properties of high-power S-band fiber oscillators and amplifiers

Jinping Hao, Hong Zhao, Dayong Zhang, Chen Zhu, Yao Li, North China Research Institute of Electro-optics (China); Ping Yan, Mali Gong, Tsinghua Univ. (China)

S-band fiber lasers, one type of ytterbium doped fiber lasers (YDFLs) which emitting in the spectral region of 1010 nm ~ 1060 nm, have drawn more and more attention especially after the proposition of tandem pump fiber lasers. The S-band laser plays an important role as the pump in a tandem pumping scheme. However, high power S-band laser output is quite difficult because of severe reabsorption. Therefore, the optical properties of S-band fiber lasers are studied and methods to achieve high power S-band laser output are presented. An S-band laser emission model based on gain comparison is built for analyzing the mechanism of laser oscillation and amplification. The model is composed of rate equations and gain comparison of several wavelengths in ASE spectrum. The gain differential between laser wavelength and ASE peak wavelength is compared to the additional gain imposed by cavity mirrors in an oscillator or the seed in an amplifier. The comparison results help in concluding the feasibility of S-band laser emission and the maximum laser power that could be obtained. Based on the model, the influences of fiber properties (including core doping level, core-to-clad ratio, and fiber length), pump power and laser power on the operation of S-band fiber lasers or amplifiers are researched. The analysis shows that fibers with lower doping level, larger core-to-clad ratio and shorter length, seed with higher power, are more helpful in realizing high power S-band

laser output. Also, the profile of oscillator is found more suitable in building high power S-band lasers than that of amplifier.

9266-13, Session 3

Fiber laser at 2 μm for soft tissue surgery

Atasi Pal, Aditi Ghosh, Debasis Pal, Ranjan Sen, Central Glass and Ceramic Research Institute (India)

Strong water absorption at 2 μm generated recent interest in lasers at this wavelength for soft-tissue surgery. Water being the main constituent of biological tissues, 2 μm lasers produce localized substantial heating, allowing very precise incision of biological tissues by vaporizing tissues with adequate hemostasis and leave minimal collateral damage (width <5 μm) and additionally suppress the bleeding, during laser cutting, by coagulation. Thulium-doped fiber laser operating at around 2 μm is emerging as the latest technology capable to replace current Ho-YAG laser. Focusing this application area, a fiber Bragg grating-based all-fiber continuous-wave cladding pumped thulium-doped fiber laser is configured. The operating wavelength of laser is 1.95 μm according to the centre wavelength of the grating- pair targeting the higher water absorption. The thulium-doped active fiber with octagonal-shaped inner cladding is pumped at 808 nm with six laser diodes through a combiner. The total pump power at the common end of the combiner is 17 W. The length of the active fiber is optimized according to the fiber design, reflectivity of the grating pair and the available pump power. The unabsorbed pump power at the end of low reflective grating is eliminated through splicing a matched single clad fiber. The laser signal power of 3.3 W with slope efficiency of 23% (against lunched pump power) is achieved. The linear variation of laser power with pump power offers scope of further power scaling. Optimization of the fiber design to enhance the efficiency is in progress.

9266-14, Session 3

780W narrow linewidth all fiber laser with sinusoidal phase modulation

Liming Zhang, North China Research Institute of Electro-optics (China)

High power narrow linewidth fiber lasers are extensively applied in coherent detection and power spectrum beam combination etc. In high power fiber laser, the limiting factor of narrow linewidth output is analyzed. The influence of Stimulated Brillouin scattering effect and sinusoidal phase modulation suppressing method are studied. The linewidth of a single frequency laser is broadened from 1MHz to 2.9 GHz by sinusoidal phase modulation technology. The output power of single frequency laser is 50mW. And through three stage fiber amplified, the central wavelength 1064.34nm, linewidth of 2.9 GHz and power of 780W are achieved respectively. The optical-optical efficiency is 79%. And the beam quality is $M_x2 = 1.44$ and $M_y2 = 1.43$. The distributing characteristic of longitudinal mode, under every modulating coefficient, is measured. And the result is the same as theoretical result. The increasing of longitudinal mode number, controlling of longitudinal mode spacing and reducing power spectrum density by sinusoidal phase modulation are proved to be viable. Then Stimulated Brillouin Scattering threshold is promoted. Finally, the output power is promoted a lot. The output power of this laser is only limited by pump power. If the pump power is increased, the higher output power of narrow linewidth fiber laser will be achieved.

9266-15, Session 3

Powerful 2 μm all-fiber laser sources pumped by Raman fiber lasers

Xiong Wang, Pu Zhou, Hanwei Zhang, Xiaoxi Jin, Xiaolin Wang, Hu Xiao, Zejin Liu, National Univ. of Defense Technology (China)

We present novel and powerful pump schemes for fiber laser sources operating near 2 μm , which employing high power Raman fiber lasers (RFLs) to provide sufficient pump light. Firstly, we demonstrate a Tm-doped fiber laser (TDFL) pumped by two RFLs at 1173 nm. The output power of the TDFL reached 96 W with slope efficiency of 0.42, and the central wavelength located at 1943.3 nm. This is the first TDFL with 100 W-level output power pumped by RFLs around Tm³⁺ ions' -1200 nm absorption band. Secondly, we demonstrate a Ho-doped fiber laser (HDFL) employing a 1150 nm RFL as pump source. The 1150 nm RFL provided 110 W pump power and the output power of the HDFL reached 42 W with slope efficiency of 0.37. The lasing wavelength covered from 2046.8 nm to 2049.5 nm with optical signal-to-noise ratio more than 30 dB. This is the first HDFL pumped by a 1150 nm RFL and the highest output power achieved at this pump band. In the last, we present a high power Ho-doped fiber (HDF) superfluorescent source (SS) pumped by a 1150 nm RFL. The SS's output power reached 1.5 W, and the full width at half maximum was about 30 nm. This is the highest output power achieved in HDF as far as we know. The results above indicate promising and powerful pump schemes to achieve higher power output in fiber lasers near 2 μm , which also can be further improved by optimizing the parameters of the lasers.

9266-16, Session 3

A compact pulse-tunable fiber laser based on pulse-pumped high-gain cavity

Hongdan Wan, Nanjing Univ. of Posts and Telecommunications (China); Zhiming Lu, Alcatel-Lucent Shanghai Bell Co. Ltd. (China); Hongchun Lv, Jin Wang, Nanjing Univ. of Posts and Telecommunications (China)

We demonstrate a simple and novel pulsed fiber ring laser based on an pulse-pumped, high gain, compound fiber cavity. A single-mode, heavily Er-doped fiber with a very high-gain per unit fiber length (-1.1?dB/cm) was used as the gain medium. The laser resonator was as short as 0.2 m. The pump system consists of a 980 nm LD (driven by a pulsed electric driver) and was thermally stabilized by an automatic temperature controller. The pump pulses coupled into the ring cavity had a maximum peak power of about 800 mW. The pulse-pumped laser was actively controlled by pulse-modulation of the pump LD as well as the adjustment of the intracavity loss through a variable optical attenuator in the cavity. The proposed laser generates tunable lasing pulses with μs pulse width in kHz repetition rate down to one shot operation. Dynamical amplification process such as the relaxation oscillation and tunable property of the pulse-pumped high gain cavity is investigated experimentally and theoretically. The pulsed operation without intracavity modulators makes the proposed laser more compact and cost effective. The lasing pulses are highly stabilized which makes it an ideal pulsed laser for space applications and seeding source for high power amplifications.

9266-17, Session 3

Towards high-power random fiber laser

Hanwei Zhang, Pu Zhou, Haibin Lv, Hu Xiao, Xiaolin Wang, Xiaojun Xu, National Univ. of Defense Technology (China)

Random laser possesses the character of plenty of modes oscillation at the same time owing to the feedback of random medium. It can be found in many applications of display, remote sensing and even tumour diagnostics. It has also attracted a great deal of attention as a fundamental physical phenomenon at the field of laser physics. However, in traditional bulk materials random lasers, the threshold to obtain laser operation is relatively high and lacking lasing directionality due to the 2-dimensional or 3-dimensional configuration. In 2007, de Matos et. al achieved the random laser in optical fiber, which comes true one dimension random laser.

Recently, a new type of random fiber laser based on Raman gain and distributed Rayleigh feedback was proposed, where light experiences feedback as well as amplification in the same passive fiber. In this paper, we pay much attention to the generation of high output power by this "mirror less" cavity. Raman and Yb gain used to amplify the random laser have both been discussed. Such configuration can be a candidate to obtain high power fiber laser without using FBGs. Moreover, physical process of the distributed feedback (DFB) random laser may be different when power increases. Finally, we achieve more than 73 W random laser output by using 300 m passive fiber as Raman gain medium as well as random feedback. And we also first report the Watt-level Yb-doped random fiber laser, which also has the potential to power scaling.

9266-18, Session 4

Strong-field tunneling ionization: from theory to application (*Invited Paper*)

Yunquan Liu, Peking Univ. (China)

Tunneling ionization of atoms is one of the fundamental processes in strong-field physics. Since the benchmark theory developed by Keldysh, there are numerous works to investigate the strong-field tunnelling ionization. In this contribution, I will present our recent experimental efforts on tunneling ionization in strong laser fields. First, we have measured photoelectron angular distributions (PADs) and observed that the yields of near-zero momentum electrons in strong-field tunneling ionization regime are much suppressed. We show that the tunneled electrons released in a certain window of initial field phases and transverse velocities are injected into the Rydberg elliptical orbits and become stabilized against ionization. Second, we have measured photoelectron angular distributions of noble gases in intense elliptically polarized laser fields, which indicate strong structure-dependent Coulomb asymmetry. We theoretically disentangle the effect of direct ionization and multiple forward scattering on Coulomb asymmetry in elliptical laser fields and quantify the roles of the ionic potential and initial transverse momentum. There is no evident initial longitudinal momentum spread at the tunnel exit according to our semiclassical simulation. At last, I will present the intriguing applications using strong-field tunneling ionization. We shows that, for single ionization, the ionization from the inner orbitals of HOMO-1 and HOMO-2 has very important effect on strong-field ionization of molecules. Using attosecond angular streaking by circularly polarized laser fields, we have measured the angular tunneling probability from inner orbitals of O₂ in strong laser fields. The molecular inner orbitals can be imaged by strong-field tunneling ionization.

9266-19, Session 4

Attosecond photoionization for reconstruction of bound electron wave packets (*Invited Paper*)

Candong Liu, Zhinan Zeng, Ruxin Li, Zhizhan Xu, Shanghai Institute of Optics and Fine Mechanics (China); Mauro Nisoli, Politecnico di Milano (Italy)

We present a method for the characterization of bound electron wave packets generated by a broadband excitation pulse. The technique is based on the photoionization of the electron wave packet by a delayed isolated attosecond pulse and on the measurement of the ionization asymmetry parameter in the direction of the probe pulse polarization, which depends on the pump-probe delay and on the photoelectron energy. By numerically solving the fully three-dimensional time-dependent Schrödinger equation we show that Fourier analysis of the two-dimensional ionization asymmetry parameter, displaying a complex interference pattern, enables a clear observation of quantum beats between pairs of stationary states involved in the generation of the wave packet. An analytical model confirms that the quantum beats signal encodes the weight of each stationary state, thus suggesting a feasible approach for the complete characterization of the relative population ratio of the excited state components of the wave packet. Moreover, an approach based on the further analysis of quantum beats is proposed to retrieve the lifetime added to each excited state.

9266-20, Session 4

The propagation properties of an ultraintense laser pulse in the linear down-ramp density plasma

Ming-Ping Liu, Yu-Zhong Qian, Nanchang Univ. (China)

The equations of dielectric constant and spot size with interaction of laser in linear down-ramp density plasma are obtained. It has investigated the self-focusing of intense laser in linear down-ramp density plasma. The change of wake field that is caused by the gradient of electron density is studied with the paraxial approximation. It is shown that the effects of density scale, the initial density and laser intensity for the spot size are discussed. The results may be significant theoretically to the mechanism of self-focusing of intense laser in the linear down-ramp density of plasma.

9266-21, Session 4

Research on chirped pulse stimulated Raman scattering in ethanol

Xiaoyang Guo, Xiao Zou, Yi Xu, Xiaoming Lu, Cheng Wang, Yanqi Liu, Yanyan Li, Yuxin Leng, Ruxin Li, Shanghai Institute of Optics and Fine Mechanics (China)

Optical parametric chirped-pulse amplification (OPCPA) technology has shown remarkable development over the last 20 years. Second harmonics of a single-mode, single-frequency Nd:glass laser with a wavelength of 527 nm is a proper choice for OPCPA pump pulse. OPCPA systems based on KDP or DKDP crystals mostly work at 1053 nm (in degeneracy) or at 910 nm to obtain broadband amplification. To obtain broadband 1053 nm seed pulse, there are two usual ways of using nonlinear converters such as optical parametric amplifiers (OPAs) and stimulated Raman scattering (SRS) with a femtosecond 800 nm laser. The Raman media possess the advantage of possible frequency shift of less than 1000 cm⁻¹ with high energy efficiency

makes it a promising way. However, in the femtosecond regime effects such as self-phase modulation, self-focusing, and continuum generation become inevitable. In order to remove these competing nonlinear processes, the approach based on SRS of a chirped pulse with hundreds of picosecond duration accompanied by subsequent temporal compression of the Stokes component is proposed. In this paper, we report a generation of 10.6% conversion efficiency near 1053 nm first order Stokes pulse in stimulated Raman scattering pumped using 800 nm Ti:sapphire based femtosecond pulse that is stretched to 460 ps, obtained by use of a single pass ethanol Raman shifter. The Stokes pulse almost maintains the bandwidth of the pump and is compressed to ~10 ps using a mismatched grating-pair. The spectral characteristic of the Raman pulse is calculated and the results explain the observed transient features.

9266-40, Session Post

Numerical simulation of laser-induced interfacial wave on the transparent solid/solid interface

Liping Xue, Yan Zhao, Nanjing Univ. of Science and Technology (China)

In this paper, the finite element method is used to simulate the laser generated interfacial wave on the transparent solid/solid interface in the thermoelastic region. Typical calculation is performed for the configuration of quartz glass bond to tungsten. Transient waveforms of laser-generated interfacial waves are presented. The simulations can provide theoretical guideline for the understanding of interfacial wave propagation.

9266-41, Session Post

Recent progress of the Integration Test Bed (ITB)

Junpu Zhao, Wenyi Wang, Xuejun Fu, Jun Tang, Yanwen Xia, Lin Chen, Wei Han, Yue Liang, Sen Li, Dong Gao, Feiyue Yan, Honghuan Lin, Ji Chen, Dehuai Chen, Qihua Zhu, Kuixing Zheng, Feng Jing, Wanguo Zheng, Xiaofeng Wei, China Academy of Engineering Physics (China)

The Integration Test Bed (ITB) is a large-aperture single-beam Nd:glass laser system, built to demonstrate the key technology and performance of the laser drivers. It uses two multipass Slab amplifiers. There are four passes through the main amplifier and three passes through the booster amplifier. The output beam size is 360mm by 360mm, at the level of 1% of the top fluence. The designed output energy of ITB at 1053nm is 15kJ in a 5ns flat-in-time pulse, the third harmonic conversion efficiency is higher than 70%. ITB has been completed in July 2013. A series of experiments demonstrated that laser performance meets or exceeds original design requirements. It has achieved maximum 19.6kJ in a 5ns pulse at 1053nm. Based on a pair of split third harmonic generation KDP crystal, third harmonic conversion efficiency of about 70% has been obtained at mean fluence 8.4J/cm² with 5ns flat-in-time pulse.

9266-42, Session Post

Spectral broadening and inhibition of amplitude frequency modulation in Nd:glass regenerative amplifier

Yuqi Zhang, Xue Pan, Jiangfeng Wang, Shanghai Institute of Optics and Fine Mechanics (China)

In order to broaden the spectrum of laser pulse and reduce the gain narrowing effect in Nd:glass regenerative amplifier to realize the ambition of inhibiting amplitude frequency modulation, proper quartz birefringence crystal plate is inserted into the cavity. The influence factors of central wavelength, depth of modulation and range of modulation are obtained theoretically. The width of the spectrum is broadened by controlling all the factors. Two kinds of thickness, 5mm and 6mm, are inserted into the regenerative amplifier cavity. The results of theoretical calculation and experiment both show that the effect of spectrum widening is evident, which reduces the gain narrowing effect to some extent. The amplitude frequency modulation resulted from gain narrowing effect is inhibited when the central wavelength deflects about 1nm. At the same time, the inhibited effect is simulated according to theoretical model. The results in combination with the former experiment results of compensation outside the cavity show that inhibited effect is remarkable. And the method is a potential effective technique for amplitude frequency modulation inhibition.

9266-43, Session Post

Wavefront aberration analysis of slit spatial filtering system

Guotan He, Xiang Zhang, Han Xiong, Baoxing Xiong, Xiao Yuan, Soochow Univ. (China)

Slit spatial filtering system consists of four cylindrical lenses and two orthotropic slits, which can significantly enlarge the focal area by changing the original focal spot into focal line. It's beneficial in solving of pinhole closure due to the decrease of focal area.

Wave-front aberrations become a more important concern in slit filtering system comparing with traditional pinhole spatial filter. According to actual needs the wave-front aberration function is expanded in square aperture. Matlab numerical calculation has been used to analysis the effect on slit spatial filtering system from several kinds of geometrical aberrations, which are spherical aberration, coma, astigmatism, field curvature and distortion, etc. Fast Fourier Transform (FFT) was used to take place of diffraction integral in the calculation to save time. The effect of aberrations on the system was judged by the light field parameters — relative change in peak intensity, intensity irradiated on slit-1 and slit-2 as well as the near-field modulation and the near-field contrast of the output beam. It is proper to consider the value of one particular type of aberration that makes the relative change of any light field parameters reach to 10% as the tolerance of the aberration. According to calculation results, each aberration has different tolerance. Ranked from large to small, they are in turn the astigmatism, field curvature, distortion, spherical aberration and coma. The tolerance of coma is as small as 0.01%. A scheme that distribute different values of aberrations to different lenses was putted out to make sure that the values of aberrations are in the range of optical process and the relative change of all light field parameters are less than 10% at the same time.

9266-44, Session Post

Volume-discharge formed in SF6 and C2H6 mixtures without preionization

Ge Zhang, Nanyang Polytechnic (China)

A new approach to obtain glow discharge in working mixtures of non-chain HF laser has been brought forward. The most advantage of the approach is without pre-ionization, so the contamination of pre-ionization will not happen and the laser equipment is compact and simple. It is found, if the cathode surface is equally rough, we can obtain uniform volume-discharge

in SF₆ mixtures without any pre-ionization, and dispense with uniform electric field electrode profile. The form of Self-Sustained Volume Discharge (SSVD) is a Self-Initiated Volume Discharge (SIVD). We show here the possibility of obtaining SIVD with a uniform energy deposition in a system of electrodes with non-uniform electric field. Experiments show that, with rough cathode and even anode, a volume discharge is forming in non-uniform electric-field without pre-ionization in SF₆ and C₂H₆ mixtures. At the beginning of the discharge, many diffuse channels attached to bright circular cathode spots, then, diverge towards the anode, with the channels overlapping, form a spatially uniform glow discharge. SIVD has been performed at a total mixture pressure up to 8kPa and energy deposition up to 200J/l. We also report measurements of the V-I characteristics of SIVD with SF₆ and C₂H₆ mixtures at pressure up to about 8kPa. The experimental results indicate that SSVD in SF₆ and C₂H₆ mixtures develops in the form of SIVD is promising for creation of high energy and pulse-periodic HF laser.

9266-45, Session Post

Experimental comparison of the cutting speed and quality for mild and stainless steel sheets with fiber and CO₂ lasers

Victor B. Shulyatyev, Anatoly M. Orishich, Alexandr Golyshev, Alexandr G. Malikov, Khristianovich Institute of Theoretical and Applied Mechanics (Russian Federation)

Recently, fiber lasers found wide application for metal cutting along with CO₂ lasers. Multiple experiments show that the cutting results by two types of lasers differ in basic characteristics, namely, cutting speed and cut quality.

This work presents with the experimental comparison of the low-carbon steel and stainless steel cutting by the fiber and CO₂ lasers under the condition of the maximal cut quality. The surface roughness and absence of dross is accepted as the quality criterion. The dependence of the cut surface roughness on cutting parameters was analyzed for stainless steel sheets of 3 and 5 mm and mild steel sheets of 5, 10, 16 mm. The optimal speed at which the roughness is minimal was found.

During the oxygen-assisted laser cutting of low-carbon steel, the optimal speed correlating with the minimal roughness, is higher in the case of the CO₂ laser, the laser power being the same. The surface roughness is lower in the fiber laser case. The maximal cutting speeds are approximately similar for both lasers. During the fusion cutting of stainless steel, the minimal roughness is observed at the maximal cutting speed, both for the fiber and CO₂ laser. The roughness value averaged by the sheet thickness is close for both lasers, whereas the maximal cutting speed for the fiber laser is above the maximal cutting speed of the CO₂ laser at the same beam power.

For the oxygen-assisted laser cutting, the empirical relations were found which connect the cutting speed and laser power associated with the minimal roughness, with the cut sheet thickness, for the cutting processes by the fiber and CO₂ laser.

9266-46, Session Post

Influence trend of temperature distribution in skin tissue generated by different exposure dose pulse laser

Ning Shan, The Chinese People's Armed Police Force (China)

Laser is widely applied in military and medicine fields because of its excellent capability. In order to effectively defend excess damage by laser, the thermal processing theory of skin tissue

generated by laser should be carried out. The heating rate and thermal damage area should be studied. The mathematics model of bio-tissue heat transfer that is irradiated by laser is analyzed. And boundary conditions of bio-tissue are discussed. Three layer FEM grid model of bio-tissue is established. The temperature rising induced by pulse laser in the tissue is modeled numerically by adopting ANSYS software. The changing trend of temperature in the tissue is imitated and studied under the conditions of different exposure dose pulse laser. The results show that temperature rising in the tissue depends on the parameters of pulse laser largely. In the same conditions, the pulse width of laser is smaller and its instant power is higher. And temperature rising effect in the tissue is very clear. On the contrary, temperature rising effect in the tissue is lower. The cooling time induced by temperature rising effect in the tissue is longer along with pulse separation of laser is bigger. And the temperature difference is bigger in the pulse period.

9266-47, Session Post

Efficient bending compensation of large mode area fiber

Ya-Xian Fan, Farida Souaci, Li-Bo Yuan, Harbin Engineering Univ. (China)

For high-power fiber lasers and amplifiers, improving mode area is a key target in current research on microstructure and solid Large-mode-area (LMA) fibers. While much research has been developed to achieve very large mode areas fibers, many difficulties arise, such as bending losses, mode deformation, and high order modes suppression. The main obstacle which remains difficult to confront in LMA fibers is bending distortion. When a conventional LMA fiber is coiled, it will generally suffer large bending distortion, and the mode area will contract accordingly, which would significantly affect laser or amplifier performances for some of the LMA fibers. In this report, we proposed a simple and efficient way for bending compensation in LMA fiber. A periodic structures machined inside the cladding of a coaxial step-index LMA fiber to compensate the deformation, bending loss and mode-coupling effects. Without the structure, the bending losses are very low at large bending radius. When the bending radius reduces, there is a rapid increase of losses. In particular, for smaller bending radius (less than 20cm), the fundamental mode deforms severely, and cannot normally transmit in the core. The numerical simulation results showed that the design not only efficiently improves the effective mode area, but also the fundamental mode bending loss is resistant. Even at bending radius as small as 5cm, the fundamental mode can transmit normally in the fiber with an increased mode area scaling. Furthermore, the LMA fiber with the structure can be flexibly manufactured by conventional fiber manufacturing approaches and recent etching technologies.

9266-48, Session Post

Gain Raman effect in an erbium-doped fiber laser

Lei Li, Jiangsu Normal Univ. (China)

Classical erbium-doped fiber laser can be operated in a wide wavelength range from 1550 to 1600 nm. However, further extending the emission spectrum would be difficult due to the limited gain spectrum of the gain medium. In the paper, we propose a new method to achieve the wavelength shift by the gain Raman effect in the erbium-doped fiber (EDF), which would be of great interest for novel wavelength emission of Er-fiber laser. Based on this method, we design a common configuration of fiber laser with 9 m EDF as the gain medium. In the experiment, the central emission wavelength can be tuned

to 1613.5 nm, and stable ultra short pulses were obtained, with a signal to noise of more than 60 dB. The emission light of the fiber laser located at the edge of the gain spectrum of the EDF, the 3 dB spectrum of the laser was about 2.3 nm. The pulse width was about 1.9 ps. It is found in the experiment that the reabsorption of the amplified spontaneous emission of the gain medium would result in the wavelength red-shift. Such results demonstrated the potentially extended applications of fiber lasers as a seed source without complex frequency conversion or the requirement for novel gain medium.

9266-49, Session Post

7-mJ 70-W nanosecond linear-polarized thulium-doped fiber laser in all-fiber format

Jianlong Yang, Yao Wang, Geng Zhang, Yulong Tang, Jian-Qiu Xu, Shanghai Jiao Tong Univ. (China)

We demonstrate a nanosecond all-fiber MOPA with linear-polarized output at 2040 nm, seeded by an in-band-pumped gain-switched thulium-doped fiber laser, which can directly output tens-of-microjoules pulses with designable pulse duration and Gaussian-like pulse profile. After only two stages of amplification, we achieve an average power of 70 W at a pulse width of 114 ns and a repetition rate of 10 kHz, corresponding to a pulse energy of 7 mJ and a peak power of 61.4 kW. Benefit from the on-site polarization control technique we proposed, a polarization extinction ratio (PER) of 25 dB at the highest output is also obtained. To the best of our knowledge, this is the highest power nanosecond all-fiber laser reported at 2- μm waveband and the PER is also a record among high-power fiber lasers.

9266-50, Session Post

High-power continuous-wave ytterbium-doped fiber oscillator at 1018 nm

Renli Zhang, Univ. of Chinese Academy of Sciences (China) and Academy of Opto-Electronics (China); Yuhao Xue, Hong Zhang, Xiaobo Feng, Wupeng Gong, China South Industries Research Academy (China); Yong Bi, Academy of Opto-Electronics (China)

Ytterbium-doped fiber lasers (YDFLs) that operate from 1.0 to 1.2 μm are well known for their outstanding characteristics, which include excellent power conversion efficiency and the broad gain bandwidth. 1018 nm YDFLs have attracted many attentions for the use of tandem pumping, which is regarded and preliminarily demonstrated to be an ideal scheme for power scaling beyond multi-kilowatt level. We have demonstrated a 1018 nm continuous wave fiber oscillator pumped by LDs operating at 976 nm. Two kinds of Ytterbium-doped dual-clad fibers, 15/130 μm fiber and 25/250 μm fiber, are employed separately in the experiments. 67 W total output power with the 15/130 μm fiber for 100 W of pump power is achieved with a slope efficiency of 67%. And with the 25/250 μm fiber, 276 W total output power is generated for 360 W of pump power with a slope efficiency of 76%. To the best of our knowledge, this is the highest output ever reached by a dual-clad fiber oscillator at this wavelength that ever reported in open detail.

9266-51, Session Post

All-fiber designed narrow line-width 1.55 μm double cladding fiber lasers

Hongxin Su, Zhiyang Wu, Lijing Xu, Hebei Univ. (China)

Lasers operating in the eye-safe spectral region around 1.55 μm have numerous applications in many fields, such as fiber communication, free space optical communication, remote sensing lidar and coherent measurement. By the virtue of high lasing efficiency and high power potential in the 1.55 μm spectral region, Er³⁺/Yb³⁺ co-doped double cladding fiber lasers (EY-DCFLs) have been paid great attention and developed rapidly in the past years. In this paper, to develop 1.55 μm high power lasers with compactness, narrow spectral line-width and high wavelength stability suitable for practical applications, EY-DCFLs are built in all-fiber configuration with different parameters and the output characteristics are investigated experimentally. The experimental setups are composed of Er³⁺/Yb³⁺ co-doped double-clad gain fiber, multimode 976nm pump laser diode, double-clad fiber Bragg gratings (FBGs) and (1+1) \times 1 side pump couplers. To optimize the output characteristics, FBGs with narrow band width and different reflectivity are applied as output reflectors, and forward-pump manner and backward-pump manner are performed respectively. We find that as the efficiency and the spectral stability are considered simultaneously, EY-DCFL with low reflective FBG output mirror and in backward-pump manner is more desirable, which is in good agreement with theoretical simulation. In the optimized all-fiber EY-DCFL, the maximum output power with an optical-optical efficiency more than 25% is up to 2W, and the center wavelength is defined at 1550.8nm by the FBG with a line-width about 0.03nm.

9266-52, Session Post

High-power high-efficiency picosecond 355nm ultraviolet laser based on La₂CaB₁₀O₁₉ (LCB) crystal

Chao Yan, Yuye Wang, Degang Xu, Tianjin Univ. (China)

A high-power high efficiency picosecond (ps) 355 nm ultraviolet (UV) laser was reported based on the nonlinear optical crystal of type-I phase-matching La₂CaB₁₀O₁₉ (LCB) which possesses the characteristic of non-hygroscopicity. The high-power third harmonic generation was successfully achieved from a 1064 nm ps fundamental laser. The maximum output power of 7.81 W of 355 nm UV laser was obtained from 35.2 W 1064 nm ps laser (80 MHz repetition rate, 10 ps pulse width) with optical conversion efficiency of 22.2%. The experimental results show that the LCB crystal has a promising prospect in generating high-power high efficiency UV laser.

9266-53, Session Post

High-power PPMgLN intracavity doubled green laser

Yan Qi, Yong Bi, Yu Wang, Boxia Yan, Academy of Opto-Electronics (China); Rongrong Jiang, Beijing Phoebus Vision Optoelectronic Co., Ltd. (China)

The experimental setup of the LD end pumped intracavity doubled Nd:YVO₄/PPMgLN green laser at 532 nm is shown in Fig.1. Three mirror folded cavity is used. The pump source is a CW 20 W fiber-coupled laser diode array. The laser crystal is an a-cut Nd:YVO₄ crystal with the size of 3 mm(W) \times 3 mm(H) \times 6mm(L). The left side of the laser crystal is anti-reflection coated at 808 nm and high-reflection coated at 1064 nm as one mirror of the

cavity, the right side of Nd:YVO₄ is anti-reflection coated at 808 nm and 1064 nm. A plano-concave mirror (M1) with 50mm curvature radius is adopted in compact folded three-mirror as the output mirror, the concave surface is high-reflection coated at 1064 nm and high-transmission coated at 532 nm. The radius of plano-concave mirror M2 is 200mm, the concave surface is high-reflection coated at 1064 nm and 532 nm. A z-cut 5mol% MgO doped LiNbO₃ sample of 6.9 μm domain period and 50% duty cycle along the entire crystal length is adopted as the frequency doubler, both sides of the PPMgLN are anti-reflection coated at 1064 nm and 532 nm.

As a 1 mm-thick, 2 mm-long 5mol % MgO-doped quasiphase matched PPMgLN crystal is used intracavity frequency doubled, a 6.93 W Watt-level high power 532 nm laser is obtained with a pump power of 20 W at 808 nm, the optical-to-optical conversion efficiency is about 34.7%.

9266-54, Session Post

Pump couplers in a series connection

Xiao Chen, Tsinghua Univ. (China)

The coupling efficiency of the pump coupler determines the pump light injection capacity of a laser system. We have designed a pump coupler in a series connection, of which two or more pump couplers are spliced together through signal fibers to form a new pump coupler with high coupling efficiency and high output power. In the experiment, 3?1 end-pumping couplers and (2+1)?1 side-pumping couplers were made respectively and the two couplers were spliced to form a series connection. Six LDs with output power of 200 W respectively were spliced with the six pumping arms of the new pump coupler. A total output power of this series connection pump coupler was 1160 W, corresponding to a coupling efficiency as high as 98%. The loss of signal light was less than 0.4%.

9266-55, Session Post

Uniformity of pump intensity distribution in diode-array side-pumped laser rod

Wenwen Liu, Yanxiong Niu Sr., Haixia Liu, Caili Wang, Haisha Niu, Da Man, BeiHang Univ. (China)

Diode-pumped solid-state lasers are high efficiency, long lifetime, compact and reliable, so they have been covering a wide range of applications. Thermal effect is a major limiting factor in scaling the average power of high-power solid-state lasers, and it has been a critical issue in designing diode-pumped solid-state lasers. The uniform pump intensity distribution in laser rod can weaken the influence of thermal effects in lasers, and the research of improving the pump distribution uniformity has attracted a great deal of attention. People usually establish a model of single diode-bar pumped laser rod to calculate the distribution. However, for diode-array pumped laser rod, the model is limited and the calculation results have deviation with the actual pump distribution, which cannot reflect the real working conditions in lasers.

In this paper, the theoretical model of diode-array pumped laser rod is built. Based on the actual working environment of diode-array side-pumped Tm:YAG laser rod, the expression of pump intensity distribution in the laser medium is deduced. Additionally, the influence of total pump power, pump structure, Tm:YAG rod characteristic parameters and pump beam radius on pump intensity distribution are simulated and analyzed. Moreover, the parameters are optimized in order to obtain the optimistic results which are efficient to improve the uniformity of pump distribution. The results show that when the pumping distance from diode-array to the rod's surface is 3mm, the distance between two rows of diode-bars is 1mm, the absorption

coefficient is 330m⁻¹, the pump beam width is 2.5mm, the pump intensity distribution of five-way pumped laser rod is improved, and then the thermal effects could be weakened. The presented results can provide theoretical guidance to design and optimization of high-power lasers.

9266-56, Session Post

Design and fabricate large scale gold coated pulse compression grating for Ti: sapphire laser

Chaoming Li, Soochow Univ. (China)

Large scale broad bandwidth pulse compression grating which is used in the femtosecond Ti: sapphire laser is studied. The groove density of gold coated laser pulse compression grating is 1740lp/mm. The working wavelength of gold coated grating is from 700nm to 900nm and its deviation angle is 10 degree. By using rigorous coupled wave theory, a series of calculating results with different profiles of gold coated laser pulse compression grating, such as rectangular, trapezoidal, sin, semi-sin are provided in the paper. In addition, the fabrication process redundancy is also given. Generally, there are two ways to fabricate gold coated pulse compression gratings. One way is by depositing gold film on the photoresist mask. The other way is to transferring the photoresist mask microstructure into the glass substrate to obtain the glass mask by using ion etching technology. Then the glass mask is coated with gold to fabricate gold coated pulse compression gratings. By using holographic recording method, and optimization of process parameters (including the photoresist thickness control, exposure dose, developing concentration control and time control etc.), a gold coated laser pulse compression grating with 200mm?400mm scale has been fabricated. The -1st diffraction efficiency of this gold coated grating reaches 94%(TM@808nm).

9266-57, Session Post

Analysis of the refractive index change of optical waveguide in LiNbO₃ using a femtosecond laser

Shihan Yang, Zhang Liang, Xuesong Lin, Feng Jie, Jun-Jiang Chen, Zigang Zhou, Southwest Univ. of Science and Technology (China)

We used a commercially available 75 MHz regeneratively amplified laser system emitting 50 femtosecond pulses of energies up to 3nJ at a wavelength of 800 nm. All waveguides were fabricated by focussing the femtosecond pulse train polarised parallel to the x-axis to a distance of approximately 125 μm below the sample surface using a 0.65 NA, ?40 microscope objective and translating the sample along the y axis. To find the optimum waveguide fabrication parameters the translation speed was varied from 2 to 100 μm/s. We introduces a method of measuring the refractive index of optical waveguide in ten micrometer. Using CCD to measure the two-dimensional near-field light intensity distribution of the output cross-section of the waveguide, by measuring the two-dimensional near-field light intensity distribution of the output cross-section of the waveguide can be calculated the two-dimensional distribution of refractive index of waveguides. The context detailedly gives measurement results about femtosecond laser inducing the near-field intensity of lithium niobate optical waveguide cross-section and calculations of refractive index of optical waveguide. The results show that the refractive index of waveguides showed a large central, gradually reduce and the change of refractive index in the range of 0.001. This method is of great significance to measure the optical waveguide refractive index distribution.

9266-58, Session Post

Fabrication of lithium niobate-based low-loss bend optical waveguide

Xin Li, Ang Llu, Qiu Yu, Jie Feng, Jun-Jiang Chen, Xuesong Lin, Shihan Yang, Zi-gang Zhou, Southwest Univ. of Science and Technology (China)

In this paper, by using tightly focused femtosecond laser pulses with repetition rate 76 MHz, pulse duration 50 fs, average out power 270mW, and the focus lens' NA is 0.65. We put forward a structure of waveguide that bent it to be 1/4 round, and research it by make experiments. Under the above conditions, when the vertical scanning speed of the laser system is 0.8 mm / s, the width of the bend optical waveguide is about 10 μ m, the loss reaches a minimum value about 1dB/cm when the bend way's radius is about 5mm. Based on the experimental results of the above parameters, we can manufacture a 1/4 round vertical bend fiber coupler, the device can be applied to the connection between the chips or inter-level optical. The results showed that the bend lithium niobate waveguides can be applied in the field of optical communication and has important implications for the production of low loss, low cost and small size optical waveguide gratings, vertical fiber coupler, optical switches and other devices.

9266-59, Session Post

Design of high-efficiency broadband pulse compression device based on composite transmission grating with high damage threshold

Xinrong Chen, Soochow Univ. (China); Chaoming Li, Soochow Univ (China)

A novel pulse compression device has been developed for femtosecond Ti: sapphire laser at 800nm center wavelength with 700nm-900nm bandwidth. This new kind of composite pulse compression device consists of two fused silica transmission gratings with 1250lp/mm and 3300lp/mm respectively and these two fused silica transmission gratings are located in two optical surfaces of the same fused silica plate. With an appropriate design, it can achieve high diffraction efficiency and high transmittance in a broad-bandwidth range. Owing to use anti-reflection transmission gratings with high space frequency (3300lp/mm), it can avoid the diffraction aberration due to coating antireflection film on one surface of the fused silica plate. In addition, because the whole device is made of fused silica, this new composite pulse compression device will be expected to have high laser damage threshold. The diffraction efficiency with different grating groove (rectangular or trapezoidal) and different polarization states (TE or TM) is provided and the corresponding process tolerance range which is useful in device manufacturing is given also. The calculation results show that: the -1st diffraction efficiency of 1250lp/mm grating at 800nm can reach 97% and the transmittance of 3300lp/mm grating up to 99.9%.

9266-60, Session Post

Characteristics of nonlinear imaging of broadband laser stacked by chirped pulses

Youwen Wang, Kaiming You, Liezun Chen, Shizhuan Lu, Zhiping Dai, Xiaohui Ling, Hengyang Normal Univ. (China)

Nanosecond-level pulses of specific shape is usually generated by stacking chirped pulses for high-power inertial confinement fusion driver, in which nonlinear imaging of scatterers may

damage precious optical elements. We present a numerical study of the characteristics of nonlinear imaging of scatterers in broadband laser stacked by chirped pulses to disclose the dependence of location and intensity of images on the parameters of the stacked pulse. It is shown that, for sub-nanosecond long sub-pulses with chirp or transform-limited sub-pulses, the time-mean intensity and location of images through normally dispersive and anomalously dispersive self-focusing medium slab are almost identical; While for picosecond-level short sub-pulses with chirp, the time-mean intensity of images for weak normal dispersion is higher than that for weak anomalous dispersion through a thin nonlinear slab; the result is opposite to that for strong dispersion in a thick nonlinear slab; Furthermore, for given time delay between neighboring sub-pulses, the time-mean intensity of images decreases with chirp of the sub-pulse increasing; for a given pulse width of sub-pulse, the time-mean intensity of images decreases with the time delay between neighboring sub-pulses increasing; additionally, there is a little difference in the time-mean intensity of images of the laser stacked by different numbers of sub-pulses. Finally, the obtained results are also given physical explanations.

9266-61, Session Post

Development of a sub-petawatt ultrashort laser facility

Xiaodong Wang, Qihua Zhu, Jingqin Su, Na Xie, Dongbin Jiang, Kainan Zhou, Xiaojun Huang, Xiaoming Zeng, Yi Guo, Li Sun, Qing Li, China Academy of Engineering Physics (China)

The paper presents the development of a sub-petawatt ultrashort laser facility, i.e. the upgraded super intense laser for experiment on the extremes (SILEX-I). The laser mainly consists of a femtosecond front-end system, a pulse filter based on cross-polarized wave (XPW) generation, three Ti:sapphire amplifiers with output powers greater than 5TW, 50TW, and 500TW respectively, and a compressor. The cross-polarized wave (XPW) generation technique was employed to improve the temporal contrast. To improve the power density on the target, a pair of achromatic lenses was designed to compensate astigmatism and an adaptive optical system was utilized to correct wavefront aberrations further before each shot. A high beam quality and image-relayed pump system was designed to pump the last two Ti:sapphire amplifiers.

9266-62, Session Post

Short pulse diagnostic for multi-petawatt laser facility

Qingwei Yang, Shanghai Institute of Optics and Fine Mechanics (China); Yanhai Wang, College of Sciences, Hebei University of Science and Technology (China); Xinglong Xie, Ailin Guo, Haidong Zhu, Jun Kang, Ping Zhu, Jianqiang Zhu, Shanghai Institute of Optics and Fine Mechanics (China)

In femtosecond multi-petawatt laser facility (e.g. 150J, 30fs, 290mm*290mm, 5PW), real-time accurate measurement is crucial for calculating focused intensity and helpful in inertial confinement fusion and laser-driven plasma accelerators experiments. In the short pulse diagnostic, there are many difficulties, for example as following: 1) For the femtosecond laser pulse (e.g. 30fs), any inserted optical elements in measuring optical path will cause the pulse broadening and some measurement error; 2) For a large diameter beam (e.g. 290mm*290mm), the chromatic aberration caused by the shrink beam device in the measuring optical path will make the

measurement error; 3) For a single real-time measurement, the material dispersion introduced by transmission sampling optical path will make the measurement error.

In order to meet the requirements of short pulse diagnostic in the multi-petawatt laser facility, a careful design of the diagnostic scheme, such as the theoretical analysis of the above difficulties and the corresponding solutions, is one of key problems in the building of this laser system. In this paper, based on the detailed analysis on mirror transmission sampling effects on measurement of pulse, the chromatic aberration caused by the shrink beam device effects on measurement of pulse, the residual dispersion symbols of the system effects on the measurement results and the corresponding solutions, a short diagnostic scheme suitable for the multi-petawatt laser facility is designed.

9266-63, Session Post

Analysis of chirped-pulse-amplification system based on Offner triplet stretcher and transmission grating

Lin Li, Soochow Univ. (China)

Chirped pulses amplification is a method which makes it possible to minimize the nonlinear effects and the risk of damage in the amplifier by stretching an ultra-short pulse prior to amplification. In CPA systems the seed pulse is temporally broadened by stretcher (e.g. Martinez or Offner stretcher). After the amplification the chirped pulse is compressed when it passes through a negative delay consisting of a pair of parallel gratings. In this paper, we deduce precise electric field expression of second and third order dispersions for Gaussian pulse. It is concluded that third order dispersion compensation not only can avoid pulse broadening, but also eliminate oscillation in the pulse edge. Next, we present an analytical phase expression for an Offner triplet telescope stretcher based on ray tracing. Under the condition of paraxial approximation, the expression reveals that Offner stretcher is the conjugation of a grating pair compressor. Through theoretical analysis and numerical simulation, the real-imaging procession exhibits some deviation compared to paraxial approximation, which can be attributed to the uncompensated spherical aberration of Offner stretcher. Finally, the stretched and amplified pulses are compressed by a diffraction grating compressor based on transmission gratings. By using transmission gratings, our compressor provides higher throughput and optical damage resistance than metallic reflection gratings. We can adjust the incident angle and perpendicular distance between gratings to completely compensate the second and third order dispersion of Offner stretcher in the central wavelength.

9266-64, Session Post

Numerical simulation of different pulse width of long-pulsed laser on aluminum alloy

Mingxin Li, Guangyong Jin, Juan Bi, Gui-bo Chen, Changchun Univ. of Science and Technology (China)

This simulation is based on the interaction between single pulsed laser with different pulse width and different peak energy and aluminum alloy material. By comparing the theoretical simulation data and the actual test data, we discover that: the theoretical simulation curve is well consistent with the actual experimental curve, this two-dimensional model is with high reliability; when the temperature at the center of aluminum alloy surface increases and evaporation happens after the surface temperature at the center of aluminum alloy surface reaches boiling point and later the aluminum alloy material sustains in the status of equilibrium

vaporization; the keyhole appears on the surface of the target, an increment of the keyhole, the maximum temperature at the center of aluminum alloy surface gradually moves inwardly. This research may provide the theoretical references to the understanding of the interaction between millisecond pulsed laser and many kinds of materials, as well as be beneficial to the application of the laser materials processing and military field.

9266-65, Session Post

The similarities and differences between coherent beam combination and mode-locking

Maohua Jiang, Peng Zhang, Renjiang Zhu, Yu Zhang, Chongqing Normal Univ. (China)

Coherent beams combination(CBC) is a very important way to reach high power output with good beam quality, the key problem in CBC is how to control the phase error between each beam. And mode-locking is also a very important way to achieve pulse output in laser technology, the key problem of mode-locking is phase-locking. This paper discussed the similarities and differences between CBC and mode-locking from principles, aims, methods, natures, trends and so on. It has been find that CBC effects on the modulation of the spatial plane, in order to concentrate the energy in a much smaller area, and the mode-locking effect is modulated in time, in order that the energy is concentrated in a smaller time range.

9266-66, Session Post

Longitudinally-excited CO2 laser with tail-free short pulse

Kazuyuki Uno, Kazuma Dobashi, Tetsuya Akitsu, Univ. of Yamanashi (Japan); Takahisa Jitsuno, Osaka Univ. (Japan)

With the rapid development of CO2 laser technology, CO2 lasers (9.2-11.4 μm) have been applied in industrial applications and medical treatments. Many excitation systems have been used for CO2 lasers. We focus on the longitudinal excitation scheme to realize a low-cost, portable, maintenance-free, and warm-up-free industrial CO2 laser. In the longitudinal excitation scheme, the excitation discharge is in the direction of the laser axis, and the electrodes are well separated and have small discharge cross-section. The scheme does not require a strong preionization or a fast gas flow system. The long discharge length provides a large discharge impedance, but the laser system produces a short-pulse CO2 laser by controlling the discharge.

The laser tube was consisted of a 60-cm-long discharge tube or a tandem tube that was constituted by connecting two 30-cm-long discharge tubes with an intermediate electrode. The laser system was consisted of the laser tube, an optical cavity with a ZnSe output coupler with a reflectivity of 85% and a high-reflection mirror, a pulse power supply producing -600 V, a step-up transformer, a storage capacitance, and a spark-gap switch with a trigger system. The laser system produced a short laser pulse without pulse tail like Q-switched CO2 lasers. The tandem-tube scheme produced a short laser pulse by lower charging voltage than the single-tube scheme. In this work, the maximum peak intensity was 312 kW at the pulse width of 60 ns (FWHM) and the output energy of 18.7 mJ.

9266-67, Session Post

Simulation of wavefront sensorless correction based on Stochastic Parallel Gradient Descent algorithm

Gang Wang, yudie zhang, CETC-11 (China)

Stochastic Parallel Gradient Descent (SPGD) algorithm can optimize the system exhibition firsthand without using of wavefront sensor, it predigests the adaptive optic system. Based on SPGD algorithm, a model with 32 element demorphable mirror was simulated, the capability of correct toward static aberration and convergence of SPGD algorithm are analysed, the relationship of gain coefficient, stochastic perturbation amplitude are discussed, an adaptive adjustment of gain coefficient is proposed, and it can improve convergence rate effectively.

9266-68, Session Post

Comparison of different Nd doping concentrations in YAG crystal

Kai Li, Guochun Zhang, Yicheng Wu, Technical Institute of Physics and Chemistry (China)

Nd:YAG crystal is one of the most frequently used laser crystal used in diode-pumped solid-state laser. However, the laser output performances may vary a lot for different Nd doping concentrations and different manufacturers. In this paper, the performances of YAG crystals with different Nd doping concentrations, 0.5%, 0.7%, 0.8% and 1.0%, are compared. A side-pumped laser module is used, in which the 808nm bars have a total power of 400W. The actual concentration, absorption coefficient, and fluorescence lifetime at different site of the crystals are measured. The power, pulse width, and laser mode at different repetition frequencies are tested. The peak power density is calculated to compare different doping concentrations. It's concluded that 0.5% Nd doping concentrations has the best performance, in which the largest power, rather small pulse width, and the largest peak power density are obtained.

9266-22, Session 5

Research of quasi-three-level thermal effect of diode-side-pumped Tm:YAG crystal

Yanxiong Niu Sr., Caili Wang, Wenwen Liu, Haisha Niu, Da Man, BeiHang Univ. (China)

The combination of volumetric heating of the laser material by the absorbed pump radiation and surface cooling required for heat extraction leads to a no uniform temperature distribution in the rod. With the coactions of pump field and coolant, the temperature gradient is formed within laser working medium, and then the thermal effects including thermal lens, thermal stress birefringence, etc. They all seriously restrict the output characteristics of laser. The uniform temperature field distribution in laser working medium weakens the influences of thermal effects in laser. The thermal effect of Tm:YAG laser generated by laser-diode pumping the Tm:YAG crystal is analyzed. After considering the quasi three-level structure of the crystal, a more actual temperature field in the crystal is obtained by revamping the heat conversion coefficient. The thermal effects mechanics were analyzed at first, and then the physical and mathematical thermal analysis models were established based on the theoretical knowledge of thermal effects in LD side-pumped Tm:YAG laser, the Tm:YAG crystal's temperature and thermal stresses distribution was simulated by using MATLAB software.

The method can be applied to the laser thermal effect research of quasi three-level and three-level. The analysis and the result can be referred to the thermal effect research of the solid state laser end-pumped by the LD and the optimal design of resonant cavity.

9266-23, Session 5

High-power 1060-nm super large cavity semiconductor lasers

Shaoyang Tan, Teng Zhai, Wei Wang, Ruikang Zhang, Dan Lu, Chen Ji, Institute of Semiconductors (China)

The design and realization of high power single-mode ridge waveguide 1060-nm semiconductor lasers with super large cavity are reported. The lasers consist of compressively strained double InGaAs/GaAs quantum wells and a GaAs/AlGaAs separate confinement vertical structure. A super large vertical optical cavity is employed to realize low internal loss, large optical spot size and low vertical optical divergence angle. The material composition and thickness of waveguide layers and claddings layer are optimized systematically. The active layer is detuned from the center of the waveguide and thickness of cladding layers is optimized to guarantee single mode lasing of the large optical cavity. The large vertical cavity laser structure with thickness of 4 μm allows the lasers having a low internal loss of less than 0.6/cm, a large optical spot size about 1 μm and a vertical divergence angle about 20 degree. For lateral optical confinement, a double trench ridge waveguide is employed to maintain single-lateral-mode operation. Based on the optimization, 1.5 W continue wave optical power is achieved for broad area lasers with 1-mm cavity length. Narrow stripe ridge waveguide lasers of 1-mm cavity length with single mode current and optical power of 700 mA and 340 mW, respectively, is obtained. Suggestions for further improvements in terms of single mode power and applications of the high power semiconductors are discussed.

9266-24, Session 5

Investigation of physical features of both static and flowing-gas diode-pumped rubidium vapor lasers

Juhong Han, You Wang, Wei Zhang, He Cai, Liangping Xue, Hongyuan Wang, Guofei An, Southwest Institute of Technical Physics (China)

A diode-pumped alkali lasers (DPAL) is a new kind of laser source which can offer laser radiation with high efficiency and little thermally-induced effects at the near-infrared wavelength region. By constructing the theoretical algorithms of kinetic and fluid dynamic analyses, the thermal features and output characteristics of a DPAL have been systematically evaluated for both static and flowing-gas statuses. The corresponding temperature distributions are calculated for different waists and powers of a pump beam. The results are thought to be useful for realization of a high-powered DPAL in the future.

9266-25, Session 5

High average power passively Q-switched laser by using Nd:YAG/Cr:YAG/YAG composite crystal

Siqi Zhu, Jinan Univ. (China)

A high average power passively Q-switched 1064 nm laser by

using Nd:YAG/Cr:YAG/YAG composite crystal were reported. The average output power of 1064 nm was measured with 85% initial transmission of Cr:YAG. When the maximum pump power was 187.5 W, the maximum average output power of 83.68 W at 1064 nm is obtained. By frequency doubling the 1064 nm laser output in a KTP nonlinear crystal, 27.2 W green laser pulses at 532 nm with the corresponding pulse width of 210 ns and the repetition rate of 21.2 kHz are produced under the maximum pump power. The 532 nm laser single-pulse energy is 1.28 mJ and the peak power is 6.1 kW. And the optical-to-optical conversion efficiency of pump light to frequency-doubling light is 14.72%.

9266-26, Session 5

High-power high-beam quality Nd:YVO4 slab laser pumped with high duty cycle quasi-continuous wave laser diode stacks

Yang Liu, North China Research Institute of Electro-optics (China)

Diode end-pumped solid state lasers have been shown to be compact, efficiency sources with high beam qualities, which are widely used in industry and research such as micromachining and efficient harmonic generation. And slab lasers, because of great thermal management, have great potential to get high power with high beam quality. In this paper, we use the quasi-continuous wave laser diode stacks as the pumping source, which have the duty cycle of 20%, also with the pulse width of 200 ns and repetition of 1kHz. To improve the beam quality of the slab laser, we use the innovate resonator to restrain the high order modes in the slab laser. In the vertical direction, a stable resonator is used, and the pumped region matches well with the TEM00 mode, and in the horizontal direction, we use the unstable resonator to improve the beam quality. And in the vertical direction, the size of the beam in the resonator is calculated with different thermal lens, which shows that the TEM00 size in the resonator can matches the pumping size in a large thermal range. Using this configuration, with Nd:YVO4 as the slab gain media, 101 W output power is obtained when the pumping power is 216.5W with the repetition of 1kHz, the optical-to-optical efficiency and slope efficiency are 46.7% and 51.14%, respectively. The beam quality M2 factors in the unstable direction and the stable direction are 1.36 and 1.56 respectively at the output power of 101 W.

9266-27, Session 5

Theoretical analysis of wavelength-switchable diode-side-pumped Tm:YAG laser

Caili Wang, Yanxiong Niu Sr., Wenwen Liu, Haisha Niu, Da Man, BeiHang Univ. (China)

The high-power lasers at Tm:YAG Laser have attracted great research attention and it have been extensively investigated recently because of its attractive applications in the areas of medical treatment, optical communications and effective pump sources for optical parametric oscillators. In the Tm³⁺ doped YAG crystal, the Tm³⁺ ions are excited into the 3H4 state from 3H6 state by absorbing pump radiation at ~ 785 nm, and the ions then relax down to the upper lasing level 3F4. The laser radiation takes place between the lower Stark level of 3F4 and the higher Stark level of 3H6. The considerable phonon broadening and high multiplicity of the Stark levels of the 4f electron provides tunability from 1.87 to 2.16 μm. We presented an analysis for the performance of side pumped quasi-three-level laser oscillators. Taking into account reabsorption loss, we present a theoretical model studies of quasi-three-level laser with particular attention given to the Tm:YAG laser. Equation for Tm:YAG quasi three-level

laser system is founded, and a formula of the threshold pump power of the laser is described. The threshold pump power with different emission wavelengths versus the transmission of the output coupler is discussed, and we also analysis the influence on the threshold pump power with different emission wavelengths affected by the crystal length. With the same pump power, a lower transmission of the output coupler would result in a higher intracavity intensity. As a result, the lower laser sub-level within 3H6 ground state manifold has higher reabsorption loss and therefore, the higher Stark sub-level within 3H6 ground state manifold has a lower laser threshold and longer laser wavelength.

9266-28, Session 6

Femtosecond laser microchannels fabrication based on electrons dynamics control using temporally or spatially shaped pulses (*Invited Paper*)

Xueliang Yan, Jie Hu, Xiaowei Li, Bo Xia, Pengjun Liu, Beijing Institute of Technology (China); Yongfeng Lu, Univ. of Nebraska-Lincoln (United States); Lan Jiang, Beijing Institute of Technology (China)

With ultrashort pulse durations and ultrahigh power densities, femtosecond (fs) laser presents unique advantages of high precision and high quality fabrication of microchannels in transparent materials. In our study, by shaping fs laser pulse energy distribution in temporal or spatial domains, localized transient electrons dynamics and the subsequent processes, such as phase changes, can be controlled, leading to the dramatic increases in the capability of fs laser microchannels fabrication. In water-assisted fs laser drilling, by temporally shaping the fs laser pulses into pulse trains, the enhancements of up to a 56 times higher material removal rate and a 3 times larger maximum drilling depth are obtained, as compared with unshaped fs laser processing. The temporally shaped fs laser pulse trains can also significantly enhance the etching rate of the fused silica and eliminate the dependence of etching rate on laser polarization in the microchannels fabrication with the method of fs laser irradiation followed by chemical etching. A 10 times higher etching rate and 3-5 times greater processing speeds can be achieved by double pulses in homogeneous photo-modification regime. As the pulse energy increases, nanogratings are formed inside the photo-modification zone. Double pulses can effectively change the morphology of nanogratings, resulting in 7 times greater maximum aspect-ratios of three-dimensional microchannels. Besides, high-aspect-ratio (~300:1) and small-diameter (2.0-2.5 μm) holes are drilled in polymethyl methacrylate by spatially shaping fs laser pulses into zero-order nondiffracting Bessel beams, which have a much longer depth of focus than the Rayleigh range generated by Gaussian beams.

9266-29, Session 6

Direct diode lasers for material processing applications: beam shaping and power scaling

Klaus Reinecke, LIMO Lissotschenko Mikrooptik GmbH (Germany)

First application notes were published for cutting of metal sheets of up to 4 mm thickness by means of high power diode lasers during last couple of years. The power level used for these experiments was typically in the range of 1 kW to 2 kW.

This paper presents approaches of high power diode lasers of up to 8 kW based on conventional, highly reliable and well tested principles and components - namely passively cooled laser diode

bars, coarse wavelengths coupling and fiber delivery. The clue of power scaling of these systems is to apply special, asymmetric, noncircular beam shaping. The beam parameter product of the laser light is manipulated accordingly. It allows the generation of spot geometries which inherently support the interaction processes of the laser light with materials as metals.

First results in material processing are presented. The main focus is on cutting applications. The new laser configurations allow cutting of mild- and stainless steel of thicknesses exceeding 8 mm with high quality of the cutting kerf. Furthermore, the potential of no circular focus geometries is shown in experiments for surface modifications.

9266-30, Session 6

Ultraviolet pulsed laser micromachining of Si and SiC wafer

Litao Qi, Mingxing Li, Haipeng Lin, Jinping Hu, Qingju Tang, Chunsheng Liu, Heilongjiang Institute of Science and Technology (China)

This paper provides an investigation of the ablation behavior of single crystal 4H-SiC and 6H-SiC to improve the manufacturability and high-temperature performance of SiC using laser applications. Ultraviolet pulsed laser (266nm and 213nm) micromachining of 3C-SiC wafer was investigated. The purpose is to establish suitable laser parametric regime for the fabrication of high accuracy, high spatial resolution and thin diaphragms for high-temperature MEMS pressure sensor applications. Etch rate, ablation threshold and quality of micromachined features were evaluated. The governing ablation mechanisms, such as thermal vaporization, phase explosion, and photomechanical fragmentation, were correlated with the effects of pulse energy. The etch rate and the ablation threshold is obtained with ultraviolet pulsed laser ablation. The results suggested ultraviolet pulsed laser's potential for rapid manufacturing. In addition, the etch rates were substantially higher than those achievable in various reactive ion and electrochemical etching methods. Excellent quality of machined features with little collateral thermal damage was obtained in the lower pulse energy range. The leading material removal mechanisms under these conditions were discussed.

9266-31, Session 6

Temperature fields during the long-pulse laser irradiating aluminium alloy plate

Wei Zhang, Changchun Univ. of Science and Technology (China)

Based on Von Mises yield criterion and elasto-plastic constitutive equations, an axisymmetric finite element model of a Gaussian laser beam irradiating a metal substrate was established. In the model of finite element, the finite difference hybrid algorithm is used to solve the problem of transient temperature field. Moreover, distributions as well as histories of temperature fields were obtained. On the foundation of theoretical analysis, transient of temperature field in 7A04 aluminium alloy plate under the pulse train of long-pulse laser irradiation is simulated and calculated. Finite element analysis software COMSOL is used to simulate the Temperature during the pulse train of long-pulse laser irradiating 7A04 aluminium alloy plate.

By the analysis of the results, it is found that because of the good thermal conductivity of 7A04 aluminum alloy, thermal diffusion is extremely quick after laser irradiate. As a result, for the multi-pulsed laser, 7A04 aluminum alloy will not produce obvious temperature accumulation when the laser frequency is less than or equal to 10 Hz.

The result of this paper provides theoretical foundation not only for research of theories of 7A04 aluminium alloy and its numerical simulation under laser radiation but also for long-pulse laser technology and widening its application scope. Comparison of the numerical results with the reported experiments results shows the availability of the finite element method.

Key words: Temperature field , Pulse train, Long-pulse laser?COMSOL

9266-33, Session 7

Injecting parameters design and performance test of the pre-igniter for continuous wave DF/HF chemical lasers

Bing Huang, Shengfu Yuan, Lijia Yang, Xiaoting Fang, National Univ. of Defense Technology (China)

Igniter is an integral part of the combustion driven continuous wave (cw) DF / HF chemical laser. Usually, aviation spark plug is used as the igniter, and in the combustion chamber the sparkplug-igniter directly contacts with the strong oxidizing gas with high temperature and high pressure, which would badly ablate the igniter. Then Combustion-driven cw DF/HF chemical lasers cannot be inflamed successfully because the sparkplug-igniter is intolerant of ablation, especially after long-time operation. This problem seriously affected the reliability of the lasers. In this paper, a pre-igniter is designed as a new ignition system to produce F2 to inflame the lasrs, based on the principle that high-intensity spontaneous combustion will happen when F2 mixes with H2. Firstly, the injecting parameters of the pre-igniter were designed, then the results of NF3 and H2 reacting with different mole ratios were calculated by CEA software. The operation reliability of the pre-igniter, the mole concentration of F2 in the mixing gas, and the equilibrium temperature were validated by a series of experiments. The experimental results were consistent with the calculated data: with the mole ratio of NF3 to H2 increasing, the equilibrium temperature decreased gradually and finally leveled off; the mole concentration of F2 in the mixing gas first increased and then decreased, achieving the maximum of about 40% when the mole ratio of NF3 to H2 was about 3.2. Experimental results showed that the pre-igniter performed reliably and could produce high output of F2. The ignition system with a pre-igniter and a spark plug could provide a new alternative for combustion-driven CW DF/HF chemical laser.

9266-34, Session 7

Characteristic optimization of 1.55- μ m InGaAsP/InP high-power diode laser

Qing Ke, Shaoyang Tan, Teng Zhai, Ruikang Zhang, Dan Lu, Chen Ji, Institute of Semiconductors (China)

A comprehensive design optimization of 1.55- μ m high power InGaAsP/InP board area lasers is performed aiming at increasing the internal quantum efficiency (IQE) while maintaining a low internal loss of the device as well . The P-doping profile and separate confinement heterostructure (SCH) layer bandgap are optimized respectively with commercial software Crosslight. Analysis of lasers with different p-doping profiles shows that, although heavy doping in P-cladding layer increases the internal loss of the device, it ensures a high IQE because higher energy barrier at the SCH/P-cladding interface as a result of heavy doping helps reduce the carrier leakage from the waveguide to the InP-cladding layer. The results also show that the carrier leakage current density increases faster with lower P-doping value in InP-cladding layer and higher band gap value in SCH layer. The band gap and thickness of the

SCH layer are also optimized for high slope efficiency. Smaller band gap helps reduce the vertical carrier leakage from the waveguide to the P-cladding layer, but the corresponding higher carrier concentration in SCH layer will cause some radiative recombination, thus influencing the IQE. And as the injection current increases, the carrier concentration increases faster with smaller band gap, therefore, the output power saturates sooner. The width of the waveguide is also increased to reduce the internal loss without the occurrence of higher-order transverse mode. An optimized band gap in SCH layer of approximately 1.127eV and heavy doping up to $0.7 \times 10^{18}/\text{cm}^3$ at the SCH/P-cladding interface are identified for our high power laser design, and we achieved a high IQE of 92% and internal loss of 4.7/cm for our design.

9266-35, Session 7

Broadband generation by multiple four-wave mixing process due to ASE Q-switching in high-power double-clad Ytterbium-doped fiber amplifier

Sourav D. Chowdhury, Nishant Shekhar, Maitreyee Saha, Ranjan Sen, Mrinmay Pal, Central Glass and Ceramic Research Institute (India)

High power cladding pumped fiber amplifiers are used for amplifying low power continuous wave and pulsed seed sources. Depending on the splice loss, saturable absorption effect of the double clad active fiber and the pump power the system can show intrinsic lasing and self-pulsing. The pulses originate from passive Q-switching of the amplified spontaneous emission (ASE) due to saturable absorption effect, resulting in broadband spectral output. Here the amplifier setup consists of a 5.5m double clad, double D shaped Ytterbium doped fiber pumped at 976nm by multi-mode laser diodes, a single clad passive fiber is used for excess pump absorption and a 99.9:0.1 splitter for monitoring in OSA. We observe broadband output from 1060nm to 1700nm and red light pulsing with and without a CW seed. The broadband is not continuous but contains discrete multiple wavelengths. It is generated by multiple four-wave mixing process with maximum broadening efficiency near 1300nm which is the zero dispersion wavelength for silica fiber. The visible red light generates from cascaded four-wave mixing of the already generated multiple wavelengths. The generated intense pulses travel both in forward and backward direction and have enough high peak power and energy to damage splice points and fiber components even through isolator connected before the amplifier block. Under the presence of a sufficient seed the self-pulsing and broadband generation is often suppressed. But with increased pump powers the system can again self Q-switch and generate broadband.

9266-36, Session 8

Self-pumped stimulated Brillouin scattering of high-power super-Gaussian shaped laser pulses

Xuehua Zhu, Henan Polytechnic Univ. (China); Yulei Wang, Harbin Engineering Univ. (China); Zhiwei Lu, Harbin Institute of Technology (China)

In this paper, we investigated theoretically and experimentally the self-pumped stimulated Brillouin scattering of super-Gaussian shaped 3ns laser pulses transmitting in the Brillouin active medium FC-40. A frequency-doubled high power Nd:glass laser system with the wavelength of 527nm is used as the pump source, and the laser pulses are nearly flat-top shaped. According

to Fourier transform theory, there is a sideband in the frequency domain of the flat-top laser pulses. When the collimated laser pulses irradiated onto the surface of the rear cell window, partial of the pulse is reflected to transmit in the opposite direction. The Stokes component within the weak feedback pulse, whose frequency difference with the main frequency of the pump pulse equals to Brillouin shift of the nonlinear medium, can be amplified by the forward-transmitted pump laser. The physical geometry is similar to the traditional "Brillouin-amplifier" with a weak seed injected in the other side of the medium. When the pump energy is higher than some certain value (so called SBS threshold), the SBS process will be established from the randomly distributed thermal noise within the Brillouin medium. To distinguish the feedback initiated SBS component with the noise initiated at high pump energy condition, the length of the medium cell (60cm) is designed to be longer than half of the spatial length corresponding to the laser pulse-width (~35cm in FC-40). Both the results of simulation and that of experimental shows that the weak feedback of the cell window reduced the SBS threshold for nearly 2 folds.

9266-37, Session 8

Optical parametric amplification for few-cycle IR pulse generation using a collinear geometry

Qingbin Zhang, Zuofei Hong, Peixiang Lu, Huazhong Univ. of Science and Technology (China)

A novel compact dual-crystal optical parametric amplification (DOPA) scheme, collinearly pumped by a Ti:sapphire laser (0.8 μm), is theoretically investigated for efficiently generating broadband IR pulses at non-degenerate wavelengths (1.2 μm , 1.4 μm and 1.8 μm , 2.1 μm). By inserting a pair of barium fluoride (BaF₂) wedges between two thin λ -barium borate (BBO) crystals, the group velocity mismatch (GVM) between the three interacting pulses can be compensated simultaneously. In this case, the obtained signal spectrum centered at 1.3 μm is nearly 20% broader and the conversion efficiency is increased, but also the pulse contrast and beam quality are improved due to the better temporal overlap. Furthermore, sub-two-cycle idler pulses with carrier-envelope phase (CEP) fluctuation of sub-100-mrad root mean square (RMS) can be generated.

On the other hand, a degenerate dual-pump optical parametric chirped-pulse amplifier (OPCPA) for generation of few-cycle intense pulses centered at 1.6 μm is theoretically proposed. By adding the optimized linear chirp to the two pump pulses from Ti:sapphire source and carefully adjusting the delays between the two pumps and seed, the long- and short-wavelength components of the seed pulse are efficiently amplified during the parametric process. Our simulations show that a broadband spectrum spanning from 1.3 μm to 1.9 μm is attained with a conversion efficiency of 15.3%. Signal pulse with a near transform-limited (TL) duration of 11.6 fs can be achieved by simply removing the linear chirp from the output signal. Besides, the compressed signal beam manifests good quality both spectrally and temporally.

9266-38, Session 8

Investigation on the formation of second-order-hot-image-like fringes

Yonghua Hu, Guohui Li, Shaobo Zhang, Yi Shen, Hunan Univ. of Science and Technology (China)

It is well known that second-order hot-image will be produced for a scatterer with phase modulation. However, when the number of scatterer is larger than one, the interaction between

the scattered waves will lead to new nonlinear propagation phenomena. In this paper, the nonlinear imaging propagation from two parallel wirelike phase-typed scatterers is investigated through computer simulation and some interesting propagation phenomena are demonstrated. Under certain conditions, there is no intense second-order hot image fringe in the predicated plane half-distance from the medium to the scatterer, but there are other two intense fringes whose in-beam positions are some distance deviated from those of the scatterers. These intense fringes are called second-order-hot-image-like fringes in this paper. When compared with the corresponding single scatterer case, the intensity level of the fringes are close to that of second-order hot image fringe, and there are also hot image fringes, but their intensities are much lower. The influence of the phase modulation depth of the scatterers on the propagation for both double and single scatterer cases is also investigated. First, as the phase modulation depth increases, the fringe intensity changes same as second-order hot image fringe does and their intensities keep very close to each other. Second, in a certain value range of phase modulation depth, the fringe intensity decreases at first and then increases but the hot image intensity changes inversely around an intensity level. Third, in the Kerr medium, the maximum intensity of the beam in the double scatterer case is higher than that in the single scatterer case except for the phase modulation value section around 3 rad.

9266-39, Session 8

Finite element simulation of laser-induced ultrasonic wave in layered structure

Yan Zhao, Liping Xue, Nanjing Univ. of Science and Technology (China)

Ultrasonic field in layered structure excited by a nanosecond pulsed laser irradiation is numerically simulated by finite element method. Typical calculation is executed for a configuration of a zirconium nitride (ZrN) thin film with different thickness on a steel substrate. The waveforms of surface acoustic wave are presented and the dispersion properties of surface waves in two-layered structure are analyzed by the method of phase spectral analysis, and the results show that the surface wave is anomalous dispersive with the higher frequencies propagating fast than the lower frequencies, and that with the decrease of film thickness, the dispersion of surface wave becomes more serious.

Conference 9267: Semiconductor Lasers and Applications VI

Thursday - Saturday 9 -11 October 2014

Part of Proceedings of SPIE Vol. 9267 Semiconductor Lasers and Applications VI

9267-1, Session 1

Novel InGaAlAs/InGaAlAs quantum well multimode-interferometer-Fabry-Perot laser diode (*Invited Paper*)

Hua Yang, Brian Corbett, Tyndall National Institute (Ireland); Frank H. Peters, Tyndall National Institute (Ireland) and Univ. College Cork (Ireland)

Single mode lasers are an indispensable component in communication systems for generating the optical signals. They are typically based on distributed feedback (DFB) or distributed Bragg reflector (DBR) lasers due to their robust single mode behaviour. However, the lasers require submicron gratings which must be generated using electron beam or holographic lithography, and may also require a second epitaxial growth, both of which are time consuming and costly. Slotted Fabry Perot (SFP) lasers have been reported as an alternative option which demonstrate comparable single mode performance and can be fabricated using only photolithographic techniques and no regrowth. In this paper, we demonstrate a novel single-mode multimode-interferometer-Fabry-Perot (MMI-FP) laser in which a multimode interferometer is inserted in the conventional FP laser waveguide to generate single wavelength emission.

Simulations were done using FIMMWAVE commercial software in the design and the principle was analysed with the experimental result. A fabricated AlInGaAs/AlInGaAs quantum well MMI-FP laser with single output arm shows a SMSR of 25dBm at 1567.15nm wavelength and also tunability in a certain range with injection current. Also the laser with three output arms can be used to generate coherent source by injection locking to the MMI-FP LD. The fabrication of the proposed laser device is as simple as that of the standard FP laser which significantly eases the processing enabling an increase in the yield and a reduction in the cost.

9267-2, Session 1

MOCVD growth of InAs/InGaAsP/InP quantum dots and their laser applications (*Invited Paper*)

Tao Yang, Shuai Luo, Feng Gao, Institute of Semiconductors (China)

InAs/InP quantum dot (QD) lasers have recently attracted considerable attention as they can emit in a wide wavelength range from 1.3 μm to 2.1 μm , which has promising prospects in optical fiber communication, gas detection, biomedical applications etc. In this talk, we'll introduce our research progress in the growth of InAs/InP QDs by MOCVD and their lasers. In particular, by optimizing the growth parameters, the emission wavelength of the QDs can be tuned in the wavelength range from 1.3 to 1.9 μm . By employing a double-cap procedure with two growth temperatures to grow the capping layer, the PL characteristics of the QDs can be significantly improved, including a dramatically reduced PL linewidth from 124 meV to 87 meV, an enhanced PL peak intensity, and improved PL distribution uniformity across wafer surface. Based on the optimized growth condition, lasers working in different wavelength under continuous wave mode have been demonstrated. In particular, the 1.5 μm as-cleaved laser can work at up to 110 $^{\circ}\text{C}$ and has a high characteristic temperature (T_0) of 245 K between 20 and 50 $^{\circ}\text{C}$. To the best of our knowledge, this T_0 achieved here is the highest reported so far for InP-based semiconductor lasers. Moreover, to take advantage of the wide

gain spectrum of the active region arising from the large size dispersion of the QDs, a tunable external cavity QD laser with a large wavelength tuning range of 144 nm has been obtained.

9267-3, Session 1

Simultaneous five-state lasing from intermixed InAs/GaAs quantum dot laser

Mohammed A. Majid, Hala H. Alhashim, Mohammed Zahed Mustafa Khan, Tien Khee Ng, Boon S. Ooi, King Abdullah Univ. of Science and Technology (Saudi Arabia)

Self-assembled InAs/GaAs quantum dots (QDs), utilized as active media in semiconductor lasers, have attracted considerable interests for the fabrication of high performance optoelectronic devices due to their superior properties such as ultra-low and temperature stable threshold current density, high-speed operation, and low frequency chirping. QD lasers with broadband lasing spectrum are highly desirable for applications in mode-locking, fiber-optic sensing and low-coherence imaging. Furthermore, bias controlled multimode lasing covering a broad wavelength band have been realized a potential in wavelength switching, read and write operations, and a source for wavelength division multiplexing. Recently, experimental observation of simultaneous lasing in steady state via ground state, first excited state and the second excited state in QD lasers have been reported. However, to our knowledge, there is no experimental investigation of multistate lasing from post-growth intermixed QD laser. In this work, by utilizing a high current density and appropriate choice of cavity lengths, in an intermixed modulation p-doped multi-stack InAs QD laser structure, we observed simultaneous five-state lasing at room temperature in the very important wavelength range of 1030 to 1125 nm (frequency doubling for green light generation). We attribute the multistate lasing to the significant reduction in the energy separation of electronic states, high carrier population in the QD states as well as long relaxation time from high energy level to lower energy levels. Owing to the increased degeneracy of excited states and 2D InGaAs wetting layer (metamorphic QD/ quantum well levels), the threshold current density of the simultaneous five-state lasing was higher.

9267-4, Session 2

VCSELs: Enabling technologies from access to terabit interconnects (*Invited Paper*)

Werner H. Hofmann, Technische Univ. Berlin (Germany)

The Vertical-Cavity Surface-Emitting Laser (VCSEL) has developed from an exotic device-concept to a mature device technology enabling novel products like the laser-mouse. Other application fields are communication and sensing.

VCSELs feature a very short optical cavity and only a very small amount active media has to be pumped compared to typical edge-emitters.

Modal properties can be defined at levels of dedicated distributed feed-back laser diodes. Featuring a designed cavity with Bragg-reflectors, mode-filters or even high-contrast gratings can be used. This yields a low-cost laser-diode with superior modal behavior which can be operated up to the thermal roll-over. Together with a well-designed mode-gain offset or detuning, very temperature-stable devices with intrinsic power limiter can be realized.

VCSELs have been developed in various configurations and emission wavelengths so far. 850-nm devices are matched to multi-mode fibers. These devices have the longest research history and are now commercially available from single-mode sources for laser mice to high-speed arrays for active optical cables.

Long-wavelength devices emitting at 1.3 μm and up, have application as directly modulated devices as coarse-wavelength division multiplexing and passive optical.

Very recently, optical interconnects for application in supercomputers moved into the center of attention. VCSELs are the natural candidate for this emerging mass-market.

Novel nanophotonic structures, so called can replace the thick top-mirror of VCSELs saving epitaxial thickness and cost. Additionally, this kind of reflector can ensure single-mode emission of larger aperture devices or define the cavity mode by structuring different patterns, making VCSEL arrays for wavelength-division-multiplexing feasible.

9267-5, Session 2

Nonlinear dynamics of polarization switching of a 1550-nm vertical-cavity surface-emitting laser under orthogonal optical injection

Jian-Jun Chen, Zheng-Mao Wu, Guang-Qiong Xia, Southwest Univ. (China)

In recent years, vertical-cavity surface-emitting lasers (VCSELs) are becoming increasingly attractive for promising applications in all-optical signal processing due to their inherent advantages over edge-emitting lasers (EELs), such as low threshold current, single-mode operation, high speed, circular output beam, high compactness, and so on. For short-wavelength VCSELs, previous reports demonstrated that by introducing orthogonal injection light into a VCSEL, a rich variety of nonlinear dynamical behaviors can be generated while the polarization switching (PS) and bistability may be observed. Recently, much more attention has been focus on the analysis of nonlinear dynamics in long-wavelength VCSELs emitting at 1550nm since this waveband VCSELs are low cost optical sources and power efficient devices in local and access networks. At present, some experimental investigations on nonlinear dynamics and PS of a 1550nm VCSEL subject to orthogonal optical injection have been conducted, however corresponding detailed theoretical analysis is still scarce.

In this work, by utilizing modified spin-flip model (SFM) of VCSELs extended to account for the noise and orthogonal optical injection in a 1550nm VCSEL, different bifurcation scenarios including periodic oscillation, injection locking and chaotic oscillation, in combination with time series and power spectra, can be observed. Detailed mappings of polarization-resolved nonlinear dynamical states are calculated to unveil a rich variety of dynamical scenarios for different scanning routes of injected power in the parameter space of injected power and frequency detuning, and show that the dynamical states and PS are critically dependent on the scanning routes of the injected power.

9267-6, Session 2

Design of high-power and narrow divergence angle photonic crystal surface-emitting lasers

Xiaojie Guo, Yufei Wang, Aiyi Qi, Lei Liu, Fan Qi, Wanhua Zheng, Institute of Semiconductors (China)

We design photonic crystal (PC) array surface emitting lasers

with large-area coherence. The structure has six-fold rotational symmetry. By finite-difference time-domain method, the far-field characteristics of the individual element and the array are simulated. The coherent PC array has lower far-field divergence angles and higher power compared to those of individual elements. Such PC array exhibits strong leaky coupling which has high mode stability and high intermodal discrimination, which shows great potential for high output power and low divergence in-phase surface laser emitting.

9267-7, Session 3

Detailed comparison of performance of a Fabry-Perot semiconductor laser under both strong- and weak-injection (Invited Paper)

Yali Zhang, Xuebao Peng, Shangjian Zhang, Yong Liu, Univ. of Electronic Science and Technology of China (China)

Optically-injected semiconductor lasers have attracted great attention for many years due to their simplicity in configuration but with rich performance in behavior, which can be find wide application in several ways. There has been extensive work on the injection-locking effect in kinds of semiconductor lasers, such as distributed feedback (DFB) lasers, Fabry-Perot (FP) lasers, and vertical cavity surface emitting lasers (VCSEL). Wherein, FP semiconductor lasers have drawn more interest as cost-effective colorless transmitters used in the WDM-PON.

In this paper, we numerically and experimentally investigate and compare the performance of a FP semiconductor laser under both strong- and weak-injection conditions in detail. The dynamics of the electronic and carrier density are simulated based on the rate equation model with injection term for the above two conditions, respectively. The numerical simulation results prove that the optically injection-locked FP semiconductor laser, featured in operating at a single-longitudinal mode, will become stable in the injection-locking region under the above two conditions. Nonetheless, the former arrangement can achieve stability faster than the latter for it can suppress relaxation oscillations effectively whatever the frequency detuning is.

Further, it is experimentally provided about the dynamic injection-locking map and the property of side-mode suppression ratio (SMSR) for the optically injection-locked FP semiconductor laser under strong optical injection with comparison to the weak injection arrangement. Associated experiment phenomena are observed and qualitatively discussed. Our experiments show that quite different dynamics are obtained in the two modes of operation, with weak-injection arrangement offering overall benefits in terms of more complicated dynamics and potential application.

9267-8, Session 3

Influence of the nonlinear gain on the stability limit of a semiconductor laser with external optical feedback

Yuanlong Fan, Yanguang Yu, Jiangtao Xi, Univ. of Wollongong (Australia); Huiying Ye, Zhengzhou Univ. (China)

Dynamical stability analysis of a single mode semiconductor laser (SL) under external optical feedback (EOF) system has been attracted an extensive attention by scholars in the past few decades due to the broad applications of an SL with EOF, such as optical communication, data recording and sensing. When the system determinant has no zeros in the right side of the S-plane, the system is thought as stable. For a DC biased

SL with EOF, the stability limit of the system is reached when the constant laser output just transits into periodic oscillation followed by other instabilities, including quasi-periodic oscillation, low frequency fluctuations (LFFs) and chaos. To determine the stability limit, the condition of the transition should be studied. Many relevant works have been conducted in the past decades. However, the influence of the nonlinear gain effect on the stability limit has escaped attention. Nonlinear gain effect is an important factor for describing the dynamic behaviors of an SL with EOF. The inclusion of nonlinear gain can provide a good agreement between numerical results and experimental results. In this paper, our analysis starts from the L-K equations. Firstly, a new and accurate system determinant is derived with the inclusion of nonlinear gain. Then by varying the parameters of the system, we observe the root locus of the system determinant, from which, the stability limit of an SL with EOF system is obtained. Finally, the influence of the nonlinear gain on the stability limit is investigated and a number of interesting discoveries are presented.

9267-9, Session 3

High side-mode suppression ratio laser output by single sideband injection locking of semiconductor lasers

Wang Jian, Shanghai Institute of Optics and Fine Mechanics (China)

High side-mode suppression ratio (SMSR) and higher optical power output of laser is successfully realized by single side band injection locking of distributed feedback laser (DFB). This method is of great potential in the application of fast optical frequency sweep signal generation. Compared to that acquired from direct carrier suppressed single sideband (CS-SSB) modulation, the SMSR of the injection locked slave laser by single sideband injection locking is much higher (32.5dB to 12dB at best), and the power of the injection locked slave laser output is 11dB higher (-22dBm to -33.5dBm) than converting directly from CS-SSB modulation. The variation of SMSR and locking bandwidth of the slave laser as optical injection ratio changes is also researched.

9267-10, Session 3

Dynamic behaviors of a broad-area diode laser with lateral-mode-selected external feedback

Mingjun Chi, Paul M. Petersen, Technical Univ. of Denmark (Denmark)

Broad-area diode lasers (BALs) are attractive light sources for various applications due to their high output power, high electro-optical efficiency, compactness, low cost and easy operation. However, BALs suffer from poor spatial beam quality in the slow axis owing to the broad emitter aperture in this direction. External feedback with lateral-mode selection is an effective approach to improve the spatial coherence of BAL in this direction. But complex dynamics may be induced in the BAL by the external feedback.

In this abstract, we investigate the dynamics of a BAL with lateral-mode selected external feedback experimentally by measuring the far-field profile, intensity noise spectrum and time series of the output beam. The mode-selection is achieved by adjusting a stripe mirror at the pseudo far-field plane. Different dynamic behaviors are observed when different lateral modes are selected. When the mirror is aligned correctly and high-order modes are selected, in most of the cases periodic dynamics corresponding to a single roundtrip external-cavity loop is

observed, but the dynamic behavior disappears in some case; when the zero-order mode is selected, dynamics corresponding to a double roundtrip external-cavity loop is observed. When the stripe mirror is not aligned perfectly and high-order modes are selected, a dynamic behavior like pulse-package oscillations is observed, which consist of a frequency component of the single roundtrip external-cavity loop modulated by periodic low-frequency fluctuations (LFFs), and this phenomenon is normally observed in diode lasers with short optical feedback, not long optical feedback like our case.

9267-11, Session 4

Fiber-connected position localization sensor network (*Invited Paper*)

Shilong Pan, Dan Zhu, Jianbin Fu, Tingfeng Yao, Nanjing Univ. of Aeronautics and Astronautics (China)

Position localization has drawn great attention during the past few decades due to its wide applications in many areas such as radars, sonars, electronic warfare, wireless communications and so on. Photonic approaches to realize position localization can achieve high-resolution, which provides also the possibility to move the signal processing from each sensor node to the central station, thanks to the low loss, immunity to EMI and broad bandwidth brought by the photonic technologies. In this paper, we present a review on the recent works of position localization based on photonic technologies. A fiber-connected UWB sensor network using optical time-division multiplexing (OTDM) is proposed to realize high-resolution localization and a spatial resolution as high as 3.9 cm is achieved. The complex signal processing from each UWB sensor node is moved to the central station, making the sensor network very simple. In addition, more complex algorithm can be adopted to achieve higher accuracy. A wavelength-division multiplexed (WDM) fiber-connected sensor network is also demonstrated. Since the received signals are separated in the wavelength domain, the proposed system is suitable for both pulsed and non-pulsed signal source localization, independent of the format of the emitted signal. The signals from the emitter received by different sensors can be identified by different optical carriers, and no clock synchronization or parameter estimation is required at the sensor nodes, which greatly simplifies the entire system. A spatial resolution of less than 17 cm is achieved in a proof-of-concept experiment for two-dimensional localization of a wireless fidelity (WIFI) signal.

9267-12, Session 4

High-speed time-stretch imaging system based on multi-wavelength laser source (*Invited Paper*)

Hongwei Chen, Fangjian Xing, Cheng Lei, Minghua Chen, Sigang Yang, Shizhong Xie, Tsinghua Univ. (China)

Ultrafast microscopic imaging has attracted more and more attentions in many application fields. The temporal resolution is considerably restricted by charge-coupled device (CCD) or complementary metal oxide semiconductor (CMOS) imaging technique. Many high speed imaging techniques in scientific research, such as time-resolved pump-probe technique or high-speed streak camera, are reconstructed by repeated pulsed illuminations and only suitable for capturing an event that can be recreated exactly the same way multiple times. Recently, serial time-encoded amplified microscopy (STEAM) is demonstrated as a novel optical imaging technique that can achieve high frame rate (~10MHz) in real time. The key element in STEAM is the high performance optical source, it requires a broadband spectrum and high degree of shot-to-shot temporal amplitude stability to

ensure the field of view and image quality.

We propose a novel time-stretch imaging system using multi-wavelength source. Unlike ultra-short pulse source, the pulse width is irrelevant to spectral bandwidth. So it can provide different profile of power distribution at whole spectrum, while with different pulse shapes and repetition rate at the same time. With this new method, a surface scanning imaging system has been demonstrated at scan rate of 80MHz with 20 discrete wavelengths. Also, by waveband-division technique, we achieve a surface scanning imaging system at scan rate of record 2GHz with 15 discrete wavelengths. As far as we know, this is the first time that the temporal resolution of real-time line scan imaging system reaches 500ps.

This work was supported by National Program on Key Basic Research Project (973) 2012CB315703, by the NSFC 61322113, 61335002, 61120106001, 61271134, 61090391, 61132004, and by National Program for Support of Top-notch Young Professionals.

9267-13, Session 4

Photonic generation of phase-modulated microwave signals (*Invited Paper*)

Wei Li, Institute of Semiconductors (China)

This paper reviews recent progress of our group on the generation of phase-modulated microwave signals. Binary phase-modulated microwave signals with pulse or continuous wave (CW) modes have been generated using a single external modulator. Moreover, we have also generated arbitrary phase-modulated microwave signals using a single dual-drive Mach-Zehnder modulator. In addition, all-optical binary phase-modulated microwave signal can be generated based on cross-polarization modulation in a highly nonlinear fiber. These techniques features outstanding performances, simple architecture, and flexible tunability.

9267-14, Session 5

Recent advances in photonic temporal integrator (*Invited Paper*)

Ming Li, Ninghua Zhu, Institute of Semiconductors (China); Jianping Yao D.D.S., Univ. of Ottawa (Canada); José Azaña, Institut National de la Recherche Scientifique (Canada)

In the past tens of years, information technology has witnessed a tremendous progress in optical communication systems, which are superior to electronic systems in many applications [1-7]. As a result of their severe speed limitation, traditional electronic systems cannot afford a high signal processing speed, and thus they are limited to offer a broad operation bandwidth. A photonic temporal integrator is a basic building block to create more complex signal processing and computing optical platforms. Such a device performs the temporal integral of an arbitrary input optical signal, which has many important applications such as optical dark soliton detection, pulse-shaping, optical memory and photonic analog-to-digital conversion.

Several kinds of photonic temporal integrators have been proposed and experimentally demonstrated based on different optical components and systems, including fiber Bragg grating (FBG), ring resonator and a time-spectrum convolution system. A real time and single-shot ultra-fast photonic time-intensity integrator for arbitrary temporal waveforms has been proposed and demonstrated based on a time-spectrum convolution system [8]. A photonic temporal integrator with an ultra-wide integration time window implemented based on a photonic integrated circuit (PIC) in an InP-InGaAsP material system consisting of semiconductor optical amplifiers (SOAs) and current-injection

phase modulators (PMs) was proposed and experimentally demonstrated [9]. A photonic temporal integrator based on an integrated active Fabry-Perot (FP) cavity is proposed and theoretically investigated [10].

9267-15, Session 5

Photonic generation of ultra-wideband signals and its applications based on semiconductor laser (*Invited Paper*)

Mingjiang Zhang, Taiyuan Univ. of Technology (China)

Ultra-wideband (UWB) technology has attracted considerable interests due to its wide applications. In order to distribute UWB signals over the optical fiber, it is highly desirable that the UWB signals can be generated directly in the optical domain.

We propose and demonstrate a method to generate UWB signals in optical domain based on the chaotic dynamics of an optically injected semiconductor laser with optical feedback. The spectrum of the UWB signals is in full compliance with FCC spectral mask, and the experimental results are qualitatively consistent with the simulated results.

Moreover, a UWB radar system for remote ranging based on microwave-photonic chaotic signal generation and fiber-optic distribution is proposed and demonstrated experimentally. The target ranging is achieved at the central office by correlating the echoed signal with reference signal. We experimentally realize a detection range of 8 m for a free-space target after 24 km remote distance, and achieve a ranging resolution of 3 cm for single target and 8 cm for double targets.

Furthermore, a high-accuracy microwave-photonic sensor for remote water-level monitoring based on chaotic laser is proposed and demonstrated. The water-level measuring is accomplished through cross correlation between reference signal and probe signal at the central office. The remote water-level monitoring system with a high resolution of 2cm and 24 km remote distance is achieved and the height of water surface can be displayed in real time.

9267-16, Session 5

Measuring high-frequency responses of an electro-optic phase modulator based on dispersion-induced phase modulation to intensity modulation conversion (*Invited Paper*)

Shangjian Zhang, Heng Wang, Xinhai Zou, Yali Zhang, Shuang Liu, Yong Liu, Univ. of Electronic Science and Technology of China (China)

Electro-optic phase modulation can eliminate bias drifting and generate inherent out-of-phase sidebands compared with Mach-Zehnder intensity modulation, which has attracted significant interest in microwave photonic signal processing. In phase modulation systems, the frequency responses of the optical phase modulator, including modulation index and half wave voltage, influence the overall high frequency performance, which should be critically characterized to evaluate and optimize the system. However, optical phase modulators only change the optical phase, which makes it difficult to measure directly the modulation efficiency with developed intensity sensitive instruments.

As we know, when a phase modulated signal propagates along the length of a dispersive fiber, the fiber dispersion acts as an optical phase filter and spectrally alters the relative phasing of the phase modulated signal, causing the phase modulation

to become intensity modulation. In this talk, we investigate the phase modulation to intensity modulation conversion in dispersive fibers in the context of measuring frequency responses of electro-optic phase modulators, and demonstrate two typical measurements with fold-back path and cascade path. The measured responses achieve an uncertainty of less than 2.8% within 20 GHz frequency range. Our measurements show stable and repeatable results because the optical carrier and its phase-modulated sidebands are affected by the same fiber impairments. The proposed method requires only dispersive fibers and works without any small-signal assumption, allowing swept frequency measurement with high resolution and accuracy by a vector network analyzer, which benefits from the high resolution and swept frequency of developed electrical domain measurement techniques.

9267-20, Session Post

All-optical clock recovery for 100 Gb/s RZ-OOK signal after 25 km transmission using a dual-mode beating DBR laser

Liqiang Yu, Institute of Semiconductors (China)

In spite of the current dominance of coherent optical transmission using electronic digital signal processing, the need for clock recovery is still high in all-optical network. All-optical clock recovery (CR) is regarded as a crucial technique for optical signal processing applications, such as 3R regeneration, optical time-division demultiplexing, and modulation format conversion. Among the various techniques for all-optical clock recovery, schemes based on monolithic dual-mode beating lasers (MDMBL) are attractive technologies due to their advantages in compact size, low-cost, low-power consumption and integration possibilities with other components. Here, we report an all-optical clock recovery (AOCR) for 100 Gb/s RZ-OOK signal using a novel mode-beating distributed Bragg reflector (DBR) laser with dual-mode output. In our previous, it has been demonstrated that both the working wavelengths and mode spacing of the dual-mode laser can be tuned when the currents injected into the DBR laser are adjusted.

Based on an injection-locking of the 100-GHz-spacing dual-mode DBR laser, a 100-GHz optical clock is recovered. Timing jitter (<1 ps) derived from both phase noise and power fluctuation is measured by an optical sampling oscilloscope (OSO). Furthermore, clock recovery is also realized for the 100 Gb/s signal after 25 km transmission. After the 25-km SMF (5-dB loss) transmission, the signal-to-noise ratio (SNR) of the signal drops from 18 dB to 5.2 dB. The dependence of the timing jitter on the input power is investigated. The lowest timing jitter of 665 fs is realized when the input power is 3 dBm.

9267-28, Session Post

Long-wavelength InP/GaAs-based InGaAsP lasers at 1550nm

Xiaobo Li, Beijing Univ. of Posts and Telecommunications (China)

Metamorphic growth of InGaAsP/InGaAs multiple quantum wells (MQWs) laser structure on GaAs (001) substrate is achieved via two-step growth and thermal cyclic annealing (TCA) in a Low-pressure (LP) metal organic chemical vapor deposition (MOCVD) system. A 15nm thick LT InP buffer is grown at 450°C and the temperature of thermal cyclic annealing (TCA) is changed from 300°C to 700°C for three times. The active regions are consisted by four 5nm In_{0.53}Ga_{0.47}As quantum wells and five 10 nm In_{0.25}Ga_{0.75}As_{0.54}P_{0.46} barriers, and its photoluminescence (PL) peak is 1538nm at room temperature. The root mean square (RMS) roughness values are 0.97nm in a 10²×10² m² scanning

area and 0.26nm in a 1²×1² m² scanning area. The device size is 300²×500² m, and the P electrode width is 30² m and the cavity length is 500² m. A pulse wave room-temperature (RT) threshold current is 160 mA. Through calculating, threshold current density is 1.06KA/cm³. The series resistance of the laser is 0.7 Ω and the power slope efficiency is 0.13mW/mA. Multi-longitudinal mode with a peak wavelength of 1549nm is presented and full width at half maximum (FWHM) of the envelope is 3nm when the pulsed injection current is 500 mA.

9267-31, Session Post

Thermal conductivity of multiple layers in vertical-external-cavity surface-emitting laser

Renjiang Zhu, Maohua Jiang, Yiping Liang, Dingke Zhang, Yuting Cui, Peng Zhang, Chongqing Normal Univ. (China)

Thermal property of multiple layers including distributed Bragg reflector (DBR) and multiple quantum wells (MQWs) used in semiconductor gain element is crucial for the performance of vertical-external-cavity surface-emitting lasers. For the purpose of more reasonable semiconductor wafer designing, so to improve the thermal management of laser, accurate thermal conductivities of DBR and MQWs are under considerable requirement. The in-plane and cross-plane thermal conductivities of the above multiple layers were calculated by the use of non-equilibrium molecular dynamics (NMD) method, and simulated results were compared with reported data. Whereas the diameter of pump spot is much larger than the total thickness of MQWs and DBR, and heat flow in a vertical-external-cavity surface-emitting laser is mainly axial and quasi-one-dimension, therefore the cross-plane thermal conductivities of MQWs and DBR was focused. The cross-plane thermal conductivity of AlAs/AlGaAs DBR, as an example, was computed, the influences of Al composition and interfacial roughness on the cross-plane thermal conductivity were analyzed, and an optimized DBR configuration was proposed. For the strained MQWs, which not only provides gain to the laser wavelength, but also works as the heat source in the active region, the cross-plane thermal conductivity was modeled, the effects of the stress, the strain compensate layer, and the depth of barrier on the cross-plane thermal conductivity were discussed. Using the calculated thermal conductivity, temperature rise of a vertical-external-cavity surface-emitting laser was simulated, and the theoretical results are in good agreement with experiment.

9267-32, Session Post

Numerical analysis of thermal effects in semiconductor disk lasers with water cooling

Renjiang Zhu, Chongqing Normal Univ. (China); Yingjun Pan, Chongqing Univ. (China); Maohua Jiang, Peng Zhang, Chongqing Normal Univ. (China)

Based on the heat transfer model of semiconductor disk lasers (SDLs) with water cooling, the temperature distribution of SDLs including distributed Bragg reflector (DBR), multiple quantum wells (MQWs), welding layer and heat sink has been calculated under different conditions of heatsink with the finite element method. Calculations show that the use of high convective heat transfer coefficient of water-cooled microchannel heatsink can significantly reduce the temperature of MQWs, but due to the high thermal resistance in series with the heat transfer path, making the microchannel heatsink heat dissipation performance saturated; under reasonable convective heat transfer coefficient, microchannel heat sink has a optimum

thickness, which indicates the importance of heat diffusion before dissipation of epitaxial wafers with the materials of high thermal conductivity, in which when microchannel convective heat transfer coefficient is $5\text{Wcm}^{-2}\text{K}^{-1}$, the heat dissipation performance of silicon carbide microchannel heatsink is about the 1.5 times the silicon.

9267-33, Session Post

Band structural design and spectral characterization for the active region of interband cascade laser

Junliang Xing, Yu Zhang, Juan Wang, Yongping Liao, Yingqiang Xu, Zhichuan Niu, Institute of Semiconductors (China)

GaSb-based interband cascade laser (ICL) with high output power and beam quality at any operating temperature have demonstrated a promising alternative in the range 3–5 μm . The active regions comprising AlSb/InAs/GaxIn $_{1-x}$ Sb/InAs/AlSb quantum wells (QWs) with a type II band alignment have been a mature design. Injected electrons are confined in InAs layer and injected holes in the other side GaxIn $_{1-x}$ Sb layer. The spatial separation of carriers and the strain effects in GaxIn $_{1-x}$ Sb layer suppress Auger recombination, which is favorable for the low threshold current and high temperature T_0 . However, the separation significantly reduces the electron-hole wavefunction overlaps of the active region. We insert an InAs layer to a GaxIn $_{1-x}$ Sb layer and design a new active region. The inserting InAs layer extends the hole wavefunction to electron well. The design allows for electron-hole wavefunction overlaps (15.58%) is greater than the former (14.662%). The insertion of InAs layer can be precisely controlled the bandgap of the active region.

Two samples with different structure investigated in this paper were fabricated on Te-doped (001) oriented GaSb substrates using Gen-II solid-source MBE system which is equipped with As and Sb valved cracker. The room temperature photoluminescence (PL) spectra confirm the results of our band calculations and the high-resolution X-ray diffraction (HRXRD) illustrate the insertion doesn't reduce the crystal quality. Due to the introduction of additional interfaces, the integrated PL intensity of the new one is smaller than the former.

9267-34, Session Post

Fabrication of 1.79 μm InGaAs/InP integrated laser with butt-coupled passive waveguide utilizing selective wet etching

Junping Mi, Hongyan Yu, Lijun Yuan, Song Liang, Qiang Kan, Jiaoqing Pan, Institute of Semiconductors (China)

We investigated the etching method especially for the InGaAs multiquantum-well laser, which usually works in the wavelength range of 1.6–1.9 μm , with a butt-coupled waveguide for the first time. Two different etching ways were demonstrated, which are reactive-ion-etching (RIE) followed by selective wet etching and selective wet etching only. For the first method, after RIE to define a vertical etched facet without undercut of the active layer, the wafer was etched by selective solution for 10s to relieve the RIE damage. However, the scanning electron microscope (SEM) photograph showed that there was a void and defects in the interface between the active region and the waveguide layers after regrowth. These lead to diffraction and radiation loss and reduce the couple effective. For the latter method, the wafer was etched only by a different selective solution for moderate time. The SEM photograph showed an ideal butt-coupled shape in the regrown waveguide layer. The regrown waveguide layer was free from the visible defects, which is essential for the fabrication of

an integrated laser. Using the latter method, we also fabricated a 1.79 μm integrated laser with 300 μm active region and 100 μm waveguide region. The L-I characteristics of lasers with and without waveguide were demonstrated. For the integrated laser, the threshold current and slope efficiency were 40 mA and 0.05 mW/mA, respectively. It is demonstrated that this simple and effective technology can be successfully applied to fabricate integrated long-wavelength photonic devices with InGaAs/InP materials.

9267-35, Session Post

MBE growth and fabrication of 2. μm InGaAsSb/AlGaAsSb laser

Yu Zhang, Institute of Semiconductors (China)

2. μm InGaAsSb/AlGaAsSb compressively strained quantum wells laser has been grown and fabricated. Antimonide laser with 1.5 mm \times 90 μm without AR/HR emitted 528 mW of continuous wave output power at 2 μm . And 2.4 μm laser without AR/HR output 195 mW at room temperature.

9267-36, Session Post

A compact dual-wavelength laser for portable Raman spectrometer

Zhijian Cai, Wenlong Zou, Xiaoru Wei, Jianzhi Ju, Jianhong Wu, Soochow Univ. (China)

Portable Raman spectrometers have been widely used in biochemical tests and security inspections. One big challenge of this kind of device is how to reject the fluorescence disturbance, especially for some organic samples, such as food additives, drugs and explosives. Shifted-excitation difference Raman spectroscopy (SERDS) is a recently developed technique to discriminate Raman signal from fluorescence background, and has been proven to be able to get clean Raman spectrum with high signal-to-noise ratio. In order to apply SERDS onto a portable Raman spectrometer, it's necessary to employ a special laser source with multiple wavelength. This paper proposed a compact laser system design based on the principle of external cavity diode laser, which uses only one external cavity feedback grating for two laser diodes to generate two slightly spaced wavelengths. The two wavelengths can be switched on alternatively by all-electrical controller. Without any mechanical moving parts, this laser system is more stable and can be integrated into a portable Raman spectrometer. Using the proposed laser, some organic samples were tested on a SERDS system. The results shown that the dual-wavelength laser can be used to reject fluorescence effectively in Raman spectroscopy.

9267-37, Session Post

Design and optimization of a widely-tunable semiconductor laser for blood oxygenation and blood flow measurements

Yafei Feng, Jian-Jun He, Zhejiang Univ. (China)

A method for measuring blood oxygenation and blood flow rate using a single widely tunable semiconductor laser is proposed and investigated. It is shown that a 700-nm-band tunable laser gives the highest sensitivity for blood oxygen measurement. The structure of the laser is designed, which comprises two coupled cavities that form V-shaped branches with a 2 \times 2 half-wave optical coupler at the closed end. The lengths of the two

cavities are designed to be 182 μm and 191 μm , respectively, corresponding to a length difference of 5%. The coupler is designed to have a π -phase difference between the cross-coupling and self-coupling so as to produce synchronous power transfer functions. High single-mode selectivity is achieved by optimizing the coupling coefficient. The threshold difference between the lowest threshold mode and the next lowest threshold mode is 5.4 cm^{-1} when the normalized cross-coupling coefficient is 0.0183. By employing the Vernier effect, the tunable range of the laser can reach 8 nm theoretically, which is sufficient for the blood oxygenation measurement in the 700-nm-band by using the Beer-Lambert law. With the feature of high single-mode selectivity, the laser can be used at the same time to measure the blood flow rate based on the Doppler principle. The laser does not involve any grating or epitaxial regrowth, which offers significant advantage of fabrication simplicity. Its compactness, easy wavelength control and easy integration with photodetectors make it very promising for portable health monitoring devices.

9267-38, Session Post

An asymmetric sampled Bragg grating structure for improving semiconductor laser efficiency

Yating Zhou, Gang Wang, Hong Zhu, Jun Lu, Changzhou Institute of Technology (China); Xiangfei Chen, Nanjing Univ. (China)

Generally, in order to improve the output efficiency of an DFB semiconductor laser, coating its one end-facet with high-reflection coating and the other end-facet with anti-reflection coating is a good method. However, in a monolithically integrated photonic transmitter chip, relying on butt-joint or selective area epitaxial growth technology, an optical power monitor array, multi-wavelength laser array, modulator array, semiconductor optical amplifier array and array waveguide multiplexer are successively integrated together. Therefore, coating the two end-facets of a laser in such a chip is too difficult to implement.

In the past few years, reconstruction-equivalent-chirp (REC) technique is proposed to fabricate DFB lasers. Fabricating DFB lasers with the same performance, true π phase shift grating in conventional E-beam lithography method is substituted for π equivalent phase shift (EPS) sampled Bragg grating (SBG) in REC technique. The required process precision is lowered by one or two orders of magnitude, thus REC technique has advantages in large-scale commercial application of high-performance and low-cost DFB lasers.

We proposed and numerically studied an asymmetric SBG semiconductor laser, in which the SBG is divided into two sections with the same length but different sampling duty cycle. The results from our study show that arbitrary magnitude EPS can be introduced into the proposed structure. Relying on regulating sampling duty cycles in the two sections, the output laser power ratio from the two end-facets can be adjusted according to actual requirement. With this method, without coating end-facets the output efficiency of such an SBG semiconductor laser can be improved.

9267-39, Session Post

The effect of Zinc diffusion on extinction ratio of MQW electroabsorption modulator integrated with DFB laser

Daibing Zhou, Ruikang Zhang, Huitao Wang, Baojun Wang, Jing Bian, Xin An, Lingjuan Zhao, Hongliang Zhu, Chen Ji, Wei Wang, Institute of Semiconductors (China)

Monolithically integrated electroabsorption modulated lasers (EML) are widely being used in the optical fiber communication systems, due to their low chip, compact size and good compatible with the current communication systems. In this paper, we investigated the effect of Zinc diffusion on extinction ratio of electroabsorption modulator (EAM) integrated with distributed feedback laser (DFB).

EML was fabricated by selective area growth (SAG) technology. The MQW structure of different quantum energy levels was grown on n-type InP buffer layer with 150nm thick SiO₂ parallel stripes mask by selective area metal-organic chemical vapor deposition (MOCVD). A 35nm photoluminescence wavelength variation was observed between the laser area ($\lambda_{\text{PL}}=1535\text{nm}$) and modulator area ($\lambda_{\text{PL}}=1500\text{nm}$) by adjusting the dimension of parallel stripes. The grating ($\lambda=1550\text{nm}$) was fabricated in the selective area. The device was mesa ridge structure, that was constituted of the DFB laser, isolation gap and modulator. The length of every part is 300 μm , 50 μm , and 150 μm respectively.

Two samples were fabricated with the same structure and different p-type Zn-doped concentration, the extinction ratio of heavy Zn-doped device is 12.5dB at -6V. In contrast, the extinction ratio of light Zn-doped device is 20dB at -6V, that was improved for approximate 60%. The different Zn diffusion depth into the MQW absorption layer was observed by Secondary ion mass spectrometer (SIMS). The heavy Zn-doped device diffused into absorption layer deeper than the light Zn-doped device, that caused the large uniformity of the electric field in the MQW layer. So the extinction ratio characteristics can be improved by optimizing the Zn-doped concentration of p-type layer.

9267-40, Session Post

Tunable π -coupled-cavity semiconductor laser monolithically integrated with monitoring photodiodes using deeply etched reflective trenches

Xiaolu Liao, Zhejiang Univ. (China)

We present a 1560-nm-band digitally wavelength tunable π -coupled-cavity semiconductor laser monolithically integrated with two waveguides based monitoring photodiodes (MPD) through deeply etched reflective trenches. The reflective trenches are designed to be 1.16 μm wide, about three quarters of the wavelength, and are deeply etched through the waveguide with a depth larger than 4 μm . Due to the high reflectivity of the etched trenches, a low threshold current of 19mA is achieved. Using a single electrode control, wavelength tuning of 22 channels at 100GHz spacing with SMSR above 35 dB is obtained. The relationship between the photocurrents of the two MPD at the two waveguide branches and the laser output power from the coupler side is investigated as a function of the wavelength. Since the optical gain in the channel selector cavity changes with the tuning current, the optical power emitted from the channel selector cavity is different from that emitted from the fixed gain cavity. As a result, the variations of the generated photocurrents at the two MPDs with the wavelength are different, and they do not reflect the variation of the output power from the coupler side. However, it is found that the average of the two MPD currents is proportional to the output power. Based on a calibrated responsivity coefficient of 0.12A/W, the output power can be derived from the average of the two MPD currents with a deviation less than 0.5dB for all wavelengths. The responsivity and the dark currents are investigated as a function of the MPD waveguide length under different bias voltages in order to optimize the MPDs. Since the integrated tunable laser with MPDs is very compact and does not involve any grating or epitaxial regrowth, it is suitable for low-cost multifunctional photonic applications for access and data center networks.

9267-41, Session Post

One-dimensional photonic crystal lasers with narrow vertical divergence and wavelength stabilization

Yun Liu, Lei Liu, Hongwei Qu, Wanhua Zheng, Institute of Semiconductors (China) and State Key Lab. on Integrated Optoelectronics (China)

Edge-emitting laser diodes operating at 900nm are designed and fabricated with an epitaxial one-dimensional photonic crystal (PC). PC structure consists of the p-waveguide, the active quantum layers, the n-waveguide and the n-cladding layer. The energy band of the PC is shown in terms of normalized frequency and the internal angle in the high index layer. PC structure and the optimized p-cladding of the lasers confine one tilted optical mode at a certain angle. The fundamental mode extends more vertically due to the photonic band modulation at the angle perpendicular to the interface of PC. Experimentally, broad-area lasers with 100 μ m width and 500 μ m cavity length with output power of 0.79W show a narrow vertical far-field divergence of 10 $^\circ$, and a small thermal shift (d λ /dT \approx 0.08nm/K) in continuous wave operation.

9267-17, Session 6

Multi-dimensional signal processing in high-speed optical communication systems (Invited Paper)

Anlin Yi, Lianshan Yan, Zhiyu Chen, Bin Luo, Wei Pan, Lin Jiang, Southwest Jiaotong Univ. (China)

"Multi-dimension", including multi-level modulation formats and multi-dimensional multiplexing schemes, is one of the essential characteristics of future high-speed, high-capacity and long-distance optical fiber transmission systems. Meanwhile, (all-) optical signal processing is regarded as the key enabler for future all-optical networks. However, the conventional signal processing is facing great challenges, such as complicated structures, high cost and low performance. Therefore, signal processing for multi-dimensional signal would be significantly valuable for the future optical fiber transmission systems. In this paper, we review some kinds of signal processing techniques for multi-dimensional signals, especially for PDM signals with traditional or "multi-dimension" modulation formats, utilizing different nonlinear effects in highly nonlinear fiber (HNLF). It is including signal regeneration by using counter-propagating scheme or nonlinear polarization-diversified loop, wavelength conversion based on cross phase modulation (XPM), format conversion and optical signal to noise ratio (OSNR) monitoring based on four wave mixing (FWM). Recent experimental demonstration results are presented and discussed, which might be some supporting techniques for higher speed optical communication systems in near future.

9267-18, Session 6

SOA based optical signal processing for multi-dimensional multiplexing system (Invited Paper)

Yu Yu, Huazhong Univ. of Science and Technology (China)

Optical signal processing is a key function in providing flexible management and interface for different fiber-optic communication networks. Recently, multiple multiplexing techniques, i.e. the wavelength division multiplexing (WDM),

the polarization division multiplexing (PDM) and the space division multiplexing (SDM), are utilized simultaneously to further increase the transmission capacity. As a result, the corresponding signal processing should be compatible with the multi-dimensional multiplexing system.

The semiconductor optical amplifier (SOA) had been considered as a promising candidate for optical signal processing, due to the small footprint, the high nonlinearity and potential for integration. However, the SOA was well-known for the significant cross-talk if works with multiple wavelengths and polarization, resulting in the incompatibility in future optical networks. By selectively enhance the specific nonlinear effects while restraining the undesired ones, we propose and demonstrate various parallel optical signal processing functions for multi-dimensional multiplexing signals based on a single SOA, including the modulation format conversion, the signal regeneration, the clock recovery and so on. Furthermore, we also present some all-optical signal processing functions for multi-dimensional signals by using other integrated devices as well as the SOA.

9267-19, Session 6

Behavioral modeling and digital compensation of nonlinearities in DFB lasers for multi-band directly-modulated radio-over-fiber systems (Invited Paper)

Jianqiang Li, Chunjing Yin, Hao Chen, Feifei Yin, Yitang Dai, Kun Xu, Beijing Univ. of Posts and Telecommunications (China)

The traditional radio access networks (RAN) suffer from severe problems in service quality, power consumption, and cost efficiency. Therefore, an evolved network architecture namely C-RAN has been envisioned by China Mobile and well recognized by the wireless communications community. The C-RAN framework suggests a unified network solution for smooth evolution and good compatibility, which prevents deploying multiple wireless communication systems over separate network infrastructures. As for the network architecture, the C-RAN concept relies on distributed antenna systems (DAS) which consist of a central unit (CU) and multiple remote antenna units (RAUs). The so-called fronthaul connections between CU and RAUs are commonly enabled by optical fiber links. Directly-modulated radio-over-fiber (ROF) links can serve as a low-cost option to make fronthaul connections between CU and RAUs. However, it has been realized that the legacy and emerging wireless communication standards will coexist for a long time to support diverse user terminals and demands. At the same time, different standards are working at different discrete allocated frequency bands. Therefore, most of the major mobile operators worldwide are facing a multi-band multi-standard environment in practical RAN deployment. In this regard, it is strongly necessary to investigate multi-band multi-standard directly-modulated ROF systems.

As is known, directly-modulated radio-over-fiber (ROF) systems often suffer from inherent nonlinearities from directly-modulated lasers. Unlike ROF systems working at the single-band mode, the modulation nonlinearities in multi-band ROF systems can result in both in-band and cross-band nonlinear distortions, which ultimately limit the link performance and RF power transmitting efficiency for downlink. In order to address this issue, we have recently investigated the multi-band nonlinear behavior of directly-modulated DFB lasers based on memory polynomial model and orthogonal polynomial model. Based on these models, an efficient multi-dimensional baseband digital predistortion technique was developed and experimentally demonstrated for linearization of multi-band directly-modulated ROF systems.

9267-21, Session 6

Super-Nyquist signal transmission and digital signal processing (*Invited Paper*)

Junwen Zhang, Fudan Univ. (China); Jianjun Yu, Fudan Univ (China); Nan Chi, Fudan Univ. (China)

Super-Nyquist, also known as Fast-than-Nyquist (FTN), signal generation based on optical or electrical spectrum shaping methods has been demonstrated to be an efficient scheme for future high-capacity transmission systems. Super-Nyquist signal demodulations based on maximum a posteriori (MAP) or maximum likelihood sequence estimation (MLSE) on receiver side have been demonstrated in 100G, 200G and 400G systems, which enables PDM-QPSK transmission with 4bit/s/Hz net spectral efficiency (SE) at lower OSNR requirement and longer transmission distance. Further studies also show the highly filtering-tolerant advantage of the super-Nyquist signal when using the 9-QAM-based multi-modulus equalization. This feature is quite useful for signals transmission under the aggressive optical filtering in multiple reconfigurable optical add-drop multiplexers (ROADMs) transmission link. In this paper, a novel DSP scheme for this optical super-Nyquist filtering 9-QAM like signals based on multi-modulus equalization (MMEQ) without post filter are proposed and experimentally demonstrated, which directly recovers the Nyquist filtered QPSK to a 9-QAM like signal. We first successfully transmitted 100-GHz-grid, 20 channels single-carrier 440-Gb/s super-Nyquist 9-QAM-like signal over 3600-km ultra-large effective-area fiber (ULAF) at record a net SE of 4b/s/Hz (after excluding the 7% hard-decision FEC overhead). The highly filtering-tolerant performance of the 9-QAM like super-Nyquist signal is also experimentally demonstrated. Using this scheme, we then successfully transmit 10 channels 440-Gb/s signal over 3000-km ULAF and 10 cascaded ROADMs with 100-GHz-grid based on the single-carrier ETDM 110-GBaud QPSK. It is the highest baud rate of all-ETDM signal reported with the highest net SE at this baud rate for PDM-QPSK signal.

9267-22, Session 7

Mid-infrared pulsed fiber lasers operating at 3 μ m region (*Invited Paper*)

Yong Liu, Jianfeng Li, Hongyu Luo, Heping Li, Xiaojun Zhou, Univ. of Electronic Science and Technology of China (China)

Mid-infrared pulsed fiber lasers with centered wavelength from 2 to 5 μ m have attracted substantial attention owing to their potential applications in laser microsurgery, defence, material processing, nonlinear frequency conversion, etc. We reported our recent achievements at 3 μ m pulsed fiber lasers by utilizing Q-switching, gain switching methods respectively. Firstly, we presented a passively Q-switched Ho³⁺-doped ZBLAN fiber laser operating at ~2971 nm, using a reversely designed semiconductor saturable mirror (SESAM) acted as a saturable absorber. The obtained maximum pulse energy of 6.65 μ J only limited by the maximum pump power was also one of the highest levels from passively Q-switched fiber lasers at this wavelength range, and corresponding pulse repetition rate and duration were 47.6 kHz and 1.68 μ s, respectively. In addition, a cascaded dual wavelength pulsing mechanism i.e., Q-switching induced cascade transition gain switching was demonstrated to 3.0 μ m and 2.07 μ m pulsed laser, by using an external electrically driven acoustic-optical modulator into a Ho³⁺-doped ZBLAN fiber laser cavity. The achieved 2.07 μ m gain switched pulse train was almost clamped at the same repetition rate as 3.0 μ m Q-switched pulse train yielding maximum pulse energy of 6.4 μ J and 21.7 μ J, narrowest duration of 460 ns and 350 ns, respectively. To sum up, the above

achievements would be beneficial for further development of mid-infrared pulsed fiber lasers.

9267-23, Session 7

Blue shift of laser mode in photonic crystal microcavity

Pengchao Zhao, Zhigang Feng, Fan Qi, Aiyi Qi, Yufei Wang, Wanhua Zheng, Institute of Semiconductors (China)

We report the first demonstration of blue shift of optical pumping photonic crystal (PhC) laser. A femtosecond laser was used to pump the InGaAsP based two dimensional photonic crystal laser at room temperature. Linear dependence of the resonance wavelength with respect to the pump power is observed: $d\lambda/dP = -1.5 \times 10^{-2}$ nm/W. Blue shift of overall 1.1nm was obtained with the increase power of pump laser. These results are in agreement with theoretical expectation while the carrier-induced index change is introduced into the PhC semiconductor laser. It shows a possibility that by proper wafer design and careful optimization, we may obtain wavelength stable photonic crystal laser, which is important in photonic integration.

9267-24, Session 7

The influence of AlN buffer layer on AlGaIn/AlN/sapphire epitaxial layer

Deng Xie, South China Normal Univ. (China); Yi Ting He, Zhi-Ren Qiu, Sun Yat-Sen Univ. (China); Ting Mei, South China Normal Univ. (China) and Northwestern Polytechnical Univ. (China); Shuchang Wang, Xiong Zhang, Southeast Univ. (China); Zhe Chuan Feng, National Taiwan Univ. (Taiwan)

Aluminum gallium nitride thin film have been under intense investigation over the past few years for its excellent performance in microwave power applications, such as high linearity, high breakdown field, and high speed. These properties are directly related to crystalline quality of the film. For more flexible tuning of the bandgap, AlGaIn films with high Al content are needed. With metal-organic chemical vapor deposition (MOCVD) technique, high quality AlGaIn thin film with Al content up to 60% can be grown on sapphire using an AlN buffer layer. Here, we discuss the grown condition of AlN buffer dependent AlGaIn crystal performance by combining various non-destructive characterization methods, from which detail optical and structural properties of the films could be discussed quantitatively.

Two set of AlGaIn films with Al content varying from 20 at.% to 62 at.% were grown on sapphire with a low temperature AlN (LT-AlN) of several nanometers as nucleation layer. Except that, set B has a nominally 140 nm high temperature AlN (HT-AlN) buffer grown after LT-AlN layer. By combining variable angle spectroscopic ellipsometry (VASE) and optical transmittance data modeling, set B is found to have a larger and steeper bandgap. Meanwhile, the existence of a thin transition layer is regarded as the reason of bandtail annihilation in AlGaIn layer of set B. Roughness layer thickness deduced by atom force microscope in good accordance with the VASE modeling result. However, X-ray diffraction and Raman spectrum shows a broader peak for set B, which indicates an existence of amorphous phase. Due to discussions above, we argue that blue shift of band gap in set B could be an evidence of Stark shift caused by nano-crystalline structure in the amorphous region.

9267-25, Session 7

FPGA based design for real-time measurement of alpha factor

Zhenghao Liu, Yanguang Yu, Qinghua Guo, Jiangtao Xi, Jun Tong, Sheng Tong, Univ. of Wollongong (Australia)

The alpha factor, also known as linewidth enhancement factor (LEF), is a fundamental characteristic parameter of a semiconductor laser (SL) and has great importance in SL applications as well. Self-mixing Interferometry (SMI) is considered both efficient and accurate for alpha factor measurement. However, most existing signal processing algorithms used for SMI signals are implemented on a PC by using Matlab or other programming software, the whole structure of SMI sensing system is cumbersome and the measurement is in low speed. Field-programmable gate arrays (FPGA) is an attractive method to handle both high throughput and adaptability to the real-time digital signal processing. In this work, we build a FPGA based alpha measurement system by using SMI technique. The sensing signal from the SMI system is feed into a FPGA development system for high speed processing, from which the alpha factor can be obtained. Considering the issue of noise reduction, a high-performance filtering method and effective data selection algorithms are combined to optimise the measurement accuracy on the frequency-domain based alpha measurement method. The corresponding FPGA design includes noise reduction block, normalisation block, phase unwrapping block, FFT (Fast Fourier Transform) block, alpha calculation and data selection block. Both simulation and hardware co-simulation show that the SMI system with our FPGA design can achieve fast and reliable alpha factor measurement.

9267-26, Session 8

Integrating periodic microstructures in organic optoelectronic devices (Invited Paper)

Hong-Bo Sun, Jing Feng, Yue-Feng Liu, Yan-Gang Bi, Jilin Univ. (China)

Microstructures with wavelength to subwavelength-scale periodicity have played important roles in optical and optoelectronic devices, particularly in optical fibers, distributed feedback lasers, LEDs and solar cells etc. through manipulating the generation and propagation of photons in materials. We have investigated systematically the fabrication of microstructures in organic optoelectronic devices and their effects on improving the device performance. The waveguide and surface plasmon-polariton (SPP) modes that were generally lost in conventional bottom-emitting OLEDs have been successfully recovered by employing the microstructure, and a much enhanced light extraction has been observed. The introduction of the periodic corrugation into the top-emitting OLEDs (TOLEDs) is effective in relieving the tradeoff between device lifetime and efficiency, through the coupling of the SPPs associated with the Ag cathode and the microcavity modes. A microstructured cavity with periodically and gradually changed cavity length has been introduced into the TOLEDs and exhibited its effects in eliminating the angular dependence of the emission wavelength and intensity. Dual-periodic corrugations which excite the SPPs resonance at two separate wavelengths have been introduced into the metallic electrodes of the white organic light-emitting devices (WOLEDs) to realize a broadband light extraction. Moreover, the enhanced light absorption has also been realized by integrating microstructures in organic solar cells.

References

[1] Y. Bai, J. Feng, Y. F. Liu, J. F. Song, J. Simonen, Y. Jin, Q. D. Chen, J. Zi, H. B. Sun. "Outcoupling of trapped optical modes in

OLEDs with one-step fabricated periodic corrugation by laser ablation", Org. Electron. 12, 1927 (2011).

[2] Y. G. Bi, J. Feng, Y. F. Li, Y. Jin, Y. F. Liu, Q. D. Chen, and H. B. Sun. "Enhanced efficiency of organic light-emitting devices with metallic electrodes by integrating periodically corrugated structure" Appl. Phys. Lett. 100, 053304 (2012).

[3] Y. Jin, J. Feng, X. Zhang, Y. Bi, Y. Bai, L. Chen, T. Lan, Y. Liu, Q. Chen, and H. B. Sun. "Solving efficiency-stability tradeoff in top-emitting OLEDs by employing periodically corrugated metallic cathode", Adv. Mater. 24, 1187 (2012).

[4] Y. F. Liu, J. Feng, Y. G. Bi, J. F. Song, Y. Jin, Y. Bai, Q. D. Chen, and H. B. Sun. "Omnidirectional emission from top-emitting organic light-emitting devices with microstructure cavity", Opt. Lett. 37, 124 (2012).

[5] Y. G. Bi, J. Feng, Y. F. Li, X. L. Zhang, Y. F. Liu, Y. Jin, H. B. Sun. "Broadband light extraction from WOLEDs by employing corrugated metallic electrodes with dual periodicity" Adv. Mater. 25, 6969 (2013).

[6] Y. Jin, J. Feng, M. Xu, X. L. Zhang, L. Wang, Q. D. Chen, H. Y. Wang, H. B. Sun, "Matching photocurrent of sub-cells in double-junction organic solar cells via coupling between surface-plasmon-polariton and microcavity modes", Adv. Opt. Mater. 1, 809 (2013).

9267-27, Session 8

Narrow linewidth 1.55 μ m directly-modulated distributed-feedback laser (Invited Paper)

Jinjin Guo, Jianguo Liu, Ninghua Zhu, Wei Chen, Institute of Semiconductors (China)

We fabricated a narrow linewidth 1.55 μ m directly-modulated distributed-feedback (DFB) laser. The laser exhibits an output power of 14mW at 100mA, flat frequency response with -3 dB bandwidth of 18 GHz, the third-order intermodulation distortion (IMD3) with 39.8dBm, narrow optical linewidth with 181kHz, and RIN below -135.7dB/Hz in the 0.1-10GHz range along with the high side-mode suppression ratio (>52dB). We also experimentally verified the modulation bandwidth, linearity, and linewidth is related to the bias current. The characteristics of the laser, namely sufficient modulation bandwidth, high linearity, low relative intensity noise (RIN) and narrow linewidth, make it the perfect candidates for high dynamic directly modulated analog optical link.

9267-29, Session 8

An ultra-wideband optical frequency comb generator based on semiconductor quantum dot F-P cavity

Wenhui Sun, Jianguo Liu, Wen-Ting Wang, Jinjin Guo, Wei Chen, Ninghua Zhu, Institute of Semiconductors (China)

An ultra wideband optical frequency comb (OFC) generator based on semiconductor Quantum dot F-P cavity is packaged by our group. The free spectral range (FSR) of the OFC can be tunable from 97GHz to 100GHz and the pulse width of the 100GHz OFC is 1.2ps. The full span of the OFC spectra is 80nm with a Gaussian shaped, and in span of 10nm, the flatness of the OFC can be limited to 1.7dB. The OFC has the advantages of small volume, simple and compact structure, low power dissipation, and has an ultra-wide bandwidth and flat spectrum, which can be used in the field of arbitrary waveform generation, channel information processing, and optical frequency division multiplexing.

9267-30, Session 8

Validate the parameters in HITRAN through the experiment of H₂O based on direct absorption spectroscopy technology

Shao Jie, Liming Wang, Zhejiang Normal Univ. (China)

High-resolution absorption measurements of H₂O using direct absorption spectroscopy (DAC) technology were made to acquire the spectroscopic parameters of High Resolution Transmission Molecular Absorption Database (HITRAN database). The most important spectral parameters such as line position, line intensity, lower state energy, air-broadened, half width self-broadened half width, temperature-dependence coefficient for air-broadened half width which widely used in the researchers and study, was calculated from the integrated absorbance area at the different temperature from 296K to 1273K of the spectrum near 1397nm based on the distributed feedback (DFB) laser. From the result of experiment, the calculated spectral parameters was compared with the literature values from HITRAN database, and the causes of a little disagreement was analyzed objectively. Using the calculated spectral parameters, the combustion byproduct H₂O in the combustion region were determined to verify the measured spectroscopic parameters and to demonstrate the feasibility of the diode laser sensors for temperature measurement. The work in this paper are expected to be helpful in the supply of the sufficient accuracy spectral parameters in the practical measurement for the industrial applications.

Conference 9268: Optics in Health Care and Biomedical Optics VI

Thursday - Saturday 9 -11 October 2014

Part of Proceedings of SPIE Vol. 9268 Optics in Health Care and Biomedical Optics VI

9268-1, Session 1

Optical molecular imaging of immune response (*Invited Paper*)

Qingming Luo, Britton Chance Ctr. for Biomedical Photonics (China) and Wuhan National Lab. for Optoelectronics (China) and Huazhong Univ. of Science and Technology (China)

Optical molecular imaging is the most promising tools for investigating the function and motility of immune cells in vivo. Immuno-Optimaging as a new interdisciplinary research area has been developed for a decade. Here, we developed a multi-scale optical imaging approach to evaluate the spatio-temporal dynamic behavior and properties of immune cells from the whole field of organs to the cellular level at the inflammatory site: the recruitment of leucocytes was directly visualized using whole-field fluorescent imaging at the organ and tissue levels; the dynamic distribution of the leukocytes was directly visualized using large-scale scanning microscopy at the single-cell level; the motility and migration dynamics of leukocytes were visualized in real time and analyzed using time-lapse confocal imaging or two-photon excitation microscopy at the single-cell level with high temporal resolution. Meanwhile, some multi-color labeling mouse models based on the exogenous labeling with fluorescent protein and the endogenous labeling with fluorescent dye were established. The dynamic properties and function of immunocytes in the immune response (e.g., the delayed type hypersensitivity reaction and tumor immunotherapy) were visually investigated using multi-scale optical molecular imaging techniques combined with the multi-color labeling mice model.

9268-3, Session 1

Noninvasive retinal oxygen-metabolic quantification through integrated photoacoustic ophthalmoscopy with optical coherence tomography

Wei Song, Harbin Institute of Technology (China) and Northwestern Univ. (United States); Wenzhong Liu, Qing Wei, Northwestern Univ. (United States); Rui Zhang, Harbin Institute of Technology (China); Hao F. Zhang, Northwestern Univ. (United States)

Integrated photoacoustic ophthalmology (PAOM) and optical coherence tomography (OCT) is a newly-developed multimodal ophthalmologic imaging technology, which provides complementary retinal anatomical information by detecting both optical-absorption and optical-scattering contrasts in the retina. However, accurately measuring oxygen metabolism in the retina is essentially critical for fundamental pathophysiological investigation, and even early-stage clinical diagnosis and treatment of many blinding diseases, such as diabetic retinopathy, retinal degeneration, and glaucoma. To quantitatively determine dynamic oxygen consumption in the retina at a microscopic level, we combined spectroscopic PAOM and Doppler spectral-domain OCT (SD-OCT) for functional imaging of retinal metabolic rate of oxygen (MRO₂). PAOM at multi-wavelength excitation measured the oxygen saturation (sO₂) in major retinal vessels taking advantage of the wavelength-dependent optical absorption characteristic of oxy- and deoxy-

hemoglobin. Simultaneously, SD-OCT mapped the blood flow rate based on the Doppler shift induced from moving red blood cells. We demonstrated the integrated ophthalmologic imaging system for in vivo quantifying the retinal MRO₂ in wild-type rat eyes. The integrated PAOM and SD-OCT is a unique imaging modality for extracting both anatomical (vessel size and density) and functional (sO₂ and blood flow) parameters in the retina; therefore, it may open up new window for fundamental research and clinical care of human vision disorders in the future.

9268-4, Session 1

The evaluation and planning of light dose in photodynamic therapy for port wine stain

Fengjuan Zhang, Xiaoming Hu, Beijing Institute of Technology (China)

Photodynamic therapy (PDT) is one of the best available treatment for dermatology, especially for port wine stains (PWS), in which the efficacy is associated with many factors, such as the light dose, the photosensitizer concentration, the oxygen concentration, and so on. Accurate control of the light dose will be able to help doctors develop more effective treatment protocols, and reduce the treatment cost.

Considering the characters of PWS and other dermatoses, a binocular vision system composed of a camera, a digital projector and a computing unit is designed. The system was calibrated at first to get the parameters of the vision system, and an accurate 3D modeling of patients was achieved using a gray coding structured light. The coordinates of the point clouds are calculated based on coding and decoding technology of the gray and optical triangulation. Subsequently, each 3D point is fit on the surface by a nearest neighbor algorithm and the surface pieces can be obtained. At the end, the surface normal, areas and other related parameters of small polygons are analyzed, so the irradiance on the surface at a given angle can be assessed, and the optimum angle for the treatment can be solved and optimized by the doctor.

The paper verified the above processes with a human head model and compared the reconstructed 3D model with the scan outcome of 3D scanner. The result shows that the approach proposed is practicable, and may be used to improve the doctors in quantitatively assessing the therapeutic effect and making the rehabilitation program.

9268-5, Session 1

Optical coherence tomography: A potential tool for prediction of treatment response for port wine stains after photodynamic therapy

Jie Zhen, Beijing Institute of Technology (China); Ying Gu, Beijing Institute of Technology (China) and Chinese PLA General Hospital (China); Chengming Wang, Tsinghua Univ. (China); Ying Wang, Chinese PLA General Hospital (China); Defu Chen, Beijing Institute of Technology (China)

Background: Response of port wine stain (PWS) to Photodynamic therapy treatment?PDT?is variable and dependent

on treatment setting used and anatomic site as well as on size and depth of ectatic vessels. Optical coherence tomography (OCT) is a non-destructive imaging modality. OCT images reveal the layered structure of the upper part of the skin. PWS skin structures such as blood vessel diameter and depth in different anatomic sites are showed in the OCT images.

Objectives: In this study, the possible role of PWS skin structure in the response to PDT was assessed.

Methods: Fifty children with PWS underwent OCT evaluation in cheek, zygomatic area, preauricular and temporal region before the first PDT and after three months, meanwhile treatment outcomes characterizing the degree of fading were evaluated. Blood vessels diameter and depth of PWS was measured in the OCT images.

Results: Compared with that of before PDT, the vessels diameter and depth became small and the number of vessels obvious decreasing after PDT. The ectatic vessels diameter was obvious bigger in the cheek which had slightly poorer outcomes than other areas.

Conclusions: The PWS skin structures evaluated by the OCT images have significant influence of the treatment outcomes. Some typical structures respectively have poor and excellent outcomes after first PDT. This research help clinic doctors predict which patients will benefit from treatment. The OCT will be a potential tool for prediction of treatment response for PWS after Photodynamic therapy.

9268-104, Session 1

Label-free optical imaging of tissue morphology and microcirculations in vivo in 3D (*Invited Paper*)

Ruikang K. Wang, Univ. of Washington (United States)

Optical coherence tomography (OCT) is a new medical imaging modality that is capable of creating high resolution (micron-scale) subsurface image of tissue microstructure. Recently, we have supplemented the microstructural OCT images with additional contrast mechanisms such as blood flow imaging using the static and dynamic (Doppler) speckle effects, which provide us the ability to perform label-free optical microangiography (OMAG) of microcirculatory tissue beds. The ability to visualize tissue blood flow at the microcirculation level is important in a variety of biomedical applications, some of which (along with the OCT basics and the enabling technologies) will be highlighted in this talk. Examples using OMAG to delineate the dynamic blood perfusion, down to capillary level resolution, within living tissue will be given, including cerebral blood flow in small animals and retinal blood flow in humans.

9268-6, Session 2

Fiber-optic nonlinear endomicroscopy towards clinical applications (*Invited Paper*)

Wenxuan Liang, Gunnsteinn Hall, Kristine Glunde, Zaver Bhujwalla, Johns Hopkins Univ. (United States); Katherine Luby-Phelps, Mala Mahendroo, The Univ. of Texas Southwestern Medical Ctr. at Dallas (United States); Ming-Jun Li, Corning Incorporated (United States); Xingde Li, Johns Hopkins Univ. (United States)

The past decades have witnessed increasing interest in the field of nonlinear endomicroscopy, including two-photon

fluorescence (TPF) and second-harmonic generation (SHG). Various prototypes have been attempted to translate these powerful imaging modalities into biomedical and clinical benefits. Beneath the intuitive basic ideas of delivering light to and from the distal probe where beam scanning is implemented, multiple major technical challenges have to be overcome in order to construct a practically applicable, robust and high-performance endomicroscopy system. We have systematically investigated these obstacles and brought up innovative solutions to achieve broadening-free optical-fiber delivery of femtosecond laser pulses, effective beam focusing through a high-NA miniature objective, robust beam scanning mechanism, and efficient collection of emission photons. Built around a single piece of customized double-clad fiber and a miniature objective, our newly-developed fiber-optic nonlinear endomicroscopes demonstrate unprecedented fine resolution and high detection sensitivity, yielding high-quality intrinsic TPF and SHG images with a safe level of excitation power (~20-30 mW). With its capability to visualize clearly subcellular structures on various biological tissues, the endomicroscope has exhibited promising results in preliminary studies with various disease models. Through SHG imaging, it can access the cervical collagen structure and its changes during pregnancy, which can be useful for preterm birth prediction. The TPF modality, further extendable with lifetime measurement, can provide both anatomical and physiological information which is valuable for early diagnosis of cancerous tissues (e.g. breast cancer). These initial results demonstrate our endomicroscopes' strong potential for a broad range of in vivo and clinical applications.

9268-7, Session 2

Visualization of brain circuits by recovering GFP fluorescence from plastic status (*Invited Paper*)

Shaoqun Zeng, Britton Chance Ctr. for Biomedical Photonics (China)

In a cellular phone, the information flow is present in real functional connections. Similarly, in our brains, information is transmitted within and between neural circuits through functional neuronal connections based on axonal projections. Revealing the axonal projection of a single neuron is essential to understand the brain functions, in terms of health and disease. The axon is less than 1 μm in diameter, whereas its projection length may exceed 1 cm. Consequently, tracing a single axon within the centimeter range in three dimensions (3D) is challenging. Here we propose a new optical imaging method to obtain high-resolution brain images with high-throughput, and demonstrated using a thy1-YFP H mouse brain as an example. This method provides a new starting point to image large scale fluorescence-labeled specimen in resin embedding manner.

9268-8, Session 2

Solutions on high-resolution multiple configuration system sensors

Hua Liu, Luoyang Institute of Electro-Optical Equipment (China)

To break the optical diffraction limit, to achieve an improved resolution, based on studies of single molecule microscopy in the field of traditional and the modern domain, we develop the method of continuous zoom multiple configuration, and the establishment of a micro lens array and core optics as the main component in a system to attempt to establish model by

novel principle on resonance energy transfer and high accuracy localization by which between the principle and application of molecular resonance, as well as single molecule positioning technology, the system resolution can be improved with a level of a few nanometers. A comparative study on traditional design methods and their advantages and disadvantages of the implementation mechanisms can demonstrate that the dialectical relationship and their balance is important, among Merit function, Optimization algorithms and Model parameterization. The effect of system evaluated criterion that Modulation Transfer Function (Modulation Transfer Function, the MTF), Energy concentration (Radial Energy Analysis, REA), diffusion (Spot Diagram, RMS) and other aspects and other qualitative criteria can support our arguments. And the results can be used as basis for the development of new products.

9268-9, Session 2

Sub-diffraction resolution pump-probe microscopy with shot-noise limited sensitivity using laser diodes

Takayoshi Kobayashi, Jun Miyazaki, The Univ. of Electro-Communications (Japan)

We have demonstrated that sub-diffraction resolution pump-probe imaging with shot-noise limited sensitivity can be carried out using conventional laser diodes with a balanced-detection scheme. The cost of LD was 50 times lower than in the Ti:sapphire laser-based system. Furthermore, LD is maintenance free and power consumption and space occupied by the instruments were reduced in comparison with the mode-locked laser-based system. Blue, red and near-infrared laser diodes are readily available, as they are widely used in optical disks and in optical communication. In recent years, tremendous advances have been made in green-emitting (500-532 nm) InGaN-based LD technology, achieving an output power of more than 100 mW. Furthermore, green to yellow (543-570 nm) LDs with ~3 mW power can be used at room temperature. By incorporating these LDs, our method becomes applicable to various types of probe molecules. Thus, this method offers new opportunities for studying the nanostructures and properties of biological tissues.

9268-10, Session 2

A photoelastic modulator-based birefringence imaging microscope for measuring biological specimens

Baoliang Wang, John Freudenthal, Andy Leadbetter, Jacob Wolf, Hinds Instruments, Inc. (United States); Solomon Segal, Saint Louis Univ. School of Medicine (United States)

The photoelastic modulator (PEM) has been applied to a variety of polarimetric measurements.¹ However, nearly all such applications use point-, or scanning point-measurements. The main challenge for employing PEMs in camera-based imaging instruments is that PEMs modulate at high frequencies (tens of KHz). The slow frame rate of the camera will average out any specific polarization information that is carried on the modulation frequency of the PEM. Hence there are only a very limited number of studies for PEM-camera imaging polarimeters.²⁻⁴ In this paper, we report the working principle and systematic test results for a PEM-camera birefringence imaging microscope. This instrument contains a simple microscope with low magnifications

at 2X, 5X and other customized options, two PEMs, a modest resolution camera (4 megapixels) and light-emitting diode (LED), triggered by a field-programmable gate array (FPGA). The key is to pulse the LED light source in synchrony with the modulation frequencies of the PEMs so that the camera only receives light pulses carrying specific polarization information. We will show measurement of several standard birefringent samples as instrument calibration. Furthermore, we describe applications of this instrument in resolving birefringence found in various biological specimens containing birefringent molecules.⁵ Among the most frequently studied biological molecules with birefringence are collagen, enamel, congo-red-stained amyloid, and myelin. Myelin is a lipoprotein found in the nervous system, particularly in the white matter. Myelin wraps around the elongated part of neuronal cells known as axons, forming cable-like structures coated with an insulating (myelinated) cuff. Axons (also termed fibers) tend to form thicker bundles with millions of myelinated axonal fibers known as white matter tracts. White matter tracts containing myelin are characteristically birefringent. Since other parts of the brain tissue are not as rich in myelin as the white matter tracts, there is significant contrast between myelinated and non-myelinated brain tissue in birefringence imaging. Novel applications of this PEM-based birefringence imaging microscope to both research communities and industrial applications are being tested.

Selected references

1. B. Wang, "Polarimetry" in Handbook of Optical Metrology: Principles and Applications, T. Yoshizawa, Ed. (CRC Press, 2009); 2nd Edition, in print (2014).
2. P. Gleyzes, A. C. Boccara and H. Saint-Jalmes, Optics Letters, 22 (20), 1529 (1997).
3. C.Y. Han and Y.F. Chao, Rev. Sci. Instrum. 77, 023107 (2006).
4. S. Alali, T. Yang, and I. A. Vitkin, Optics Letters, 38 (16), 2997-3000 (2013).
5. N.M. Kalwani et al. Qualitative polarized light microscopy of unstained cochlear sections, Journal of Biomedical Optics 18(2), 02621 (February 2013)

9268-11, Session 2

Direct comparing the performance of low-light cameras in super-resolution localization microscopy

Zeyu Zhao, Luchang Li, Ze Hu, Zhen-Li Huang, Huazhong Univ. of Science and Technology (China) and Britton Chance Ctr. for Biomedical Photonics (China)

Super-resolution localization microscopy, including the popular PALM and STORM, depends on imaging of thousands or even tens of thousands individual single molecules to realize a super-resolution image. On the other hand, with the rapid advance in the field of low-light detectors, a large number of commercial cameras is suitable of imaging the weak fluorescence from single molecules, thus making it important and even confusing in selecting a suitable low-light detector for super-resolution localization microscopy. Although many studies have been reported to quantify the performance of the low-light detectors in super-resolution localization microscopy, these studies are carried out in an indirect manner. As a consequence, the conclusions are vulnerable to the influence of the experimental conditions.

In this talk, we will introduce a direct method for quantifying the performance of low-light detectors in super-resolution localization microscopy. In this method, we consider the

influence of a variety of experimental factors on the quality of the performance comparison. We further select two commercial EMCCD and sCMOS cameras as representative low-light detectors and present a direct comparison. We believe that this study can provide useful information for selecting a suitable low-light detector for super-resolution localization microscopy.

Keywords: super-resolution microscopy, single molecule localization, low-light detector, EMCCD, sCMOS

9268-12, Session 2

Size-dependent amplitude and phase distribution under a high NA objective

Xin Hong, Huan Liu, Dalian Univ. of Technology (China)

The interactions between light and sub-wavelength sized dielectric particles have been paid more attentions especially in biotechnology and photonics. Single sub-wavelength sized dielectric particle is difficult to directly detect and size using optical methods because it do not show obvious spectral resonances in the visible light region and provide a low index contrast to the index of the surrounding medium compared to similar sized metallic particle under resonance. Base on Mie scattering method, we calculate the electrical field distribution scattered by a single dielectric particle which is focused by a high numerical aperture (NA) objective. We present the individual dielectric particle's amplitude and phase distribution simulation and experimental images with different radii for the first time, and analyze these images to distinguish the individual dielectric particle size, especially in phase aspect. We acquire the main diagonal and counter-diagonal phase curves from the different phase distribution images and dwell on these phase curves. Meanwhile the theoretical result indicates a size dependent amplitude and phase distribution, which agrees well with the experimental measurement. This method provides a way to evaluate the particles size down to the range of less than diffraction limitation.

9268-13, Session 3

Antimicrobial blue light inactivation of infecting organisms (Invited Paper)

Tianhong Dai, Massachusetts General Hospital (United States)

Drug resistance, also known as antimicrobial resistance, is a quickly growing and extremely dangerous health threat. The use of antimicrobial drugs is the single most important factor leading to drug resistance. As a result, there is a pressing need for the development of new treatment approaches. The objective of this study was to investigate the feasibility of a novel non-pharmacological approach, antimicrobial blue light, for inactivation of infecting organisms.

A blue light LED with a peak emission at 415 nm was used. Representative infecting organisms *Pseudomonas aeruginosa*, *Acinetobacter baumannii*, and *Candida albicans* were studied. In vitro studies showed that all the organisms were significantly more susceptible (tens of fold) to blue light inactivation than human keratinocytes. Transmission electron microscopy revealed blue light-mediated ultrastructural damage in microbial cells. Fluorescence spectroscopy and high-performance liquid chromatography (HPLC) confirmed the presence of endogenous porphyrins, which are assumed to be responsible for the antimicrobial activity of blue light. No elevated resistance to blue light inactivation was observed after 10 cycles of sub-

lethal inactivation of the organisms. In vivo animal studies demonstrated that, a single exposure of blue light at 55.8 J/cm² significantly reduced the microbial burden (16-100 fold) in 3rd degree mouse burns, and saved the lives of mice in the event of potentially lethal infections. No significant DNA damage was detected using TUNEL assay in mouse skin after a blue light exposure of 195 J/cm².

In conclusion, antimicrobial blue light is potentially an effective and safe approach for inactivation of infecting organisms.

9268-14, Session 3

Activity-dependent global photobiomodulation on an organism (Invited Paper)

Timon Cheng-Yi Liu, South China Normal Univ. (China)

The global photobiomodulation (PBM) on an organism was studied in terms of function-specific homeostasis (FSH) and scale-free functional network in this paper. FSH is a negative-feedback response of a biosystem to maintain the function-specific conditions inside the biosystem so that the function is perfectly performed. A function in/far-from its FSH is called a normal/dysfunctional function. The quality of an FSH is called the functional fitness of the FSH-maintained normal function. The order of a normal function can be decided in terms of its functional fitness. A normal/dysfunctional FSH-specific stress disrupting the FSH is called a successful/chronic stress. The external activities and internal functions of an organism can be divided into essential, special non-essential and general non-essential ones in terms of their respective effects on organism mortality, life-span or longevity, respectively. Health may be defined to be a state of an organism in which all the essential and special non-essential functions are normal or their stresses are successful. Suboptimal health may be defined to be a state of a disease-free organism in which only some special non-essential functions are dysfunctional in comparison with its healthy state. The level of health or suboptimal health can be decided in terms of its normal function order. Disease may be defined to be a state of an organism which is not in both health and suboptimal health. The global PBM of health, suboptimal health or disease suggested that the PBM may depend on the organism activities.

9268-15, Session 3

Photophysical properties and photo-induced intermolecular electron transfer of a novel aryl benzyl ester dendritic axially-substituted silicon (IV) phthalocyanine

Xiuqin Chen, Yiru Peng, Fujian Normal Univ. (China)

Photodynamic Therapy (PDT) had been intensively investigated as a new technology for diagnosis and treatment of malignant cancer or macular degeneration. The efficacy of PDT mainly depended on the behavior of the photosensitizer, including its efficiency for generation reactive oxygen species and selectivity for accumulation in the tissues. Phthalocyanines have been regarded as the second generation photosensitizers. However, because of their π - π interaction and hydrophobic characteristics, stacking of phthalocyanines in aqueous media is particularly strong. The aggregation obviously shortened its triplet state lifetime and reduced fluorescence quantum yield, leading to a

decrease in photodynamic therapy efficiency and limiting their great potential application in photodynamic therapy.

In order to obtain higher PDT efficacy, the structure of dendritic phthalocyanines were proposed. The substitution of large dendritic wedges expanded π - π conjugated structure of phthalocyanine rings and prevented the aggregation. Constructing a dendrimer around a phthalocyanine core could reduce the aggregation behavior and improve its photophysical property.

In this paper, the photophysical property of an aryl benzyl ester dendritic axially substituted silicon (IV) phthalocyanine was studied by steady and time-resolved spectroscopic methods. The steric hindrance of dendritic structure can reduce the aggregation efficiently and lead to super photophysical property. The photoinduced intermolecular electron transfer between this novel macromolecule and benzoquinone was studied. The results showed that the fluorescence emission of this dendritic phthalocyanine could be quenched by BQ. Therefore, this novel dendritic phthalocyanine was an effective new electron donor and transmission complex could be used as a potential artificial photosynthesis system. It would be a promising third-generation photosensitizer for photodynamic therapy.

9268-16, Session 3

Role of laser fluence in protein synthesis of cultured dorsal root ganglion neurons following low-level laser irradiation

Liqin Zheng, Fujian Normal Univ. (China)

Low level lasers have been used to relieve pain in clinical for many years. But the mechanism is not fully clear. In animal models, adenosine and its receptors especially adenosine A1 receptors have been reported involving in the transmission and modulation of nociceptive signals. So the objective of this study was to establish whether low level lasers with different laser fluence could stimulate the synthesis of adenosine A1 receptor in cultured primary dorsal root ganglion neurons (DRG neurons). The primary DRG neurons were isolated from healthy Sprague Dawley rats (8-12 weeks of age) and spread on 48-well plates specially used for confocal microscopy. 24 hours after spreading, cells were irradiated for two consecutive days with three different wavelength (658 nm, 785 nm, 830 nm) at the energy density of 1-6 J/cm² respectively. Controls were not exposed to lasers, but were kept under the same conditions as the irradiated ones. The synthesis of adenosine A1 receptor after laser irradiation was detected by immunofluorescence, and the changes of it were evaluated using confocal microscopy and Image J software. The results showed that all of the three lasers could promote the synthesis of adenosine A1 receptors in DRG neurons. And irradiation of 4-6 J/cm² increased the synthesis of adenosine A1 receptors, whereas little changes were observed after irradiation of 1-3 J/cm². These results demonstrated that laser irradiation could modify protein synthesis in a dose or fluence dependent manner, and indicated that low level laser irradiation might achieve the analgesic effect through adenosine A1 receptors.

9268-17, Session 3

A new laser technology in ophthalmology for glaucoma treatment

Olga I. Baum, Emil N. Sobol, Evgenii M. Shcherbakov, Institute on Laser and Information Technologies (Russian Federation)

A new approach to increase of uveoscleral outflow path under thermo-mechanical effect of laser radiation have been presented. Experiments have been performed with 40 minipig eyes in-vitro and with 20 rabbit eyes in-vivo using an Erbium doped glass fiber laser of 1.56 microns in wavelength. Laser settings providing substantial alterations in light scattering correlate well with laser parameters required for significant increase of water permeability resulting in normalization of the intraocular pressure.

Light Scattering and Atomic Force Microscopy measurements have been used to study alteration in scleral structure due to non-uniform laser heating.

Rarefaction of the collagen structure in the laser affected zone and formation of sub-micron pores have been clearly recognized.

Substantial increase of water permeability of eye tissues can be a novel approach to normalize the intraocular pressure. The results obtained are the basis of a new effective method for glaucoma treatment.

9268-18, Session 3

The simulation of light distribution in photodynamic therapy for port wine stains

Xiaoming Hu, Shiyu Zhang, Beijing Institute of Technology (China)

Photodynamic Therapy is regarded as the best treatment for port wine stains, which has the main side effect of various degrees of pain (mild to moderate) during the illumination. Though the cooling and cold water have been used to reduce such pain, there is still no scientific evidence for these relief. In this paper, a realistic skin model is built to simulate the distribution of light under treatment, which help to control the light dose and temperature, and improve the clinical results. Comparing with the general parallel skin model, a curving stratum basale layer is used in this paper, and various blood vessel configurations such as single and multiple vessels with horizontally and vertically oriented, curve vessels, various vessel size and various radius of curvature of stratum basale layer are simulated. The results shows a more realistic modelling for modeling the thermal damage and help to relief the pain in the processes.

9268-19, Session 3

In vitro sensitivity of Candida spp to hematoporphyrin monomethyl ether-mediated photodynamic inactivation

Yucheng Wang, Chinese PLA General Hospital (China) and Nankai Univ. (China); Ying Wang M.D., Ying Gu, Chinese PLA General Hospital (China)

Background: An increasing prevalence of Candida infections has emerged with the wide use of immune-suppressants and antibiotics. Current antifungal drugs exhibit low efficiency and high toxicity to the normal organs. Photodynamic inactivation (PDI) provides an alternative therapeutic strategy involving

the use of photosensitizer (PS) and light irradiation. This study evaluated PDI effects against strains of *C. albicans*, *C. parapsilosis*, *C. glabrata*, and *C. krusei*, using the PS of hematoporphyrin monomethyl ether (HMME), which is a novel PS clinically approved in China.

Methods: Suspensions ($\sim 10^6$ CFU/ml) were incubated with seven HMME concentrations (0.25-50 μ M) for 30 min followed by 532-nm laser irradiation for 10 min at 40 mW/cm². Viability of cells was assayed by CFU counting. Furthermore, fetal calf serum (10%) and singlet oxygen quencher NaN₃ (100 mM) was respectively added to the suspension of *C. krusei* to evaluate their roles in PDI process.

Results: Among the four species, *C. albicans* was the most sensitive to PDI, 4 log₁₀ killing was achieved at the concentration of 7.5 μ M. *C. glabrata* was the most resistant, only at concentrations above 25 μ M, log reduction was observed. PDI effect was inhibited by both of serum and NaN₃.

Conclusions: HMME-mediated PDI was able to effectively kill some strains of *Candida* in our experimental conditions, mainly through a Type II photoprocess. However, the effect can be intensively impaired by the presence of serum. Thus, there might be a long way before HMME can be used in fighting against *Candida* in real infectious foci.

9268-20, Session 4

Development of portable optical device for rapid virus detection (*Invited Paper*)

Daxiang Cui, Shanghai Jiao Tong Univ. (China)

Herein, we reported that, in recent years, our group designed and fabricated a series of portable optical devices for ultrasensitive quantitative detection of pathogens combined with quantum dot-labeled lateral flow strips. The CCD-based readers were designed, and fabricated, the quantitative analysis software was developed and optimized. The different kinds of quantum dots were fabricated, and were used to label antibody, and develop a series of quantum dot-labeled lateral flow strips for detection of HBV, HPV and Cag A. The device used 365-nm ultraviolet LED as the excitation light source, and captured the test strip images through an acquisition module. Then, the captured image was transferred to the computer and was processed by a software system. A revised weighted threshold histogram equalization (WTHE) image processing algorithm was applied to analyze the result. For example, CdS quantum dot-labeled lateral flow strips for detection of CagA were prepared. One hundred sera samples from clinical patients with gastric cancer and healthy people were prepared for detection, which demonstrated that the device could realize rapid, stable, and point-of-care detection, with a sensitivity of 20 pg/mL. The device is also granted to medical apparatus certification by china government.

9268-21, Session 4

Photothermal effect of single-wall carbon nanotubes

Naiyan Huang, Chinese PLA General Hospital (China) and The BC Cancer Agency Research Ctr. (Canada); Hequn Wang, The BC Cancer Agency Research Ctr. (Canada); Jianhua Zhao, The BC Cancer Agency Research Ctr. (Canada) and The Univ. of British Columbia (Canada); Harvey Lui M.D., The Univ. of British Columbia (Canada); Mladen Korbelik, The BC Cancer Agency Research Ctr.

(Canada); Haishan Zeng, The BC Cancer Agency Research Ctr. (Canada) and The Univ. of British Columbia (Canada)

Background and Objectives: Single-wall carbon nanotubes (SWNTs) with strong optical absorption in the broad visible and near IR offer unique advantages for photothermal cancer therapy. As the first step, the objective of this study is to observe its photothermal property related with irradiation time, laser power density, and the concentration of SWNTs.

Study Design/Materials and Methods: SWNTs water solutions of different concentrations (0.125, 0.0625, 0.0312, 0.0156, 0.00781, and 0 mg/ml - pure water) placed 0.3 ml (close to the tumor volume) of each into individual wells of a 96 well culture plate. Then irradiated each well with 785 nm laser at two different power density levels: 100 mW/cm² and 200 mW/cm². During the continuous light irradiation, the temperatures of the solution were monitored by an IR thermometer (non-contact measurements).

Results: The temperature of SWNTs solution increases proportionally with the SWNTs concentration and laser power density. In every experiment, the temperature increases quickly with time in the first few minutes and eventually reaches a plateau at about 10 minutes. Temperature increases of 10 to 15 degrees Celsius are easily achievable.

Conclusions: single-walled carbon nanotubes have good absorption at 785nm, and could generate enough heat to destroy cancer cells. It should be a good candidate of photothermal therapy agents.

9268-22, Session 4

Synthesis of folate receptor-targeted photosensitizers for one- and two- photon excited photodynamic therapy

Yanyan Fang, Xiaopu Wang, Yuxia Zhao, Feipeng Wu, Technical Institute of Physics and Chemistry (China)

A series of amphiphilic benzylidene cycloalkanes ketone photosensitizers with or without folate receptor-targeted agent were designed, synthesized and applied in photodynamic therapy (PDT) and two-photon excited PDT (2PE-PDT) processes. Polyethylene glycol were introduced in these photosensitizers to improve their lipid-water partition coefficients. Their linear and nonlinear photophysical properties were studied. The results showed that all compounds exhibited appropriate lipid-water partition coefficients, high reactive oxygen yields, and large two-photon absorption cross-section. The introduction of the folate receptor-targeted agent had no obvious influence on the photophysical properties of corresponding compounds. In vitro studies were conducted using MCF-7 cells (FR+), Hela cells (FR+) and A549 cells (FR-), which represented different levels of folate receptor (FR) expression. All of them showed low dark toxicity and superior PDT and 2PE-PDT effects compared with the clinical drug PSD-007 (a mixture of porphyrins). What's more, folate receptor-targeted photosensitizers achieved higher accumulation and more excellent PDT and 2PE-PDT effects in MCF-7 cells (FR+) and Hela cells (FR+) than photosensitizers without folate receptor-targeted agent and PSD-007. The photo-cytotoxicity of these photosensitizers showed no obvious differences in A549 cells (FR-).

9268-23, Session 4

Sunscreen nanoparticles titanium dioxide and zinc oxide thermal influence on skin at sunlight radiation

Ilya V. Krasnikov, Alexey Y. Seteikin, Amur State Univ. (Russian Federation); Alexey P. Popov, Univ. of Oulu (Finland)

Skin protection against excessive doses of solar radiation causing skin cancer is a challenging task. Skin is a multilayered structure consisting of layers with specific physical properties [1]. The superficial skin layer (stratum corneum) serves as a natural protecting barrier for deeper-located layers containing living cells. From the optical point of view, its function is to prevent penetration of ultraviolet (UV) radiation into epidermis and dermis. In order to increase intrinsic protection of these layers by the upper-located stratum corneum, sunscreens containing chemical light-absorbing components were developed [2].

A mathematical model developed by the authors was applied to simulate sunlight radiation absorption and heat transfer processes in the sunscreen-treated skin [3]. The focus was on the effect of size and concentration of TiO₂ and ZnO nanoparticles for UV protection. Energy of the absorbed light is released mainly in the form of heat, making consideration of heat load an important issue.

In this research, we consider the effect of nanoparticles (of various sizes) embedded into the superficial layer of skin on distribution of absorbed light density and skin surface temperature dynamics at sunlight irradiation. The sunlight comprised by range of wavelengths from 310 to 800 nm with weighted contribution of each wavelength. This causes overestimation of the heat load due to exclusion of longer wavelengths from the consideration.

[1] V.V. Tuchin, Handbook of Optical Biomedical Diagnostics (SPIE, Bellingham, 2002).

[2] A. Popov, A. Priezzhev, J. Lademann, R. Myllylä, Journal of Quantitative Spectroscopy and Radiative Transfer, 112(11), 1891-1897 (2011).

[3] I. Krasnikov, A. Popov, A. Seteikin, R. Myllylä, Biomedical Optics Express, 2(12), 3278-3283 (2011).

9268-43, Session Post

In vivo photoacoustic computed tomography with compressed sensing

Jing Meng, Qufu Normal Univ. (China); Chengbo Liu, Liang Song, Shenzhen Institute of Advanced Technology (China)

Capable of imaging optical absorption contrast with extremely high sensitivity at multiple scales, photoacoustic computed tomography (PACT) is becoming a powerful in vivo imaging tool for many preclinical and clinical applications, such as the imaging of tumor angiogenesis, cardiovascular atherosclerosis and breast cancer. However, one challenge to translate PACT into the clinic is that, the amount of data acquired with current PACT systems is usually huge, making real-time data acquisition, transmission, and reconstruction difficult to achieve. Compressed sensing (CS) is able to recover sparse signals with fewer measurements than that required by the Nyquist sampling theorem. In this work, we present two novel CS-based imaging strategies developed for PACT and photoacoustic microscopy (PAM), respectively. (1) CS with partially known support (CS-PKS) has been developed for a high-frequency PACT system; (2) A CS-based virtual-detector method has been developed to reconstruct the out-of-focus

regions in a low-frequency deep-penetration PAM system. In vivo imaging experiments of the rat-back vasculature and human hand have been performed, demonstrating that: compared with traditional backprojection PACT reconstruction, (1) CS-PKS has produced high-quality in vivo photoacoustic images with three-fold less measurements for PACT system; (2) CS-based virtual-detector method has recovered regions ~4-mm out-of-focus in PAM with higher resolution and contrast-to-noise ratio, leading to an effective increase of the depth-of-focus of PAM. Based on the current studies, CS-based PACT has been shown to possess a great potential for enabling the development of truly high-speed and low-cost photoacoustic imaging technology for a broad range of biomedical applications.

9268-44, Session Post

High-speed quantitative interferometric microscopy-based phase imaging cytometer

Liang Xue, Shanghai Univ. of Electric Power (China); Nan Sun, Shanghai Institute of Quality Inspection and Technical Research (China); Keding Yan, Nanjing Univ. of Science and Technology (China); Yin Wang, Sun Yat-Sen Univ. (China); Fei Liu, Nanjing Agricultural Univ. (China); Shouyu Wang, Nanjing Univ. of Science and Technology (China)

Imaging of cells with high speed and accuracy in a completely non-invasive manner is a challenging task. In order to realize real time phase measurement as well as large amount cell detection, here, we have proposed a phase imaging cytometer based on quantitative interferometric microscopy. Driven by gravity, phase distributions of flowing biological cells are measured by quantitative interferometric microscopy combined with ultra-high speed CMOS camera. The phase imaging cytometer could realize high throughput phase detecting and statistical analysis with high detecting speed. Moreover, with the measured data by cytometer, the statistical characteristics of biological cells are obtained which can be reference for biological analysis and disease detection. We believe the proposed high speed quantitative phase imaging system is of great potential in applications for basic and clinical research.

9268-45, Session Post

Common-path OCT for endoscopic medical imaging

Yi Wang, Xiaodong Chen, Ji Leng, Ting Wang, Xiaojie Chen, Junwei Li, Dao Yin Yu, Tianjin Univ. (China)

Endoscopically guided biopsy is currently the main method for detection of internal organ diseases on clinic. The usage of optical coherence tomography (OCT) in endoscopically guided biopsy makes it possible to achieve non-invasive and high-resolution imaging of biological tissue in vivo, revealing both pathological changes on the surface of mucosa and inside the mucosa, which is essential for early diagnosis.

Conventional OCT bases on low-coherence interferometer which has two arms and locates pathological changes with optical path length between the two arms. Common-path OCT has only one arm and use the reflected light of probe as reference light. But these setups cannot be used in endoscopically guided biopsy for its small optical path length varying scope, which makes it hard for OCT endoscope to get effective tomography of organs.

To solve the discussion above, we built up a common-path OCT for endoscopically guided biopsy in this paper. Our system is nearly the same with common-path OCT reported before but using reflected light of sample surface as reference light. Then the imaging scope will not be influenced by the location of probe inside the body.

In this paper, we described the theory and setup of our common-path OCT firstly, and then experimented with different biological samples. The results proved the validity of our system being used in endoscopically guided biopsy.

9268-47, Session Post

Identification of the boundary between normal breast tissue and invasive ductal carcinoma during breast-conserving surgery using multiphoton microscopy

Tongxin Deng, Yuting Nie, Fujian Normal Univ. (China); Yuane Lian, Fujian Medical Univ. (China); Yan Wu, Fujian Normal Univ. (China) and Jimei Univ. (China); Fangmeng Fu, Chuan Wang, Fujian Medical Univ. (China); Jianxin Chen, Fujian Normal Univ. (China)

With the development of recognition about biological characteristics of breast cancer and the improvement of early diagnosis techniques of breast cancer, great changes have taken place in the local treatment of breast cancer. Breast-conserving surgery has become an important way of surgical treatment for breast cancer. The purposes of breast-conserving surgery is not only to reduce the chance of postoperative local recurrence of tumor but also to conserve normal breast tissue as much as possible. Lesions residue is the most important reason for the local recurrence, so it is very vital to identify the boundary between normal and cancerous breast tissue during breast-conserving surgery. To avoid local residual carcinoma after surgery, the surgical margin has to undergo intraoperative frozen procedures and routine pathological procedures which usually are time-consuming. Multiphoton microscopy (MPM), based on two-photon excited fluorescence (TPEF) and second harmonic generation (SHG), has the ability to noninvasively visualize tissue architecture in real time. In this study, MPM is used to image the microstructures of normal human breast tissue and invasive ductal carcinoma of breast. The fresh, unfixed, and unstained slice specimens are examined by MPM. MPM images are compared with the corresponding Hematoxylin and Eosin (H&E) stained images. In this work, MPM can reveal the cellular morphology and organization structure of normal human breast tissue and invasive ductal carcinoma of breast respectively. Our results show that MPM has the ability to distinguish normal from cancerous breast tissue thus identifying the boundary between normal and cancerous breast tissue. With the development of miniature, real-time MPM imaging technology, MPM should have great application prospects during breast-conserving surgery.

9268-48, Session Post

Surface-Enhanced Raman Scattering(SERS) Spectroscopic Analysis of Herba Houttuyniae Decoction

Weiwei Chen, Jia Lin, Fujian Normal Univ. (China); Hao Huang, Fujian Univ. of Traditional Chinese Medicine (China); Shangyuan Feng, Fujian Normal Univ. (China); Yun Yu, Duo Lin, Fujian Univ. of Traditional Chinese Medicine (China); Rong Chen, Fujian Normal Univ. (China)

The normal Raman spectra and surface-enhanced Raman scattering (SERS) spectra of herba houttuyniae decoction(HHD) were tested and analyzed. The characteristic SERS bands of HHD were tentatively assigned. There was no Raman signal in normal Raman spectra of HHD. However, as a result of the silver colloid enhanced effects on the Raman scattering of HHD, we observed that the SERS spectra of HHD had primary thirteen SERS peaks such as 538, 620, 686, 730, 955, 1030, 1231, 1240, 1325, 1400, 1472, 1564 and 1651 cm^{-1} , and there were six strong signals at 538, 620, 730, 955, 1325 and 1400 cm^{-1} bands. The results showed that the SERS spectroscopy might provide a new kind of high-sensitive, accurate, easy, and rapid detecting method for traditional Chinese medicine.

9268-49, Session Post

Assessment of dental demineralization of yellow race based on fluorescence spectrum

Zhenlin Zhan, Fujian Normal Univ. (China)

Dental caries, also known as tooth decay or a cavity, is the most prevalent chronic disease in dentistry, which is seriously threatening human oral health. Generally, a tooth is in a constant state of back-and-forth demineralization and remineralization between the tooth and surrounding saliva. When demineralization exceeds saliva and other remineralization factors, the mineral content is progressively broken down, producing dental caries. If carious lesions could be detected early enough, intervention methods can be applied to reverse the caries process. In this study, the demineralization status at different acid-etch time is monitoring based on fluorescence spectrum. Human molar in vitro of yellow race is used in the study and immersed in 0.3% citric acid to simulate the oral natural demineralization. According to acid-etch time, samples are divided into four group: ?10 min, ?20 min, ?40 min and ?60 min. The normal untreated specimen is set as control group. The fluorescence spectrum before and after treatment are measured and analysed. The result shows that fluorescence spectrum could be efficiently used to monitor the demineralization status of human dentin. The relative fluorescence intensities of dental tissue excited under 260, 330 and 400 nm decrease with the increase of acid-etch time, though there is no new constituent formed after demineralization.

9268-50, Session Post

Detection of liver cancer tissue using silver nanoparticles-based surface-enhanced Raman spectroscopy

Fadian Liao, Qiuyong Ruan, Juqiang Lin, Fujian Normal Univ. (China); Yongyi Zeng, Fujian Medical Univ. (China); Ling Li, Zufang Huang, Peng Lu, Rong Chen, Fujian Normal Univ. (China)

Early hepatocellular carcinoma without obvious symptoms is hard to detect and diagnose. In our work, we achieved the Raman signal of liver normal tissues and hepatocellular carcinoma tissues by using silver nanoparticles based surface enhanced Raman spectroscopy(SERS), respectively. The sample tissue was under frozen section at -20°C sliced into $20\ \mu\text{m}$. The mean Raman spectra of two groups are roughly similar. But the peaks intensity of hepatocellular carcinoma tissues at 722 cm^{-1} and 1049 cm^{-1} are obviously higher than those of normal tissues. Some peaks of hepatocellular carcinoma tissues appeared to have shifted. Besides, Raman peaks at 1004 cm^{-1} had disappeared in normal tissue. The above data suggested that SERS spectra

can feature liver normal tissue and hepatocellular carcinoma tissue. Principal component analysis (PCA) coupled with linear discriminant analysis (LDA) was performed on the measured data. There were three most diagnostically significant PCs (PC3, PC9, and PC15, $p < 0.05$) for discriminating these two groups. The diagnostic sensitivity and specificity both were 84.6%. The whole analysis of each sample needs less time-consumed and cost than other traditional methods in detecting and diagnosing HCC. The preliminary result suggests that SERS spectra can be a potential medical technology to detect and diagnose HCC.

9268-52, Session Post

Enhancement display of veins distribution based on binocular vision and image fusion technology

Peng Liu, Guangdong Univ. of Technology (China) and Guangzhou Institute of Advanced Technology (China); Si Di, Jian Jin, Guangzhou Institute of Advanced Technology (China); Liping Bai, Guangdong Univ. of Technology (China)

The capture of veins distribution is important for some applications, such as medical care and identification. Therefore, it has become a popular topic in the field of biomedical imaging. Usually, people capture the picture of veins distribution by infrared imaging because hemoglobin can absorb the infrared light strongly. But the display result is similar with that of a gray picture. To some degree, it is unreal for doctors or nurses. In this paper, we develop a binocular vision system to carry out the enhancement display of veins under the condition of keeping actual background color. The binocular system is consisted of two adjacent cameras. A visible band filter and an infrared band filter are placed in front of the two lenses, respectively. Therefore, the pictures of visible band and infrared band can be captured simultaneously. After that, a new fusion process is applied to the two pictures, which related to histogram mapping, principal component analysis and modified bilateral filter fusion. The final result shows that the veins distribution can be displayed clearly. At the same time, the background color of the hand is unchangeable. Besides, correlation coefficient, average gradient and average distortion are selected as the parameters to evaluate the image quality. By comparing the parameters, it is evident that our novel fusion method is prior to some popular fusion methods such as Gauss filter fusion, IHS fusion and bilateral filter fusion.

9268-53, Session Post

High-speed quantitative interferometric microscopy with fast pixel shifting phase unwrapping algorithm

Mingfei Xu, Yanke Shan, Nanjing Agricultural Univ. (China); Liang Xue, Shanghai Univ. of Electric Power (China); Shouyu Wang, Nanjing Univ. of Science and Technology (China); Fei Liu, Nanjing Agricultural Univ. (China)

Quantitative interferometric microscopy is an important method for observing biological samples such as cells and tissues. In order to obtain continuous phase distribution of the sample from the interferogram, phase extracting and phase unwrapping are both needed in quantitative interferometric microscopy. Phase extracting includes fast Fourier transform method and Hilbert transform method, etc., almost all of them are rapid methods. However, traditional unwrapping methods such as least squares algorithm, minimum network flow method, etc. are

time-consuming to locate the phase discontinuities which lead to low processing efficiency. Other proposed high-speed phase unwrapping methods always need at least two interferograms to recover final phase distributions which cannot realize real time processing. Therefore, high-speed phase unwrapping algorithm for single interferogram is required to improve the calculation efficiency. Here, we propose a fast phase unwrapping algorithm to realize high-speed quantitative interferometric microscopy, by shifting mod 2π wrapped phase map for one pixel, then multiplying the original phase map and the shifted one, then the phase discontinuities location can be easily determined. Both numerical simulation and experiments confirm that the algorithm features fast, precise and reliable.

9268-54, Session Post

Quantitative interferometric microscopic cytometer with expanded principal component analysis method

Shouyu Wang, Nanjing Univ. of Science and Technology (China) and Nanjing Agricultural Univ. (China); Ying Jin, Keding Yan, Liang Xue, Nanjing Univ. of Science and Technology (China); Fei Liu, Nanjing Agricultural Univ. (China); Zhenhua Li, Nanjing Univ. of Science and Technology (China)

Quantitative interferometric microscopy is used in biological and medical fields and a wealth of applications are proposed in order to detect different kinds of biological samples. Here, we develop a phase detecting cytometer based on quantitative interferometric microscopy with expanded principal component analysis phase retrieval method to obtain phase distributions of red blood cells with a spatial resolution $\sim 1.5 \mu\text{m}$. Since expanded principal component analysis method is a time-domain phase retrieval algorithm, it could avoid disadvantages of traditional frequency-domain algorithms. Additionally, the phase retrieval method realizes high-speed phase imaging from multiple microscopic interferograms captured by CCD camera when the biological cells are scanned in the field of view. In this paper, both numerical simulation and experiments are presented which prove the expanded principal component analysis based quantitative interferometric microscopic cytometer could realize phase imaging of biological samples. We believe this method can be a powerful tool to quantitatively measure the phase distributions of different biological samples in biological and medical fields.

9268-55, Session Post

Novel optimization method for multi-dimensional breast photoacoustic tomography

Meng Cao, Jie Yuan, Xiaojun Liu, Nanjing Univ. (China); Xueding Wang, Univ. of Michigan Medical School (United States); Guan Xu, Paul L Carson, University of Michigan (United States)

Photoacoustic tomography (PAT) is an effective optical biomedical imaging method which is characterized with nonionizing and noninvasive, presenting good soft tissue contrast with excellent spatial resolution. To build a multi-dimensional breast PAT image, more ultrasound sensors are needed, which brings difficulties to data acquisition. The time complexity for multi-dimensional breast PAT image reconstruction also rises tremendously. Compressive sensing (CS) theory breaks the restriction of Nyquist sampling theorem and is capable to

rebuild signals with fewer measurements. In this contribution, we propose an effective optimization method for multi-dimensional breast PAT, which combines the theory of CS and an unevenly, adaptively distributing data acquisition algorithm. With this method, the quality of our reconstructed breast PAT images are better than those using existing multi-dimensional breast PAT system. To build breast PAT images with the same quality, the required number of ultrasound transducers is decreased by using our proposed method. We have verified our method on simulation data and achieved expected results in both two dimensional and three dimensional PAT image reconstruction. In the future, our method can be applied to various aspects of biomedical PAT imaging situation such as early stage tumor detection and in vivo imaging and monitoring.

9268-56, Session Post

Experimental demonstration of a fresnel-reflection-based optical fiber biosensor coated with polyelectrolyte multilayers

Wenjie Yu, China Jiliang Univ. (China)

We report that the end facet of an optical fiber can be coated with polyelectrolyte multilayers (PEM) of polycation (diallyldimethyl ammonium chloride) and polyanion(styrenesulfonate sodium salt) (PDDA+PSS)_n (n is the number of bilayers), which functions effectively as a fresnel-reflection based biosensor. The experimental setup includes a broadband light source, a 3dB coupler, and an optical spectrum analyzer. Biotin and streptavidin are deposited onto the multilayers-coated end facet sequentially. The light intensity change due to variation of external refractive index is monitored. When the concentrations of streptavidin changes from 0.1mg/ml to 1mg/ml, a linear relationship between the concentration of streptavidin and the reflected optical power at the wavelength of 1530nm is observed. The sensitivity increases from -1.6262?10⁻³ dB/ppm to -4.7852 ?10⁻³ dB/ppm, when the number of PEM increases from 1 to 2. Then we confirm the best optimization bilayers of PEM are 9 through experiment. Selectivity and repeatability of our proposed optical fiber biosensor are verified. When bovine serum albumin (BSA) is added instead of streptavidin, the obtained spectra overlaps with that of biotin's. The final end facet coated with PEM and biotin-streptavidin can be cleaned using microwave vibration or aqua regia. The microwave vibration method is utilized due to security concern. The optical spectra changes back to the initial one of the optical fiber in air. In conclusion, a fresnel-reflection based optical fiber biosensor with good sensitivity, selectivity and repeatability is proposed. This biosensor has the advantages of simple structure, low cost and reliability.

9268-57, Session Post

Multi-sample-based adaptive photoacoustic tomography image optimization method

Wenchao Li, Jie Yuan, Xiaojun Liu, Nanjing Univ. (China); Xueding Wang, Paul L. Carson, Univ. of Michigan Medical School (United States)

Photoacoustic tomography (PAT) is an effective optical biomedical imaging method which is characterized with non-ionizing and noninvasive, presenting good soft tissue contrast with excellent spatial resolution. In the process of PAT, it is mandatory demanded that the power of illumination sources must be limited to ensure safe tissue exposure. Also, because biological tissue

is a highly scattering medium for electromagnetic waves in the optical spectral range, photons will undergo quick scattering and attenuation. Thus the detected photoacoustic (PA) signals are usually of low signal-to-noise ratio (SNR), which is a key factor deteriorating the image quality in PAT. This contribution introduces a multi-sample based adaptive approach to optimize the quality of PAT images. We have explored the relationship of PA signals between different sample processes, and theoretically illustrated its advantage in increasing the SNR of PA signals and furthermore improving the photoacoustic image quality. With this method, we are capable of dramatically reducing the noise and in addition, some detail information in PAT images that used to be buried can be discovered. We carry out both ex vivo and in vivo experiments to validate the effectiveness of our proposed method. The results show that, with our proposed method, the image quality can be effectively improved, which indicate its universality in PAT.

9268-58, Session Post

Fluorescence spectrum analysis of peanut oil mixed with gutter oil

Minghui Chen, Hoo Lee, Shanghai Institute for Minimally Invasive Therapy (China)

Using the fluorescence spectroscopy on rapid detection of gutter oil. The experiment uses different excitation wavelength fluorescence to analyze the peanut oil. Comparing the pure peanut oil and the peanut oil contains 95%, 90%, 80%, 60%, 40% proportions of gutter oil in data collecting, real-time measurement and fluorescence spectra characteristics. The results shows that the fluorescence characteristics of pure peanut oil and the peanut oil containing different proportions of gutter oil have large differences, especially in fluorescence intensity. In the vicinity of the excitation wavelength of 375 nm, the oil's fluorescence intensity is inversely proportional to the content of the gutter oil, particularly when the volume fraction of gutter oil has more than 5%, the sags are the most significantly. Using the advantages of fluorescence spectroscopy's non-contact and high sensitivities, which can be used as the basis to fast detect and determine whether the peanut oil has incorporated with gutter oil.

9268-59, Session Post

Comparison of 1470nm laser and 1470nm laser heat head for ex vivo kidney tissue cutting: a preliminary study

Zhentian Zhou, Zhiyuan Liang, Capital Medical Univ. (China)

Purpose: Compare of the efficiency of 980nm laser and 980nm laser point heat source for tissue cutting in vitro porcine tissue. Method: We designed a laser point heat source head that convert light energy into thermal energy by the absorbing medium. Fresh muscle tissue was harvested from a pig at necropsy and then placed on a platform of uniform rotation. The same power of 980nm laser and 980nm laser point heat source was used to cutting the tissue, respectively. The depth of the traces after cutting was measured and then calculated the volume of tissue vaporization. Result: 980nm laser point heat source has a deeper cutting depth and a larger volume of tissue vaporization compared with 980nm laser. Conclusion: 980nm laser point heat source was better for tissue cutting. This study indicate that we might be able to make laser which have a low tissue absorption coefficient to obtain good results for tissue cutting through the

laser point heat source.

9268-60, Session Post

Research of the types of applicable people and the statistical characteristics of hand vein image

Haifeng Yang, Xiaoping Yang, Tianjin Univ. of Technology (China)

Hand vein image has been widely used in biological recognition, auxiliary medical and other fields. People with age, height, weight, gender differences have distinction in fat thickness of the back of hand, so the contrast and sharpness of their hand vein images are different too, which may affect the results of applications. In this paper, a hand vein image acquisition system is given and the hand vein images of people from the age of 3 to 60 are obtained in various conditions. The effect on the images caused by ages, genders, BMI (body mass index) and FMI (fat mass index) are researched and the statistical characteristics of the images are analyzed. The types of applicable people are also proposed for applications.

9268-61, Session Post

The simulation of the recharging method of active medical implant based on Monte Carlo method

Xianyue Kong, Yong Song, Qun Hao, Jie Cao, Xiaoyu Zhang, Pantao Dai, Wansong Li, Beijing Institute of Technology (China)

The recharging of Active Medical Implant (AMI) is an important issue for its future application, and more and more AMI have been implanted into human body in medical field. As a result, medical monitoring as well as treatment can be implemented within human body. However, the current battery technologies fail to meet the requirements of AMI completely. In this paper, a method for recharging active medical implant using wearable incoherent light source has been proposed, which has the characteristics of low cost, small size, etc. Firstly, the models of the proposed method are developed, which include the models of incoherent light source and the skin tissue, in which the LED light source model with planoconvex lens is used for simulating the incoherent light source, while the skin tissue model is used for simulating the transmission process of incoherent light. Secondly, the recharging processes of the proposed method have been simulated by using Monte Carlo (MC) method. Finally, based on the discussions of the simulation results, some important conclusions have been achieved, which show that the energy decreases from 5.8333 J to 0.5906 J with the increasing of z from 1.25 mm to 12 mm in the fat layer, while, approximate 0.5 J optical energy can arrive at the muscle layer. The results indicate that the proposed method will help to result in a convenient, safe and low-cost recharging method, which will promote the application of this kind of implantable device.

9268-62, Session Post

$^{13}\text{CO}_2/^{12}\text{CO}_2$ isotopic ratio measurements for breath diagnosis with a 2 μm diode laser

Mingguo Sun, Hongliang Ma, Zhensong Cao, Kun Liu, Guishi Wang, Lei Wang, Qiang Liu, Xiaoming Gao, Chinese Academy of Sciences (China)

The validity and practicability of the diagnosis of helicobacter pylori by detecting the $^{13}\text{CO}_2/^{12}\text{CO}_2$ isotopic ratio with diode laser spectroscopy as a non-invasive diagnostic method has been illustrated by many groups. A laser spectrometer based on a distributed-feedback semiconductor diode laser at 2 μm in combination with sensitive wavelength modulation detection was developed to measure the changes of $^{13}\text{CO}_2/^{12}\text{CO}_2$ isotopic ratio in exhaled breath sample with 4% CO_2 concentration. It is characterized by a simplified optical layout, in which a single detector and associated electronics are used to probe CO_2 absorption. The CO_2 absorption spectra were recorded in a 10 cm long optical multi-pass cell with 27 m optical length, and 280 cm^3 volume using balanced detection, which eliminates the influence of laser power fluctuation and CO_2 absorption in ambient. The cell pressure was controlled at 20 Torr by a pressure controller with a precision of 0.1 Torr, and the temperature was stabilized at 30 $^\circ\text{C}$ with an accuracy of ± 0.03 $^\circ\text{C}$ and precision of 0.01 $^\circ\text{C}$, both are actualized by PID-feedback circuits. The signal-to-noise ratios (SNR) were remarkably raised with a digital filter program organized with Labview software. The best 13 σ precision of 0.2 % was achieved, which already satisfies the requirement of gastroenterology breath tests.

9268-63, Session Post

Homing peptide guiding optical molecular imaging for the diagnosis of bladder cancer

Xiao Feng Yang, Jian-zhi Pang, Jie-hao Liu, Yang Zhao, Xing-you Jia, Jun Li, Reng-xin Liu, Wei Wang, Zhen-wei Fan, Zi-qiang Zhang, San-hua Yan, Jun-qian Luo, Xiao-lei Zhang, Shanxi Medical Univ. (China)

Background

The limitations of primary transurethral resection of bladder tumor (TURBt) have led the residual tumor rates as high as 75%. The intraoperative fluorescence imaging offers a great potential for improving TURBt have been confirmed. So we aim to distinguish the residual tumors and normal mucosa using fluorescence molecular imaging formed by conjugated molecule of the CSNRDARRC bladder cancer homing peptide with fluorescent dye. The conjugated molecule was abbreviated Fluo-ACP. In our study, we will research the image features of Fluo-ACP probe targeted bladder cancer for fluorescence molecular imaging diagnosis for bladder cancer in vivo and ex vivo.

Methods

After the Fluo-ACP probe was synthesized, the binding sites, factors affecting binding rates, the specificity and the targeting of Fluo-ACP labeled with bladder cancer cells were studied respectively by laser scanning confocal microscope (LSCM), immunofluorescence and multispectral fluorescence ex vivo optical molecular imaging system.

Results

The binding sites were located in nucleus and the binding rates were correlated linearly with the dose of probe and the grade of pathology. Moreover, the probe has a binding specificity with

bladder cancer in vivo and ex vivo. Tumor cells being labeled by the Fluo-ACP, bright green spots were observed under LSCM. The tissue samples and tumor cells can be labeled and identified by fluorescence microscope. Optical molecular imaging of xenograft tumor tissues was exhibited as fluorescent spots under EMCCD.

Conclusion

The CSNRDARRC peptides might be a useful bladder cancer targeting vector. The Fluo-ACP molecular probe was suitable for fluorescence molecular imaging diagnosis for bladder cancer in vivo and ex vivo.

9268-64, Session Post

Detection of protein kinases P38 based on reflectance spectroscopy with N-type macroporous silicon microcavities for diagnosing hydatidosis hydatid disease

Xiao-yi Lv, Xinjiang Univ. (China); Guodong Lv, Xinjiang Medical Univ. (China); Zhenhong Jia, Jiajia Wang, Xinjiang Univ. (China); Jiaqing Mo, Xinjiang Univ (China)

Detection of protein kinases P38 of *Echinococcus granulosus* and its homologous antibody have great value for early diagnosis and treatment of hydatidosis hydatid disease. Protein kinases P38 and its homologous antibody were prepared by our co-operative group from key laboratory of Xinjiang hydatid institute of the first teaching hospital of Xinjiang medical university. The conventional methods for quantitatively determining protein kinases P38, such as ELISA, are sensitive but require labeling with a fluorescent probe. Also, they are time-consuming and suppress specific hybridization.

In recent years, reflectance Spectroscopy analysis with porous silicon has been employed widely for determining antigen-antibody. Various complicated PSi-based photonic configurations have emerged particular advantages, such as microcavities, Bragg mirrors and waveguides. In this experiment, N-type macroporous silicon microcavities have been successfully fabricated without KOH etching or oxidants treatment that reported in other literature. We observed the changes of the reflectivity spectrum before and after the antigen-antibody reaction by N-type macroporous silicon microcavities. The binding of protein kinases P38 and its homologous antibody causes red shifts in the reflection spectrum of the sensor, and the red shift was proportional to the protein kinases P38 concentration with linear relationship. This research lays the foundation for early diagnosis and treatment of hydatidosis hydatid disease and developing sensitive label-free optical immunosensors for determining any other antigen or antibody.

9268-65, Session Post

High-speed high-stability wavelength-swept source for optical coherence tomography

Minghui Chen, Univ. of Shanghai for Science and Technology (China)

The design and development of the swept laser for optical coherence tomography is presented. It is manifested by a semiconductor optical amplifier, a fiber coupler, two fiber isolators, a semiconductor optical amplifier (SOA) and an acousto-optic tunable filter (AOTF) for frequency tuning within a unidirectional all-fiber ring cavity. Light output from the coupler is further amplified and spectral shaped by a booster SOA terminated at both ends with two isolators. The total loss

in ring cavity is 8.2 dB. The gain SOA provides fiber-to-fiber small signal gain of 22.2 dB with saturation output power of 9.0 dBm. The developed laser source provides up to 100 kHz over a full-width wavelength tuning range of 140 nm at center wavelength of 1308 nm with an average power of 8 mW, yielding an axial resolution of 5.4 μm in air for OCT imaging. Theoretically, the measurement principle and the feasibility of the system are analyzed. Implementing the laser source in swept source based OCT (SS-OCT) system, real-time structural imaging of biological tissue is realized.

9268-66, Session Post

An active timing controlled-gate fluorescence lifetime imaging microscopy using an ultrafast picosecond diode laser

Yang Liu, Chinese Academy of Sciences (China)

We report a time-gated fluorescence lifetime imaging microscopy (FLIM) using a home-made active timing-controlled device and an ultrafast picosecond diode laser. This system could utilize more precise synchronization between laser excitation pulse and ICCD gate combining low timing-jitter diode laser with high precise timing control unit. Two flexible trigger signals for laser source and intensifier gate could adjust time sequence with picosecond precision compared with conventional passive delay adjustment. The importance of the adjustable repetition rate of this laser source is discussed with respect to noise reduction and precision in the lifetime determination, illustrating a further significant advantage over conventional mode-locked solid-state lasers. This FLIM system instrument could satisfy a wide temporal dynamic range demand for various biological applications.

9268-67, Session Post

Texture analysis on basal cell carcinoma caused by excessive ultraviolet radiation

Shulian Wu, Hui Li, Yuxia Wang, Xiaoxiao Zheng, Fujian Normal Univ. (China)

Texture feature is significant internal visual features of images. It includes the arrangement of surface structure and the order of the organization. It reflects the quality of images with phenomenon recurring visual characteristics. In our study, the images during the process of basal cell carcinoma (BCC) irradiated by excessive ultraviolet radiation in the hairless mouse were monitored by skin detector in vivo. A box-counting algorithm and gray level co-occurrence matrix were applied to determine the texture feature in order to evaluate the BCC damage. Then, the morphology characteristics obtained from histological analysis which is a golden criterion was analyzed for comparative with the texture analysis. And then, the relation between morphology and texture feature was established. The results help us to further understand the mechanism of BCC from texture feature.

9268-68, Session Post

An improved non-local means filter for denoising in brain magnetic resonance imaging based on fuzzy cluster

Bin Liu, Xinzhu Sang, Shujun Xing, Bo Wang, Beijing Univ. of Posts and Telecommunications (China)

Image denoising is crucial for medical imaging and diagnosis which will directly affect the subsequent image processing results and quality. Optimal denoising methods should not only preserve edges best but also eliminate noise without artifacts. Image denoising methods, which can improve image quality without compromising imaging processing speed, have attracted intense research interests.

Non-local means(NLM) is one of the classical algorithms for image denoising, which exhibits an outstanding performance for image denoising of brain Magnetic Resonance Imaging(MRI). However, the calculation time and the continuous degree of the boundary are the main drawbacks. Fuzzy cluster method, which is the non-surveillance clustering algorithm, can greatly reduce the computational time and retain more information of the primitive image. An improved method, which combines fuzzy cluster strategy and NLM method, is presented to achieve noise removing and detail enhancement simultaneously.

T1-weighted synthetic MR images of human brain from the 'BrainWeb' website (3D brain MRI spatial resolution is 181*217*181 and slice thickness is 1mm) are used in our experiments. Different levels of Rician noise(1%-7% respectively) are added to the original brain MRI in which to create noisy images.

Three important performance metrics are evaluated in our experiments which is root mean square error(RMSE), peak signal-to-noise ratio(PSNR) and computational time. Quantitative and qualitative results show that our proposed method can not only suppress the noise more effectively but also well preserve the continuous edge and detailed structure for brain MRI compared with the NLM denoising method. In addition, the computational time is greatly reduced.

9268-69, Session Post

Measurement of the mid-infrared spectroscopic imaging of whole human face by portable apparatus (size: 50*50 mm, weight: 200 g)

Wei Qi, Ichiro Ishimaru, Akira Nishiyama, Kenji Wada, Satoru Suzuki, Pradeep Kumara Wijesekara Abeygunawarhana, Yo Suzuki, Masaru Fujiwara, Tsubasa Saito, Kagawa Univ. (Japan)

In the daily living space, measurement of the biological-substance distributions such as sebum can be realized by the proposed method of imaging-type 2-dimensional Fourier spectroscopy. The proposed method is a near-common-path phase-shift interferometer, has the strong robustness for mechanical vibrations. So, the spectrometer can be produced as very simple optical configuration without anti-vibration mechanism. Therefore, the spectrometer's size can be controlled under the 50*50mm and the weight is only about 200 gram. Moreover, the phase shifter is a core part of the spectrometer, and it is constructed by the bimorph type actuator which is depending on the vibration control of the piezoceramic in proposed method.

It is appropriate as the actuator of the phase shifter from the evaluation results of the actuator straightness and position accuracy. As we know, the Fourier spectroscopy has high light utilization efficiency. Additionally, in proposed method we do not use optical part to limit the field angle, which is different about the conventional FT-IR. So, light utilization efficiency is higher than FT-IR. Therefore, the low price microbolometer can be used in the optics as the imaging sensor. From the above reasons, the low-cost, compact and high portability spectrometer can be produced using proposed method. Furthermore, take advantage of the 2-dimensional spectral imaging which can be obtained by proposed method. If a hyperboloidal mirror is installed as objective lens, omnidirectional spectroscopic images can be obtained.

In this report, we demonstrated the feasibility of the middle infrared spectroscopic imaging of whole human faces without active illuminations.

9268-70, Session Post

Miniaturized endoscopic probe for optical coherence tomography with a tiny magnet driving device

Ziwei Pang, Jigang Wu, Shanghai Jiao Tong Univ. (China)

Optical coherence tomography (OCT) is a high-resolution biomedical imaging system with important applications in clinical diagnosis. In the past two decades, various endoscopic probes for OCT have been developed to extend its application into imaging of internal organs. We propose a side-imaging endoscopic probe design for optical coherence tomography by exploiting a tiny radially magnetized metal piece. In the probe design, the OCT light source is coupled into the probe by a single-mode fiber, then focused by a gradient-index (GRIN) lens attaching to the fiber tip. The focused light beam is reflected by a mirror of cylindrical wedge shape and focused at the side of the probe. The mirror is attached to a magnetized metal piece with a short steel wire using epoxy. For OCT scanning, we use magnetic field generated by a larger magnet externally to drive the rotation of the magnetized metal. The reflection mirror will thus be rotated accordingly and scan the beam around the side of the probe. Compare with other probes, our probe design has two distinct advantages: 1) The exit beam will be unobstructed during 360 degree circumference scanning because there are no connecting wires in the scanning part. 2) In principle, the probe can be made very tiny because of the simple structure consisting only the single-mode fiber, GRIN lens, reflection mirror and the magnetized metal piece.

We have made a prototype of the probe with diameter of 1.4 mm and perform preliminary OCT imaging experiments to verify its performance.

9268-71, Session Post

Mueller matrix characterization on anisotropy in tissue simulating phantoms

Yunfei Wang, Graduate School at Shenzhen, Tsinghua Univ. (China) and Tsinghua Univ. (China); Nan Zeng, Graduate School at Shenzhen, Tsinghua Univ. (China); Yihong Guo, Graduate School at Shenzhen, Tsinghua Univ. (China) and Tsinghua Univ. (China); Hui Ma, Graduate School at Shenzhen, Tsinghua Univ. (China)

Most of real tissues have anisotropic microstructures or anisotropic optical features. The variation of tissue anisotropy can be an effective character to describe some abnormal conditions in tissues, so it is meaningful for the extraction and comparison of parameters for anisotropy evaluation. Polarization scattering methods and measurements have shown important potential for early diagnosis, and several anisotropic tissue models and characterization parameters have been present in our previous papers. In this paper, based on our previously proposed sphere-cylinder scattering model, we simulate and investigate the propagation and scattering of polarized light in tissue phantoms using polarization-sensitive Monte Carlo simulation. Focusing on anisotropic tissues, we consider two type disturbance of highly ordered cylindrical elements: cylinders with a distribution of the orientation angle and the existence of the isotropic elements like spheres. By analyzing the corresponding backscattering Mueller matrices with the changes of structural parameters in our tissue model, we extract a characteristic parameter to describe the symmetry of certain Mueller matrix elements. According to the simulation, the characteristic is less sensitive to the size of cylindrical scatterers, and is especially suitable for the case of detecting the small scale isotropic perturbation in a highly anisotropic medium. The simulation and experimental results present in this paper confirm the feasibility of this new anisotropy factor to measure the degree of tissue anisotropy, and imply the validity of applying it in distinguishing some pathological changes.

9268-72, Session Post

Laser Doppler line scanner for monitoring skin blood perfusion changes in port wine stains during vascular-targeted photodynamic therapy

Defu Chen, Beijing Institute of Technology (China); Ren Jie, Ying Wang, Ying Gu, Chinese PLA General Hospital (China)

Vascular-targeted photodynamic therapy (V-PDT) is known to be an effective therapeutic modality for the treatment of port-wine stains (PWS). Monitoring the PWS microvascular response to the V-PDT is crucial for improving the effectiveness of PWS treatment. The objective of this study was to use laser Doppler technique to directly assess the skin blood perfusion changes in PWS before and during V-PDT treatment. In this study, 30 patients with PWS were treated with V-PDT. A commercially laser Doppler line scanner (LDLS) was used to record the skin blood perfusion of PWS immediately before and at 1, 3, 5, 7, 10, 15, 20 min during V-PDT treatment. Our results showed that there was substantial inter- and intra-patient perfusion heterogeneity in PWS lesion. Before V-PDT, the comparison of blood perfusion in PWS and contralateral healthy control normal skin indicated that PWS blood perfusion could be larger than, or occasionally equivalent to, that of control normal skin. During V-PDT, the blood perfusion in PWS significantly increased after the initiation of V-PDT treatment, then reached a peak within 10 minutes, followed by a slowly decrease to a relatively lower level, which was still larger than the perfusion value before V-PDT. Furthermore, the time for reaching peak and the subsequent magnitude of decrease in blood perfusion varied with different patients. In conclusion, the LDLS system is capable of assessing skin blood perfusion changes in PWS during V-PDT, and has potential for elucidating the mechanisms of PWS microvascular response to V-PDT.

9268-73, Session Post

Rose Bengal and green light (RGX): Second-generation approach for cornea cross-linking to inhibit progression of cornea ectatic disorders

Hong Zhu, Wellman Ctr. for Photomedicine (United States) and Shanghai Jiao Tong Univ. (China); Irene E. Kochevar, Massachusetts General Hospital (United States)

Purpose. We have developed a collagen cross-linking technology using Rose Bengal (RB) plus green light (RGX) for strengthening cornea. The goals of this study were to evaluate the corneal stiffening and potential effects on ocular structures.

Methods. Corneas of young Dutch belted rabbits treated with 0.1% RB and 0.25W/cm² green light for 6.6 min. Retina safety was evaluated by fundus fluorescein angiography (FFA) on days 3, 7 and 28 after treatment. After eyes were harvested on day 1 and 28, NBT staining was used to assess thermal damage on iris, cornea stiffness was measured by tensiometry, keratocyte number and retinal outer nuclear layer (ONL) thickness on H&E sections was calculated.

Results. RGX increased the average cornea stiffness by 2.7-fold on day 1 and by 1.6-fold on day 28 compared to controls. No change in NBT staining in the iris was observed after RGX. RGX did not alter the number of keratocytes and ONL thickness. FFA on days 3, 7 and 28 did not show any damage in the retina.

Conclusions. RGX treatment substantially increases cornea stiffness and is safe for the retina and iris. These results suggest that RGX is a viable approach for treat ectatic cornea diseases.

9268-74, Session Post

In vivo monitoring rat skin wound healing using nonlinear optical microscopy

Chen Jing, Xiaoqin Zhu, Fujian Normal Univ. (China)

Normal cutaneous wound healing is a dynamic and orderly process, involving several events that lead to blood clotting, formation of granulation tissue, collagen deposition, and finally tissue remodeling. Common clinical methods to diagnose wounds may cause extra damage and even more delayed healing when biopsies are taken. Therefore, noninvasive assessment methods of the wound healing process are of paramount importance to treatment. In this work, nonlinear optical microscopy based on two-photon excited fluorescence and second harmonic generation were employed for imaging and evaluating the wound healing process on rat skin in vivo. The morphology and distribution of specific biological markers in cutaneous wound healing such as collagens, blood vessels and hair were clearly observed at 1, 5 and 14 days post injury from the high-resolution nonlinear optical images. We found that the disorder of native collagen existed in the exposed surfaces of wound at day 1 was covered with regenerative collagen on day 5, which was thin and organized. By day 14, the thick and dense collagen bundles appear more randomly oriented at the original margin of the wound, similar to normal dermis collagen bundles. In addition, the autofluorescence signals which obtained on the first day were originated from the blood clot containing inflammatory and blood cells. And the new vessels of granular appearance can be identified at day 5, revealing the formation of granulation tissue.

Importantly, our results demonstrated that this technique has the ability to provide more accurate and comprehensive information for the physiological states of normal wound healing process on intravital rat skin. Advantages in instrumentation may lead to the application of nonlinear optical microscopy for noninvasive clinical detection and treatment.

9268-75, Session Post

The structural assessment of 3D-printed porous hydrogel scaffolds using optical coherence tomography

Pei Tu, Ling Wang, Enming Xu, Hangzhou Dianzi Univ. (China)

One of the main challenges in tissue engineering is the fabrication of porous scaffolds with complex architectures. Three-dimension (3D) printing technique is an attractive method to produce scaffolds with tight pore size distributions and controlled geometries for tissue engineering applications. It is generally known that the design, geometry optimization and structural assessment of 3D-printed macroporous scaffolds are very important for successful integration in tissue engineering. And there have been increasing demands for imaging techniques to help in its optimal design, which are capable of assessing complex three-dimensional structure with high resolution in situ and at larger depths in highly-scattering scaffolds. In our study, 3D-printed hydrogel scaffolds were designed in distinct geometries including rectangular pores and different pore sizes. Three dimensional optical coherence tomography (OCT) was applied for nondestructive imaging and quantitative characterization of the scaffold structures. High-resolution OCT revealed the automatic image analysis methods to quantify the spatially-resolved morphometric parameters such as pore size. The measurements were compared to the theoretical design parameters, and the poor geometric control of hydrogel scaffolds with smaller pores was found. Cell distributions of cell-mixed porous hydrogel scaffolds with different morphological design parameters were also characterized in order to demonstrate structural optimal design further. The results indicated that OCT can be a promising tool to evaluate the 3D printing process and help optimize scaffold fabrication.

9268-76, Session Post

In-vivo dynamic analysis zonal difference of hepatobiliary metabolism in chronic hepatic diseases

Chih-Ju Lin, National Taiwan Univ. (Taiwan)

In vivo dynamic analysis hepatobiliary metabolism was a novel subject to understand hepatic functions. The phenomenon of hepatobiliary metabolism was non-uniform in hepatic lobule, and liver diseases would cause hepatic functional variation. In this study, molecular probe of 6-carboxyfluorescein diacetate (6-CFDA) was hydrolyzed by intracellular esterase into fluorescent 6-carboxyfluorescein (6-CF) and 6-CF was excreted to canaliculi, whole 6-CFDA metabolism would investigated with two-photon fluorescence microscopy. Normalization of 6-CF metabolic curve, the mean results of liver fibrosis and fatty liver were similar to control liver. But periportal hepatocytes, hepatocellular 6-CF retain of fatty liver was about 30% of control and liver fibrosis. This result shows that the membrane transporter may increase in chronic liver diseases.

9268-78, Session Post

Multiphoton microscopic imaging and quantifying of fibrotic focus in invasive ductal carcinoma of the breast

Sijia Chen, Yuting Nie, Fujian Normal Univ. (China); Yuane Lian, Fujian Medical Univ. (China); Yan Wu, Fujian Normal Univ. (China); Fangmeng Fu, Chuan Wang, Fujian Medical Univ. (China); Jianxin Chen, Fujian Normal Univ. (China)

During the proliferation of breast cancer, the desmoplastic can evoke a fibrosis response by invading healthy tissue. Fibrotic focus (FF) in invasive ductal carcinoma (IDC) of the breast had been reported to be associated with significantly poorer survival rate than IDC without FF. As an independent prognosis indicator, it's difficult to obtain the exact fibrosis information from traditional detection method such as mammography. Multiphoton imaging based on two-photon excited fluorescence (TPEF) and second-harmonic generation (SHG) has been recently employed for microscopic examination of unstained tissue. In this study, multiphoton microscopy (MPM) was used to image the fibrotic focus in invasive ductal carcinoma tissue. The morphology and distribution of collagen in fibrotic focus can be demonstrated by the SHG signal. Quantification analysis was also made to further characterize the grade of fibrosis in fibrotic focus, which be greatly related to the metastasis of breast cancer. Our result suggested that the MPM can be efficient in identifying and assessing the extent of fibrosis of the fibrotic focus in IDC. Combining with pathology analysis and other detecting methods, MPM owns potential in becoming an advanced histological tool for detecting the fibrotic focus in IDC and collecting prognosis information, which may guide the subsequent surgery option and therapy procedure for patients.

9268-79, Session Post

Initiation efficiency and cytotoxicity of a series of water-soluble benzylidene cyclopentanone photo-initiators for two-photon polymerization of bio-compatible materials

Xiaopu Wang, Yanyan Fang, Qianli Zou, Technical Institute of Physics and Chemistry (China) and Univ. of Chinese Academy of Sciences (China); Yuxia Zhao, Feipeng Wu, Technical Institute of Physics and Chemistry (China)

The 3D fabrication of bio-compatible materials under an aqueous environment is a fundamental requirement for tissue engineering. In this work, a series of polyethylene glycol (PEG)-, carboxylate anionic group- or pyridyl cationic group-functionalized benzylidene cyclopentanone photoinitiators were synthesized. Their water-solubility, photophysical properties and cytotoxicity were investigated. Using eosin as reference, their initiation efficiencies in water-soluble photoactive formulation (SR610 with 20% of DI water) excited by one- or two-photon were studied. The results showed that the water-solubility of X2 and X3 were much better than those of other four compounds. There were no significant differences between each other for the linear and nonlinear photophysical properties of six compounds. Four PEG-functionalized compounds presented lower cytotoxicity than those of Y1 and P1. Using these compounds as photoinitiators directly, 3D micro-structures fabricated by two-photon

polymerization of water-soluble acrylate all could be achieved. In addition, their threshold energies were all lower than 0.5 mW. However, the rigidity of 3D micro-structures was affected by the water-solubility of these photoinitiators. 3D micro-structures built by formulations containing X2 and X3 would collapse easily. Conversely, other 3D microstructures could sustain very well. This work proves that B2 and B3 have extensive application prospects in 3D fabrication for tissue engineering.

9268-80, Session Post

Time-resolved multicolor two-photon excitation fluorescence microscopy of living cells

Wei Zheng, Shenzhen Institute of Advanced Technology (China)

Multilabeling which maps the distribution of different targets is an indispensable technique in many biochemical and biophysical studies. Endogenous fluorophores, such as reduced nicotinamide adenine dinucleotide (NADH), flavin adenine dinucleotide (FAD), keratin, and tryptophan, have provided contrast agents for imaging metabolism and morphology of living cells. Therefore, two-photon excitation fluorescence (TPEF) microscopy of endogenous fluorophores combining with in vivo fluorescence labeling techniques such as genetically encoded fluorescent protein (FP) and fluorescent dyes staining could be a powerful tool for imaging living cells. However, the challenge is that the excitation and emission wavelength of these endogenous fluorophore and fluorescent labels are very different. A multi-color ultrafast source is required for the excitation of multiple fluorescence molecules. In this study, we developed a two-photon imaging system with excitations from the pump femtosecond laser and the selected supercontinuum generated from a photonic crystal fiber (PCF). Multiple endogenous fluorophore, fluorescent proteins and fluorescent dyes were excited in their optimal wavelengths simultaneously. A time- and spectral-resolved detection system was used to record the TPEF signals. This detection technique separated the TPEF signals from multiple sources in time and wavelength domains. Cellular organelles such as nucleus, mitochondria, microtubule and endoplasmic reticulum, were clearly revealed in the TPEF images. The simultaneous imaging of multiple fluorophore in vivo will greatly aid the study of sub-cellular compartments and protein localization.

9268-81, Session Post

Pulse wave detection and analysis based on swept source optical coherence tomography

Yihui Shen, Hui Li, Fujian Normal Univ. (China)

Pulse diagnosis is an important method of traditional Chinese medicine. The doctors diagnose the patient's physiological and pathological status through the palpation of radial artery for radial artery pulse information. Optical coherence tomography (OCT) is an important tool for medical optical research. The swept source optical coherent tomography (SS-OCT) imaging speed is up to 200 frames per second with the spatial resolution of 25um in our research. Current conventional diagnostic devices only function as a pressure sensor to detect the pulse wave which can just partially reflect the doctors feeling and lose large amounts of useful information. The research will study

microscopic changes of the surface skin above radial artery in the form of images based on OCT. The deformation of surface skin in a cardiac cycle which was caused by arterial pulse is detected by OCT. The patient's pulse wave is calculated through image processing. It is found that it is good consistent with the result conducted by pulse analyzer. The real-time patient's physiological and pathological status can be monitored. This research provides a kind of new method for pulse diagnosis of traditional Chinese medicine.

9268-82, Session Post

Quantitative changes of collagen in human normal breast tissue and invasive ductal carcinoma using nonlinear optical microscopy

Weiqiang Li, Yan Wu, Fujian Normal Univ. (China); Yuane Lian, Fangmeng Fu, Chuan Wang, Fujian Medical Univ. (China); Jianxin Chen, Fujian Normal Univ. (China)

Multiphoton microscopy (MPM), based on two-photon excited fluorescence (TPEF) and second-harmonic generation (SHG), provides a glimpse of real-time biology, making it suitable for applications in almost all the areas of biomedical research and clinical study. Especially, MPM imaging of collagen plays a key role in noninvasive diagnoses of human tissue. During the course of the experiment, we observed an interesting phenomenon which TPEF signal of collagen in human invasive ductal carcinoma of breast tissue becomes much weaker than the normal breast tissue, but the SHG signal of collagen does not get an obvious change. In order to explain the phenomena, this paper emphasizes on the intensity of TPEF and SHG signal from collagen in human invasive ductal carcinoma of breast tissues and normal breast tissue. Further, we respectively obtain the intensity spectral information from collagen in the above two tissues with all parameter unaltered. Our quantitative results show that the intensity of TPEF from collagen in human invasive ductal carcinoma of breast tissue is much lower than the normal breast tissue. According to the theoretic analysis, it was concluded that the intensity of TPEF declined due to the reduction of the quantum yield when the collagen was intruded by cancer cells. However, the invasion of cancer cells make no difference on decisive factor of SHG. Our theoretical analysis bring more detailed information about intensity of SHG and TPEF from collagen in the above two tissues.

9268-83, Session Post

Simulation of stimulated emission depletion intensity distribution by scalar integral

Jianling Chen, Xiaogang Chen, Hongqin Yang, Zewen Qiu, Hui Li, Shusen Xie, Fujian Normal Univ. (China)

Stimulated emission depletion (STED) optical nanoscopy can achieve super-resolution fluorescence imaging, by suppressing fluorescence on the peripheral of excitation center with $0-2\pi$ vortex phase modulation. Previously, the STED intensity distribution at the focal plane and the derived expression of resolution are generally analytical described by vectorial integral. To overcome the complex and multifarious of the vector calculation, we proposed scalar integral method and used the Collins-Huygens integral to analytically describe the peak intensity, the central intensity of the doughnut spot and

the resolution of STED nanoscopy. We verified our method by comparing our results with vector theory. And we found it agreed well with vector theory under the high STED power, which was commonly used experimental conditions for high resolution. Our method provides a fast and convenient way to evaluate the performance of STED with vortex phase modulation.

9268-84, Session Post

Microfluidics-integrated cascaded double-microring resonators for label-free biosensing

Yangqing Chen, Fang Yu, Chang Yang, Mingyu Li, Longhua Tang, Jinyan Song, Jian-Jun He, Zhejiang Univ. (China)

Recently, cheap silicon-on-insulator (SOI)-based biosensors have been demonstrated that allow fast and accurate quantitative detection of biologically relevant molecules for applications in medical diagnostics and drug development. However, whereas the SOI sensor can be made cheaply, the cost of sample and reagents required are normally ineffective, and an high precise spectrometer is typically required to accurately monitor the resonance wavelength shift in the sensor's transmission spectrum. To address this issue, we reported a highly-sensitive optical biosensor based on cascaded double-microring resonators with integration of microfluidic chips and then explored their label-free biosensing capability. The sensor is based on SOI wafer, consisting of cascaded double-microring resonators to improve the sensitivity by using the Vernier effect. The optical chip is integrated into lab-on-a-chip using of epoxy glue to bond the microfluidic network to the optical chip. The lab-on-a-chip system allows for fast and leak-tight assembly of spaced fluidic interconnects and can reduce the amount of samples or reagents required for testing and analysis. The sensing capability can be investigated by the detection of numerous biological targets. Herein we performed multiple tests measuring the binding capacity of the antibody on the surface, using biotin-avidin. Furthermore, we detected recognition for the non-target molecules using casein. These experiments demonstrate as-resulted biosensing chips have a good reliability for detection and the significantly resonance wavelength shift in the nanometer level without high precise spectrometer, which improve the sensitivity relative to the reported biosensor with the picometer level shift. Further benefit may be realized in the future through integration of light source and photodiodes on the SOI optical chip, which leads to portable devices to enable on-site testing.

9268-85, Session Post

Spectroscopic studies of the interaction between tetra-substituted aluminum phthalocyanines and bovine serum albumin

Yiru Peng, Yipeng He, Liqin Zheng, Yide Huang, Pingping Lin, Hongqin Yang, Fujian Normal Univ. (China)

Serum albumin, the most abundant plasma protein in mammalian blood, shows significant effects on delivery and therapeutic efficacy of drugs, therefore, the investigation of binding interaction between serum albumin and drugs is vital and necessary. In the present study, the binding interaction of two aluminum(III) phthalocyanine(AIPc) derivatives, tetrasulfonate- and tetra-(p-sulfoazophenyl-4-aminosulfonyl)-substituted AIPc(complex 1 and 2), with bovine serum albumin (BSA), one of the most widely studied plasma proteins, was investigated by

UV-Visible absorption and fluorescence spectroscopy. Addition of BSA to the Pc complexes in buffered aqueous solution led to an altered aggregation behavior of the studied Pcs, which could be obviously observed through the remarkable changes in their Q-band absorption spectra. On the other hand, the intrinsic fluorescence of BSA was significantly quenched by the static quenching mechanism when titrating these complexes with the serum albumin solution. The interaction between BSA and the Pcs complexes caused conformational alterations of BSA according to fluorescence data. Besides, binding constants and binding sites were obtained and binding ability between the Pc complexes and serum albumin was assessed. Our results suggest that complex 1 and 2 readily interact with BSA whereas the latter shows more affinity (with higher binding constant value) to the serum albumin, implying the stretched space chain substituents of complex 2 may contribute to their transportation in the blood.

9268-87, Session Post

Energy threshold of efficacy and safety laser mode for creation very high-density peptide arrays

Olga I. Baum, Emil N. Sobol, Institute on Laser and Information Technologies (Russian Federation); Alexander Nesterov-Muller, Karlsruher Institut für Technologie (Germany)

The development of new the methods for diagnosis of the immune system and the type of the new tissue which grows as a result of laser-activated regeneration of biological tissues is of current interest at this time.

Purpose of this work to present one of such method, which based on the creation of very high-density peptide arrays using laser impregnation of amino acids from the polymer into the surface layer substrate.

The theoretical model for the laser-induced heterogeneous pulse periodic heating of polymer with amino acids have been constructed.

The theoretical calculation of the upper and lower thresholds of the selective surface fusing amino acids, which allows to optimize the laser parameters for efficient impregnation of a linker amino acid substrate layer of micro-particles while preserving their functionality based on the thermal conductivity equation.

The typical three-dimensional distribution of temperature field inside the polymer with amino acids along the direction of laser irradiation have been constructed.

On the bases of the result obtained the theoretical calculation for the energy threshold of efficacy and safety laser mode for impregnation of amino acids with the preservation of their functionality to create very high-density peptide arrays have been found.

9268-88, Session Post

Influence of static pressure on dynamic characteristics of laser-induced cavitation and hard-tissue ablation under liquid environment

Chuanguo Chen, Xuwei Li, Xianzeng Zhang, Zhenlin Zhan, Shusen Xie, Yixuan Yang, Fujian Normal Univ. (China)

Several studies have demonstrated that laser-induced hard tissue ablation effects can be enhanced by applying an additional

water-layer on tissue surface. However, the related mechanism has not yet been presented clearly. In this paper, the influence of static pressure on dynamic characteristics of cavitation induced by pulse laser in liquid and its effect on bovine shank bone ablation were investigated. The laser source is fiber-guided free-running Ho:YAG laser with wavelength of 2080 nm, pulse duration of 350 μ s and energy of 1600 mJ. The tissue samples were immersed in pure water at different depths of 11, 16, 21, 26 and 31 mm. The working distance between the fiber tip and tissue surface was fixed at 1 mm for all studies. The dynamic interaction between laser, water and tissue were recorded by high-speed camera, and the morphological changes of bone tissue were assessed by stereomicroscope and OCT. The results showed that many times expansion and collapse of bubble were observed, more than four pulsation periods were accurately achieved, most energy (account for only 2% of radiation energy) focuses on the first period and the bubble became more and more irregular in sharp. The internal temperature of bubble reached 70° much larger than water temperature 20°. The volume (175.5-130.4 mm³), longitudinal length (7.49--6.74 mm) and transverse width (6.69--6.08 mm) of bubble were slowly decreased while volume (0.0461--0.0124 mm³) of ablation craters were drastically reduced, with static pressure increasing. The results also presented that the water-layer on hard-tissue surface can not only reduce thermal injury but also improve lubricity of craters, although the water-layer reduced ablation efficiency.

9268-89, Session Post

Influence of liquid medium with different absorption coefficient on bovine bone tibia ablation induced by CO₂ laser

Xuwei Li, Chuanguo Chen, Xianzeng Zhang, Zhenlin Zhan, Shusen Xie, Fujian Normal Univ. (China); Qinglin Wu, First School of Sanming (China)

Liquid-assisted laser ablation has been investigated in laser surface cleaning, laser osteotomy, and dental tissue ablation. However, the actual mechanism of liquid-assisted ablation is not clear yet. The purpose of this study was to investigate the influence of liquid medium with different absorption coefficient and the liquid thickness on laser ablation efficiency. A pulsed CO₂ laser ($\lambda=10.64 \mu\text{m}$, $\tau_p=5 \text{ ms}$) was employed to ablate bovine bone tibia under different liquid environments (pure water with $\alpha=817 \text{ cm}^{-1}$ or liquid with ink volume of $\alpha=926 \text{ cm}^{-1}$). The thickness of liquid layer varied from 0.6 mm to 2 mm. The applied pulse power level was set at 5 w and each crater was produced with six laser pulses. Morphological deformation and crater dimensions were measured by optical microscope and optical coherence tomography (OCT) system respectively. The dynamic process of ablation was monitored with a high speed camera. The results showed that the ablation cross-section area produced with various levels of pure water thickness (0.6, 0.8, 1 and 2 mm) were lower than under another liquid, and the ablation depth gradually decreased as the water layer becoming thicker. The biggest cross-section area in liquid thickness of ink was 0.8 mm, then the ablation depth decreased quickly as the liquid layer thicker than 0.8 mm. Thermal damage could be observed for both groups, but less seen in pure water.

9268-90, Session Post

Monitoring the effect of low-level laser therapy in healing process of skin with second harmonic generation imaging techniques

Xiaoman Zhang, Biying Yu, Hui Li, Fujian Normal Univ. (China)

The 632nm wavelength low intensity He-Ne laser was used to irradiated on 20 rats which have skin wound. The dynamic changes and wound healing processes was observed with nonlinear spectral imaging technology. We observed that:(1) The wound healing process was accelerated by the low level laser therapy(LLLT);(2)The new tissues produced SHG signals. Collagen content and microstructure differed dramatically at different time points along the wound healing. Our observation shows that the low intensity He-Ne laser irradiation can accelerate the healing process of skin wound in rats, and Second harmonic generation imaging technique can be used to observe wound healing process, which is useful for quantitative characterization of wound status during wound healing process.

9268-91, Session Post

Ocular damage induced by pulsed 1.338 μm laser radiation

Zai-Fu Yang, Beijing Institute of Radiation Medicine (China); Hongxia Chen, Chinese PLA General Hospital (China); Jiarui Wang, Luguang Jiao, Xiaomin Jing, Jinggeng Yang, Beijing Institute of Radiation Medicine (China)

The ocular damage effects of penetrating near infrared lasers (1.15-1.4 μm) have attracted much attention in recent years. However, little is known about the ocular damage effect on 1.338 μm wavelength. The goal of this research effort was to identify the corneal and retinal damage effects induced by 1.338 μm laser. The experiment was performed on chinchilla grey rabbit for retinal damage and New Zealand rabbit for corneal damage. The pulse duration was 5ms. For corneal damage, the incident laser spot diameter was 5 mm, the radiant exposure was between 19.8 and 33.6 J/cm², the exposed sites were clinically evaluated for presence of lesions at 1h and 24h post-exposure. For retinal damage, the laser spot diameter on cornea was 5 mm, the radiant exposure was between 3.31 and 5.74 J/cm², the exposed sites were clinically evaluated with direct ophthalmoscope at 1h, 24h and 48h post-exposure. The ED₅₀ was calculated with probit analysis method. Corneas and retinas were collected at 24-h and 48-h endpoint respectively and prepared for microscopic evaluation. Results showed that the corneal ED₅₀ was 27.0J/cm² (95% confidence interval 25.8-28.1 J/cm²) at 1-h checkpoint. The retinal ED₅₀ was determined to be 4.83J/cm² (95% confidence interval 4.60-5.05J/cm²) at 1-h and 4.60J/cm² (95% confidence interval 4.31-4.86J/cm²) at 24-h checkpoint. Histological section showed that the threshold lesion of both retina and cornea has the characteristics of full-thickness damage.

9268-92, Session Post

In vivo differentiation of photo-aged epidermis skin by texture-based classification

Xiaoman Zhang, Cuncheng Weng, Hui Li, Fujian Normal Univ. (China)

Two sets of in vivo female cheek skin epidermis images were analyzed through gray level co-occurrence matrix (GLCM) and fast Fourier transform (FFT). One set was derived from women in their 20s and the other from women more than 60 years of age. GLCM was used to evaluate the texture features of the regions of interest within the cheek epidermis, and texture classification was subsequently performed. During texture classification, 25 images (320×240 pixels) in each age set were randomly selected. Three texture features, i.e., energy, contrast, and correlation, were obtained from the skin images and analyzed at four orientations (0°, 45°, 90°, and 135°), accompanied by different distances between two pixels. The textures of the different aging skins were characterized by FFT, which provides the dermatoglyph orientation index. The differences in the textures between the young and old skin samples can be well described by the FFT dermatoglyph orientation index. The texture features varied among the different aging skins, which provide a versatile platform for differentiating the statuses of aging skins.

9268-93, Session Post

Neuron location in whole brain imaging with single-cell resolution: staining study

Xiangning Li, Huazhong Univ. of Science and Technology (China) and Wuhan National Lab. for Optoelectronics (China); Hui Gong, Qingtao Sun, Miao Ren, Huazhong Univ. of Science and Technology (China)

Whole brain imaging is becoming an increasingly important tool in both neural research and clinical care. A range of imaging technologies now provide unprecedented sensitivity that we can map the whole brain in much greater detail than previously possible. Moreover, high-throughput optical imaging is critical to obtain large-scale neural connectivity information of brain, the location of neurons in the whole brain and the fine structures of every encephalic region are required. Micro-optical sectioning tomography system is enabling us to identify neural networks involved in cognitive processes with visualization of brain structure and function with submicron resolution from the level of individual neuron to the whole brain. However, sectioning the fluorescence sample sometimes induces tears between adjacent tiles and causes difficulties in continuous fiber tracing from fluorescence imaging. To acquire the location of neurons in whole brain imaging simultaneously, we performed neural dyes and staining methods screening. Together with fluorescence micro-optical sectioning tomography imaging system, our modified staining methods enable the visualization of whole brains with single-cell resolution and neuron location information.

9268-94, Session Post

The photodynamic efficacy of hematoporphyrin monomethyl ether mediated by 457nm laser on human umbilical vein endothelial cells in vitro

Haixia Qiu, Hongyou Zhao, Jing Zeng, Ying Wang M.D., Naiyan Huang, Ying Gu, Chinese PLA General Hospital (China)

Vascular photodynamic therapy (V-PDT) has showed promising result in some vascular disease, such as port wine stains, AMD, esophageal varices and radiation gastroenteritis, et al, and vascular endothelial cell is target of V-PDT. This study was conducted to characterize the accumulation of hematoporphyrin monomethyl ether (HMME) which is a new domestically produced second generation photosensitizer in human umbilical vein endothelial cells (HUVEC) in vitro. At the same time, the PDT inactivation effect of a potential V-PDT light source: the 457nm laser was investigated comparing with that of the 532nm laser. The absorption of HMME by HUVEC was observed by fluorescence spectrophotometry. The cellular viability was determined by MTT assay. The uptake of HMME in HUVEC correlated positively with the incubation concentrations, and increased with the increasing of incubation times. HMME-PDT could kill the HUVEC effectively both by 457nm laser and 532nm laser, the inactivation rate was increased with the increasing concentrations of HMME, while the survival rates of 457nm laser was higher than that of 532nm laser at the same HMME concentration. These results suggested the 457nm laser has the potential to be the light source for V-PDT, but the PDT effect of 457nm laser may not be better than that of the 532nm laser.

9268-95, Session Post

Dynamic visualization of hydrophobic and hydrophilic solutes in oleic-acid enhanced transdermal delivery

Te-Yu Tseng, National Cheng Kung Univ. (Taiwan); Kung-Bin Sung, Chiu-Sheng Yang, National Taiwan Univ. (Taiwan)

Considerable efforts have been directed towards gaining an extensive understanding of transdermal delivery. Until today, fewer studies on dynamics of solutes transporting across stratum corneum have been reported. This study is focused on investigating dynamics of sulforhodamine B (SRB) and rhodamine B hexyl ester (RBHE) molecules transporting across ex-vivo human stratum corneum with and without oleic acid enhancement. With two-photon fluorescence microscopy employed as a non-invasive tool, fluorescence imaging stacks of stratum corneum are recorded and further analyzed for characterizations of solutes distribution. Oleic acid enhances penetrations of both SRB and RBHE in the transdermal delivery. However, the mechanisms of enhanced delivery are different in that for SRB, enhancement of probe delivery is achieved by the disruption of stratum corneum by oleic acid, leading to increased SRB penetration. RBHE tend to form vesicles with oleic acid, which first fuse and then become integrated with the stratum corneum, releasing RBHE in the process. Furthermore, dynamic quantifications of transport enhancement can be achieved with the use of Fick's Second Law. Dynamic monitoring of solutes transporting across the stratum corneum is an effective method

for understanding dynamic phenomena in transdermal delivery of probe molecules, leading to improved delivery strategies of molecular species for therapy purposes.

9268-96, Session Post

Monitoring vascular distribution and quantifying blood flow velocity in mouse by using optical coherence tomography

Jian Gao, Xiao Peng, Wei Yan, Bin Yu, Qi Wang, Junle Qu, Hanben Niu, Shenzhen Univ. (China)

Optical coherence tomography (OCT) is widely used in biomedical imaging. As an optical imaging technology, OCT is non-invasive, has high resolution and high sensitivity. Furthermore, Doppler OCT (ODT) combines Doppler effect with OCT technology, leading to simultaneously obtain both high-resolution images of tissue structure and hemodynamics. In this study, we built a spectral domain OCT system by using broadband light-source and fast spectrometer. Theoretically, transverse resolution, axial resolution and the depth of imaging system are 10.23 μ m, 6.8 μ m and 2.58mm, respectively. By imaging nude mouse model with dorsal skin window chamber, we obtained the complicated vessel distribution and the velocity of several main vessels at different depths in a short time. In the next step, we will optimize the imaging system by using a faster spectrometer, in order to calculate velocity vector of vessels at higher resolution.

9268-97, Session Post

Monitoring blood flow in live mouse with dorsal skin window chamber model by using video-rate two-photon excited fluorescence imaging system

Qi Wang, Xiao Peng, Wei Yan, Bin Yu, Jian Gao, Junle Qu, Hanben Niu, Shenzhen Univ. (China)

Cancer is one of the most deadly diseases of human. Recently, bacterial therapy is becoming a promising method for cancer treatment. Some results indicated that bacteria could specifically target the microenvironment of solid tumor, but the underlying mechanism is still unclear. To clarify the mechanism, the measurement of blood flow in live animals with high spatial resolution and imaging speed is crucial in the study of cancer and development of bacterial vector in cancer therapy. However, there are several challenges for traditional imaging methods to successfully achieve the goals, including limited imaging depth, slow speed and low sensitivity. Here, we propose a high speed two-photon excited fluorescence imaging system with two fluorescence detection channels. Two-photon excitation allows for in situ excitation and high spatial resolution. The long-wavelength excitation also decreased the photo damage to the animal during long term observation. Moreover, we developed a specially designed platform for imaging dorsal skin window chamber of the nude mouse model. By using the entire system, we obtained video rate two-photon excited fluorescence images of blood flow as well as vessel walls of tumors embedded in the window chamber of the nude mouse model. Finally, we detected the changes of velocity of blood flow before and after the bacterial therapy in the tumors of the mouse cancer model. In conclusion, our imaging system can provide useful information for monitoring tumor angiogenesis and drug therapy effects.

9268-98, Session Post

Characterization of secreted proteins in HepG2 and LO2 cells by Raman spectroscopy

Qiuyong Ruan, Fadian Liao, Juqiang Lin, Jinyong Lin, Zufang Huang, Nenrong Liu, Rong Chen, Fujian Normal Univ. (China)

Secreted proteins, the promising source of biomarkers for early detection and diagnosis of cancer, have received considerable attention. Raman spectroscopy and principal component analysis (PCA) were used to characterize the secreted proteins collected from the cell cultures of human hepatoma cell line HepG2 and normal human liver cell line LO2 in this paper. We found the major difference of secreted proteins Raman spectra between HepG2 and LO2 cells were in the range of 1200cm⁻¹-1800cm⁻¹. Compared with LO2 cells, some significant changes based on secondary structure of secreted proteins in HepG2 cells were observed, including the increase in the relative intensity of the band at 1004cm⁻¹, 1445cm⁻¹, 1674cm⁻¹ and the decrease at 1074cm⁻¹. These variations of Raman bands indicated that the species and conformation of secreted proteins in HepG2 cells changed. The measured Raman spectra of the two groups were separated into two distinct clusters with no overlap and high specificity and sensitivity by PCA. These results show that the combination of Raman spectroscopy and PCA analysis may be a powerful tool for distinguishing the secreted proteins between human hepatoma cells and normal human liver cells, provide a new thought to analyze the secreted proteins from cancer cells and find a novel cancer biomarker.

9268-99, Session Post

Optical functional imaging of retina using stimulus-evoked intrinsic optical signals

Yuhong Yang, Shuangyun Shao, Beijing Jiaotong Univ. (China); Bei Tian, Xueqian Guo, Capital Medical Univ. (China)

Intrinsic optical signals (IOSs) detection technology is a noninvasive optical detection method with high temporal resolution and spatial resolution. It can detect the changes of optical signals caused by reflection, scattering and transmission in tissues. Without dying and fluorescently labeled markers on tissues, IOSs detection technology is a promising method to detect retinal function without influence on normal activities of organism. Slow IOSs of retina reflect the activities in inner retina and the middle layer of retina, and fast IOSs of retina stem from activities of inner retina. In this paper, IOSs detection technology was introduced to detect retinal function. An IOSs' detection system was built to detect fast IOSs. The retinal image was captured through a fast CMOS camera. The retina was illuminated by infrared light that was continuously on for the duration of the experiment. The visible light was presented to stimulate the retina. The IOSs changes are small when compared to background illumination. To reveal the optical changes, the system was optimized to improve signal-to-noise ratio and different ICA algorithms was introduced to extract IOSs. The experimental results showed that the detection system is suitable to obtain the morphology and the functional status of retina and IOSs detection technology is an effective and reliable noninvasive method to study changes of function of retina.

9268-100, Session Post

Dual illumination OCT at 1050nm and 840nm for whole eye segment imaging

Shanhui Fan, Shanghai Jiao Tong Univ. School of Medicine (China); Lin Qin, Shanghai Jiao Tong Univ. (China); Cuixia Dai, Shanghai Institute of Technology (China); Chuanqing Zhou, Shanghai Jiao Tong Univ. (China)

We present an improved dual channel dual focus spectral domain optical coherence tomography (SD-OCT) with two illuminations at 840nm and 1050nm for three dimensional (3D) and dynamic full eye imaging from the cornea to retina. By adjusting the divergences of the two probing beams, the light beam of 1050nm was focused at anterior segment for anterior segment imaging while the light beam of 840nm was focused at retina for retinal imaging. In addition, with the implantation of full resolved complex (FRC) method, the imaging depth of anterior segment OCT can be doubled for the whole anterior segment imaging. The two light beams were coupled by a dichroic mirror in the sample arm, which can effectively minimize the loss of sample information. And with optimization of the delivery optics, the scan paths of 1050nm and 840nm light beam can be separated, which can extend the scan range of retina and improve the retinal image quality. The axial resolution for 1050nm and 840nm OCT was 10 μ m and 8 μ m in air, respectively. And the dual illumination approach can avoid the deterioration of transverse resolution when using single beam approach. Finally, we demonstrated the feasibility of this imaging system for simultaneous imaging in vivo of the whole anterior segment (e.g. cornea, limbus, iris, and lens) and retina at unaccommodated and accommodated states in healthy volunteers.

9268-101, Session Post

A denoising module based on the wavelet and empirical mode decomposition for photoacoustic microscopy

Yi Du, Lin Li, Xinyu Chai, Chuanqing Zhou, Shanghai Jiao Tong Univ. (China)

In this research work, we set up a denoising module to improve the imaging result for the photoacoustic microscopy (PAM) by improving the signal noise ratio and spatial resolution. This module contains a series of data processing methods to reduce the noise from the tissues and the machine. And this module is adaptive to different imaging systems and occasions because of these methods' intrinsic characteristics and the parameters those decided according to the data in the process. In this module, firstly data's length is limited because each system has its own imaging depth capacity and data outside this length is noise. And data is filtered in frequency domain with the Wiener adaptive filter according to bandwidth of the imaging system. Secondly the data is presented in time-frequency domain with different time-frequency analysis methods such as Wigner-Ville related methods. With the aid of this presentation in time-frequency domain, we can set down denoising parameters according to the characteristics of this data and this also makes the denoising module adaptive. Thirdly the data is denoised using wavelet and empirical mode decomposition (EMD) methods. These two methods demonstrate strong denoising capacity in the data processing field and are very suitable for data from processing real biological tissues. With decided parameters, wavelet and EMD methods are decided and all the data is denoised automatically to get the best imaging effect instead of processing each data manually with different methods. This

denoising module improves the imaging quality and has adaptive ability to reach the best effect for different PAM imaging occasions.

9268-102, Session Post

OCT imaging enhancement of ovarian cancer using gold and gold/silver nanorods

Yi Wen Shi, Shanghai Jiao Tong Univ. (China); Shanhui Fan, Shanghai Jiao Tong Univ. School of Medicine (China); Shuhui Chen, Xia Jiang, Qingliang Zhao, Daxiang Cui, Chuanqing Zhou, Shanghai Jiao Tong Univ. (China)

For OCT imaging, enhancing contrast efficiency will lead to significant improvements in the detection limits in cancer. Recently, noble metal nanoparticles are considered to be better contrast agents than traditional ones, especially for gold and silver. Silver nanoparticles have more attractive optical properties than gold nanoparticles. But they are employed far less because of its poor chemical stability. In this paper, we introduced our recent progress on a new application of using gold/silver alloy nanoparticles as OCT contrast agents in the detection of ovarian cancer. The scattering properties and sensitivity of silver were investigated. By means of tuning LSPR wavelengths of the nanoparticles, they were able to match the central wavelength of light used in OCT. The cytotoxicity of these materials were also studied with the MTT assay. Before carrying out animal experiments, we conducted a number of studies to analysis the different performances of alloy nanoparticles and gold nanorods in vitro. It has been sufficiently demonstrated that the alloy nanoparticles revealed stronger OCT signals than gold nanorods because of the better scattering properties. Then we moved on to animal experiments. We directly compared the contrast enhancement of gold/silver alloy nanoparticles and gold nanorods. Furthermore, the signal to noise ratio (SNR) of these two materials were also measured. Details of the different scattering properties of these two materials were discussed. This study contributes a new kind of contrast agent in OCT imaging, which has a profound effect on drug delivery and further therapeutic action.

9268-103, Session Post

Photoacoustic signal simulation and detection optimization based on laser-scanning optical-resolution photoacoustic microscopy

Lin Li, Yi Du, Qingliang Zhao, Qian Li, Xinyu Chai, Chuanqing Zhou, Shanghai Jiao Tong Univ. (China)

Laser-scanning optical-resolution photoacoustic microscopy (LSOR-PAM) has higher scanning speed than other mechanical scanning photoacoustic systems with a 2-D galvanometer scanner and stationary unfocused ultrasonic transducer, which is important for clinical applications, especially for ophthalmology. The refraction and attenuation of laser generated photoacoustic signal in different tissue mediums and coupling agents can cause inhomogeneous signal strength and direction distribution, therefore, the transducer characteristics and position decide the efficiency and field of view (FOV) of photoacoustic signal detection. In this study, we simulate the photoacoustic signal generation, propagation and detection in compound medium models with different tissue parameters using k-space method

based on LSOR-PAM imaging principle. The results shows a clear distance related signal strength attenuation because of the wave diffusion and tissue attenuation coefficient. According to tissues and water acoustic impedance, the energy transitivity reduce quickly when signal incidence angle is large, which means the transducer tilted a large angle with vertical direction of the sample will detect much weaker signal, but a larger angle may provide bigger FOV of the scanning area due to the distance chances between transducer and acoustic source and signal wave contacts with the transducer surface. Our study provide a method for photoacoustic signal detection optimization for different tissue medium condition based on LSOR-PAM, which is beneficial for PAM imaging optimization of fundus and other complex tissue structure.

9268-24, Session 5

Noninvasive monitoring of circulating melanoma cells by photoacoustic flow cytometry (*Invited Paper*)

Xunbin Wei, Shanghai Jiao Tong Univ (China)

Melanoma, a malignant tumor of melanocytes, is the most serious type of skin cancer in the world. It accounts for about 80% of deaths of all skin cancer. For cancer detection, circulating tumor cells (CTCs) serve as a marker for metastasis development, cancer recurrence, and therapeutic efficacy. Melanoma tumor cells have high content of melanin, which has high light absorption and can serve as endogenous biomarker for CTC detection without labeling. Here, we have developed an in vivo photoacoustic flow cytometry (PAFC) to monitor the metastatic process of melanoma cancer by counting CTCs of melanoma tumor bearing mice in vivo. To test in vivo PAFC's capability of detecting melanoma cancer, we have constructed a melanoma tumor model by subcutaneous inoculation of highly metastatic murine melanoma cancer cells, B16F10. In order to effectively distinguish the targeting PA signals from background noise, we have used the algorithm of Wavelet denoising method to reduce the background noise. The in vivo flow cytometry (IVFC) has shown a great potential for detecting circulating tumor cells quantitatively in the blood stream. Compared with fluorescence-based in vivo flow cytometry (IVFC), PAFC technique can be used for in vivo, label-free, and noninvasive detection of circulating tumor cells (CTCs).

9268-25, Session 5

Characterizing the microstructure of living cells and tissues using Mueller matrix polarimetry (*Invited Paper*)

Hui Ma, Shenzhen Key Laboratory of Minimally Invasive Medical Technology, Tsinghua University, (China)

It has been demonstrated in many recent publications that polarization imaging is potentially a powerful tool for biological studies and clinical diagnosis. Since the scattered polarized photons carry rich information on the size, shape and density of the scatterers and the optical properties of both the scatterers and their ambient media, polarization imaging allow detailed quantitative characterization of the micro- and macro- structure, as well as the optical properties of the non stained living cells and tissues. A Mueller matrix transforms the polarization states between the incident and the scattering lights and provides a comprehensive characterization of the polarization properties of the sample. However, it is often not convenient to use the

Mueller matrix in actual applications. A Muller matrix element may contain contributions due to various polarization-sensitive processes and often does not exhibit explicit connections to the structural features of the sample.

In this report, we demonstrate our recent efforts to disentangle the structural information encoded in the Mueller matrix elements. We carried on Monte Carlo simulations using an extended sphere-cylinder scattering model which approximates the complicated anisotropic biological samples to solid spheres and infinitely long cylinders embedded in an ambient medium. By varying the parameters of both the scatterers and the ambient medium, we are able to examine in detail the connections between these structural parameters and the Mueller matrix elements. We also propose different Mueller matrix transformation techniques to obtain sets of new polarization parameters which are functions of the Mueller matrix elements but respond explicitly to different parameters of the scatterers and the ambient medium in the scattering model. The validity of both the scattering model and the Mueller matrix transformation techniques are supported by experiments on phantoms of very simple structure and on different types of biological tissues, such as skeletal muscle, skin, fat and liver tissues. .

9268-26, Session 5

Tissue optical clearing window for blood flow monitoring (*Invited Paper*)

Dan Zhu, Huazhong Univ. of Science and Technology (China)

The tissue optical clearing (TOC) technique could significantly improve the biomedical optical imaging depth, but most current investigations are limited to in vitro studies. For in vivo applications, the TOC method must provide a rapid treatment process, sufficient transparency, and safety for animals, which makes it more difficult. Recently developed innovative optical clearing methods for in vivo use show great potential for enhancing the contrast and resolution of laser speckle contrast imaging (LSCI) for blood flow monitoring. This paper gives an overview of recent progress in the use of TOC for vascular visualization with LSCI. First, the principle of TOC-induced improvement of LSCI and a quantitative analysis method for evaluating the improvement are described briefly. Second, the paper introduces transparent windows, including various skin windows and a cranial window, that permit LSCI to monitor dermal or cortical blood flow, respectively, with high resolution and contrast. Third, preliminary investigations of the safety of TOC demonstrate that the transparent skin window is switchable, which enables LSCI to repeatedly image blood flow. However, research on in vivo TOC is currently less advanced than that on in vitro TOC. Future work should focus on developing a highly effective, safe method and extending its applications

9268-27, Session 5

Venule vasoconstriction correlated with local singlet oxygen generation during vascular targeted photodynamic therapy (*Invited Paper*)

Buhong Li, Lisheng Lin, Fujian Normal Univ. (China); Defu Chen, Chinese PLA General Hospital (China); Yirong Li, Fujian Normal Univ. (China); Ying Gu, Chinese PLA General Hospital (China)

We have recently developed a novel configuration of near-infrared sensitive InGaAs camera that enables directly image

the singlet oxygen luminescence generated in blood vessels in a dorsal skinfold window chamber model in vivo during vascular targeted photodynamic therapy (V-PDT). In this study, the diameters and blood flow of blood vessels before and immediately after V-PDT and 20, 40 and 60 mins thereafter were quantitatively monitored using a white-light microscope, and the vasoconstriction of venules was correlated to the local singlet oxygen generation, which can be directly determined from the recorded singlet oxygen luminescence images. The obtained data show that the arterioles completely constricted, while more than 50% venules with a significant constriction after V-PDT. Furthermore, the vasoconstriction of venules in specific regions of interest (ROIs) within treated area strongly correlated with the local singlet oxygen generation. Our data suggest that the singlet oxygen luminescence based dosimetry is effective for evaluating V-PDT.

9268-28, Session 5

Hybrid-modality high-resolution Imaging: for diagnostic biomedical imaging and sensing for disease diagnosis

Vadakke M. Murukeshan, Lim Hoong Ta, Nanyang Technological Univ. (Singapore)

Biomedical optics which is an interdisciplinary branch of science and technology uses optics for improving the basic understanding of biological processes, enhancing the diagnostic efficiency and treatment of human diseases. From this perspective, medical diagnostics in the recent past has seen the challenging trend to come up with dual and multi modality imaging for implementing better diagnostic procedures. The changes in tissues in the early disease stages are often subtle and can occur beneath the tissue surface. In most of the cases, conventional types of medical imaging may not be able to detect these changes easily. Each imaging modality has its own advantages and limitations and one cannot fit one single modality for all diagnostic applications. Therefore the need for a multi or hybrid modality imaging arises.

Combining more than one imaging modality overcomes the limitation of individual imaging method and integrates the respective advantages into a single setting. This paper in this context will be focusing on the research and development of a multi modal imaging platform combining optical and photoacoustic imaging modalities for disease diagnosis in colon and eye. Photoacoustic imaging is used as the second modality as it can offer deeper penetration depth compared to optical imaging. The optical engineering and research challenges in developing the multi modality platform will be discussed followed by initial results validating the proposed scheme. The proposed scheme offer high spatial and spectral resolution imaging and is expected to offer potential biomedical imaging solutions.

The authors acknowledge the financial support received through A*STAR-SERC 1121480003 and COLE-EDB funding.

9268-29, Session 5

Mapping the microvascular and the associated absolute values of oxy-hemoglobin concentration through turbid media via local off-set diffuse optical imaging

Chen Chen, Lehrstuhl für Photonische Technologien (Germany)

Imaging resolution of diffuse optical imaging (DOI) could hardly achieve that of a similar functional system like spectroscopic

OCT. In this work, we delivered a new approach of local off-set DOI with the emphasis on resolving micron-scale targets and evaluating the absolute values of oxy-hemoglobin concentration through turbid media. Principally, the local off-set should overturn the boundary conditions of the modified Beer-Lambert Law. Experimental results have confirmed the feasibility of address both two challenges. Prospectively, it could be utilized to map the microvascular and associated oximetry under an in-vivo skin, and ultimately to monitor a tumor progression in skin.

9268-31, Session 5

Diffraction tomographic phase microscopy

Peng Xiu, Xin Zhou, Cuifang Kuang, Xu Liu, Zhejiang Univ. (China)

3D refractive index distribution of cell samples is important information to describe the live state of the cells. Traditionally we use interference microscope to observe the refractive index of samples and we can only acquire an average result along the illumination angle. To overcome this gap, tomographic phase microscopy proposes a new method to observe the 3D refractive index distribution by detecting the phase images at different angles and reconstructing the 3D image by Radon algorithm. The working principle of tomographic phase microscopy[1] (TPM) is just like the CT technology, but the light at 633nm can't go through the sample along a district line like X-ray, even if the sample are immersed in liquid whose refractive index is nearly equal to the sample[2]. Moreover, when light goes through sample, diffraction can't be avoid, which lead to the phase images consist of the information of diffraction light and the transmission light which may affect each other.

Here, we demonstrate for the first time that diffraction tomographic phase microscopy (DTMP) can be used to improve the quality of 3D refractive index image. At one illumination angle, we change the focal plane of objective lens between the top and the bottom of the sample and we can get two phase images which record common transmission light phase but different diffraction light phase. Then we make a difference between the two images and we will acquire the phase information introduced by the sample between the top and bottom planes. When the illumination angle changes, we can get the right phase information of the sample between two fixed focal planes at different angle, as a result the resolution and signal to noise rate of the 3D refractive index image we reconstruct are higher than the traditional TPM. Our findings further enhance the performance of TPM microscopy and widen its applications in scientific researches.

9268-33, Session 5

Multifunctional superparamagnetic nanoshells: combing two-photon luminescence imaging, surface-enhanced Raman scattering, and magnetic separation

Xiulong Jin, Ni Kong, Haiyan Li, Jian Ye, Shanghai Jiao Tong Univ. (China)

Core-shell nanoparticles offer a unique platform to combine multifunctions in a single particle, which shows great potential in biomedical field. In this work, we will present a new kind of multifunctional superparamagnetic nanoshells (Fe₃O₄@SiO₂@Au), which were composed of a core of iron oxide

(Fe₃O₄) cluster, a thin shell of Au and a silica (SiO₂) layer in between. The obtained multifunctional nanoparticles exhibiting superparamagnetic and plasmonic optical properties can simultaneously be employed for two-photon luminescence (TPL) imaging, surface-enhanced Raman scattering (SERS) and magnetic separation. We have also used extensive characterization tools and simulation method including transmission electron microscopy (TEM), zeta-potential measurement, superconducting Quantum Interference Device (SQUID) magnetometer, UV-Vis spectrometer, and finite difference time domain (FDTD) simulation method to well investigate their morphology, magnetic and optical properties. In addition, the Fe₃O₄@SiO₂@Au nanoparticles may have potential applications such as the enhanced MRI imaging and photothermotherapy.

9268-34, Session 6

Multi-modality super-resolution optical microscopy (*Invited Paper*)

Peng Xi, Xusan Yang, Zhiping Zeng, Xuanze Chen, Peking Univ. (China); Yujia Liu, Macquarie Univ. (Australia); Hao Xie, Peking Univ. (China)

Optical microscopy has been routinely applied to explore a vast variety of biological phenomena in life sciences. However, conventional optical microscopy has met grand challenges in discerning fine structures inside biological cells due to the resolution barrier bestowed by optical diffraction, which hinders the optical microscopy to reveal fine details below 200nm. The typical feature size of sub-cellular organelles is around several to several tens of nanometers.

In the past decades, a series of super-resolution optical microscopy techniques have been invented. Based on the mechanism of surpassing the resolution barrier, they can be categorized into two: (1) targeted modulation, such as stimulated emission depletion microscopy (STED),¹ reversible optically linear fluorescence transitions microscopy (RESOLFT),² saturated structured illumination microscopy (SSIM),³ or (2) randomized blinking/fluctuation modulation, such as photoactivated localization microscopy (PALM) and stochastic optical reconstruction microscopy (STORM),^{4,5} Super-resolution Optical Fluctuation Imaging (SOFI) ⁶⁻⁸, etc. Here we present several key progress on our study with super-resolution, such as the comparison with STED and SIM in the imaging of organic fluorophore⁹ and fluorescent nanodiamonds¹⁰, PALM/SOFI imaging of photoswitchable fluorescent protein and quantum dots, etc.

1 Hell, S. W. & Wichmann, J. Breaking the diffraction resolution limit by stimulated emission: stimulated-emission-depletion fluorescence microscopy. *Optics letters* 19, 780-782 (1994).

2 Grotjohann, T. et al. Diffraction-unlimited all-optical imaging and writing with a photochromic GFP. *Nature* 478, 204-208 (2011).

3 Gustafsson, M. G. Nonlinear structured-illumination microscopy: wide-field fluorescence imaging with theoretically unlimited resolution. *Proceedings of the National Academy of Sciences of the United States of America* 102, 13081-13086 (2005).

4 Shroff, H., Galbraith, C. G., Galbraith, J. A. & Betzig, E. Live-cell photoactivated localization microscopy of nanoscale adhesion dynamics. *Nature Methods* 5, 417-423 (2008).

5 Rust, M. J., Bates, M. & Zhuang, X. Sub-diffraction-limit imaging by stochastic optical reconstruction microscopy (STORM). *Nature methods* 3, 793-796 (2006).

6 Dertinger, T., Colyer, R., Iyer, G., Weiss, S. & Enderlein, J. Fast, background-free, 3D super-resolution optical fluctuation imaging (SOFI). *Proceedings of the National Academy of Sciences* 106, 22287-22292 (2009).

7 Dertinger, T. et al. in *Nano-Biotechnology for Biomedical and Diagnostic Research* 17-21 (Springer, 2012).

8 Geissbuehler, S., Dellagiacomma, C. & Lasser, T. Comparison between SOFI and STORM. *Biomedical optics express* 2, 408-420 (2011).

9 Liu, Y. et al. Achieving $\lambda/10$ Resolution CW STED Nanoscopy with a Ti: Sapphire Oscillator. *PLoS One* 7, e40003 (2012).

10 Yang, X. et al. Sub-diffraction imaging of nitrogen-vacancy centers in diamond by stimulated emission depletion and structured illumination. *RSC Advances* 4, 11305-11310, doi:10.1039/C3RA47240J (2014).

9268-35, Session 6

Dynamic fluorescence lifetime imaging of liver cell apoptosis (*Invited Paper*)

Junle Qu, Wei Yan, Xiao Peng, Jing Qi, Shenzhen Univ. (China)

In last ten years, two-photon excited fluorescence lifetime imaging (FLIM) has become a powerful tool in biology and biomedical studies. Till now, most of the FLIM imaging systems employ galvo-mirrors to scan the laser spot across the biological samples, which has limited the imaging speed. This method does not allow for fast functional event detection in live biological samples. Here, we report a dynamic fluorescence lifetime imaging system that is based on a pair of acousto-optic deflectors (AOD) for the random regions of interest study in the sample. In our experiment we used dye Rhodamine-6G to stain liver cancer HepG2 cells. then we used TNF-alpha to induce apoptosis in HepG2 cells and recorded the change of fluorescence lifetime of Rhodamine-6G. We found that the fluorescence lifetime of Rhodamine-6G in the HepG2 cells increased during cell apoptosis. The experimental result demonstrated that our system can dynamically monitor the changing process of the regions of interest in live biology samples, and Rhodamine-6G is a promising probe for monitoring apoptosis in live cancer cells.

9268-36, Session 6

Multimodal imaging with multiphoton microscopy and optical coherence tomography (*Invited Paper*)

Shuo Tang, Tom Lai, The Univ. of British Columbia (Canada)

Multiphoton microscopy (MPM) and optical coherence tomography (OCT) are two important and complementary imaging techniques. By combining them together, we can develop a powerful system which can take the advantages of both techniques while compensate for their individual limitations. Multiple contrasts can be acquired, such as the two-photon excited fluorescence (TPEF) and second harmonic generation (SHG) contrasts determined by the biochemical compositions, and the scattering contrast from changes of refractive index; Large field-of-view (FOV) and high resolution can both be achieved, where OCT can scan over a large FOV at fast speed while MPM can provide cellular level high-resolution imaging.

We have developed a multimodal MPM/OCT system which can acquire co-registered MPM and OCT images. The OCT modality can acquire cross-sectional images of layered tissue structures over several millimeters in lateral and ~1mm in axial at 100 frames-per-second. The MPM modality can provide a high-resolution

of 0.5 μ m in lateral and 2 μ m in axial. With the multimodal MPM/OCT, a fast screening with the OCT can be performed to find abnormal tissue regions, and the MPM can then be applied to examine the identified regions for more detailed analysis based on the cellular and extracellular matrix structures. The multimodal MPM/OCT has been applied to image cornea and other tissues. Detailed structure of corneal layers and quantitative information of its thickness and refractive index are obtained. The multimodal MPM/OCT is demonstrated to be an important tool for label-free imaging which can obtain a sufficient set of parameters for reliable tissue analysis.

9268-37, Session 6

Wide field-of-view microscopy using compressive sensing

Jie Wang, Jigang Wu, Shanghai Jiao Tong Univ. (China)

In conventional microscope, resolution and field of view are often a trade-off, i.e., better resolution generally implies more limited field of view. Focus-grid-based wide field-of-view microscope has been developed to break this trade-off, where a two-dimensional focus grid is used to scan the sample while the transmission of each focus through the sample is recorded during the scanning and then used to reconstruct the transmission image of the sample according to the scanning pattern. The imaging resolution and field of view will be determined by the focal spot size and the focus grid area along with the scanning mechanism independently, thus break the abovementioned trade-off.

In the wide field-of-view microscopy, the whole sample area has to be scanned with at least Nyquist-frequency sampling in order to reconstruct the image. In order to reduce the acquisition data, we propose a novel scanning mechanism using compressive sensing (CS). Many research have demonstrated that CS can be used successfully with normal biological images because of its sparsity in carefully chosen transform domains. Compared with the two-dimensional focus-grid scanning, we propose to use less focal spots randomly to linearly scan the sample where the scanning lines cover only a portion of the sample. The image of the sample is then reconstructed in wavelet domain using the principle of CS. Our preliminary studies show that 75% of scanning lines is enough to reconstruct a decent image. Thus we can reduce the acquisition data which allow for simpler scanning mechanism and data acquisition.

9268-38, Session 6

Methods for super-resolution imaging based on PSF engineering

Yue Fang, Cuifang Kuang, Xu Liu, Zhejiang Univ. (China)

Confocal laser scanning microscopy was first promoted to eliminate the effects caused by scattering light in the detection of samples, but its attainable resolution is still within the diffraction limit. Several attempts have been made to break the diffraction limit by reducing the size of the point spread function (PSF) of the system, the so-called point-spread-function (PSF) engineering method.

Stimulated Emission Depletion (STED) microscopy uses two overlapping synchronized laser beams of which the excitation beam's PSF was sharpened by the de-excitation beam's PSF which has a doughnut-shaped pattern. Based on STED and the concept of fluorophores' lifetime, time-gated STED (g-STED) microscopy has been proposed by collecting photons after detection delay in STED microscopy. The subtractive imaging technique is another effective method to achieve resolution and contrast enhancement based on PSF engineering. Through properly shaping the PSF by subtraction, the subtractive PSF has been demonstrated sharpened, while better resolution and

SNR can be obtained in the subtractive image with a proper subtractive parameter.

We examine the optical principles of PSF engineering, and make detailed statements on how each method enables super-resolution using these principles. Giving a comparison among these methods, we summarize major advances and weak points of each method. In addition, we discuss the influence of the subtractive parameter on resolving ability in different subtractive methods. Biological applications and promising new developments have also been emphasized.

9268-39, Session 6

Measurement of refractive index distribution of biotissue by scanning focused refractive index microscopy

Tengqian Sun, Qing Ye, Xiao Wan Wang, Jin Wang, Zhi-Chao Deng, Jian-Chun Mei, Wen-Yuan Zhou, Chun-Ping Zhang, Jianguo Tian, Nankai Univ. (China)

A novel scanning focused refractive-index microscopy (SFRIM) technique is presented. With a focused laser serves as the light source, we combine the derivative total reflection method (DTRM), microscopy and the scanning technique together to obtain the refractive-index profiles (RIP) of objects. The refractive index (RI) accuracy is 0.002. The central spatial resolution of SFRIM achieves 1 μ m, smaller than the size of the focal spot. Results of measurements carried out on cedar oil and a gradient-refractive-index (GRIN) lens agree well with theoretical expectations, thereby verifying the accuracy of SFRIM. Refractive index distributions of biotissue are measured by this microscopy. The use of SFRIM opens up possibilities for RIP measurement in many applications, including optical waveguides, photosensitive materials and devices, the study of the photorefractive effect, and RI imaging in biomedical fields.

9268-40, Session 7

Multi-scale functional and molecular photoacoustic imaging in vivo (Invited Paper)

Liang Song, Shenzhen Institute of Advanced Technology (China)

While super-resolution imaging has broken through the optical diffraction limit to enable our visualization of the sub-cellular world in live cells, photoacoustic imaging has broken through the optical diffusion limit to allow us seeing intact biological tissue in vivo at an unprecedented depth (up to several cm) with rich optical contrasts. As a result, photoacoustic imaging can provide anatomic, functional, and molecular information on biological tissue at multiple scales from organelles to organs. In this talk, we will present our development of acoustic- and optical-resolution photoacoustic microscopy and endoscopy technologies that can offer multi-scale molecular and functional information about intact biological tissue. In conjunction with optically absorbing molecular probes, acoustic-resolution photoacoustic microscopy can penetrate deep to provide a macroscopic view of the disease status. On the other hand, their optical-resolution counter-part can offer optical-diffraction limited spatial resolution to visualize microscopic vascular functional changes using endogenous contrast. Example applications of the developed technologies in molecular and functional imaging of cancer and atherosclerotic plaques will be discussed.

9268-41, Session 7

High-resolution dual-modality ocular imaging (*Invited Paper*)

Changhui Li, Peking Univ. (China)

We developed a prototype dual-modal ocular imaging system integrating photoacoustic and ultrasound imaging modalities. This system successfully imaged the murine eyes in vivo, including iris, retina, retinal pigment epithelium, and choroid. Our results demonstrated that this system has a great potential in the diagnosis of human's various ocular diseases.

9268-42, Session 7

Optical coherence tomography imaging of microfluidic pattern with different refractive index contrast

Zhixiong Hu, National Institute of Metrology (China)

Optical coherence tomography (OCT) technology is analogous to ultrasound imaging, except that OCT employs light instead of sound. The non-invasive imaging method works by projecting light on test target and detecting the backscattering from the underlying layers. As the OCT technology is based on optical interference, the internal structural features and inhomogeneities induced by different refractive index contrast could be detected and displayed in the form of a gray scale or false color image. In this paper, a microfluidic device with internal micro-fabricated pattern including resolution test bars was produced and measured by a spectral domain OCT instrument. The internal dimensions of the lab-on-chip device were determined using the OCT imaging technology and were in agreement with results obtained with conventional microscope and surface profiler. In order to study the effect of different refractive index contrast on OCT imaging, fluid with various refractive indexes was injected into the microfluidic channel respectively, and the acquired OCT images of the internal microfluidic pattern were analyzed. The results demonstrate that optical coherence tomography could be used as a new metrology tool to determine the internal channel dimensions of lab-on-chip devices. Furthermore, the experiment results reveal the relations between the refractive index contrast and OCT image quality.

Thursday - Saturday 9 -11 October 2014

Part of Proceedings of SPIE Vol. 9269 Quantum and Nonlinear Optics III

9269-1, Session 1

Measurement-based noiseless linear amplification for quantum communication *(Invited Paper)*

Ping Koy Lam, The Australian National Univ. (Australia)

Entanglement distillation is an indispensable ingredient in extended quantum communication networks. Distillation protocols are necessarily non-deterministic and require advanced experimental techniques such as noiseless amplification. Recently it was shown that the benefits of noiseless amplification could be extracted by performing a post-selective filtering of the measurement record to improve the performance of quantum key distribution. We apply this protocol to entanglement degraded by transmission loss of up to the equivalent of 100km of optical fibre. We measure an effective entangled resource stronger than that achievable by even a maximally entangled resource passively transmitted through the same channel. We also provide a proof-of-principle demonstration of secret key extraction from an otherwise insecure regime. The measurement-based noiseless linear amplifier offers two advantages over its physical counterpart: ease of implementation and near optimal probability of success. It should provide an effective and versatile tool for a broad class of entanglement-based quantum communication protocols.

9269-2, Session 1

Quantum theory of optical sensing: estimation, control, and fundamental limits *(Invited Paper)*

Mankei Tsang, National Univ. of Singapore (Singapore)

Following the seminal work by Helstrom on quantum detection and estimation theory, we have discovered fundamental quantum limits to the detection and estimation of time-varying waveforms using dynamical systems, such as optomechanical force sensors and magnetometers. These limits, in the form of Helstrom bound, quantum Cramer-Rao bound, and quantum Ziv-Zakai bound, generalize well known inequalities in classical statistics and were applied to quantum dynamical systems for the first time to our knowledge. We have also invented quantum noise cancellation and optimal signal processing techniques useful for the attainment of such limits and, in collaboration with experimentalists at the University of Tokyo, performed a quantum optics experiment that demonstrates waveform estimation near the quantum Cramer-Rao bound.

9269-3, Session 1

Quantum secure direct communication on-site detection of eavesdropper and obliteration of information leakage before eavesdropping detection *(Invited Paper)*

Gui Lu Long, Tsinghua Univ. (China)

Classical cryptography does not have the capability of on-site detection of eavesdropper, nor obliteration of information leakage before eavesdropping detection. There have been many great lessons in history where big loss or even defeat was resulted from ignorance of breaking of secret codes.

Quantum communication has the capability of on-site detection of eavesdropper. Quantum key distribution detects eavesdropper

on-site by inspecting the error rate from channel sampling. It cannot obliterate information leakage during the sampling process, hence can only distribute random keys. The legal users communicate random numbers in quantum key distribution. If no eavesdropper is found, the communicated random numbers will be used as keys after some post-processing. If eavesdropping is found, they will abandon the transmitted data. In this way, they can guarantee eavesdropper does not have any information about the key, and hence the secret information in latter communications of transmitted messages.

Started from 2000, quantum secure direct communication has become a hot area of research in quantum communication. It can not only detect eavesdropper on-site, but also obliterate information leakage during the sampling process. Hence it can communicate secret messages directly. In addition, it can carry out tasks that cannot be completed by quantum key distribution, for instance, quantum voting, and quantum bidding and so on. It is also compatible with future all-quantum network technology.

In this invited talk, the brief history, the principles, and several pioneering protocols and future perspective will be presented.

9269-4, Session 1

Single-photon-level quantum image memory based on cold atomic ensembles

Dongsheng Ding, Univ. of Science and Technology of China (China); Zhi-yuan Zhou, Bao-Sen Shi, Guang-Can Guo, university of science and technology of China (China)

The abilities of storing single photons are now being actively explored due to its more important application of quantum networks. Encoding photon with orbital angular momentum state (OAM) significantly increases their information-carrying capability and network capacity. Constructing such quantum memories operating in OAM state is interesting and a challenge thing. Via electromagnetically induced transparency memory method, the first experiment storing a true single photon carrying orbital angular momentum (OAM) in a cold atomic ensemble is demonstrated. The non-classical pair correlation between trigger photon and retrieved photon is retained, and the spatial structure of input and retrieved photons exhibits strong similarity. More importantly, the coherence of single-photon is preserved during storage. The ability to store spatial structure at the single-photon-level is a key step towards building high-dimensional quantum networks.

9269-5, Session 2

Loss tolerance and verification in remote entanglement sharing *(Invited Paper)*

Geoff J. Pryde, Griffith Univ. (Australia)

Photons provide an excellent means of sharing entanglement between remote parties. In order to use this entanglement for quantum information science and technology, it is necessary to overcome the adverse affects of loss and also to be able to verify entanglement in communications or network scenarios. We investigated several techniques to address these issues.

The existence of strong nonlocal correlations between distant parties can be tested without trusting the measurement devices used, or the parties themselves. This leads to device-independent unconditionally secure quantum information tasks, but requires loophole-free Bell inequality violations, with their challenging requirements on detection and transmission efficiency. An easier test, EPR-steering, can tolerate high losses, but requires complete

trust in one party and their equipment. We have demonstrated how to overcome this limitation in using EPR-steering for device-independent entanglement verification.

We also investigated other methods to combat loss in remote entanglement sharing. We experimentally demonstrated how noiseless-amplification-type techniques can be used to improve the transmission of a quantum channel. Together with mode teleportation or entanglement swapping, the channel can be used to transmit information or share correlations.

One might imagine that the nonlocal effects observed in entanglement swapping experiments are somehow stronger than those generated in usual Bell tests, because of the initial independent and uncorrelated nature of the particles that ultimately become entangled. Other experimental work in our lab tests this "bilocal" proposition by comparing nonlocal effects generated in entanglement swapping experiments with those generated in tests of Bell's inequality.

9269-6, Session 2

Quantum computing using spins and photons (*Invited Paper*)

Chaoyang Lu, Jian-Wei Pan, Univ. of Science and Technology of China (China)

Single-photon sources based on semiconductor quantum dots offer distinct advantages for quantum information, including a scalable solid-state platform, ultrabrightness and interconnectivity with matter qubits. A key prerequisite for their use in optical quantum computing [1] and solid-state quantum networks is a high level of efficiency and indistinguishability. In this talk, I will describe our recent experiments on generating pulsed single photons from single quantum dots under true s-shell excitation [2]. Pi pulse-excited resonance fluorescence photons show a vanishing (~1%) two-photon emission probability and a Hong-Ou-Mandel interference visibility of ~97%, which were used to demonstrate high-fidelity quantum controlled-NOT gate. Then I will describe methods of robust generation of single photons using adiabatic rapid passage [3], and creation of bandwidth-tunable single photons from spin-flip Raman transitions, and high-visibility (~87%) quantum interference between single photons from two coherently pulsed driven quantum dots at a distance [4]. Finally, I will discuss our more recent results of generating Greenberger-Horne-Zeilinger-type spin-photon entanglement [5] and quantum state transfer between single photons and single spins [6].

References:

- [1] Pan et al. Rev. Mod. Phys 84, 777 (2012); Cai et al. Phys. Rev. Lett. 110, 230501 (2013).
- [2] He et al. Nature Nanotechnology 8, 213 (2013).
- [3] Wei et al. submitted
- [4] He et al. Phys. Rev. Lett. 111, 237403 (2013)
- [5,6] He et al. Manuscript submitted (2013).

9269-7, Session 2

Heralded optical quantum states and their storage in optical cavities (*Invited Paper*)

Jun-ichi Yoshikawa, Kenzo Makino, Yosuke Hashimoto, Akira Furusawa, The Univ. of Tokyo (Japan)

Highly nonclassical optical quantum states, characterized by a negative Wigner function, have been so far created probabilistically with heralded schemes. The usability of the probabilistic states will be greatly improved if we could store them until they are required. We recently succeeded

in such an experiment for a heralded single photon state by using a concatenated cavity system. Two optical cavities are concatenated, where one is a memory cavity to store a quantum state inside, and the other, placed at the output of the memory cavity, is a shutter cavity to control the release from the memory cavity. Photons in the memory cavity are rapidly ejected only when the resonance of the shutter cavity is tuned to the frequency of the photons, and otherwise stored inside. Therefore, when quantum entanglement is created and shared between two frequency modes inside the memory cavity by parametric down conversion, it is possible to eject one mode promptly while keeping the other mode. A projective measurement by a photon detector on the ejected mode results in probabilistic and heralded shrinkage at the stored mode into a single photon state through the quantum correlation. Once a quantum state is successfully created and stored in such a way inside the memory cavity, it can be released on demand by quickly shifting the resonance of the shutter cavity. In the talk, we will present this experiment, and other related experiments using heralded quantum states.

9269-8, Session 2

The classification of quantum symmetric-key encryption protocols

Chong Xiang, China Information Technology Security Evaluation Ctr. (China); Li Yang, Institute of Information Engineering (China) and Data Assurance and Communication Security Ctr. (China); Peng Yong, Dongqing Chen, China Information Technology Security Evaluation Ctr. (China)

The classification of the quantum private key encryption protocol is presented. According to whether five elements of a quantum private key encryption protocol: plaintext, ciphertext, key, encryption algorithm and decryption algorithm are quantum ones, there are 32 different kinds of combination. Among them, 5 kinds of protocols have already been constructed and studied, and 21 kinds of them are impossible to be built, the last 6 kinds of them are not constructed efficiently yet.

In our work, the examples of the 5 feasible protocols will be given, the classical private key encryption is one of them. It is pointed out that while using the quantum key to construct the protocol, the shared private key is always an entangled state instead of two quantum states which are in the same states, this is different from the classical situation, so it is hard to extend a quantum protocol to be a multi-protocol. Then it is shown that 21 kinds of protocols are impossible to be constructed with the basic characteristics of quantum mechanics. The last 6 kinds of them can be built extend from the 5 feasible ones, but they are also said to be inefficient ones, because these extensions will reduce the efficiency of the encryption and give no advantage. So they can be built somehow, but there is no efficient one exists.

9269-9, Session 3

Photonic interferometer with quantum correlation (*Invited Paper*)

Florian Hudelist, Jia Kong, Cunjin Liu, Jietai Jing, East China Normal Univ. (China); Zeyu J. Ou, Indiana Univ.-Purdue Univ. Indianapolis (United States); Weiping Zhang, East China Normal Univ. (China)

Traditional interferometers usually consist of beam splitters for wave splitting and recombination.

These interferometers are widely used for precision measurement. Their sensitivity for phase measurement is limited

by the shot noise, which can be suppressed with squeezed states of light.

Here, we study a new type of interferometer in which the beam splitting and recombination elements are parametric amplifiers which generate the quantum correlation of photons in the beams. We observe an improvement of 4.1 ± 0.3 dB in signal-to-noise ratio due to the photon correlation compared to a traditional interferometer under the same operating condition, which is 1.6 times enhancement in rms phase measurement sensitivity beyond the shot noise limit. Combined with squeezed state technique for shot noise suppression, this interferometer promises further improvement in sensitivity. Furthermore, because nonlinear processes are used in this interferometer, we can couple a variety of different waves and form new types of hybrid interferometers, opening a door for many applications in metrology.

9269-10, Session 3

Current development of experimental investigation of squeezed light and its applications (*Invited Paper*)

Genta Masada, Tamagawa Univ. (Japan)

Squeezed light is a nonclassical state of the electro-magnetic field and has noise suppressed below the standard quantum limit in one quadrature component while increased in the other. One of the important applications of squeezed lights is quantum enhanced sensing such as gravitational wave detector with ultimate resolution. Another important application is continuous variables quantum teleportation which utilizes two mode squeezed lights as an essential resource for quantum entanglement. Finally we are interested in quantum radar as a novel application of two mode squeezed lights, for example, quantum illumination. In these applications the final outcome is limited by squeezing level. So it is important to generate highly squeezed light.

Experimental investigation of squeezed light began in the 1980s. Over the past few decades a considerable number of the experiments have been performed to generate highly squeezed lights. One of the successful methods is utilization of a sub-threshold optical parametric oscillator (OPO) which includes a nonlinear optical crystal for the second order nonlinear interaction. We will introduce current experimental results utilizing an OPO with a bow-tie configuration and show that improvements of optical losses and nonlinearity of the crystal are important factors to generate highly squeezed lights.

A simple method to generate two mode squeezed lights is combining two independent squeezed lights by using a beam splitter with the relative phase of 90 degrees between each optical field. We will also introduce recent experimental realization of generation of two mode squeezed lights and verification of quantum entanglement by utilizing a photonic chip.

9269-11, Session 3

Multiplexing continuous-variable quantum information in optics (*Invited Paper*)

Seiji Armstrong, The Australian National Univ. (Australia) and The Univ. of Tokyo (Japan); Meng Wang, Peking Univ. (China); Run Yan Teh, Swinburne Univ. of Technology (Australia); Qihuang Gong, Qiongyi He, Peking Univ. (China); Jiri Janousek, Hans A. Bachor, The Australian National Univ. (Australia); Margaret D. Reid, Swinburne Univ. of Technology (Australia); Ping Koy Lam, The Australian National Univ. (Australia); Shota Yokoyama,

Ryuji Ukai, Chanond Sornphiphatphong, Toshiyuki Kaji, Shigenari Suzuki, Jun-ichi Yoshikawa, Hidehiro Yonezawa, The Univ. of Tokyo (Japan); Nicolas C. Menicucci, The Univ. of Sydney (Australia); Akira Furusawa, The Univ. of Tokyo (Japan)

Large entangled systems have been recently demonstrated in various optical platforms. In these experiments, quantised optical modes (qumodes) with continuous-variable encodings are made to propagate on the same optical channel. This leads to highly scalable architectures for quantum networks utilising entanglement. Qumodes have thus far been multiplexed in three domains: the spatial domain [ref1,ref2], the time domain [ref3], and the frequency domain [ref4,ref5]. In this talk I will present experiments performed in the first two domains and discuss relevant advantages and limitations.

Spatial-mode multiplexing was performed in the Bachor Group [ref1]. By overlapping orthogonal spatial modes onto one optical beam, we define our qumodes to be linear combinations of different spatial regions of the beam. A multi-photodiode homodyne detector then discriminates between 8 spatial regions of the beam, leading to basis of 8 independent qumodes. We emulate various linear optics networks and measure a variety of entangled mode bases with full control over virtual beam-splitters. This highly efficient programmable quantum network was recently used in order to demonstrate the first observations of multipartite Einstein-Podolsky-Rosen steering [ref2]. By inducing asymmetries in the network we reveal the directional monogamy of steering, and demonstrate one-sided device-independent quantum secret sharing.

While successful, the spatial-mode multiplexing demonstrations do not scale well. In order to create arbitrarily large entangled states we employed a theoretical proposal by Menicucci [ref6], and by multiplexing qumodes in the time domain we generated the largest entangled state reported to date, in the Furusawa Group [ref3]. The generated cluster state may be used for universal measurement-based quantum computing.

1 S. Armstrong et al., Programmable quantum networks. *Nature Commun.* 3, 1026 (2012).

2 S. Armstrong et al., Multipartite Einstein-Podolsky-Rosen steering and genuine tripartite entanglement with optimised networks. Under review (2014).

3 S. Yokoyama et al., Ultra-large continuous-variable cluster states multiplexed in the time domain. *Nature Photon.* 7, 982 (2013).

4 J. Roslund et al., Wavelength-multiplexed quantum networks with ultrafast frequency combs. *Nature Photon.* 8, 109 (2014).

5 M. Chen, N. Menicucci, O. Pfister, Experimental realization of multipartite entanglement of 60 modes of a quantum optical frequency comb *Phys. Rev. Lett.* 112, 120505 (2014).

6 N. Menicucci, Temporal-mode continuous-variable cluster states using linear optics. *Phys. Rev. A* 83, 062314 (2011).

9269-12, Session 3

Determination of the hyperfine structure constants of $4D_{5/2}$ state of Rb-85 atoms

Junmin Wang, Jie Wang, Huifeng Liu, Guang Yang, Baodong Yang, Jun He, Shanxi Univ. (China)

High-precision measurement of atomic hyperfine structure (HFS) plays an important role in tests of fundamental physical constants and insights into atomic structure. The HFS splittings of $4D_{5/2}$ state of Rb-85 atoms are measured precisely based on double-resonance optical-pumping (DROP) spectra in a ladder-type ($5S_{1/2}$ - $5P_{3/2}$ - $4D_{5/2}$) Rb-85 atomic system. The frequency interval calibration is performed by employing a wideband fiber-pigtailed phase-type electro-optic modulator (EOM) together with a high-finesse Fabry-Perot (F-P) cavity to cancel the

error arising from nonlinearity of laser frequency scanning. The magnetic dipole HFS constant A and the electric quadrupole HFS constant B of Rb-85 $4D_{5/2}$ state are determined to be $A = ?$ (16.801±0.005) MHz and $B = ?$ (4.978±0.004) MHz, respectively. The values of A and B are 3 times and 25 times more accurate than previous measurements in laser-cooled atoms using interferometric method, respectively. This work provides a simple method to precisely measure excited-state HFS in heavy atoms that may be of interest for parity non-conserving (PNC) measurements.

9269-13, Session 3

Investigation of a novel two-color magneto-optical trap with cesium atoms

Baodong Yang, Jie Wang, Huifeng Liu, Guang Yang, Jun He, Junmin Wang, Shanxi Univ. (China)

We present investigations of a novel two-color cesium (Cs) magneto-optical trap (MOT) configuration with the counter-propagating two-color cooling beams in Cs $6S_{1/2}$ - $6P_{3/2}$ - $8S_{1/2}$ (852.3nm +794.6nm) atomic system. Based on conventional 3D MOT due entirely to the 852.3nm cooling laser' scattering forces from $6S_{1/2}$ - $6P_{3/2}$ transition, one of six 852.3nm cooling beams is replaced with 794.6nm cooling beam which couples $6P_{3/2}$ - $8S_{1/2}$ excited-state transition. We find interesting and counter-intuitive phenomena: this two-color MOT configuration can cool and trap Cs atoms from the negative-detuning side to the positive-detuning side of the two-photon resonance without the precooling. This two-color MOT configuration can be more easily realized compared with the previous two-color MOT configuration with a pair of 794.6nm cooling beams replacing a pair of 852.3nm cooling beams, which traps atoms at the two-photon positive detuning point only when the power of 794.6nm cooling laser is strong enough. This two-color MOT can be applied to a completely background-free detection of cold atoms' fluorescence. The technique demonstrated here is also very promising to direct generation of two-color (761.1nm + 894.6nm) correlated photons based on a diamond-level four-wave mixing. Furthermore, our two-color Cs MOT configuration may be very helpful for deeply understanding of the two-color MOT and relevant applications.

9269-14, Session 3

Fiber-based nonlinear quantum optical devices

Xiaoying Li, Tianjin Univ. (China)

For the traditional optoelectronic information technology which is based on the classical electromagnetic theory, the ability of operating and utilizing the stream of photons is approaching its classical limit. From the perspective of the law of development of science and technology, a promising approach of surpassing the classical limit is to introduce the quantum technology into the field of optoelectronic information processing, including the optoelectronic imaging, detection, communication and sensing etc.. On the other hand, quantum information science and technology has made a great achievement in recent years, however, many quantum devices, such as the quantum light sources, often suffer from the drawbacks of large dimension, high cost, and the difficulties in operation and maintenance, which impeded its practical application.

In this paper, we investigate the realization of the quantum optical devices which are low cost, compact, and ease in operation and maintenance by using the $\chi^{(3)}$ nonlinearity in optical fiber. We first present the work on generating the quantum light source in both discrete variable and continuous variable states. Using the pulse pumped spontaneous four wave

mixing in various kinds of fibers, we have obtained the entangled photon pairs with different wavelength and degree of freedom, and heralded sources of single photons with high purity and high efficiency; while using the high gain four wave mixing in optical fiber, we have realized the pulsed twin beams, whose noise fluctuations of both the sum of the phase quadratures and the difference of amplitude quadrature are lower than the short noise limit. We then demonstrate the application of our quantum light source in precision measurement.

9269-15, Session 4

Genuine multipartite Einstein-Podolsky-Rosen steering for continuous variables (Invited Paper)

Qiongyi He, Peking Univ. (China)

We develop the concept of genuine N -partite Einstein-Podolsky-Rosen (EPR) steering. This nonlocality is the natural multipartite extension of the original EPR paradox. Useful properties emerge that are not guaranteed for genuine multipartite entangled states. In particular, there is a close link with the task of one-sided device-independent quantum secret sharing. We derive inequalities to demonstrate multipartite EPR steering for Gaussian continuous variable (CV) states in loophole-free scenarios.

We show that it is possible to obtain genuine multipartite EPR steering in very different sorts of systems to those so far predicted for multipartite Bell nonlocality. We have formalized the meaning of genuine multipartite EPR steering, and derive criteria to detect it. Here, we show how to verify N -partite steering for CV Gaussian systems both in optical systems and in multimode hybrid optomechanical systems, giving efficiency bounds to do so conclusively. Our results show that the hybrid quantum system - atomic ensemble inside of pulsed cavity optomechanical system, will be a promising candidate to test the signature of quantum correlations among the multimode massive objects and will be also useful to explore the Schrodinger cat states using the atomic ensemble and mechanical oscillator.

9269-16, Session 4

Light-control-light displays (Invited Paper)

Xiangping Li, Swinburne Univ. of Technology (Australia)

As one of the most important aspects of information technology, optical displays of three-dimensional (3D) objects with fast speed and high-definition are highly desired. In this regard, holography invented by Dennis Gabor provides a revolutionary way to reconstruct 3D light fields of objects with amplitude and phase information, which leads realistic 3D view without eyewear. Through digitally generating discrete phase modulations and removing the physical recording process, spatial light modulators have enormously motivated the experimental demonstration of digital holographic display. However, such an electrically driven spatial light modulator is intrinsically slow and can only facilitate a phase modulation in a region of a few tens of wavelengths, which is detrimental to the motivation of all-optical displays. On the other hand, the nonlinear interaction of femtosecond pulsed beams with optical materials leads to ultra-fast photoresponse and paves the way for all-optical light-control-light devices. Under the tightly focusing condition, the strong electric field by a femtosecond pulse can facilitate a large and fast refractive-index change in graphene based nanocomposites. In addition, the localized phase modulation within a diffraction-limited focal region can be controlled by the intensity of a tightly focused femtosecond pulse to form holographic correlations. Applying this feature, we demonstrate light-control-light holographic display of a 3D object in graphene based nanocomposites. The

demonstrated holographic display by a femtosecond pulse paves a new way for optical tele-display as well as many advanced all-optical manipulations.

9269-17, Session 4

Investigation of slow light using independent control light in Rb vapor cell

Sunwoo Heo, Seunghyun Hwang, Donghyun Lee, Byoung Seung Ham, Gwangju Institute of Science and Technology (Korea, Republic of)

In order to remotely control the signal light, the experimental system is consisted of two independent light sources. There is no connection between two lasers. Each laser uses locking system based on LIR (Lock-In Regulator). The signal and control pulses for this experiment are made by AOMs (Acoustic-Optic modulators) with PTS and DDG. And the temperature of Rb vapor cell housed μ -metal is controlled by heating tape based on PID system. The more the cell temperature increases, the more the number of atoms in cell responses with light. If the cell temperature becomes higher than the specific point, signal beam would be decreased, because many atoms get out of resonant frequency as the cell temperature increases. However, it is possible to long-term light storage in optical buffer memory, because the group delay of signal pulse increase as the cell temperature increases. Based on this principle, we observed the increase of group delay as a function of the cell temperature from 20 μ s to 130 μ s, and the decrease of signal beam when the cell temperature is higher than 50 μ s. And also, we found that the FWHM (Full Width at Half Maximum) of signal beam decreases as the cell temperature increases more than 50 μ s. We will discuss the tendency of this research in detail at SPIE Asia.

9269-36, Session Post

Interactive identification protocol based on a quantum public-key cryptosystem

Chenmiao Wu, Li Yang, Institute of Information Engineering of Chinese Academy of Sciences (China)

We define a quantum public-key cryptosystem by a quadruplet $(\{f_i\}_{i \in I}, \{(|\psi_k\rangle_{r,s}\rangle_{\sin\{0,1\}^{O(n)}}\}, E, D)$ which contains a set of private-keys $\{f_i\}_{i \in I}$, a set of public-keys $(|\psi_k\rangle_{r,s})$, quantum encryption algorithm E and quantum decryption algorithm D . The quantum public-key cryptosystem is adopted in our interactive identification protocols. Compared with classical public-key cryptosystem, one private-key in our protocols corresponds to an exponential number of public-keys.

We propose two interactive identification protocols. Basic protocol runs in two phases: set-up phase and authentication phase. In set-up phase, fundamental parameters will be established. Authentication phase contains two-round transmission. Participant does operation with quantum computing of Boolean function. Basic protocol ensures completeness and soundness. Through numerical experiment, we show that basic protocol leaks information about prover's private-key. We modify basic protocol with random string and random Boolean permutation. The first message send by verifier, he does computation with his random Boolean permutation:

$$U_{\text{Verifier}}(|\psi\rangle_{R_1, R_2}) \otimes |0\rangle_{R_3} = \sum \alpha_{\{m\}} |\text{mangle}_{R_1\} |F_{\{k\}} \oplus r_{\text{Prover}} \rangle_{R_2} |F_{\text{Verifier}} \rangle_{R_3}$$

Then verifier sends the first two registers to prover. Prover computes with her private key?

$$U_{\{k\}} (\sum \alpha_{\{m\}} |\text{mangle}_{R_1\} |F_{\{k\}})$$

$$(m) \oplus r_{\text{Prover}} \rangle_{R_2} = \sum \alpha_{\{m\}} |\text{mangle}_{R_1\} |F_{\{k\}} \oplus F_{\{k\}} \oplus r_{\text{Prover}} \rangle_{R_2} = \sum \alpha_{\{m\}} |\text{mangle}_{R_1\} |r_{\text{Prover}} \rangle_{R_2}$$

and sends the first register back to verifier. Verifier finally disentangles all the registers and checks prover's identity. During two-round transmission, transmitted messages are both in ultimate mixed states. Legitimate participants and attacker are unable to get any useful information about private-key by measuring such states. Modified protocol achieves completeness, soundness and property of zero-knowledge which ensures that identification will not provide any useful information about private-key.

9269-37, Session Post

Tripartite steering in hybrid optomechanical systems

Meng Wang, Qiongyi He, Peking Univ. (China)

The concepts of genuine tripartite entanglement and quantum steering in a three-mode optomechanical system are investigated. The system is composed of an atomic ensemble located inside a single-mode cavity formed by a fixed semi-transmitted mirror and a movable fully reflective mirror. The cavity mode is driven by a short laser pulse and is assumed to experience a fast damping due to its coupling to an external reservoir through the semi-transparent mirror, and has a nonlinear parametric-type interaction with the mirror and a linear beamsplitter-type interaction with the atomic ensemble. Three-mode quantum states are found which allow both entanglement and Einstein's nonlocality (quantum steering) to be genuinely shared among the modes, even though there is no direct interaction of the mirror with the atomic ensemble. Both entanglement and steering are tested by a simple unified criterion. Especially, the steering of the mirror by the cavity mode and atomic ensemble addresses the question of mesoscopic local reality for a massive system. Furthermore, we distinguish between genuine tripartite steering and a stronger form of steering called collective tripartite steering which exists when a given mode is steered collectively by the remaining modes, not by each of the remaining modes alone. We then show that the idea of collective steering may provide a resource in a hybrid quantum network for one-sided device-independent quantum secret sharing.

9269-38, Session Post

Design an active imaging system using squeezed state light

Xu-ling Lin, Beijing Institute of Space Mechanics and Electricity (China); Siwen Bi, Institute of Remote Sensing and Digital Earth (China); Song Yang, Zhiqiang Wu, Pengbin Zhang, Beijing Institute of Space Mechanics and Electricity (China); Chao Wang, Beijing Institute of Space Mechanics & Electricity (China); Ningjuan Ruan, Beijing Institute of Space Mechanics and Electricity (China); Ci Jian, Beijing Institute of Space Mechanics & Electricity (China)

Squeezed light is an important non-classical light field. In this paper, we demonstrated a designed active imaging system which use squeezed state light instead of coherent light as light source. The squeezed state light is generated by utilizing the degenerate optical parametric amplifier based on periodically poled KTiOPO4 crystal. In order to obtain better imaging results, microlens arrays are used for homogenizing the squeezed light. We describe experiment setup and present some design result.

9269-39, Session Post

Electromagnetically-induced transparency in the four-level system driven by bichromatic microwave field

KeJia Sun, Lijun Yang, Su heng Zhang, Xiaomin Feng, Hebei Univ. (China)

We investigate the nonlinear behaviors of the electromagnetically induced transparency (EIT) resonance subject to bichromatic driving field in a four-level atom system. The four-level system consists of three hyperfine levels within an electronic ground state and an excited state level. An EIT resonance can be obtained when two hyperfine levels are coupled to the common excited state level by a coupling field and a weak probe field. In case that an additional microwave field drives the third transition between the other hyperfine level and the lower level related to probe field, the EIT feature associated with probe is split into a doublet structure. The new aspect of the present work is to replace the single driving field by a bichromatic microwave driving field to perturb the EIT feature. We study that the effect of the strength and frequency of bichromatic driving field on the EIT resonance characteristics in the four-level system. The probe absorption spectrum is obtained by solving the density matrix equation through the numerical analysis. We restrict the study to a special case where one component of the bichromatic driving field is resonant with corresponding transition and the other is detuning in frequency by the Rabi frequency of the resonant field. It can be seen that the result is that each EIT of the doublet structure obtained with a single driving field will itself be split into two EIT windows. The characteristics of the EIT doublets are determined by the strength of the bichromatic driving field, and the doublet splitting originates from the microwave driving field induced dynamic Stark effect. In addition a physical account of their behaviors is given in terms of a dressed state picture.

9269-40, Session Post

Sub-Poissonian light generation in a coupled quantum dot-photonic molecule system

Yuanan Zhang, Zhongyuan Yu, Wen Zhang, Yumin Liu, Yongxin Yin, Xi Liu, Beijing Univ. of Posts and Telecommunications (China)

We theoretically investigate the photon statistics in a cavity quantum electrodynamics system of a single quantum dot (QD) coupled to photonic molecule. Our previous work [Wen Zhang et al, Phys. Rev. A 89, 043832 (2014)] has shown that QD-bimodal cavity system can generate ultrastrongly sub-Poissonian light by regulating the ratio between driving strengths of two cavity modes. Here we study two coupled single-mode nanocavities with a QD coupling to one of them as a photonic molecule system by numerically solving the master equation. Statistical character of photon emission is presented by evaluating the zero-delay second-order correlation function $g_2(0)$. When both cavities with/without QD are driven, we find the sub-Poissonian character can be optimized by regulating the ratio between driving strengths of each cavities. Besides, the intercavity coupling strength induced by photonic molecule scheme can reduce $g_2(0)$ of the system significantly. The physical mechanism of both effects is to optimize the combination of super-Poissonian and coherent light which results in sub-Poissonian light generation. Meanwhile, we present the dependences of other system parameters on the photon statistics. As a result $g_2(0)$ can be reduced up to several orders of magnitude with proper system parameters compared with the QD coupled one-mode-cavity system. This coupled single QD-photonic molecule

system can be used to realize nonclassical light generation and quantum information processing at the single photon level.

9269-42, Session Post

Evolution of the TC model two entangled atoms without rotating wave approximation

Jingpei Feng, Xuezhao Ren, Lei Li, Shu He, Southwest Univ. of Science and Technology (China)

Using coherent states orthogonal expansion method and concurrence, the impacts of initial state and coupling strength on the degrees of entanglement between two atoms in Tavis-Cummings model are studied without rotating-wave approximation. The initial states of two identical atoms are prepared in anti-symmetric singlet and triplet states. The evolution of entanglement between two atoms is comparatively studied, with and without rotating-wave approximation. Our results show that when the initial state of the two atoms in an anti-symmetric state, the entanglement between two atoms reaches its maximum value. When the initial state of the two atoms is in a non-entanglement state, no entanglement happens under rotating-wave approximation. And in consideration of the non-rotating-wave terms, periodic entanglements are produced. But entanglement evolutions for atoms in ground state and excited state are quite different. With the increase of the coupling strength, the curve of concurrence under rotating-wave approximation is smooth, while small irregular jagged structure appears without rotating-wave approximation.

9269-43, Session Post

Interference resonant propagation and spectral properties of double femtosecond chirped Gaussian pulses in three-level $[\lambda]$ -type atomic medium

Zhendong Wang, Rongfang Ji, Jing Xiao, Jianling Ma, Tingting Liu, Taishan Univ. (China)

The interference resonant propagation and spectral properties of a superposition of two femtosecond chirped Gaussian pulses with equal pulse area and same size but opposite sign of the chirp coefficient (C) in a three-level $[\lambda]$ -type atomic medium is investigated by using the numerical solution, which is obtained by the finite-difference time-domain method and the iterative predictor-corrector method for the full Maxwell-Bloch equations. It is found that, for the double pulses with smaller area, $(2\pi, 2\pi)$ double pulses, the pulse splitting occurs when the value of the $|C|$ is smaller, and only the variation of pulse shape is present but the pulse splitting no longer occur when the value of the $|C|$ increases to a certain value; New high frequency component doesn't basically appear and the strength of the spectral component near the central frequency decreases considerably but the strength of blue shift component is not varied obviously with the value of $|C|$ increasing. For the double chirped pulses with larger areas, the case of pulse splitting is similar to that of $(2\pi, 2\pi)$ pulses, but the strength of the spectral component with higher frequency increases evidently comparing with the case of $(2\pi, 2\pi)$ double pulses. Moreover, the value of the $|C|$ also has an obvious effect on population, different population evolutions can be achieved by adjusting the value of $|C|$.

9269-44, Session Post

Spatial emission characteristics from electron oscillation driven by circularly-polarized laser pulses

Youwei Tian, Gao Yu, Nanjing Univ. of Posts and Telecommunications (China); Yuanyuan Wang, Jingxia Jiang, Qiuyuan Zhang, Nanjing University of Posts & Telecommunications (China)

Recent advances in ultrashort intense laser technology has created the exciting field of "High Field Science." Laser pulses and electron interaction can be studied in the relativistic regime and highly nonlinear physical phenomena are brought to light. Up till now, the interaction of free electrons with intense laser field has been studied by many authors and various nonlinear phenomena have been found, such as figure-8 orbits, harmonic generation, nonlinear Thomson scattering in pulse laser and continuous wave of laser field, etc. The main motivation to study these phenomena stems from the prospect of producing table-top particle acceleration and x-ray source. Scattering of continuous wave of laser light at higher intensity is well known and one can obtain solution of the classical motion of an electron in a plane wave for the case of constant continuous illumination and apply it for calculating the harmonic power. The full spatial characteristics of the radiation emission due to electron oscillations in the cases of circularly polarized laser pulse did not receive enough attention in previous studies. In this paper, we have investigated characteristics of spatial distribution of emission with a single electron model in the cases of circularly polarized femtosecond laser pulses with different intensities. The results show that the angular distribution of radiated emission is more and more directed forward with the increase of laser intensity. These phenomena are governed by the electron dynamics and properties of the circularly polarized femtosecond laser pulses.

9269-45, Session Post

Efficient seeded third order parametric down conversion in optical microfibers

Jianyu Zhang, Yunxu Sun, Harbin Institute of Technology (China)

Third order parametric down conversion (TPDC) for triple photons generation (TPG) is a challenging research. Although there are many researchers focusing on the TPDC, the small efficiency annoyed the scientists. The main problem is the difficulty of realizing phase matching between the fundamental wave and harmonic wave because of the large frequency span between two waves. Stimulated Raman scattering, stimulated Brillouin scattering and Kerr effect also contribute to the phase mismatching, which make TPDC more complicated. Besides, the tiny third order nonlinearity leads to small effects of TPDC.

The phase matching condition of TPDC can be obtained by intermodal dispersion of optical microfibers, with a diameter as half of the signal wavelength. Intermodal dispersion between pump and signal waves in different modes can compensate material dispersion between these two waves.

Based on the merits mentioned above, optical microfibers have been studied and utilized for a range of nonlinear applications. The coupled-wave equations (CWE) are used for describing the interaction of those two waves under continuous wave condition. TPDC is precisely a quantum process, which is the interaction between the pump field and vacuum state. However, seeded TPDC (sTPDC), a seed light introduced, can be described precisely by classical CWE. We explore the process of sTPDC inside microfiber by solving CWE numerically.

The advantage of sTPDC in optical microfiber is that the effects of different nonlinear terms can be engineered by the microfiber structure in order to achieve maximum efficiency. However, the relationship among maximum efficiency, microfiber structural parameters, and laser power has not been fully investigated yet. And some structures for enhancing the TPDC should be explored.

9269-46, Session Post

Composite soliton-dipole pairs in parity-time symmetric optical lattices

Lijuan Ge, Univ. of Science and Technology of Suzhou (China)

Recently, the study of Parity-Time (PT) symmetric optical lattices has attracted considerable attention in the field of the propagation of solitary waves, due to the reasons that PT-symmetry is realizable by the careful distribution of gain and loss media in a wave guide array and has lead to the first experimental observations of the properties. Generally, solitons exist only at special values of the propagation constant in a system containing gain and loss. However, due to the remarkable properties of PT potentials, which can admit all-real linear spectra, solitons could exist at continuous ranges of the propagation constant. So far, soliton families in PT-symmetric periodic potentials with defects and in PT-symmetric nonlinear potentials have been well investigated.

Fundamental solitons, with a single extremum in the intensity distribution and transversely constant phase, are the lowest-order localized structures. The structure of a dipole, comprising two dominant out-of-phase peaks packed together by the force acting between them, also attracted much attention in PT-symmetric optical lattices. Many contributions have been made in the propagation of composite soliton-dipole pairs in nonlinear media. But the properties of composite soliton-dipole pairs are not very clear in PT-symmetric optical lattices.

In this paper we consider systematically the propagation of composite soliton-dipole pairs in PT-symmetric optical lattices. The existence and stability of the vector solitons are analyzed in PT-symmetric periodic potentials (optical lattices). Although dipole solitons are linearly unstable in a lot portion of their existence region, the fundamental component of composite soliton-dipole pairs can dramatically enhance the stabilization of the dipole beam. We also investigate the nonlinear evolution of composite soliton-dipole pairs under perturbations.

9269-47, Session Post

Four-photon resonant nondegenerate eight-wave mixing in a dressed atomic system

Jing Gao, Yu Cui, Hebei Univ. (China); Xiaohang Li, North China Electric Power Univ. (China); Jiang Sun, Hebei Univ. (China)

We report a four-photon resonant nondegenerate eight-wave mixing (NEWM) in a dressed N-type six-level system. In the presence of a strong coupling field, the four-photon resonant NEWM spectrum exhibits Autler-Townes splitting. It also leads to either suppression or enhancement of the NEWM signal. This technique provides a spectroscopic tool for measuring not only the resonant frequency and dephasing rate but also the transition dipole moment between two highly excited atomic states.

Compared to two-photon resonant nondegenerate four-wave mixing and three-photon resonant nondegenerate six-wave mixing in dressed atoms, which had been reported by us, four-photon resonant NEWM spectrum is more complicated and can

provides information about the relaxation of higher-order atomic coherence, and so is particularly suitable for studying highly excited atomic states with high sensitivity. One of the difficulties of high-order wave mixing is that complex beam geometries are usually required to satisfy the phase-matching conditions. Moreover, the nonlinear signal decrease by several orders of magnitude with increase in the order of nonlinearity of the interaction. It is different from other high-order wave mixing effects, phase matching in four-photon resonant NEWM in a dressed atomic system depends on k_1 , k_4 and k_4' only and is not very critical. At the same time, the generation of the NEWM signal is quite efficient due to the multiple resonance with the atomic transition frequencies.

9269-48, Session Post

Supercontinuum generated in a dispersion-flattened photonic crystal fiber

Xingliang Li, Shumin Zhang, Mengmeng Han, Huaxing Zhang, Hong Yang, Ting Yuan, Hebei Normal Univ. (China)

We have experimentally investigated supercontinuum generated by using different pulse dynamics patterns as the pump pulses. These patterns, which include conventional mode-locked single pulse, condensed phase pulses and pulsed bunches, were all directly produced from a mode-locked erbium-doped fiber laser based on a multi-layer graphene saturable absorber. The strong third-order optical nonlinearity of graphene and all fiber cavity configuration led to the multi-pulses operation states at a low pump power. A flat supercontinuum with 20-dB width of 550 nm from 1200 nm to 1750 nm have all been obtained by seeding the amplified conventional mode-locked single pulse and condensed phase pulses into a segment of photonic crystal fiber. On the other hand, experimental results also show that the pulsed bunches was not conducive to form a flat supercontinuum.

9269-49, Session Post

Nonlinear dynamics evolution of the VCSEL polarization mode in the optical fiber

Linfu Li, Guizhou Minzu Univ. (China); Jian-Jun Chen, Xinjiang Medical Univ. (China)

Compared with conventional edge-emitting laser, vertical-cavity surface-emitting lasers (VCSELs) has many advantages, such as single longitudinal-mode operation, low threshold current, circular output beam with narrow divergence, low cost and etc. Therefore, vertical-cavity surface-emitting lasers can be used as an ideal light source for optical chaotic communication. There were many reports on the synchronization characteristics of two VCSELs. However, we have noticed that most of relevant works usually focused on the synchronization properties of the direct coupling of two VCSELs, the impact that signal transmission and evolution characteristics in the fiber channel is less considered. Considering the practical utility, The realization of high-speed long-distance optical fiber communication, is more practical value.

In this paper, based on the spin-flip model (SFM), the nonlinear output and dynamics evolution of a vertical cavity surface emitting lasers(VCSEL) subject to external optical injection in optical fiber were numerical investigated. The evolution characteristics of different linear polarization mode(i. e., x and y linear polarization mode) also the signal transmission in fiber channel were analyzed. Action of self-phase modulation(SPM) and chromatic dispersion of optical fiber on evolution of polarization mode signal is analyzed in detail?At last?the evolution characteristics of the phase?the slowly varying field

amplitude of the different linear polarization mode transmission in optical fiber are numerically simulated?respectively. This research work will supply a theoretical guide for long distance chaotic telecommunication based on the VCSEL.

9269-50, Session Post

Observation of harmonic polarization locked vector solitons in a fiber laser based graphene saturable absorber

Mengmeng Han, Shumin Zhang, Xingliang Li, Huaxing Zhang, Hong Yang, Ting Yuan, Hebei Normal Univ. (China)

The dynamics of harmonic polarization locked vector solitons have been experimentally obtained in a mode-locked fiber laser based graphene saturable absorber. The fundamental repetition frequency of our laser is 14.34 MHz, corresponding to the cavity length of 14.4 m. With carefully adjusting the PCs in extra- and intro-cavity, the polarization locked vector solitons from 1th to 5th could be formed. Both the frequency-locked and phase-locked of the two vector soliton patterns are all observed. The central wavelengths of two polarization axes for one order vector solitons lie in the same point, and the pulse height is equal basically. By comparing the dynamics of the six different orders vector solitons, we also find that with the increase of the vector soliton order, the soliton pulse duration becomes narrow. The signal to noise ratio of our system can achieve ~51 dBm, which indicates that the laser operation in a high stability condition.

9269-51, Session Post

Optimal design of dissipative-soliton fiber lasers

Huaxing Zhang, Shumin Zhang, Xingliang Li, Mengmeng Han, Hong Yang, Ting Yuan, Hebei Normal Univ. (China)

We have numerically investigated dissipative solitons fiber lasers with the central wavelength at 1060 nm by using the cubic complex Ginzburg-Landau equation, and we have analyzed the effects of different parameters, which include spectral filter bandwidth, cavity length, and nonlinear phase shifts. Firstly, we investigated the effect of spectral filter bandwidth (SF-BW) on the output characteristic (pulse shape, pulse duration, spectral shape, spectral width, pulse energy, pulse peak power). We found the best SF-BW = 8 nm for generating high energy pulses by varying the SF-BW while the other parameters kept constant. In order to further validate the best SF-BW, we only changed the length ratio (between the single-mode fiber and the gain fiber) from 3 to 4, the results showed that the best SF-BW was still 8 nm. Then, we investigated the effect of cavity length by varying the first single-mode fiber length in the cavity while the SF-BW kept the best 8 nm. We found the best length ratio ~6.5 for generating high energy pulses. The results showed that a 8-nm-wide spectral filter and a ~6.5-length ratio will be benefit to obtain a high-energy pulse fiber laser. In the last, we investigated the effect of nonlinear phase shifts on the output features by varying the pump power. Further more, by using optimal parameters (a 8-nm-wide spectral filter and a ~6.5-length ratio), the single pulse energy can reach ~20 nJ with the pulse width of 10 ps, and can be chirped to 80 fs with 240 kW peak power.

9269-52, Session Post

Widely-tunable fiber optical parametric oscillator

Hong Yang, Shumin Zhang, Xingliang Li, Mengmeng Han,

Huaxing Zhang, Ting Yuan, Hebei Normal Univ. (China)

On basis of numerical simulation and analytical treatment, a widely-tunable fiber optical parametric oscillator by using a 50 cm photonic crystal fiber as the gain medium based on modulation instability and time-dispersion-tuned technique in the negative dispersion regime is demonstrated. The spectral tuning range of signal and idle light was from 1256 to 1361 nm and from 1801 to 2025 nm while fixing the pump wavelength at 1550 nm, separately. This phenomenon can also be demonstrated by slightly tuning the pump wavelength from 1540 to 1565 nm. Detailed numerical simulation was performed to understand the pulse dynamics in the laser cavity. We believe that the proposed concept is useful for the researching of fiber optical parametric oscillator.

9269-53, Session Post

The preset grating effect for mutually-pumped phase conjugator

Lin Ma, Zhihua Kang, Ninghua Zhang, Jifang Liu, Shunxiang Shi, Xidian Univ. (China)

The preset grating effect of Mutually pumped phase conjugator (MPPC) means photorefractive gratings generated in MPPC still maintains for a long time when the incident pumped light stop incidence due to the nature of photorefractive effect. And this grating is a preset grating for the next MPPC. The preset grating will affect the next mutually pumped phase conjugation effect, promoting or inhibiting. It has promoting effect and overcomes the slow response process of photorefractive effect. Its study has a significant value on the applications of MPPC in the fields such as heterodyne detection, adaptive optics and optical communications.

Based on the four-wave mixing mechanism and light fanning effect, the preset grating of MPPC is investigated in theory and experiment. After establishing a mutually pumped phase conjugation effect model, the variation of MPPC output response with time is simulated for different scattering seed value. It shows that preset grating can enhance the fan light intensity on the need channel when it satisfies Bragg condition, equivalently, increase the values of seed light. Preset grating also can shorten MPPC response time. In experiment when both the incident light intensity are in nW level, the research on bird-wings MPPC is done with or without the existence of a preset grating and the variation of MPPC reflectivity with time is obtained in two cases. The comparative results show that the experiment is in agreement with theoretical simulation. What is described in this paper has both theoretical and practical value on the application of MPPC on optical heterodyne detection.

9269-54, Session Post

Infrared-to-visible upconversion emission of Yb³⁺/Ho³⁺ co-doped GdVO₄

Yunfeng Bai, Heilongjiang Institute of Technology (China)

GdVO₄ crystals is a suitable host material for doping with rare ions. Considering its good mechanical and thermo-optical, GdVO₄ is also considered to be a promising laser material. As far as we know there is few optical research about Yb³⁺/Ho³⁺ co-doped GdVO₄ crystals. Infrared-to-visible upconversion emission intensities are investigated in Yb³⁺/Ho³⁺ co-doped GdVO₄ crystals. Two distinctive emission bands associated with the Ho³⁺ ion are observed in green and red regions. The green emission between 530nm and 570nm is due to the transitions from ⁵F₄ and ⁵S₂ excited states to the ⁵I₈ ground state. The red emission observed between 630 and 670nm arises from the ⁵F₅/⁵I₈ transition. There is no extinction even with strong

excitation power. That indicated Yb³⁺/Ho³⁺ co-doped GdVO₄ crystals is a promising material for Infrared-to-visible and Infrared-to-Infrared laser material.

9269-55, Session Post

Theoretical research on period microstructure induced by femtosecond laser in transparent dielectric based on nonlinear optics theory

Shuwei Fan, Yan Zhang, Xi'an Jiaotong Univ. (China)

Femtosecond lasers have opened a new field for microfabricating due to their unique advantages of super strong power and super short pulse. Researchers have paid more attention to period microstructure induced by femtosecond laser in transparent material. However, physical mechanisms of inducing period microstructure was not clear yet. This paper did some researches on the physical mechanism of period microstructure induced by femtosecond laser. Main work was as follow:

Physical process of femtosecond laser propagation in dielectric was described by Non Linear Schrodinger (NLS) equation. The math model of NLS was built and were solved by alternative direction implicit method.

The influence of nonlinear effects of femtosecond laser propagation in transparent dielectric such as self-focusing, GDV, MPA, plasma defocusing and interface aberration were analyzed. The electric field distribution along with the direction of laser propagation was simulated with different optical power intensity and different pulse time in different locations.

Also, by employing electromagnetic diffraction theory, the influence of interface aberration on laser field distribution was analysed. Research showed that interface aberration changed optical energy distribution and had obvious influence on location and length of the period void array.

Considering both the nonlinear effects and interface aberration, the influence of several parameters on period microvoid were researched. It was showed that laser power and focusing depth had obvious influence on the produced period microvoid array. Simultaneously, the simulation results with different focusing lens numerical aperture demonstrated that the period microvoids could be produced more easily with bigger numerical aperture and deeper focus length.

9269-56, Session Post

Numerical investigation of a novel two-stage structure to compress spectrum and suppress pedestal employing a DIF interconnected with a HNLF-NOLM

Ying Chen, State Key Lab. of Electronic Thin Films and Integrated Devices (China)

A novel all-fiber spectral compression scheme is proposed and demonstrated, which is based on a two-stage structure employing a dispersion increasing fiber interconnected with a nonlinear optical loop mirror. Five sorts of DIF with different distribution of dispersion coefficient is analyzed one by one in the two-stage scheme. Numerical simulation result shows Logarithmic DIF is suitable for the two-stage scheme, obtain a SCR as high as 10.93 without a Raman self-frequency soliton shift under the condition of soliton number is equal to 1.4.

9269-57, Session Post

Two-dimensional distributions of supramolecular chirality at the air/water interface by in situ surface second harmonic generation linear dichroism

Xiaoyu Wang, Li Lin, Beijing Institute of Technology (China); Lu Lin, Zhen Zhang, Zhou Lu, Yuan Guo, Institute of Chemistry (China)

A method that based on Second Harmonic Generation(SHG) was used to investigate supramolecular chirality formed by achiral molecules at air/water interface. The sample we measured is a complex monolayer formed by CTAB and TPPS. The S-polarized SHG intensity was measured as a function of the incident fundamental wave polarization angles. Data fitting and comparative analysis of all the series of experimental data indicated that supramolecular chirality of complex monolayer was already present at the air/water interface before transferred on the solid substrate and the distributions of supramolecular chirality are inhomogenous in space.

9269-18, Session 5

Lowest levels detection by photo-association of the O_g - pure long-range state of Cs2 (Invited Paper)

Yichi Zhang, Shanxi Univ. (China)

We demonstrated a high sensitive detection technique to detect the two missing lowest levels ($v=0$ and 1) of the O_g - pure long-range state of Cs2. The two missing lowest levels are theoretically predicted by O. Dulieu, et al. [Phys. Rev. A 75, 052501 (2007)], which have not yet been observed in previous experiments. The photoassociation spectroscopy of ultracold cesium atoms with rotational structure presents clear identification of missing lowest levels. We represent the potential curves for the external well of the O_g - ($6S_{1/2}+6P_{3/2}$) pure long-range state in cesium molecules. The agreement between experimental and theoretically calculated energy positions would improve the precision of potential well. Values of radiative lifetimes and of the $6p2P_{1/2}$ and $6p2P_{3/2}$ atomic levels and van der Waals coefficient $C_6 = 6852\ 25$ a.u. of ground state cesium molecule are extracted, respectively.

9269-19, Session 5

Nanoscale magnetic resonance spectroscopy using a single nitrogen-vacancy center in diamond (Invited Paper)

Susumu Takahashi, The Univ. of Southern California (United States)

Magnetic resonance (MR), such as nuclear magnetic resonance (NMR) and electron paramagnetic resonance (EPR), can probe the local structure and dynamic properties of various systems, making them among the most powerful and versatile analytical methods. However, their intrinsically low sensitivity precludes MR analyses of samples with very small volumes; e.g., more than 10¹⁰ electron spins are typically required to observe EPR signals at room temperature. A vast improvement in the current limits of MR will enable the imaging of structures and conformational changes of molecules in solution at the single molecule level.

A nitrogen-vacancy (NV) center in diamond is a promising candidate for applications of nanoscale magnetic sensing as well as for investigation of fundamental quantum sciences

because of its unique properties including capability to detect a NV center, long decoherence time even at room temperature, stable fluorescence and biocompatibility. Here we will present our high-field/-frequency approach to use a single NV center in diamond to measure MR spectrum of nanoscale surrounding spin environments. We will discuss surface properties of diamond as well as application of double electron-electron resonance spectroscopy to detect surrounding electron spins.

1. E.E. Romanova, R. Akiel, F.H. Cho and S. Takahashi, Grafting nitroxide radicals on nanodiamond surface using click chemistry. J Chem Phys A, 2013 Jun; 117(46): 11933-9.

9269-20, Session 5

Two-photon polarization spectroscopy with Cs and Rb ladder-type atomic system and promising frequency reference of telecom laser

Junmin Wang, Baodong Yang, Huifeng Liu, Jie Wang, Guang Yang, Jun He, Shanxi Univ. (China)

The dense wavelength-division-multiplexing (DWDM) protocol for optical fiber telecom has remarkably increased the communication capacity of telecom network. But to meet the fast increasing demands for larger capacity and higher speed optical fiber telecommunications, DWDM maybe go to super DWDM with much narrower telecom channels in near future. Although nowadays the femto-second optical frequency comb has much more precision, it is too complicated, too huge-volume and too expensive for telecom applications. To explore simple, robust, transportable and direct 1.5 μ m optical frequency reference is very important for directly calibrating telecom channel and avoiding crosstalk between neighboring channels.

The cesium (Cs-133) $6P_{3/2} - 7S_{1/2}$ transition (1470nm) locates the vicinity of 204.00 THz channel in S band, while the rubidium (Rb) $5P_{3/2} - 4D_{5/2}$ transition (1529nm) locates the vicinity of 196.00 THz channel in S band. These atomic transitions are good candidates for telecom frequency reference. Based on the $6S_{1/2} - 6P_{3/2} - 7S_{1/2}$ (852nm + 1470nm) ladder-type 133Cs atomic system and the $5S_{1/2} - 5P_{3/2} - 4D_{5/2}$ (780nm + 1529nm) ladder-type Rb-87 atomic system, we extended the conventional polarization spectroscopy (PS) to the two-photon polarization spectroscopy (TPPS) to access hyperfine transition between excited states. The physical essences of PS and TPPS are the unsymmetrical atomic populations on the Zeeman sublevels of ground state for PS and those of the intermediate excited state for TPPS due to optical pumping, and the circular birefringence induced by this anisotropic characteristic. TPPS scheme can provide modulation-free dispersive signals for above-mentioned 1470nm and 1529nm excited-state transitions, which are very suitable for frequency discriminating to stabilize 1470nm and 1529nm telecom lasers. Frequency stabilized 1470nm and 1529nm telecom lasers have been setup and investigated experimentally. Preliminary results of laser frequency stability will be presented.

These lasers also can be utilized to explore the possibility to realize new two-color magneto-optical trap (TC-MOT) with (852nm + 1470nm) two-color cooling lasers for Cs-133 atoms and with (780nm + 1529nm) two-color cooling lasers for Rb-87 atoms, and to explore the possibility to generate 852nm + 1470nm (780nm + 1529nm) correlated photons by employing the four-wave mixing process in cold or hot Cs-133 (Rb-87) atomic ensembles. Because the 852nm (780nm) photons allow quantum information storage and readout with Cs-133 (Rb-87) atomic ensemble, and the 1470nm (1529nm) photons allow low-loss transmission in a telecom fiber network, so the 852nm + 1470nm (780nm + 1529nm) correlated photons are very useful quantum resources for implementing the quantum network or the distributed quantum information processing system.

9269-21, Session 5

Flexible multi-functional mode-locked fiber laser delivering conventional soliton and dissipative soliton

Dong Mao, Northwestern Polytechnical Univ. (China)

We report the simultaneous generation of conventional soliton (CS) and dissipative soliton (DS) in a mode-locked fiber laser exploiting chirped fiber Bragg grating and four-port circulator. Light propagation in cavity has two optional routes with different lengths and dispersion. By appropriately setting the polarization controller (PC), CS centered at 1550 nm and DS centered at 1562 nm are generated in the same laser. The CS has no spectral sidebands with the bandwidth of 0.28 nm and the duration of 15.1 ps, while the DS shows a quasi-rectangular spectrum with a bandwidth of 9.5 nm. The duration of the DS is 7.3 ps, and the pulse can be compressed to 0.55 ps in single-mode fiber. Our numerical results are in good agreement with the experiments and clearly reveal the formation mechanisms of the CS and DS. Compared with constructing independent CS laser and DS laser, the proposed scheme significantly reduces the cost and is attractive for ultrafast optics.

9269-22, Session 5

Efficient phase-matched third harmonic generation from mid-IR to near-IR regions in a double asymmetric plasmonic slot waveguide

Tingting Wu, Nanyang Technological Univ. (Singapore) and Harbin Institute of Technology (China); Yunxu Sun, Perry Ping Shum, Xuguang Shao, Tianye Huang, Nanyang Technological Univ. (Singapore)

Recent years, the research of mid-infrared (mid-IR) photonics has inspired increasingly interest due to their potential applications in a wide variety of areas, including free-space communications, chemical or biological sensors, environmental monitors, thermal imaging, IR countermeasures and medical procedures. On the other hand, third harmonic generation (THG) has been demonstrated to be a versatile tool to realize high speed optical performance monitoring of in-band OSNR and residual dispersion. The mid-IR light sources based third-order frequency conversion opens an entirely new realm of nonlinear interactions. Nevertheless, rare experimental or analytical THG modeling has been published. In this work, we theoretically investigate the possible efficient phase-matched THG in a double symmetric plasmonic slot waveguide (DAPSW) based on a mid-IR light source. Nonlinear organic material DDMEBT with third-order susceptibility of $\chi(3) = 1.7 \times 10^{-19} \text{ m}^2/\text{V}^2$ is integrated into the top metallic slot region as the main slot core medium. Silicon (Si) is used to fill the bottom metallic slot region. Silver (Ag) is considered to be the metal medium due to its low Ohmic loss. The needed phase-matching condition (PMC) is satisfied between the zeroth mode at fundamental frequency (FF) and the first mode at third harmonic (TH) by appropriate designing the waveguide geometrical parameters. The associated parameters such as the width and height of the slot, pump-harmonic modal overlap, figure-of-merit (FOM), pump power and detuning have been numerically investigated in detail. Finally, the conversion efficiency comes up to 1.69×10^{-5} with pump power of 1 W and the corresponding waveguide length is 10.8 μm .

9269-23, Session 5

Interactions of dark solitons in nonlocal media with competing nonlinearities

Ming Shen, Shanghai Univ. (China)

Despite their diversity, the interaction of solitons is always universal, i.e., they exhibit particle-like behavior. However, the interactions of bright and dark solitons is fundamentally different. For the bright solitons, they may attract, repel, and even form bound states, depending on their relative phase. On the contrary, the interaction of dark solitons is always repulsive. Recently, the interactions of solitons have been investigated in media with spatially nonlocal nonlinearity. Nonlocality can provide a long-range attractive force between solitons, leading to the formation of stationary bound states of both out-of-phase bright solitons as well as dark solitons.

In recent years the studies of interactions of solitons have been extended to nonlocal media with competing nonlinearities. The competing nonlinearities are induced by different physical processes and contribute to the overall nonlinear response of the medium. The competing nonlocal nonlinearities strongly affect properties of individual solitons. In particular, the velocity of dark solitons can be affected by the degree of nonlocality. The local quintic contribution to nonlocal cubic nonlinearity has profound effects on the bright and dark solitons in the regime of weak nonlocality. Recently we have revealed that the local quintic contribution to nonlocal cubic nonlinearity can support unique dark soliton solutions with their width being independent of the degree of nonlocality in the limit of strong nonlocality.

In this paper, we investigate the interactions of dark solitons in nonlocal media with competing nonlinearities. It is shown that the self-defocusing (self-focusing) competing nonlinearity will strengthen (weaken) the attractive interaction. These results obtained by variational approach are confirmed numerically with split step Fourier transform-based beam propagation.

9269-24, Session 5

Research progress on molecular orbital tomography based on high-order harmonic generation

Xiaosong Zhu, Meiyan Qin, Yang Li, PeiXiang Lu, Wuhan National Lab. for Optoelectronics (China)

When molecules are irradiated by intense femtosecond laser pulses, high-order harmonics are generated. It has been shown that, after recording the high-order harmonic spectra of molecules, the molecular orbital can be imaged by using a reconstruction algorithm. This is called the molecular orbital tomography (MOT) [Nature 432, 867 (2004)]. However, the existing method still has some problems for molecular orbitals with some structures, such as the asymmetric molecular orbitals and the ones with twofold mirror antisymmetry. To overcome these problems, we propose to control the high-order harmonic generation process by using the combined laser field with a strong driving pulse and its second harmonic control pulse. In this way, the one-direction recollision condition can be satisfied for the imaging of an asymmetric molecular orbital. We also developed a modified reconstruction algorithm to overcome the nodal plane problem in the imaging of molecular orbital with twofold mirror antisymmetry, by performing the reconstruction process in the rotating molecular frame instead of the fix laboratory frame.

Moreover, in the traditional MOT theory, the plane-wave approximation is applied, because of which the stability of MOT has been questioned since it was proposed. To address this problem, we developed a theory to retrieve the valence molecular orbital directly utilizing a molecular continuum

wave-function which takes into account the influence of the parent ion field on the continuum electrons. This is done by projecting the continuum wave-function on to plane wave basis set before performing the Fourier transform necessary for the reconstruction.

9269-25, Session 5

Controlled square optical bottle beam generated by symmetrical Airy beam induced by continuously-regulable phase

Denghui Li, Qian Yixian, Xueting Hong, Xiaowei Shi, Zhejiang Normal Univ. (China)

We theoretically and experimentally investigate the generation of square optical bottle, which are generated by double Airy beam induced by binary phase pattern. A regulable linear factor is introduced into phase function to modulate flexibly the size of optical bottle. Numerical simulations are performed and experimental results also show that Gaussian beam can be shaped into square optical bottle by a tunable binary cubic phase pattern. The linear factor can vary the region size of zero or low intensity of optical bottle. It is believed that the intriguing characteristic of square optical bottle can be applied in many applications such as optical tweezers, atom trapping and manipulating.

9269-26, Session 6

Extremely short pulses in VUV, XUV, and x-ray ranges via perturbation of resonant interaction (*Invited Paper*)

T. Akhmedzhanov, Texas A&M Univ. (United States); V. Antonov, Institute of Applied Physics (Russian Federation) and Texas A&M Univ. (United States); F. Vagizov, Texas A&M Univ. (United States) and Kazan Physical-Technical Institute (Russian Federation); R.N. Shakhmuratov, Kazan Physical-Technical Institute (Russian Federation); Yevgeny V. Radeonychev, Institute of Applied Physics (Russian Federation) and Texas A&M Univ. (United States); Olga Kocharovskaya, Texas A&M Univ. (United States)

An efficient method to produce extremely short pulses in VUV, XUV and X-ray ranges has been suggested recently [1-3]. It is based on strong perturbation of the resonant interaction of a quasi-monochromatic high-frequency radiation with a medium via modulation of the frequency or de-cay rate of the resonant atomic/nuclear transition. Modulation of the X-ray recoilless nuclear transition can be realized via vibration of the resonant medium due to the Doppler effect [1], while modulation of the VUV or XUV atomic transition frequency can be achieved via the time-dependent Stark shift produced by the strong control IR field [2]. Modulation of the decay rate can be produced via tunnel or barrier-suppressed ionization of an excited state of the resonant transition [3]. The possibility to form both trains and isolated subfemtosecond VUV pulses and attosecond XUV pulses in atomic gases has been predicted [2,3]. Trains of nearly transform-limited 14.4keV nanosecond pulses, constituting the frequency combs with a fixed frequency interval and phase-matched spectral components, have been produced and the possibility to control the waveforms of the individual gamma-photons has been demonstrated [1].

We will discuss also the appearance of the novel interference effects, and, in particular, modulation induced transparency, in the infrared pump - XUV probe experiments [4] and the recently suggested and demonstrated technique to produce single,

double and triple gamma-ray pulses [5].

References

1. F. Vagizov, V. Antonov, Y.V. Radeonychev, R. N. Shakhmuratov, O. Kocharovskaya, Nature, 508, 80, (2014).
2. V. A. Antonov, Y. V. Radeonychev, O. Kocharovskaya, Phys. Rev. A 88, 053849 (2013).
3. V. A. Antonov, Y.V. Radeonychev, O. Kocharovskaya, Phys. Rev. Lett. 110, 213903 (2013).
4. T. Akhmedzhanov, V. Antonov and O. Kocharovskaya, submitted.
5. F. Vagizov, R. N. Shakhmuratov, V. Antonov, Y.V. Radeonychev and O. Kocharovskaya, under preparation.

9269-27, Session 6

Sub-diffraction resolution optical imaging and manipulation of nitrogen vacancy center in diamond (*Invited Paper*)

Fang-Wen Sun, Univ. of Science and Technology of China (China)

As a potential candidate for quantum computation and metrology, the nitrogen vacancy (NV) center in diamond has attracted wide attentions. Here we show the experimental techniques to image and manipulate NV centers with sub-diffraction resolution. We have realized a quantum statistical image (QSI) of single quantum emitters with Hanbury Brown-Twiss interferometer. The quantum measurement method based on the quantum nature of antibunching photon emission has been developed to detect single particles without the restriction of the diffraction limit. By simultaneously counting the single-photon and two-photon signals with fluorescence microscopy, the images of nearby nitrogen-vacancy centers in diamond at a distance of 8.5 (2.4) nm have been successfully reconstructed. Furthermore, to manipulate the adjacent NV centers, we used the optimized optical manipulation of charge states of NV centers and developed the charge state depletion (CSD) microscopy with sub-diffraction resolution. The electron spin states dynamics of adjacent NV centers were selectively controlled and detected. The above experimental techniques can be used for nanoscale sensing for electromagnetic field and biology. Also they had high potentials in the study of the spin state quantum coherent dynamics with controllable environment and the interaction between coupled spin systems in diamond for nanoscale quantum information techniques.

9269-29, Session 6

Rogue wave statistics of emergent localized structures in spontaneous modulation instability

Shanti Toenger, FEMTO-ST (France) and Univ. de Franche-Comté (France); Goëry Genty, Tampere Univ. of Technology (Finland); Frédéric Dias, Univ. College Dublin (Ireland); Miro Erkintalo, The Univ. of Auckland (New Zealand); John M. Dudley, Univ. de Franche-Comté (France) and FEMTO-ST (France)

We use numerical simulations of the stochastic nonlinear Schrödinger equation (NLSE) to investigate the statistics of emergent intensity peaks in the chaotic field generated from spontaneous modulation instability (MI) excited from a continuous wave background with low amplitude noise. Analytic descriptions of Akhmediev breathers (AB), higher-order breathers, and Kuznetsov-Ma (KM) dynamics, are shown

to provide excellent local descriptions of the properties of spontaneously-generated localized structures in chaotic MI field. Good agreements are obtained by a direct comparison of the structures, as well as an indirect comparison of the peak intensity and the full width at half maximum (FWHM) relation from each spontaneously emergent localized structures, with the analytical ones. Several statistical analyses on the intensity of these spontaneously emergent soliton on finite background (SFB) solutions are performed and the results are compared, shown to be significantly different. We emphasize that the intensity peak detection over a full two-dimensional time-space window of the field evolution, rather than just at a fixed distance, is the appropriate measure to detect rogue wave events in the NLSE. The most extreme of the "rogue" events in the tails of the peak intensity histogram are exclusively associated with higher-order breather solutions of the NLSE, in particular the collisions of three breathers. The corresponding spectrums of these extreme collisions are vastly broadened, exceeding the regular spectral broadening due to MI, confirming the complex dynamics involved.

9269-30, Session 6

Multilayer-graphene micro-sheets: Ultralow-power active control of polarization-insensitive metamaterial-induced transparency

Cuicui Lu, Peking Univ. (China)

Electromagnetically-induced transparency analogue in metamaterials has great potential applications in the field of integrated photonic devices and ultrahigh-speed information processing chips. However, two obstacles restrict its practical applications, i.e., the metamaterial-induced transparency effect is highly incident polarization dependent and it is difficult to realize ultrafast and ultralow-power active control of metamaterial-induced transparency simultaneously. Here, we experimentally realize polarization-insensitive metamaterial-induced transparency by using a gold nanoprism trimer with a symmetrical configuration as the meta-molecule. Moreover, an ultralow-power and ultrafast all-optical control of metamaterial-induced transparency is realized by using multilayer-graphene micro-sheets/polycrystalline indium-tin oxide as the nonlinear medium. An ultralow threshold pump intensity of 4 kW/cm² and an ultrafast response time of 25.3 ps were reached simultaneously. Compared with previous reports, the threshold pump intensity is reduced by six orders of magnitude, while an ultrafast response time of picoseconds order is maintained. It attributes to three aspects. First, the tremendously enlarged thickness of multilayer-graphene micro-sheets results in exceedingly enhanced interaction between light and graphene. Second, the hot-electron injection from gold nanoprisms into ITO film and strong quantum confinement effect provided by the nanoscale ITO crystal grains make polycrystalline ITO possess excellent third-order optical nonlinearity. Third, there was enormous electric field distribution near the end faces of gold nanoprisms when the pump light wavelength is near to the surface plasmon polariton resonances. This work not only opens up the possibility for realizing quantum solid chips based on metamaterials, but also offers a strategy for constructing photonic materials with large nonlinearity and ultrafast response simultaneously.

9269-31, Session 6

Achieving 130mW@397.5nm single-frequency violet laser via cavity-enhanced frequency doubling with a tapered amplifier boosted 795nm DBR diode laser

Yashuai Han, Xin Wen, Jiandong Bai, Baodong Yang, Yanhua Wang, Jun He, Junmin Wang, Shanxi Univ. (China)

We present experimental results on the frequency doubling of a tapered amplifier (TA) boosted 795nm DBR diode laser. Using a 20-mm long PPKTP bulk crystal in a bowtie-type four-mirror ring cavity for enhancement frequency doubling, single-frequency 397.5 nm tunable violet laser with stable output power of 130 mW is realized with a mode-matched 795 nm laser power of 416 mW, corresponding to a doubling efficiency $\eta = 31\%$. In scanning mode, the maximum violet power raises up to ~ 180 mW. Scanning the injection of seeding DBR diode laser, we observed the saturation absorption spectroscopy (SAS) of D1 transitions of Rb-85 and Rb-87 atoms. This indicates that the 795 nm laser can be tuned continuously around 8.5 GHz. Thus, the tunability of 397.5 nm violet laser is proved.

We also briefly discussed the residual violet absorption induced thermal instability and dephasing, which limit the doubling efficiency and power stability in continuous-wave mode at high incident power. The stability of output power at 397.5 nm is measured at different fundamental laser power in continuous-wave mode. We observed the degradation of violet power at high incident power, which might be caused by thermal instability. The beam profile of violet laser is measured in agreement with TEM₀₀-mode Gaussian beam.

The generated 397.5 nm violet laser with moderate output power paves the road to the realization of squeezed vacuum state at 795 nm, based on the method of optical parametric oscillator (OPO). And further more, we can generate bright 795 nm tunable polarization squeezing light, which can be used to improve detection sensitivity of atomic magnetometer and atomic spin gyroscope. Meanwhile, when the fundamental laser is tuned to 793.676 nm, the output violet laser corresponds to $40\text{Ca}^+ 4S_{1/2} - 4P_{1/2}$ transition (396.838nm), which can be applied in laser cooling and manipulation of 40Ca^+ ions.

9269-41, Session 6

Recent progress of laser cooling for neutral mercury atom

Kangkang Liu, Ruchen Zhao, Xiaohu Fu, Jinmeng Hu, Yan Feng, Zhen Xu, Yuzhu Wang, Shanghai Institute of Optics and Fine Mechanics (China)

Mercury is the heaviest stable atom that could be laser cooled, and have a large nuclear charge number. So it has a distinct advantage in quantum precision measurement such as fine-structure constant α and permanent electric dipole moment. Due to its insensitivity of black body radiation, atomic mercury is a good candidate of optical clock. Here we report our recent development of laser cooling of neutral mercury atom. By cooling the mercury source to about -70 °C, an ultra-high vacuum system was realized to produce ultracold mercury atoms. The commercial frequency quadrupled semiconductor laser is locked on the cooling transition (1S₀-3P₁ transition, wavelength of 253.7 nm) by sub-Doppler frequency modulation spectroscopy. By the modification with feed-forward method, the UV laser becomes faster tunable and more stable. A folded beam configuration was used to realize the magneto-optical trap (MOT) because of the shortage of cooling laser power, and the ultracold mercury atoms were observed by fluorescence detection. All of six rich abundant isotopes have been all observed, the atom number is about

1.5 \times 10⁵ with density of 4.2 \times 10⁸ /cm³ for 202Hg. With optical shutter and the programmable time sequence, the temperature of ultracold atoms can be measured by time of flight method. To enhance the laser power, a 1015 nm fiber laser amplifier was developed, which can work at room temperature. After two stages of frequency doubling about 75 mW of 253.7 nm UV laser were generated, and the saturated absorption spectroscopy of mercury atom was also observed. More power of UV laser could help to trap more atoms in the future. These works laid a good foundation to realize the mercury lattice clock.

9269-32, Session 7

A flat lens by negative refraction in nonlinear optics (*Invited Paper*)

Jianjun Cao, Yuanlin Zheng, Xianfeng Chen, Wenjie Wan, Shanghai Jiao Tong Univ. (China)

A flat lens utilizing negative refraction contrasts sharply with traditional lenses for its unique ability to focus light at the nanoscale. In linear optics, such negative refraction can only occur in materials with designed spatial dispersion such as metals, meta-materials and photonics crystals, all of them are difficult to fabricate, suffer high loss and work only in microscale if for imaging applications. In nonlinear optics, alternative approaches to achieve negative refraction are proposed using third order nonlinearity, e.g. phase conjugation and four-wave mixing. However, up to now, few experiments have realized imaging functionality at the macro-scale. Here we demonstrate a new type of flat lens by negative refraction using the degenerate four wave mixing (4WM) process. We realize direct nonlinear image (of different color) of the original target behind a thin lens with a strong pump beam at frequency ω_1 and a probe beam at frequency ω_2 which carrying the original image. A signal beam at frequency $2\omega_1 - \omega_2$ is negatively refracted with respect to the input probe beam and form the final image. By using this effect, we further realize imaging in non-collinear and collinear configuration. Clear images formed by the 4WM wave are observed. Our methods show that a planar nonlinear medium can act as a flat lens, which is desired in imaging systems and may find further applications in super resolution imaging.

9269-33, Session 7

Dynamic dissipative cooling and polariton pair generation in strong coupling optomechanics (*Invited Paper*)

Yong-Chun Liu, Peking Univ. (China); Chee Wei Wong, Columbia Univ. (United States); Qihuang Gong, Yun-Feng Xiao, Peking Univ. (China)

Cooling of mesoscopic mechanical resonators represents a primary concern in cavity optomechanics, which enables not only the fundamental test of quantum theory and the exploration of the quantum-classical boundary but also important applications in quantum information processing and precision metrology. We demonstrate that cavity dissipation can be viewed as a resource. By dynamically controlling the cavity dissipation, it is able to significantly accelerate the optomechanical cooling process and reduce the cooling limit by 2 to 3 orders of magnitude. The dynamic dissipation control provides new insights for tailoring the optomechanical interaction and offers the prospect of exploring the quantum regime of mesoscopic mechanical devices.

Usually, the cavity optomechanical system is dominated by linear interaction, while the nonlinearity is extremely weak. We show the resonant enhancement of nonlinearity by orders of magnitude. We take advantage of light-enhanced linear optomechanical coupling to create the normal mode splitting, and through

frequency matching the nonlinear interaction becomes resonant, which greatly boosts the nonlinearity. Such nonlinear interaction offers a promising way for manipulating photons and phonons, and generating mesoscopic quantum states.

9269-34, Session 7

Observation of a novel two-state behavior in the supercontinuum generation of coupled saturable nonlinearity

Nithyanandan Kanagaraj, Pondicherry Univ. (India)

Supercontinuum generation (SCG) is the phenomenon of generating ultrabroad band spectrum has been the subject of intense research in the last few decades. Owing to its potential application in diverse field such as frequency metrology, optical coherence tomography, ultra-short pulse compression, sensor technique, fiber characterization etc., the SCG in the modern days has been recognized as the "White-light laser". The physics underlying SC generation is now generally well understood; the primary mechanism of generating broadband source is identified as soliton fission (SF) and modulational instability (MI). Former is the well-known mechanism of generating high quality broadband spectrum driven by the soliton dynamics. Latter is the MI induced SCG (MI-SCG), where the initial dynamics are governed by the noise, which lead to the breakup of the pulses similar to the case of SF. In principle, each material possesses an upper power threshold at which the nonlinear response of the medium saturates, such medium is referred as the saturable nonlinear medium (SNL). The power threshold at which nonlinear response of the medium saturates is known as the saturation power. Lyra et al, reported the different functional form of the SNL, out of which ESN is observed to generate the broadest spectrum at relatively shorter distance than the known kind of SNL. Thus, we study the MI induced SCG in the ESN system and report the novel two state behavior in the SCG. We identify and discuss the salient features of ESN and its cutting edge over the other functional form of saturable nonlinearities. An exact dispersion relation is obtained using LSA and the MI analysis is performed. Unlike the conventional Kerr type nonlinearity, the critical modulational frequency (CMF - frequency corresponding to the instability window) does not monotonously increases, rather behaves in a way, such that the increase in power increases the CMF up to the saturation power, and further increase in power decreases the CMF. This is due to the fact that the effective nonlinearity in ESN follows in a unique such that there exist two different powers at which the nonlinearity register same value. Because of which, the MI spectrum is identical at two different powers (i.e) input power (P) above and below saturation power (Ps). Following the MI analysis, we study the SCG numerically using split-step Fourier method. The evolution of spectral bands is studied for different input power and it is observed that the spectrum is nearly identical at two different input powers, corresponding to the constant nonlinear factor. Also, the maximum enhancement of SCG (SCG at shortest distance) is observed only at P = Ps and for all combination of powers the SCG gets inevitable suppressed. This we observe as the unique feature of ESN system and represent as the two state behavior in the SCG. Thus we brings to the light that the dynamics of SCG in ESN are indeed unique and offers rich information which could be useful in many applications.

9269-35, Session 7

Image blurring and deblurring using two biased photorefractive crystals in the frequency domain

Haiyong Gan, Chong Ma, Zhixu Sun, Tao Xu, Jianwei Li, Nan Xu, National Institute of Metrology (China); Jinjin

Wang, Feng Song, Nankai Univ. (China); Chuanxiang Sheng, Ming Sun, Li Li, Nanjing Univ. of Science and Technology (China)

In an imaging system based on a coherent source of moderate power density, images can be blurred when a biased photorefractive crystal is applied at the focal point of the imaging lens. In the frequency domain of the original images, the intensity patterns are diffracted through the photorefractive crystal with varied bias voltage. The high intensity region, which is usually the center or low frequency region of the intensity patterns, is more readily focused or defocused, resulting in blurred images in perception. Such blurred images could not be simply recovered by defocusing methods, which can only indistinguishably focus or defocus the whole intensity patterns. However, the blurred images may be deblurred to certain extent for recovery if a second photorefractive crystal with bias voltage is employed at the focal point of a tandem imaging system. The mechanism of deblurring is similar to that of blurring: the blurred images are transferred through the frequency domain again using an imaging lens, where the second biased photorefractive crystal diffracts the intensity patterns to revert the sensitive region where previously gets focused or defocused. In this work, theoretical analyses are presented in detail to explain the blurring-deblurring mechanism using two biased photorefractive crystals and compatible experimental results are obtained and illustrated. Considering the blurring and deblurring function subgroups of the experiment setup can be potentially developed into encryption and decryption units compatible with far field propagation, the technology presented herein may be promising to find applications in secure laser-based free-space communication systems.

Conference 9270: Optoelectronic Devices and Integration V

Thursday - Saturday 9 -11 October 2014

Part of Proceedings of SPIE Vol. 9270 Optoelectronic Devices and Integration V

9270-1, Session 1

LD and LED manufacture with nanoimprint process *(Invited Paper)*

Wen Liu, Univ. of Science and Technology of China (China)

As the application of nanophotonics increasing in various fields, the critical dimension becomes smaller and smaller, the pattern complexity becomes higher and higher. Nanoimprint Lithography (NIL), with the advantages of high resolution, low cost, high throughput and high flexibility, has become one of the most promising research interest in micro and nano fabrication.

We presentation a few improvements on NIL itself and demonstrates its application in DFB laser array and light emitting diode (LED) chip manufacturing. Including specific experiment program for each step of NIL: proposing the method of E-beam lithography combining with electroforming to fabricate the metal stamp in order to greatly increase the life of stamp. Soft mold ultraviolet (UV) imprint process is present to improve the yield of large area imprint. A multi-layer mask method is layer mask method developed.

Based on these technologies, monolithic integrated 4 channel DFB array with MMI coupled has been fabricated successfully. The average threshold current is less than 10mA, the side-mode suppression ratio(SMRS) is larger than 50dB. The monolithic integrated 16 channel DFB array with AWG coupled has also been fabricated. Another work is using NIL to fabricate nano patterned sapphire substrate (nPSS) in order to enhance the output efficiency. The photoluminescence (PL) output efficiency of the modified chip is nearly doubled compared with ordinary chip, and after packaging the output power increase by 22.6%.

9270-2, Session 1

Realization of low temperature transparent a-IGZO based TFT devices for flexible sensing transistors

Yuanjie Li, Xi'an Jiaotong Univ. (China); Yanghui Liu, Ningbo Institute of Materials Technology & Engineering (China); Feng Yun, Xi'an Jiaotong Univ. (China)

Transparent amorphous oxide semiconductors (TAOS) have attracted considerable technological interests because of their high mobility (10-30 cm²/Vs), large-area uniformity and low temperature deposition capability. In particular, amorphous InGaZnO (a-IGZO) is regarded as a promising active channel material for flexible thin film transistors (TFTs)-driven display and sensors. In this work, TFT devices with the bottom gate structure have been fabricated with the nanocolumnar SiO₂ film of ~800 nm by plasma-enhanced chemical vapor deposition (PECVD) as the gate dielectric layer on indium-tin-oxide (ITO) glass substrates. The ITO/SiO₂/IZO capacitor structure was also fabricated to characterize the capacitance-frequency properties of SiO₂ gate dielectric. A nickel shadow mask was placed directly above the SiO₂ dielectric layer with a distance of ~50 μm. Subsequently, a 147 nm thick IGZO layer was sputtered on the SiO₂/ITO/glass substrate using a commercial IGZO target at room temperature by RF sputtering. During deposition, the IGZO layer diffracts into the shadow region of the nickel mask and a thin IGZO channel layer is self-assembled simultaneously. Optical transmission spectra of the TFT arrays on glass substrates were characterized using a UV/Visible spectrometer system. The electrical characteristics of the devices were measured by a Keithley semiconductor parameter analyzer and precision impedance analyzer in dark. Enhancement-mode IGZO/SiO₂/ITO

transparent TFT devices with field effect mobility of 10.5 cm²/Vs, VT of 0.7 V, subthreshold swing (SS) of 70 mV/dec and Ion/Ioff of 1.5x10⁶ have been achieved in this work.

9270-3, Session 1

Characteristic optimization of 1.55-μm InGaAsP MQW lasers for direct modulation applications

Guo Fei, Chen Ji, Ruikang Zhang, Dan Lu, Institute of Semiconductors (China)

We have investigated 1.55-μm InGaAsP strained multi-quantum-well (MQW) lasers on InP for direct modulation applications using the commercial laser simulator PIC3D. The strained quantum-well differential gain is deduced from the material gain computation based on the 4?4 kp method considering valence mixing effect. The differential gain in InGaAsP strained multiple quantum well (MQW) lasers varies from 41.46 to 9.13 ?10⁻¹⁶ cm² within the carrier concentration from 1?10⁻¹⁸ cm⁻³ to 5?10⁻¹⁸ cm⁻³, showing a reciprocal attenuation with the carrier concentration. The physical mechanisms affecting the laser dynamic characteristics such as Auger recombination, vertical electron leakage effect including their dependence on temperature are considered in the simulation. The influence of barrier height is analyzed and a tradeoff has to be determined because too high barriers will result in more nonuniform carrier distribution in the active regions, increasing the Auger recombination rate severely and the vertical current leakage outside the QWs will increase dramatically at lower barrier height. The 1.55-μm DFB laser is fabricated and characterized its dynamic properties using 8510C Network Analyzer. The epitaxial structure was grown on an n-InP buffer via metal organic chemical vapor deposition (MOCVD). The MQWs composed of 6 compressive strain quantum wells and 7 barriers with the optimized bandgap of 1.03 eV were sandwiched between the two 100 nm InGaAsP separate confinement heterostructure (SCH) layers. A ridge waveguide structure is formed by wet-etching process. The threshold current of the DFB laser is around 30mA and the resonance frequency of 11 GHz and 3-dB bandwidth in excess of 14.5 GHz at 90mA injection current.

9270-4, Session 1

Simulation and experiment of 1310nm high-speed InGaAsP/InP EAM

Huitao Wang, Institute of Semiconductors (China)

We report systematic modelling of 1310 nm InGaAsP/InP electroabsorption modulators. The modulator is a reverse biased p-i-n diode, in which the MQW structure is composed of several InGaAsP/InGaAsP quantum wells. By a 3D finite element software PICS3D, we have comprehensively investigated the internal physical mechanism of the modulator, which includes the red shift of the absorption edge with the reverse bias and the absorption intensity, which could be derived from the normalized overlap integral between the energy levels for the electrons and the holes. The absorption spectrum on wavelength and the reverse bias voltage is analyzed, which provide us with both the extinction ratio and the transimission loss for a special operating wavelength. Key design parameters such as barrier height and quantum well width are optimized for extinction ratio, and confirmed by parallel experimental studies. What's more, the RF performance has been investigated in detail. The junction capacitance, the series resistance and the parasitic capacitance

(mostly the bonding pad) are studied systematically. A ridge structure model is analyzed for high speed performance, in which the important parameters, such as the ridge width, the cavity length, the area of the bonding pad and the thickness of polyimide (or BCB) under the bonding pad, are optimized for over 20GHz 3dB bandwidth. The cavity length is optimized by making compromise between the extinction ratio and the RF performance. In conclusion, the design parameter space of the 1310nm EAM has been systematically explored. Our work should provide a firm basis for 1310nm InGaAsP/InP EAM device design optimization for optical datacom applications.

9270-5, Session 1

InP-based terahertz devices and integrated circuits

Zhi Jin, Institute of Microelectronics (China)

The high carrier mobility and rich energy band alignment of InP-based materials make them a good choice in the applications for terahertz devices and circuits. We have designed and fabricated InP-based heterostructure bipolar transistors (HBTs), high electron mobility transistors (HEMTs) and Schottky diodes for terahertz monolithic integrated circuits. Through the energy band tailoring, the energy band spike between the base and collector of InP-based DHBT is eliminated. The current gain cutoff frequency (f_T) of more than 200 GHz and maximum oscillation frequency (f_{max}) of more than 300 GHz has been achieved. f_{max} reaches 600 GHz in the common-base configuration. The HEMT with lattice matched InGaAs channel has f_T of more than 270 GHz and f_{max} of 521 GHz, when the gate length is 80 nm. The Schottky diode has cutoff frequency of 4.5 THz. The devices have been used to design and fabricate terahertz monolithic integrated circuits (TMICs). Low noise amplifier, voltage-controlled oscillator, frequency multiplier, and mixer with operation frequency of more than 0.1 THz have been demonstrated.

9270-6, Session 1

Light manipulation for organic light-emitting diodes

Jianxin Tang, Soochow Univ. (China)

Organic optoelectronic devices, including organic light-emitting devices (OLEDs) and organic solar cells (OSCs) have been attracting considerable interest as next-generation lighting source and renewable energy applications. Significant progress on the device performance of OLEDs and OSCs with nearly 100% internal quantum efficiency has been made in recent years via the incorporation of new materials, morphology control, interface engineering, and device fabrication processes. However, further improvement in efficiency remains a daunting challenge due to limited light extraction or absorption in conventional device architectures. Here we report a universal method of optical manipulation of light by integrating a dual-side bio-inspired moth's eye nanostructure with broadband anti-reflective and quasi-omnidirectional properties for use in the performance improvement of organic optoelectronic devices of various material systems. Light out-coupling efficiency of OLEDs with stacked triple emission units is over 2 times that of a conventional device, resulting in drastic increase in external quantum efficiency and current efficiency to 119.7% and 366 cd/A at a luminance of 1,000 cd/m² without introducing spectral distortion and directionality. Similarly, the light in-coupling efficiency of OSCs is increased 20%, yielding an enhanced power conversion efficiency of 9.33%. The light-coupling enhancement in OLEDs and OSCs with MEN is the combined result of both the two-dimensional sub-wavelength structures and the continuously tapered morphology on the patterned surface with a superior gradient refractive index profile at the interface. The light is

therefore manipulated in all azimuthal directions over the entire emission wavelength range. The optical simulations provide an understanding of optical manipulation of light out-coupling and in-coupling process in OLEDs and OSCs. Note also that the method developed here brings about an invaluable advantage, which enables the processing compatibility with the high-throughput large-area roll-to-flat and roll-to-roll manufacturing techniques in future mass production of low-cost organic optoelectronic devices.

REFERENCE

1. L. Zhou, Q. D. Ou, J. D. Chen, S. Shen, J. X. Tang,* Y. Q. Li, S. T. Lee, *Sci. Rep.* 2014, 4, 4040.
2. J. D. Chen, L. Zhou, Q. D. Ou, Y. Q. Li, S. Shen, S. T. Lee, J. X. Tang,* *Adv. Energy Mater.* 2014, DOI: 10.1002/aenm.201301777.
3. P. P. Cheng, L. Zhou, J. A. Li, Y. Q. Li, S. T. Lee, J. X. Tang,* *Org. Electron.* 2013, 14, 2158-2163.
4. D. D. Zhang, X. C. Jiang, R. Wang, H. J. Xie, G. F. Ma, Q. D. Ou, Y. L. Chen, Y. Q. Li, J. X. Tang,* *ACS Appl. Mater. Inter.* 2013, 5(20), 10185-10190.

9270-7, Session 1

1.2-GHz gated single-photon detector with simple filtering

Junliang Liu, Chunfang Zhang, Yongfu Li, Shandong Univ. (China); Zuqiang Wang, Shandong University (China)

A 1.2 GHz gated infrared single photon detector based on InGaAs/InP avalanche photodiode (APD) is described. The APD is working in Geiger-mode, gated by 1.2 GHz sine wave signal with an amplitude of 10 V_{pp}, cooled by a 4-stage Peltier cooler with fan-cooling. A group of simple 12th order Bessel LC low-pass filters are used to suppress the capacitive response of the avalanche diode by > 60 dB. The detection efficiency, dark count probability and after-pulse probability of the detector were 15.46%, 7.85%¹⁰-6 /gate and 2.53%, respectively. The detector is based on commercially available inexpensive devices and can be manufactured easily.

9270-8, Session 2

Effect of surface ligands on the performance of organic light-emitting diodes containing quantum dots

Sergey V. Dayneko, National Research Nuclear Univ. MEPhI (Russian Federation); Dmitriy A. Lypenko, A.N. Frumkin Institute of Physical Chemistry and Electrochemistry (Russian Federation); Pavel Linkov, National Research Nuclear Univ. MEPhI (Russian Federation); Alexey R. Tameev, A.N. Frumkin Institute of Physical Chemistry and Electrochemistry (Russian Federation); Igor L. Martynov, Pavel S. Samokhvalov, Alexander A. Chistyakov, National Research Nuclear Univ. MEPhI (Russian Federation)

Quantum dots (QDs) have numerous applications in optoelectronics due to their unique optical properties. Novel hybrid organic light-emitting diodes (OLEDs) containing QDs as an active emissive layer are being extensively developed. The performance of QD-OLED depends on the charge transport properties of the active layer and the degree of localization of electrons and holes in QDs. In this regard, the type and the density of the ligands presented on the QD surface is very important.

We have fabricated OLEDs with a CdSe/ZnS QD active layer. The fabricated OLEDs contain hole and electron injection layers

consisting of poly(9-vinyl carbazole) and ZnO nanoparticles, respectively. The energy levels of these materials ensure efficient injection of charge carriers into the QD emissive layer.

In order to enhance the charge transfer to the active QD layer and thereby increase the OLED efficiency, the QD surface ligands (tri-n-octyl phosphine oxide, TOPO) were replaced with a series of aromatic amines and thiols. The substituents were expected to enhance the charge carrier mobility in the QD layer. Surprisingly, the devices based on the original TOPO-coated QDs were found to have the best performance, with a maximum brightness of 500 Cd/m² at 10 V. We assume that this is due to a decrease in the charge localization within QDs when aromatic ligands are used. We conclude that the surface ligands considerably affect the performance of QD-OLEDs, efficient charge localization in QD cores being more important for good performance than a high charge transfer rate.

9270-9, Session 2

Flexible amorphous oxide thin-film transistors on polyimide substrate for AMOLED

Zhiping Xu, Min Li, Miao Xu, Jianhua Zou, Junbiao Peng, Wang Lei, Yong Cao, South China Univ. of Technology (China)

Flexible substrates are tend to deform during heat/cold circle, thus cause misalignment problem in subsequent process. It is necessary to bond the flexible substrate on a rigid carrier substrate during the device fabricating process, and then de-bond the flexible substrate with the display device on it when the whole process is finished. But it's a big tradeoff of stably bonding the substrate on carrier which have to withstand ion bombardment, etchant corrosion, high temperature treatment, and UV exposure while the flexible substrate can be de-bonded easily when the fabricating process is finished. Many methods had been proposed to solve this problem, such as Laser Release technology developed by Phillip, heat generator technology by Samsung, adhesive technology by LG, and release layer technology by Industry Technology Research Institute. Here, we proposed an easy technology of de-bonding polyimide substrate from rigid carrier substrate. A surface isolation layer is deposited on the carrier prior to the coating of PI film. It will prevent forming of chemical bond between polyimide and the carrier. After fabricating process of MOTFTs with a highest temperature of 350°, the PI substrate with TFTs was de-bonded from the carrier substrate without significant deterioration in electrical properties.

9270-10, Session 2

Construction of novel host materials based on 1, 2, 4-thiadiazole and applications to phosphorescent organic light-emitting diodes

Lei Wang, Huazhong Univ. of Science and Technology (China)

A series of host molecules for phosphorescent organic light-emitting diodes (PhOLEDs) have been designed and synthesized via introducing 1, 2, 4-thiadiazole as an electron-transport moiety. By means of changing the side functional groups and linkage mode, the photophysical and electrochemical properties of these materials could be gradually tuned. Firstly, by incorporating 1,2,4-thiadiazole with typical hole-transporting carbazole moieties, a series of bipolar hybrids, o-CzTHZ (2,5-bis(2-(9H-carbazol-9-yl)phenyl)-1,2,4-thiadiazole), m-CzTHZ (2,5-bis(3-(H-

carbazol-9-yl)phenyl)-1,2,4-thiadiazole), and p-CzTHZ (2,5-bis(4-(H-carbazol-9-yl)phenyl)-1,2,4-thiadiazole), were synthesized. All the hybrids exhibit high glass transition temperatures ($T_g \geq 167^\circ$) and show good thermal and morphological stability in films. Moreover, a remarkable electroluminescent (EL) performance can be observed in devices hosted by o-CzTHZ with a high external quantum efficiency (?EQE) reaching up to 26.1%, which is still over 20% even at the high luminance of 10000 cd/m². Secondly, to further understand the relationship between the linkage mode of bipolar hosts and the device performances, another series of hybrid, 3-CzTHZ (3-(4-(9H-carbazol-9-yl)phenyl)-5-(4-(tert-butyl)phenyl)-1,2,4-thiadiazole) and 5-CzTHZ (5-(3-(9H-carbazol-9-yl)phenyl)-3-(4-(tert-butyl)phenyl)-1,2,4-thiadiazole), were synthesized. A direct comparison reveals that the thiadiazole/carbazole hybrids with the substituent situated at the 3- position of 1, 2, 4-thiadiazole show the merits of low turn-on voltage and high power efficiency, which are 2.6 eV and 94.8 lm/W, respectively, while the substitution at 5-position is more beneficial to achieve high current efficiency and external quantum efficiency, which are 93.9 cd/A and 26.3 %, respectively. Finally, we found 1,2,4-thiadiazole could also be used to construct excellent electron-transport type hosts. By fine tuning the electron transporting properties, devices hosted by BzCzTHZ (5-(2-(9H-carbazol-9-yl)phenyl)-3-bromo-1,2,4-thiadiazole) and DBzTHZ (3,5-bis(3-(1-phenyl-1H-benzo[d]imidazol-2-yl)phenyl)-1,2,4-thiadiazole) achieve maximum power efficiencies (?p, max) of 90.8 and 100 lm/W, corresponding to maximum quantum efficiency (?EQE, max) of 22.6 and 25.4%, respectively. Above all, 1, 2, 4-thiadiazole is an excellent moiety for constructing host materials to phosphorescent organic light Emitting diodes.

9270-11, Session 2

Electro-optical line cards with multimode polymer waveguides for chip-to-chip interconnects

Long Xiu Zhu, Hui Juan Yan, Jinhua Wu, TTM Technologies, Inc. (China); Marika P. Immonen, TTM Technologies, Inc. (Finland); Peifeng Chen, TTM Technologies, Inc. (China); Tarja Rapala-Virtanen, TTM Technologies, Inc. (Finland)

Power consumption and scaling the performance and quantity of electrical interconnects for data traffic inside boards and backplanes are one of the critical barriers envisaged in next-generation Data Center (DC) and High-Performance Computing (HPC) applications.

In this paper, we report developments of electro-optical PCBs (EO-PCB) with low-loss (<0.05dB/cm) polymer waveguides. The paper focuses emulator boards designed to simulate a line card product with embedded optical chip-to-chip and chip-to-module lines. Our results shows successful fabrication of complex waveguide structures part of hybrid EO-PCBs utilizing production scale process on standard board panels. Test patterns include 90° bends of varying radii (40mm - 2mm), waveguide crossing with varied crossing angles (90°-20°), cascaded bends with varying radii, splitters and tapered waveguides. Full ranges of geometric configurations are required to meet practical optical routing functions and layouts. Moreover, we report results obtained to realize structures to integrate optical connectors with waveguides. Experimental results are shown for MT in-plane and 90° out-of-plane optical connectors realized with coupling loss < 2dB and < 2.5 dB, respectively. These connectors are crucial to realize efficient light coupling from/to TX/RX chip-to-waveguide and within waveguide-to-fiber connections in practical optical PCBs.

Moreover, we show results for fabricating electrical interconnect structures e.g. tracing layers, vias, plated vias top/bottom and through optical layers. Process compatibility with accepted practices and production scale up for high volumes are

key concerns to meet the yield target and cost efficiency. Results include waveguide characterization, transmission loss, misalignment tolerance, and effect of lamination. Critical link metrics are reported.

9270-12, Session 2

Dual gratings for broad band light trapping in thin film solar cell

Shouqiang Zhang, Univ. of Electronic Science and Technology of China (China); Xiaowei Guo, Photoelectric Information Institute (China)

The conversion efficiency of thin film silicon solar cell is still much below that of silicon solar cell due to low optical absorption. Light trapping techniques can enhance the optical absorption in solar cells. To enhance absorption efficiency in thin film silicon solar cells, here we investigate a dual grating light trapping structure in which top grating acts as antireflection layer and bottom grating as light diffusion layer. All the calculations are based on the rigorous coupled wave theory. The influence of each grating period, depth and duty cycle on light absorption was firstly studied. We found the solar cell with only top grating perform good absorption in the blue and green light while the cell with bottom grating exhibit better in red light. Combining top and bottom grating leads to the cell obtaining a significant absorption improvement. After optimizing the dual grating structure, the cell can achieve the absorption enhancement over entire solar spectrum approaching to the theory limit. The parameters are: when silicon height of 2000nm, top grating height of 180 nm, top grating cycle of 300nm, bottom grating height of 180nm and bottom grating cycle of 600nm.

9270-14, Session 3

Comparison of the amplification potentials in silicon-core and silicon-nitride-core Er³⁺polymer hybrid slot waveguides (Invited Paper)

Samuel Serna, Weiwei Zhang, Xavier Le Roux, Laurent Vivien, Eric Cassan, Institut d'Électronique Fondamentale (France)

Optically pumped Er³⁺ doped Al₂O₃ waveguide amplifiers have been developed in recent years with net gain in the order of 15dB. High performance organic waveguides doped with Er³⁺ nanoparticles have been also reported with net gain of around 10dB/cm. Nevertheless, several open issues still remain uninvestigated, including the best pumping scheme, i.e. 1.48μm versus 0.98μm in silicon-compatible waveguides and the most appropriate waveguide geometries to enhance the gain while maintaining the linear losses at a low level. In this context, CMOS compatible Er³⁺ doped polymer hybrid slot waveguides with either a high (Si/SiO₂) or a medium (Si₃N₄/SiO₂) core/cladding index contrast have been investigated by using a 4-level and 6-level spectroscopic models pumping at wavelength of 1.48μm and 0.98 μm, respectively. In the Si₃N₄ scheme, double slot waveguides have been found to be an alternative option to simultaneously confine the λ=980nm and the λ=1530nm wavelengths in single-mode conditions. This configuration allows integrating Yb co-doped Er³⁺ polymers which strongly enhance its effective absorption cross-section. On the other hand, high index contrast silicon slot waveguides (i.e. with a Si core) can only be used at the pumping wavelength of 1.48μm due to the strong Si light absorption at λ=0.98μm. A comparison between the Si and Si₃N₄ amplifiers under 1.48μm pump wavelength in a single slot disposition shows net gains around 20dB when considering a similar linear loss level of 5dB/

cm. The required slot waveguide lengths for Si/Si₃N₄ are then around 40mm. The main difference between the two options is due to silicon nitride's lower index contrast properties: in Si₃N₄ waveguides, around 4 times larger pump power is required to obtain the same optical net gain. On the contrary, in the 0.98μm pumping regime, due to Yb³⁺ sensitization, the pumping power required in Si₃N₄ double slot waveguides for optimum performance is reduced more than 10 times for the same gain as Si and Si₃N₄ single slot waveguide with a pumping beam of 1.48μm.

9270-15, Session 3

Analysis of wavelength detuning, injected power, and injected mode effect on Fabry-Perot laser diode

Dongying Zhang, Nanjing Univ. (China); Bikash Nakarmi, Nanjing Univ. (China) and KAIST (Korea, Republic of); Xuping Zhang, Nanjing Univ. (China)

Basic characteristics of wavelength locked FP-LD are analyzed theoretically and results are presented by the simulation of a theoretical model of the FP-LD. We use fourth-order Runge-Kutta to solve the rate equation of injection locked FP-LD which has been studied by many researchers. But most of the research are either focused only on wavelength detuning or modes of injected beam. Hence we analyze the effect of wavelength detuning, modes of injected beam, injected power on the FP-LD. With these analysis we can conclude the required wavelength detuning, mode for injection, required injected beam power and others depending upon applications. We model FP-LD theoretically and analyze output spectrum without injection locking which contains photon number of each mode and carrier density along with gain spectrum. We added the injected beam term to the rate equation in one or more modes to obtain the spectrum of wavelength locked FP-LD. Injection locked phenomena is observed with sufficient on/off contrast ratio. Various parameters such as wavelength detuning, injected beam power, bias current, temperature and injected modes are changed to analyze output power and spectrum. Analysis on hysteresis width is done by changing the wavelength detuning, and injected mode number to see the effect on hysteresis width which is important to find proper wavelength detuning, injected power and mode of injected beam required for the different application such as switching, memory and others. The analysis will help to find effective parameters to meet the demand of power effective optical devices for future optical networking system.

9270-16, Session 3

Spectrum width control of square-wave pulses in a passively mode-locked fiber laser

Mei Li, Lixin Xu, Guoliang Chen, Chun Gu, Xianming Zhang, Biao Sun, Jian Lin, An-Ting Wang, Univ. of Science and Technology of China (China)

The Yb-doped passively mode-locked figure-8 fiber laser generates square-wave pulse with narrow spectrum width, typical 3-dB bandwidth less than 0.1nm. While the Yb-doped NPR fiber laser can generate square-wave pulse much wider than the figure-8 laser. It's strange that the two passively mode-locked fiber laser are all based on the additive pulse mode-locking and all generate square-wave pulse, however, the square-wave pulse generated by the two lasers have distinctly different spectrum. To explain this phenomenon we added couplers with different coupling ratio to the bidirectional ring of a figure-8 fiber laser and analyzed the laser output. The results show that a higher output

coupling ratio leads to square-wave pulse with lower peak power and narrower spectrum bandwidth. We think that a higher output coupling ratio leads to stronger peak power clamping effect, thus the peak power of the square-wave pulse gets lower and the corresponding spectrum band width is narrower due to a weaker nonlinear effect.

9270-17, Session 3

All-fiber tunable multiwavelength erbium-doped fiber laser based on nonlinear optical loop mirror and Lyot birefringence fiber filter

Jiajun Tian, Harbin Institute of Technology (China); Yuan Li, Harbin Institute of Technology (China); Mingran Quan, Harbin Institute of Technology (China)

We have proposed and demonstrated an all-fiber tunable multiwavelength erbium-doped fiber laser based on the nonlinear optical loop mirror (NOLM), and Lyot birefringence fiber filter (BFF). Accurately, the peak location of the lasing line can be tuned in the free spectrum range (FSR) of the Lyot BFF. The intensity-dependent loss (IDL) induced by the NOLM is used to suppress the mode competition of erbium-doped fiber, and guarantees stable multiwavelength operation at room temperature. The number and the spectral region of the lasing lines can be controlled by regulating the working state of the NOLM. Moreover, a fine controlling the lasing lines number in a fixed wavelength is achieved by changing the pump power. The results may find useful applications in optical communication and fiber sensing.

9270-18, Session 3

All-fiber bidirectional mode-locked and wavelength-tunable ring laser by using graphene

Jian Lin, Univ. of Science and Technology of China (China)

An all-fiber bidirectional passively mode-locked laser with a graphene-based saturable absorber has been presented. Two stable pulse trains in opposite directions are delivered simultaneously from the ring cavity. The counterpropagating pulses show different central wavelengths, pulse durations, and repetition rates. By using a tunable filter, the central wavelengths of both pulses can be tuned in a wide range. Our results show that the graphene mode locked fiber lasers provide a compact, user friendly and low cost wavelength tunable bidirectional ultrashort pulse source

9270-19, Session 3

Tunable multiwavelength erbium-doped fiber laser based on a modified dual-pass Mach-Zehnder interferometer and nonlinear optical loop mirror

Jiajun Tian, Mingran Quan, Yuan Li, Harbin Institute of Technology (China)

To achieve fine tunable operation, an all-fiber multiwavelength erbium-doped fiber laser based on a modified dual-pass Mach-Zehnder interferometer (MDMZI) and a nonlinear optical loop mirror (NOLM) is proposed and demonstrated. The tunable operation of the channel-spacing switching, the peak location

adjusting, the wavelength tunability and the spectral region controlling can be perfectly realized by regulating polarization controllers and the pump power. To be more precise, up to 27 stable lasing lines with 0.3 nm spacing and 14 lasing lines with 0.6 nm are obtained at room temperature via controlling the working state of MDMZI. Moreover, the number and the spectral region of the lasing lines can also be accurately controlled by adjusting the polarization controller and QWP of the NOLM.

9270-20, Session 3

A wavelength conversion circuit for active multi-spectral detection

Yanyan Kang, Shaokun Han, Baowei Li, Wenzhe Xia, Beijing Institute of Technology (China)

Active multi-spectral detection technology is used to acquire the information of the targets such as spectrum, distance, intensity, and location and so on. So the active multi-spectral detection technology becomes one of the main trends of development of detection system in the future. Based on the analyzing the theory of streak tube lidar active multi-spectral detection system, we design a wavelength conversion circuit which can be applied to implement wavelength conversion in the streak tube lidar in the active multi-spectral detection. Through the O-E-O conversion mode, the wavelength of laser echo signal which contains the target information is transformed into another wavelength which represents the spectral peak response wavelength of the stripe tube photocathode. The simulation results show that when the input laser echo signal wavelength is 1.55 μ m, and the after-converted wavelength is 0.85 μ m, the photon conversion efficiency can reach 2.2×10^{-6} , the signal to noise ratio can reach 19.3 dB. And when the target distance or the signal bandwidth increases, the signal to noise ratio will decrease accordingly.

9270-21, Session 4

Performance improvement for long range BOTDR sensing system based on high extinction ratio modulator (Invited Paper)

Yixin Zhang, Xuelin Wu, Lan Xia, Zhoufeng Ying, Xuping Zhang, Nanjing Univ. (China)

Billouin optical time domain reflectometer (BOTDR) sensing systems are capable of measuring the temperature and strain along the entire length of sensing fiber with one-end access. Generally, an electro-optic modulator (EOM) is used to convert a continuous-wave light into short probe pulse. However, the leakage light the EOM induced by its finite extinction ratio (ER) may degrade the performance of BOTDR sensing system, especially for long range measurement. In this paper, a novel configuration of modulator based on synchronous EOM and optical switch (OS) is presented. The proposed configuration has the following advantages. First, the insert loss of OS is less than 1dB, therefore the feedback signal is almost 20dB higher than traditional method, resulting in higher ER locking speed and stability. Second, most power of probe pulse is removed from feedback. Therefore the input of stabilizer will mainly consist of leakage light, which can avoid ER variation caused by the impact response of probe pulse, especially when the ER value is already in high level. Third, the isolation ratio of OS itself can provide extra suppression on leakage light, which is capable to obtain high ER probe pulse together with the EOM. Experimental results have shown that the performance of a long distance BOTDR sensing system can be improved with the proposed high ER modulator. At the end of a 48.5km sensing fiber, the maximum temperature uncertainty of has been reduced from 5.2% to 0.8% under 25m spatial resolution after we improved the ER of probe pulse from 35dB to 65dB.

9270-22, Session 4

Research of range image on non-scanning LADAR based on APD arrays

Baowei Li, Shaokun Han, Beijing Institute of Technology (China)

Compared to scanner imaging lidar, non-scanning LADAR plays a more prominent role in the militarily imaging scenarios. Non-scanning LADAR has many advantages, such as structure simplicity, high reliability, imaging efficiency and etc. However the range accuracy is low. This paper proposes a technique to use a designed delay line module in the APD array LADAR systems, which could significantly improve the range accuracy in all channels. A semiconductor laser is used as light source. A 5*5 APD array detector is adopted as the sensitive unit. A 25 channel parallel amplifier circuit is designed to process the signal with bandwidth 240MHz. Field Programmable Gate Array (FPGA) is used to process these 25 signals paralleled, with a delay line module designed, to significant improve the ranging accuracy. The clock frequency of FPGA is 400MHz with accuracy 2.5ns. The delay lines module are used to measure part of pulse flying time, which is shorter than the clock cycle and could not be directly measured by the clock, and that is the cause of the ranging accuracy. Every delay cell is 46ps, total timing accuracy is less than 500ps. By using above technique, a short distance imaging experiment is presented and get the 5*5 pixels range image. The result is analyzed together with the factors, which influence the accuracy of ranging image, it shows the ranging accuracy of each pixel is 10cm. And Some advanced methods are proposed to improve the accuracy of the system in the future.

9270-23, Session 4

Compact microfluidic sensing by detecting effective phase shift in fiber Bragg grating

Guanghui Wang, Minghui Tang, Nanjing Univ. (China); Ho-Pui A. Ho, The Chinese Univ. of Hong Kong (Hong Kong, China); Xuping Zhang, Nanjing Univ. (China)

A compact microfluidic refractive index sensor fabricated by drilling hole in the middle section of a fiber Bragg grating (FBG) is reported herein. The laser-drilled hole provides a microfluidic channel for the aqueous sample to pass through while at the same time permits coupling of the interrogating light to detect the target analyte. The reported sensor takes advantage of the fact that a small phase shift in the central region of the grating will result in a very sharp peak in the FBG stop-band. The phase shift can be related to a range of possible perturbations inside the microfluidic channel, including passage of cells, beads and a shift in the concentration of certain fluidic component. The amount of wavelength shift of the peak in the FBG stop-band represents the change in the refractive index inside the microfluidic channel. Simulation results indicate very favorable sensor signal characteristics such as large wavelength shift and sharp reflection dips. The reported microfluidic phase shift FBG sensor could be a good candidate for portable flow cytometry applications.

9270-24, Session 4

An integral imaging method for depth extraction with lens array in an optical tweezer system

Shu-Lu Wang, Wei-Wei Liu, Univ. of Science and

Technology of China (China); An-Ting Wang, Univ of Science and Technology of China (China); Yin-Mei Li, Hai Ming, Univ. of Science and Technology of China (China)

In this paper, an integral imaging method for depth extraction and optical tweezers are integrated in a single microscopy system by inserting a lens array into the optical train, and the optical performance of the system is analyzed. In which, the optical tweezer subsystem is built by using a solid laser (532nm), and the modulated, focused beam of light form a light trap to capture tiny specimens (0.5µm diameter). Otherwise, the microscopic integral imaging subsystem is composed of a microscope objective (100x, oil), a lens array (150x150 array with 0.192mm unit size and 9mm focal length) and a high resolution (1280x1024) monochrome charge coupled device (CCD). Pre-magnified by the microscope objective, the specimens captured by the light trap and the ambient of specimen cell form multiple images through the lens array on the CCD. A single photograph of a series of multiple image units have recorded perspective views of the specimens, and the differences between adjacent image units is synthetically analyzed to extract the depth information of the field. Aberration is considered as an interference factor hence a filter is used against the chromatic aberration. In addition, a hemocytometer is used as a frame (with the spatial frequency of 20 /mm), and with the optical tweezers' measurable translation, monochromatic aberration such as curvature and distortion of the field has been corrected. With the 100x microscope objective, and CCD with 10µm size pixels, the depth resolution of the system can reach to 0.8µm. The ability that the depth calculated from a single graph allows further research of real-time 3D information extraction of moving and living biological specimen controlling by optical tweezers.

9270-25, Session 4

Closed-loop experiment of resonator integrated optic gyro with triangular wave phase modulation

Yichuang Tang, Huilan Liu, Yinzhou Zhi, Lishuang Feng, Junjie Wang, BeiHang Univ. (China)

A closed-loop RIIOG scheme based on triangular wave phase modulation is proposed. The closed-loop system includes a distributed feedback fiber laser (DFB-FL), an isolator, an integrated optical modulator (IOM) which combines the Y-branch, polarizer, and phase modulators (PM1/2) into a chip, an optic waveguide ring resonator (OWRR), two InGaAs PIN photodetectors (PD1/2), a frequency locking module and a feedback/signal detection module. The light wave is split into two beams by the Y-branch, one passes through PM1, the other passes through PM2, both of which are modulated by triangular wave, and then launch into the OWRR, where one light wave travels clockwise (CW) and the other counterclockwise (CCW). The output light waves are detected by PD1 and PD2. The output of PD2 is demodulated by the frequency locking module to lock the frequency of the DFB-FL to the CCW resonant frequency. The output of PD1 is demodulated by the feedback/signal detection module to generate digital serrrodyne wave with a frequency resolution of 0.023 Hz, which is superimposed upon the modulation triangular wave to compensate the resonant frequency-difference between the CW and CCW light waves in the OWRR. The frequency control word (FCW) is proportional to the shifted frequency, which is readout as the gyro output.

Experimental results show that the proposed scheme can realize the closed-loop RIIOG employing only an IOM, which has the advantage of miniature size. A bias stability of 0.42°/s is achieved. Moreover, good linearity and large dynamic range are also experimental demonstrated.

9270-26, Session 4

Resonator integrated optical gyro employing external cavity laser diode

Lishuang Feng, Ming Lei, Yinzhou Zhi, Junjie Wang, BeiHang Univ. (China)

Resonator integrated optical gyro (RIOG) incorporates the characteristic of no moving parts of optic gyro and the micro fabrication technique of MEMS, which is widely investigated. The conventional basic structure of the RIOG based on ECLD includes ECLD, optical isolator (ISO), integrated optical modulator (IOM) which combines the Y-branch, polarizer, and phase modulator (PM) into a chip, IOR made of SiO₂, InGaAs optoelectronic detector (PD), and a signal detection/control module. The light wave is split into two beams by Y-branch, which are modulated by triangular waveforms. Then launched into IOR through coupler C3, where one light wave travels CW and the other one CCW. Then the output light waves are directed into PD1 and PD2 through couplers C2 and C1, respectively. Which are demodulated by the signal detection/control module to lock the frequency of the ECLD to the CCW resonant frequency. The demodulated signal from CW provides a RIOG output. The structure of the RIOG based on current modulation is shown, the PMs are removed and the ECLD is driven by square waveforms to modulate the light wave frequency. The RIOG test setup based on ECLD is constructed and the phase and current modulation scheme, are selected. The performances, such as zero bias stability and dynamic range, are tested. We can get the conclusion that the former has a advantage of high accuracy, but the latter has a advantage of miniature size.

9270-13, Session Post

Colour tunable micro-display based on LED matrix

Bin Xue, Hua Yang, Institute of Semiconductors (China)

LEDs are the subject of intensive research activity which is driven by the prospects as a promising light source. Thanks to the development in epitaxial growth, chip fabrication and packaging of LEDs, emission spectral of the device is capable of covering the visible spectrum. Besides lighting, LEDs offer a wide range of potential applications including display. As we all know, display technology is developing tremendously and the market is huge. LED has been playing an important role in the deployment of LCD display as back light source. Due to their characteristics?potential application of LEDs in display market can be expanded. In contrast with LCD, LEDs display has better contrast ratio, higher response rate etc which makes LEDs along with other self-illumination technologies an ideal candidate in making display panel.

Due to the popularization of HD and Ultra HD standard, display panel with better image quality is needed which means the number of pixels of the panel needs to be increased and the size of each pixel needs to be reduced.

As far as full-color LED display panel is concerned, typical pixel sizes range from 1mm to 25mm and the pixel is based on conventional SMD packaged LED product. The technology basically requires the application of chip moulder and wire bonder to assembly a large amount of SMD packaged full-color LED modules onto a substrate to form the display panel. In this paper, we demonstrated a color tuneable micro display panel based on a 16*16 and 32*32 LED matrix with typical pixel size of 0.7 and 0.5mm respectively. Benefit from the application of COB package, a micro LED matrix display panel was obtained by mounting LEDs directly onto an isolating substrate with metalized pads before the matrix was connected to control unit. Comparable brightness of the LED matrix emitting at different colors was achieved by adjusting the input current.

9270-47, Session Post

Comparison of the photo-emission behavior between negative electron affinity InGaAs and GaAs photocathodes

Muchun Jin, Benkang Chang, Nanjing Univ. of Science and Technology (China); Zeng Yugang, Changchun Institute of Optics, Fine Mechanics and Physics (China); Yijun Zhang, Jing Guo, Nanjing Univ. of Science and Technology (China)

In view of the important application of vacuum semiconductor materials in night vision system, two types of reflection-mode photocathodes—extended red InGaAs photocathode and standard GaAs photocathode were prepared by metal organic chemical vapor deposition. Differences in photoemission behavior, namely the activation process and quantum efficiency decay have been investigated using a multi-information measurement system. The activation experiment shows that a surface negative electron affinity state for the InGaAs photocathode can be achieved harder than GaAs photocathode by the Cs-O two-step activation. Besides, a quantum efficiency decay experiment shows that the InGaAs photocathode exhibits a shorter lifetime in a demountable vacuum system than the GaAs photocathode. The striking difference in the activation process and quantum yield decay between the InGaAs and GaAs photocathodes can be explained by comparing of the energy band structures and the state of negative electron affinity. The experimental phenomenon indicates that as the band gap decreases, the surface potential barrier to vacuum increases, requiring a bigger change in the vacuum level position relative to the bulk conduction band minimum to achieve a negative electron affinity emitter. This implies that the narrow band gap InGaAs photocathode doesn't need a long lifetime to return to a positive electron affinity state in comparison with the wide band gap GaAs photocathode.

9270-48, Session Post

Spin velocity measurement for space debris from periodic signatures with active and passive illumination

Xue Li, Ming Li, Liang-liang Wang, Beijing Institute of Tracking and Telecommunication Technology (China)

Space debris is a hidden threat for space craft, and even centimeter-level debris may cause a great damage to space craft. Measurement for spin velocity is an important method for identification of space debris from functioning crafts as space debris usually has a bigger spin velocity because of control failure. Ground-based observation uses CCD to get the target images, and the obtained light curve shows some signatures about periodicity and then spin velocity, which helps to identify the debris from functioning space craft. Active illumination and passive illumination are different ways to measure spin velocity. Limited by the illumination angle and locations of observation stations, a single station can only measure debris of a certain orbit arc. A possible solution is combining stations of different locations to get the target images of more orbit arcs. In this paper, space debris of different properties and conditions are both theoretically analyzed and simulated with a ray tracing method by Tracepro. Positions of stations and the sun are converted into the target body coordinate system and the converting matrix shows the change of target attitude and its scattering cross section. Based on the converting matrix, the scattered light intensity received by CCD on ground stations is theoretically calculated. Here, light sources for active and passive measurement are laser of 532nm and the sun, respectively. In the ray tracing simulation method, light is presented by a visible way as light rays, and only some basic laws of geometrical optics and

material properties of targets are needed. Light intensity can be symbolized by the number of received rays. Observing stations of Kunming (China), Herstmonceux (UK) and Greenbelt (USA) are used as scattered stations to get light curves of debris of different orbit arcs. Six orbital elements are used to get the orbits of debris, and some different altitudes (taking debris of NORAD 17590, 20509, 23769 for examples) are simulated. Standard atmosphere model is used to reduce the atmospheric absorption and refraction, and in the simulation, a piece of frosted glass of a certain absorption coefficient and refraction index is set to simulate the atmospheric influence. For comparison, a three-axis stabilized cooperative satellite is simulated with both active and passive measurement. And different spin velocities, different surface materials (take Aluminum alloy, Titanium alloy, Ti3Al, Nb5Si and CMC as typical space materials), and different sizes are simulated. Simulation results show a consistency of light curves with theoretical results, which has periodic signatures resulted from the periodic change of scattering cross section. Although there are some periodic signatures for cooperative targets, the periodic change is much slower than debris. And different visible signatures for different target materials provide a method to recognize different debris. Spin velocities obtained from stations of different locations verifies the possibility of multi-station measurement and full-orbit measurement.

9270-49, Session Post

Passively mode-locked Er-doped fiber laser based on a semiconductor saturable absorber mirror

Meng Wang, Cong Chen, Qi Li, Kaiqiang Huang, Haiyan Chen, Yangtze Univ. (China)

Ultrashort pulses have versatile applications in high speed all optical communication, ultrafast spectroscopy, biomedical diagnostics, medicine, military, optical information processing and laser remote sensing. Passively mode-locked fiber lasers with the advantage of compact and flexible geometry construction, low cost and stable pulses output with the pulse duration of sub-ps, have attracted a lot of attention in recent years. Nonlinear polarization rotation (NPR), nonlinear amplifying loop mirror (NALM) and saturable absorbers (SAs) are the mainly techniques to achieve the passive mode-locking in fiber laser. Recently, the mainstream of mode-locking is using the SAs, a device that possesses an intensity-dependent response to favor optical pulse formation over continuous-wave lasing. The common SAs are semiconductor saturable absorber mirror (SESAM), single-wall carbon nanotubes (SWCNTs), and graphene. In our previous work, we did some theoretical and experimental researches on ring cavity CW and Q-switched fiber lasers with a SESAM SA.

In this presentation, a ring cavity passively mode-locked fiber laser using a SESAM as SA and a fiber Bragg grating as dispersion compensator, is proposed and experimental demonstrated, its output performance is discussed. Stable mode-locking spectrum with 3dB bandwidth of 3.2nm, center wavelength of 1555.8nm and average output power of 0.32mW is observed at the pump power of 110mW. The pulse repetition rate is 25 MHz, as determined by the cavity length of ~8m. In case of the output sech² transform-limited pulses, the output pulses duration of 0.79ps and single pulse energy of 12.64pJ are obtained.

9270-50, Session Post

Theoretical revision of quantum efficiency formula for thin AlGaAs/GaAs photocathodes

Cheng Feng, Nanjing Univ. of Science and Technology

(China)

With the advantages of high quantum efficiency, low dark current and narrow energy spread, negative electron affinity (NEA) AlGaAs/GaAs photocathodes have been widely applied in the weak light detection and high energy physics. Modern low-light-level night vision device is developed toward the features of high sensitivity and broadband spectral response. Besides, achieving high quantum efficiency and good stability for thin photocathodes is an important topic in the research of favorable electron source. However, there exist the limitations of conventional quantum efficiency formulae for both transmission-mode (t-mode) and reflection-mode (r-mode) exponential-doped GaAs photocathodes in some cases. The revised quantum efficiency formulae of the t-mode and r-mode photocathodes have been solved from the one-dimensional continuity equations, wherein the built-in electric field in the GaAs layer and the electrons generated from the AlGaAs layer are considered. According to the revised formulae, we analyze the effects of some relational performance parameters, such as the thicknesses of GaAs layer and AlGaAs layer, and the interface recombination velocity on the quantum efficiency for t-mode and r-mode photocathodes in combination with the conventional formulae. The results show that the main contribution of photoelectrons generated from AlGaAs layer to quantum efficiency in the shortwave (i.e. high incident photon energy) region, depends on the factors including cathode thickness and interface recombination velocity. Investigation into the influence of AlGaAs layer to the quantum efficiency would provide theoretical guidance for the improvement of blue-extended effect of t-mode AlGaAs/GaAs photocathodes, which facilitates the ability of target detection in the desert terrain or marine environment.

9270-51, Session Post

Efficiency analysis of parallelized wavelet-based FDTD model for simulating high-index optical devices

Rong Ren, Jin Wang, Xiyan Jiang, Yunqing Lu, Ji Xu, Nanjing Univ. of Posts and Telecommunications (China)

The finite-difference time-domain (FDTD) method, which solves time-dependent Maxwell's curl equations numerically, has been proved to be a highly efficient technique for numerous applications in electromagnetics. Despite the simplicity of the FDTD method, this technique suffers from serious limitations in case that substantial computer resource is required to solve electromagnetic problems with medium or large computational dimensions, for example in high-index optical devices. In our work, an efficient wavelet-based FDTD model has been implemented and extended in a parallel computation environment, to analyze high-index optical devices. This model is based on Daubechies compactly supported orthogonal wavelets and Deslauriers-Dubuc interpolating functions as biorthogonal wavelet bases, and thus is a very efficient algorithm to solve differential equations numerically. This wavelet-based FDTD model is a high-spatial-order FDTD indeed. Because of the highly linear numerical dispersion properties of this high-spatial-order FDTD, the required discretization can be coarser than that required in the standard FDTD method. In our work, this wavelet-based FDTD model achieved significant reduction in the number of cells, i.e. used memory. Also, as different segments of the optical device can be computed simultaneously, there was a significant gain in computation time. Substantially, we achieved speed-up factors higher than 30 in comparisons to using a single processor. Furthermore, the efficiency of the parallelized computation such as the influence of the discretization and the load sharing between different processors were analyzed. As a conclusion, this parallel-computing model is promising to analyze more complicated optical devices with large dimensions.

9270-52, Session Post

A 3D optoelectronic integrated chip utilizing CMOS post-backend process

Zan Zhang, Beiju Huang, Zanyun Zhang, Chuantong Cheng, Xurui Mao, Hongda Chen, Institute of Semiconductors (China)

The integration of optical devices and electronic integrated circuits is a main issue for optoelectronic convergence. In this work, a CMOS post-backend process flow is utilized to demonstrate a 3-D monolithic optoelectronic integrated chip. The chip is composed of two layers, an integrated chip as electronic layer and a silicon nitride waveguide device layer as photonic layer above electronic layer. The electronic layer contains micro-heaters and control circuits fabricated in the CSMC commercial 1 μ m CMOS process. The photonic layer contains Si₃N₄ grating couplers and microring add-drop filters. By thermal tuning the photonic devices with micro-heaters, the interaction between the electronic layer and the photonic layer can be achieved. The photonic layer is fabricated by CMOS post-backend process. First, a 4 μ m SiO₂ layer is deposited on the surface of the IC chip act as under cladding for waveguide structure. Then, after Chemical Mechanic Polishing (CMP) of the SiO₂ cladding, 400 nm Si₃N₄ is deposited and waveguide structure is patterned to form the photonic layer. The cross-section of the waveguide is 400 nm \times 1 μ m. Finally, the upper SiO₂ cladding is deposited and bonding pad windows are etched. All the dielectric layers are deposited by PECVD method with a temperature below 400 $^{\circ}$ C, which will do no harm to the performance of the IC chip.

9270-53, Session Post

Polymer waveguide-based hybrid optoelectronic integration technology

Jinbin Mao, Lingling Deng, Xiyan Jiang, Rong Ren, Yumeng Zhai, Jin Wang, Nanjing Univ. of Posts and Telecommunications (China)

While monolithic integration especially based on InP appears to be quite an expensive solution for optical devices, hybrid integration solutions using cheaper material platforms are considered powerful competitors because of the high freedom of design, yield optimization and relative cost-efficiency. Among them, the polymer planar-lightwave circuit (PLC) technology is regarded attractive as polymer offers the potential of fairly simple and low-cost fabrication, and of low-cost packaging. In our work, polymer PLC was fabricated by using the standard reactive ion etching (RIE) technique, while other active and passive devices can be integrated on the polymer PLC platform. Exemplary polymer waveguide devices was a 13-channel arrayed waveguide grating (AWG) chip, where the central channel crosstalk was below -30dB and the polarization dependent frequency shift was mitigated by inserting a half wave plate. An optical 90-degree hybrid was also realized with one 2 \times 2 multi-mode interferometer (MMI). The excess insertion losses are below 4dB for the C-band, while the transmission imbalance is below 1.2dB. When such an optical hybrid was integrated vertically with mesa-type photodiodes, the responsivity of the individual PD was around 0.06 A/W, while the 3 dB bandwidth reaches 24 - 27 GHz, which is sufficient for 100Gbit/s receivers. Another example of the hybrid integration was to couple the polymer waveguides to fiber by applying fiber grooves, whose typical loss value was 0.2 dB per-facet over a broad spectral range from 1200-1600 nm.

9270-54, Session Post

Activation process of GaAs photocathodes using SAES cesium and oxygen dispensers

Yijun Zhang, Yuan Xu, XinLong Chen, Guanghui Hao, Muchun Jin, Cheng Feng, Benkang Chang, Nanjing Univ. of Science and Technology (China)

In recent years, negative-electron-affinity (NEA) GaAs-based photocathodes have found widespread applications in vacuum devices for photoelectric detection and electron sources for high-energy physics. To achieve NEA state, the atomically clean cathode surface must be activated by work-function-lowering materials, typically such as cesium (Cs) and oxygen (O). In view of the required computer-control of evaporation flow rates, the solid O dispenser instead of gaseous oxygen is used in our daily experiments just as the regular Cs dispenser. In order to compare the activation effect between our original dispensers and untried SAES dispensers, the Cs and O dispensers supplied by SAES group were applied to activate epitaxial reflection-mode GaAs photocathodes. The SAES Cs dispenser is a mixture of a cesium chromate salt and a reducing agent zirconium-aluminum alloy powder while the O dispenser is of another component as silver oxide rather than barium peroxide. Through a series of Cs-O activation experiments with the co-deposition technique, it is found that the appropriate evaporation current passed through Cs dispenser and O dispenser should exceed 3.8A and 7.8A respectively. The unsatisfactory feature for the SAES dispenser is that the O dispenser released effectual oxygen gas more slowly than the original O dispenser, which was adverse to the first Cs/O alternate activation. To change this unfavorable phenomenon, an effective activation method was proposed which could bring out the desired symmetry of photocurrent curve shape during the whole Cs/O alternate activation process. This proposed activation method for SAES dispensers could provide guidance for the normalization of activation craft.

9270-55, Session Post

Post-digital image processing for systems based on micro-lens array

Chaiyuan Shi, Feng Xu, Soochow Univ. (China)

Owing to the feature of small, thin and lightweight, the imaging systems based on microlens array have become a popular area of research. However, current imaging systems based on microlens array have insufficient imaging quality. It can't meet the practical requirements. This means that post-digital image processing for image reconstruction from the low-resolution sub-image sequence is particularly important. In general, the post-digital image processing includes two parts: the accurate estimation of the motion parameters between the sub-image sequence and the reconstruction of high resolution image. In this paper, given the fact that the preprocessing of the unit images of each small lens can make the edges of the reconstructed high-resolution image clearer, the low-resolution images are preprocessed before the post-digital image processing. Then, after the processing of the pixel rearrange method, we get the high-resolution image. From the high-resolution image, we find that the edges of the reconstructed high-resolution image are clearer.

9270-56, Session Post

Micro-cavity lasers with large device size for directional emission

Chang-ling Yan, Changchun Univ. of Science and Technology (China)

Optical micro-cavities, which can confine light in a small mode volume with high quality factors, have become an important platform not only for optoelectronic applications with densely integrated optical components, but also for fundamental studies such as cavity quantum electrodynamics and nonlinear optical processes. Micro-cavity lasers have low threshold current densities, but their optical power output is very low due to total internal reflection of the whispering gallery modes WGMs and their far-field profiles are isotropic. To overcome the intrinsic problems of micro-disk lasers, several types of deformed structures were proposed, which are typically stadium-shaped lasers, bow-tie mode lasers, and spiral-shaped lasers. Recently, a limaçon-shaped micro-cavity has been proposed as a promising resonator shape for micro-cavity lasers with attractive properties such as a directional emission and a high cavity Q-factor. And the light output power of the micro-cavity laser is still a concerned question for nearly all the device applications. In this paper, we presented the limaçon-shaped cavity laser with large device size, and fabricated this type of micro-cavity laser with quantum cascade laser material due to its lack of surface recombination and inherently in-plane, transverse magnetic (TM) mode emission. The micro-cavity laser with device size of about 120 μ m was fabricated by using InP based InGaAs/InAlAs quantum cascade lasers material at about 10 μ m emitting wavelength, and the micro-cavity lasers with large device size were characterized with light output power, the far-field pattern, threshold current, and Q factor.

9270-57, Session Post

Room temperature ammonia vapor sensing properties of transparent single-walled carbon nanotube films

Sellaperumal Manivannan, Shobin L. R., National Institute of Technology, Tiruchirappalli (India)

Carbon nanotube (CNT) networks are identified as potential substitute and surpass the conventional indium doped tin oxide (ITO) in transparent conducting electrodes, thin-film transistors, solar cells, and chemical sensors. Among them, CNT based transparent gas sensors gained more interest because of its need in environmental monitoring, industrial pollution control, and detection of harmful gases in warfare or for averting security threats. The properties of CNT networks such as high surface area, low density, high thermal conductivity and chemical sensitivity open the path for gas sensing applications. Commercial unsorted single walled carbon nanotubes (SWCNTs) were purified by thermal oxidation and acid treatment processes and dispersed in N-methyl pyrrolidone. Optically transparent films are realized on glass from dispersed SWCNTs using dynamic spray coating process at 200°C. The films were characterized by scanning electron microscopy, raman and UV-vis-NIR spectroscopy techniques. Ammonia vapor sensing properties of the films are studied at room temperature by measuring the change in resistance against the concentration from 0 to 1000 ppm. The sensor response is increased logarithmically in the concentration ranging from 0 to 500 ppm with the detection limit 0.007 ppm. The high electron donating nature of ammonia molecule to the SWCNTs produced the fast, reversible and selective response. The response and recovery times were measured to be 57 and 397 sec respectively for 62.5 ppm ammonia vapor with 90% optical transparency at 550 nm SWCNTs films.

9270-60, Session Post

Improvement of spatial resolution for BOTDR by subdividing Brillouin signal

Jiayun Dong, Weiwei Zhan, Feng Wang, Xuping Zhang, Nanjing Univ. (China)

In this paper, we propose a subdivision method to improve the spatial resolution of Brillouin optical time-domain reflectometry (BOTDR). An energy density distribution (EDD) is derived based on the facts of that the detected Brillouin signal is determined by the pulse width of the probe pulse and the response time of detection system. The fiber which generates the detected Brillouin signal is divided into short segments with equal length and the sub Brillouin signal generated from each segment is extracted out of the detected Brillouin signal based on the EDD. So the Brillouin frequency shift (BFS) of shorter fiber can be obtained and a higher spatial resolution is achieved. We also use a cross correlation algorithm to enhance the signal-to-noise ratio (SNR) of the Brillouin signal before the subdivision procedure. A spatial resolution of 0.05 m in a 500 m sensing fiber is obtained by using 10 ns probe pulse which break through the limitation of the phonon life time in fiber.

9270-61, Session Post

Supercontinuum generation in two kinds of chalcogenide microstructured optical fibers

Weiqing Gao, Jigang Hu, Yuan Li, Huaili Qiu, Zijun Yuan, Feng Gao, Hefei Univ. of Technology (China); Zhongchao Duan, Takenobu Suzuki, Yasutake Ohishi, Toyota Technological Institute (Japan)

Chalcogenide microstructured fibers (MOFs) have great advantages for supercontinuum (SC) generation in mid-infrared (MIR) region, because they possess the properties of high nonlinearity and wide transmission window, simultaneously. The nonlinear parameters of chalcogenide MOFs can be higher by several tens or hundreds than those of silica, fluoride and tellurite fibers depending on the material components and fiber structures. Chalcogenide MOF can be transparent from visible up to the infrared region of 12 or 15 μ m depending on the compositions. In this paper, we demonstrate the SC generation in two kinds of suspended-core chalcogenide MOFs with different material components and fiber structures. One is an As₂S₃ MOF (Fiber I) with three-hole structure. The other is an As₂S₅ MOF (Fiber II) with four-hole structure. For Fiber I, the SC range of 3020 nm (from 1510 to 4530 nm) were obtained in a 2.4 cm fiber, when pumped by the wavelength at 2500 nm. The SC extends to the wavelengths longer than 4 μ m. For Fiber II, the SC range of 4280 nm (from 1370 to 5650 nm) is generated in a 4.8 cm fiber when pumped by the wavelength at 2300 nm, which covers more than two octaves. Compared to the SC generated in Fiber I, the SC spectral range in Fiber II has been increased by more than 1200 nm due to the better transmission property of the As₂S₅ glass; the SC extends to the wavelengths longer than 5 μ m.

9270-62, Session Post

The effect of processing conditions on recombination dynamics in polythiophene-fullerene bulk heterojunction solar cells

Weimin Li, Jinchuan Guo, Bin Zhou, Xin Wang, Li Li, Shangxu Li, Shenzhen Univ. (China)

To investigate the effect of processing conditions on recombination dynamics, poly (3-hexylthiophene):[6,6]-phenyl-C61-butyrac acid methyl ester (P3HT:PCBM) based bulk heterojunction solar cells were fabricated with different spin speed and dry rate. Trap density is determined by analyzing capacitance dependence on bias voltage (C-V) and frequency (C-f) of devices. The C-V and C-f characteristics show that processing conditions such as the slower growth rate assists the formation of self-organized ordered structure in the P3HT/PCBM blend system and lead to reduction in total trap density, however, fast grown active layer results in higher trap density owing to the structure disorder. The dependence of open circuit voltage on the light intensity reveals that for slower grown active layers with lower trap densities, bimolecular (Langevin) recombination is the major loss mechanism at high light intensity and trap-assisted (Shockley-Read-Hall, SRH) recombination dominates at low light intensity, however, for faster grown active layers, trap-assisted recombination is aggravated by the presence of high trap density and dominates the bimolecular recombination at all light intensity, leading to loss of photocurrent and lowering of fill factor. This study shows that a correlation is observed between processing conditions, trap density, recombination mechanism and property of solar cells. Processing condition affects the performance of devices as it has an influence on trap density that finally determines recombination mechanism and strength.

9270-63, Session Post

Ultra-broadband supercontinuum generation in fluoride glass by filamentation

Meisong Liao, Shanghai Institute of Optics and Fine Mechanics (China); Yasutake Ohishi, Toyota Technological Institute (Japan)

The mid-IR supercontinuum (SC) light source is in demand for many chemical, biological, medical, and astronomical applications. It is of great significance to develop a mid-IR SC light source whose spectrum is wide and flat.

We obtained ultra-broadband mid-IR SC by using a piece of fluoride glass through filamentation. Though the SC generation by filamentation needs a powerful laser chain to be the pump source, it has some advantages in comparison with that based on fiber. First, the optical path length in the glass can be very short due to the adopted high pump power. The negative influence of accumulated loss can be reduced greatly, so the transparent range of glass is much larger than fiber. Secondly, it is convenient in light-coupling, and the coupling efficiency can be high. In comparison with it, the coupling of the small core (usually the core is small to ensure a high nonlinearity) mid-IR glass fiber is troublesome. Thirdly, the glass piece is cost-effective, and can be fabricated easily.

We obtained a SC spectrum covering 0.2-8.0 μm by using a 32mm-thick fluoride glass sample. The 3 dB bandwidth covers 1.15-4.76 μm . The 20 dB bandwidth spans from 0.39 to 7.4 μm . The glass thickness, optical path, and pump conditions are optimized to enable the SC to be as wide as possible. This work shows that the SC generation through filamentation in bulk glass can be an effective way to obtain an ultra-broadband mid-IR light source, which will find various applications in mid-IR regions.

9270-64, Session Post

Deposition rate-dependent trap density and its effect on the performance of organic solar cells based on CuPc/C60

Weimin Li, Jinchuan Guo, Bin Zhou, Shangxu Li, Xin Wang,

Li Li, Shenzhen Univ. (China)

To investigate the effects of deposition rate on device performance, the CuPc (40nm) / C60 (45nm) double-layer heterojunction organic photovoltaic devices were fabricated by varying CuPc layer growth rate of 0.1 $\text{\AA}/\text{s}$, 1 $\text{\AA}/\text{s}$, 10 $\text{\AA}/\text{s}$, 20 $\text{\AA}/\text{s}$, respectively. The experimental results show that the deposition rate affects the property of organic solar cells and the higher deposition rate can lower the short-circuit current density (J_{sc}), the fill factor and the energy conversion efficiency of organic solar cells. This reveals that slower growth rate leads to reduction in total trap density, and these traps are responsible for lower performance of organic solar cells. To understand the effect of processing conditions such as deposition rate on the density of trap, sandwiched devices based on single layer of copper phthalocyanine (CuPc) between two metal electrodes have been used and traps due to structural disorder have been introduced by selecting different deposition rate of 0.1 $\text{\AA}/\text{s}$, 20 $\text{\AA}/\text{s}$, respectively. The trap density in the layer of CuPc is determined by analyzing capacitance dependence on bias voltage (C-V) and frequency (C-f) of devices. The C-V and C-f characteristics show that the higher deposition rate produces these traps in the CuPc layer and these defects affect the capacitance characteristics. Therefore, it becomes imperative to understand the processing condition such as deposition rate to be able to defect-engineer the organic solar cells for achieving higher performance.

9270-65, Session Post

Analytical beam-width characteristics of distorted cat-eye reflected beam

Yanzhong Zhao, Congmiao Shan, Yonghui Zheng, Laixian Zhang, Hua-yan Sun, Equipment Academy of PLA (China)

Most optical lenses have detectors fixed on their focal plane, so the laser beam that irradiates on optical window can be reflected along the entrance way. Such is "cat-eye effect". The active detection system based on cat-eye effect has been used on battlefield, but still develops slowly, because its performance is difficult to be analysed quantitatively, especially the beam-width parameters of reflected light. Therefore, based on the approximate three-dimensional analytical formula for laser beam passing through cat-eye optical lens, and by using the definition of second order moment, Gamma function and its solving and integral functions, the analytical expression of beam-width of distorted cat-eye reflected beam is deduced in this paper.

Then, the laws that divergence angle and astigmatism degree of the reflected light varies with incident angle, focal shift, aperture size, and centre shelter ratio are achieved by numerical calculation, and analyzed. The results show that the cat-eye reflected beam likes a beam transmitted and collimated by the target optical lens, and has some characteristics same as that of Gaussian beam. The main distribution and evolve characteristics are decided by the incident angle and structure parameters of the target optical lens, which are similar to the effects of expand aperture and axis incline on the divergence angle of expanding laser. The astigmatism is mainly caused by incidence angle.

Totally, by using these analytical formulas, the cat-eye reflected beam can be studied easily and expediently, and then the active detection system can be analyzed and designed quantitatively and directly.

9270-66, Session Post

Assessment of reliability of a code of optical rotary encoders with the serial interface

Maksim S. Nikolaev, Yuri V. Filatov, Petr A. Pavlov, Saint

Petersburg Electrotechnical Univ. "LETI" (Russian Federation)

Now more and more digital optical rotary encoders with a serial output code are widely adopted. In this regard there is a need of an assessment of precision characteristics of such converters.

As means of calibration and checking of such sensors the dynamic laser go-niometer with the ring laser as a reference angular sensor is used.

The complete error of the converter e consists of an error of quantization e_1 and an error of angular position measurement at the moment of the code change e_2 . The error of quantization e_1 is evenly distributed on the interval.

Existing techniques of an assessment of precision characteristics of rotary en-coders with a parallel code are based on measurement of an angular error of the moments of the code change with post processing of the obtained data.

Unlike encoders with a parallel code at serial reading the data collection is carried out on demand in the arbitrary instant of time and is not attached to code changes. In such way, only the complete error e can be measured and in this connection there is a need of development of an assessment techniques of precision characteristics of such encoders. As such characteristics can be used, in particular, such parameters, as a root mean square deviation of angular positions of code changes and reliability of a code.

Root mean squared deviation of an error e_2 can be obtained by determination using processing of sampling of values of the complete error e . The assessment of reliability of a code can be determined by the frequency of hit of an error e in i -th quantum. It is necessary to develop a technique of receiving representative sampling of the complete error e for realization of these algorithms of processing.

9270-67, Session Post

Theoretical investigation of modal gain control for six-mode erbium-doped fiber amplifiers

Zujun Qin, Guilin Univ. of Electronic Technology (China)

Mode division multiplexing (MDM) has been regarded as one of the potential approaches to further increase single fiber transmission capacity. Multimode optical amplifiers capable of amplifying all the guided modes are desirable to extend the transmission distance of MDM systems. For such amplifiers, controlling of modal gain over all modes is of importance to minimize the degradation of signal performance. In the manuscript, we propose a numerical model to investigate multimode erbium-doped fiber amplifiers (MM-EDFAs) to manipulate the mode-dependent gain (MDG) across six weakly guided modes at the signal wavelength, i.e., LP01s, LP11as, LP11bs, LP21as, LP21bs, and LP02s. In the modeling scheme, several sections of EDF with optimized doping profiles and thus different MDG characteristics are cascaded in structure to control the gain of the six spatial signal modes simultaneously. The mode contents of the pump are also optimized enabling another freedom to control the MDG. According to the simulation, a six-mode EDFA with the average gain greater than 18dB and the MDG less than 2.5dB has been designed only by concatenated two sections of EDFs with different Er³⁺ spatial distribution in the core.

9270-68, Session Post

Mode-locked erbium-doped fiber laser using graphene-covered-microfiber as saturable absorber

Shenggui Fu, Bojun Zhou, Shandong Univ. of Technology (China); Mingming Luo, Zhi Wang, Yange Liu, Nankai Univ. (China)

Graphene has been widely investigated in applications of fiber lasers for its excellent characteristics of wavelength-independent absorption, ultrafast recovery time, and low absorption intensity. Many different types of saturable absorbers based on graphene have been proposed before, and however, this area stays hot and urgently needs to be improved in perspectives of the fabricating cost and working performance.

In our work, a mode-locked Er-doped fiber laser using graphene-covered-microfiber (GCMF) as saturable absorber is demonstrated. The GCMF has excellent interaction between the propagating light and graphene film via its large evanescent field. This saturable absorber introduces no extra losses for its all-optical structure and is easier to fabricate compared to other graphene-based fiber saturable absorbers.

In the experiment, we adopted 3m Er-doped fiber as the gain media, and an isolator was used to ensure the unidirectional light propagation. A PC was used to adjust the polarization state of incident light. By improving the side-pump power and adjusting the PC, we successfully achieved pulse trains with a repetition rate of 1.7 MHz, which matches well with the length of the cavity. As we further improved the pump power to 160 mW, stable mock-locking phenomenon was observed on the oscilloscope. The pulse width was measured by using an autocorrelator, and 380 fs pulse width was obtained. By tuning pump power and polarization states in the laser cavity, stable Q-switching, Q-switched mode-locking, and continuous-wave mode-locking can be achieved in our experiments.

The GCMF has been proven to be an effective saturable absorber in our experiment. Because the graphene film absorbs light from the evanescent field, GCMF can be adopted in mode-locking fiber lasers of higher power.

9270-69, Session Post

Analysis of the effects of the air gap thickness on the transmittance of e-ray on with deviated optical axes

Bai Xin, Northwest Institute of Nuclear Technology (China)

Taking Glan-Taylor prism with deviated optical axes for example, double beam interference in the air gap are considered in detail, e-ray transmittance varies with the air gap thickness by deviated optical axes is analyzed. Finally, the formula for the transmittance of e-ray in the air gap are obtained when the prism optical axes have departure angles from their ideal directions. The suitable thickness of air gap will improve the e-ray transmissivity, in order to design an optimum prism.

9270-70, Session Post

An effective coding design for improving the performance of LED lighting based optical communication system

Na Yang, Yu Nian Zou, Yi Yang, Yun-Cui Zhang, Sheng De Li, Dalian Polytechnic Univ. (China); Yoshinori Namihira, Univ. of the Ryukyus (Japan)

In order to combine LED lighting with optical communication system well, an effective coding design plugged in a time interval which is selected through theoretical calculation is proposed in the paper. In this way a stable environment for illumination will be provided and the brightness will be improved. Results of the experiment verify that the coding design is effective.

9270-71, Session Post

Thermal influence of phosphor to GaN-based white LEDs

Zichao Zhou, Institute of Semiconductors (China); Lixia Zhao, Institute of Semiconductors, CAS (China); Pengzhi Lu, Huaiwen Zheng, Junxi Wang, Yipeng Zeng, Institute of Semiconductors (China)

In this study, we quantitatively investigate the influence of phosphor to the thermal properties of white LEDs. We find that although the junction temperature of white LEDs is higher than corresponding blue LEDs, due to the high thermal conductivity of the phosphor, it will help to improve the thermal dissipation and lower the thermal resistance of white LEDs. Based on this, a heat transfer model has been proposed, which has also been confirmed by simulation analysis. While for white LEDs with remote phosphors, although the lower junction temperature can help to improve performance and reliability, the thermal resistance has not been improved. The heat generated by phosphors is isolated by the silicone and this would increase the phosphor temperature and lead to a different degradation mechanism after a long time stress.

9270-72, Session Post

Combination characteristics analysis of LED array

Benjian Shen, Academy of Military Medical Sciences (China)

It has been proved that LED with special waveband has great useful in biological applications, such as to conduct the growth and development of spinach, to induce carotenoid accumulation in filamentous fungus-*Colletotrichum gloeosporioides* and to kill some special bacteriums. Unlike the LED used in road illumination, the LED used in biology research requires not only high average output power but the illumination uniformity in small area. However, because the output power of a single LED is very small, it is necessary to use multiple LED to form LED array to enhance the brightness and improve the uniformity. In this paper, the combination characteristics of LED array with rectangle distribution and hexagonal distribution are numerical analyzed and compared for the first time to our knowledge. The relationships between the peak intensity of the combining LED array and the propagate length are researched, and the effects of LED separation distance and the viewing angle on the peak intensity of LED array are simulated. The uniformity of the LED array is investigated. In simulation, the total number of the LED is 169, corresponding to the rectangle distribution with dimension of 13*13 and hexagonal distribution with 7 rings. The simulation results show that the peak intensity of the LED array with rectangle distribution is smaller than that with hexagonal distribution in the same parameters. The peak intensity of the LED array decreases with the increase of the propagate length and/or the separation distance. However, the peak intensity of the LED array increases with the increase of the viewing angle of the LED, and the peak intensity with hexagonal distribution is larger than that with rectangle distribution when the viewing angle is larger. The uniformity can be improved by optimizing the separation distance or viewing angle. The results can be guided for LED array design.

9270-27, Session 5

Wavelength-swept lasers and their application to fiber-optic sensors (*Invited Paper*)

Min Yong Jeon, Myeong Ock Ko, Byeongkwon Choi, Yong Seok Kwon, Chungnam National Univ. (Korea, Republic of)

The wavelength swept laser (WSL) is a promising optical source in optical coherence tomography, optical fiber sensor, and optical beat source generation. It is demonstrated by employing a narrowband wavelength-scanning filter, such as a fast rotating polygonal-scanner-filter, a diffraction grating on a galvo-scan mirror, or a fiber Fabry-Perot tunable filter (FFP-TF). The speed of the conventional WSL is limited by both the tuning speed of the filter and laser cavity lifetime. Many kinds of WSLs have been developed in order to improve the scanning rate and scanning bandwidth. Specially, a Fourier domain mode-locked WSL with the FFP-TF is developed to increase the scanning speed of the swept laser. In this presentation, I will review the several applications of the WSL, which is used in optical coherence tomography, dynamic fiber-optic sensor, and frequency-swept optical beat source generation.

9270-28, Session 5

Brillouin optical time domain analysis based on three-wavelength lightwaves

Yuangang Lu, Xue Wang, Cunlei Li, Xuping Zhang, Nanjing Univ. (China)

A novel scheme of distributed fiber sensor based on Brillouin optical time domain analysis (BOTDA) operating on multi-wavelength lightwaves is presented. The probe and pump lightwaves of the BOTDA both contain three wavelengths with small equal-wavelength spacing. For the three pairs of probe and pump wave whose frequency difference is equal to the Brillouin frequency shift (BFS), stimulated Brillouin scattering (SBS) process occurs synchronously. The system impairments imposed by fiber dispersion and nonlinearities are analyzed theoretically. A three-wavelength BOTDA sensor is demonstrated experimentally and it provides 9.2dB electrical Signal-Noise-Ratio enhancement compared to a conventional single-wavelength BOTDA sensor.

9270-29, Session 5

Dynamic strain variation measurement with STFT-based BOTDR sensing system

Yixin Zhang, Guojie Tu, Zhoufeng Ying, Xuping Zhang, Lidong Lv, Nanjing Univ. (China)

Distributed optical fiber sensors based on Brillouin scattering have attracted significant interest in the past few decades since they can detect temperature and strain simultaneously along the entire length of sensing fiber. Traditional Brillouin sensing systems usually require a time-consuming frequency scanning to obtain Brillouin spectrums, which restricts the application of traditional systems to static measurement only. In this paper, a novel configuration of sensing system based on short time Fourier transform (STFT) has been proposed and demonstrated. Dynamic strain measurement was achieved with Brillouin optical time domain reflectometry (BOTDR) sensing system. Unlike traditionally frequency scanning method, our system sampled the Brillouin backscattering signal directly after it has been down converted to intermediated frequency (IF) region. The Brillouin spectrums were reconstructed with STFT from the recorded time domain data continuously without dead-time, providing much

higher refreshing rate. To the best of our knowledge, this is the first time that STFT was applied to a BOTDR sensing system for measuring speed enhancement. The proposed method extends the application realm of BOTDR sensor, allowing distributed dynamic strain variation measurement with single-end structure. A 16.7 Hz strain variation upon a 12m section was successfully detected at the end of a 270m sensing fiber with 4m spatial resolution and 45% uncertainty.

9270-30, Session 5

Reduced graphene oxide coated optical fiber for methanol and ethanol vapor detection at room temperature

Kavinkumar T. Thangavelu, Dillibabu Sastikumar, Sellaperumal Manivannan, National Institute of Technology, Tiruchirappalli (India)

Since the successful isolation of single layer of graphene from graphite by mechanical exfoliation method, attracted a great attention due to its unique structural, optical, mechanical and electronic properties. This makes the graphene as a promising material in many possible applications such as energy-storage, sensing, electronic, optical devices and polymer composite materials. High quality of reduced graphene oxide (rGO) material was prepared by chemical reduction method at 100°C. The structural and optical properties of the rGO sheets were characterized by FT-IR, micro Raman, powder XRD and UV-vis-NIR techniques. FT-IR reveals the absence of oxygen functional groups on rGO due to the reduction process. Powder XRD shows the broad peak at $2\theta=24.3^\circ$ corresponding to interlayer spacing of 3.66Å which is smaller than the graphene oxide. UV-vis-NIR spectrum of rGO displays the absorption peak at 271 nm indicates the reduction of GO and the restoration of C=C bonds in the rGO sheets. The Clad removed and rGO coated commercial PMMA optical fiber is investigated for methanol and ethanol vapors detection in the concentration ranging from 0 to 500 ppm at room temperature. The spectral characteristics along with output intensity modulation of clad removed and rGO coated fiber results reveal the potential of methanol and ethanol vapor sensing properties of the fabricated sensor. The results will be presented.

9270-31, Session 5

High-precision fiber Bragg grating wavelength demodulation system based on spectrum segmentation

Gang Yang, Guoliang Xu, Guojie Tu, Lan Xia, Nanjing Univ. (China)

A high precision fiber Bragg grating wavelength demodulation system based on spectrum Segmentation is proposed and experimentally demonstrated. F-P etalon is added into the traditional F-P filter method to dynamical calibrate the read out value of filter wavelength, which can eliminate measurement errors caused by the temperature drift effect, the peristaltic effect of F-P filter. Besides the ASE spectral characteristics and etalon are used to segment the wavelength for demodulation, which can greatly reduce the effects of the nonlinear effect of F-P filter to improve the demodulation accuracy of wavelength and enhance the stability of the demodulation system. The result shows, the stability of the system is 0.65pm, the resolution is 0.23pm, the linearity of temperature is 0.9999.

9270-32, Session 6

Electrowetting-based adaptive vari-focal liquid lens array for 3D display (Invited Paper)

Yong Hyub Won, KAIST (Korea, Republic of)

Electrowetting is a phenomenon that can control the surface tension of liquid when a voltage is applied. This paper introduces the fabrication method of liquid lens array by the electrowetting phenomenon. The fabricated 23x23 lens array has 1mm diameter size with 1.6 mm interval distance between adjacent lenses. The diopter of each lens was -24-27 operated at 0V to 50V. The lens array chamber fabricated by Deep Reactive-Ion Etching (DRIE) is deposited with IZO and parylene C and tantalum oxide. To prevent water penetration and achieve high dielectric constant, parylene C and tantalum oxide ($\epsilon=23-25$) are used respectively. Hydrophobic surface which enables the range of contact angle from 60 to 160 degree is coated to maximize the effect of electrowetting causing wide band of dioptric power. Liquid injection into each lens chamber was proceeded by two different ways. First way was self water-oil dosing that uses cosolvent and diffusion effect, while the second way was micro-syringe by the hydrophobic surface properties. To complete the whole process of the lens array fabrication, underwater sealing was performed using UV adhesive that does not dissolve in water. The transient time for changing from concave to convex lens was measured <33ms (at frequency of 1kHz AC voltage.). The liquid lens array was tested unprecedentedly for integral imaging to achieve more advanced depth information of 3D image.

9270-33, Session 6

Wave guiding by low refractive-index strips on surfaces of Chalcogenide glass thin films

Yanfen Zhai, Wei Zhang, Yiyong Huang, Tsinghua Univ. (China)

Chalcogenide glass (ChG) waveguides offer large third-order nonlinearities, low two-photon absorption and negligible free carrier absorption, which are preferred in developing on-chip integrated nonlinear devices. Although ChG films can be fabricated easily by several ways, including thermal evaporation, sputtering, chemical vapor deposition and laser deposition and so on, lift-off process and etch process on ChG films are difficult due to their mechanical and thermal properties.

In this paper, we proposed and demonstrated a simple ChG waveguide structure, guided by low refractive-index strips on the surfaces of planar ChG films. Theoretical analysis shows that it supports single quasi-TE mode transmission in 1550nm band with high nonlinearity. In vertical direction the light field is confined in the ChG film, while in the in-plane direction to the film, the propagation direction of the mode is guiding by the low refractive index strip on the surface. Since the lift-off process and etching process are avoided in this structure, its fabrication is highly simplified. Samples of this surface guiding ChG waveguides are fabricated, in which the ChG films are deposited by the thermal evaporation and the low refractive index SU8 strips are fabricated by UV lithography. Its transmission properties are measured by the cut-off method, showing a waveguide attenuation of 0.67dB/mm and a coupling loss with optical fibers of ~8dB/facet. It provides a simple way to realize high quality ChG waveguides, which has great potential in developing nonlinear photonic devices.

9270-34, Session 6

Birefringence compensated arrayed waveguide grating

Jun Zou, Xiang Xia, Zhejiang Univ. (China); Tingting Lang, China Jiliang Univ. (China); Jian-Jun He, Zhejiang Univ. (China)

A birefringence compensation technique based on angled star couplers in arrayed waveguide grating (AWG) is proposed and experimentally demonstrated both in low-index-contrast and high-index-contrast material systems. A 16-channel AWG with 100GHz channel spacing for DWDM application is designed and fabricated in silica-based low-index-contrast waveguide. The experimental results confirm that the polarization-dependent wavelength shift (PD λ) can be tuned by varying the incident/diffraction angle at the star couplers and a birefringence-free property can be achieved without additional fabrication process as compared to conventional AWG. A further validation of this technique is demonstrated in high-index-contrast silicon-on-insulator waveguide, in combination with different diffraction orders for TE and TM polarizations. An ultra-compact birefringence-compensated AWG with cross-order design for triplexer application is designed and fabricated. The PD λ is reduced from about 370nm to less than 2.5 nm for wavelength channels at 1490-1550nm. A birefringence compensated silicon nanowire AWG for CWDM optical interconnects is also fabricated. The theoretical and experimental results show that the PD λ can be reduced from 380-420 to 0.5-3.5 nm, below 25% of the 3 dB bandwidth of the channel response.

9270-35, Session 6

The 1 \times 5 optical splitters based on silicon photonic crystal cascaded self-collimation ring resonators

Yuanyuan Lin, Fujian Normal Univ. (China); Xiyao Chen, Minjiang Univ. (China); Junzhen Jiang, Biao Chen, Zexuan Qiang, Yishen Qiu, Hui Li, Fujian Normal Univ. (China)

In this paper, the 1 \times 5 optical splitters (OSs) based on 2D air-hole type silicon photonic crystal embed cascaded self-collimation (SC) ring resonators (CSCRR) was proposed. The 1 \times 5 OSs consist of eight beam splitters, which are formed by varying the radii of the air holes. With self-collimation effect, we can manipulate the light's propagation in the OSs. Here we consider TM modes. Utilizing multiple-beam interference theory, the theoretical transmission spectra at different outputs were analysed. These transmission spectra can help us to set the radii of eight splitters properly, for we can control the light coming out from five ports with the light-intensity ratio we need. Meanwhile these outputs' transmission spectra were investigated by the finite-difference time-domain (FDTD) method. The simulation results have a good agreement with the theoretical prediction. The 1 \times 5 OSs is not only small-size but low-loss which will have practical applications in photonic integrated circuits.

9270-36, Session 6

Series-coupled double-ring resonators with asymmetric radii for optical channelizers

Xiaowen Gu, Dan Zhu, Shilong Pan, Nanjing Univ. of Aeronautics and Astronautics (China) and State Key Lab. of Millimeter Waves (China)

A series-coupled double-ring resonator with asymmetric radii is presented and analyzed to achieve filtering response with large free spectral range (FSR), small passband width (tens of MHz) and small shape factor simultaneously for use in microwave photonic channelizer. By introducing differentiation of the two radii to realize a vernier effect, the FSR of the resonator filter can be extended while maintaining the small passband width and the small shape factor. And with the slightest differentiation of the two radii while maintaining the extended FSR, the smallest passband width and the smallest shape factor will be realized. An optical filter with and FSR of 29.444 GHz, a 3-dB bandwidth of 96 MHz and a shape factor of 3.17 is obtained.

9270-37, Session 6

Theoretical investigation of polarization-dependent devices based on the critical guiding condition of SOI waveguide

Zhoufeng Ying, Guanghui Wang, Xuping Zhang, Nanjing Univ. (China); Ho-pui Ho, The Chinese Univ. of Hong Kong (Hong Kong, China)

With the increasing demand for information, integrated silicon photonics technology has been highly valued. Among them, silicon on insulator (SOI) has advantages of low cost, process maturity, and IC technology compatible, making it to be one of the most competitive integrated optoelectronic platforms. However, due to its highly polarization-dependent performance, polarization-selective devices are essential on SOI platform. In this paper, we analyze the critical guiding condition of SOI waveguide as well as the hybrid plasmonic waveguide (HPW). Based on the different critical guiding condition for both polarizations, we propose several polarization-selective devices on SOI platform, including polarizer, polarization beam splitter (PBS) and polarization rotator. Firstly, an ultracompact and broadband TE-pass polarizer based on HPW is proposed. The optimized design has an active region as small as 0.8 μ m, which is the shortest polarizer reported until now. Secondly, a PBS based on asymmetrical directional coupling is designed, consisting of two silicon waveguides with different dimension and different critical guiding condition. The PBS owns the minimal effective coupling length of only 1.52 μ m. Similarly, a polarization rotator based on multimode interference with the effective length of only 2.3 μ m is also proposed. Simulation results show that the designed devices have excellent optical properties, and the sizes of the devices achieve a great breakthrough.

9270-38, Session 6

Aspheric lens based imaging receiver for multi-input and multi-output visible light communication

Qiuqi Ju, Zhongcheng Liang, Jin Wang, Xueming Liu, Tingting Yang, Nanjing Univ. of Posts and Telecommunications (China)

Visible light communication (VLC) has been regarded as a promising solution in short-range intelligent communication system. To achieve a larger transmission capacity and a stronger transmission reliability of the VLC system, the multi-input multi-output (MIMO) technique is a promising candidate. However, one of the key issues in implementing the MIMO technique is the multipath inter-symbol interference. The multipath inter-symbol interference is induced by the noise signal coming from the reflection in the environment and the crosstalk between different channels. In this paper, we propose a novel imaging receiver for the MIMO VLC system. This imaging receiver uses aspheric lens coated with reflecting films to focus the light onto a small area

photodetector. Thus, the optical power of the focused light on the photodetector is much stronger than those of the reflection component. According to experimental results, the power of reflection component is at least 7 dB (electrical) lower than that of the weakest line-of-sight (LOS) component received, which means that the reflection noise could be neglected compared with the LOS component. Furthermore, signals from different LEDs could be separated, which mitigate the channel crosstalk dramatically, and thus reduce multichannel interference. The simulation results in this paper shows the distribution of optical power on the imaging plane for various receiving positions and low correlation between all channels. We can find that the optical power density becomes stronger than non-imaging system and the interference is substantially decreased. Signal-to-noise ratio (SNR) and bit error rate (BER) of the system are also optimized. Analysis about the optical system is given in this paper.

9270-39, Session 6

Sub-wavelength focusing of cylindrical vector beams by a 1D metallic photonic crystal plano-concave lens

Yi Zhong, Jin Wang, Ji Xu, Nanjing Univ. of Posts and Telecommunications (China)

The fine manipulations of cylindrical vector beams (CVBs) based on metallic microstructures, such as sub-wavelength focusing, have entered many interdisciplinary areas, and the important applications have been found in many fields including optical micromanipulation, super-resolution imaging, micro-machining and so on. But so far, the sub-wavelength focusing of azimuthally polarized beams is encountered, since the manipulation mechanisms rely heavily on the excitation of surface plasmon polaritons, which brings the polarization limitation.

We theoretically investigated the focusing behavior of CVBs in 1-D metallic photonic crystals (MPCs). The simulation results show that a 1-D MPC plano-concave lens can focus cylindrical vector beams into scale of sub-wavelength. The negative refraction at the interface between the air and the 1-D MPC is analyzed at the frequencies corresponding to the second photonic band, which makes the 1-D MPC has the ability to focus higher Fourier components of light beams. The cylindrical plano-concave structure is constructed to focus the radially and azimuthally polarized beams simultaneously. The behavior is demonstrated by Finite Element Method (FEM). The shape of focusing field can be tailored, by changing the polarization ratio of the incident beams. In addition, the effective sub-wavelength focusing phenomenon can also be realized in variety of wave ranges, by choosing the proper materials and adjusting the parameters. We believe that it's the first time to realize the simultaneous sub-wavelength focusing of radially and azimuthally polarized beams, the application of which is quite promising in broad prospects.

9270-40, Session 7

Excess signal transmission with dimming control pattern in indoor visible light communication systems (*Invited Paper*)

Jian Chen, Nanjing Univ. of Posts and Telecommunications (China)

In traditional dimming control system using pulse width modulation (PWM) combined with M-QAM OFDM scheme, OFDM signal is only transmitted during "on" period. To guarantee the communication quality, reduction of duty cycle will cause increased symbol rate or added LED power. This means system BER performance degradation and power consumption. In order to solve the defects of the traditional dimming scheme, we

propose a new dimming control scheme in indoor visible light communication, which combines OFDM signal and multi pulse position modulation (MPPM) light pulse well with each other. By means of dividing traditional PWM pulses into MPPM pulses with the same duty cycle, the pattern effect of MPPM pulses is utilized, which makes excess signal transmission possible. Simulation results shows that when reducing the brightness of LED the required symbol rate using dimming control pattern is not higher than the traditional PWM scheme and LED power is also reduced, which satisfies both system reliability and energy effectiveness under constant high data rate and bit error rate (BER) less than $1E-3$.

9270-41, Session 7

Demonstration of 20 Gb/s polarization-insensitive wavelength switching system using a HNLF

Feng-Chen Qian, Xi'an Institute of Optics and Precision Mechanics (China) and Univ. of Chinese Academy of Sciences (China); Xiaoping Xie, Xi'an Institute of Optics and Precision Mechanics (China); Yalin Ye, Yu Wen, Xi'an Communication Institute (China)

All-optical switches can avoid expensive high-speed electronics in the 'optical-to-electronic-to-optical' (OEO) conversion system. We propose a simple, flexible, polarization-insensitive all-optical lightpath switching system for free-space optical communications (FSO), which generates the multiplexed bits stream for data base rates up to 20Gb/s or higher rate in OTDM. The switching system is composed of all-optical wavelength conversion (AOWC) and tunable optical bandpass filter (TOBF). AOWC is implemented using highly nonlinear fiber (HNLF) based on four-wave mixing (FWM) with transparent optical wavelength multicast by multi-wavelength conversion. For demonstration purposes, we build a 20Gb/s optical network, which is composed of 3 nodes with 4 input port by 4 output port wavelength-based switching system and OTDM system. Transmitter can multiplex eight 2.5Gb/s tributary signals into one 20Gb/s optical data stream by an simple actively mode-locked fiber ring laser (AML-FRL) with repetition frequency tunable and modulators. Receiver will realize 20 Gb/s OTDM data stream to 2.5Gb/s via a HNLF ring. The experimental setup space link distance is over 10 meters. We aim at demonstrating that there are solutions for the required functionalities in a high-speed OTDM and switching system for FSO network. The system will also be shown to be able to operate in longer distance links at higher data rate, and the results of experiments can be used for reference in the design of ultra-high speed FSO network.

9270-42, Session 7

Optically-powered active sensing system for internet of things

Chen Gao, Jin Wang, Long Yin, Jian Jiang, Hongdan Wan, Nanjing Univ. of Posts and Telecommunications (China)

Internet Of Things (IOT) drives a significant increase in the extent and type of sensing technology and equipment. Sensors, instrumentation, control electronics, data logging and transmission units comprising such sensing systems will all require to be powered. Conventionally, electrical powering is supplied by batteries or/and electric power cables. The power supply by batteries usually has a limited lifetime, while the electric power cables are susceptible to electromagnetic interference. In fact, the electromagnetic interference is the key issue limiting the power supply in the strong electromagnetic radiation area and other extreme environments. The novel

alternative method of power supply is power over fiber (PoF) technique. As fibers are used as power supply lines instead, the delivery of the power is inherently immune to electromagnetic radiation, and avoids cumbersome shielding of power lines. Such a safer power supply mode would be a promising candidate for applications in IOT. In this work, we built up optically powered active sensing system, supplying uninterrupted power for the remote active sensors and communication modules. Also, we proposed a novel maximum power point tracking (MPPT) technique for photovoltaic power converters. In our system, the actual output efficiency greater than 40% within 1W laser power. After 1km fiber transmission and opto-electric power conversion, a stable electric power of 210mW was obtained, which is sufficient for operating an active sensing system.

9270-43, Session 7

Investigation on the BER performance of the space laser communication system with a power EDFA

Mi Li, Wenxiang Jiao, Xuping Zhang, Shandong Dong, Yuejiang Song, Yuangang Lu, Nanjing Univ. (China)

For a space laser communication system with an EDFA as a power amplifier, the performance of its BER deteriorates because the EDFA's characteristics are badly impacted by space radiation. As is investigated in this paper, small divergence-angle, lower than 30°rad, assures that the BER is lower than 1E-20 although the increase of radiation dose from 0Gy to 250Gy leads to 20 orders of magnitude increase of the BER. Such perfection results from our selection of optimal parameters. In the case of zenith angle, the BER increases smoothly when the zenith angle is lower than 10 degrees. After the point of 10 degrees, however, the BER starts its linearly fast increase. Increasing the radiation dose makes the BER increase and such evolution trend more smooth. Moreover, the increase of receiving diameter leads to linear reduce of BER. It is interesting to note that the evolution becomes nonlinear in region of low receiving diameter when we change the divergence-angle to a higher value 60°rad. Besides, suffering radiation makes the nonlinearity mentioned above more apparent. Another try to change the zenith angle to higher value 45° does not show obvious nonlinear effect but it worsens the performance of BER quite a lot. Commonly, the impact of radiation will reach its saturation when the dose of radiation continues to increase. The work will benefit the design of practical space laser communication system with EDFAs.

9270-44, Session 7

Optical generation of tunable microwave and millimeter waves by using asymmetric fiber Bragg grating Fabry-Perot cavity fiber laser

Cong Chen, Meng Wang, Qi Li, Kaiqiang Huang, Haiyan Chen, Yangtze Univ. (China)

Optical generation of microwave or millimeter waves has attracted great interests due to its potential applications in satellite communication, radio-over-fiber network, remote sensing, radar systems and wireless communication links. Till now many possibilities have been proposed to generate microwave and millimeter wave signals, such as such as Brillouin scattering, harmonic frequency locking, MZ interferometric modulator, Self-Heterodyne Method, Injection-Locked Four-Wave-Mixing Conjugate Modes in a Semiconductor Laser, dual-transmission-band fiber Bragg grating (FBG) filter, and single mode fiber FP cavity with pulse laser injection. All of them, Heterodyne Method is a typical and useful one. Furthermore, a dual-wavelength fiber

laser used to generate microwave and millimeter wave signals in stead of two independent lasers is a good method, two kinds of cavity structures, ring cavity and linear cavity, are available. In the category of linear cavity, the uniform and chirped fiber Bragg gratings based Fabry-Perot (F-P) cavity are commonly used.

In this presentation, we propose and experimentally demonstrate a novel optical generation of microwave and millimeter wave signals by using asymmetric fiber Bragg grating FP cavity dual-wavelength fiber laser, dual-wavelength emission can be achieved with wavelength separation of 0.6nm corresponding to the millimeter wave signal at 75GHz. By appropriately adjusting the operation temperature of intracavity FBG, the frequency of millimeter wave signal generated can be tunable. Our experimental results demonstrate the new concept of optical generation of microwave and millimeter wave signals by using asymmetric fiber Bragg grating FP cavity dual-wavelength fiber laser and the technical feasibility.

9270-45, Session 7

On-chip optical pulse shaper for arbitrary waveform generation using optical gradient force

Shasha Liao, Huazhong Univ. of Science and Technology (China); Shucun Min, Wuhan National Lab. for Optoelectronics (China); Jianji Dong, Huazhong Univ. of Science and Technology (China)

Integrated optical pulse shaper opens up the possibility for the realization of ultrahigh-speed and ultra wide-band linear signal processing with compact size and low power consumption. We propose a silicon monolithic integrated optical pulse shaper using optical gradient force which is based on the eight-path finite impulse response. A cantilever structure is fabricated in one arm of the Mach-Zehnder interferometer (MZI) to act as an amplitude modulator. The phase shift feature of waveguides is analyzed with the optical pump power and five typical waveforms are demonstrated with the manipulation of optical force. Unlike other pulse shaper schemes based on thermo-optic effect or electro-optic effect, our scheme is based on a new degree of freedom manipulation, i.e., optical force, so no microelectrodes are required on the silicon chip which can reduce the complexity of fabrication. Besides, the chip structure is suitable in commercial silicon on insulator (SOI) wafers, which have a top silicon layer of about 220nm.

9270-73, Session 7

Optical properties of (1-x)Pb(Zn_{1/3}Nb_{2/3})O₃-xPbTiO₃ single crystals

Chongjun He, Huiling Hu, Nanjing Univ. of Aeronautics and Astronautics (China); Hong Jia, Suihua Univ. (China); Jiming Wang, Kongjun Zhu, Youwen Liu, Nanjing Univ. of Aeronautics and Astronautics (China)

Optical properties of (1-x)Pb(Zn_{1/3}Nb_{2/3})O₃-xPbTiO₃ (PZN-xPT, x=5%, 9% and 12%) single crystals have been comprehensively investigated. The PZN-xPT single crystals used in this study were grown using a high temperature flux method. Refractive indices (n_{ij}) were measured by the Brewster's angles (θ_B=tan⁻¹n) at different wavelengths. Dispersion equations of refractive indices were obtained. After poled along [001] direction, the transmittance of PZN-12%PT single crystal is more than 65% from 0.5 to 5.8 μm, which is much higher than that of PZN-5%PT and PZN-9%PT single crystals. PZN-12%PT has a tetragonal phase, its spontaneous polarization P_S is along [001] direction. After poling, it could form a single domain structure. Orientation and

temperature dependences of the electro-optic coefficient were investigated at He-Ne laser by the Senarmont compensator method. Large effective electro-optic coefficient ($r_c = 430$ pm/V) was observed in [001]-poled PZN-9%PT crystal. More importantly, r_c of tetragonal PZN-12%PT is about 130 pm/V, which is almost unchanged in a temperature range -20-80 °C. The r_c of PZN-xPT single crystals are much higher than that of widely used electro-optic crystal LiNbO₃ ($r_c = 20$ pm/V). These excellent optical properties make the PZN-xPT single crystals promising candidates for electro-optic modulation applications.

Conference 9271: Holography, Diffractive Optics, and Applications VI

Thursday - Saturday 9 -11 October 2014

Part of Proceedings of SPIE Vol. 9271 Holography, Diffractive Optics, and Applications VI

9271-1, Session 1

Nonlinear ray optics and nonlinear dynamics: a phase-space approach *(Invited Paper)*

George Barbastathis, Massachusetts Institute of Technology (United States) and Shanghai Jiao Tong Univ. (China); Hanhong Gao, Massachusetts Institute of Technology (United States)

Ray optics expresses light propagation in terms of the evolution of the normals to the wavefront. This evolution has been known since the time of W. R. Hamilton (1805-1865) to be derivable from conservation principles, similar to the trajectories of systems subject to mechanical or other force potentials; and the canonical phase-space, as defined by H. Poincaré (1854-1912) and, later, by E. P. Wigner (1902-1995) has been known to be the most complete, if redundant, representation of such evolutions even in nonlinear dynamical systems. Nonlinear optics, however, as a discipline has traditionally shied away from any kind of ray representations, perhaps due to concern over rigor or fear of oversimplification. In this talk, I will review how Wigner's version of phase-space reconciles wave and corpuscular optics and generalize the concept of "rays" to describe even nonlinear optical phenomena, such as self-focusing beams and solitary waves, more intuitively and vividly.

9271-2, Session 1

Diffractive optics for short wavelengths and short pulses *(Invited Paper)*

Jürgen Jahns, FernUniv. Hagen (Germany); Thordis Vierke, FernUniversität in Hagen (Germany); Manfred Musigmann, FernUniv. Hagen (Germany); Stephan Lindorfer, FernUniversität in Hagen (Germany)

During the past 20-30 years, diffractive optics has matured from an emerging technology to a field with numerous commercial applications. And yet, there is still plenty of room for interesting research and novel concepts. Here, we discuss two topics: nano focusing at EUV and x-ray wavelengths and spatio-temporal shaping of ultrashort pulses.

Focusing and imaging of EUV and x-ray radiation (i.e., at wavelengths from approximately 0.1 - 100 nm) has many applications, for example, in astronomy, advanced lithography and the life sciences. Different approaches exist, using refractive and diffractive optics. Diffractive approaches includes specific structures such as the "photon sieve" and, as a recent example, a Fresnel zone plate with structured rings. Here, the concepts behind these elements will be described and a diffraction-theoretical analysis will be presented.

The second topic to be addressed is the use of diffractive elements for the shaping of ultrashort optical pulses. Shaping in the spatial domain includes, for example, the generation of vortex beams. A diffractive implementation of a vortex beam is achieved by a so-called spiral axicon. Diffraction, however, leads to strong chromatic dispersion which causes a problem for ultrashort pulses. Here, we consider dispersion compensation by the combination of refraction and diffraction.

9271-3, Session 1

High-efficiency broadband reflective metasurface and plasmonic hologram application *(Invited Paper)*

Din Ping Tsai, Academia Sinica (Taiwan); Wei Ting Chen, National Taiwan Univ. (Taiwan); Kuang-Yu Yang, Ecole Polytechnique Fédérale de Lausanne (Switzerland); Chih-Ming Wang, National Dong Hwa Univ. (Taiwan); Yao-Wei Huang, Pin Chieh Wu, National Taiwan Univ. (Taiwan); Greg Sun, Univ. of Massachusetts Boston (United States); Shulin Sun, Lei Zhou, Fudan Univ. (China); Ai Qun Liu, Nanyang Technological Univ. (Singapore)

Holograms are the optical devices to reconstruct images by recovering amplitude and phase of light, which show many applications in our daily life. Recently, the metasurfaces, an array of sub-wavelength antenna, show the abilities to manipulate both the amplitude and phase of incident electromagnetic wave in a wide electromagnetic region from visible to microwave frequencies. Here, we realized a high-efficiency broadband 4-level phase plasmonic meta-hologram by reflected metasurface made of subwavelength 6?6 gold cross nano-antennas of 16 different shapes which is designed and fabricated in optical frequencies. As a result, the reconstructed images of meta-hologram exhibit far more efficient (reaches 18% for 780 nm illumination), polarization-controlled dual images with high contrast, functioning for both coherent and incoherent light sources within a broad spectral range (bandwidth ?880 nm) and under a wide range of incidence angles. The reflective hologram has a number of advantages such as simple fabrication process, low metal absorption, broad working spectral range, and greater tolerance to variation of incident angle and light incoherence. By combining with the techniques of tunable metasurfaces, meta-hologram can potentially be used to realize active hologram that works at arbitrary electromagnetic wave region.

9271-4, Session 1

Applications of diffractive optical elements for optical measurement techniques *(Invited Paper)*

Frederik Schaal, Tobias Haist, Christof Pruss, Wolfgang Osten, Institut für Technische Optik (Germany)

Diffractive optical elements insert a high degree of freedom for phase and spectral behavior in optical designs. This enables new and compact optical sensors. We show several recent applications which benefit from unique properties of diffractive optical elements. The applications include: field aberration correction e.g. of microscope objectives, 200 channel microscope objective integrated optical addressing system, tunable polarisation control, diffractive/refractive hybrid optics for high efficiency beam shaping, high precision freeform testing and deflection angle enlargement of spatial light modulators.

9271-5, Session 1

3D display with glasses-free based on micro-nano-approach and system (*Invited Paper*)

Linsen Chen, Soochow Univ. (China) and SVG Optronics (China)

The developments of new devices and advanced materials with micro-nano structures perform significant roles in accelerating the progress of ultra-thin 3D display with glasses-free. Composite sub-wavelength optics and nano-structure devices with functional designs have become the trends in the novel display industries. Recently, 3D display with glasses-free has been promoted by advanced nano-manufacturing technologies. One of the critical questions for the nano-patterning is the huge data processing capability requirement. For example, the 27 inches size of 3D images, the data should be as big as 15Tb. Of course, the large size micro-nano-molding technologies for the roll-to-roll nano-imprinting and induced-assembly are also very difficult. The most important question for commercialization of 3D display is how to fabricate the directional nano-structures and replicate the them to on the flexible substrates in cost-effective?

The topics will include an introduction to approaches of sub-wavelength grating waveguide devices for 3D display. A pixelized tunable interference lithography approach and system have been described for achieving the sub-wavelength gratings in pixels. The pitch and direction of sub-wavelength grating in pixel can be changed from 200nm to 500nm with the sub-nanometer accuracy according to the design of grating distribution design of 3D display. Therefore, with this technology, the 3D images and sub-wavelength light guide plates can be easily fabricated to goal the real colorful 3D effects. The example of micro-nano-light guide films for 3D display units has been introduced based on the nano-patterning and roll-to-roll nano-imprinting technologies. The strategies to push the 3D display ahead have been introduced for either the research work, or the industrial applications. The glasses-free 3D display has shown powerful vital force in industry field. There are lots of opportunities to be collaborated together for 3D display.

9271-6, Session 2

Holographic video of real-world scenes based on multi-modal data capture (*Invited Paper*)

Malgorzata Kujawińska, Tomasz Kozacki, Konstantinos Falaggis, Robert Sitnik, Warsaw Univ. of Technology (Poland)

Holographic capturing of large scenes in an open space is difficult or even impossible to realize at the present stage of the technology. This is the reason why multi-source 3D data capture has to be employed in order to generate complex hologram and holographic video. For the purpose of this work we had captured three different types of 3D objects: a series of high quality cloud of points with texture (x,y,z:RGB) captured for variable in time real 3D object, a series of digital holograms of moving 3D object and a set of 2D images of a background. This individual data is converted into Fresnel holograms. All inputs have to be composed into a multi-modal digital hologram. The assembly process is based on the superposition of individual holograms. The composition is started from the furthestmost distant object (background). Then this holographic field is refocused to the reconstruction plane of the second input hologram and the holograms are merged in the subsequent sharp reconstruction planes. The two merged inputs: are joined basing on the thresholding mask. The mask divides holographic field into two regions: one region corresponds to the new holographic input

with sharp image, while the second one to the refocused field of the background hologram. For the propagation we employ angular spectrum method. The process is repeated for all of the holographic inputs, finishing with the propagation to the hologram plane. As in a holographic video all these operations have to be performed many times in real time, the automating and accelerating of processing procedures are discussed and the present efficiency of the procedures is reported.

9271-7, Session 2

Recent holographic display: devices and applications (*Invited Paper*)

Juan Liu, Yongtian Wang, Beijing Institute of Technology (China)

Holographic display has been widely used in various fields, including the planar holographic waveguide, the full-color holographic 3D printer, and dynamic holographic three-dimensional (3D) display, and so on. In this presentation, we will firstly overview various holographic display methods. We will then present three recent developed devices in our lab for holographic display: holographic waveguide display, 3D stereo-holographic display, and 3D real-time holographic display. Basic problems and primary solutions are included in this presentation.

9271-8, Session 2

3D holographic reconstruction by the angular spectrum based on phase-only spatial light modulator (*Invited Paper*)

Liangcai Cao, Yan Zhao, Hao Zhang, Qingsheng He, Guo Fan Jin, Tsinghua Univ. (China)

A three dimensional computer generated holographic display by angular spectrum method based on a phase-only spatial light modulator (SLM) is proposed. The proposed method is more computationally efficient compared with the point source algorithm. Objects consists of multiple slices, i.e., medical images from computational tomography(CT), can be easily modeled by the angular spectrum. It is demonstrated that 3D structure can be built through the superposition of computer generated phase holograms originally from parallel discrete planes at different depths. An angular spectrum algorithm for the computer generated phase holograms from all the slices is proposed. Then the superposed phase hologram is uploaded to the phase-only SLM. Coherent light illumination is applied to the SLM and the 3D reconstruction is observed by a camera. The reconstructions testified that the pure-phase hologram could reconstruct 3D slice images. The phase holograms is capable of higher diffraction efficiency than the amplitude hologram. It could also help to avoid the complicated coding of amplitude hologram from the complex amplitude and avoid the twin image during the reconstruction.

9271-9, Session 3

Polarization multiplexed Debye diffraction-limited multifocal array

Haoran Ren, Xiangping Li, Min Gu, Swinburne Univ. of Technology (Australia)

Diffraction-limited multifocal arrays based on phase-only modulation by a high numerical aperture (NA) objective are essential for applications requiring high-throughput parallel laser processing such as imaging, direct laser writing and

optical data storage. Meanwhile, as one of fundamental aspects, polarization of light plays a deterministic role in controlling light-matter interactions. As such, there is an increasing interest in manipulating not only the intensity distributions but also the polarization states in the individual foci of a multifocal array. Despite that the Jones calculus can be applied in the manipulation both of polarization and phase in a single paraxial beam; it cannot generate a multifocal array with individually variant polarized foci by a high NA objective. To date, it is still a compelling obstacle to individually tailor the polarization states in a multifocal array by a high NA objective. We propose a novel phase-only modulation enabling us to individually manipulate the polarization states in a highly uniform diffraction-limited multifocal array by a high NA objective. The vectorial Debye diffraction theory is used to calculate both the intensity and the polarization distributions in the focal region and a weighting factor is further applied to adaptively improve the uniformity in a multifocal array. The multifocal arrays with variable polarization states in individual foci and high polarization purity have been experimentally verified through applying the phase-only modulation method to parallel imaging of gold nanorods. Consequently, the method has been successfully applied to dynamic parallel polarization multiplexed storage where multiple polarization channels can be recorded simultaneously.

9271-10, Session 3

Polarization holography and its characteristics (*Invited Paper*)

An'an Wu, Xiaodi Tan, Jinliang Zang, Ying Liu, Jue Wang, Xiao Lin, Beijing Institute of Technology (China); Tsutomu Shimura, The Univ. of Tokyo (Japan); Kazuo Kuroda, Beijing Institute of Technology (China) and Utsunomiya Univ. (Japan)

In recent years, a detailed and useful tensor theory of polarization holography was proposed. This theory is based on the photoinduced change of the dielectric tensor of the polarization sensitive materials. It is expressed as a function of the electric field in a general form. Using this expression, the vectorial coupled wave equations that describe the interaction of incident waves during the propagation in polarization holograms are derived. The characteristics of the reconstruction of the polarization holography are studied on the basis of the tensor theory. The result is that, in general, the polarization state of the reconstructed signal is different from the recorded signal. However, if a special condition is satisfied, it can be reconstructed faithfully by the illumination of the original reference wave. And, in this condition, if we use the orthogonal reference wave to reconstruct, some interesting phenomena will occur. Also the phenomena are different when the polarization states of the waves we used to record are different. In this paper, we focus on the characteristics of the reconstruction of the polarization holography using the circularly polarized wave. Based on the tensor theory, we derived its properties theoretically. We discuss the special condition that the signal can be faithfully reconstructed. And in this condition we found that the reconstruction wave is disappeared when we use the orthogonal reference wave to reconstruct. Related experimental results show consistent trends with the theoretical results as well.

9271-11, Session 3

Precise optical simulation for volume holographic storage based on VOHIL model (*Invited Paper*)

Ching-Cherng Sun, Yeh-Wei Yu, National Central Univ. (Taiwan)

Holographic data storage is capable to perform not only high-density and long-life storage but also optical parallel readout. Besides, the volume-holographic disc has an advantage of EM pulse resistance to makes it more secure. As a result, volume holographic storage is regarded as one of the major solutions for the era of big data. In order to deal with the complicated calculation of the holographic data storage system, VOHIL model is used for calculating the diffraction condition of a volume hologram under weak coupling. The model is simpler and more effective comparing to couple mode theory and Born's approximation. Based on VOHIL model, analytic solution for collinear holographic storage system, off-axis shift-multiplexing holographic storage system, and even random phase encoding storage system were proposed. According to the clear physics insight shown by the analytic solution, we keep proposed system optimization methods and novel solutions in the past ten years. For collinear system, we proposed reference with lens array modulation, which approaches the best SNR of the world. For off-axis shift-multiplexing holographic storage system, we proposed methods to compensate the pixel migration, to reduce the radial cross-talk, and to improve the longitudinal shift selectivity.

9271-12, Session 3

Gold nanosphere-doped photopolymer for volume holography

Liangcai Cao, Chengmingyue Li, Zheng Wang, Qingsheng He, Guo Fan Jin, Tsinghua Univ. (China); Yuan Luo, National Taiwan Univ. (Taiwan)

Due to its attractive properties of low cost, large refractive index changes and high dimensional stability, photopolymer has been extensively used in holographic applications such as holographic data storage, holographic display and holographic optical elements. In this work, we firstly propose a novel gold nanosphere doped photopolymer for volume holography. Nanospheres with the diameter of 6-8 nm are evenly dispersed inside a thick photopolymer with thermo-polymerization method. The holographic properties can be greatly enhanced during the two-beam holographic exposure with the doping of the gold nanospheres. Both the photophysical and photochemical mechanism of the gold nanosphere doped photopolymer are analyzed and discussed during holographic grating formation. The applications of the photopolymer for volume holographic recording and reconstruction systems are also experimentally demonstrated.

References:

1. Chengmingyue Li, Liangcai Cao*, Jingming Li, Qingsheng He, Guofan Jin, Shiman Zhang, and Fushi Zhang, "Improvement of volume holographic performance by plasmon-induced holographic absorption grating," *Applied Physics Letters*, 102, 061108 (2013).
2. Chengmingyue Li, Liangcai Cao*, Qingsheng He, and Guofan Jin, "Holographic kinetics for mixed volume gratings in gold nanoparticles doped photopolymer," *Optics Express*, 22, 5017-5028 (2014).

9271-13, Session 3

Reflection grating in collinear holographic storage system

Yeh-Wei Yu, Shuai Xiao, Ching-Cherng Sun, National Central Univ. (Taiwan)

Collinear holographic storage system is simple and stable, and thus has more potential in commercialization. Due to the reflection layer inside the disc of collinear system, the reflection

beam and transmission beam cause reflection grating inside the disc. The optical behaviors of the reflection grating are exactly different from the transmission grating. However, the behavior of reflection grating has never been discussed by literatures. In this paper, we propose the optical model of reflection grating of collinear holographic storage system. The paraxial analytic solution is derived out based on VOHL theorem and Fresnel diffraction approximation. By the analytic solution, we are able to analyze both point spread function and wavelength selectivity of the reflection grating. Accordingly, we find the point spread function for both reflection grating and transmission grating are the same, but the wavelength selectivity of reflection grating are higher than transmission grating. The analysis result benefits the development of collinear holographic storage system.

9271-14, Session 3

Polarization-based all-optical logic operations in volume holographic photopolymer

Chengmingyue Li, Liangcai Cao, Chengmingyue Li, Qingsheng He, Guo Fan Jin, Tsinghua Univ. (China)

The emergence of optical signal processing systems demands all-optical logic devices with high speed and parallel signal processing [1]. Holographic technology has the unique advantages to implement all-optical logic devices for its intrinsic nature of fast transfer rate and high parallelism [2]. In the past decades, holographic all-optical logic operations were realized either based on intensity with high energy depletion or in the holographic crystal and photorefractive film [3-4]. Its further application on devices is limited by the complex fixing process of the holographic crystal and external electronic control of the photorefractive film. Compared with these two types of material, holographic photopolymer is an optimum medium for practical holographic applications due to its large capacity, dry real-time processing and low cost [5]. In this letter, we report on all-optical logic AND, OR and NAND operations manipulated by polarization in a volume holographic photopolymer. The polarization-based all-optical logic implementation on two input pages is analyzed theoretically with the theory of polarization volume holographic grating. To accurately represent the output optical operations, the polarization properties of this photopolymer with the thickness of 1 mm are characterized for holographic recording and reconstruction process. Then two input pages are recorded simultaneously in this photopolymer through a dual-channel polarization holographic architecture. By changing the polarization state of the diffraction beam, all-optical logic AND, OR and NAND operations could be implemented in the volume holographic photopolymer. This polarization-based all-optical logic operations in the volume holographic photopolymer may pave a way for practical all-optical logic devices with high speed and large information capacity.

9271-15, Session 4

Lasing from Penrose quasicrystal made by holographic polymer-dispersed liquid crystals (Invited Paper)

Dan Luo, South Univ. of Science and Technology of China (China); Xiaowei Sun, Nanyang Technological Univ. (Singapore)

Quasicrystals, which possess only long-range order and orientation symmetry but not translation symmetry, was firstly observed by D. Shechtman in Al-Mn metallic alloy [1]. Lasing, generated from photonic quasicrystals (PQCs) fabricated by semiconductor materials, have been reported to generate

possible unlimited lasing modes due to the arbitrary order of their rotational symmetry while only limited mode existing in photonic crystals (PCs) [2].

Due to electrically switchable/tunable optoelectronic properties, liquid crystals/polymer composite have received substantial attention. Different kinds of periodic/non-periodic structures such as grating, photonic crystals and photonic quasicrystal have been realized through holography lithography based on holographic polymer dispersed liquid crystals (H-PDLCs). Despite the low index contrast, which forbids the exist of complete bandgaps, lasing from photonic crystals made by H-PDLCs is still possible due to low group velocity dispersion and local field enhancement [3].

In this paper, we report the lasing from photonic Penrose quasicrystal made by H-PDLCs. The lasing presented here shows excellent linear polarization property and relative low pumping threshold comparing to that from photonic crystal made by H-PDLCs. A wide directional dependence of lasing is also achieved. These properties make laser based on H-PDLC photonic quasicrystal promising for a new type of an all organic tunable miniature lasers.

References:

- [1]. M. Notomi, H. Suzuki, T. Tamamura, and K. Edagawa, Phys. Rev. Lett. 92, 123906 (2004).
- [2]. T. J. Bunning, L. V. Natarajan, V. P. Tondiglia, and R. L. Sutherland, Annu. Rev. Mater. Sci. 30, 83 (2000).
- [3]. R. Jakubiak, V. P. Tondiglia, L. V. Natarajan, R. L. Sutherland, P. Lloyd, T. J. Bunning, and R. A. Vaia, Adv. Mat. 17, 2807-2811 (2005).

9271-16, Session 4

Transport of intensity equation: a new approach to phase and light field

Chao Zuo, Qian Chen, Nanjing Univ. of Science and Technology (China); Anand K. Asundi, Nanyang Technological Univ. (Singapore)

Phase is an important component of an optical wavefield bearing the information of the refractive index, optical thickness, or the topology of the specimen. Phase retrieval is a central problem in many areas of physics and optics since the phase of a wavefield is not accessible directly. The most well-established method for obtaining quantitative phase is through interferometry, such as digital holography. However, this class of methods relies on coherent illumination, therefore, plagued with problems of speckle that prevent the formation of high quality images. On a different note, quantitative phase can be retrieved by transport-of-intensity equation (TIE) using only object field intensities at multiple axially displaced planes. TIE has been increasingly investigated during recent years due to its unique advantages over interferometric techniques: it is non-interferometric, works with partially coherent illumination, computationally simple, no need to phase unwrapping, and does not require a complicated optical system. In this presentation, we will talk about some recent new developments in TIE phase retrieval: including its fast numerical solution, treatment of boundary problem and the low-frequency artifacts, and two configurations for dynamic phase imaging. We also reexamine TIE in terms of phase-space optics, demonstrating the effect of partially coherent illumination on phase reconstruction, and connecting it to light field imaging at the geometry optics limit.

9271-18, Session 4

Polarization-insensitive and bandwidth-adjustable anisotropic dynamic gratings based on erbium-doped fiber

Pan Xu, National Univ. of Defense Technology (China)

We demonstrated a polarization-insensitive and bandwidth-adjustable anisotropic dynamic grating based on Er-doped fibers by utilizing phase modulation technology. A Faraday rotator mirror attached to the end of the Er-doped fiber guarantees the feedback light is orthogonally polarized to the entrance light, and then these two orthogonal polarized waves form an anisotropic dynamic grating. The polarization insensitive property of the dynamic grating is also maintained by using the Faraday rotator mirror and is validated experimentally. Experimental results show that varying the amplitude of phase modulation can adjust the reflection bandwidth of the anisotropic dynamic grating, and the fitting control coefficient is about 5MHz/rad.

9271-19, Session 5

Holographic generation of non-diffractive beams (Invited Paper)

Byoung-ho Lee, Dawoon Choi, Keehoon Hong, Seoul National Univ. (Korea, Republic of); Kyoung-Youm Kim, Sejong Univ. (Korea, Republic of)

An Airy beam is a non-diffractive wave which propagates along a ballistic trajectory without any external force. Although it is impossible to implement ideal Airy beams because they carry infinite power, so-called finite Airy beams can be achieved by tailoring infinite side lobes with an aperture function and they have similar propagating characteristics with those of ideal Airy beams. The finite Airy beam can be optically generated by several ways: the optical Fourier transform system with imposing cubic phase to a broad Gaussian beam, nonlinear generation of Airy beams, curved plasma channel generation, and electron beam generation. In this presentation, a holographic generation of the finite Airy beams will be discussed. The finite Airy beams can be generated in virtue of holographic technique by 'reading' a hologram which is recorded by the interference between a finite Airy beam generated by the optical Fourier transform and a reference plane wave. Moreover, this method can exploit the unique features of holography itself such as successful reconstruction with the imperfect incidence of reference beam, reconstruction of phase-conjugated signal beam, and multiplexing, which can shed more light on the characteristics of finite Airy beams. This method has an advantage in that once holograms are recorded in the photopolymer, a bulky optics such as the SLM and lenses are not necessary to generate Airy beams. In addition, multiple Airy beams can be stored and reconstructed simultaneously or individually.

9271-20, Session 5

Beam shaping with multiple-powered phase masks

Dengfeng Kuang, Nankai Univ. (China); Thierry Lépine, Univ. Jean Monnet Saint-Etienne (France); Jianliang Tian, Nankai Univ. (China); Paul Dufouleur, Univ. Jean Monnet Saint-Etienne (France)

Cubic phase mask has been demonstrated to generate finite energy Airy beam by modulating a Gaussian beam [1] and to extend the depth of imaging field [2]. We present multiple-powered phase masks to convert a plane wave beam into

different shaped beams, which shall be very useful for atomic guiding and optical manipulation. We use a micro-objective lens, a pinhole and a focusing lens to convert the incident Gaussian laser beam to a plane wave and then we use an aperture to limit the beam diameter. A transmitting spatial light modulator (SLM) is employed to impose the multiple-powered phase masks. The shaped beams are generated and observed before and after the Fourier plane of a converging lens. The experimental results and the simulation results with Zemax are compared. With the squared phase mask, a hollow beam is obtained before the Fourier plane of the converging lens and a highly focused beam is obtained after the Fourier plane. With the fourth-power phase mask, a highly focused point is formed on the Fourier plane, then a beam lattice with strong light spots on the four corners is generated after the Fourier plane and the beam lattice has different size on different observing distances. With the fifth-power phase mask, an approximately diffraction-free and self-bending beam is generated over long propagation distances (more than 30 cm).

References

[1] G. A. Siviloglou, J. Broky, A. Dogariu and D. N. Christodoulides, "Observation of accelerating Airy Beams," Phys. Rev. Lett. 99, 213901 (2007).

[2] Edward R. Dowski and W. Thomas Cathey, "Extended depth of field through wave-front coding," Appl. Opt. 34, 1859-1866 (1995).

9271-21, Session 5

Axial multifocal spots generated by sectored phase-only modulation under tight focusing condition

Linwei Zhu, Meiyu Sun, Ludong Univ. (China); Junjie Yu, Shanghai Institute of Optics and Fine Mechanics (China); Zhigang Li, Jiannong Chen, Ludong Univ. (China)

We propose a method for generating axial multifocal spots (AMS) with a high numerical aperture (NA) objective. The AMS is generated by using phase-only modulation at the back aperture of the objective. Without using any iteration algorithm, the modulated phase distribution is directly calculated by an additional phase analytical formula with different focal distances. By dividing the back aperture of the objective into multi sectorial zones and applying the corresponding additional phase with different focal distances, the axial multifocal spots can be generated. Numerical simulation shows that the numbers of the axial focus depends solely on the different phase distribution calculated by different focal distances. By engineering the phase pattern with different focal distances, axial multifocal spots with different spacing can be created. Furthermore, combined with vortex phase, the AMS with specific shape spots can be created. In addition, the AMS focused by incident beams of circular polarization, radial polarization and angular polarization are also studied. This kind of AMS may be found applications in optical imaging, especially in three-dimensional (3D) biological imaging, and also be attractive in multi-plane optical trapping.

9271-22, Session 5

Modulation of rotationally symmetric mask on the focusing of azimuthally polarized beams

Peng Li, Northwestern Polytechnical Univ. (China)

The unique focusing properties of cylindrical vector (CV) beams have been extensively studied over the past years, owing to their wide applications in optical trapping, super-resolution imaging,

as well as superfine processing. Recently, more research interest focus on the tight focusing of azimuthally polarized (AP) beams. Beyond the extraordinary intensity distribution in focal field, the polarization and transversal energy flow distribution are much richer and have displayed very interesting issues. It has been proposed that the AP beams obstructed by rotationally symmetric obstacles take place energy flow redistribution in the focal region, and the AP beams modulated by spiral phase and sector obstacle exhibit controllable polarization singularities conversion. In this paper, we explore theoretically the focusing dynamics of AP beams transmitted from rotationally symmetric masks, by connecting the tunable polarization and energy flow distribution with the angular diffraction. Our results show that, for an N-fold symmetric composite mask, each single-segment aperture gives rise to pair of circularly polarized components with opposite handedness, and each circularly polarized component has its own set of orbital angular momentum (OAM) sidebands which occupy the angular positions $\theta = \pm 2\pi/N$, the interference of circular polarizations carrying opposite OAM give rise to the generation abundant polarization properties.

9271-23, Session 5

Transformation of top-hat distribution from Gaussian laser beam using a kinoform

Shiyuan Yang, Seiichi Serikawa, Kyushu Institute of Technology (Japan)

In general, it is often used to transform a Gaussian laser beam to a Top-hat distribution with a series of lenses, but it is not a good Top-hat distribution because of the structure of lenses. In this study, the authors suggest a new method to transform a Gaussian laser beam to a Top-hat distribution using a phase-only computer-generated hologram so-called kinoform. In order to obtain a good Top-hat distribution, it is necessary to use some dummy area as a freedom to reduce the errors in the Top-hat region. We use an iterative dummy area algorithm to optimize the distribution of kinoform. Simulation results show that a plane-wave-near-field Top-hat distribution region can be obtained. We also find that the quality of Top-hat distribution depends on the Gaussian radius and the ratio of Top-hat region and the dummy area. Detail relationships are simulated for various Gaussian radius, sizes of Top-hat region and the dummy area.

9271-24, Session 5

Holographic techniques applied in the generation of statics and dynamics special non-diffractive beams

Marcos R. R. Gesualdi, Tarcio de Almeida Vieira, UFABC (Brazil); Michel Zamboni-Rached, Univ. Estadual de Campinas (Brazil)

In this work, we present the experimental generation of statics and dynamics special Non-Diffractive Beams (Bessel beams, Airy beams, Frozen Waves and others) using holographic techniques. First, the experimental realization of these NDBs was obtained using a holographic setup for the optical reconstruction of computer generated holograms (CGH), based on a 4-f Fourier filtering system and a spatial light modulator (SLM), where CGHs were first computationally implemented, and later electronically implemented, on the SLM for optical reconstruction. For other hand, the photorefractive holography was used for generation of NDBs. The experimental results are in agreement with the corresponding theoretical analytical solutions and hold excellent prospects for implementation to many applications such as optical tweezers, tractor beams systems, optical bistabilities,

optical high-intensity waves and others in optics and photonics areas.

References:

- [1] Vieira, Tarcio A. ; GESUALDI, MARCOS R. R. ; Zamboni-Rached, Michel . Frozen waves: experimental generation. *Optics Letters*, v. 37, p. 2034-2036, 2012.
- [2] Vieira, Tarcio A. ; Zamboni-Rached, Michel ; Gesualdi, Marcos R.R. . Modeling the spatial shape of nondiffracting beams: Experimental generation of Frozen Waves via holographic method. *Optics Communications (Print)*, v. 315, p. 374-380, 2014.
- [3] Vieira, Tarcio A. ; Gesualdi, Marcos R.R. ; Zamboni-Rached, Michel . Experimental Generation of Frozen Waves in Optics: Control of Longitudinal and Transverse Shape of Optical Non-diffracting Waves. In: H. E. Hernández-Figueroa, E. Recami and M. Zamboni-Rached. (Org.). *Non-Diffracting Waves*. 1ed.: Wiley-VCH Verlag GmbH & Co. KGaA, 2013, v. , p. 417-431.

9271-25, Session 6

Demonstration of an autostereoscopic three-dimensional light-emitting diode display using diffractive optical elements sheet

Ping Su, Graduate School at Shenzhen, Tsinghua Univ. (China); Pengli An, Tsinghua Univ. (China); Jianshe Ma, Graduate School at Shenzhen, Tsinghua Univ. (China); Lixiang Han, Zhenbo Ren, Tsinghua Univ. (China); Mao Jie, Shanghai Huanding Television Technology Co., Ltd. (China)

The autostereoscopic three-dimensional (3D) light-emitting diode (LED) displays with traditional light splitting elements (LSE; lenticular lens and parallax barrier) are suffering from a large distance from the LSE and the LED display panel. An autostereoscopic three-dimensional (3D) light-emitting diode (LED) display system using a diffractive optical elements (DOEs) sheet as the light splitting element is proposed. For a specified application, the DOE with a proper magnification factor is designed. In order to making the DOEs periodically arranged to reduce processing difficulty and the viewing zones equally-spaced, the column spacings of the LED display panel are non-equal. There is a one-to-one correspondence between the DOEs and the columns of the LED display panel, and the thickness of the proposed display panel is $k+1$ times (k is the number of viewing zones) smaller of that of the existing technology. A roller mold is fabricated by diamond turning, and 100mm-wide DOE sheet is acquired by nanoimprinting. With precisely truncating and splicing of the DOE sheets, a 12m² autostereoscopic LED display prototype is finally developed. The thickness of the prototype is 57.7mm, which makes the installation of a outdoor display possible. The experimental result shows that the proposed method is a potential autostereoscopic technology for the large area LED displays.

9271-26, Session 6

Glasses-free large size high-resolution three-dimensional display based on the projector array (Invited Paper)

Xinzhu Sang, Beijing Univ. of Posts and Telecommunications (China)

Normally, it requires a huge amount of spatial information to increase the number of views and to provide smooth motion parallax for natural three-dimensional (3D) display similar to real life. To realize natural 3D video display without eye-wears,

a huge amount of 3D spatial information is normal required. However, minimum 3D information for eyes should be used to reduce the requirements for display devices and processing time. For the 3D display with smooth motion parallax similar to the holographic stereogram, the size the virtual viewing slit should be smaller than the pupil size of eye at the largest viewing distance. To increase the resolution, two glass-free 3D display systems rear and front projection are demonstrated based on the space multiplexing with the micro-projector array and the special designed 3D diffuse screens with the size above 1.8 m² × 1.2 m. The displayed clear depths are larger 1.5m. The flexibility in terms of digitized recording and reconstructed based on the 3D diffuse screen relieves the limitations of conventional 3D display technologies, which can realize fully continuous, natural 3-D display. In the display system, the aberration is well suppressed and the low crosstalk is achieved. 64 views and 32 views 3D video displays are realized.

9271-27, Session 6

Binocular three-dimensional measurement system using a Dammann grating

Kun Liu, Shubin Li, Yanyang Li, Jin Wang, Yancong Lu, Shengbin Wei, Shaoqing Wang, Changhe Zhou, Shanghai Institute of Optics and Fine Mechanics (China)

In this paper, we develop a binocular three-dimensional measurement system using a Dammann grating. A laser diode and a two-dimensional Dammann grating are employed to generate a regular and square laser spot array. Dammann array illuminator is placed between the two cameras and narrowband-pass filters are embedded in the project lens to eliminate the interference of background light. During the measurement, series laser spot arrays are projected toward the object and captured by two cameras simultaneously. Similar to stereo vision of human eyes, stereo matching will be performed to search the homologous point which is a pair of image points resulting from the same object point. At first, the sub-pixel coordinates of the laser spots are extracted from the stereo images. Then stereo matching is easily performed based on a fact that laser spots with the same diffraction order are homologous ones. Because the system has been calibrated before measurement, single frame three-dimensional point cloud can be obtained using the disparity between homologous points by triangulation methods. At last, three-dimensional point clouds belong to different frame which represent different view of the object will be registered to build up an integral three-dimensional object using our improved ICP algorithm. On one hand, this setup is small enough to meet the portable outdoor applications. On the other hand, measurement accuracy of this system is better than 0.3 mm which can meet the measurement accuracy requirements in most situations.

9271-28, Session 6

Three-dimensional holographic imaging of a real diffusely reflective object with conversion to horizontal-parallax-only hologram

Taegeun Kim, You Seok Kim, Sejong Univ. (Korea, Republic of)

Recently, speckle free recording of a diffusely reflective object is demonstrated using optical scanning holography. In this technique, the complex diffracted field of a real object is extracted without speckle noise. This makes it possible to process the complex diffracted field numerically without background, twin image and speckle noise. In this presentation, we review

recent progress of three dimensional holographic imaging system which includes off-axis hologram converting process. This process converts the complex diffracted field into an off-axis hologram that is suitable to be presented using a conventional amplitude-only spatial light modulator.

9271-29, Session 6

A time-sequential autostereoscopic 3D display using a vertical line dithering for utilizing the side lobes (Invited Paper)

Hee-Jin Choi, Minyoung Park, Sejong Univ. (Korea, Republic of)

In spite of the developments of various autostereoscopic 3D technologies, the inferior resolution of the realized 3D image is a severe problem that should be resolved. For that purpose, a time-sequential 3D display is developed to provide 3D images with higher resolution and attracts much attention. Among them, a method using a directional backlight unit (DBLU) is an effective way to be adopted in liquid crystal display (LCD) with higher frame rate such as 120Hz. However, in the conventional time-sequential system, the insufficient frame rate results a flicker problem which means a recognizable fluctuation of image brightness. A dot dithering method can be a good solution for reducing that problem but it was impossible to observe the 3D image in side lobes because the image data and the directivity of light rays from the DBLU do not match in side lobes.

In this paper, we propose a new vertical line dithering method to expand the area for 3D image observation by utilizing the side lobes. Since the side lobes locate in the left and right position of the center lobe, it is needed to arrange the image data in LCD panel and directivity of the light rays from the DBLU to have continuity in horizontal direction. Although the observed 3D images in side lobes are flipped ones, the utilization of the side lobes can increase the number of observers in horizontal direction.

9271-30, Session 6

Unwrapping stepped objects using reduced-phase dual-illumination technique

Behnam Tayebi, Yonsei Univ. (Korea, Republic of)

We propose a common path, off axes, single shot and single wavelength phase imaging technique for measuring high phase transparent objects without using unwrapping process. A grating between a laser and the object is used to make beams with different angle, which determines the measurement range of the microscope. The grating pitch and magnification of the lens system before the sample affect the angle. The angle inside the object is changed according to Snell's law; therefore, final angle is related to the refractive index of the object. Magnification of the lens system after sample will control the modulation frequency of microscope. The interference pattern is constructed at CCD plane and convey information of the sample. For a phase below the measurement range of the microscope, the reconstructed phase is not wrapped. By increasing the measurement range accuracy of the system will drop; therefore the magnification of the lenses must choose carefully to obtain optimal phase. The ability of this technique is demonstrated by reconstructing phases of two transparent step objects with 150 and 510 micrometers height without using unwrapping algorithms.

9271-31, Session 7

Experimental Investigation of reconstruction guarantee in compressive Fresnel holography

Fan Wu, Yuhong Wan, Tianlong Man, Xiaole Guo, Beijing Univ. of Technology (China)

Compressive sensing (CS) offers a mathematical framework which allows us to reconstruct the original data from many fewer measurements than suggested by Shannon's sampling theorem. In recent years, compressive sensing has been successfully applied in digital holography (DH), formulated holography as a compressive sensing problem, thus the reconstruction of hologram is inverted as the decompress and solving the minimization problem. The original information can be reconstructed accurately when the reconstruction conditions is guaranteed in different physical scheme and recording set-up. In this paper, the reconstruction conditions are investigated both theoretically and experimentally in near-field Fresnel propagation regime. The effect of recording distance on the physical properties of Fresnel wave propagation as the sensing operator and the coherence parameter are demonstrated, and then show their effect on reconstructed image quality. The experiments are designed and implemented based on off-axis phase shift digital holography using Mach-Zehnder interferometric recording set-up. The reconstruction was carried out using two-step iterative shrinkage/thresholding algorithm (TwIST) to decompress. We have randomly sampled the holograms which are recorded at different z and found the required minimal number of samples (M) for obtaining the reconstructed images with acceptable PSNR. Based on the investigation, the recording distance affects the coherence parameter. When the recording distance z is given, the limitation of sampling ratio (M/N) is considered and the qualities of reconstructed images are demonstrated experimentally.

9271-32, Session 7

A 3D acquisition method for holographic display

Weirui Yue, Shanghai Institute of Optics and Fine Mechanics (China); Jingdan Liu, Beijing Institute of Technology (China); Guohai Situ, Shanghai Institute of Optics and Fine Mechanics (China)

It is well known that holographic display can provide 3D scenes with continuous viewpoints and free of accommodation-convergence conflict. So far most of the research in this area focuses on the display end, leaving the acquisition end merely explored. For holographic content acquisition, one needs to capture the scene in 3D. Ways to do this include the traditional optical holography and integral imaging. However, optical holography suffers from serious speckle while integral imaging has a long march to increase the resolution. In this paper, we propose a technique based on a variation of the transport of intensity equation to calculate the "phase" information of a scene from its defocused intensity captured by a color camera under white light illumination. With the defocused phase and intensity data at hand, we can calculate the infocused wavefront of the scene, and further encode it into a computer generated hologram for subsequent holographic display. We demonstrate the proposed technique by simulation and experimental results. Compared with existing 3D acquisition techniques for holographic display, our method may provide better viewing experience due to the free of speckle in the acquisition stage, as well as the fact that the resolution does not limited by the microlenslet.

9271-33, Session 7

4D imaging based on the Fresnel Incoherent Correlation Holography

Xia Shi, Bin Yuan, Wufeng Zhu, Fengying Ma, Zhengzhou Univ. (China)

Fresnel incoherent correlation holography (FINCH) is one of the three-dimensional imaging techniques which records holograms under incoherent illumination. A spatial light modulator (SLM) was used to split the incoherent light reflected/emitted from each object point into two spatial self-coherent spherical beams with different curvatures, and the interference fringes was recorded by a CCD. Based on the theoretical and simulation research, a mathematical model of FINCH system using dual diffractive lenses on a spatial light modulator has been established. We obtained the specific forms of the point spread function, the axial magnification and the resolution. The results show that the system can realize the recording and reconstruction of 3D object rapidly in a single channel and motionless way. This technique can be applied in real-time 3D display, microscopic imaging and other areas. We present a new idea of 4D imaging, and the numerical simulation of three channel color holographic imaging is given. One 4D imaging system based on electrically tunable FP filter is proposed too, and we discuss the key problem of this new technique at last.

9271-34, Session 7

LED holographic imaging by spatial-domain diffraction computation of textured models

Ding-Chen Chen, Xiao-Ning Pang, Yi-Cong Ding, Yi-Gui Chen, Jian-Wen Dong, Sun Yat-Sen Univ. (China)

Unavoidable speckle noise on reconstructed image in laser-based holography system has been a serious problem in holographic display, due to both the temporal and spatial coherence of laser. Employing partially coherent light in optics experiment is an effective way to reduce the speckle noise and thus enhance the signal-to-noise ratio. In this talk, we will show you the analysis on the coherence of input light, which will affect the quality of the reconstructed image by computer generated hologram (CGH). The correlation between the coherence of light and the image quality is theoretically investigated. We use LED light source with band-pass filters and spatial filters to achieve different levels of coherence. The experimental results show high agreement with our analysis on the correlation. On the other hand, we previously proposed a full analytical diffraction computation for encoding the CGH of polygonal model. Although it is a high efficient way, the unexpected fringes inside each triangle of the model can be obviously seen, and it generates negative impressions to human beings. In the talk, we will also show you how to eliminate these unexpected fringes by introducing fast Fourier transform instead of analytical Fourier transform. Affine transform is also applied to the Rayleigh-Sommerfeld diffraction. In conclusion, we propose the LED-based holographic imaging system, in order to improve the quality of the holographic imaging.

9271-35, Session 7

Full parallax stereo holography research-based computer generated holography

Gao Bin Yan, Jia Yu, Huiping Liu, Tian Wang, Jincheng Wang, Ocean Univ. of China (China)

This paper studies the method of three-dimensional dynamic

holographic display and proposes a new method that combines CGH and holographic stereogram. While making CGH of a real three-dimensional object, the propagation of diffracted object light wave front is a very complicated problem, a large amount of the data computation is need. Furthermore, resolution requirements of the recording material are up to tens of thousands of lines per millimeter, the current spatial light modulator technology is not able to meet the requirement. The CGH and holographic stereogram are combined in our method in the following steps: firstly, a set of perspective 2D pictures are acquired from a virtual 3D objects in computer according to the full parallax principle, secondly, the original images are processed with certain image transform method and new sequences of 2D images are generated, then the CGH is generated while a sequence of Fresnel holograms are calculated one by one with each of the new image sequence acting as the object, and finally every Fresnel hologram of the sequence acts as a holographic stereogram unit and all of them together form a whole 3D image. Due to the high cost of high-resolution SLM, instead of making dynamic holographic displaying system, experiment are carried out only by making the hologram to verify the feasibility of our method. The Fresnel hologram is recorded on holographic plate by projected lithography, the size of the pixel of the image projected is about 0.3 microns, a hologram is produced with the area of one square centimeter and stereo 3D effects is generated successfully which verifies the correctness and feasibility of our method. With the development of SLM technology, while the CGH made by this method is displayed on a high- resolution SLM, the 3D dynamic holography will be achieved.

9271-17, Session Post

Synchronization control for ultrafast laser parallel microdrilling system

Zhongsheng Zhai, Hubei Univ. of Technology (China) and Univ. of Liverpool (United Kingdom); Zheng Kuang, Jinlei Ouyang, Dun Liu, Walter Perrie, Stuart Edwardson, Geoff Dearden, Univ. of Liverpool (United Kingdom)

Ultrafast lasers have been widely used in material micro-processing with the advantage of very little thermal damage. Parallel micro-processing has been seen significant developments in ultrafast laser fabrication, thanks to Spatial Light Modulators (SLM) which can split a single beam to multiple beams through Computer Generated Holograms (CGHs). However, without fully synchronizing the CGHs playing with the scanning, the flexibility of the processing was largely reduced.

To overcome this limitation, a synchronization control method is presented in this paper. It was achieved by using two application control software: SAMLight and LabVIEW. SAMLight was used to control the laser and the scanning galvanometer to implement micro-processing, while a control program developed with LabVIEW was used to control the SLM and a motion stage. Synchronization signals, communicated between the two programs were routed by a National Instruments (NI) device USB-6008. We demonstrated that the synchronized system could easily and automatically finish complex fabrication in a short time.

Additionally, a fully synchronized ultrafast laser parallel micro-drilling processing using diffractive multiple annular shaped beams is demonstrated. The multiple annular beams, generated by superimposing multi-beam CGH onto a diffractive axicon CGH, can drill multiple holes at one time. Different patterns can be continuously obtained by changing the CGHs through synchronization control. This drilling way is an optical trepanning and it avoids huge laser energy waste with attenuation. The results show that the synchronized processing is over 300 times faster than the traditional mechanical trepan drilling, moving a small laser spot in the larger orbit.

9271-69, Session Post

Mathematical simulation of the space-variant lens array used for retina-like image sensor

Tao Liu, Yong Song, Qun Hao, Fan Fan, Jie Cao, Yufei Zhao, Beijing Institute of Technology (China)

A novel retina-like image sensor based on space-variant lens array is proposed. Using the space-variant lens array, the proposed sensor reduces the redundancy corresponding to the peripheral region of the photosurface. On the other hand, the proposed sensor can transfer an image from Cartesian coordinate system to log-polar coordinate system, which results in an important characteristic of special rotation and scaling invariance property. To solve the problems of previous research on the retina-like image sensor, we propose a retina-like image sensor based on space-variant lens array with the characteristics of high speed, high sensitivity and big planar array, etc., in which a space-variant lens array is used for performing log-polar mapping. In this paper, the mathematical simulation of the space-variant lens array used for retina-like image sensor is introduced. Firstly, we developed and verified the mathematical models of the space-variant lens array. Secondly, the relationships among the parameters of the space-variant lens have been simulated and discussed. Finally, some important conclusions are deduced, which will help to result in a novel retina-like image sensor with the characteristics of high speed, high sensitivity and big planar array, etc.

9271-70, Session Post

Crystal growth and holographic properties of In:Ce:Cu:LiNbO₃

Tao Zhang, Harbin Engineering Univ. (China)

A series of In:Ce:Cu:LiNbO₃ crystals with various level of In doping were prepared using the Cz equipment with a resistance furnace. The crystal holographic properties with optical damage resistance ability, sensitivity and dynamic range were measured by means of two-beam coupling light path. Based on the principle of angle-fractal multiplexing, using diode-pumped solid-state laser (DPL) instead of huge ionized argon laser, a compact volume holographic data storage system has been constructed by using In:Ce:Cu:LiNbO₃ crystal as the storage medium. The storage of 1000 images is realized.

9271-71, Session Post

Measurement of sub-pixel image motion based on joint transform correlator

Xueting Hong, Yixian Qian, Xiaowei Shi, Zhejiang Normal Univ. (China)

An effective approach to measure image motion is presented based on joint transform correlator (JTC), in order to measure the sub-pixel image motion caused by satellite attitude instability or vibration. Firstly, the high-speed CCD is used to capture image sequences, which are preprocessed by wavelet edge detection. Next the acquired image edge sequences are optically calculated by JTC, and an improved correlation peak is obtained. Lastly a modified centroid algorithm is proposed to get more accurate motion measurement. Motion measurement based on optical correlation is discussed, and the optical experiment system is also set up. The experimental results show that the measurement error is as low as 0.02 pixels, the accuracy is improved greatly.

9271-72, Session Post

Optical receiving antenna for indoor visible light communication based on holographic optical element

Longhui Wang, Tian Lan, Beijing Institute of Technology (China)

This paper presents a novel method for the design and production of the optical receiving antenna, the hologram called a holographic optical element (HOE), which has the dual function of gathering beam and filtering ambient wave, is made on holographic material by using the principle of interference and diffraction. The angular selectivity, spectral selectivity and diffraction efficiency at any point of the novel optical receiving antenna can be analyzed by Kogelnik coupled-wave theory and k vector closed legitimate, and further the performance of the system has done a theoretical analysis. Compared with the combination of a converging lens and a filter of the conventional optical receiving antenna, features such as small size, light weight, and low cost of the HOE make it the best choice of the optical receiving antenna for indoor visible light communication system.

9271-73, Session Post

Reflective flat lens with a surface plasmonic metasurface formed by rectangular annular arrays

Ruibin Li, Chinhua Wang, Soochow Univ. (China)

Sub-wavelength metallic metasurface devices attract increasing interests as a mean to control the interactions between light and metals by exciting surface plasmon polaritons (SPP) resonance related to the periodicity of the structure and localized surface plasmon (LSP) resonance related to the shape effects of the structure. It has been proven that the LSP resonance is accompanied by a phase shift between the incident and the transmitted or reflected waves, from which arbitrary form of desired wavefronts, such as spherical wavefront can be implemented if microstructures on the surface are properly designed. Two important challenges in metasurface lenses are the generation of a total phase of 2π and the as high as possible focusing efficiency. Transmissive plasmonic lenses have been proposed with different type of structures, however, the focusing efficiency of those devices worked in transmitted field is very low due to the optical losses or the absorption of the metallic thin film of light. In this paper, a reflective planar plasmonic lens is proposed. It is formed by an array of spatially varying sub-wavelength rectangular annular patterned in the upper Au film of the metal-insulator-metal (MIM) structure. The reflected phase ($0-2\pi$) and amplitude can be well controlled by manipulating the width of the annular gaps and the length of the MIM cavity which incurs the localized surface plasmonic resonance. A lens has been realized through an optimized design at a wavelength of $1.55\mu\text{m}$, which can generate a spherical wave-front with the desired spatial phase discontinuity modulation in the reflected field. The numerically simulated results using the Finite Difference Time Domain (FDTD) method show that the focal length can be precisely controlled with the theoretical value, and the spot size at focus plane is close to the theoretical diffraction limit. The focusing efficiency is up to 50%, and it can also work in the case of oblique incidence.

9271-74, Session Post

All-optical fabrication of blazed grating on P-cyclic-azoMMA film

Lixiong Xu, Jianhong Wu, Jian WANG, Xinrong Chen, Soochow Univ. (China)

Blazed grating is a key diffractive optical element in spectrometer. It has been manufactured on a novel polymer with cyclic-azobenzene pendants (P-cyclic-azoMMA) by all optical fabrication with two steps, which is different from traditional holographic ion beam etching technology. Firstly, use two interfering Kr^+ laser beams with the most efficient RCP+LCP polarization to inscribe symmetric surface relief gratings on polymer film and then make a single laser beam with polarization perpendicular to the grating grooves irradiate slantly to induce blazed asymmetric structure. In order to precisely control the profile of blazed grating, the influences of the height of symmetric surface relief grating, the slant angle of single linearly polarized light and laser irradiation time were researched in the experiment. The calculation demonstrates that -1st order reflective diffraction efficiency of blazed gratings is similar to that of ideal triangle blazed grating.

9271-75, Session Post

Research on distortion invariant in optical correlation detection and recognition technology

Xiaowei Shi, Yixian Qian, Xueting Hong, Zhejiang Normal Univ. (China)

It is difficult to detect and recognize moving target for optical correlator owing to the image information containing various rotation and scale variation, though optical processing owns the advantage of high-speed, large capacity and real-time. An efficient approach was proposed to improve correlation peak and enhance recognition performance of target based on Fourier-Mellin transform, by which optical correlator are not sensitive to the distortion of image information, and it will alleviate greatly the complexity of image recognition. We have also constructed an detection and recognition system based on optical joint correlator, the computer simulations and experimental results show that the proposed method has got sharp correlation peak and improved the detection performance.

9271-76, Session Post

Theoretical analysis for 3D surface reconstruction by square-pattern projection via cross gratings

Nan Sun, Shanghai Institute of Quality Inspection (China); Keding Yan, Nanjing Univ. of Science and Technology (China); Liang Xue, Shanghai Univ. of Electric Power (China); Shouyu Wang, Nanjing Univ. of Science and Technology (China)

3-D surface reconstruction is an important modeling method for 3-D printing technique. However, most of the 3-D modeling methods are contact-type and linear pattern projection, which cannot meet the requirements of transient surfaces. In this paper, an improved square-pattern projecting method via cross gratings is introduced for 3-D surface reconstruction. The proposed method could obtain the shape information in two vertical directions from single projection simultaneously. Comparing with

other traditional modeling methods, the proposed method is more effective and convenient.

9271-77, Session Post

Combined volume phase holographic gratings used as a beam splitter in near-infrared waveband

Xizhao Zhang, Qijing Mei, Minxue Tang, Soochow Univ. (China)

With the intrinsic advantages of high diffraction efficiency, signal to noise ratio, wavelength and angle selectivity, and low scattering, absorption, volume phase holographic gratings (VPHGs) have been widely used for spectroscopy, telecommunications, astronomy and ultra-fast sciences.

In this paper, a novel kind of beam splitter which is consisted of a transmission VPHG and a reflection VPHG as core components and used in near-infrared waveband is proposed. The design idea of the device is described in detail. Based on the Bragg condition and the rigorous coupled wave analysis (RCWA), diffraction properties in near-infrared waveband of the transmission and reflection VPHGs recorded in dichromated gelatin (DCG) are studied theoretically. As an example, two wavebands that need to be separated in near infrared spectrum region are taken into account. One that from 1.574 μm to 1.617 μm centered at 1.596 μm will be diffracted by the reflection grating, and the other that from 1.636 μm to 1.682 μm centered at 1.659 μm will be diffracted by the transmission grating. The diffraction efficiencies of the gratings are calculated and optimized by applying coupled wave theory and G-solver software, respectively. The recording setup is also designed for further experiments. The effects of the recording and reconstruction setup parameters, the amplitude of the index modulation (n) and the thickness (d) of the gelatin layer, and the polarization state of reconstruction beams on the diffraction efficiency properties of the gratings are calculated and analyzed. This kind of beam splitter is prospected to be used in spectrometers for greenhouse gases monitoring.

9271-78, Session Post

Optical encryption of three-dimensional information with digital holography

Yinghong Liu, Weimin Jin, Zhejiang Normal Univ. (China); Xin Yang, Soochow Univ. (China)

At present, most of the optical encryption technologies are achieved through computer simulation and studies by means of optical experiments are very rare. The decryption using optical method will be very difficult because of the precise setup of optical devices. An encryption method combining optical holography recording with simulated decryption on computer is proposed. A digital hologram of 3D object and a hologram of key information are recorded by optical method. The 3D object is Fourier transformed by lens and passed through the phase mask which is placed at the Fourier transform plane and imaged onto the CCD camera by the 4-f optical system. The reference wave passes through another phase mask by the 4-f optical system to keep the spatial coherence. During the decryption process, the useful information in the two holograms is obtained by filtering in spectrum domain. And the object information can be derived with the useful information we obtained before. The security of the system is enhanced by the phase mask which the reference wave transmits through as a new added key. An optical system is required for recording the digital holograms, optical encryption with two random phase masks represent a convenient way to secure 3D information. Furthermore, in this way, the method allows us to avoid electronic transmission of the key if this is

desired to increase security. Optical experiments results are presented.

9271-79, Session Post

Directional light-guide devices with continuously variable-spatial frequency sub-micron grating structures for autostereoscopic display applications

Wenqiang Wan, Linsen Chen, Yimin Lou, Soochow Univ. (China)

Autostereoscopic displays is a promising three dimensional display technology for its convenience and compatibility with current display systems which has attracted considerable attention, We describe a autostereoscopic display system with full-parallax using directional light-guide device with continuously variable-spatial frequency sub-micron grating structures in detail. The structure of sub-micron grating pixels(SMGPs)which have been optimized is given.The grating parameters for each pixel which can diffract light from the incident beam with the incidence angle 60° under the total internal reflection condition to a specific viewing point is calculated such as grating period and its angular orientation.The first-order diffraction efficiency is 1%-15% when the depth of grooves of SMGPs changes at 50-500nm and duty cycle at 0.1-0.9. A method of implementing SMGPs based on a ultraviolet continuously variable-spatial frequency photolithography process has been proposed. We fabricate 2-inch night directions backlight with partial grating pixel coverage, The pitch of grating pixel vary at 441-578nm under illumination by a collimated 650nm LED light source. The properties of SMGPs are investigated by measurements of diffraction angle and diffraction efficiency. Improving the uniformity of diffraction intensity is discussion.

9271-80, Session Post

High immersive three-dimensional tabletop display system with high dense light field reconstruction

Mengqing Zheng, Xunbo Yu, Songlin Xie, Xinzhu Sang, Chongxiu Yu, Beijing Univ. of Posts and Telecommunications (China)

Three-dimensional (3D) tabletop display is a kind of display mode with wide range of potential applications which provides the viewer with a vivid 3D scene or object. During the past decades, a great progress has been made for 3D displays. Auto-stereoscopic 3D displays with the liquid crystal display device and the lenticular sheet provide an easy method to realize the glass-free 3D display, which normally distributes the pixels of the LCD device to 5-11 view-points. Here, an auto-stereoscopic tabletop display system is designed to provide the observers with high level of immersive perception. To improve the freedom of viewing position, the eye tracking system and a set of active partially pixelated masks are utilized. The light intensity distribution and crosstalk of parallax images are measured respectively to evaluate the rationality of the auto-stereoscopic system. In the experiment, the high immersive auto-stereoscopic tabletop display system is demonstrated, together with the system architectures including the hardware and the software. A new semiautomatic calibration method is presented which extracts the common area at the same time. The size of common area to be displayed is controllable and the boundary condition to reach max size is investigated. For the transport part, processing the data in common area only makes real-time become possible and a parallel register is designed in the receiver of transport part to synchronize frames of different views. Finally,

the experimental results illustrate the effectiveness of the high immersive auto-stereoscopic tabletop display system.

9271-81, Session Post

Comparison of digital holography and iterative methods of wavefront reconstruction

Igor Shevkunov, Nikolai V. Petrov, Nikolay S. Balbekin, National Research Univ. of Information Technologies, Mechanics and Optics (Russian Federation)

In this paper, we compared iterative and digital holography methods of wavefront reconstruction. Digital holography is a recognized reliable method of full recovery of the wave field by the use of the reference beam and interference; iterative same recovery methods do not use the reference wave and the wave front is recovered by a certain set of intensity distributions and mathematical processing. The main difficulty of holography is to use the reference wave, i.e. it is need to separate of radiation on two fronts, and then mix them again, complicating a experiment. In iterative restoration techniques is not necessary to use a reference wavelength that minimizes the number of tools required. As a result, we compared contrast and sharpness of reconstructed images of objects, produced by these different methods.

9271-82, Session Post

The resolution of Fresnel incoherent correlation holography

Wufeng Zhu, Xia Shi, Fengying Ma, Zhengzhou Univ. (China)

Fresnel incoherent correlation holography (FINCH) is one of the methods for recording digital holograms of 3D samples under incoherent illumination. The FINCH does not scan the object neither in the space nor in the time. Therefore, it can generate the hologram rapidly without sacrificing the system resolution. This method has been successfully applied to white reflective holographic imaging, multicolor holographic of 3D fluorescence objects and 3D microscopic imaging. In FINCH system, the spherical wave from a point of a 3D object propagates and incidents to a spatial light modulator (SLM) which a phase mask is mounted on, and then the optical beam is split into a plane wave and a spherical wave or two spherical waves. The two waves interfere with each other and the interference pattern is recorded by CCD. The hologram of the 3D object is created by incoherent superposition of the interference pattern from each point of the 3D object. A series of holograms within stepped phase differences are obtained to suppress the twin images and bias term in the image reconstruction. In this article, the processes of optical recording, digital reconstruction and the point spread function of the classic FINCH system were described in detail. The reconstruction images of three letters of "Z", "W" and "F", each of which has a different distance from the collimating lens, were simulated and realized by experiments based on the FINCH system. The improved image resolution was observed when using double quadratic phase masks on the SLM compared with using single quadratic phase mask.

9271-83, Session Post

Coupled Dammann grating

Shaoqing Wang, Changhe Zhou, Shengbin Wei, Kun Liu, Shanghai Institute of Optics and Fine Mechanics (China)

A coupling method of Dammann gratings to generate dense spots array is presented, and the grating period matching condition is proposed. In this paper, one 3×3 Dammann grating is coupled with one 64×64 Dammann grating to generate uniform 192×192 spot arrays, where the 3×3 spots array generated by the 3×3 grating, are used as nine incident lights of the 64×64 grating. Because Dammann grating is type of binary-phase grating, the groove depth of these gratings should be carefully controlled otherwise the higher order diffractive light of 3×3 grating will deteriorate the quality of the final 192×192 spots array generated by 64×64 grating. In the meantime, only if the angle between the +63th and the -63th diffractive beam of 64×64 grating equals to the beam splitting angle of 3×3 grating, the uniform 192×192 spots array can be obtained. In our experiment, one 3×3 Dammann grating with period of $3.9 \mu\text{m}$ and one 64×64 Dammann grating with period of $500 \mu\text{m}$, which are design for 650nm laser, are fabricated of fused silica. These two grating's periods satisfy the grating period matching condition, and their groove depth are carefully controlled to 710nm . Experimental results show that by coupling these two Dammann gratings together, 192×192 spots array with uniformity better than 15% are finally obtained, and the higher order diffractive lights are almost eliminated. In this paper, the influence of the fabrication errors of Dammann grating on the coupled spots array is also analyzed.

9271-84, Session Post

Effect of multiple circular holes Fraunhofer diffraction for the infrared optical imaging

Chunlian Lu, He Lv, Yang Cao, Zhisong Cai, Xiaojun Tan, Harbin Engineering Univ. (China)

With the development of infrared optics, infrared optical imaging systems play an increasingly important role in modern optical imaging systems. Infrared optical imaging is used in industry, agriculture, medical, military and transportation. But in terms of infrared optical imaging systems which are exposed for a long time, some contaminations will affect the infrared optical imaging. When the contamination contaminate on the lens surface of the optical system, it would affect diffraction. The lens can be seen as complementary multiple circular holes screen happen Fraunhofer diffraction. According to Babinet principle, you can get the diffraction of the imaging system. Therefore, by studying the multiple circular holes Fraunhofer diffraction, conclusions can be drawn about the effect of infrared imaging. This paper mainly studies the effect of multiple circular holes Fraunhofer diffraction for the optical imaging. Firstly, we introduce the theory of Fraunhofer diffraction and Point Spread Function. Point Spread Function is a basic tool to evaluate the image quality of the optical system. Fraunhofer diffraction will affect Point Spread Function. Then, the results of multiple circular holes Fraunhofer diffraction are given for different hole size and hole spacing. We choose the hole size from 0.1mm to 1mm and hole spacing from 0.3mm to 1mm . The infrared wavebands of optical imaging are chosen from $1\mu\text{m}$ to $5\mu\text{m}$. We use the MATLAB to simulate light intensity distribution of multiple circular holes Fraunhofer diffraction. Finally, three-dimensional diffraction maps of light intensity are given to contrast. We can use the results to analyze effect of multiple circular holes Fraunhofer diffraction for the infrared optical imaging.

9271-85, Session Post

Characteristics measurement methodology of the large-size autostereoscopic three-dimensional light-emitting diodes display

Pengli An, Tsinghua Univ. (China); Ping Su, Graduate School at Shenzhen, Tsinghua Univ. (China); Changjie Zhang, Cao Cong, Tsinghua Univ. (China); Jianshe Ma, Graduate School at Shenzhen, Tsinghua Univ. (China)

Large-size autostereoscopic three-dimensional (3D) light-emitting diode (LED) displays are commonly used in outdoor or large indoor spaces, and have the properties of long viewing distance and relatively low light intensity at the viewing distance. The instrument used to measure the characteristics (crosstalk, inconsistency, viewing angles, etc.) of the displays should have long working distance and high sensitivity. In this paper, we propose a methodology for characteristics measurement based on a distribution photometer with a working distance of 5.76m and the illumination sensitivity of 0.001 mlx. A display panel holder is fabricated and attached on the turning stage of the distribution photometer. Specific images are loaded on the displays separately, and the luminance data at 5.76m to the panel is measured. Then the data is transformed into the light intensity at the best viewing distance. According to the definition of the characteristics of the 3D displays, the crosstalk, inconsistency, viewing angles, etc. could be calculated. The test results of the characteristics of an autostereoscopic 3D LED display are proposed.

9271-86, Session Post

2D POLICRYPS realized via amplitude modulated spatial light modulator

Chen Lin, Zhang Bin, Haitao Dai, Tianjin Univ. (China)

The polymer liquid crystal polymer slices (POLICRYPS), which is a structure made of perfectly aligned alternative liquid crystal films separated by slices of almost polymer, has been reported. POLICRYPS devices can achieve higher diffraction efficiency (as high as 98%) with low scattering loss and power consumption due to the completely phase separation.

In this paper, we reported a 2D polymer liquid crystal polymer slices 'POLICRYPS' devices fabricated with the maskless lithographic system based on amplitude-modulated spatial light modulator (aSLM) illuminating with visible light. The complete phase separation can be realized during visible light radiation exposing. The samples were prepared by filling the syrup of prepolymer and nematic LC into the ITO glass cell (with alignment layer on both sides) and then exposing to the illumination pattern (formed by the maskless lithographic system). The prepolymer was composed by monomer, photoinitiator and other auxiliaries. NOA 61 (Norland) is used as monomer, and two photoinitiators (RB and IRG784) and three kinds of liquid crystal (PO616A, E7 and E48) were used for comparison. Furthermore, the preparing conditions, such as exposure time, ambient temperature, and the ratio between LC and prepolymer, were also optimized to achieve completely phase separation. Besides, we studied the electric-optical properties of the POLICRYPS holographic grating.

9271-87, Session Post

Polarization-multiplexing imaging for phase-only object in dual-wavelength digital holography

Yifei Chen, Zhe Wang, Zhuqing Jiang, Yunxin Wang, Lu Rong, Beijing Univ. of Technology (China)

Dual-wavelength digital holography can retrieve the synthetic phase map of object structure free of 2π discontinuities via recording two holograms with two small difference wavelengths. Compared to conventional digital holography, dual wavelength digital holography can be applied to achieve phase imaging of objects that have a high aspect ratio. In this paper, a polarization-multiplexing off-axis dual-wavelength digital holography is proposed. The structure of a groove grating is measured by using the polarization-multiplexing dual-wavelength digital holographic system with a common optical path configuration. Two half wave plates are used to change the polarization state of two light beams of wavelengths 671nm and 656nm. The two wavelengths share the same optical path in a Mach-Zehnder interferometer, and then are split into two paths by a beam splitter placed after the interferometer. Two polarizers are placed each in front of two CCDs to select the corresponding polarization wavelength from dual-wavelength beams. In the experiment, two holograms of the grating each with respect to the wavelengths 671nm and 656nm is recorded by two CCDs, and then the two phase maps corresponding to the two wavelengths are reconstructed by numerical simulation of diffraction process of the holograms, respectively. The phase image of beat-wavelength is obtained by subtracting two phase images directly. Thus, the phase map of the grating is achieved by using the polarization-multiplexing dual-wavelength digital holography in the off-axis optical setup. The experimental results demonstrate the feasibility of the system, and show it can provide a real-time solution for measuring 3D profile information.

9271-88, Session Post

Effect of dummy area in the generation of computer-generated hologram to improve the reconstruction diffraction efficiency

Yuki Misaki, Yosuke Koga, Shiyuan Yang, Seiichi Serikawa, Kyushu Institute of Technology (Japan)

In most cases of the generation of computer-generated hologram, a zero-valued dummy area is usually added to the desired object in order to avoid the disturbance of high order reconstruction. The high order reconstruction not only disturbs the zero order reconstruction but also decreases the zero order reconstruction diffraction efficiency. In this study, we show a method to improve the zero order reconstruction diffraction efficiency by using a finite dummy area. According to the structure of a general computer-generated hologram, that is each calculated computer-generated hologram point has the same square size, then the high order reconstruction is the product of the zero order reconstruction and a sampling function with a scale factor. We use computer simulation to show the effect of dummy area in the improvement of the zero order reconstruction diffraction efficiency. According to our simulation results, we find that the zero order reconstruction diffraction efficiency increases as increasing the size of dummy area. In addition, we also find that the on-axis reconstruction has a higher reconstruction diffraction efficiency than the off-axis ones.

9271-90, Session Post

Measurements of small displacements with real-time holographic interferometry

Ma H. Huan D.V.M., Nanjing Univ. of Science and Technology (China)

Because the performance of the material components can be usually reflected by strain and stress distribution, the accurate detection method of stress deformation and stress distribution of arbitrary shape material components have important significance in materials engineering applications. Optical measurement method is one of methods to analyze material stress and deformation because of its many advantages. Holographic interference is an effective experimental method of modern material stress distribution detection. The basic methods of holographic interference are as follows: single exposure (real-time), double exposure, continuous exposure (time-average), three beams single exposure, nonlinear recording holographic interference, holographic wave-front shearing interference, holographic Moire fringe technique and so on. There are many applications about holographic interference measurement.

This paper describes a brief introduction to the theory and experiment concerning real-time holographic interferometry from the point of view of dynamic displacement measurements, and the application of holographic single exposure is mainly studied. Small displacement is collected by CCD camera and then processed by computer automatically. Due to the amplifying effect of Moire fringe, measurement accuracy is high by adopting subdivision technique to Moire fringe. Experiments show that this method has many merits as follows: simple principle, real-time, accurate and so on. Therefore, it is very important in practical engineering field.

9271-91, Session Post

A tunable dual-core photonic crystal fibers for broadband dispersion compensation

Xu Cheng, Beijing Univ. of Posts and Telecommunications (China)

A dual-core polymer-filled photonic crystal fiber (PCF) is designed for the broadband dispersion compensation based on the asymmetric mode coupling. The two-concentric-core structure is obtained by introducing an inner high-index silica core and an outer low-index polymer core.

A full-vector finite-element method (FEM) with a scattering boundary condition is used to investigate the loss, the effective index of the guided mode, and the group velocity dispersion. As an accurate numerical mode solver, the full-vector FEM method is more efficient in the analysis of this dual-core PCF when the complete coupling happens.

By varying the sizes of air holes, a desired structure can be achieved. The PCF shows a broad bandwidth over the entire C band and a very high negative dispersion from -1070 to -1450 ps/(nm²km) due to the leaky mode coupling between the fundamental inner core mode and high order outer core mode.

Furthermore, the polymer-filled outer core shows a good tunable property while the refractive index of the outer core is adjusted artificially, such as temperature control. It can be seen that the index moves to smaller value with the raise of the temperature. When the refractive index of the polymer decreases from 1.4078 to 1.4036 gradually, the dispersion curve shifts and the curve shape does not show any obvious change. Besides, the dispersion curves cover the whole C band and have a numerical value from -720 to -1850 ps/(nm²km). So it can be well used for the broadband dispersion compensation timely.

To our knowledge, this tunable broadband dispersion compensation fiber has never been proposed before. This fiber

has a larger potentially application for dynamical dispersion compensation in wavelength-division-multiplexing (WDM) systems.

9271-92, Session Post

The image quality of varied line spacing plane grating by computer simulation

Shouqiang Sun, Weiping Zhang, Lei Liu, Guangxi Univ. (China)

Varied line spacing plane gratings have the features of self-focusing, aberration-reduced and easy manufacturing, which are widely applied in synchrotron radiation, plasma physics and space astronomy, and other fields. Many researchers have deeply studied them from different aspects in these years. In the study of diffracting imaging, the optical path function is expanded into maclaurin series, aberrations are expressed by the coefficient of series, most of the aberration coefficients are similar and the category is more, can't directly reflects image quality in whole.

The paper will study on diffraction imaging of the varied line spacing plane gratings by using computer simulation technology, for a method judging the image quality visibly. In this paper, light beam from some object points on the same object plane are analyzed and simulated by ray trace method, the distance each diffraction light deviates from principal ray is calculated, the value of radius of blurred spot on image plane is given. According to the size of dispersion spot of object point, the weighting factor is determined. The evaluation function is set up, which can fully scale the image quality. In addition, based on the evaluation function, the best image plane is found by search algorithm. Finally, the reliability of simulation is validated by comparing the simulation data and experiment data.

9271-93, Session Post

Production of optical accelerating regular polygon beams and their optical characteristics

Chen Chen, Zhijun Ren, Zhejiang Normal Univ. (China)

Accelerating beams with a beam shape given by Airy function are observed for the first time in 2007. Accelerating Airy beams are a kind of unique beams because of curved propagation trajectory for their main lobes during propagation of the beams in free space, therefore their shapes are similar to the shape of rainbows. As new-style energy source of laser, accelerating beams can be regarded as new tool use for scientific research in optical community. In practical applications, people need various kinds of accelerating beams with different topological structures and accelerations according to different requirements. Based on catastrophe theory, one family of so-called accelerating "regular polygon beams" was theoretically introduced, seeing Opt. Lett. 35, 4118 (2010). Such accelerating beams have odd numbers (three, five, seven, and so on) of high-intensity accelerating peaks (also called main lobes). For example, one regular trigon beam has three accelerating sample points in contrast to an Airy beam that has only one accelerating sample point. Further, one regular pentagon beam has even five accelerating sample points.

Based on Thom's elliptic umbilical singularity, we design pivotal phase-only masks to generating accelerating regular polygon beams. By using the diffractive phase grey-scale map written onto a spatial light modulator, we experimentally obtain some optical regular polygon beams. Their optical topological structures and propagation characteristics are investigated subsequently. Moreover, we have given the mechanism of controlling acceleration and ballistic trajectory of main lobes of regular polygon beams according to practical requirements.

9271-94, Session Post

Eigenfunction methods of partially coherent light which transmits in a multimode optical fiber

Lihui Yang, Yishen Qiu, Gaoming Li, Baocheng Lin, Hui Li, Fujian Normal Univ. (China)

The study of the transmission of partially coherent light in a multimode optical fiber is important in understanding mode noises and the speckle characteristics. Since the temporal and spatial coherence of the illuminant affect the spatial coherence of output light from a multimode optical fiber in different ways, the physical laws governing the propagation of partially coherent light in free space are not applicable to that in a multimode optical fiber. In this communication, an eigenfunction-based methodology is developed to describe the mutual intensity of light in a multimode optical fiber. The method consists of three steps: 1) obtain the coherence for input light by casting the mutual intensity in canonical form in a representation furnished by its eigenfunctions; 2) expand the input eigenfunctions according to the modes of a multimode fiber and derive the correlation matrix for output light based on the input temporal coherence and modal dispersion. And then diagonalizing this correlation matrix yields N_f nonzero eigenvalues; 3) define the product of input coherence and N_f as the output coherence from a multimode optical fiber. According to this methodology, a convenient way of calculating speckle contrast for output light from a multimode fiber will be offered.

9271-37, Session 8

Denoising in digital holography reconstruction by using contourlet transform

Xiangchao Zhang, Hao Zhang, Xiaoying He, Min Xu, Fudan Univ. (China)

Digital holographic microscopy is a very promising measurement method for micro-structured components. The quality of reconstruction of measured surface from digitally recorded holograms is critical to the measurement accuracy. Due to the disturbance in environment and imperfection of optical components, the reconstructed surface topography will be affected. The holograms contain salient features of the measured surfaces and some fine-scaled interferometric fringes, as a result the most widely used Fourier transform or wavelet based noise removal methods may break down these signals over a wide range in the frequency domain, making the signal and noise mixed together and difficult to be separated.

In this paper we propose a new noise removal method. The contourlet transform is composed of bases oriented at various directions in multiple scales with a redundancy rate. It has excellent capability in the sparse representation of sharp borderlines between smooth regions. Then features in different directions in each scale can be well separated in the contourlet domain, and the coefficients corresponding to the primary features concentrate on several terms. Thus the salient structures of large scales, interferometric fringes of medium scales and random noise of fine scales can be separated successfully, at the same time preserving sharp edges well. From the view point of practical applications, this method is straightforward and flexible to use, and computationally efficiently compared to nonlinear optimization algorithms and model learning based methods.

Experimental examples are presented. Compared with conventional Gaussian filtering and wavelet filtering methods, the contourlet transform is superior in terms of noise removal, feature preserving and flexibility for the reconstruction of digital holography.

9271-38, Session 8

Iterative digital in-line holographic reconstruction with improved resolution by data interpolation

Mingjun Wang, Jigang Wu, Shanghai Jiao Tong Univ. (China)

??Digital in-line holography (DIH) is a lensless imaging technique that can be used to build low-cost and compact imaging systems. In DIH, the in-line hologram is recorded by a CMOS or CCD sensor and later used to reconstruct the image of the sample. The imaging resolution is determined by the system numerical aperture provided that the pixel size is smaller than the required Nyquist criteria for sampling distance. In the case of short sample-to-sensor distance, pixel size is often a limiting factor for the resolution. To solve this problem, we propose to use iterative method along with data interpolation for the holographic reconstruction. Proof-of-concept numerical simulations have been done to show the effectiveness of our method.

In our algorithm, the optical field is propagated back and forth between the sample plane and the sensor plane while using the measured intensity and a priori information about the sample as constraints, following Gerchberg-Saxton and Fienup's methods. The iteration will converge and we can get both intensity and phase information of the sample. Before the iteration, the intensity data matrix measured by the sensor is interpolated to enlarge the matrix dimension and thus effectively reduce the pixel size. During the iteration, we apply the sensor plane constraints on only the measured intensity location but not the interpolated data location. In our simulation, we observed that during the iteration, the interpolated data will be changed reasonably and we can finally reconstruct the sample image with better resolution.

9271-39, Session 8

Automatic angular-spectrum filtering algorithm in dual-wavelength digital holography

Zhe Wang, Zhuqing Jiang, Yifei Chen, Yuhong Wan, Beijing Univ. of Technology (China)

Dual-wavelength digital holographic microscopy (DHM) has emerged as a quantitative phase imaging method without the usual phase unwrapping for detection of phase discontinuity. This phase imaging method involves in the generation and combination of two phase maps respective to two wavelengths in a digital holography system. For an off-axis lens-less digital holography algorithm, it is required to extract the Fourier transform spatial frequency domain data from each hologram of two individual wavelengths. A reconstruction procedure typically consists of Fourier transform, angular-spectrum filtering and free-space diffraction. In most cases, the angular-spectrum filtering is usually performed by manual processing. In this paper, we present an automatic angular-spectrum filtering algorithm for phase reconstruction in dual-wavelength digital holography system with a common optical path configuration. The major procedure of automatic angular-spectrum filtering for dual-wavelength phase imaging consists of two steps: excluding the zero-order region of Fourier spectrums, and locating the center of order +1 region of the angular spectrums for two individual wavelengths. In the proposed method, only if the center of the order +1 spectrum region of either of one wavelength is figured out, the center of the order +1 spectrum region respective to another wavelength can be calculated out according to the relationship between the angular spectrums of two wavelengths. The phase map of an object is retrieved with the automatic angular spectrum-filtering algorithm, which demonstrates that

the automatic angular spectrum-filtering algorithm is feasible and effective. It provides an efficient solution for angular-spectrum filtering in real time dual wavelength digital holographic microscopy.

9271-40, Session 8

Incoherent digital holographic adaptive optics with enhanced operation speed

Xiaole Guo, Tianlong Man, Yuhong Wan, Beijing Univ. of Technology (China)

Incoherent digital holographic adaptive optics (IDHAO) is a new technology of wavefront sensing and correction. In the traditional adaptive optics, the true image is encoded by the aberration, and the key aberration is extracted using the guide star information. The IDHAO system dispenses with the hardware lenslet arrays and deformable mirrors of conventional systems. As some algorithms such as phase unwrap can be adopted, the dynamic range of deformation measurement is essentially unlimited. Wavefront sensing can be achieved by recording digital holograms of incoherent objects and a guide star while aberration can be compensated with appropriate numerical algorithm. However, in this type of IDHAO system, the process of the wavefront sensing needs to record digital holograms of object and a guide star independently which reduces the speed of sensing. In this paper, we present a method for enhancing the operation speed of the IDHAO. It is shown that for a discrete object, the hologram of guide star can be extracted from the hologram of incoherent object. For reconstruction, the hologram of objects can be compensated digitally by using the complex conjugate of the hologram of guide star. The dependence of wavefront compensation on the size of guide star hologram is analyzed quantitatively. This approach is investigated theoretically and experimentally based on the basic principle of the self-referenced spatially incoherent holography. The process is seen to be effective under various ranges of parameters, such as aberration type and strength.

9271-41, Session 9

Ring beam experiment with a phase-only spatial light modulator

Qi Li, Xue Ma, Harbin Institute of Technology (China)

The phase-only liquid crystal spatial light modulator (SLM) is a real-time electro-optic device capable of modulating the phase of an optical wavefront in space. SLMs have been harnessed for beam shaping. A phase-only spatial light modulator has been used to transform a single-mode He-Ne laser into a ring-shaped pattern. But intensity in beam center is generally high. In this paper, the improved method is investigated. The experimental results showed that a given single-mode laser beam could be converted into a ring-shaped intensity distribution which corresponds to our designation.

9271-42, Session 9

Lensless microscope based on iterative in-line holographic reconstruction

Jigang Wu, Shanghai Jiao Tong Univ. (China)

We propose a lensless microscopic imaging technique based on iteration algorithm with known constraint for image reconstruction in digital in-line holography. In our method, we introduce a constraint on the sample plane as known part in the lensless microscopy for iteration algorithm in order to eliminate

the twin-image effect of holography and thus lead to better performance on microscopic imaging. We evaluate our method by numerical simulation and built a prototype in-line holographic imaging system and demonstrated its capability by preliminary experiments.

Phase retrieval algorithm based on iteration between sample plane and detection plane is one of the important image reconstruction methods to suppress the twin-image of in-line holography. A popular method is to choose a threshold to define the sample support, which was used as constraint in the iteration. However, the threshold might need to be changed according to specific type of the samples. In our approach, we eliminate the need to choose a threshold manually and thus suitable for different types of samples.

In our proposed setup, a carefully designed photomask used to hold the sample is under illumination of a coherent light source. The in-line hologram is then recorded by a CMOS sensor. In the reconstruction, the known information of the illumination beam and the photomask is used as constraints in the iteration process. The improvement of image quality because of suppression of twin-images can be clearly seen by comparing the images obtained by direct holographic reconstruction and our iterative method.

9271-43, Session 9

Quasi-confocal volume holographic microscopy with random speckle illumination

Hsi-Hsun Chen, National Taiwan Univ. (Taiwan); Vijay Raj Singh, SMART-Singapore MIT Alliance for Research & Technology (Singapore); Yuan Luo, National Taiwan Univ. (Taiwan)

The aim of this research is to improve the optical sectioning ability of 4-f volume holographic imaging (VHI) via random laser speckle illumination. VHI has been proposed as a novel 4-f imager to acquire scanning-free and multi-depth images with wide field of view by setting a volume hologram (VH) on Fourier plane. Due to the finite thickness of VH, VH could discriminate the wavefront of probe waves with different angular and wavelength. These properties lead that VH grating can not only perform as a wavelength filter, but a multi-focal lens which could project the multi-depths images onto the different lateral location on CCD sensor. However, the optical sectioning ability of VHI still suffers from the corresponding point spread function (PSF) along z axis which is similar with PSF of traditional 4-f imager. Hence, compared with confocal microscopy, the quality of acquired images is blurred owing to considerable out-of-focus signal. To tackle this issue, HiLo computational scheme with laser speckle illumination is adapted. The HiLo method needs to take two images, one from uniform illumination and another from speckle illumination. Owing to statistical contrast feature of speckle field associated with PSF, the speckle image could provide the out of background rejection but with lower resolution (Lo). The higher resolution (Hi) information would be compensated by operating a high pass filter to image from uniform illumination. Therefore the fusion of Hi and Lo image could achieve the high resolution image with optical sectioning even for DC area. By means of HiLo computational method, VHI shows the multi-depths images of volumetric object, such as biological tissue, with quasi-confocal sectioning performance.

9271-44, Session 9

Holographic line beam scanner with liquid crystal on silicon modulator

Jian-Tsung Chen, Cheng-Huan Chen, National Tsing Hua

Univ. (Taiwan); Chung-Li Tsai, Po-Chi Hu, Chia-Ming Jan, Metal Industries Research & Development Ctr. (Taiwan)

A laser scanning device can be used for contour or pattern reconstruction with associated image processing or recognition algorithm. For a better accuracy or accommodating to a high efficiency algorithm, the laser beam often needs reshaping to a specific pattern, such as a line beam, or homogenization so as to reduce the spatial variation of the device performance. In addition, a scanning mechanics is normally inevitable. Both beam shaping and scanning module take quite a volume in the whole system, which could be an issue for the applications in which miniature device is highly desired. In this paper, a holographic scanner has been proposed to perform both laser beam shaping and scanning function. A pure phase modulation liquid crystal on silicon (LCOS) device is used for implementing the dynamic hologram. The LCOS has a pixel size of 3.74 μ m, and provides 16 phase level with a full phase depth of 2 π . A line beam with 20mm and uniformity up to 70% is generated and it is scanned back and forth in the orthogonal direction of the line with a stroke of 20mm. The scanning line pattern is generated based on iterative Fourier transform algorithm (IFTA) and the first diffraction order pattern is exploited with the zero order being blocked and absorbed so that the noise in the scanning line pattern is minimized. The proposed scheme is a compact and versatile solutions for patterned laser beam scanning devices.

9271-45, Session 9

A 2D absolute linear encoder

Chunlong Wei, Changhe Zhou, Jianyong Ma, Xiansong Xiang, Yancong Lu, Yanyang Li, Jin Wang, Wei Jia, Junjie Yu, Shanghai Institute of Optics and Fine Mechanics (China)

In recent years, 2D linear encoder becomes more and more attractive because of its unique advantages. Although the present 2D linear encoder is incremental based on diffractive grating, 2D absolute linear encoder based on images analysis of grating maybe the same useful. A 2D absolute linear encoder is developed in this paper which can measure the absolute position along the moving axis (X-axis & Y-axis) of precision linear stage simultaneously. Abbe errors can be greatly eliminated compared with the 2D arrangement composed of two 1D absolute linear encoder. The optical configuration is simple and effective, which includes one source, one collimation lens, one image lens, one prism, one 2D CCD camera, one 2D grating scale. The 2D grating scale is encoded with absolute encode by means of a new type of laser writing technique. Different period grating scales are tested. It is confirmed that the prototype 2D absolute linear encoder has a nanometer resolution. Further design scheme of a 2D absolute linear encoder based on diffractive grating is presented and discussed.

9271-46, Session 9

Digital holographic Michelson interferometer for nanometrology

Vladimir Y. Venediktov, Saint Petersburg Electrotechnical Univ. "LETI" (Russian Federation); Sergey A. Pulkin, Saint-Petersburg State Univ. (Russian Federation); Alexander A. Sevrygin, Saint Petersburg Electrotechnical Univ. "LETI" (Russian Federation)

The paper considers the dynamic holographic interferometry schemes with amplification (multiplication) of holographic fringes and with correction for distortions, imposed by the

interferometer scheme elements. The use of digital microscope and of the matrix light modulator with direct addressing provides the completely digital closed-loop performance of the overall system for real-time evaluation of nano-scale objects size. Considered schemes were verified in the laboratory experiment, using the Michelson micro-interferometer, equipped by the USB-microscope and digital holography stage, equipped by the Holoeye spatial light modulator.

9271-47, Session 9

Measurement of refractive index profile of optical fiber using the dual wavelength diffraction phase microscope

Mohammadreza Jafarfard, Yonsei Univ. (Korea, Republic of)

In this research, we demonstrated the use of Dual Wavelength Diffraction Phase Microscopy (DW-DPM) with the inverse Abel transform for accurately obtaining the refractive-index profile of an optical fiber. This nondestructive imaging analysis technique can provide high precision measurement of the refractive-index information of the fiber. This technique has been found to be attractive in that it gives a nondestructive, fast, reliable and robust method of characterizing the refractive index with good precision and accuracy.

The simultaneous dual-wavelength measurement was performed with a Dual Wavelength Diffraction Phase Microscopy based on a transmission grating and a spatial filter that form a common-path imaging interferometer. With a combined laser source that generates two-color light continuously, a different diffraction order of the grating was utilized for each wavelength component so that the dual-wavelength interference pattern could be distinguished by the distinct fringe frequencies.

Using dual wavelength algorithm, we solved phase wrapping problem caused by large size of optical fiber sample and final phase image was obtained without 2- π ambiguity. After obtaining the phase image, the index profile was extracted by the inverse Abel transform of the phase profile. Because the classic formula of the inverse Abel integration is vulnerable to the measurement errors in the vicinity of the origin, we used an alternative calculation method that utilized the Fourier transform. In order to remove the background phase that originated from the index difference between the cladding and the surrounding medium, the background phase was calculated from the phase data of the cladding to make the core phase profile that could be directly transformed to the index profile of the core without the full phase image that includes the whole cladding part. We compared our result with perform data and we found a good agreement between two measurement results in terms of the overall shape of the profile and the peak value of the index difference.

9271-48, Session 10

Design and applications of digital diffractive gratings (Invited Paper)

Changhe Zhou, Shubin Li, Shaoqing Wang, Shengbin Wei, Wei Jia, Chunlong Wei, Yancong Lu, Shanghai Institute of Optics and Fine Mechanics (China)

Recent achievements in simplified modal method, three-dimensional imaging, high precision grating are reported. Simplified modal method is now realized as a powerful tool for the close-to-wavelength gratings, simplified modal method is developed to analyse the slanted gratings, it is found that slanted gratings can be explained as the rectangular gratings with the simple equations obtained from simplified modal method,

and there are even-to-odd modes conversion in the slanted grating which usually doesn't happen in a rectangular grating. Three dimensional imaging using Damman grating for array illumination is built as a miniaturized apparatus for capturing three-dimensional information of a human face statue. We fabricated a series of high precision gratings, we also built an optical measurement system for evaluating the pitch uniformity of the fabricated gratings. The pitch uniformity is measured to be 400nm and the peak-to-valley position accuracy is 1.5 micron in the whole range up to 60 mm. Recent achievements reflect our current effort toward to the practical applications of digital diffractive gratings.

9271-49, Session 10

Intuitive surface-wave model of surface Bloch modes on periodically-perforated metallic surfaces and their relations with the extraordinary optical transmission (Invited Paper)

Haitao Liu, Xin Zhang, Nankai Univ. (China); Ying Zhong, Tianjin Univ. (China)

We build up an intuitive microscopic surface-wave model for the surface Bloch mode (SBM) on metallic surfaces patterned with a periodic array of subwavelength holes [1]. The SBM is also called a spoof surface plasmon when metals approach perfect electric conductors at THz or microwave frequencies. Both the complex propagation constant and the field distribution of the SBM can be quantitatively reproduced by the model. With the model the SBM is found composed of surface waves on flat metallic surfaces, the surface plasmon polariton (SPP) and the quasi-cylindrical wave (QCW) launched by every individual holes in the array, which shines new light on the design of perforated metallic surfaces as plasmonic metamaterials. We also establish explicit relations between the macroscopic SBM picture and the microscopic surface-wave picture for explaining the extraordinary optical transmission (EOT) through subwavelength metallic hole arrays. Analysis with the model shows that the SBM is tightly related with the EOT through a complex pole of the in-plane wave vector, at which the SBM and the EOT possess similar field distributions expressed as superpositions of the SPPs and QCWs. Our analysis bridges the gap between the macroscopic view in terms of a resonant excitation of SBMs and the microscopic view in terms of the multiple scattering of flat-interface surface waves for interpreting the EOT, or more general, the rich variety of phenomena related to the seminal topic of Wood's anomaly of metallic gratings.

[1] X. Zhang, H. T. Liu, Y. Zhong, Phys. Rev. B, in press.

9271-50, Session 10

Metal/multilayer-dielectric coated grating for chirped pulse amplification laser system

Hui Chen, Tsinghua Univ. (China)

Diffractive gratings are key elements of chirped pulse amplification laser systems. In these applications the gratings should have high diffraction efficiency, high laser induced damage threshold (LIDT), and large spectral bandwidth. Gratings consist of grooves etched into a dielectric substrate and coated with first a highly-reflecting metallic layer and then a multilayer dielectric thin-film stack may meet these requirements. However, in reality after each layer is deposited, the new top surface of the grating deviates from the previous one, and at the end the final top surface of the grating may be significantly different from the

initial substrate surface in both groove shape and groove depth. The deformation of layer interface profiles reduces the diffraction efficiency and affects the LIDT of gratings. In this work, the deformation process for a particular thin-film deposition method was studied by means of scanning electron microscopy. On basis of the experiment data, a profile evolution model was proposed. Diffraction efficiency and bandwidth performance of metal/multilayer-dielectric coated gratings was numerically optimized for various initial substrate grating profiles by changing the dielectric layer thicknesses.

9271-51, Session 10

Mode analysis of beam splitter for slanted grating

Shubin Li, Changhe Zhou, Yancong Lu, Kun Liu, Jin Wang, Yanyang Li, Jun Wu, Shanghai Institute of Optics and Fine Mechanics (China)

Beam splitters are widely used in various optical modern systems for separating optical wave into different directions. We have proposed a novel slanted grating for beam splitter at the central wavelength of 1550nm, which can be used in the optical communication. With the simulated annealing algorithm, beam splitter slanted grating can be optimized by using the rigorous coupled wave analysis (RCWA). The diffraction process can be analyzed by the simplified modal method. The simplified modal method, without complicated calculation, reduces the difficult diffraction process into a vividly and physical modal. We have derived an analytical expression which can provide an insightful physical description of the simplified modal method for the slanted grating. Compared with the rectangular grating, the slanted grating has the asymmetric physical structure. Therefore, the odd grating mode can also be excited in the slanted grating under normal incidence. The odd grating mode, which only exists in the asymmetric structure, plays the role of breaking the symmetric field distribution in the output plane. The physical analytical expression of mode conversion and coupling for the slanted grating can be obtained to interpretation the asymmetric field distribution. Numerical results obtained by the rigorous coupled wave analysis verified the validity of the simplified modal method. We expect the modal method for the slanted grating set forth in this work should be helpful for the tremendous potential application of the slanted grating.

9271-52, Session 10

The high divergent 2D-Dammann grating

Jin Wang, Jianyong Ma, Changhe Zhou, Shubin Li, Yancong Lu, Yanyang Li, Kun Liu, Shanghai Institute of Optics and Fine Mechanics (China)

The Dammann grating is the standard binary-phase grating which can create a finite array of uniform intensity spots in the direction of one-dimension as well as two-dimension. The diffraction angles of traditional Dammann gratings are quite small which is about the milliradian level. However gratings with large diffraction angles more than 10 degrees are needed in some cases. It's known that the diffraction angles are related to grating period. To obtain the large diffraction angles, the period should be small when they are compared with wavelength, which means that the subwavelength high divergent Dammann grating couldn't be designed by the traditional scalar diffractive theory. Hence we design the 2D-Dammann grating by the vector theory and compare the results between scalar theory and the vector one. In addition, the small period of grating increases the difficulties of fabricating. So we fabricate the 2D-Dammann gratings by direct laser writing (DLW) instead of traditional manufacturing method. As we know the direct laser writing (DLW) technique has become

a well-established, flexible and multi-functional method of micro manufacturing technology with the advantages of low costs and high flexibility. Then the method of ICP etching is used to obtain the high divergent 2D-Dammann grating. In this paper we design and fabricate a 3?3 high divergent 2D-Dammann grating with period of 3.906?m at wavelength of 850nm.

9271-53, Session 10

Fabricating high-spectral resolution flat-field concave grating with compensation concave lens

Qian Zhou, Rui Tian, Kai Ni, Jinchao Pang, Jinchao Zhang, Graduate School at Shenzhen, Tsinghua Univ. (China)

Flat-field concave diffraction grating (FCDG) is the key component of a portable grating spectrometer, which integrates three optical properties: dispersion, imaging, and flat spectral image in a single optical device. FCDG with high spectral resolution has more widely applied range. However, there is a long-standing fabrication problem that the distance between the two recording light sources is often very short, causing mechanical interference, sometimes even makes it impossible. This problem restricts the applications of FCDG.

In this paper, a method to increase the distance between the two recording light sources is proposed by using a compensation concave lens. Compensation concave lens can achieve spectral resolution results almost the same as that of the two original recording light sources, what's more, the wide spectrum FCDG can be accomplished. The operation process of our method can be described as follows: First, we calculated the coordinate of two original recording points with Matlab. In this step, high spectrum imaging quality which is affected by optical resolution is our goal, and the design requirements of FCDG, which contains wavelength range, entrance aperture and spectrum surface length are included in Matlab program. Second, we calculated the new recording points by the principle of paraxial imaging. In this step, the new recording points imaging on the compensation concave lens, the original recording points and the new recording points are image points and object points respectively. Finally, we performed system modeling, simulation, and optimizing the aberrations in Zemax by using the above new recording points. A theoretical analysis is given to show that the proposed method can ensure the spectral image quality and greatly reduce the fabrication difficulty.

9271-54, Session 11

Pitch evaluation of high-precision gratings

Yancong Lu, Changhe Zhou, Chunlong Wei, Wei Jia, Xiansong Xiang, Yanyang Li, Junjie Yu, Shubin Li, Jin Wang, Kun Liu, Shengbin Wei, Shanghai Institute of Optics and Fine Mechanics (China)

Optical encoder and laser interferometer are two primary solutions in nanometer metrology. As the precision of encoder depends on the uniformity of grating pitches, it is essential to evaluate pitches accurately. We use a CCD image sensor to acquire grating image for evaluating the pitches with a high precision. Digital image correlation technology is applied to filter the noises. We propose three algorithms with different noises for detecting the pitches of grating with peak positions of correlation coefficients. Numerical simulation indicated the average of pitch deviations from the true pitch and the pitch variations are less than 0.025% and 0.025% for these three algorithms when the ideal grating image added with salt and pepper noise, speckle noise, and Gaussian noise. Experimental results demonstrated that our method can measure the pitch of the grating accurately,

for example, our home-made grating with 20?m period has 500nm peak-to-valley uniformity of the averaged period with 40nm standard deviation during 35mm range. Another measurement illustrated that our home-made grating is 40nm peak-to-valley uniformity with 10nm standard deviation. This work verified that our lab can fabricate high-accuracy gratings which should be interesting for practical application in optical encoder.

9271-55, Session 11

Miniature pulse compressor with double-line-density gratings

Yanyang Li, Wei Jia, Changhe Zhou, Shanghai Institute of Optics and Fine Mechanics (China); Xiaona Yan, Shanghai Univ. (China); Shubin Li, Yancong Lu, Kun Liu, Jin Wang, Shanghai Institute of Optics and Fine Mechanics (China)

Femtosecond laser technology is one of the frontiers in the fields of nonlinear optics, advanced manufacturing etc. The method of femtosecond pulse compression is an important research content. To compress the femtosecond pulse, we need to use negative dispersive elements to compensate the positive dispersion of Ti: sapphire crystal and other optical elements. For this purpose, we propose a miniature double-line-density grating pair in which the line density of the second grating is twice of the first one, so the output pulse propagates along the way back. The density of the gratings is high, which will have a high diffraction efficiency and can compensate a high GVD (group velocity dispersion) in a small distance. For the first grating is transmitted and the second one is reflective, the device will not occlude the beam propagation. With the pair of the gratings, the input positive chirped 89fs pulse is neatly compressed into the Fourier transform limited 44fs pulse with no spectral spatial walk off and dispersion. It can be used for compression in laser cavity or out of the cavity. The gratings are easy to adjust and the structure is simple and compact, which has widespread interest in practical applications.

9271-56, Session 11

Single-track absolute position encoding method based on spatial frequency of stripes

Xiansong Xiang, Yancong Lu, Chunlong Wei, Changhe Zhou, Shanghai Institute of Optics and Fine Mechanics (China)

A new method of single-track absolute position encoding based on spatial frequency of stripes is proposed. Instead of using pseudorandom-sequence arranged stripes as in conventional situations, this kind of encoding method stores the location information in the frequency space of the stripes, which means the spatial frequency of stripes varies with position and indicates position. This encoding method has a strong fault-tolerant capability with single-stripe detecting errors. The method can be applied to absolute linear encoders, absolute photoelectric angle encoders or two-dimensional absolute linear encoders. The measuring device includes a CCD image sensor and a microscope system, and the method of decoding this frequency code is based on FFT algorithm. This method should be highly interesting for practical applications as an absolute position encoding method.

9271-57, Session 11

Demonstrating and optimizing the dual dispersion and focusing functionality of grating-Fresnel lens

Qian Zhou, Jinchao Zhang, Kai Ni, Jinchao Pang, Rui Tian, Graduate School at Shenzhen, Tsinghua Univ. (China)

As optical spectroscopy plays a vital role in many of modern science and engineering, there is a growing need for developing an inexpensive and miniature spectrometers. Many attempts have been tried to solve the issue, such as concave gratings and volume holographic spectroscopy.

Grating-Fresnel is a hybrid device that fuses the functions of a grating and Fresnel lens into a single device. Two major advantages are obvious. First, it has a large numerical aperture which result in a more compact spectrometer without significantly sacrificing the resolution. Second the device has planar surface which allows for low-cost mass production by replicating from a master pattern. A PDMS based hybrid grating and Fresnel lens (G-Fresnel) device has been demonstrated by Chuan Yang in The Pennsylvania State University. The G-Fresnel device was fabricated by using PDMS based soft lithography. Although the resolution was determined to be 1.4nm at 476.6nm, some problems which came from the gratings still exist. Low sensitivity and narrow spectral bandwidth are the major ones. In this paper, we try to design a transmission type G-Fresnel device in which a varied line-spacing grating is used. The varied line-spacing plane grating can effectively eliminate the aberration by controlling the line space. At the same time, the Fresnel lens are designed specially to try to get the best resolution. In order to improve the resolution and sensitivity, the grating will have a blaze angle and the length between Fresnel lens and gratings will be optimized.

9271-58, Session 11

A portable flat-field concave grating spectrometer with high resolution

Qian Zhou, Jinchao Pang, Kai Ni, Rui Tian, Graduate School at Shenzhen, Tsinghua Univ. (China); Jinchao Zhang, Graduate School at Shenzhen, Tsinghua Univ. (China)

Flat-field concave diffraction grating can be the only optical component of a grating spectrometer. Thus, flat-field concave diffraction grating determines the quality of the spectrometer directly. The two most important performance parameters which characterize a spectrometer are the resolution and the sensitivity. But for the portable grating spectrometer, the volume is also a key parameter. At present, the resolution can be improved by increasing the number of CCD or by using multiple grating, while these methods will increase the volume of spectrometers. This will seriously limit the use of the portable grating spectrometer.

In this paper, a novel method is introduced to increase the resolution while maintain the volume of the spectrometer by using a mirror. The key of this method is to divide the whole waveband into two wavebands. For the actually light path, the two CCDs detected the short wave and the long waves separately are located in different position and have different orientation. But in order to control the volume of the instrument, these can be realized on one CCD by using a mirror. By this way, we not only can effectively control the size of instrument, but also introduces more adjustable parameters to further improve the resolution. The position and orientation of the mirror can be calculated by the actual optical path. Furthermore, a light barrier is used to avoid the mutual influences of the two wavebands. For the determination of various parameters, we take two steps: First, we generally determine the value of these parameters according to

the optical path function equation. Secondly, we use the software of ZEMAX to further optimize the parameters. According to the result of simulation, the resolution of the spectrometer is 2-4times better than that of the current works.

9271-59, Session 12

Low rank matrix completion algorithms analysis and application in phase retrieval

Zhang Fen, Zhang Q. Bing, Anhui Univ. (China); Cheng Hong, Anhui Univ. (China); Zhang Cheng, Anhui Univ. (China); Wei Sui, Anhui Univ. (China)

Phase is an inherent characteristic of any wave field. Statistics show that greater than 25% of the information is encoded in the amplitude term and 75% of the information is in the phase term. Existing Probe can only record the amplitude of diffraction field directly. The information of phase is lost. The technique of using amplitude of diffraction field to reconstruct wave field is called phase retrieval. Solving phase retrieval problem via non-convex procedures relies on additional information of signal, and can only get local optimal solution. The phase retrieval problem of no additional information is solved in the paper. The approach is to formulate it as one of finding the rank-one solution to a system of linear matrix equations via convex relaxation. So only solving a matrix completion problem can capture the phase information with high probability, and it is a global optimal solution. Several methods are reviewed for low-rank matrix completion, such as Singular Value Thresholding (SVT), OPTSPACE, Fixed Point Continuation with Approximate (FPCA) SVD and TFOCS. The first is to summarize its core ideas, main steps of all algorithms and how these different algorithms are related to each other. Then, Numerical experiments are performed on synthetic data give the analysis at run-time performance and other aspects of convergence of these methods. Finally, the TFOCS package of matrix completion algorithms is used for the problem of phase retrieval, and experimental results demonstrate its effectiveness and correctness.

9271-60, Session 12

Design method of DOE with large diffraction angle (Invited Paper)

Hui Pang, Chongqing Institute of Green and Intelligent Technology (China) and Institute of Optics and Electronics (China); Shaoyun Yin, Chongqing Institute of Green and Intelligent Technology (China); Guoxing Zheng, Wuhan Univ. (China); Qiling Deng, Lifang Shi, Institute of Optics and Electronics (China); Chunlei Du, Chongqing Institute of Green and Intelligent Technology (China)

Design methods of diffractive optical elements (DOE) are almost based on the Fraunhofer diffraction theory. However, when the diffraction angle of the target pattern is large, the paraxial condition no longer holds and the actual result will deviate from the target. In this situation, the Rayleigh-Sommerfeld diffraction theory should be used. But, this theory is not suitable for fast Fourier Transform, and the calculation procedure is quite time consuming. In this paper, a pre-distortion correction method is proposed. By comparing the Rayleigh-Sommerfeld diffraction and the Fraunhofer diffraction, the difference between the diffraction patterns is calculated in the situation of large diffraction angle and the correction method of diffraction pattern is given for traditional DOE design method. The method is used for the design of DOE generating a laser keyboard, which verifies the feasibility and practicability of the method.

9271-61, Session 12

Synthesis of depth-map computer generated holograms (CGH) without dark line defects

Jin-young Roh, Yohan Park, Sujin Choi, Eunkyong Moon, Jaebeom Kwon, Dajeong Im, Hwi Kim, Korea Univ. Sejong Campus (Korea, Republic of)

The dark line defect problem associated with the depth-map computer generated holograms (CGH) is addressed. The physical origin of the dark line defect in the depth-map CGH is analyzed. We propose a novel depth-map CGH synthesis method for generating photo-realistic holographic three-dimensional images without the dark line defects. The proposed algorithm is verified with numerical and experimental results.

9271-62, Session 12

Single-phase modulator for colorful spatial distribution reconstruction

Jing Zhu, Qiang Song, Jian Wang, Fang Zhang, Weirui Yue, Guohai Situ, Xi Bao Yang, Huijie Huang, Shanghai Institute of Optics and Fine Mechanics (China); Jianguo Li, Lenovo (China)

Two potential solutions involving micro-mirror scanning and holographic method are both developed corresponding to a fast growing demand for micro- and pico-projections. Compared with beam scanning technique, diffractive method has three main advantages: to avoid local defects and obstructions and to provide stable images because of a collective forming of the image by all pixels of the light modulator; high efficiency due to redirection of light into the desired locations; laser eye-safety with strongly divergent wavefronts. Recently, two kinds of diffractive modulators are developed for colorful image: volume medium holography and three spatial modulators. The former method can form a fine full parallax viewing with white light reconstruction, while the last method can realize real-time holographic display by using three phase modulators irradiated by red, green and blue laser beam separately and to compose a final color hologram. However, both two methods are relatively expensive because of the phase recording media and make difficulties in real applications. One of the possible solutions is to use just one single diffractive phase modulator. Both multi exposure color switching and spatially separated methods are employed based on single phase modulator. The former approach resulted in flickering images and a rainbow effect because of low refresh frequency of current commercial spatial light modulators (SLM). The spatially separated method involves a segmentation which means part range of the hologram is used and showed viewing obstructions or ghost images. Therefore, full dynamic range of the phase modulator totally used simultaneously for three laser beam with segmentation are very important for a truly color reconstruction.

This report shows how to reconstruct the full color image with only single phase modulator based on a modified Gerchberg Saxton (GS) algorithm. In our approach, the phase distribution of the modulator is recovered by reconstructing the three primary color images together within a GS iterative loop. The most important issue of the approach is that the three primary color images are established at special distances to the image plane in the algorithm. Then the wave front is propagated through each of these three color separation planes at different wavelength and back to the hologram for a loop. As a result, the color image can be reformed in the image plane with the designed hologram by applying the three wavelength lasers irradiation with spatial overlap. Moreover, the contrast ratio and the speckles visibility is depending on the repeated number of the loop.

When considering real time projection application, an outside-window amplitude freedom method is employed in the algorithm to save the calculation time. In this modification, the amplitude outside the setup window is modified with a dynamic factor to increase the contrast ratio of the image. The performed numerical simulations have proven that the new technique allows one to successfully display a fully color image with both high resolution and high phase retrieval speed by use of GPU. This method has potential application for real-time pico-display in wearable display device.

9271-64, Session 13

Toward high-quality computational holography for the display of deep 3D scene (Invited Paper)

Masahiro Yamaguchi, Tokyo Institute of Technology (Japan)

The advantage of holography in 3D display applications is the reproduction of 3D images with all the depth cue of human vision, especially the reproduction of deep 3D scene. For the realization of holographic 3D display, the technique for calculating hologram is a key issue as well as the development of high-resolution display devices. Conventional techniques for calculating hologram based on the diffraction from point sources or polygons generate holograms of high-resolution 3D scene, but rendering various appearances of an object, such as occlusion, specular reflection, transparency or translucency, and iridescent colors, is not easy by wavefront-based rendering. On the other hand, advanced rendering techniques are available in the field of computer graphics based on light-ray information. Although ray-based rendering can be applied to the hologram calculation, it loses the resolution in the image far from the hologram plane. Thus, we have been developing a technique for calculating holograms by using ray-based rendering without loss of resolution. In the proposed method, a ray-sampling (RS) plane is defined near the object, and the wavefront from the object is computed by ray-based rendering and ray-to-wavefront conversion. The method can also be easily applied to the hologram calculation from real objects, using scanning camera array or integral imaging. By defining multiple RS planes, it is possible to generate hologram that reconstructs deep 3D scene. The method for suppressing speckle noise in the hologram calculated by using RS plane is presented as well.

9271-65, Session 13

Generation of phase-only hologram (Invited Paper)

Peter W. M. Tsang, City Univ. of Hong Kong (Hong Kong, China)

The rapid advancement of computing and optical technologies in the past decade has enabled the numerical generation, as well as acquisition of medium size digital holograms at video rate. However, as a digital hologram is a complex image, it will require a pair of spatial light modulators (SLM) to display its orthogonal (real/imaginary, magnitude/phase, or phase/phase) components. Such optical setup is complicate, requiring precise alignment between the SLMs and other optical accessories. Although a complex hologram can be converted into an off-axis, amplitude-only hologram by mixing with a reference beam so that it can be displayed with a single SLM, the reconstructed image is accompanied with the zeroth-order diffraction and the twin image. To overcome these problems, investigation on the generation of phase-only hologram (POH) has been an area of interest for many years. Being different from a complex hologram, a POH can be displayed with a single phase-only SLM.

In addition, the reconstructed image is inherently free from the zeroth-order diffraction and the twin image, and also exhibits higher optical efficiency as compared with the amplitude-only hologram. In this talk, the author will review a number of modern methods for the generation of phase-only holograms. Albeit the differences in the methodologies, these works share the common objective of enhancing the computation efficiency, as well as simplifying the optical setup of the display system. Subsequently, the author will present a novel approach for the generation of POH. Experimental results will be illustrated to demonstrate the feasibility of the proposed method.

produce accurate depth information as well as viewer-position-dependent effects. The hologram is spatially partitioned into many holographic elements to achieve perspective views and corresponding depth maps according to their positions. Accurate accommodation cue and occlusion effect can be created, and computer graphics rendering techniques can be employed in the CGH generation to enhance the image fidelity. A binary-amplitude hologram with 400 million pixels is fabricated by an electron-beam lithography system, and the diffraction angle is above 30 degrees during optical reconstruction. Numerical simulation and optical experiment are performed, and the experimental results show our proposed method can reconstruct a realistic 3D image with an accurate sensation of depth.

9271-66, Session 13

Diffractive optical elements with freeform apertures

Yunlong Sheng, Univ. Laval (Canada)

Binary phase holograms fabricated by e-beam lithography and micro-optics mass replicable in plastic are widely used in the Head Mounted Displays (HMDs), laser and holographic projectors for structured illumination for the 3D sensing, robot vision, virtual interface display, gesture sensing, motion sensing in Kinect for Xbox One. The hologram generated in the computer (CGH) is usually designed as a matrix of pixels. When the CGH is fabricated with e-beam lithography, the later has much higher definition (50 nm for instance) depending on the e-beam machines. The only constraint is the minimum feature size, e.g. minimum distance between two features on the mask, which can be in microns. Therefore, an e-beam CGH should be designed with a very small pixel size (50 nm) although still respecting the minimum feature size constraint. In this way the number of the pixels and the number of degree of freedom in the design is dramatically increased to several billion pixels. In order to fully explore the very high number of degree of freedom we have proposed the CGH of triangle, polygonal, trapezoidal or orthogonal apertures and several design optimization approaches. An overview on this technique and some recent realizations will be presented in the conference.

9271-67, Session 13

The accelerated algorithm of polygon computer-generated hologram synthesis

Dajeong Im, Hwi Kim, Korea Univ. Sejong Campus (Korea, Republic of)

Computation time is a crucial matter to solve in polygon computer-generated hologram synthesis. We propose the fast calculation algorithm of polygon computer-generated hologram by reducing effective area of two-dimensional Fourier transform of a triangle.

9271-68, Session 13

Calculation for high-resolution computer-generated hologram with fully-computed holographic stereogram

Hao Zhang, Yan Zhao, Liangcai Cao, Guo Fan Jin, Tsinghua Univ. (China)

A high-resolution full-parallax computer-generated hologram (CGH) is created to reconstruct a photorealistic three-dimensional (3D) scene. Fully-computed holographic stereogram is introduced to generate the CGH, which integrates physically based method and holographic stereogram based method to

Thursday - Friday 9 -10 October 2014

Part of Proceedings of SPIE Vol. 9272 Optical Design and Testing VI

9272-1, Session 1

Light scattering characterization of optical components: BRDF, BTDF, and scatter losses *(Invited Paper)*

Sven Schröder, Alexander Finck, Fraunhofer-Institut für Angewandte Optik und Feinmechanik (Germany); Dina Katsir, Aektar Ltd. (Israel); Uwe Zeitner, Angela Duparré, Fraunhofer-Institut für Angewandte Optik und Feinmechanik (Germany)

Light scattering caused by imperfections of optical components can critically affect the performance of optical systems in terms of losses and image degradation. Because of the numerous potential sources of scattering such as roughness, surface and sub-surface defects, bulk inhomogeneities, as well as coatings, scattering properties must be carefully specified and measured at the wavelengths of application. Bidirectional Reflectance and Transmittance Distribution Functions (BRDF / BTDF) are used to quantify the angle resolved scattering properties. The data can be used as an input for optical engineering software just as FRED, ASAP, ZEMAX for stray light modeling. In addition, analyzing the scattered light can provide valuable information about the relevant imperfections. The presentation provides an overview of instrumentation for light scattering measurements at wavelengths ranging from the visible to the extreme ultraviolet and the infrared spectral regions. Examples of applications will be discussed ranging from superpolished mirrors to diffraction gratings, interference coatings, and black absorbing coatings.

9272-2, Session 1

Extremely-small red-green-blue beam combiners for compact projection-type displays *(Invited Paper)*

Toshio Katsuyama, Akira Nakao, Kosuke Ogawa, Kenta Tsujino, Kohei Takahata, Univ. of Fukui (Japan)

Laser beam combiners, which can be used for compact projection-type displays, are reviewed and a newly-proposed extremely-small laser beam combiner composed of optical waveguides and optical couplers is described. Here, the laser beams with three RGB (Red-Green-Blue) primary colors are combined into one single beam by using the laser beam combiner. Such combiners are classified into three categories, i.e., a mirror-prism type, an optical fiber type and an optical waveguide type. The mirror-prism type combiners are composed of the mirrors and/or prisms for combining the laser beams. The optical fiber type combiners use the optical couplers made of optical fibers. On the other hand, optical waveguide-type combiners, which are based on the optical waveguides, are particularly useful because they enable us to construct extremely small laser combiners integrated with laser sources.

Here, we proposed and analyzed a new integrated waveguide-type red-green-blue (RGB) beam combiner that can contribute to a miniaturization of the compact projection-type displays such as an eyewear projector. The essential point of this beam combiner is that it is composed of three individual waveguides for RGB light inputs, and three directional couplers. The combined output light can be obtained from the single waveguide. The waveguide supports the single mode transmission. The efficiency for output light is as high as 96%, and the size is as small as 0.06778 mm. In addition, the small dependence of the output efficiency on the wavelength and the relatively large fabrication tolerance are obtained.

9272-3, Session 1

A design of UV-LED system to obtain high power density in specific distance working-plane *(Invited Paper)*

Renyuan Li, Xiuhui Sun, Jian Gou, Wentao Cai, Chunlei Du, Shaoyun Yin, Chongqing Institute of Green and Intelligent Technology (China)

With the advantages of low cost, small volume, low energy consumption, long service life and environment friendly, the application of UV-LED has attract widespread concern among academia and industry researchers, especially in the field of ink printing industry. However, how to get high power density in specific distance working plane is a technical problem need to be solved eagerly. This paper presents a design solution to reduce the Etendue of the lighting system and therefore obtain high power density. The design uses UV-LED array as the light source, and uses a freeform surface collimating lens array to collimate this light source. In order to improve the energy sufficiency of the system, multipoint fitting-based freeform surface lens design for UV-LED extended sources is proposed to design collimating free-form lens for UV-LED extended source in this work. The freeform surface collimating lens array is placed in front of the UV-LED extended sources array. And a non-spherical lens is used in the optical path to focus the light beam. In the simulation, a light source module with the size of 50mm * 50mm has been designed, and obtained power density up to 8W/cm² in the specific working plane with the working-distance of 3cm. This design is expected to replace the existing mercury lamp-based UV light sources and solve the problem in the application of UV-LED ink printing field.

9272-4, Session 1

Design of directional light source for blue phase LCD

Che Yen Lin, King Lien Lee, Po-Yu Tsai, Jie Wen Chen, National Taipei Univ. of Technology (Taiwan)

Directional light source has been used widely in backlight modules of 3D stereoscopic display and a vertical-field-switching blue phase liquid crystal display. The blue phase LCD can exhibit a better efficiency by using a large oblique incident angle (Cheng et al., 2011). For submitting the directional light source of a large oblique incident angle, we design a new backlight module at top and bottom microstructures of light guide plate. Results of the research substantially present the incident angle 59° of oblique light source and provide a higher uniformity 74.8% of illumination. Therefore, the new backlight module can cut down a prism film, up diffusion and down diffusion; we will reduce a cost of material and procedures of manufacture.

A light guide plate with microstructures at the bottom was proposed, it can produce oblique light source which emit at 40°. The objective of our research is to design microstructures at the top of light guide plate for increasing the angles of oblique light source and provide higher uniformity of illumination. In this work, we divide a light guide plate into four zones and distribute the microstructures by different linear equations in each zone, then simulate the backlight system by optical software, TracePro. The best simulation result in this paper shows that the output rays mainly emit at 59° and the uniformity is 74.8%. The contrast ratio of the blue phase liquid crystal display is 1163. Consequently, we substantially increase the angles of oblique light source and provide a better uniformity of illumination for a backlight module, which can produce more oblique light source to a vertical-field-switching blue phase liquid crystal display for improving the

efficiency of liquid crystal display. Meanwhile, this manner offers related companies to cost down and increase benefit.

[1] H. C. Cheng, J. Yan, T. Ishinabe, and S. T. Wu, "Vertical field switching for blue-phase liquid crystal devices," *Appl. Phys. Lett.*, vol. 98, pp. 261102, Jun. 2011.

9272-5, Session 1

Flexible polymer light-emitting diode employing graphene as anode

Wei Luo, Chongqing Institute of Green and Intelligent Technology (China) and Chongqing Univ. (China); Weimin Chen, Chongqing Univ. (China); Chongqian Leng, Haofei Shi, Chunlei Du, Chongqing Institute of Green and Intelligent Technology (China)

Transparent conducting electrodes play a vital role in organic optoelectronic devices. Conventional transparent conductor indium tin oxide (ITO) is troubled with the ease of brittleness, expensive rare source and indium diffusion problem, making an urgent need to find an alternative material. Graphene, the most advanced 2D nanomaterial, rivals ITO with combined extremely excellent optical, electrical and mechanical properties. Here we report the fabrication of a polymer light emitting diode employing graphene as anode by solution process. The graphene on PET substrate is modified through interfacial engineering to obtain a patterned uniform film, which yields a composite electrode with high work function, high optical transmission and low sheet resistant. Emission layer MEH-PPV is spin coated on the composite electrode followed by evaporating the LiF/Al cathode. The resulting device exhibits high electroluminescence efficiency, which is attributed to our high quality graphene and good chemical doping. Also it can survive a good performance after one thousand bending tests, manifesting its wonderful flexibility. Such polymer light emitting diode employing this green and smart graphene anode will promote the development of organic electroluminescent and photovoltaic devices toward a flexible and wearable era.

9272-6, Session 1

Feedback modification strategy for designing a freeform optical surface with given illumination pattern

Yuhao Chen, Zhaofeng Cen, Xiaotong Li, Yun Dong, Zhejiang Univ. (China)

In order to achieve a uniform illumination distribution confined to a given rectangular region, a feedback modification strategy is introduced in the design of free-form optical surface. The whole process of this strategy includes two steps: solving the initial structure and feedback process.

To solve the initial surface, we first divide the source space along its longitude and latitude direction with uniform angle. Because the energy of each longitude and latitude micro-belt of free-form surface and each corresponding micro-belt on the target plane is equal, the target plane can be divided into grids, and then the mapping relationship of source space and target space is constructed. By using Snell's Law and tangent plane iterative method, we obtain the coordinates of all grid nodes and an initial freeform surface can be constructed.

As we known, the initial optical surface is designed with point light source, the first simulation result may have a large deviation from expectation because of the extended LED source. To solve this problem, we use a feedback modification strategy. During the feedback process we design specific algorithm. In every round of feedback, we use simulation result as well as given illuminance

distribution of last round to improve solved optical model of next round. In our experiment, this method is proved to be efficient, the shape of illumination spot is dramatically improved and the uniformity is promoted from less than 20% to up to 80% after eleven times feedback. The optical free-form surface constructed with this strategy has a smooth shape, which make great convenience for manufacture.

9272-7, Session 2

Three-dimensional image formation based on scanning with a floating real image (Invited Paper)

Daisuke Miyazaki, Osaka City Univ. (Japan)

Stereoscopic three-dimensional (3-D) display technology is expected to advance visual interface technology utilizing optical techniques. The development of auto-stereoscopic display techniques has recently become active to avoid the use of bothersome 3-D glasses. The achievement of natural depth perception is an important issue for 3-D display technique. In addition, floating image formation is effective to enhance realistic sensation of a 3-D image, and to gain accessibility for direct interactive operation to the image with fingers or 3-D pointing devices.

We have proposed several types of 3-D display systems based on real image formation with optical imaging elements. A volumetric display generates a floating 3-D image by arranging light spots in the air, which satisfies all the criteria of stereoscopy. We have developed several volumetric display systems using two kinds of optical imaging elements, concave mirrors and micro-mirror array devices. A dihedral corner reflector array (DCRA) is a novel a micro-mirror imaging element, which can form a plane-symmetrical real image without image distortions. A real image is moved by an optical scanner to scan a volume.

As another type of an autostereoscopic 3-D display technique, we have been developing floating multi-viewpoint display systems. The multi-viewpoint imaging can be implemented by using multiple projectors or a high-frame-rate single projector and an optical scanner. We used a DCRA device to form a floating real image and images of exit pupils for providing multiple viewpoints. It is possible to expand the viewing area to 360 degrees around a floating image.

9272-8, Session 2

3D goes digital: from stereoscopy to modern 3D imaging techniques (Invited Paper)

Norbert Kerwien, Carl Zeiss AG (Germany)

Visual perception is the most important sense to experience our environment. Since our surrounding is three-dimensional, the ability to see in 3D is critical for orientation. As early as the 19th century, the English physicist Charles Wheatstone realized that we use the parallax of binocular vision to gain depth perception of our environment. The binocular disparity of the two retinal 2D images in our eyes is the basis for our brain to form a 3D image, known as stereopsis. Based on this discovery, Wheatstone also constructed the first stereoscope, establishing the basis for stereoscopic 3D imaging. In the years that followed, many optical instruments were influenced by these basic ideas. Examples include binoculars, rangefinders, stereo-microscopes, airborne cameras, stereo cameras, head-mounted displays, autostereoscopic imaging techniques, 3D cinema, and more.

The advent of digital technologies also revolutionized 3D imaging. Powerful readily available sensors and displays combined with efficient pre- or post-processing enable new

methods and applications for 3D imaging. Examples span a wide range of areas, including 360°-photography to enrich product presentations on the web, light field cameras to take pictures from different perspectives and focal points in one shot, modern methods of digital 3D reconstruction to improve 3D metrology, and much more.

This paper draws an arc from basic concepts of 3D imaging to modern digital implementations, picking out instructive examples during its 175 years of history.

9272-9, Session 3

Imaging microscopy by phase-contrast engine: retardation-modulated differential interference contrast microscope (*Invited Paper*)

Masahide Itoh, Hiroshi Ishiwata, Univ. of Tsukuba (Japan)

Differential interference contrast (DIC) microscopes are commonly used for observing objects' phase distribution. The DIC microscope is a powerful means of revealing detailed structures in living cells and small steps on the surfaces. Current DIC microscopes have high sensitivity and high resolution. However, DIC microscopes have a drawback in that, they are unable to make quantitative measurements of the phase distribution of the phase object. We have developed the retardation-modulated DIC (RM-DIC) microscope and it is able to make a quantitative measurements of the phase distribution of a phase object.

In the field of biology and medicine, observation object of the microscope has been changing from the thin specimen to the thick living tissue. Furthermore, observation of the internal structure of a living tissue is also desired by low invasion. However, the real structure of a phase object with three-dimensional distribution such as a living tissue is difficult to observe, because of the influence of the phase distribution before and behind of observation position.

We enabled observation of the internal structure of living tissue without stain, by adding a new function to reduce the influence of phase distribution before and behind to our RM-DIC microscope system.

9272-10, Session 3

Phase-contrast scanning optical microscopy for biological tissues (*Invited Paper*)

Masaki Hisaka, Osaka Electro-Communication Univ. (Japan)

Phase-contrast imaging of living tissues is important for investigating biological structures and functions. A phase-contrast scanning optical microscope using annular illumination and active image processing have been developed. This microscope has some features such as separate phase and amplitude imaging, reducing nonlinear imaging components and aberration-free imaging for rotationally invariant aberrations. A laser beam irradiated tissue samples annually, and CCD camera with an annular aperture captured an annular shape distribution. The constructed oblique images was Fourier-transformed, and a figure-8-shaped spatial frequency filter with the sign correction (+i, ?i) were applied to extract the linear phase-contrast imaging components. The reconstructed spectrum superposed with figure-8-shaped different azimuthal spectra was inversely Fourier transformed, and the phase-contrast cross-sectional images such as structures of cell nucleus and the outer wall of hepatocyte

were obtained. We also evaluated the imaging features of lateral and axial spatial resolutions in three-dimensions.

9272-11, Session 3

Integrated phase-shifting digital holography using statistical approach (*Invited Paper*)

Nobukazu Yoshikawa, Kazuki Kajihara, Takaaki Shiratori, Saitama Univ. (Japan)

The integrated phase-shifting method can change the phase continuously in a short time. This property is preferable in terms of phase stability. However, in the integrated phase-shifting method, it may be difficult to control the phase-shift using a low-cost system because it requires real time operation.

In this study, we propose a statistical generalized phase-shifting digital holography using integrating method. The relative phase-shift can be estimated by the statistical method using three holograms taken by the integrating method. The statistical method is not necessary to control the amount of the phase-shift strictly.

We confirm the feasibility of the proposed method and investigate the relationship between the relative phase-shift amount and speed of moving mirror by experiments. The results indicate that the phase randomness of the diffraction field of the object holds enough regardless of the integration process. Recording time of the proposed method was considerably decreased because the stabilization time of the moving mirror is not needed. The estimated phase-shift values of the proposed method were almost the same as those of the step phase-shifting method though the recording time is considerably reduced. The method is easily implemented using a simple phase shifter because precise controls and calibrations of the phase shifts are not necessary.

9272-12, Session 3

High-precision three-dimensional coordinate measurement with subwavelength-aperture-fiber point diffraction interferometer

Daodang Wang, China Jiliang Univ. (China); Yangbo Xu, College of Metrology and Measurement Engineering, China Jiliang University (China); Xixi Chen, Fumin Wang, China Jiliang Univ. (China); Ming Kong, College of Metrology and Measurement Engineering, China Jiliang University (China); Jun Zhao, China Jiliang Univ. (China)

With the development of ultra-precise machining technique, three-coordinate measurement has got wide application in the field of high-precision even ultra-high-precision measurement. To overcome the accuracy limitation due to the machining error of standard parts in measurement system, a three-dimensional coordinate measurement method with subwavelength-aperture-fiber point diffraction interferometer (PDI) is proposed, in which the high-precision measurement standard is obtained from the ideal point-diffracted spherical wavefront instead of standard components. On the basis of the phase distribution demodulated from point-diffraction interference field, high-precision three-dimensional coordinate measurement is realized with numerical iteration optimization algorithm. The sub-wavelength-aperture fiber is used as point-diffraction source to get precise and high-energy spherical wavefront within high aperture angle range, by which the conflict between diffraction wave angle and energy in traditional PDI can be avoided. Besides, a double-iterative

method based on Levenberg-Marquardt algorithm is proposed to realize precise reconstruct three-dimensional coordinate. The analysis shows that the proposed method can both reach the measurement precision and repeatability accuracy better than microns within a 200?200?300 (in unit of mm) working volume. This measurement method does not rely on the initial iteration value in numerical coordinate reconstruction, and also has high measurement precision, large measuring range, fast processing speed and preferable anti-noise ability. It is of great practicality for measurement of three-dimensional coordinate and calibration of measurement system.

9272-13, Session 3

Freeform metrology based on phase retrieval and computer-generated hologram

Fa Zeng, Qiao Feng Tan, Tsinghua Univ. (China); Yi Liu, China Precision Engineering Institute (China); Hua Rong Gu, Tsinghua Univ. (China); Guo Fan Jin, Tsinghua Univ (China)

Recently, interferometric null testing with computer-generated hologram has been proposed as a non-contact and high precision solution to the freeform optics metrology. However, the interferometry solution owns some typical disadvantages such as the strong sensitivity to the table vibrations or temperature fluctuations, which hinders its usage outside the strictly controlled laboratory conditions. Phase retrieval presents a viable alternative to interferometry for measuring phase and can provide a more compact, less expensive, and more stable experimental setup. In this work, for the first time we propose a novel solution to freeform metrology based on phase retrieval and computer-generated hologram (CGH). The CGH is designed according to the ray tracing method, so as to compensate the aspheric aberration related to the freeform element. With careful alignment of the CGH and the freeform element in the testing system, several defocused intensity images can be captured for phase retrieval. In this paper the experimental results related to a freeform surface with 18?18mm² rectangular aperture (its peak-to-valley asphericity equals to 193um) are reported, meanwhile, the measurement error and repeatability are both analyzed. In addition, we also have compared them with the measurement results given by the interferometry solution, so as to evaluate the validity of our solution.

9272-14, Session 4

Design and fabrication of single panoramic stereo imaging system (*Invited Paper*)

Jian Bai, Zhejiang Univ. (China)

A novel panoramic stereo imaging system with double panoramic annular lenses (PAL) combined in single optical system is introduced in this paper. The proposed system consists of two coaxial PAL units and images the surroundings on one sensor. The imaging rings are concentric. The object position can be calculated by triangulation method. The novelty of this system is that the central blind zone of one PAL unit is partly used by the other as an image zone. The stereo field of view is 60°-105°?360°. The depth extracting resolution is about 10 mm within object space distance of 500mm. The F# of the system is about 3, facilitating the system to be applied in low illumination environment. A design is presented and the depth extracting precision is analyzed.

9272-15, Session 4

Polarization aberration function for perturbed lithographic lens (*Invited Paper*)

Wei Huang, Changchun Institute of Optics, Fine Mechanics and Physics (China) and State Key Lab. of Applied Optics (China); Xiangru Xu, Mingfei Xu, Changchun Institute of Optics, Fine Mechanics and Physics (China) and Univ. of Chinese Academy of Sciences (China); Weicai Xu, Changchun Institute of Optics, Fine Mechanics and Physics (China) and State Key Lab. of Applied Optics (China); Zhaoxin Tang, Changchun Institute of Optics, Fine Mechanics and Physics (China) and Univ. of Chinese Academy of Sciences (China)

A comprehensive polarization aberration function is proposed to evaluate the imaging quality of a perturbed high NA lithographic lens. In this function, the system polarization aberration, i.e. Jones matrix, is decomposed into several basic parts as wavefront aberration, apodization, diattenuation, retardance and rotation by single value decomposition (SVD). The wavefront aberration is described by field-Zernike polynomials (FZP), and the diattenuation, as well as retardance, is described by field-orientation Zernike polynomials (FOZP). The relationship of system polarization aberration with pupil, field and manufacturing errors is established by an approximately analytical equation, which provides a possible way to analyze lens tolerance for polarization aberration.

9272-16, Session 4

Design, simulation, and experimental analysis of an anti-stray-light illumination system of fundus camera (*Invited Paper*)

Chen Ma, Dewen Cheng, Chen Xu, Yongtian Wang, Beijing Institute of Technology (China)

Fundus camera is a complex optical system for retinal photography, involving illumination and imaging of the retina. The stray light is one of the most significant problems of fundus camera because the retina is so minimally reflective that back reflections from the cornea and any other optical surface are likely to be significantly greater than the light reflected from the retina. To provide maximum illumination to the retina while eliminating back reflections, a novel design of illumination system used in portable fundus camera is proposed. Internal illumination, in which eyepiece is shared by both the illumination system and the imaging system but the condenser and the objective are separated by a beam splitter, is adopted for its higher efficiency. To eliminate the strong stray light caused by corneal center and make full use of light energy, the annular stop in conventional illumination systems is replaced by a fiber-coupled, ring-shaped light source that forms an annular beam. Parameters including size and light-emitting angle of the light source are specially designed. To weaken the stray light, a polarized light source is used, and an analyzer plate is placed after beam splitter in the imaging system. Simulation results show that the illumination uniformity at the fundus exceeds 90%, and the stray light is within 1%. Finally, a proof-of-concept prototype is developed and retinal photos of an ophthalmophantom are captured. The experimental results show that ghost images and stray light have been greatly reduced to a level that professional diagnostic will not be interfered.

9272-17, Session 4

Semi-transparent screen based on the optimization of microlens patterns for the head-up display in automobiles

Jae Yong Lee, Min Ho Shin, Young Joo Kim, Yonsei Univ. (Korea, Republic of)

Since the direct projection head-up display (HUD) provides the driving information to the driver through the screen prepared on the windshield of vehicle, it is necessary to develop a semi-transparent screen which has high and uniform reflect intensity with a reasonable transmittance at the driver's field of view (Eye-box) and driver's eyes, simultaneously. Although the semi-transparent screen can be designed to increase the reflect intensity to the driver's eyes using the micro patterns, the reflected image is not uniform at the eye-box since the windshield has usually a different tilt angle. In this study, the optical simulation and optimization of microlens patterns distribution was conducted to enhance the reflected image uniformity with keeping enough reflect intensity. The micro patterns were optimized by controlling the relative curvature and aspect ratio at the each divided section with the geometrical optical simulation. Semi-transparent screen also includes a metal coating which has a thickness to maintain the reflect intensity and transmittance of screen with the consideration of trade-off relationship. This micro pattern structure has some advantages for semi-transparent screen, including the easy control of reflectivity intensity and simple fabrication process. The uniformity of screen was measured by 9-point method suggested as a general display measurement method. From the simulation results, we obtained the enhanced semi-transparent screen which has microlens of 100 μ m radius at the sectional micro pattern distributions with different aspect ratio. Designed screen showed the improved characteristics than those of previous report with 96.01% of uniformity. In addition, the semi-transparent screen is prepared and evaluated with the optimized micro pattern distribution with the consideration for the conditions of vehicle and driver.

9272-27, Session Post

CFRP variable curvature mirror being capable of generating a large variation of saggitus: prototype design and experimental demonstration

Hui Zhao, Xuewu Fan, Zhihai Pang, Xi'an Institute of Optics and Precision Mechanics (China); Guorui Ren, Xi'an Institute of Optics and Precision Mechanics (China); Wei Wang, Yongjie Xie, Zhen Ma, Yunfei Du, Xi'an Institute of Optics and Precision Mechanics (China); Jingxuan Wei, Xidian Univ. (China); Xiaopeng Xie, Inner Mongolia Univ. (China)

Optical zoom imaging is a long history technique that could date back to 1834 and two traditional ways (optical compensation and mechanical compensation) can be used to realize optical zooming. In recent years, optical zoom imaging without introducing moving elements has been paid much attention, because this novel technique is suitable for special application fields such as mobile phone camera and space-born camera and so on.

Because conventional optical component could not change its curvature, they can only provide a fixed optical power (OP). Hence, according to the classical calculation equation of overall OP, the only way to alter focal length is to change the relative interval between components. Fortunately, VCM

(variable curvature mirror) provides one way to eliminate moving elements.

By introducing optical leveraging into system design, the slightly OP variation of VCM will be boosted to generate a big change of system focal length. However, in order to obtain enough optical magnification, VCM should provide a large variation of saggitus and this requires the corresponding component material have following characteristics: be robust enough during curvature variation, require less force to deform and have a high ultimate strength. Compared with conventional materials, CFRP (carbon-fiber-reinforced-polymer) satisfies all these requirements and is suitable for fabricating VCM. Therefore in this paper, a CFRP VCM (diameter 100mm, thickness 2mm and initial curvature radius 1740mm) is designed, fabricated and tested. The results demonstrate that this component can provide a 22.9 μ m variation of saggitus approximately, which proves that CFRP is indeed a good choice for fabricating VCM.

9272-28, Session Post

Visible- and near-infrared spectra of conical bubble sonoluminescence in water

Shoujie He, Hebei Univ. (China); Jing Ha, Agricultural Univ. of Hebei (China)

The conical bubble luminescence is a type of sonoluminescence. In this paper, it has been produced using an improved conical bubble U-tube in water. The light pulses and emission spectra of bubbles in water have been detected. Results show that several light pulses in a flash are distributed within a few hundred nanoseconds. The spectrum of conical bubble sonoluminescence for H₂O is continuum extending from visible to near infrared wavelength region, on which five apparent spectral bands are superimposed. The five spectral bands from short wavelength to long wavelength are assigned to 3 ν_1 + ν_3 combination bands (vapor phase), 2 ν_1 + ν_2 + ν_3 combination bands (vapor phase), 3 ν_3 combination bands (vapor phase), 2 ν_1 + ν_2 combination bands (vapor phase) and 2 ν_1 + ν_3 combination bands (liquid phase near boiling point). The apparent emitted vibrational spectral bands of H₂O molecules in the visible and near infrared region are firstly detected in sonoluminescence experiments which verifies the hot-spot chemiluminescence model of sonoluminescence to some extent. The obtained optical characteristics of conical bubble sonoluminescence in D₂O identify the assignment of those vibrational bands of H₂O.

9272-29, Session Post

Design of an ultra-thin dual band infrared system

Ke Du, Shanghai Institute of Spaceflight Control Technology (China); Xuemin Cheng, Graduate School at Shenzhen, Tsinghua Univ. (China); Huabao Long, Shanghai Institute of Spaceflight Control Technology (China)

Ultra-thin imaging systems using reflective multiple-fold approach have smaller volume and weight while maintain high resolution compared with conventional optical systems. The multiple-fold approach can operate within wide spectral range due to the absence of chromatic aberration and significantly extend focal distance. The approach can fulfill the need of compact, high performance dual band surveillance infrared imaging systems. In this paper, we present a dual band infrared imaging system of four-fold reflection with two air-spaced concentric reflective surfaces. The dual band IR system imaging over the SWIR and LWIR bands has 107mm effective focal length, 0.7NA, f-2 effective illumination, $\pm 4^\circ$ FOV, 50mm effective aperture with 80mm outer diameter in a 25mm total thickness,

which spectral response is 2-12 μ m. The high performance, compact system has very small size and weight which can be widely used in long range surveillance.

9272-30, Session Post

Design of testing system of conformal dome

Fu Lian Xiao, Shanghai Institute of Laser Technology (China)

The shape of conformal dome meets the demands of aerodynamics, which can make guided missile improve velocity and distance. Conformal dome will be widely used in optical seeker of weapon in the future, but it is a difficult problem to test the surface precision of conformal dome. In this paper the testing method of Offner is put forward, the designing method of Offner is also introduced. Concave aspheric surface of conformal dome can be tested by Offner optical system., in order to test concave aspheric surface of conformal dome, firstly the formula of Offner system with single lens is deducted based on the third-order aberration, secondly the initial configuration of Offner optical system is calculated with formula, field lens is also added to balance the optical system, then the data of initial configuration is optimized by optical software ZEMAX, the final result of Offner optical system with single compensating lens is obtained after optimization. With the same principle, the formula of Offner optical system with double compensating lens is deducted, the initial configuration of Offner optical system is also calculated with formula, so the final configuration of double compensating lens system is obtained after optimization. Finally Offner optical system with double compensating lens is selected to test the aspheric surface of conformal dome.

9272-32, Session Post

Design of a dual-band MWIR/LWIR circular unobscured three-mirror optical system with Zernike polynomial surfaces

Hao Zhu, Qingfeng Cui, Mingxu Piao, Chunzhu Zhao, Changchun Univ. of Science and Technology (China)

This paper discusses the optical design of an uncooled dual-band MWIR/LWIR optical system using a circular unobscured three-mirror system which is particularly suitable for wide spectral range, large aperture and small volume imaging systems. The system is designed at focal length 310mm, F-number 1.55 with field of view 1.77 $^{\circ}$ ×1.33 $^{\circ}$. A coaxial three-mirror system is calculated by the paraxial matrix as a starting point. With the condition that the focal point of each conic mirror is placed to coincide successively, elements in the system are tilted and decentered properly to make the system unobscured and the mirrors are arranged to form a round configuration for compactness. The optical path is folded inside the region surrounded by the mirrors. Zernike polynomial surfaces which are limited to be symmetric about tangential plane are used to correct aberrations and to improve the image quality. The modulation transfer function of this system is above 0.65 in MWIR band and above 0.5 in LWIR band all over the field of view at the Nyquist frequency of 20 line pairs per millimeter. The result shows that the space can be utilized efficiently, the system is compact and image quality is favorable.

9272-33, Session Post

Design and optimization of optical system for a spectrometer based on VPHT grating

Zhong Ren, Jiangxi Science and Technology Normal Univ. (China) and Nanchang Univ. (China); Guodong Liu, Zhen Huang, Jiangxi Science and Technology Normal Univ. (China)

Spectrometer is a kind of advanced analytical tool has being widely employed into varieties of field. In the traditional grating typed spectrometer, the plane and concave grating have usually been used as the spectral diffraction component, for example, the plane grating is usually used into the Czerny-Turner spectrometer. Although these spectrometers have widely applied into the practice, some drawbacks are still existed, for example, low light-passing efficiency, serious stray-light and spectral distortion, etc. With the development of holography technique and nano-superfinishing technique, holography grating has being used into the spectrometer. To overcome some drawbacks of optical system for plane and concave grating typed spectrometer, including serious aberration, worse spectral fatness and low diffraction efficiency etc, a novel optical system based on volume phase holographic transmission (VPHT) grating was designed in this paper. For this grating, its manufacture and theories were investigated, and its diffraction efficiency was numerically simulated. In order to validate this designed optical system, the spectral scaling experiment was performed and the spectral resolution reached 2nm, the calibration equation between the scaling wavelength and corresponding pixels was gotten via linear least square fitting algorithm. It was proved that the wavelength absolute value reached 1.7nm on the wavelength of 635nm, the root-mean-square error (RMSE) of full scaling wavelengths was 0.3nm. These experimental results illustrated that the design of the optical system for spectrometer based on VPHT grating is good.

9272-34, Session Post

Optical performance study of duplex Y-branch coupler with different structures

Kuang-Lung Huang, MingDao Univ. (Taiwan); Jin-Jia Chen, Te-Shu Liu, Jei Ding, National Changhua Univ. of Education (Taiwan)

Y-branch coupler has gradually become an indispensable component in present solar lighting systems to combine multiple beams collected by solar concentrators into a trunk beam or to split a trunk beam into multiple beams for distributive lighting. However, the structure of the Y-branch coupler intensively affects its optical performance, and thus many structures and the involved optical performance studies are proposed in the past years. But, most Y-branch structures only emphasize the optimized coupling angle between its two branches without concerning the influence of the obtuse angle at the joint of the branch and the trunk, and this leads to a limited optical performance.

In this paper, the duplex optical performances of various Y-branch structures, which are widely used in present solar lighting systems, will be investigated. Both optical efficiencies of beam combining and splitting for each structure will be compared. In addition, the output beam pattern distribution, which will influence the coupling efficiency into the other fiber, for each structure will also be investigated. To get better optical performance, two improved Y-branch structures are proposed further. The optical simulation results show that both optical efficiencies of beam combining and splitting with these two improved structures can achieve above 90%, while the optical efficiency of beam combining gets least 10% more efficiency than

that of the traditional structures. Furthermore, the output beam pattern distribution is also improved to have a smaller beam angle for efficiently coupling light beam into other fibers.

9272-35, Session Post

Design of blue LEDs arrays with high optical power

Pengzhi Lu, Hua Yang, Bin Xue, Huaiwen Zheng, Jing Li, Xiaoyan Yi, Junxi Wang, Guohong Wang, Institute of Semiconductors (China)

Technical progress in the field of blue light emitting diodes (LEDs) based on III-V compounds has been breathtaking during recent years around the world. With the rapid development of the device, high optical power is expected from blue LEDs in a wide range of applications such as optical-communications, medical optics and Biomedical optics. In this paper, an array of blue LEDs with high optical power is presented and discussed. Optical of the novel design is completed with the help of running simulation in TracePro to predict the performance of the module. Cree XP-E LEDs with a square reflector was used in the novel design. In addition, the length and depth of the reflector was 23.7mm and 20mm respectively. To verify the simulation results, Aluminum substrate, Copper substrate and Aluminum reflector have been made, respectively. Optical characteristics of the samples with different substrates were measured under the HAAS-2000 High Accuracy Array Spectrophotometer at room temperature. The relationship between input current (A) and optical power (mW) of the samples with Aluminum substrate and Copper substrate can be observed that the optical power of sample 2 was higher than that of sample 1 and it can be attributed to the better thermal dispersion performance of Copper. The optical power of sample 1 and sample 2 was 8126mW and 9445mW at 2A, respectively. The experiment result of sample 1 is consistent with previous simulation. Due to the better thermal characteristic of Copper substrate, the optical power of sample 2 is even higher than the simulated result.

9272-36, Session Post

Calculation of Mueller matrix for light scattering from randomly rough surface

Keding Yan, Shouyu Wang, Nanjing Univ. of Science and Technology (China); Shu Jiang, China Shipbuilding Industry Corp. (China); Liang Xue, Shanghai Univ. of Electric Power (China); Yuanyuan Song, China North Vehicle Research Institute (China); Zhengang Yan, Xi'an Modern Control Technology Research Institute (China); Zhenhua Li, Nanjing Univ. of Science and Technology (China)

Mueller matrix is a useful tool for analyzing polarization characteristics in a wealth of research fields. With Mueller matrix, the modulation effects of samples on polarization could be quantitatively analyzed and discussed. In this paper, all elements in the Mueller matrix are calculated when the lights scatter from one dimensional randomly rough surfaces at different conditions with Kirchhoff approximation method which owns high accuracy and fast calculation speed. Besides, theoretical analysis of the light scattering from randomly rough dielectrics and metal surfaces is also proposed in this paper. Moreover, with both theoretical analysis and numerical simulations, we have explained the variations of all elements in Mueller matrix, more importantly, m_{34} is highly focused which is quite a significant mark in both randomly rough dielectric and metal surfaces. To our best knowledge, it is the first time this obvious difference is both analyzed and discussed via both theoretical analysis and

numerical calculation, and is successfully explained via phase difference between incident and reflective waves. According to the analysis, more information of the target could be obtained in order to determine the characteristics of the target. The paper will be an important reference for polarization imaging in laser radar and remote sensing, etc.

9272-37, Session Post

First-order design for focal power compensation zoom system

Hengyu Li, Hongtao Cheng, Shanghai Univ. (China)

The traditional zoom system employs changing space between the each thin lens along the optical axis. However, for the inherent structure cannot change in the space between the each thin lens such as smart phone and pad optical system. This optical system is digital zoom. Zoom system which used a lens of tunable radius has been published and analyzed. Changing the radius of lens is promising in future. The liquid lens and electric wetting lens appeared. The merit is low complexity and cost, a possibility for miniaturization system, better robustness and faster adjustment in zoom systems. In the work, the principle of the variable focal power lens was analyzed. Optical zoom of compact optical system which change the lens of the radius be demonstrated. And focal power compensation zoom system character has been analyzed. We employ Gaussian optics and matrix optics to analysis a three-lens-group. The first-order design for focal power compensation zoom system design procedure was display. Meanwhile, we obtain the formula for designing this kind of zoom system. It is applied layout the optical system and design optimum for the focal power compensation zoom system.

9272-38, Session Post

Design and experimental demonstration of variable curvature mirror having a large saggitus variation

Xiaopeng Xie, Inner Mongolia Univ. (China); Hui Zhao, Xi'an Institute of Optics and Precision Mechanics (China); Guorui Ren, Xi'an Institute of Optics and Precision Mechanics (China); Jingxuan Wei, Xidian Univ. (China); Neimule Menke, Inner Mongolia Univ. (China)

Variable curvature mirror (VCM) is a simplified active optical component which can change its curvature radius as required. In order to change the curvature radius in a wide range, VCM should be capable of providing a large variation of saggitus. Besides that, the optical performance should be maintained above a reasonable level. Therefore, several problems should be solved. (1) how to obtain a large saggitus variation with less force? (2) how to distribute actuators to ensure satisfactory center deflection and optical performance at the same time. (3) how to compensate small variation of optical performance after the curvature radius has been properly changed. A prototype design of VCM is proposed in this manuscript. First, an annual ring is adhered to the back of the mirror. Second, the actuators are fixed into a solid plate and the head of actuators are connected to the annual ring. The force provided by actuators plays their effect on mirror in a uniform way through that ring. By making each actuator generate a same force, the curvature radius can be changed. Not only the analytical solutions have been derived, but also FEA(finite element analysis) is used to see if this prototype design could satisfy our requirements. According to theoretical computation and FEA results, the design is effective in achieving our requirements. Based on the design verification, the mirror and supporting structures have been fabricated and its extreme variation of curvature radius has been obtained through experimental test. The results complies with the design very well.

9272-39, Session Post

Design and simulation of flat-top microstructure fiber

Cheng Jing Wu, RongXia Liu, Xi'an Technological Univ. (China); Xu Yan, Changchun Institute of Optics, Fine Mechanics and Physics (China)

Purpose: In order to reduce the nonlinear effects in optical fiber effectively and make the energy output of the light beam much more uniformly, a flat-top beam-shaping device based on micro-structured optical fiber (MOF) has been designed in this paper. **Methods:** Output of flat-top fundamental mode is realized by introducing a low refractive index inner core in the refraction-guiding MOF. Based on this principle, output performance of the flat-top MOF is simulated and analyzed with the Rsoft. **Results:** The structure parameters of the flat-top MOF are obtained after optimization, and the diameter of the corresponding mode field is 10.37 μm , and the defect degree is 0.16%. **(Conclusions)** These results show that the flat-top fundamental mode with large mode area can be carried out in the designed MOF, and moreover, they also provide theoretical basis for the fabrication of the flat-top MOF.

9272-40, Session Post

Freeform lens design using a complementary optimization method for uniform illumination with extended LED light sources

Te-Yuan Wang, Jin-Jia Chen, National Changhua Univ. of Education (Taiwan); Kuang-Lung Huang, MingDao Univ. (Taiwan); Chuen-Ching Wang, Kao Yuan Univ. (Taiwan)

With the progress of LED technology, high power LEDs have gradually replaced traditional light sources and widely used in various indoor or outdoor lighting applications in recent years. Particularly, the large-sized integrated LEDs, for example, the chip-on-board (COB) LEDs, can obtain more luminous flux than previous LED devices to satisfy the mass requisition in future lighting applications. However, to achieve the purpose of uniform illumination, conventional point-source lens design method is inappropriate for an extended LED light source like the COB LED. Thus, to develop an effective lens design method is inevitable for applying extended LED sources to produce uniform illumination.

In this paper, we propose a simple and effective complementary optimization method to design a freeform lens for uniform illumination with extended LED sources. With this method, a primary freeform lens is first constructed based on a basic source-target energy mapping approach; then a complementary illuminance on the target plane is introduced to reform the profile of the primary freeform lens so that it can produce uniform illumination with an extended COB LED. The computer simulation results show that the illuminance uniformity of the optimized lens can be improved at least by 30% as compared with that of the primary lens; meanwhile, the optical efficiency achieves above 94% when a Cree XLamp source of 8.9-mm chip diameter is applied. To test the real effect of the proposed method, a practical measurement is also presented.

9272-42, Session Post

Study on features-based Autonomous navigation simulation optical system of Lunar Landing

Xiaoxiao Wei, Soochow Univ. (China) and Key Lab. of Advanced Optical Manufacturing Technologies of Jiangsu Province (China) and Key Lab. of Modern Optical Technologies of Education Ministry of China (China); Feng Xu, Soochow Univ. (China)

With the implementation of Mars exploration and re-entry Moon and such exploration missions, the spacecraft autonomous navigation technology based on surface features becomes a regarded key technology in the deep exploration fields. The technology is to determine the position and attitude of the spacecraft relative to lunar by imaging and matching the features of lunar surface which can ensure the pin-point landing precision. With the support of one Pre-Research Program, this paper studies the application and the basic problem involved in the spacecraft autonomous navigation. The main contents of this paper design a simulation optical system according to the working principle of features-based autonomous navigation, which is to simulate autonomous navigation real-time image located when landing of the spacecraft. The simulation optical system is composed of a dynamic target, a collimator and imaging sensor. The collimator is used to collect the dynamic target images in the process of decline, and the imaging sensor is used to obtain the dynamic images from the collimator which then feedback the image information to spacecraft. The navigation positioning parameters are obtained by image matching processing, and then the estimated errors are corrected to adjust Lander's location constantly to ensure the precision of Lander's orbit and attitude. Results show that the dynamic image optical system scheme is validated to real-time simulate the autonomous navigation landing.

9272-43, Session Post

Design of vari-focal panoramic annular lenses based on Alvarez surfaces

Yujie Luo, Jian Bai, Zhejiang Univ. (China)

We propose a novel design of vari-focal panoramic annular lenses (PAL) for the imaging of 360° surroundings with a large field of view (FOV) ranging from 35°-110° to 55°-100°, whose wavelength band is between 486 and 656 nanometers. The conventional vari-focal PAL is based on the axial shift of some optical components, which will make the blind zone larger and out of the sensing area, while our design is based on the lateral shift, which can diminish the FOV and restrict the area of blind zone to ensure the efficiency of sensor. In order to change the focal length of conventional PAL system, we introduce several pairs of free-form surfaces (Alvarez surfaces) which can be regarded as several plano-spherical lenses and change the focal power of the whole optical system, at the same time mathematically deduce the surface shape equation of them which is generalized by a cubic polynomial. As we set two different configurations (long focal length and wide angle), all of the optical parameters are designed and optimized with the help of the software (Zemax and ASAP), and the analysis of aberration, modulation transfer function and optical path difference is discussed as well.

9272-44, Session Post

Effect of environmental temperature on diffraction efficiency for multilayer diffractive optical elements in mid-wave infrared

Mingxu Piao, Qingfeng Cui, Hao Zhu, Bo Zhang,
Changchun Univ. of Science and Technology (China)

In this paper, the effect of environmental temperature change on multilayer diffractive optical elements (MLDOEs) is evaluated from the viewpoint of the diffraction efficiency and the polychromatic integral diffraction efficiency (PIDE). As environmental temperature changes, the microstructure heights of MLDOEs expand or contract, and refractive indices of substrate materials also change. Based on the changes in microstructure height and substrate material index with environmental temperature, the theoretical relation between diffraction efficiency of MLDOEs and environmental temperature is deduced. A practical 3-5 μ m Mid-wave infrared (MWIR) optical system designed with a MLDOE, which made of ZNSE and GE, is discussed to illustrate the influence of environmental temperature change. The result shows that diffraction efficiency reduction is no more than 85% and PIDE reduction is less than 50% when environmental temperature ranges from -20°C to 60°C. According to the calculated diffraction efficiency in different environmental temperatures, the MTF of hybrid optical system is modified and the modified MTF curve is compared with the original MTF curve. Although the hybrid optical system achieved passive athermalization in above environmental temperature range, the modified MTF curve also remarkably decline in environmental temperature extremes after the consideration of diffraction efficiency change of MLDOE. It is indicated that the image quality of hybrid optical system with ZNSE-GE MLDOE is significantly sensitive to environmental temperature change. The analysis result can be used for optical engineering design with MLDOEs in MWIR.

9272-45, Session Post

Correcting the wavefront aberration of membrane mirror based on liquid crystal spatial light modulator

Bin Yang, Yin Wei, Xinhua Chen, Minxue Tang, Soochow Univ. (China)

Membrane mirror is a new-concept ultra lightweight mirror for space applications. Compared with traditional mirrors, membrane mirror has the advantages of lightweight, folding and deployable, low cost and etc. Due to the surface shape of membrane mirror is easy to deviate from the design surface shape, it will bring wavefront aberration to the optical system. In order to solve this problem, a method of membrane mirror wavefront aberration correction based on the liquid crystal spatial light modulator (LCSLM) will be studied in this paper.

The principle of LCSLM is described and the property of the phase modulation is measured and analyzed firstly. Then the membrane mirror wavefront aberration correction system is designed and established according to the optical properties of a membrane mirror. The LCSLM and a Shack-Hartmann sensor are used as a wavefront corrector and a wavefront detector, respectively. The detected wavefront aberration is calculated and converted into voltage value on the LCSLM for aberration correction by programming in Matlab. When in experiment, the wavefront aberration of a glass plane mirror with a diameter of 100mm is measured and corrected for verifying the feasibility of the experiment system and the correctness of the program. The PV value and RMS value of distorted wavefront are reduced and near diffraction limited optical performance is achieved. On

this basis, the wavefront aberration of a membrane mirror with a diameter of 100mm is corrected and the errors are analyzed. It provides a means of correcting the wavefront aberration of membrane mirror.

9272-46, Session Post

A high-generating efficiency design for solar photothermal battery

Wei X. Guang, Beijing Univ. of Posts and Telecommunications (China)

We propose an improved design of the solar battery. Though solar battery has been widely used in various fields, its generating efficiency is still very low. The traditional solar battery generates power via the Photoelectric Effect. When the sun shines on the surface of solar battery, the solar battery converts the luminous energy to electric energy, whereas this process produces much heat wasted. Our device can convert luminous energy and heat energy to electric energy at the same time, so we name our device the Solar Photothermal Battery (SPB). SPB can utilize the heat to produce electricity because of the semiconductor thermoelectric materials (STM) that are adhered to the Thin Film Silicon Solar Cells (TFSSC). A small laboratory model is constructed and tested. The generating efficiency of SPB is increased by 2.6% comparing to the traditional solar battery under the equal condition. The SPB can be widely used as the roof and wall of the building to generate electricity for everyday electricity.

9272-47, Session Post

Distributed solar radiation fast dynamic measurement for PV cells

Yi Yang, Yan-zhong Yang, Donghua Univ. (China); Xi-dong Xie, Ministry of Education The People's Republic of China (China); Fang Han, Donghua Univ. (China); Xue-qin Jiang, Ministry of Education The People's Republic of China (China)

To evaluate operating characteristics of PV cells under fast dynamic irradiation relevant to stochastic moving of clouds, a solar radiation measuring array (SRMA) is introduced. The terminal nodes with low-cost fast-responded photodiode are placed in horizontal plane (x- and y- directions) to form cross topologies. This cross photodiodes structure tracks fast stochastic moving of clouds. A central node, with pyranometer, large active area photodiode and tested PV cell, is placed in the origin of the cross topologies coordinate to scale temporal envelope of solar irradiation. The terminal nodes and central node are connected by ZigBee. A tracking-quantizing algorithm developed for SRMA is proposed in this paper too. The specific designs about terminal nodes and central nodes are discussed in detail. This system is tested from May to August, 2013. The results show that SRMA could be a capable method for fast dynamic measuring about solar radiation and related PV cell operating characteristics.

9272-48, Session Post

Two-dimension lateral shearing interferometry for microscope objective wavefront metrology

Zhixiang Liu, Institute of Optics and Electronics (China) and Univ. of Electronic Science and Technology of China (China) and Univ. of Chinese Academy of Sciences (China); Tingwen Xing, Institute of Optics and Electronics (China); Yadong Jiang, Univ. of Electronic Science and Technology of China (China); Baobin Lv, Institute of Optics and Electronics (China) and Univ. of Electronic Science and Technology of China (China) and Univ. of Chinese Academy of Sciences (China); Fuchao Xu, Institute of Optics and Electronics (China)

Lateral shearing interferometry was an attractive technique to measure the wavefront aberration of high numerical aperture microscope objective lens due to its self-referencing interference, common-path interference, relaxed coherence requirements, and its suitability to high numerical apertures. By analyzing the diffraction efficiency of two type 2D gratings, the cross grating and the chessboard grating, a two dimension lateral shearing interferometer based on chessboard grating was designed for microscope objective wavefront metrology. By positioning the chessboard grating which was used as a beam splitter at the talbot distance of the objective focal plane, the wavefront after passing through the tested objective was divided and sheared in two dimension. Then the shearing interferogram, that is, Fourier image of the grating, was captured with the CCD. By applying two dimensional Fourier transform, a spatial frequency spectra of the interferogram was obtained. And then by setting a spectral band-pass filter at the +1 order part in the x direction and y direction respectively around the carrier-frequency domain, shifting the carrier-frequency spectra to the zero, executing inverse Fourier transform and unwrapping the phases, the orthogonal differential wavefronts of x direction and y direction was obtained. Zernike coefficients of the wavefront were obtained by fitting the differential Zernike polynomial to the differential wavefronts. A 10x, NA0.25 microscope objective was measured by using this lateral shearing interferometer at 632.8nm wavelength, the results showed that the wavefront of the objective was 0.755? PV, 0.172? RMS, the repeatability(3?) of RMS at random grating position was 2.3m?, the repeatability(3?) of Z5 to Z36 at random grating position was 17m?.

9272-49, Session Post

Enhancement of wireless ultraviolet communication system using FEC codes

Xiang Zhang, Yansong Zhang, Beijing Univ. of Posts and Telecommunications (China); Shuo Yang, Beijing University of Posts&Telecommunications, China (China); Feng Zhang, College of Information Engineering, North China Univ. of Technology, Beijing, China (China); Min Zhang, Qing Li, Beijing Univ. of Posts and Telecommunications (China)

We present theoretical and experimentally study on performance of typical FEC codes in wireless ultraviolet communication system.

A Monte Carlo based simulation platform with measured parameters is established to analyze performance of the FEC codes in UVC system precisely. And to test these typical FEC codes in UVC NLOS mode, elevation angle is set as set as

10°-10° and 20°-20°. In comparison with uncoded system, communication distance increases 33% with RS (31, 25), 67% with RS (15, 9), 83% with LDPC (960, 800) and 144% with LDPC (960, 480) code in the situation of 10°-10°, similarly, in the situation of 20°-20°, communication distance increases 33% with RS (31, 25), 58% with RS (15, 9), 100% with LDPC (960, 800) and 175% with LDPC (960, 480) code.

To verify the results of simulation, we implement RS (18, 10) and LDPC (960, 480) code in our UVC test-bed. Based on 10-6 BER and repeated test, in comparison with uncoded system, average communication distance increase 42% with RS code, while 94% with LDPC code in the situation of 10°-10° and increase 41% with RS code, while 116% with LDPC code in the situation of 20°-20°.

The simulation and experiment results show that UVC system with FEC code outperforms uncoded system, meanwhile, at the similar code rate, LDPC code and concatenated code can extend larger communication distance at the same BER with respect to RS code. We can also find that FEC codes are more effective in the higher elevation angles of NLOS mode.

9272-50, Session Post

Distortion control for panoramic annular lens with Q-type aspheres

Xiangdong Zhou, Jian Bai, Zhejiang Univ. (China)

As in fisheye lens, panoramic annular lens (PAL) has a big barrel distortion due to its large field of view. That has an apparent effect to its imaging performance such as pixel utilization and image resolution. If we manage to control the barrel distortion instead of only increasing it, the resulting system can gain better performance. In this paper we propose a method to control distortion that using Q-type aspheres. First, the Q-type aspherical polynomials and its advantages are introduced in the aspect of algorithm and fabrication relative to the traditional symmetrical polynomial-based aspheres. Then, an example design of PAL with Q-type aspheres using ZEMAX optical design package is presented. The designed PAL's focal length is -1.25 mm, F Number is about 5, distortion in all the fields of view are less than 1% under the f-? distortion formation. The imaging quality of the optical system approached to diffraction limit. The result shows that Q-type aspheres has certain advantage in distortion control for PAL that can enhance imaging performance.

9272-51, Session Post

The experiment to detect equivalent optical path difference in independent double aperture Interference light path based on step scanning method

Chaoyan Wang, Xin-Yang Chen, Lixin Zheng, Yuanyuan Ding, Shanghai Astronomical Observatory (China)

Fringe test is the method which can detect the relative optical path difference in optical synthetic aperture telescope array. To get to the interference fringes, the two beams of light in the meeting point must be within the coherence length. Step scanning method is within its coherence length, selecting a specific step, changing one-way's optical path of both by changing position of micro displacement actuator. At the same time, every fringe pattern can be recorded. The process of fringe patterns is from appearing to clear to disappearing. Firstly, a particular pixel is selected. Then, we keep track of the intensity of every picture in the same position. From the intensity change, the best position of relative optical path difference can be made sure. The best position of relative optical path difference is also the position of the clearest fringe. The wavelength of the infrared source is 1290 and the bandwidth is 63.6nm. In this experiment,

the coherence length of infrared source is detected by cube reflection experiment. The coherence length is 30 μ m by data collection and data processing, and that result of 30 μ m is less different from the 26 μ m of theoretical calculated. In order to further test the relative optical path of optical synthetic aperture using step scanning method, the infrared source is placed into optical route of optical synthesis aperture telescope double aperture. The precision position of actuator can be obtained when the fringe is the clearest. By the experiment, we found that the actuating step affects the degree of precision of equivalent optical path. The smaller step size, the more accurate position. But the smaller the step length, means that more steps within the coherence length measurement and the longer time.

9272-52, Session Post

Quasi-retroreflection of corner-cube with freeform surface

Shin Woong Park, Eunyoung Moon, Yohan Park, Yun Yi, Korea Univ. (Korea, Republic of); Joon-Yong Lee, Jinwoo Kim, MNTech Co., Ltd. (Korea, Republic of); Hwi Kim, Korea Univ. (Korea, Republic of)

Quasi-retroreflection of corner-cube sheets due to statistical position imperfection of the apex point is analyzed. It is assumed that the positional deviation from the ideal apex point follows the Gaussian statistics. It is shown that the obtained quasi-retroreflection distribution patterns are highly related to the statistical parameters of the fabrication tolerances and the controllability of the divergence angle of the quasi-retroreflection is manifested.

9272-53, Session Post

Wavefront reconstruction for image restoration based on generalized ridge estimation

Yang Yang, Information Engineering Univ. (China); Bo Chen, Peking Univ. (China)

In order to enhance the performance of adaptive optics image restoration, a novel wavefront reconstruction algorithm was presented that was based on generalized ridge estimation. In the view of adaptive optics image post-processed restoration, real time and fast computation are not the basic request of wavefront reconstruction, but the high-precision. On the consideration of sacrifice time for precision, it brought the idea of generalized ridge estimation (GRE) into wavefront-reconstruction algorithm, to improve the singularity of least square (LS) and restrain the enlarger of wavefront measure-error. Then, the iterative solution method was brought into wavefront-reconstruction for improving the solution of singular equation and the precision of reconstructed-PSF (point spread function). Finally, the blurred-image restoration experiment was implemented to verify the precision of reconstructed-PSF. The experiment proved that the novel algorithm which restored PSF had performed well in image restoration, and the image restoration effect of GRE-Reconstructed-PSF was 15% better than those of LS-Reconstructed-PSF.

9272-55, Session Post

Aberration resilience of azimuthally-polarized beam with a helical phase mask

Bosanta R. Boruah, Md. Gaffar, Indian Institute of Technology Guwahati (India)

An azimuthally polarized beam when passes through a helical phase mask, gives rise to a circularly symmetric focal spot which appear very similar to the focal spot of a normal linearly polarized beam with a plane wavefront. However it is noticed that common monochromatic aberrations have different degree of influences on the two types of beams, that is the azimuthally polarized beam with a helical phase mask and the linearly polarized beam with a plane wavefront. In this paper we present a detailed investigation on the effect of primary aberrations on the two types of beams. We have observed during our investigation that the azimuthally polarized beam with a helical phase mask exhibit significantly higher resilience to certain types of aberrations relative to the resilience of the normal beam. We employ vectorial diffraction theory to compute focal field components in the presence of aberrations for both the beams under both low numerical aperture and high numerical aperture conditions. In this paper we will present some of the important results to demonstrate reduced degradation of the focal volume of an azimuthally polarized beam with a helical phase mask even as certain types of aberrations are incorporated.

9272-56, Session Post

The design of an ultra-thin and multiple channels optical receiving antenna system with freeform lenses

Lingyun Zhang, Dewen Cheng, Yuan Hu, Weitao Song, Yongtian Wang, Beijing Institute of Technology (China)

Visible Light Communications (VLC) has becoming an emerging area of research since it can provide higher data transmission speed and wider bandwidth. The white LEDs are very important components of the VLC system, because it has the advantages of higher brightness, lower power consumption, and a longer lifetime, more importantly, their intensity and color are modulatable. Besides the light source, the optical antenna system also plays a very important role in the VLC system since it determines the optical gain, effective working area and transmission rate of the VLC system. In this paper, we propose to design an ultra-thin and multiple channels optical antenna system by tiling multiple off-axis lenses, each lens consists of two reflective and two refractive freeform surfaces. The tiling of multiple systems and detectors but with different band filters makes it possible to design a wavelength division multiplexing VLC system to highly improve the system capacity. The field of view of the designed antenna system is 30°, the entrance pupil diameter is 1.5mm, and the thickness of the system is under 4mm. The design methods are presented and the results are discussed in the last section of this paper. Besides the optical gain is analyzed and calculated. The antenna system can be tiled up to four channels but without the increase of thickness.

9272-57, Session Post

Angular-momentum-dependent splitting of light through the metal nanohole

Dejiao Hu, Huang Li, Yu Liu, Zhiyou Zhang, Jinglei Du, Sichuan Univ. (China)

A light beam with orbital angular momentum (OAM) has

a spiral phase distribution, its electric field distribution in the plane perpendicular to the propagating direction is $E(r, \varphi) = E_0 \exp(iL\varphi)$, where L is the topological charge which denotes the orbital angular momentum. Another component of angular momentum of spin angular momentum (SAM) associated with the handedness of the circular polarization. When these light beams carrying with total angular momentum L_t (including orbital angular momentum L_o and spin angular momentum L_s) passes through the metal nanohole, there exhibits an AM selection rule for the conservation of angular momentum in the interaction of light and plasmon structure, which leads to the splitting of polarization states in the far field. Our experiment to demonstrate this phenomenon is carrying out as follows: First, the metal nano-holes are obtained by employing the self-assembly of sparse polystyrene spheres and evaporation deposition; Then the beam carrying with OAM is obtained from a spatial light modulator (SLM) of liquid crystal; lastly, a high sensitivity CCD camera is used to detect light distribution in the far field.

9272-58, Session Post

Generation of radially- and azimuthally-polarized beams with an inner wall waveguide fiber

Yujing Zhao, Zhihai Liu, Harbin Engineering Univ. (China)

Beams with radial polarization have attracted immense attention. In this paper, a novel method for generating cylindrical vector beams with radial and azimuthal polarization is presented. We use the inner wall waveguide fiber which is a hollow annular symmetry waveguide with air layer, core layer, cladding layer.

We plate on its inner wall surface with suitable thickness (~10nm) and length (~10mm) silver film. The incident light will be polarized in the film area. There is an edge wave in the interface of metal-medium surface which characterizes as non-radiation surface-plasma waves. Only TM wave can satisfy the boundary conditions and propagate along the interface. Light in the TM polarization propagating in the optical fiber is converted into a surface-plasma wave, propagates through the coated region, and then is converted back into TM polarization wave in the fiber. TE mode will be loss in the coating area. Therefore, the coated area has a polarizing effect, and achieve polarization-selective. The generation of cylindrical vector beam is successful. Radial polarized beam is converted into azimuthally polarized beam after 90 degrees rotated. We combine the two half-wave plates (HWP). The optical axis of the first HWP is oriented at 45 deg while the optical axis of the second HWP is oriented in the horizontal direction.

The experiments results demonstrate that the output optical field distribution is cylindrical vector beams in far field.

9272-59, Session Post

Lens design based on lens form parameters using Gaussian brackets

Xiangyu Yuan, Xuemin Cheng, Graduate School at Shenzhen, Tsinghua Univ. (China)

A Gaussian bracket is defined by a recurrent expression, which can be processed conveniently and efficiently by computer programming. Generalized Gaussian Constants (GGC's) can be written with Gaussian brackets and their elements consist of a set of constituent parameters of an optical system. Applying the GGC's in the paraxial theory, ray propagation in an optical system can be simplified to matrix computation easily. Hence, using Gaussian brackets to analyze an optical system is a more efficient method.

The optical power distribution and the symmetry of the lens components are two important attributes that decide the ultimate lens performance and characteristics. Lens form parameters parameters W and S are the key criteria describing the two attributes mentioned above. Lens components with smaller W and S will have a good nature of aberration balance and perform well in providing good image quality.

Applying the Gaussian brackets, we reconstructed the two lens form parameters and the Seidel Aberration Coefficients. An initial lens structure can be analytically designed by simultaneous equations of Seidel Aberration Coefficients and third-order aberration theory. Adding the constraints of parameters W and S in the solving process, we can receive a solution with a proper image quality and aberration distribution. The optical properties and image quality of the system based on the parameters W and S are also analyzed in this article. In the method, the aberration distribution can be controlled to some extent in the beginning of design, so that we can reduce some workload of optimization later.

9272-60, Session Post

Preparation of metal nanoparticles with the help of polystyrene-spheres and vapor deposition

Shiwei Xie, Yidong Hou, Liangke Ren, Zhiyou Zhang, Fuhua Gao, Jinglei Du, Sichuan Univ. (China)

As we all best know, a number of theories and conjectures about microscopic world in atomic scale or nanometer are put forward after that modern molecular and atomic were recognized as fundamental components of matter for over one hundred years ago, except for ancient philosophy. Nanoscale science and technology have been penetrated deeply in many areas, such as metamaterials, biomedicines, optical communications, military weapons, even cosmetics and building materials, etc. In these realm, various nanostructures were manufactured, and there is a case that plasmon resonance enhanced optical absorption by metal nanostructure have been used in optoelectronic devices to improve their effect, for example, the photoelectric conversion efficiency of solar cells and performance of nanolasers.

In this work, a periodic planar structure of metal nanoparticles is designed and fabricated, in which the dimension of these particles is about 80nm. With the techniques of self-assembly of polystyrene spheres and vapor deposition of metal, the nanoparticles are made successfully after removal of the polystyrene spheres using PDMS and its electronic field of transmission with linearly polarized light incidence is simulated.

9272-61, Session Post

Polarization state control using metal nanograting

Yang Yue, Dejiao Hu, Zhiyou Zhang, Jinglei Du, Sichuan Univ. (China)

Polarizer has a very broad application both in many advanced areas, but we usually need a quarter-wave plate and an ordinary polarizer to generate polarized light, and getting different polarization state requires different devices. However, changing polarization state directly and conveniently is needed in a lot of advanced techniques. We fabricate a metallic nanograting (MNG) which can produce angle-free elliptically polarized light via rolling the direction of grating. The MNG is fabricated by means of two-time-evaporation coating on a quartz grating with metal, and the grating is made by interference lithography and reactive ion etching (RIE). We find interesting phenomena in our experiment. When incident light polarizes is perpendicular to the gratings, no

polarization state changes within both reflected and transmitted beam, and transmission energy acquires its maximum. However, when polarization direction of incident light is parallel to the gratings, almost all energy is reflected and the reflected light's polarization remains same with incident beam. What's more, if the angle between polarization direction and gratings is θ , transmitted light is linear polarized and polarization direction is perpendicular to the gratings' direction, while reflected light is ellipsoidal polarized and becomes circular polarized when θ is a particular value. In this article, we explore operating principle of the MNG and optimize the structure of it.

9272-62, Session Post

A microspectrometer based on subwavelength metal nanohole array

Jun Cui, Wuhan Univ. (China) and Chongqing Institute of Green and Intelligent Technology (China); Liangping Xia, Zheng Yang, Chongqing Institute of Green and Intelligent Technology (China); Guoxing Zheng, Wuhan Univ. (China); Shaoyun Yin, Chunlei Du, Chongqing Institute of Green and Intelligent Technology (China)

As the measuring instrument of the spectrum, spectrometer has been widely used in metallurgy, geology, petroleum chemical industry and other fields. For the purpose of adapting to the global situation, miniature spectrometer is increasingly becoming researchers' focus recently. Previous studies have shown the optical property of extraordinary transmission through metal subwavelength structure which opens another idea for the development of miniature spectrometer. In this letter, we innovatively present a spectrometer structure based on surface plasmon resonance combining an efficient spectral recovery algorithm. With carefully design, a distinctive transmittance peak with small FWHM (Full Wave at Half Maximum) is shown in the transmittance spectra of a subwavelength metal nanohole array which is acted as a filtering unit in our design. A series of the above filtering units are orderly arranged in a filter structure integrated in a microchip. A supporting spectral recovery algorithm named sparse algorithm is also presented in our design. Different from traditional recovery algorithm, the sparse algorithm can realize the spectral recovery breaking out of the limit of the filtering units' number which means that the resolution of the spectrometer structure we presented can be greatly increased. Demonstrated having the capability of high resolution, the proposed spectrometer structure with thin film feature is expected to find its application in integrated optical systems with light weight.

9272-63, Session Post

A method to calibrate pupil-fill against telecentricity

Dawei Rui, Wei Zhang, Wei Huang, Weicai Xu, Changchun Institute of Optics, Fine Mechanics and Physics (China)

For calibrating the pupil-fill of microlithographic lens, we wrote a program that combine Monte Carlo ray tracing data with sequential calculations, and implemented the code within Matlab. Code V macros are attached to a Matlab external procedure, and a component object model interface is used to connect the Code V with Matlab. The program was demonstrated to be functional and efficient in calibrating and calculating the pupil-fill through a simulation with an optimized immersion lithographic lens. The technique has benefits for not only prediction veracity during simulations, but also performance measurements during system tests.

9272-64, Session Post

Measurement of optical surfaces with a large radius of curvature and small aperture by optical profiler

Shuang Ma, Shengzhen Yi, Shenghao Chen, Zhanshan Wang, Tongji Univ. (China)

Kirkpatrick-Baez microscope is one of key diagnostic tools for researches on inertial confinement fusion. In a Kirkpatrick-Baez microscope, two orthogonal concave mirrors with a large radius of curvature and small aperture working at grazing incidence produce the image of an object by collecting X-rays in each orthogonal direction independently. Accurate measurement of optical surfaces with a large radius of curvature used in the Kirkpatrick-Baez microscope is very important to achieve its design optical properties including imaging quality, optical throughput and energy resolution. There is a severe problem in measuring an optical surface with a large radius of curvature and small aperture. The produced reflective intensity is too low to correctly test. In this paper, the modified method to measure optical surfaces with large radius of curvature and small aperture by optical profiler is presented because its measured area is close to the mirrors' aperture. Firstly, we use a standard plane surface to calibrate the reference lens before each experiment. Following, deviation of central position is corrected by the theory of Newtonian rings, and the position of zero-order fringes is derived from the principle of interference in which surface roughness has minimum values in the position of zero light path difference. The measurement results show the low relative errors and high repeatability. Eventually, the imaging experiments of Kirkpatrick-Baez microscope demonstrate that the measured results of optical surfaces with large radius of curvature and small aperture are in agreement with the design value.

9272-65, Session Post

Design of hard x-ray focusing telescope with a large field-of-view

Shenghao Chen, Baozhong Mu, Tongji Univ. (China); Shuang Ma, Tongji University (China); Zhanshan Wang, Tongji Univ. (China)

X-ray Timing and Polarization (XTP) satellite with focusing optics and advanced detectors will study Black Hole, Neutron Star, Quark Star and the physics under extreme gravity, density and magnetism. XTP is about to make the most sensitive temporal and polarization observations with good energy resolution in 1-30 keV. We present the design of XTP Telescope with a larger field of view in this paper. The initial structure design of nested conical Wolter-I telescope in X-rays is determined with the focal length $F=4.5\text{m}$, mirror length $L=100\text{mm}$, thickness $t=0.3\text{mm}$, inner and outer diameter $D_{in-out}=110-450\text{mm}$. The structural parameters are optimized by maximizing center geometrical collecting area with a self-complied Matlab software. A constant deviation gap between every two mirrors is introduced and we calculate geometrical area between on-axis and off-axis. Balancing the performance of the telescope, the final gap value is 0.06 mm. The geometrical collecting areas of on-axis decreased by 5%, the average geometrical area of off-axis is increased about 1.7% and the field of view is improved from 22° to 24° , however number of mirrors and total weight of mirrors also are decreased by 5.8%, 5.3% respectively.

9272-66, Session Post

Enhancement of light absorption in organic solar cells by using plasmonic gratings

Xiao Xiao, Zhiyou Zhang, Shiwei Xie, Yu Liu, Jinglei Du, Sichuan Univ. (China)

In recent years, organic solar cells (OSCs) have drawn intense attention due to their competitive advantages, including light weight, flexibility, etc. But the relatively low power conversion efficiency (PCE) is the main obstacle in the way of OSCs commercialization. One of main reasons that limit PCE is the mismatch between electrical transmission properties and light absorption properties in organic active layer, because organic semiconductors have inferior carrier mobility and their exciton diffusion lengths (<10nm) are far shorter than optical absorption lengths (~100nm). And fortunately, some light management technologies including surface plasmon resonance (SPR), diffraction grating, and photonic crystal have been investigated to resolve this dilemma, which could enhance light absorption in the organic active layer without increasing the active layer thickness. Among these approaches, plasmonic resonator architecture attracts many attentions of researchers because the resonance width of SPR overlaps the absorption region of organic active material, and the field decay length of SP in typical organic material coincides with the thickness of organic layer.

In this work, we numerically investigate the light absorption enhancement of OSCs by embedding metallic gratings as electrodes, including the anode and cathode. The absorption enhancement mechanism is analyzed in detail, and the effects of grating width, grating period, grating height, and incident angle are also investigated systematically. The results show the SPR of metallic gratings has an obvious improvement for light harvesting in active layer, and an enhancement factor about 100% is observed. In addition, the grating parameters (width, period, height) have a significant influence on light absorption. More details could be found in full paper.

9272-67, Session Post

Simulation modeling and analysis of segmented telescope

Zhou Liao, Institute of Optics and Electronics (China); Qi Qiu, Univ. of Electronic Science and Technology of China (China); Yudong Zhang, Institute of Optics and Electronics (China)

The Segmented Primary Mirror is the most effective way to build a giant telescope. In order to have a better understanding of the optical properties of Segmented Telescope System, Simulation modeling is necessary. the model can be built use diffraction optics or geometry optics with ray tracing. The analytical expression of the Point Spread Function (PSF) would be derived with diffraction optics. Use the model with geometry optics, can get the wavefront aberration, far-field image, Strehl ratio and Modulation Transfer Function(MTF) etc.. when analyze the impacts of various errors induced by Single Segmented Mirror of primary mirror, because the effect of the second mirror, The model with diffraction optics only could simulation the segmented primary mirror optical system. And the model with geometry optics can simulation the Segmented telescope optical system. To effective analysis the optical properties of Segmented Telescope System, it is necessary to build the model with the diffraction optics and geometry optics with ray tracing.

9272-68, Session Post

Optical design of solar-blind UV optical system for missile approach warning

Yu Chen, Changchun Univ. of Science and Technology (China)

UV warning technology is playing a very important roll in the field of military application. Based on the optimal working waveband of solar-blind UV optical system from 240nm to 280nm, an optical system is designed for missile approach warning. To enhance the received light energy, expand the detection range and simplify the system structure, aspheric surfaces and binary elements are adopted in the system. Only five elements are used to realize the focal length 50mm and field of view (FOV) 43 degrees. iKon-L 936 from ANDOR company is selected as the UV detector, which has pixel size 13.5 μ m x 13.5 μ m and active image area 27.6mm x 27.6 mm. The optional materials are very few for UV optical systems to choose from, in which only CaF₂ and JGS1 are commonly used. However, they have similar refractive indexes and Abbe numbers, which determines chromatic aberrations are not easy to be corrected. A binary surface is set at the 4th surface to help to correct the aberrations. Because this is an energy system instead of an imaging system, spot diagram, diffraction encircled energy and point spread function (PSF) are adopted as the evaluation criterion of image quality. During aberration correction, the most sensitive surfaces for spherical aberration can be set as aspheric surfaces. In this paper, the 9th and the 10th surfaces are adopted as aspheric surfaces according to multiple attempts. After optimization, the maximum RMS radius is only about 11 microns, which is much less than pixel size of the detector and 85% of the light energy from each FOV is converged within the circle of radius 6.75 microns. The image quality shows the designed system can meet the working requirements of solar-blind UV optical system. If the focal length can be decreased, the FOV of the system can be enlarged further.

9272-69, Session Post

Fabrication technology of aberration-free microlens arrays

Weiguo Zhang, Xiuhui Sun, Shaoyun Yin, Haofei Shi, Chunlei Du, Chongqing Institute of Green and Intelligent Technology (China)

Microlens arrays are the core elements of optical systems such as the laser medical equipment, semiconductor laser homogenization systems and so on. Due to the small size of the single lens in microlens arrays, it is difficult to precisely control the spherical aberration, and the spherical aberration seriously affects the quality of the microlens array imaging facula, which in turn limits in the improvement of the performance of the optical system. This article systematic studied the causes of spherical aberration of microlens arrays, and presented the photoresist absorption effect correction method, then combining with the mask-moving photolithography technology, we developed a microlens arrays fabrication technology which can eliminates the spherical aberration. Finally we used the aberration-free microlens arrays in homogenization optics system, and significantly improved the emergent spot quality of the existing optical system.

9272-70, Session Post

A high-efficiency LED portable desk lamp based on V-groove cells LGP

Shin-Hong Kuo, Chi-Feng Chen, National Central University (Taiwan)

The intensity distribution of a conventional dot pattern light guide plate (LGP) has the maximum intensity distribution at around 40-60 degrees due to light delivery. To increase the proportion of luminance in effective utilization area, diffusion sheet and brightness enhancement film have to be disposed on the light exit surface of LGP with maximum intensity distribution of light being concentrated to 0 degree. But the utilization of sheet will increase the loss of material absorption. There is about 35% of loss of total light energy and the manufacturing cost is increased as 2 BEFs and 2 diffusion sheets are added.

The research studies a new LED portable desk lamp with V-groove cells LGP. Parameters of V-groove microstructure are classified and analyzed. Influential relationship of parameters with respect to intensity distributions is provided. Also the concept of V-groove cells is provided. We utilize the density property to design microstructure by grouping 2 to 5 as one microstructure cell according to required microstructure density, such that if the light transmitted in LGP enters the V-groove cells, the impact of specific density on light will be enhanced. Therefore, the density property is utilized effectively to control distribution of intensity distributions. Moreover, we apply the microstructure design to a desk lamp. Under the condition of the similar illuminance of target area, compared with a commercially available desk lamp: the efficiency is increased by 1.2 times, the energy consumption is reduced by 1.3 times. Obviously, such unit composed of multiple V-groove microstructures may implement LGP design goal of various intensity distribution distributions, and applied to LED table lamps.

9272-71, Session Post

The deflection effect of starlight transmission in hypersonic conditions

Jing Hu, Beihang University (China); Bo Yang, Beihang Univ. (China)

When starlight navigation method is applied in the hypersonic vehicle, the complex turbulence generated around the window of star sensor causes starlight deflection, thus lead to the centroid offset of navigation star in the star-map imaging. Starting from characteristics of the flow field, the deflection effect of starlight transmission is researched to solve. At first, based on Reynolds average, the model of flow around the window was established to obtain the density distribution that can be divided into mean-time and fluctuation flow field to analysis the whole field. On this basis, the starlight is traced by using the Runge-Kutta method, while taking the principle of refraction, the evaluation index for starlight deflection is derived to characterize the deflection effect of the field. Finally, through comparative analysis to verify the applicability of the evaluation index and also study the impact on deflection effect with the follow situations: different installation locations of star sensor, different angles of incident ray, different Mach numbers and wavelenghts of starlight. The study provides the predictive information for centroid offset of navigation star in star-map pre processing to improve the efficiency of star-map matching, also provides the best choice for the work of the star sensor.

9272-72, Session Post

Analysis of error propagation in an improved zonal phase-gradient model

Bosanta R. Boruah, Biswajit Pathak, Indian Institute of Technology Guwahati (India)

Wavefront sensing and reconstruction is an important branch of optics which finds application in several areas viz. adaptive optics, phase imaging, visual optics and so on. Wavefront sensing primarily involves collection of data about the wavefront in the form of gradients in a standard Hartmann-Shack (H-S) type sensor. Wavefront reconstruction is then employed to mathematically reconstruct the wavefront from the gradient values obtained in the wavefront sensing technique. Methods for recovering wavefront phase from measurements of wavefront slope fall into two general categories: zonal and modal. In zonal wavefront reconstruction technique, slope measurement is converted into wavefront phases. The error propagation coefficient in wavefront reconstruction may be defined as the ratio of mean-square phase errors to the variance of the phase difference measurements. It is categorized into two types: wavefront difference-based (WFDB) and slope-based (SB), depending on the wavefront measurement error and wavefront slope error respectively. Owing to its superiority over other geometries in error propagation, Southwell geometry is adopted which is characterized by taking the wavefront slope measurements and wavefront estimation values at the same nodes. Recently, we showed that the Southwell estimation scheme can be further improved by blending more number of adjacent slopes and phase values. In this paper, we have attempted to analyze the error propagation in both the Southwell and improved model. The accuracy of the proposed slope geometry is elucidated based on preliminary experimental results by calculating WFDB error propagation coefficient with the least squares solution technique and is found to offer a non-negligible reduction of error propagation.

9272-73, Session Post

A novel solution for LED wall lamp design and simulation

Rui Ge, Pengxiang Liang, Weibin Hong, Kuangqi Li, Fuli Zhao, Sun Yat-Sen Univ. (China)

The model of the wall washer lamp and the practical illumination application has been established with a new design of the lens to meet the uniform illumination demand for wall washer lamp based on the Lambertian light sources. Our secondary optical design of freeform surface lens to LED wash wall lamp is based on the conservation law of energy and Snell's law can improve the lighting effects as a uniform illumination. With the relationship between the surface of the lens and the surface of the target, a great number of discrete points of the freeform profile curve were obtained through the iterative method. After importing the data into our modeling program, the optical entity was obtained. Finally, to verify the feasibility of the algorithm, the model was simulated by specialized software, with both the LED Lambertian point source and LED panel source model.

9272-74, Session Post

Smart structures on multiple configuration systems in image sensor

Hua Liu, Quanxin Ding, Luoyang Institute of Electro-Optical Equipment (China)

General contact between all kinds of image sensors has

been noticed. Inspired in order to reveal the structure of molecules in living cells scale and dynamic characteristics, to improve imaging resolution, further technical requirement is proposed in some areas of the function and influence on the development of multiple sensors. Based on the comprehensive fundamental theories to close to the diffraction limit, and so that to breakthrough diffraction limit, some correlative methods is studied, the core technology of such a system are thoroughly analyzed. Based on the theory of Gaussian optical system error distribution and comprehensive balancing algorithm; Sensor for optical systems, the results show that the solution to a wide spectrum, more field, low distortion and MTF matching problem is effective. Quality criterion, such as system Modulation Transfer Function (Modulation Transfer Function, the MTF), Energy concentration (Radial Energy Analysis, REA), diffusion (Spot Diagram, RMS) and so on are significant advantage. Methodology can change traditional design concept and to develop the application space.

9272-18, Session 5

The effect of higher-order aberrations on a radially-polarized beam (*Invited Paper*)

Bosanta R. Boruah, Md. Gaffar, Indian Institute of Technology Guwahati (India)

Radially polarized beams have cylindrically symmetric polarization profile. When focused tightly such beam gives rise to a strong axially polarized electric field component at the focus. Owing to this unique property, radially polarized beams have found applications in a number of important areas. There has been published research work on the properties of the radially polarized beam in the presence of primary monochromatic aberrations. However optical system involving such beam may also contain second order aberrations. Unfortunately there has not been any such study in the available literature. In this work we will employ vectorial diffraction theory to investigate the effect of the focal field components due to the presence of second order aberrations. We will employ FFT form of the vectorial diffraction theory to simulate various focal volume properties in the presence Zernike circular polynomials representing second order aberrations. We will also present a comparative study between the effects of primary and corresponding secondary aberrations on radially polarized beams.

9272-19, Session 5

Nanofabrication with sub-50nm features by imprinting-induced cracks

Liangping Xia, Chongqing Institute of Green and Intelligent Technology (China); Man Zhang, Institute of Optics and Electronics (China); Zheng Yang, Shaoyun Yin, Chunlei Du, Chongqing Institute of Green and Intelligent Technology (China)

Nanofabrication is the foundation in nanoscience and is a research hotspot in the last decades. A lot of nanofabrication techniques have been developed, such as photolithography, imprinting, and self-assembles. However, the fabrication of structures with sub-50nm features is not easy, high cost and low efficiency. Crack is a natural phenomenon and happened when objects shrinking, such as the land crack when drying and glass crack when quenching. In substrate/thin film systems, the crack is also exist, such an adverse effect has been tamed to produce crack channels having width as narrow as 10nm. But the crack pattern is randomly distributed without control. If the crack can be induced to form controlled pattern, it will be a potential way to fabricate nanostructures. Based on this, a cheap and easy

way to fabricate nanostructures is proposed in this work, which is the imprinting-induced nanocracks in ultraviolet (UV) curable resist layers. In this process, nanostructures are obtained by the crack of UV-curable resist due to volume shrink when solidifying, and the crack pattern is induced by imprinting. The process is theoretically analyzed and experimentally demonstrated. By finite element method simulation, the theory and parameter influence is discussed with different imprinting templates. The experimental results show that a nanochannel pattern with the width of 30nm is obtained on a UV curable resist by imprinting-induced crack.

9272-20, Session 5

A simple method generating first-order optical structure based on particle swarm algorithm

Qiang Song, Qiang Song, Jing Zhu, Xi Bao Yang, Rui Wei Yue, Shanghai Institute of Optics and Fine Mechanics (China)

Optical design is vital for advanced optical system such as hyper numerical lithography system and microscopic imaging system. The quality of optical design have the direct bearing on imaging. To date, there are various of optical structure, but there is no a simple and general approach for generating first order optical structure once the optical requirement known. In this paper, we present a general design method of generating first optical structure constrained by the control points in the Delano diagram. The Delano diagram is first presented by Delano in 1963, and he had proposed an excellent tool to calculate the first-order quantity of the optical system. According to his theory, only if the Lagrange invariant is known by designer, then all the first order quantity can all be calculated. However, he can only just calculate some simple structure. when the number of optical component is more than 3, the calculation become hard. To address this issue, we proposed a modified Delano diagram method .by constraining control points in Delano diagram with particle swarm algorithm. The modified theory is deduced by us. For simplifying the process of optical design, we also developed a GUI interface based on MFC . So the user can type the optical parameter , then the first optical structure can be generated once one type the confirm button. In the end , a specify usage is shown for verifying our software.This work can be used in symmetry optical system with the finite focal length.

9272-21, Session 5

MTF curve integral calculation method and its application in image quality evaluation

Xiao Zexin, Guilin Univ. of Electronic Technology (China); Huang Yin, Guilin Univ. of Electronic Technology (China); Shuping Ma, Guilin Univ. of Technology (China)

The optical transfer function (MTF) has been widely used in the design and manufacture of optical system. The area under the MTF curve can show image quality of the optical system directly. However, for a long time, as the evaluation index remained at the qualitative level, it has little value in practice. When the author started the research of MTF curve integral calculation method, no related literatures were available.

With the aid of the OSLO optical design software, optimized optical system structure and corresponding MTF curve discrete data are obtained by means of iterative optimization with the software. Then, the original MTF curve data are fit and interpolated by MATLAB and the integral result of the curve is calculated through the relevant numerical method. With the software programmed by the authors, the subjects planned to be evaluated can be ranked in order of image quality automatically.

This method can be used as a criterion for evaluating image quality. Application cases show that the evaluation methodology proposed by author is prompt, reliable and can be easily operated. This method is supposed to bring about a new way to evaluate the image quality of optical system with the MTF curve.

9272-22, Session 5

The investigation of large field-of-view eyepiece with multiLayer diffractive optical element

Chang-jiang Fan, Zhejiang Normal Univ. (China)

In this paper, a light-small hybrid refractive/ diffractive eyepiece for HMD is designed, which introduces a multilayer Diffractive Optical Element for the first time. This eyepiece optical system has a 22mm eye relief and 8mm exit pupil with 60° FOV. The three-layer DOE overcomes the difficulties of single-layer DOE and double-layer DOE using in the optical system, and improve the image contrast and the performance significantly due to the diffraction efficiency of the three-layer DOE is larger than 90% in wide waveband and large FOV range. The material of three-layer DOE are FCD1 for first layer, FD6 for second layer, PS for the filler layer. Moreover, the weight of the eyepiece system is only 8g, and the diameter of lens is 16mm. The MTF performance can satisfy the requirement of display with VGA resolution. Besides, the lateral color and distortion are 4.8% and 10 μ m, respectively. The properties of the helmet eyepiece system are excellent.

9272-23, Session 6

Optical metrology techniques and apparatus for lens assembly (Invited Paper)

Shuping Wang, Univ. of North Texas (United States); Chi Zhang, Colleen Davis, Mark Alt, Sanmina-SCI Corp. (United States); Zheng Ji, Univ. of North Texas (United States); Yue Han, Michael Gardner, Sanmina-SCI Corp. (United States)

Precision positioning and bonding lenses into mount/cell plays an important role for many scientific and industrial applications, requiring very precise lens alignment and high vibration and temperature stability. The ultimate goal of the project is to design an automated assembly system, which allows positioning and attaching a plano-convex lens precisely into a floating kinematic mount with submicron accuracy, for high volume production. Before developing the fully automated assembly system development of low cost prototypes with rapid turnaround time is necessary to prove the feasibility of the system components and process features. This paper presents the optical and lens design for alignment to meet the challenging position specifications. Fabrication of the prototypes and testing results and analysis are also presented. The alignment system consists of a fiber-coupled HeNe laser source, a beam profiler to monitor the beam position that is directly associated with the plano-convex lens position, an autocollimator that is used to detect the angle between the incident beam and the surface normal of the plano-convex lens, and a custom-designed aspheric lens that re-collimates incident beam into the detector. The system components as well as their interaction with each other were simulated with Zemax software and tested in an experimental setup in order to conduct tolerance study and provide specifications for the mechanical fixtures used in the system. The epoxy is used to affix the parts together in a cost effective manner for prototyping. The position accuracy of ± 3

μ m compared to the golden unit has been achieved. Further improvement for position accuracy and repeatability is proposed by using an actively stabilized beam source and laser welding technique for the future fully automated assembly system.

9272-24, Session 6

Single camera stereo vision coordinate measurement in parts' pose recognition on CMM

Chunmei Wang, Fengshan Huang, Xuesha Wang, Hebei Univ. of Science and Technology (China); Li CHEN, Hebei University of science and technology (China)

In order to recognize parts' pose on Coordinate Measuring Machine (CMM) correctly and fast, based on the translation of CMM, A single camera stereo vision measurement method for feature points' 3D coordinate on the measured parts is proposed. According to the double cameras stereo vision principle, a image of the part to be measured is captured by A CCD camera, which is driven by CMM along its X or Y axis, on two different position correspondingly. Thus, the part's single camera stereo vision measurement is realized with the proposed image matching method, which is based on the centroid offset of image edge, on two images of the same feature point on the part, and each feature point's 3D coordinate in the camera coordinate system can be obtained. The measuring system is set up, and the experiment is conducted. The feature point's coordinate measuring time is 1.818s, and the difference value, which is between feature points' 3D coordinate calculated with the experiment result and that measured by CMM in the machine coordinate system, is less than 0.3mm. This measuring result can meet parts' pose real-time recognition requirement on the intelligent CMM, and also show that the method proposed in this paper is feasible.

9272-25, Session 6

Inertially stabilized line-of-sight control system using a magnetic bearing with vernier gimbaling capacity

Zhuchong Lin, Kun Liu, National Univ. of Defense Technology (China)

Line of sight stabilization and control system is widely used in pointing and stabilizing the line of sight of optical sensors. Multi-axis gimbals configurations are commonly used for isolating disturbance from the angular motion of the base where the stabilization platform is mounted. However, in the case of large payload, nonlinear friction and the bandwidth limit of the servo loop can greatly diminish the performance of the whole system. Magnetic actuators, because of their high force per mass capability and non-friction characteristic, are promising means of achieving high-accuracy stabilization. Nevertheless, the gap between magnetic actuators and the payload is very small, which limits the slewing range of the line of sight as well as the angular motion range of the base that can be isolated.

A novel two-stage stabilization configuration is developed, which combines multi-axis gimbals configuration and magnetic actuators as well as both of their advantages. At the first stage, a multi-axis gimbals configuration is adopted to isolate the large angular motion of the base while at the second stage magnetic actuators are utilized to perform high-accuracy stabilization. A so-called "stabilizing inside and tracking outside" scheme is carried out to perform two-stage stabilization control. The

advantage of this configuration compared with conventional configuration is analyzed through analytical method with respect to both pointing accuracy and bandwidth. And the effectiveness of the design is investigated through simulation studies.

9272-26, Session 6

Design and implementation of high-power LED machine vision

Huapeng Xiao, Guangxi Normal Univ. (China); Mingdong Li, Xingyu Gao, Guilin Univ. of Electronic Technology (China); Pengbo Chen, Guilin Univ. of Electronic Technology (China)

This article pointed out the difference between machine vision LED lighting system and traditional optical instrument lighting system. By the interactive methods which integrate with synthesis design analysis and Simulation, this paper import the element of field flattening theory into traditional lighting design, making it a kind of the new flat field lighting system. The effect when it was applied to high power LED lighting system is good.

With the new design concept, through the interactive design method and the new image quality evaluation system, we have a contrast experiment on a kind of LED single lamp lighting system. The results show that the field flat lighting system is superior to the traditional one. The most distinctive feature of the new light system is that, it can improve the performance of critical

Conference 9273: Optoelectronic Imaging and Multimedia Technology III

Thursday - Saturday 9 -11 October 2014

Part of Proceedings of SPIE Vol. 9273 Optoelectronic Imaging and Multimedia Technology III

9273-1, Session 1

Illuminant spectrum estimation using a color chart and a digital color camera

Junsheng Shi, Hongfei Yu, Xiaoqiao Huang, Yunnan Normal Univ. (China)

Illumination estimation is the main step in color constancy processing, also an important prerequisite for digital color image reproduction and many computer vision applications. In this paper, a method for estimating illuminant spectrum is presented, in which a color chart and a digital color camera are used and data of spectral reflectance of each patch of the chart is given. The first step of the method is to take a photo of the chart in an illumination, the second step is to calibrate color of the camera to measure CIEXYZ of each patch of the chart, and the third step is to estimate the spectral distribution of the illumination by the Wiener estimation method using data of CIEXYZ and spectral reflectance of each patch of the chart. The results of computer simulation verified effectiveness of the presented method for estimating CIE standard illumination A and C using the given data of spectral reflectance and CIEXYZ for X-rite ColorChecker 24-color chart. The experiment was carried to estimate illumination spectrum of a typical outdoor scene using X-rite ColorChecker 24-color chart and a common color camera. To assess the performance of the method quantitatively, the well-known the goodness-fitting coefficient was used to measure the spectral match, and two uniform color spaces CIELab and CIELuv were used to assess the color match between the actual and the estimated spectrum.

9273-2, Session 1

Infrared and visible image fusion based on region of interest and Laplace pyramid

Xiong Gao, Hong Zhang, Hao Chen, Yuhu You, Ding Yuan, BeiHang Univ. (China)

Multimodal image fusion aims at fusing information from multi-sensor images of the same scene into a single image which is suitable for human perception and practical applications. Infrared and visible image fusion are widely used to enhance the infrared target and visible background details simultaneously in fused image. In this paper, we propose a region of interest-based (ROI-adaptive) fusion algorithm of infrared and visible images by using the Laplace Pyramid method. Firstly, we estimate the saliency map of infrared images, and then divide the infrared image into two parts: the regions of interest (RoI) and the regions of non-interest (nRoI), by normalizing the saliency map. Visible images are also segmented into two parts by using the Gauss High-pass filter: the regions of high frequency (RoH) and the regions of low frequency (RoL). Secondly, we down-sampled both the nRoI of infrared image and the RoL of visible image as the input of next level processing. Finally, we use normalized saliency map of infrared images as the weighted coefficient to get the basic image on the top level and choose max gray value of the RoI of infrared image and the RoH of visible image to get the detail image. In this way, our method can keep target feature of infrared image and texture detail information of visual image at the same time. Experiment results show that such fusion scheme performs better than the other fusion algorithms both on human visual system and quantitative metrics.

9273-3, Session 1

High dynamic range imaging system based on coded aperture

RenFan Wu, YiFan Huang, Beijing Institute of Technology (China); Guangqi Hou, Zhenan Sun, Institute of Automation (China)

This paper presents a novel design scheme of high dynamic range(HDR) imaging system based on coded aperture technique. The proposed system can help us obtain HDR images which have extended depth of field comparing with images captured by traditional optical imaging systems. We first adopt sparse coding algorithm to design a finite number of coded patterns. The coded patterns are placed in the entrance pupil of the system, and modulate the rays that enter in the main lens. Then we acquire independent coded image data under different exposure settings which configured by multiple exposure sampling method. Under the guide of the multiple exposure parameters, a series of low dynamic range images are decoded through reconstruction from the raw data. Finally the rapid bilateral filtering algorithm is used to fuse the decoded images to obtain a HDR image with extended depth of field. In this paper, we conduct our optical simulation experiments by using a variety of coded aperture patterns and a range of sampling density, and some quality evaluation parameters are proposed to evaluate the experimental HDR images. From the results of experiments, our novel imaging system can extend depth of field and dynamic range of raw images.

9273-4, Session 1

Light efficient design of a depth discriminative lens

Wei Yan, Jinli Suo, Qionghai Dai, Tsinghua Univ. (China)

This paper presents a light-efficient depth discriminative imaging system, which is used to retrieve the scene depth computationally. To deal with the low robustness of depth from defocus using traditional aperture, whose homogeneous defocus radius is the only cue for depth information, we propose to use inhomogeneous point spread function (PSF) instead while avoid lowering signal-noise-ratio as in aperture coding. Specifically, we propose to use two orthometric cylindrical mirrors together with two convex lenses to encode the scene depth into a cross-shaped PSF. In terms of depth discrepancy, the designed PSF are of four degrees of freedom to reconstruct scene depth and thus is of advantages depth discriminability to conventional circle or regular polygon shaped aperture. As for light efficiency, this method totally obviates the low light transmittance of coded aperture implementation which customize PSF via light blocking, so the luminous flux is much more efficient. To validate this approach, we build a prototype setup and test the performance on a series of scenes with a large depth of field (DOF), and the effectiveness of the proposed approach is validated by the superior performance in the synthetic and real data.

9273-5, Session 1

Compressive photography based on lens array with coded mask using over-complete dictionary

Yuanchao Du, Graduate School at Shenzhen, Tsinghua Univ. (China); Xingzheng Wang, Tsinghua Univ. (China); Haoqian Wang, Graduate School at Shenzhen, Tsinghua Univ. (China); Qionghai Dai, Tsinghua Univ. (China)

With the abundant information it contains, light field photography gained a significant research interest in the last two decades. Plenoptic camera records the 4D light field data by storing the spatial information and angular information. Meanwhile, it introduces the trade-off between spatial resolution and angular resolution. Hence, the spatial resolution is reduced significantly, which drop the image quality severely. We proposed a new camera design which can optimize this trade-off, by adding a coded path into the light path of the traditional plenoptic camera with lens array. And the sensor plan will record the coded image, which has been modulated in Fourier domain. High resolution 4D light field could be reconstructed from the coded image by two steps. First, train an over-complete dictionary. Implement Coresets method process the light field datasets to get 4D light field atoms. In this way the size of the training set is significantly reduced and redundancies in the train set are removed. Then use Online Sparse Coding to train an over-complete dictionary from the processed data. Second step is sparse reconstruction. Generate a random coded mask and find the place to insert it with convex optimization method. Then reconstruct the 4D light field by compressive sensing with over-complete dictionary. The proposed architecture achieve 3 advantages: the reconstructed light field has a higher resolution than the traditional plenoptic camera. A parameter to evaluate the quality of the light field reconstruction is demonstrated and our prototype performance 20% better than traditional plenoptic camera. The light field atoms used in this paper both have higher PSNR and compression ratio than the conventional basis.

9273-6, Session 1

Modeling and performance analysis for masks in infrared coded mask imaging systems

Ao Zhang, Tianjin Univ. (China) and Jiuquan Satellite Launch Ctr. (China); Jie Jin, Qing Wang, Jingyu Yang, Tianjin Univ. (China); Yi Sun, Tianjin Jinhang Institute of Technology Physics (China)

The point spread function (PSF) of imaging system with coded mask is generally acquired by practical measurement with calibration light source. As the thermal radiation of coded masks are relatively severe than it is in visible imaging systems, which buries the modulation effects of the mask pattern, it is difficult to estimate and evaluate the performance of mask pattern from measured results. To tackle this problem, a model for infrared imaging systems with masks is presented in this paper. The model is composed with two functional components, the coded mask imaging with ideal focused lenses and the imperfection imaging with practical lenses. Ignoring the thermal radiation, the system's PSF can then be represented by a convolution of the diffraction pattern of mask with the PSF of practical lenses. To evaluate performances of different mask patterns, a set of criterion are designed according to different imaging and recovery methods. Furthermore, imaging results with inclined plane waves are

analyzed to achieve the variation of PSF within the view field. The influence of mask cell size is also analyzed to control the diffraction pattern. Numerical results show that mask pattern for direct imaging systems should have more random structures, while more periodic structures are needed in system with image reconstruction. By adjusting the combination of random and periodic arrangement, desired diffraction pattern can be achieved.

9273-7, Session 2

Spatial-spectral volume holographic imaging (*Invited Paper*)

Yuan Luo, National Taiwan Univ (Taiwan)

The biggest challenge on the path towards three-dimensional imaging is to obtain spatial and spectral information of a volumetric sample in real-time. For example, Laser induced fluorescence has been developed for a variety of clinical applications. However, many of the existing biomedical imaging systems typically require scanning in two lateral dimensions as well as depth focusing. Efforts to improve scanning efficiency by optimizing the scanning algorithm or increasing the number of focal points are ongoing. However, these methods can increase system complexity and do not eliminate the need for moving parts. This talk will introduce volume holographic imaging systems to acquire spatial images with spectral selectivity and no scanning in both transverse and longitudinal directions. The imaging modality is based upon multiplexed volume holographic (MVH) gratings acting as spatial-spectral filters used in an optical imaging system. In addition, with proper multiplexed holographic pupil engineering, the MVH systems can obtain multiple depth-resolved phase-contrast imaging in real-time in a single shot. Moreover, the talk will address MVH techniques incorporating other state-of-the-art imaging methods to better manipulate light for imaging in a variety of applications.

9273-8, Session 2

Real-time automatic small infrared target detection using local spectral filtering in the frequency domain

Hao Chen, Hong Zhang, Jiafeng Li, Yuhu You, BeiHang Univ. (China); Mingui Sun, Univ. of Pittsburgh (United States)

Accurate and fast detection of small infrared target has very important meaning for infrared precise guidance, early warning, video surveillance, etc. Based on human visual attention mechanism, an automatic detection algorithm for small infrared target is presented. In this paper, instead of searching for infrared targets, we model regular patches that do not attract much attention by our visual system. This is inspired by the property that the regular patches in spatial domain turn out to correspond to the spikes in the amplitude spectrum. Unlike recent approaches using global spectral filtering, we define the concept of local maxima suppression using local spectral filtering to smooth the spikes in the amplitude spectrum, thereby producing the pop-out of the infrared targets. In the proposed method, we firstly compute the amplitude spectrum of an input infrared image. Second, we find the local maxima of the amplitude spectrum using cubic facet model. Third, we suppress the local maxima using the convolution of the local spectrum with a low-pass Gaussian kernel of an appropriate scale. At last, the detection result in spatial domain is obtained by reconstructing the 2D signal using the original phase and the log amplitude

spectrum by suppressing local maxima. The experiments are performed for some real-life IR images, and the results prove that the proposed method has satisfying detection effectiveness and robustness. Meanwhile, it has high detection efficiency and can be further used for real-time detection and tracking.

9273-9, Session 2

Texture-adaptive hyperspectral video acquisition system with a spatial light modulator

Xiaojing Fang, Jiao Feng, Yongjin Wang, Nanjing Univ. of Posts and Telecommunications (China)

Recently, a hybrid camera system, composed of an RGB camera to obtain RGB video with high spatial resolution, a gray camera, amici prism, occlusion mask and other optical element to obtain multispectral video with high spectral resolution, have been set up. A large amount of redundant image data is collected by the CCD camera in this mask-based hybrid camera system. To achieve texture-adaptive high-resolution hyperspectral video, a spatial light modulator (SLM) is introduced to replace the mask that samples data uniformly. Combining with digital imaging analysis and computational processing, sampling patterns on the SLM are generated on-the-fly according to the texture features of different scenes, which reduces the data amount effectively. First, the hybrid system with the SLM is established, texture-features detection of the RGB video is then made to determine the sampling pattern which achieves adaptive data acquisition. Finally, by using video-frame registration and spectrum information spreading algorithm, videos with both high spatial and spectral resolution are produced. In this thesis, we propose an adaptive sampling algorithm with the method of texture segmentation, Wavelet Transform (WT). With this methodology, sampling frequency differs in different texture blocks of an image. Less texture feature, less sampling points. The sampling patterns of the SLM generated by the adaptive sampling algorithm achieve to select points of scenes adaptively. We also demonstrate the effectiveness of the sampling pattern on the SLM with the proposed method, comparing with the mask-based hybrid camera system.

9273-10, Session 2

Color correction of underwater images using spectral data

Lingyan Kan, Jia Yu, Yu Yang, Huiping Liu, Jincheng Wang, Ocean Univ. of China (China)

This paper addresses the problem of color correction of underwater images using white light absorption spectrum data. Because of the attenuation of light traveling in the water, underwater imaging became a difficulty when trying to correct color loss.

The white light absorption spectrum data are measured with the absorption spectrometer at different depth, and then in CIE1931XYZ color system tristimulus values of the spectral datum are calculated. Considering the nonlinear underwater attenuate of light in different wavelength at different depths, based on Beer's law, the attenuation of tristimulus values are estimated. The color images capturing in water were saved in sRGB format, which was a standard color space. To use the attenuation of tristimulus values, the color space conversion for images from sRGB to CIEXYZ is necessary. And then images were compensated in CIEXYZ color system. Finally, the values corrected in the CIEXYZ was converted to sRGB for display. Meanwhile, except for water

absorption and scattering, the CCD of the camera also have nonlinear effects on color loss, the image acquiring system are calibrated by measuring the response curve of the camera.

Based on this method, In situ experiments are carried out in coastal water. Firstly, the spectral datum were collected underwater with the absorption spectrometer at different depth. Then, we took images which was poor quality for analysis and processing using the underwater camera. And then, by changing the intensity of light source, the response curve of camera was determined. Finally, we processed and compensated the color images.

The results show that the color of the images acquired underwater in several different coastal seawater are all well restored, which demonstrate the feasibility of our method in in-situ underwater image acquiring and processing.

9273-11, Session 2

Non-negative structural sparse representation for high-resolution hyperspectral imaging

Guiyu Meng, Guangyu Li, Weisheng Dong, Guangming Shi, Xidian Univ. (China)

High resolution hyperspectral images have important applications in many areas, such as anomaly detection, target recognition and image classification. Due to the limitation of the sensors, it is challenging to obtain high spatial resolution hyperspectral images. Recently, the methods that reconstruct high spatial resolution hyperspectral images from the pair of low resolution hyperspectral images and high resolution RGB image of the same scene have shown promising results. In these methods, sparse non-negative matrix factorization (SNNMF) technique was proposed to exploit the spectral correlations among the RGB and spectral images. However, only the spectral correlations were exploited in these methods, ignoring the abundant spatial structural correlations of the hyperspectral images. In this paper, we propose a novel algorithm combining the structural sparse representation and non-negative matrix factorization technique to exploit the spectral-spatial structure correlations and nonlocal similarity of the hyperspectral images. Compared with SNNMF, our method makes use of both the spectral and spatial redundancies of hyperspectral images, leading to better reconstruction performance. The proposed optimization problem is efficiently solved by using the alternating direction method of multipliers (ADMM) technique. Experiments on a public database show that our approach performs better than other state-of-the-art methods on the visual effect and in the quantitative assessment.

9273-12, Session 3

Big visual data analysis: challenges and solution strategies (Keynote Presentation)

Chun-Chieh J. Kuo, The Univ. of Southern California (United States)

Millions of images/videos have been created every day due to the popularity of smart phones and surveillance cameras. Due to the huge size and great diversity of visual data, big visual data analytics plays a critical role in applications such as large-scale image/video indexing, search and tagging. In this work, I will address two competing factors that have a high impact on the performance of a classification system; namely, data

diversity and data abundance. I will discuss two strategies to handle the data diversity problem. They are data grouping and decision stacking. Several examples will be given to illustrate how these two techniques work. Once the data diversity problem is well resolved, we will benefit from data abundance. More data samples allow a learning-based classifier to offer better performance. We will use a couple of examples to show the power of the proposed techniques in handling big visual data.

9273-13, Session 3

Multiplexed LED array microscope for fast gigapixel phase imaging (*Keynote Presentation*)

Laura Waller, Lei Tian, Univ. of California, Berkeley (United States)

The LED array microscope is a powerful new platform for computational microscopy, enabling a wide range of capabilities with a single hardware modification - the replacement of the source with a programmable LED array. This allows patterning of the illumination at the Fourier plane of the sample. Thus, each LED in the array corresponds to illumination of the sample by a unique angle. The central LEDs produce brightfield images, whereas outer LEDs produce dark field images. Alternatively, by sequentially taking a pair of images with either half of the source on, we obtain phase derivative measurements by differential phase contrast. Finally, a full sequential scan of the 2D array captures a 4D dataset similar to a light field, enabling all the computational processing of light field imaging (e.g. digital refocusing). We can also improve resolution by Fourier Ptychography, which uses a low NA large field of view objective, but still obtains high resolution across the entire image, resulting in gigapixel images. In previous work, a series of images was taken by sequentially turning on each single LED in the array. Here, we demonstrate a multiplexed illumination strategy in which multiple randomly selected LEDs are turned on for each image. Since each corresponds to a different area of Fourier space, the total number of images can be significantly reduced, without sacrificing image quality. Compared to sequential scanning, our multiplexed strategy achieves similar results with approximately an order of magnitude reduction in both acquisition time and data capture requirements.

9273-14, Session 4

High speed confocal microscopy using binary multiplex holograms

Bosanta R. Boruah, Ranjan Kalita, Abhijit Das, Indian Institute of Technology Guwahati (India)

Confocal microscope is a powerful imaging tool that finds applications in diverse areas. In a conventional confocal microscope a single illumination beam is scanned by using two scanner mirrors. Thus the frame rate of such a microscope is primarily determined by the scanner parameters. In this paper we describe the design and implementation of a confocal microscope where the illumination beam is modified with the help of a binary multiplex hologram. In the proposed scheme one incident laser beam gives rise to a linear array of focal spots. Generation of such a focal spot array to scan the sample plane reduces the scanning time since at an instant several locations in the sample plane are simultaneously illuminated. This leads to an increase in the frame rate of the microscope. The binary holograms also facilitate shaping the wavefront of each beam in

the array. In this paper we will present preliminary experimental results using our proposed microscope set up.

9273-15, Session 4

Implementing two compressed sensing reconstruct algorithms on GPU

Sui Dong, Jun Ke, Wei Ping, Beijing Institute of Technology (China)

In compressed sensing (CS), the reconstruction process is consuming. In this paper, we use GPU to implement the Orthogonal Matching Pursuit (OMP) and the Two-Step Iterative Shrinkage/Thresholding Algorithm (TwIST) algorithms for CS signal reconstruction.

OMP is widely used in the study of CS, since it is straightforward intuitive, and easily implemented. To speed up OMP using GPU, the bottleneck is to solve a least-square problem. We take LU and QR matrix decompositions to solve the problem. We find LU can present comparable accuracy and an obvious speed up compared with QR. In addition, we find, in the first several iterations of OMP, GPU does not improve the performance much, because the size of the least-square problem is small. Thus To fully utilize GPU, we increase the problem size and reduce the number of iterations of OMP. For example, different from the classical OMP choosing one column of the measurement matrix, we take more columns to solve the least-square problem in each iteration. After this modification, our results show a 30X acceleration using GPU compared with CPU.

OMP has been proved to perform poorly for a high-dimensional problem. To deal with this issue, in this paper, we will study the TwIST algorithm. Because only summation and matrix-vector multiplication are used in each iteration of TwIST, it is convenient to implement the algorithm on GPU. Based on our previous works, we expect to obtain a larger acceleration value by implementing TwIST on GPU over CPU than OMP.

9273-17, Session 4

High-resolution light field cameras based on a hybrid imaging system

Feng Dai, Jing Lu, Yike Ma, Yongdong Zhang, Institute of Computing Technology (China)

Compared to traditional digital SLR (DSLR) cameras, light field (LF) cameras measure not only the intensity of incoming light, but also its angle, which could be used to refocus a shot or change the viewpoint after the photo capture. As LF cameras trade a good deal of spatial resolution for extra angle information, they provide lower spatial resolution than DSLR cameras. In this paper, we show a hybrid imaging system consisting of a standard LF camera and a high-resolution DSLR, achieving both high spatial resolution and high angle resolution. Each lenslet of the LF camera could be seen as a macro pixel, corresponding to a pixel in LF image. After the co-location, the system propagates the angle information into the DSLR image, guided by the RGB color similarity and Euclidean distance between the pixel of the DSLR image and the macro pixel of the LF image. The algorithm convert each pixel of the DSLR image into the macro pixel, and get high-resolution digital refocusing images, multi-view images and the depth map. We build an example prototype using a Lytro camera and a 20 megapixel (MP) Canon DSLR camera to generate a light field with 20 MP resolutions. We evaluate the system on real-world scenes, containing occlusions and complex

non-lambertian material, demonstrating the effectiveness of our method.

9273-18, Session 5

Towards multidimensional computational imaging and reconstruction (*Invited Paper*)

Yebin Liu, Tsinghua University (China)

Imaging and Reconstruction of real-world visual information plays an important role in our everyday life and in every professional field, ranging from nono-scale microscopy in life science to magascale aerial surveillance. To facilitate the human understanding of visual information, or to capture and reconstruct scenes that cannot be seen by human eye, multidimensional imaging and reconstruction are increasingly demanded, resulting in a rapid merging of optics and information techniques. Multidimensional imaging origins from the seven dimensional light field, which contains spatial dimension, view dimension, spectral dimension and time dimension. In this talk, I will introduce our recent research progress in multidimensional imaging and reconstruction, including gigapixel imaging in pixel dimension, 3D reconstruction in view dimension, hyperspectral imaging in spectral dimension and femto-photography in time dimension. The imaging in a higher dimensional space by combing some

9273-19, Session 5

A semi-automatic 2D-to-3D video conversion with adaptive key-frame selection

Hongkai Xiong, Kuanyu Ju, Shanghai Jiao Tong Univ. (China)

To compensate the deficit of 3D content, 2D to 3D video conversion (2D-to-3D) has recently attracted more attention from both industrial and academic communities. The semi-automatic 2D-to-3D conversion which estimates corresponding depth of non-key-frames through key-frames is more desirable owing to its advantage of balancing labor cost and 3D effects. The location of key-frames plays a role on quality of depth propagation. This paper proposes a semi-automatic 2D-to-3D scheme with adaptive key-frame selection to keep temporal continuity more reliable and reduce the depth propagation errors caused by occlusion. The potential key-frames would be localized in terms of clustered color variation and motion intensity. The distance of key-frame interval is also taken into account to keep the accumulated propagation errors under control and guarantee minimal user interaction. Once their depth maps are aligned with user interaction, the non-key-frames depth maps would be automatically propagated by shifted bilateral filtering. Considering that depth of objects may change due to the objects motion or camera zoom in/out effect, a bi-directional depth propagation scheme is adopted where a non-key frame is interpolated from two adjacent key frames. The experimental results show that the proposed scheme has better performance than existing 2D-to-3D scheme with fixed key-frame interval.

9273-21, Session 5

A depth video processing algorithm for high encoding and rendering performance

Mingsong Guo, Fen Chen, Ningbo Univ. (China); Chengkai Sheng, Faculty of Information Science and Engineering, Ningbo University (China); Zongju Peng, Gangyi Jiang, Ningbo Univ. (China)

In free viewpoint video system, the color and the corresponding depth video are utilized to synthesize virtual views by depth image based rendering (DIBR) technique. Hence, high quality of depth videos is a prerequisite for high quality of virtual views. However, limited depth video capturing technologies and scene variance may result in slight or abrupt depth variation. The variation may increase the encoding bitrate and decrease the quality of virtual views. To tackle these problems, a depth processing algorithm is proposed in this paper. The algorithm includes three steps, bilateral filtering, abrupt variation detecting and abrupt variation smoothing. First, a bilateral filter is adopted to process the depth video. The filter can eliminate the slight variation and protect the edge at the same time. Then, abrupt variation is detected by an adaptive threshold which is determined by the camera parameter of each video sequence. Holes of virtual views occur when the depth values of left view change obviously from low to high in horizontal direction or the depth values of right view change obviously from high to low. Therefore, for left views, the abrupt variation in left side will be processed adaptively until no abrupt variation can be detected. Similarly, abrupt variation in right side of right views is processed. Finally, the proposed algorithm is estimated in terms of encoding and virtual view rendering. Experimental results show that the proposed algorithm can reduce the encoding bitrate by 25% while the quality of the synthesized virtual views can be improved by 0.39dB. The subjective quality of virtual view is also enhanced observably.

9273-22, Session 5

A novel virtual viewpoint merging method based on machine learning

Di Zheng, Zongju Peng, Gangyi Jiang, Fen Chen, Mei Yu, Ningbo Univ. (China)

In multi-view video system, multiple video plus depth is main data format of 3D scene representation. Continuous virtual views can be generated by using depth image based rendering (DIBR) technique. DIBR process includes geometric mapping, hole filling and merging. Unique weights, inversely proportional to the distance between the virtual and real cameras, are used to merge the virtual views. However, the weights might not the optimal ones in terms of virtual view quality. In this paper, a novel virtual view merging algorithm is proposed. In the proposed algorithm, machine learning method is utilized to establish an optimal weight model. In the model, color, depth, color gradient and sequence parameters are taken into consideration. Firstly, we render the same virtual view from left and right views, and select the training samples by using a threshold. Then, the eigenvalues of the samples are extracted and the optimal merging weights are calculated as training labels. Finally, the optimal weight model is built by using support vector machine, and used to guide the virtual views rendering. Experimental results show that the proposed method can improve the quality of virtual views for most sequences. Especially, it is effective in the case of large distance between the virtual and real cameras.

9273-23, Session 5

A foreground object features-based stereoscopic image visual comfort assessment model

Xin Jin, Gangyi Jiang, Hongwei Ying, Mei Yu, Sheng Ding, Zongju Peng, Feng Shao, Ningbo Univ. (China)

With the applications of three dimensional (3D) video services, the concern about the safety of stereoscopic 3D viewing has been under the spotlight again. 3D video products not only give the customers an immersive experience, but also bring the potential for physical discomfort, such as visual fatigue, headaches and nausea. A common view is that the visual comfort has become an important factor that hinders the wide spreading of 3D video products.

To consider the viewing safety and improve 3D content generation, this paper presents a foreground object features based stereoscopic image visual comfort assessment model. In accordance with the psychological phenomenon, object segmentation is given by means of the previously calculated disparity map, the foremost object is ascertained as the one having the biggest average disparity. Then average disparity, average width and its complexity are derived as the feature to judge image category and predict visual comfort. Experimental results show that the proposed model can achieve higher consistency between objective and subjective visual comfort scores, compared with other existing methods.

9273-33, Session Post

Light field reconstruction robust to signal dependent noise

Kun Ren, Beijing Univ. of Technology (China); Jinli Suo, Qionghai Dai, Tsinghua Univ. (China)

Coded aperture imaging system had been proven to be an effective scheme to capture and reconstruct the 4D light field data, which is quite useful for scene depth inference and refocusing. However, noise is one of the key drawbacks limiting the final reconstruction quality due to the low light transmittance. Previous attempts to suppress noise in light field reconstruction mostly focused on additive Gaussian white noise, which does not hold in real capturing and naturally affects the final performance. Research shows that the CCD sensor noise is nonlinearly related to the latent signal, so this paper proposes a new method of noise robust light field acquisition. Firstly, scene dependent noise model is studied and incorporated into the light field reconstruction framework. Then, we conduct light field reconstruction from both complete and incomplete measurements: the former can be implemented by simple matrix inversion while the latter needs an assistive over complete dictionary and sparsity prior of the reconstruction coefficients. Besides mathematical analysis and validation on synthetic data, we additionally build a prototype by hacking an off-the-shelf camera for data capturing and proof the concept. The effectiveness of introducing signal dependent noise model into light field reconstruction is validated with real data capturing on a variety of scenes.

9273-47, Session 5

Joint bit allocation for 3D video coding based on virtual view distortion

Chao Yang, Ping An, Jianxin Wang, Zhaoyang Zhang, Shanghai Univ. (China)

In multi-view plus depth (MVD) 3D video coding, texture maps and depth maps are coded jointly. The depth maps provide the scene geometry information and are used to render the virtual view at the terminal through a Depth-Image-Based-Rendering (DIBR) technique. The distortion of the coded texture maps and the coded depth maps will induce synthesized virtual view distortion. Besides the coding efficiency of texture maps and depth maps, bit allocation between texture maps and depth maps also has a great effect on the virtual view's quality. In this paper, the virtual view distortion is divided into texture maps induced distortion and depth maps induced distortion separately, models of texture maps induced virtual view distortion and depth maps induced virtual view distortion are derived respectively. Based on the depth maps induced virtual view distortion model, depth maps coding rate distortion optimization (RDO) is modified and the depth maps coding efficiency is increased. Meanwhile, we also propose a Rate-distortion (R-D) model to solve the joint bit allocation problem. Experimental results demonstrate the high accuracy of the proposed virtual view distortion model. The R-D performance of the proposed algorithm is close to the full search algorithm which can give the best R-D performance, while the coding complexity of the proposed algorithm is lower. Compared with fixed texture and depth bits ratio (5:1), an average 0.4 dB gain can be achieved by the proposed algorithm. The proposed algorithm has a high rate control accuracy with the average error less than 2%.

9273-16, Session Post

Image super-resolution via adaptive filtering and regularization

Jingbo Ren, Hao Wu, Weisheng Dong, Guangming Shi, Xidian Univ. (China)

Image super-resolution (SR) is widely used in the fields of civil and military, especially for the low-resolution remote sensing images limited by the sensor. Single-image SR refers to the task of restoring a high-resolution (HR) image from the low-resolution image coupled with some prior knowledge as a regularization term. One classical methods regularize image by total variation (TV) and/or wavelet or some other transform which introduce some artifacts. To compress these shortages, a new framework for single image SR is proposed by utilizing an adaptive filter before regularization. The key of our model is that the adaptive filter is used to remove the spatial relevance among pixels first and then only the high frequency (HF) part, which is sparser in TV and transform domain, is considered as the regularization term. Concretely, through transforming the original model, the SR question can be solved by two alternate iteration sub-problems. Before each iteration, the adaptive filter should be updated to estimate the initial HF. A high quality HF part and HR image can be obtained by solving the first and second sub-problem, respectively. In experimental part, a set of remote sensing images captured by Landsat satellites are tested to demonstrate the effectiveness of the proposed framework. Experiment results show the outstanding performance of the proposed method in quantitative evaluation and visual fidelity compared with the state-of-art methods.

9273-20, Session Post

Eye detection system based on ASM and AdaBoost for 3D monitor

Xu Bin, Nanjing Univ. (China)

With the development of technology and the improvement of people's living standard, the technology of 3D get a rapid development. As we are enjoying the entertainment from 3D display, more attention is paid on the comfort and convenience. The technology of head-tracked autostereoscopic display is born at the right moment. In head-tracked autostereoscopic display, the location of eyes is captured by camera in real time. Then corresponding images are projected to the left and right eyes of Spectator for 3D. For this reason, the accuracy and stability of eye detection determine the performance of the 3D equipment. The Adaboost algorithm boosts weak classifiers to strong classifiers based on Haar features. With the help of the integral image and cascade structure, real AdaBoost algorithm has fast computation speed and it also has a high detection rate and good robustness. ASM (Active Shape Model) algorithm is based on Point Distributed Models and approves its ability in detection accuracy. An approved eye detection algorithm is proposed in this paper, aiming at the detection of face rotation. At the same time, the accuracy and Real-time performance is also improved.

9273-45, Session Post

An improved hybrid opto-digital joint transform correlator reducing the influence of defocus on image motion measurement

Hui Zhao, Hongwei Yi, Xi'an Institute of Optics and Precision Mechanics (China); Jingxuan Wei, Xi'an Institute of Optics and Precision Mechanics (China); Xiaopeng Xie, Inner Mongolia Univ. (China)

The relative motion between object and camera will bring in image blurring that leads to irreversible information loss. The key to eliminate or reduce image blurring lies in the estimation or the measurement of image motion.

Compared with those pure digital image motion measurement methods, for example block matching or phase correlation algorithms, optical joint transform correlator (JTC) is much faster and suitable for real-time image motion measurement. So far, many types of JTC have been designed and we also make a contribution by proposing a hybrid opto-digital JTC (HODJTC) in [CHIN. OPT. LETT., Vol. 8, No. 8]. Being different from traditional JTC, only one optical Fourier transform is needed and the optically generated joint power spectrum (JPS) is used to digitally compute the image motion. However, both the JPS and the correlation image are captured by CCD camera and thus the defocus could not be avoided and will influence the measurement precision. In this case, a high measurement precision obtained through HODJTC will be counteracted by the defocus effect.

Therefore in this paper, the influence of defocus is analyzed from mathematical viewpoint using the method of stationary phase and an improved HODJTC is proposed. By introducing randomly generated defocus, a series of cross-correlation peak images is first obtained and a subsequent spatial averaging procedure is applied to these images to generate the final cross-peak image which is used to compute the defocus invariant motion value. In this way, the influence of defocus on image motion measurement is effectively reduced.

9273-48, Session Post

A real-time stereo-to-multiview system based on FPGA

Yang Zhang, Yebin Liu, Tsinghua Univ. (China)

Watching 3D videos without glasses at home is popular for its convenience. Currently, there are so little videos that can directly display on autostereoscopic TV so that a stereo-to-multiview system is of great importance. In this paper, we made a high definition stereo-to-multiview system which can display 1080p video in real-time on FPGA. This system is fully automatic without any user inputs. The system consists of disparity estimation and optimization, virtual view rendering and interweaving. In the disparity estimation step, we adopt a fast block matching method with neighbor information. Only a few predicted disparities are candidates, instead of search in all disparity spaces. This method can also deal with occlusion areas and textureless areas. In the virtual view rendering step, we take human's watching comfort into account. Disparity, disparity gradient, disparity velocity are constrained so that the disparity will not change sharply. In this way, people will not feel disgusted when watching 3D videos. We created certain solving blocks and added parallel mechanism on FPGA and the running time is greatly shortened. We tested different kinds of scenes and we found that our system performed robust on those scenes.

9273-52, Session Post

Accurate point spread function (PSF) estimation for coded aperture cameras

Jingyu Yang, Bin Jiang, Jinlong Ma, Tianjin Univ. (China); Yi Sun, Tianjin Jinhang Institute of Technology Physics (China)

Accurate PSF estimation of coded aperture cameras is a key to deblur defocus images. There are mainly two kinds of approaches to estimate PSF: blind-deconvolution-based methods, and measurement-based methods with point light sources. Both these two kinds of methods cannot provide accurate PSFs due to the limit of blind deconvolution or imperfection of point light sources. Inaccurate PSF estimation introduces pseudo-ripple and ringing artifacts which influence the effects of image deconvolution.

This paper proposes a novel method of PSF estimation for coded aperture cameras. It is observed and verified that the spatially-varying point spread functions are well modeled by the convolution of the aperture pattern and Gaussian blurring with appropriate scales and bandwidths. We use the coded aperture camera to capture a point light source to get a rough estimate of the PSF. Then, the PSF estimation method is formulated as the optimization of scale and bandwidth of Gaussian blurring kernel to fit the coded pattern with the observed PSF. We also investigate the PSF estimation at arbitrary distance with a few observed PSF kernels, which allows us to fully characterize the response of coded imaging systems with limited measurements. Experimental results show that our method is able to accurately estimate PSF kernels, which significantly improve the deblurring performance.

9273-53, Session Post

Non-intrusive gesture recognition system combining with face detection based on Hidden Markov Model

Jing Jin, Yuanqing Wang, Liujing Xu, Nanjing Univ., Xianlin Campus (China); Liqun Cao, Lei Han, Biye Zhou, Minggao Li, Navy General Hospital (China)

A non-intrusive gesture recognition human-machine interaction system is proposed in this paper. The system allows users to manipulate directly without any special equipment. It is difficult to segment user's hand from the image with complex background by existing contact-less hand location algorithms. In order to solve the hand positioning problem, depth value image of stereo image pairs and skin color image is calculated as pre-processing, and face detection is used for the front-end to narrow the search area and find user's hand quickly and accurately. According to two difference images with different zero parallax, user's hand and reference points can be detected. Hidden Markov Model (HMM) is used for gesture recognition. In this paper, four basic gesture units which are leftward, rightward, upward and downward respectively are trained as HMM models. Complex gestures which are made up of simple units in a certain order can also be decoded and recognized. At the same time, considering that these units have strong directivity in four specified directions, an improved 8-direction feature vector is proposed to quantify characteristics in order to improve the detection accuracy. The accuracy of improved direction coding method has obvious improvement than traditional direction coding method. The proposed system can be applied in interaction equipments without additional devices and special training for users, such as household interactive television.

9273-54, Session Post

Oil tank detection based on salient region and geometric features

Yuan Yao, Zhiguo Jiang, Haopeng Zhang, BeiHang Univ. (China)

Oil tank detection in remote sensing images is of very significant meaning for military scouting, due to the vital role that oil tanks play in transportation and military. Oil tanks in remote sensing images have the following characteristics: they are salient because of their larger gray values; they are likely to be circular in shape, and have distinct edges and large edge gradients. In this paper, we present a novel oil tank detection method, considering the characteristics of oil tanks by using salient region and geometric features. Firstly, we employ the saliency method (LC) to get a saliency map based on the intensity characteristic, and then use Otsu threshold to segment the saliency map into a binary image. After image segmentation, opening operation are employed as morphologic processing to remove small regions. Then we can easily get all the regions of interest (ROIs) accurately. Posture ratio, rectangularity and circularity of the ROIs are calculated to represent the shape characteristic of oil tank. Then we train a linear SVM classifier to detect the candidate regions using the 3D features. Besides, we perform a post-process to remove false alarms by rotating the candidate regions by 0, 15, 30 and 45 degrees successively, and computing the areas of the bounding rectangles of the rotated regions. We collect 20 images of complex airport and harbor scenes in Google Map to validate our method. Experimental results show that our method is more robust with respect to various disturbances compared with other methods, such as occlusion, shadow or deformation.

9273-55, Session Post

Experimental calibration of x-ray camera performance: spatial resolution, flat field response, and radiation sensitivity

Hongwei Xie, Jinchuan Chen, Linbo Li, Faqiang zhang, dingyang Chen, Institute of Nuclear Physics and Chemistry (China)

Major parameters of X-rays camera include spatial resolution, flat field response and dynamic range. Such parameters were calibrated on a pulsed X-rays source with about 0.3MeV energy. Fluorophotometric method was used for the measurement of spatial resolutions of the penetrating lights and reflecting lights. Results indicated they were both basically same. And the spatial resolution of the camera was measured with edge method. Corresponding to 10% intensity, the modulator transfer function (MTS) of the resolution was about 5lp/mm, while the size of the point spread function (PSF) was about 0.8mm. Due to the system design with both short distance and big filed of view, the flat field non-homogeneity was about 15%. In addition, because of the relatively big gain of the scintillator and MCP image intensifier and the limited detecting efficiency of the X-rays and scintillator, the image intensity of the flat field response demonstrated a big standard deviation of about 1375. Due to the crosstalk throughout the system, the maximal signal-to-noise ratio (SNR) of the X-rays camera was about 10:1. These results could provide important technical specifications for both applications of X-rays camera and data processing of other relevant images.

9273-56, Session Post

An example image super-resolution algorithm based on modified k-means with hybrid particle swarm optimization

Kunpeng Feng, Harbin Institute of Technology (China); Tong Zhou, Heilongjiang Provincial Institute of Measurement & Verification (China); Jiwen Cui, Jiubin Tan, Harbin Institute of Technology (China)

This paper presents a novel example-based super-resolution algorithm with improved k-means cluster. In this algorithm, genetic k-means with hybrid particle swarm optimization is employed to improve the reconstruction of high-resolution images and pre-processing of classification in frequency accelerates the procedure. Self-redundancy across different scales of a natural image is also utilized to build attached training set to expand example-based information. As the same time, a reconstruction algorithm based on hybrid supervise locally linear embedding is proposed which uses both training sets and high-resolution images and pre-processing of classification in frequency accelerates the procedure. Self-redundancy across different scales of a natural image is also utilized to build adequately. Experimental results indicate that patches are classified rapidly in training set processing session and the runtime of reconstruction is half of traditional algorithm at least in super-resolution session. And clustering and attached training set lead to a better recovery of low-resolution image.

9273-57, Session Post

Noise reduction for stereo matching with adaptive cost function

Hao Chen, Hong Zhang, Ding Yuan, Feiyang Cheng, BeiHang Univ. (China)

Local stereo correspondence methods give competitive results recently by using filters to aggregate the matching costs. Thanks to the edge-preserving characteristic of these filters, the depth edges can be preserved effectively. However, the pixel-based matching costs often suffer noise within highly textured regions, and the noise will remain since the smooth power of the filters is depressed near the colour edges. Hence, it seems contradictory to reduce the noise and preserve the details of edges simultaneously. Enhancing the quality of the input signal, i.e. the matching cost, is a feasible solution to the above problem. Therefore, an adaptive cost function is addressed to achieve the noise reduction in this paper. Moreover, the details of the depth information on the edges could be successfully preserved. The experimental results proved that our method could surpass other top rank local methods on the Middlebury test bed.

9273-58, Session Post

Multimodal visual dictionary learning via heterogeneous latent semantic sparse coding

Chenxiao Li, Guiguang Ding, Jile Zhou, Yuchen Guo, Qiang Liu, Tsinghua Univ. (China)

Visual dictionary learning as a crucial task of image representation has gained increasing attention. Specifically, sparse coding is widely used due to its intrinsic advantage. However typical sparse coding methods focus on visual feature alone. As the explosion of web images with textual description, text data has become another significant source of image description. Many works demonstrate that text data can markedly improve the performance of various computer vision tasks. In this paper, we propose a novel heterogeneous latent semantic sparse coding model. The central idea is to bridge heterogeneous modalities by capturing their common sparse latent semantic structure so that the learned visual dictionary is able to describe both the visual and textual properties of training data.

The model comprises three parts. First, to assign image owned tags to individual local features, we propose an elegant approach which exploits image annotation and tag ranking techniques; second, to alleviate the impact of discrepancies between visual and textual spaces, we learn a continuous high-level textual feature space to replace the original discrete one; third, to leverage text tags in visual dictionary learning, we revise the traditional sparse coding model to attain concordant sparse coding between visual and textual modalities via a common semantic concept subspace.

Experiments on two real world image datasets equipped with annotations, LabelMe and Pascal VOC 2007, are extended to demonstrate the superior performance of our model over several recent visual dictionary learning methods such as K-means and Sparse coding on both image categorization and retrieval tasks.

9273-59, Session Post

Magnifying arbitrarily selected areas of fractal Chinese characters

Wei Zhang, Zhengbing Zhang, Yangtze Univ. (China)

Fractal theory has been widely used in many fields, one of which is fractal graphics generation. Iterated Function System (IFS) is an important mathematical tool to generate fractal graphics, such as fern, Sierpinski gasket, dragon, twin Christmas trees, snowflake, tree, and crystal. IFS has also been used to generate fractal Chinese characters that are self-similar and have details at every scale. These properties make fractal Chinese characters useful in broad areas, such as digital watermark, arts, encryption, and new Chinese font. In order to show details of any given area, a fractal Chinese character magnification method is proposed in this paper to zoom in on an arbitrarily selected area. For any selected area within a fractal Chinese character, a geometric transform is done to make the selected area occupy the full display area. In addition, a magnification factor and a displacement vector relative to the display area of the fractal Chinese character are calculated with the derived formula in this paper. Then the mapping coefficients of the IFS for the Chinese character are modified according to the magnification factor and the displacement vector such that the fractal pattern of the Chinese character in the selected area can be just shown in the full display area. A modified random iteration algorithm is proposed and used to show the magnified fractal pattern of the selected area. The experimental results demonstrate that details are shown clearly with the magnification factor being up to 2000 and even more.

9273-60, Session Post

Adaptive block size selection for inter-layer backward view synthesis prediction

Li Chen, Univ. of Science and Technology of China (China); Miska M. Hannuksela, Nokia Research Ctr. (Finland); Houqiang Li, Univ. of Science and Technology of China (China)

Traditional forward view synthesis prediction enables the efficient use of depth to provide synthesized frames for texture reference in non-base layers. But asserted drawbacks of high complexity that results from edge detection, hole-filling, up sampling and down sampling in forward warping technique compromise the positive performance. Hence, backward view synthesis prediction is proposed to remove these drawbacks while maintaining the performance. However, fixed depth block used in backward view synthesis prediction limits the performance gain and the number of motion compensation operations, which is a requisite concern of complexity analysis. In this paper, a block based BVSP for inter-layer prediction with only high-level syntax changes is implemented and an adaptive depth block size selection method is proposed. The experimental results show that an average gain of 3.5% bitrate reduction was achieved and after enabling adaptive depth block size selection, this performance gain is relatively maintained while the number of motion compensation operations were reduced to a designated level.

9273-62, Session Post

Recovery phase based on quadratic programming

Juan Ge, Anhui Univ. (China)

Most of the information of optical wavefront is encoded in the phase which includes more details of the object. Conventional optical measuring apparatus can only record the intensity of light, but can not measure the phase of light directly. Thus it is important to recover the phase from the intensity measurements of the object. In recent years, the methods based on quadratic programming such as PhaseLift and PhaseCut can recover the phase of general signal exactly for overdetermined system. To retrieve the phase of sparse signal, the Compressive Phase Retrieval (CPR) algorithm combines the l_1 -minimization in CS with low-rank matrix completion problem in PhaseLift, but the result is unsatisfied. This paper focus on the recovery of the phase of sparse signal and propose a new method called the Compressive Phase Cut Retrieval (CPCR) by combining the CPR algorithm with the PhaseCut algorithm. To ensure the sparsity of the recovered signal, we use CPR method to solve a semi-definite programming problem firstly. Then apply linear transformation to the recovered signal, and set the phase of the result as the initial value of the PhaseCut problem. We use TFOCS (a library of Matlab-files) to implement the proposed CPCR algorithm in order to improve the recovered results of the CPR algorithm. Experimental results show that the proposed method can improve the accuracy of the CPR algorithm, and overcome the shortcoming of the PhaseCut method that it can not recover the sparse signal effectively.

9273-63, Session Post

Laser 3D imaging technology based on digital micromirror device and the performance analysis

Xiaochun Han, Yalan Xue, Yuanqing Wang, Nanjing Univ. (China); Liqun Cao, Lei Han, Biye Zhou, Minggao Li, Navy General Hospital (China)

Current research on scannerless three dimensional imaging LiDAR mainly focus on the phase scannerless imaging LiDAR, the multiple-slit streak tube imaging lidar and the flash LiDAR. But there are the disadvantages, such as short detection range, the complicated structure of vacuum unit and lacking the grayscale images corresponding to the three kinds of LiDAR listed above. In this paper we develop a novel 3D imaging LiDAR that works in the way of pushbroom. It converts the time of flight (TOF) into the space with digital mirror device (DMD). When pulse arrives at the DMD, the micromirrors are shifting from a status to another. Because the TOFs of pulses hit on different targets are different, there will be the streak on the focal plane array (FPA) of the sensor, which shows the relative position. The relative position of the streak can be used to reconstruct the range profile of the target. Compared with other three dimensional imaging method, this new method has the advantages of high rate imaging, large field of view, simple structure and small size. First, this article introduces the theory of digital micromirror laser 3D imaging LiDAR, and then it analyses the technical indicator of the core component. At last, it gives the process of computing the detection range, theoretically demonstrat-ing the feasibility of this technology.

9273-64, Session Post

Abnormal behaviors detection using particle motion model

Yutao Chen, Hong Zhang, Feiyang Cheng, Ding Yuan, BeiHang Univ. (China); Mingui Sun, Univ. of Pittsburgh (United States)

Human abnormal behaviors detection is one of the most challenging tasks in the video surveillance for the public security control. Interaction Energy Potential model is an effective and competitive method published recently to detect abnormal behaviors, but their model of abnormal behaviors is not accurate enough, so it has some limitations. In order to solve this problem, we propose a novel Particle Motion model. Firstly, we extract the foreground to improve the accuracy of interest point detection since the complex background usually degrade the effectiveness of interest point detection largely. Secondly, we detect the interest points using the graphics features. Here, the movement of each human target can be represented by the movements of detected interest points of the target. Then, we track these interest points in videos to record their positions and velocities. In this way, the velocity angles, position angles and distance between each two points can be calculated. Finally, we proposed a Particle Motion model to calculate the characteristic value of each frame. An adaptive threshold method is also proposed to detect abnormal behaviors. Experimental results on the BEHAVE dataset and online videos show that our method could detect fight and robbery events effectively and has a promising performance against other methods.

9273-65, Session Post

Kernel based discriminant image filter learning: application in face recognition

Lingchen Zhang, Sui Wei, Lei Qu, Anhui Univ. (China)

The extraction of discriminative and robust feature is a crucial issue in pattern recognition and classification. Before feature extraction is applied, the image is commonly preprocessed by one or more filters to enhance the useful image information or reduce the effect of illumination and noise. Generally, these image filters are designed in a handcraft or analytical way but specialized to a certain dataset. As result, only limited enhancement can be obtained and the discriminability of features is mainly depend on the performance of following feature descriptors.

In this paper, we propose a kernel based discriminant image filter learning method (KDIFL) for local discriminant feature enhancing and demonstrate its superiority in the application of face recognition. Instead of designing the image filter in a handcraft or analytical way, we propose to learn a kernel based image filter so that after filtering the intra-class difference is attenuated and the inter-class difference is amplified, thus facilitate the following feature extraction and recognition. First, the neighbor of each pixel in the training images is extracted and vectorized to form the neighbor-vector matrix (NVM). Then, the 2D-GDA is applied on the NVM to learn the transformation and generate the filtered image. In 2D-GDA, the kernel trick is employed to increase the ability of algorithm in handling the nonlinear feature space problem. Different to holistic feature extraction method such as LDA and KLDA/GDA, the proposed filter can produce more discriminative local appearance features, and the local features have been approved to be more superior to the holistic ones. We show that the proposed filter is generalized and it can be concatenated with classic feature descriptors (e.g. LBP) to further increase the discriminability and robustness of extracted features. Our extensive experiments on Yale, ORL and AR face databases validate the effectiveness and robustness of the proposed method.

9273-66, Session Post

An effective representation for action recognition with human skeleton joints

Xingyang Cai, Wengang Zhou, Houqiang Li, Univ. of Science and Technology of China (China)

With the development of depth sensor technologies, human action recognition with 3D joints is receiving a growing interest in the computer vision community. In this paper, we propose a novel method to recognize human actions using 3D human skeleton joint points. First, we represent a skeleton pose by a feature vector with three descriptors: limb orientation, joint motion orientation and body part relation. The three descriptors represent the pose with motion information, which is effective to distinguish two identical poses with different motion directions. Then, we apply data mining techniques to mine discriminative local basic motions based on the sequences of feature vectors. These local basic motions contain the discriminative motions of key joints and can well represent human actions since each human action can be divide into several local motions. Finally, we provide a new way to model and recognize human actions by these local basic motions. Experiments conducted on MSR Action3D Dataset and MSR Daily Activity3D Dataset demonstrate the effectiveness of the proposed algorithm and a superior performance over the state-of-the-art techniques.

9273-67, Session Post

A combined ASEF and pictorial structure method for facial landmark detection

Yan Wang, Sui Wei, Lei Qu, Anhui Univ. (China)

Facial landmark localization is a crucial step in many facial image analysis applications, including face recognition, expression recognition and gaze or blink detection. The efficiency and accuracy are two general requirements of landmark localization algorithm. The Average of Synthetic Exact Filter (ASEF) has exhibited its impressive performance in the application of eyes localization. However, the accuracy of ASEF will deteriorate severely when the number of landmark is large. One reason is that the relative position of facial landmarks is not intrinsic considered in ASEF. As a correlation filter, the ASEF train the filter for each landmark separately, and the landmarks are detected separately as well with corresponding filter.

In this paper, we propose a combined ASEF and pictorial structure method for facial landmark detection, where the global knowledge of landmark distribution can be efficiently considered. First, the local-maximums of the ASEF response image for each landmark are extracted as candidates. Then, with the consideration that the facial landmarks is highly stereotyped, the ASEF response of candidates for each landmark and their relative positions are evaluated by the pictorial structure model. Finally, the combination of candidates with highest score is selected as the final detection result. In pictorial structure model, the relative position relationship is learned from training data. We show that by introducing the position constraint, the detection accuracy can be highly improved. The experimental results on the BioID dataset verify the efficiency and accuracy of proposed method.

9273-68, Session Post

Text processing in real-time stereo matching system

Jianzhong Yi, Tsinghua Univ. (China); Xin Jin, Graduate School at Shenzhen, Tsinghua Univ. (China); Yebin Liu, Tsinghua Univ. (China)

Text data including texts in nature scene and artificial subtitles embedded in frames of Stereo Matching System always contains abundant information about current scene or video content. As characteristics of human vision system, texts are more likely to be focused on when we are watching 3D movies. However, texts are usually considered the same as other elements in the process of stereo matching in traditional algorithms, which leads to bad visual effects such as text blur and broken strokes. We propose a complete text processing system to extract disparity map of text pixels fast and accurately comprising three steps: text location, text matching and disparity map merging, during which we combine traditional stereo matching and text locating algorithms. First we divide images into two parts: scene and artificial subtitles, and after pre-processing separately of each part a fast stroke filter will be used to the whole images to extract response maps in which strokes get high responses and other elements including strong edges of background are usually eliminated. Then a novel generalized Hough Transform method and watershed algorithm are applied to locate text and calculate disparity maps of text pixels. Maps Merging as the last step is designed to generate the final disparity in various weighted coefficients derived from edge and response maps and to be updated using spatial pairwise information. The robustness and efficiency of our system has been verified by extensive experiments on videos of complex contents.

9273-69, Session Post

Image segmentation using an improved differential algorithm

Hao Gao, Ye Liu, Baojie Fan, Yu Jiao Shi, Nanjing Univ. of Posts and Telecommunications (China)

Image segmentation plays an important role in the field of computer vision. Among all the existing segmentation techniques, the thresholding technique is one of the most popular due to its simplicity, robustness, and accuracy (e.g. the maximum entropy method, Otsu's method, and K-means clustering). However, the computation time of these algorithms grows exponentially with the number of thresholds due to their exhaustive searching strategy. Optimization method is the process of trying to find the best possible solution to an optimization problem within a reasonable time limit. Thus, applying optimization method into segmentation algorithm should be a good choice during to its fast computational ability. As a population-based optimization algorithm, differential algorithm (DE) uses a population of potential solutions and decision-making processes. It has shown considerable success in solving optimization problems characterized by nonconvex, disjoint, or noisy solution spaces. But how to further accelerate its convergence rate and enhance its global search ability still merits further discuss. In this paper, we first propose a new differential algorithm with a balance strategy, which seeks a balance between the exploration of new regions and the exploitation of the already sampled regions. Then, we apply the new DE into the traditional Otsu's method to shorten the computation time. Experimental results of the new algorithm on a variety of images show that, compared with the EA-based thresholding methods, the proposed DE algorithm gets more effective and efficient results. It also shortens the computation time of the traditional Otsu method.

9273-70, Session Post

Haze removal based on variation of detail prior

Jiafeng Li, Hong Zhang, Ding Yuan, BeiHang Univ. (China)

In this paper, we present a novel image prior named the Variation of Detail (VD) prior to remove haze from a single input image. The VD prior is proposed according to the multiple scattering phenomenon in the propagation of light which is ignored in other methods. By adopting the VD in the haze imaging model, the thickness of the haze and optical transmission can be estimated reasonably, and consequently the high quality haze-free image is recovered. Our method is stable to the fore scene's cover. Moreover it is able to handle both color images and gray level images since our VD is based on the information of image details. Extensive experiments showed that the proposed method achieved better results than many state-of-the-art algorithms, and it can be implemented very quickly.

9273-71, Session Post

Target tracking techniques based on non-scanning imaging lidar

Chen Sui, Beijing Institute of Technology (China)

Target tracking technology is to find the moving object which needs to be tracked in a series of continuous images, and extract the moving speed, location, and characteristic of the target. In our system, we use non-scanning imaging lidar which has a resolution of 2048x2048 and a measurement accuracy of 3mm, to obtain the intensity images, amplitude images and range images of the target at the same time. In this paper, in order to obtain the target information, we take following steps to process the collected intensity images. First we extract the target characteristics including the barycenter of target and its external rectangle based on codebook model. And then we use connected domain method for further image denoising, and calculate the external rectangle and center of mass. After obtaining the target position information, we use ARM to control the electric turntable with stepper motor to drive the laser radar's

9273-72, Session Post

Modeling of polarimetric BRDF characteristics of painted surfaces

Ying Zhang, Zeying Wang, Huijie Zhao, BeiHang Univ. (China)

In this paper polarimetric BRDF models of painted surfaces coupled with various modeled atmospheric polarization characteristics were developed and the output polarization of light as a simulation of the light entering the imaging system was derived. Firstly, the polarimetric BRDF model of painted surfaces was developed according to the theory presented by G. Priest based on microfacets and the downwelled skylight polarization under various atmospheric conditions was modeled based on the vector radiative transfer model RT3 using different atmospheric parameters. Secondly, adding the modeled polarimetric factors of incident diffused skylight, the modeled polarization state of reflected light from the surfaces was achieved through integrating the directional polarimetric information of the whole hemisphere. The target-sensor path is assumed to be negligible since it is relatively short in the current imaging geometry. So the reflected light is equivalent to the light entering the imaging system. The modeled results are related to the solar-sensor geometry, atmospheric conditions and the features of the painted surfaces. Then, after achieving the modeled

results, a full-polarized imaging polarimeter based on liquid crystal variable retarders was used to measure the polarimetric data of certain painted surfaces under different weather and geometric conditions in accordance with the parameters in the model. Finally, it was found that the two results can agree well on qualitative features by comparing the measured data with modeled data under different conditions. Also, the polarization features of the surfaces are invariant with the weather conditions. This result can be used to optimally invert the surface parameters ignoring the bad weather and improve the accuracy of target detection and material classification.

9273-73, Session Post

A three-dimensional shape measurement system based on fiber-optic image bundles

Cheng Zhen, Huijie Zhao, Xiaoyue Liang, Hongzhi Jiang, BeiHang Univ. (China)

A three-dimensional shape measurement system based on multipath fiber-optic image bundles was proposed to measure three-dimensional shape of complicated objects in confined space. Multipath fiber-optic image bundles have advantage of flexibility and have the structure that one end is integrated and the other is branched. It can integrate multi-view images to a single image and split a single image into multi-view images. First, based on the principle of phase shifting which is an efficient method of non-contact measuring technique and advantages of multipath fiber-optic image bundles, the mathematical model of the multi-view measuring system was established, the parameters of the system is simulated, and hardware and software platform of the system was set up. Then, the global calibration algorithm of the measuring system is realized. The problems of poor quality images, low resolution and high noise brought by multipath fiber-optic image bundles were analyzed, after which a viable solution was proposed. Finally, tests for objects in confined space were performed by using the three-dimensional shape measurement system. As the transmission media of the system, multipath fiber-optic image bundles achieved picture's flexible acquisition and projection because of the light path which could be changed as expected. The three-dimensional shape of the object was reconstructed after data processing of multi-view images. Experimental results indicated that the system was miniature and flexible enough to measure the three-dimensional shape of complicated objects in confined space. It expanded the application range of structured-light three-dimensional shape measuring technique.

9273-74, Session Post

Image fusion driven by the analysis of sparse coefficients

Xiujuan Yu, China Waterborne Transport Research Institute (China); Hanwen Zhao, Xiaoyan Luo, Ding Yuan, BeiHang Univ. (China)

In various imaging systems, with the property of sensors, the images can capture different characteristics from the scene, but it is difficult to catch all salient scene information using only one sensor. Thus, to generate an image with more comprehensive features, image fusion for a scene is still an important yet challenging problem. This paper proposes an efficient fusion method for multiple images based on sparse representation. The main point of this paper lies in the ability to solve the fusion rules of the sparse coefficients.

The proposed fusion method consists of three main steps. First is to obtain the sparse coefficients of different source images based

on a dictionary which is trained by a classic image decomposed approach. The second step is to fusing the sparse coefficients via a serial of fusion rules. Considering the sparsity, the source coefficients can be divided into salient large and common small values. According to the analysis and comparison of permutations such as salient-salient, salient-common, common-common, the final coefficients are fused in the term of data. In the third step, the fused image can be reconstructed via combining the fused coefficients and trained dictionary.

The proposed fusion rules achieve robust performances for different kinds of sparse representation methods. Moreover, the fusion processing for the representation coefficients is resistant to the variety of the source images. We believe that the proposed scheme can be employed to many applications. Some simulation results demonstrate its effectiveness.

9273-75, Session Post

Synthesis multi-projector content for multi-projector 3D display using a layered representation

Chen Qin, National Univ. of Defense Technology (China)

Multi-projector three-dimensional display(MPD) is a kind of multi-view three-dimensional(3D) display technique which needs not wear 3D glasses or other additional equipments. The pickup subsystem of MPD is a camera array and the display subsystem of MPD consists of a projector array and a diffuser screen. Similar to integral imaging display, MPD also suffers from the pseudoscopic problem. The display phase in MPD is the reverse process of the record phase in MPD, so the reconstructed 3D images are depth reversed. It is necessary to solve the pseudoscopic problem when using MPD to produce stereoscopic image. The goal of our work is to generate the layered depth video(LDV) from a small number of camera videos, and render source images for the projector array with interactive viewing control while avoiding the pseudoscopic problem. The procedure of LDV combines algorithms of several areas in computer vision, such as camera calibration, stereo matching, depth estimating and layers separation. Once these video streams of LDV is generated, we can treat each frame of LDV as a 3D object, then render it to projector image with a tetrahedral projection transform. We also verify our approach on a 100-inch MPD system, the displayed 3D image is stereoscopic. In conclusion, our study show that using a custom tetrahedral projection transform is a solution of the pseudoscopic problem in MPD, and LDV is suitable for MPD.

9273-76, Session Post

Fiber bundle high-resolution confocal endomicroscopy for in vivo mice imaging

Ling Fu, Huazhong Univ. of Science and Technology (China)

In recent years, the development of endomicroscope is very fast. But this area is still in urgent need of high-speed and high-resolution instrument. Here we present a fiber bundle confocal endomicroscope with the lateral resolution of 2.2 μm and the imaging speed of 4 fps or 8 fps. Fiber optic probe of the endomicroscope is the key technical hurdle of the development of this instrument. The diameter of the probe is 2.6 mm, which enables its direct conjunction application to the conventional endoscopes. We have applied the endomicroscope to the gastrointestinal tract of mice. After anesthesia and intravenous injection of the 10% sodium fluorescein, the crypts of the colon could be clearly seen from the screen of the endomicroscope. The columnar epithelial cells arranged closely and the goblet cells dotted around the crypts. These are consistent with the corresponding histologic specimen. The result with the cellular

resolution shows that this endomicroscope has a great potential applications in experimental study. Because of the high-speed and high-resolution feature, the probe based fiber bundle endomicroscope, which represents the development direction of endomicroscope, has a vast potential applications in clinical and is increasingly being valued by the medical institutions.

9273-77, Session Post

Virtual assembly system of gear oil pump based on Virtools

Panpan Wang, Hong Zhang, Taiyuan Univ. of Technology (China)

Mechanical drawing is a course describing the mechanical structure with design shape, size, working principle and technical requirements of the subject. It combines the theoretical teaching and the engineering practice ability training. It is to cultivate students' space imagination, creativity and drawing skills for the purpose. Due to the particularity of this course, a lot of model animations constitute the main body of mechanical drawing course. In order to achieve better teaching effect, the students need physical models to assist themselves in learning. With the further development of higher education reform, many schools start to enlarge the recruitment and building. But due to the lack of funds, experimental facilities can't meet the needs of the increasing number of students. With the continuous development of computer and network technology, virtual reality technology is attracting more attention. It can overcome the lack of investment in laboratory of colleges and the problems of maintenance in experimental instrument. Based on the analysis of engineering drawing teaching and the characteristics of virtual reality, a virtual measuring system for mechanical part and assembly on network is developed. Three-dimensional mechanical design software, 3DSMAX and Virtools are applied in this system. It is easy to operate, not subject to time and place and has strong interaction, which improves the initiative of students and enriches the engineering drawing teaching system.

9273-78, Session Post

Coupled data association and L1 minimization for multiple object tracking under occlusion

Xue Wang, Qing Wang, Northwestern Polytechnical Univ. (China)

We propose a novel multiple object tracking framework that combines data association and L1 minimization that exploits figure/ground assignment. Though L1 trackers have showed impressive tracking accuracy, they are computationally demanding for multiple object tracking. Conventional data association methods with bounding box representation for detection suffer because of the background pixels in the target region and non-reliable detections in cluttered scenes. The proposed algorithm mediates between region correspondence and L1 trackers according to whether an occlusion is detected in the scene. Moreover, the figure/ground assignment is used to eliminate the influence of background pixels in both candidate regions for data association and target templates for L1 trackers. Figure/ground assignment is computed using robust principal component analysis for the videos with stationary background and a contour and region detector for the videos with moving background. The robust tracking performance of our approach has been validated with a comprehensive evaluation involving several challenging sequences and state-of-the-art multiple object trackers.

9273-79, Session Post

Hierarchical feature selection for erythema severity estimation

Li Wang, Univ. of Science and Technology of China (China); Chenbo Shi, Tsinghua Univ. (China); Chang Shu, Peking Union Medical College Hospital (China)

As present, PASI system of scoring is used for evaluating erythema severity, which can help doctors to diagnose psoriasis. The system relies on the subjective judge of doctors, where the accuracy and stability cannot be guaranteed. This paper proposes a stable and precise algorithm for erythema severity estimation.

Our contributions are twofold. On one hand, in order to extract the multi-scale redness of erythema, we design the hierarchical feature. Different from traditional methods, we not only utilize the color statistical features, but also divide the detect window into small window and extract hierarchical features. Further, a feature re-ranking step is introduced, which can guarantee that extracted features are irrelevant to each other. On the other hand, an adaptive boosting classifier is applied for further feature selection. During the step of training, the classifier will seek out the most valuable feature for evaluating erythema severity, due to its strong learning ability.

Experimental results demonstrate the high precision and robustness of our algorithm. The accuracy is 82.3% on the dataset which comprise 282 patients' images with various kinds of erythema. Now our system has been applied for erythema medical efficacy evaluation in Union Hospital, China.

9273-80, Session Post

Automatic segmentation of psoriasis lesions

Yang Ning, Chenbo Shi, Tsinghua Univ. (China); Li Wang, Univ. of Science and Technology of China (China); Chang Shu, Peking Union Medical College Hospital (China)

Recently, automatic segmentation of psoriatic lesions attracts more attentions, which is the key step of the computer-aided medical diagnosis. For instance, psoriatic lesions diagnosis needs to segment the area the lesion including erythema and scaling. Erythema and scaling are always accompanied with each other. However, traditional methods can only deal with one of them. In contrast, this paper presents an efficient segmentation based on support vector machine (SVM).

Our algorithm follows 4 steps. First, the polarized light is introduced on the skin's Tyndall-effect during imaging to eliminate the reflection. Second, in order to separation the erythema and scaling from normal skins, we convert the RGB color space to LAB space based on the human perception. Third, sliding window and its sub-windows are utilized to extract textural and color features. During the process, a novel description of image smoothness is proposed, so that scaling can be easily separated from other skins. Finally, we design the support vector machine for feature learning and automatic segmentation.

Experiments and results verify the robustness of our algorithm, which can segment erythema and scaling under variant illuminations, skin types and etc. On the dataset provided by Union Hospital, China, 92.7% images can be segmented precisely.

9273-81, Session Post

3D reconstruction of large target by range gated laser imaging

Sining Li, Wei Lu, Dayong Zhang, Harbin Institute of Technology (China)

We have developed a whole set of range gated laser imaging system with ~3km maximum acquisition distance, the system uses a Nd:YAG electro-optical Q-switched 532nm laser as transmitter, a double micro channel plate as gated sensor, all the components are controlled by the a trigger control unit with accuracy of subnanosecond. A imaging scheme is designed for imaging the large building ~500m away, and a sequence of images are obtained in the experiment, which are the basic data for 3D reconstruction; to improve the range resolution, we study the temporal distribution of intensity of the received signal, and use centroid algorithm for data processing. We compare the 3D image with the theoretical model, and the result is consistent.

9273-82, Session Post

A no-reference contourlet-decomposition-based image quality assment method for super-resolution reconstruction

Wei Zhang, Zhongcheng Fan, Beihua Univ. (China)

The purpose of super resolution is to increase the high-frequency components and removing the degradations caused by the imaging process. So a high quality reconstruction image should increase the amount of efficient information while keep highly similar to the original image. The existing image quality assessment methods usually measure the similarity between the low resolution image and reference image, which can not be satisfied in many actual super-resolution reconstruction applications. A no-reference image quality assessment method for super-resolution reconstruction is proposed in this paper. The basic idea is to perform a Contourlet multiscale decomposition of low resolution image and reconstructed super-image first. According to the relativity of the Contourlet coefficient, the reconstructed image is divided into sharp edges, image texture and flat region. Then, calculate the ringing intensity index of sharp edges, the blur extent index of the image texture and the directional entropy index of the high frequency components. Finally, the result to evaluate the reconstructed image quality is obtained by integrated these indexes into one total image quality index. Several experimental results using both simulated and real images demonstrate the new index is efficient and stable for evaluating the quality of the reconstructed super-resolution image. It performs well in accordance with human subjective vision.

9273-84, Session Post

Real-time Remote Three-dimensional Super-resolution Range-gated Imaging based on Inter-frame Correlation

Xinwei Wang, Institute of Semiconductors (China) and City Univ. of Hong Kong (Hong Kong, China); Yanan Cao, Wei Cui, Xiaoquan Liu, Songtao Fan, Dezhen Lu, Yan Zhou, Institute of Semiconductors (China); Youfu Li, City Univ. of Hong Kong (Hong Kong, China)

High-resolution real-time three-dimensional imaging is important in the applications of 3D video surveillance, robot vision, and automatic navigation. However, current real-time 3D imaging techniques (e.g. time-of-flight (TOF) camera, 3D flash LIDAR, and stereo imaging) have a low resolution or a short operation distance which cannot satisfy some high-resolution applications of remote sensing. In this paper, a three-dimensional super-resolution range-gated imaging based on inter-frame correlation is proposed to realize high-resolution flash 3D imaging. In this method, gate images with triangular range-intensity profiles are grasped by the convolution of laser pulse and sensor gate pulse, and then depth information collapsed in 2D images can be reconstructed by spatial-temporal inter-frame correlation of two overlapped gate images. Since a CCD/CMOS with a gated image intensifier is used as an image sensor to collect echo signal reflected by targets under pulsed laser illumination, 3D imaging with a resolution of about 1000²1000 full-frame pixels can be realized within a frame. To improve the real time performance, inter-frame correlation is used. A 3D scene is reconstructed by the spatial-temporal correlation between the current frame and the previous frame, and thus a 3D point cloud frame is generated at video rates corresponding to CCD/CMOS utilized. Compared with super-resolution depth mapping under trapezoidal range-intensity profiles, range accuracy and precision are improved. Finally, some proof experiments are demonstrated in this paper.

9273-85, Session Post

Improved sequential search algorithms for classification in hyperspectral remote sensing images

Songyot Nakariyakul, Thammasat University (Thailand)

Two new sequential search algorithms for feature selection in hyperspectral remote sensing images are proposed. Since many wavebands in hyperspectral images are redundant and irrelevant, the use of feature selection to improve classification results is highly needed. First, we present a new generalized steepest ascent (GSA) feature selection technique that improves upon the prior steepest ascent algorithm by selecting a better starting search point and performing a more thorough search. It is guaranteed to provide solutions that equal or exceed those of the classical sequential forward floating selection algorithm. However, when the number of available wavebands is large, the computational load required for the GSA algorithm becomes excessive. We thus propose a modification of the improved floating forward selection algorithm which is more computationally efficient. Experimental results for two hyperspectral data sets show that our proposed algorithms yield better classification results than other suboptimal search algorithms.

9273-86, Session Post

Image feature point detection method based on the pixels of high-resolution sensors

Xingchun Liu, Zhe Wang, Zhipeng Hu, BeiHang Univ. (China); Jiancheng Zhang, Beijing Institute of Technology (China)

Through analyzing the characteristic of high resolution image obtained by high resolution sensor when the size of sensor is fixed, a new fast feature point detecting method is put forward. Firstly, select the one of images to be matched as a reference image; secondly, sample points in fixed step in all directions of the coordinates of this image, and take its 4-neighborhood point as judgment auxiliary point of the feature point, that is the feature information be described by 4-neighborhood feature of the sampling point; then select extreme points as candidate feature points by preset threshold calculation ; finally, add up the average deviation of the above candidate feature points in the horizontal and ordinate direction, and obtain a descending order of the above summation values, then by further filtering to select the accurate feature points for image matching. So, these feature points in this algorithm have local extreme characteristic, and these extreme values are excellent extreme points in a certain threshold condition, and have a large amount of information. At last, through the discussion of the principle of the method and the analysis of various experimental results can be seen, the new method fully considers the characteristic of high resolution sensor, compared with the traditional feature points extraction algorithm, no longer to traverse the redundant points, So it reduce the algorithm complexity, and achieve more quickly and efficiently extraction. At the same time, this algorithm has a good adaptability and accuracy on translation, rotation and stretch of image, which accuracy can reach above ninety percent.

9273-87, Session Post

Research of indoor positioning techniques based on visible light communication

Shumo Li, Ajian Hu, Dawei Zhang, Huazhong Univ. of Science and Technology (China); Andong Wang, Wuhan Univ. of Technology (China)

Indoor positioning system based on visible light communication has gained popularity due to the widespread introduction of white LED. Visible light positioning (VLP) has the advantages such as no radiofrequency interference, power saving and huge available bandwidth which has not been used yet. This paper introduces the current situation of VLP and analyzes three typical VLP techniques: triangulation, scene analysis and proximity. Triangulation includes TOA, TDOA, AOA and RSS. TOA utilizes the time from the transmitter to the receiver to calculate the distance. The algorithm is quite simple but accurate synchronization of all the transmitters and receivers can be much difficult. AOA measures the angles of arriving signals and finds the intersection of all direction lines. No synchronization is needed but the positioning accuracy will decrease when the receiver moves further. RSS develops a path loss model to build the relationship between the optical path and the light intensity loss. However, due to the unpredictable variation power of the transmitters and the multipath effects, the positioning accuracy will also decline dramatically. TDOA technique is discussed in detail since it is the most promising method. TDOA measures the time difference of arrival to get the position of the receiver, so there is no need to be synchronized between the transmitter and the receiver. Then comprehensive performance comparisons of these techniques including accuracy, precision, complexity, robustness, and cost are presented. Finally, conclusions and

prospects are made. There are also some problems remained to be solved and new techniques are in urgent need.

9273-89, Session Post

Monte Carlo simulation of echo signal in airborne laser underwater detection

Cheng Hua, Wang Hua Chuang, Fu Cheng Yu, Song Qing Huan, Xu Bo, Institute of Optics and Electronics (China)

This paper analyzed the shortcomings and defects of the Monte Carlo simulation method in airborne laser underwater detection at home and abroad, and puts forward a new simulation idea and simulates the whole formation process of echo signals, which is of simple principles and high efficiency. We make analysis of the transmission of laser in air and through air into seawater, the transmission of laser in seawater, the reflection at the sea bottom and the transmission of laser through seawater into air. In this paper, firstly the receiver is regarded as a circular receiver above seawater, then computes the direction of photons out of seawater, finally estimate whether the photons are received by the receiver according to the direction of photons.

9273-90, Session Post

Asymmetric multiview image coding based on feature matching

Wenjun Tao, Huihui Bai, Meiqin Liu, Yao Zhao, Beijing Jiaotong Univ. (China)

In this paper, we propose a method of feature matching based two-stage three-dimensional (3D) image coding with hierarchical reconstruction quality. Here, take three views labeled by C1, C2, C3, as an example to present the proposed scheme. At the encoder, asymmetric coding mode is designed for main view and its neighboring views. For the main view C2, H.264 intra coding can be applied to obtain high reconstruction quality. For its neighboring views C1 and C3, the novel coding mode is proposed in this paper and it contains two stages. In the first stage, we extract SIFT feature descriptors of C1, C2, C3, respectively, and then calculate transformation matrix (3×3 size) between views by RANSAC and SIFT feature descriptors. The generated transformation matrix between C1 and C2 can be labeled by H21 and the transformation matrix between C1 and C3 can be labeled by H23. The parameters of transformation matrix can be coded by very low bit rate to produce the bit stream in the first stage. At the decoder, H21 and H23 can be used respectively to transform C2 to achieve the preliminary reconstruction of C1 and C3. In the second stage, the residues are obtained from the preliminary reconstructed images and original images, which can be applied to improve the performance. The experimental results have shown that the proposed scheme can reach a very high compression ratio. Furthermore, with the change of the compression ratio, the proposed scheme can achieve more stable image reconstruction quality.

9273-92, Session Post

Image restoration for underwater laser imaging

Huachuan Huang, Southwest Univ. of Science and Technology (China) and China Academy of Engineering Physics (China) and Nanjing Univ. of Science and Technology (China); Keding Yan, Nanjing Univ. of Science and Technology (China); Zhengang Yan, Xi'an Modern

Control Technology Research Institute (China); Rongbo Wang, China Academy of Engineering Physics (China); Zhenhua Li, Nanjing Univ. of Science and Technology (China); Zeren Li, China Academy of Engineering Physics (China)

Laser imaging under water is of great significance in underwater search, marine science, and military, etc. However, traditional underwater laser imaging is often of poor quality with noises and blurs, moreover, the resolution of the image will also decrease. In order to obtain clear underwater images with high resolution and quality, here, we have designed and realized an image restoration approach. Through calculating point spread function and modulation transfer function of the imaging system, high resolution and quality images could be recovered from directly obtained images under water. In this paper, based on the introduction to the imaging system and image restoration algorithm, the experiment is established by setting the imaging system under water in the lake to capture the underwater targets. With the proposed underwater image restoration approach, images of high quality could be retrieved which proves that the method is able to identify the target -10 meters away under water.

9273-93, Session Post

Annular ring-like stream 3D images display analysis

Junewen Chen, Chung Hua Univ. (Taiwan)

An annular ring-like stream of aerosol or fluid, 3D images display, 360° view of objects, hardwareless display system without a concrete and definitive screen. Images that are projected on annular ring-like stream of aerosol or fluid can penetrate into the layer-like aerosols and thus displays 3D image are analyzed in detail. The real interactive results of models show is demonstrated using our non-concrete-type, 360°-view, 3D displays.

9273-94, Session Post

Small infrared object detection and extraction in complex sea-sky background based on wavelet and curvelet transform

Xiangyu Kong, Nanjing Univ. of Science and Technology (China)

In the border and coastal defense warning system, infrared target detection under the sea and sky background is the key technology to find and recognize intrusive targets. Due to the complexity of the noise signal in sea-sky background, while the distant infrared small targets under the sea and sky background usually appear around sea-sky-line, in order to reduce the amount of computation, sea-sky-line detection is needed firstly. And then we detect the object in sea and sky region.

In this paper, wavelet tool is used to detect the sea-sky-line. Since wavelet transformation can decompose the original image in the spatial domain and the frequency domain at the same time, it is good at edge detection. We utilize the characteristic that the sea-sky-line is continuous and linear in low-frequency of infrared image to edge detect the sea-sky-line in the level 3 horizontal wavelet coefficients. The sea-sky-line can be found easily, the sea-sky-line is continuous and linear in low-frequency of infrared image.

Then curvelet transform is used to sparse represent the object region which is detected before, and identify the small infrared object. Because curvelet transform coefficients contain the information of scale, orientation, and spatial locations of the

image, they give more detail information about small targets. Curvelet transformation is applied on the original image, and binaryzation image is obtained by thresholding the coefficients. Then the potential targets are detected.

As a result, the algorithm can perform well that the moving infrared targets are recognized near the sea-sky-line even in complex sea-sky background.

9273-95, Session Post

A fast high-dynamic range algorithm based on HSI color space

Jiancheng Zhang, Xiaohua Liu, Liquan Dong, Yuejin Zhao, Ming Liu, Beijing Institute of Technology (China)

This paper presents a fast High Dynamic Range algorithm based on HSI color space. To keep hue and saturation of original image and conform to human eye vision effect is the first problem, first, convert the input image to XYZ(CIEXYZ) color space, and then convert the image data in XYZ color space to HSI color space which include intensity dimensionality. To raise the speed of the algorithm is the second problem, use integral image figure out the average of every pixel intensity value under a certain scale, as local intensity component of the image, and figure out detail intensity component. Although average filter has a defect, may lost details and has spreading effect, but image composition algorithm can eliminate this defect. To adjust the overall image intensity is the third problem, we can get an S type curve according to the original image information, adjust the local intensity component according to the S type curve. To enhance detail information is the fourth problem, adjust the detail intensity component according to the curve designed in advance. The weighted sum of local intensity component after adjusted and detail intensity component after adjusted is final intensity. Converting synthetic intensity and other two dimensionality to output color space can get final processed image. This paper propose an algorithm which not only consider over visual effect, but also reconstruct details of extreme bright and extreme dark area. Experimental results show result and speed are superior to other algorithm.

9273-96, Session Post

Amplitude and phase of single nanoparticle calculated using finite-difference time-domain method

Xin Hong, Huan Liu, Dalian Univ. of Technology (China)

The optical detection and characterization of single nanoparticles has significant application in biomedical optical imaging. The finite-difference time-domain (FDTD) has been a very powerful tool to solve electromagnetic scattering calculations. In this work, we present a model to calculate the electric amplitude and phase field distribution of single nanoparticle by using finite-difference time-domain (FDTD) method. It is found that, for small size nanoparticle, the FDTD method is rigorous to calculate the light scattering field of the single nanoparticle. We model the light-nanoparticle interaction by using a liner polarization light to illuminate the single nanoparticle through immersion oil and glass substrate. The illumination is set as a cone of plane waves limited by the aperture of the objective. While the single nanoparticle is difficult to directly detect because of its strong size dependence, causing the weak scattering field from single nanoparticle. So the scattering field summarized on a single detector is amplified by heterodyne interference with a reference light. The amplitude and phase distribution of particles with different diameters ranging from 50 nm to 2 micron are calculated. As a result, the diverse changes of single nanoparticles' amplitude and phase images can

be as a measurement means to evaluate the nanoparticles size. The numerical calculation agrees well with the experiment.

9273-97, Session Post

Selective feature learning for hand-held 3D object recognition

Shuqiang Jiang, Shuang Wang, Xiong Lv, Institute of Computing Technology (China)

Object recognition has wide applications in the area of human-machine interaction and multimedia retrieval. However, it is still a great challenge to obtain reliable recognition result for the 2D images, due to the problem of visual polysemic and concept polymorphism. Recently, with the emergence and easy availability of RGB-D equipment such as Kinect, this challenge could be relieved because the depth channel could bring more information. A very special and important case of object recognition is hand-held object recognition, as hand is a straight and natural way for both human-human interaction and human-machine interaction. In this paper, we study the problem of 3D object recognition by proposing a method of selective deep feature learning. The motivation of this work lies in two aspects. On the one hand, hand-craft features have shown its weakness compared with the automatic feature learning, especially deep feature learning. On the other hand, discriminative feature selection could be of many useful to obtain effective 3D image representation for recognition. This work has three steps. At first, hand-held object segmentation is implemented by using depth cues and human skeleton information. Second, a selective feature learning method based on point-wise gated Boltzmann machines is used. Then a training model is established to recognize 3D hand-held objects both at the category level and instance level. Experimental results show the effectiveness of the proposed method.

9273-98, Session Post

An auto-gain control algorithm for EMCCD based on dynamic gray-level

Yuehong Qian, Wenwen Zhang, Nanjing Univ. of Science and Technology (China); Jingjing Liu, Nanjing University of Science & Technology (China); Feng Chen, Qian Chen, Guohua Gu, Nanjing Univ. of Science and Technology (China)

In low light level imaging, Electron Multiplying CCD (EMCCD) is regarded as the array detecting device as usual, but the images will be too bright or too dark under different gains. Due to this phenomenon, we analyze the characteristics of the captured images of EMCCD and then present an auto-gain control algorithm based on dynamic gray-level to overcome this shortage. The algorithm first anticipates the current illumination situation and then predicts the desired gain of the next image by exposure function. Meanwhile, we adopt not only the mean value but also the histogram of the image as the controlling parameters to adjust the multiply gain. Thus the appropriate gain can be achieved and the gray distribution of an image can quickly converge to optimal range. The experiments demonstrate that the algorithm is able to provide a better solution for low-light-level images by auto-gain control. Compared to the method of fixed value adjustment, the automatic gain algorithm here is more adaptive.

9273-99, Session Post

A flexible design for coded aperture snapshot spectral imager

Lizhi Wang, Xidian Univ. (China); Dahua Gao, Xidian Univ. (China) and Air Force Engineering Univ. (China); Chao Li, Danhua Liu, Guangming Shi, Xidian Univ. (China)

By the success of compressive sensing (CS), coded aperture snapshot spectral imager (CASSI) computationally obtains 3D spectral images from 2D compressive measurement. In CASSI, each pixel of the detector captures spectral information only from one voxel in each band with binary weights (i.e., 0 or 1), which limits the variety of superposition relationship among the 3D voxels in the underlying scene. Moreover, the correspondence of each pixel of detector to each pixel of coded aperture cannot be readily achieved in the presence of dispersive prism, due to the small pixel sizes of these elements (often in micrometer). In this paper, we propose a flexible design to improve the performance of CASSI with currently employed optical elements in CASSI. Specifically, the proposed design integrates a kind of flexible alignment relationship along the coded aperture, the dispersive prism and the detector. Each measurement of the detector is manifested as the summation of several voxels in each band with random decimal weights and different measurements corresponds to overlapped voxels, which provides more sufficient superposition relationship of the scene information. This flexible design favors the sensing mechanism better satisfy the requirement of CS theory. Furthermore, the proposed design greatly reduces the alignment complexity and burden of system construction. Preliminary result achieves improved image quality, including higher PSNR and better perceptual effect, compared to the traditional design.

9273-100, Session Post

High-accuracy hole-filling for Kinect depth maps

Jianxin Wang, Ping An, Yifan Zuo, Zhixiang You, Zhaoyang Zhang, Shanghai Univ. (China)

Hole filling of depth maps is a core technology of the Kinect based visual system. In this paper, we propose a hole filling algorithm for Kinect depth maps based on separately repairing of the foreground and background. There are two-part processing in the proposed algorithm. Firstly, a fast pre-processing to the Kinect depth map holes is performed. In this part, we fill the background holes of Kinect depth maps with the deepest depth image which is constructed by combining the spatio-temporal information of the pixels in Kinect depth map with the corresponding color information in the Kinect color image. The second step is the enhancement for the pre-processing depth maps. We propose a depth enhancement algorithm based on the joint information of geometry and color. Since the geometry information is more robust than the color, we correct the depth by affine transform in prior to utilizing the color cues. Then we determine the filter parameters adaptively based on the local features of the color image which solves the texture copy problem and protects the fine structures. Since L1 norm optimization is more robust to data outliers than L2 norm optimization, we force the filtered value to be the solution for L1 norm optimization. Experimental results show that the proposed algorithm can protect the intact foreground depth, improve the accuracy of depth at object edges, and eliminate the flashing phenomenon of depth at objects edges. In addition, the proposed algorithm can effectively fill the big depth map holes generated by optical reflection.

9273-101, Session Post

Orientation selectivity-based structure for texture classification

Jinjian Wu, Xidian Univ. (China); Weisi Lin, Nanyang Technological Univ. (Singapore); Guangming Shi, Yazhong Zhang, Liu Lu, Xidian Univ. (China)

Since the human visual system (HVS) is highly adaptive to extract structure for image understanding, local structure, e.g., local binary pattern (LBP), is widely used in texture classification. However, LBP is too sensitive to disturbance, which returns low classification accuracy for noise contaminated textures. In this paper, we introduce a novel structure for texture classification. Researches on cognitive neuroscience indicate that the arrangement of excitatory and inhibitory cortex cells arise orientation selectivity in a local receptive field, with which the primary visual cortex performs visual information extraction for scene understanding. Inspired by the orientation selectivity mechanism, we investigate the orientation similarities among neighbour pixels for local structure description. By imitating the arrangement of the excitatory and inhibitory cells, the correlations between a pixel and its local neighbors are binarized, and the spatial correlation is represented with a set of binary values, which is called the orientation selectivity pattern. Finally, taking both the orientation selectivity pattern and the luminance contrast of a pixel into account, a novel structural descriptor is created. Experimental results on texture classification demonstrate that the proposed structural descriptor is much more robust than LBP to disturbance.

9273-102, Session Post

The CCD image data processing for the application of atmosphere lidar

Zhigang Li, Linwei Zhu, Ludong Univ. (China); Zhishen Liu, Ocean Univ. of China (China)

The charge coupled device (CCD) can be used as the detector for lidar receiving system. In this paper, we introduce the application of CCD detector used in atmosphere lidar system for doppler shift and aerosol scattering detection in boundary layer. The system performance due of the detector influence was analyzed. Based on the improvement of the image data retrieval method, a detailed processing simulation for the retrieval of atmosphere information is presented, the results comparison and data error analysis was carried out. This work is useful for the improvement of data accuracy of lidar using CCD as photoelectric detector.

9273-103, Session Post

Research of image haze removal system based on DaVinci DM6467T processor

Zhuang Liu, Institute of Semiconductors (China)

Video monitoring system (VMS) has been extensively applied in domains of target recognition, traffic management, remote sensing, auto navigation and national defence. However the VMS has a strong dependence on the weather, for instance, in foggy weather, the quality of images received by the VMS are distinct degraded and the effective range of VMS is also decreased. All in all, the VMS performs terribly in bad weather. Thus the research of fog degraded images enhancement has very high theoretical and practical application value.

A design scheme of a fog degraded images enhancement

system based on the TI DaVinci processor is presented in this paper. The main function of the referred system is to extract and digital cameras capture images and execute image enhancement processing to obtain a clear image.

The processor used in this system is the dual core TI DaVinci DM6467T?ARM@500MHz+DSP@1GHz?. A MontaVista Linux operating system is running on the ARM subsystem which handles I/O and application processing. To process video and image, it uses the VISA APIs provided by the Codec Engine. The Codec Engine, in turn, uses services such as DSP/BIOS Link and protocols such as xDAIS and xDM to communicate with a pre-configured Codec Engine Remote Server on the DSP subsystem. The DSP handles signal processing and the results are available to the ARM subsystem in shared memory.

The system benefits from the DaVinci processor so that, with lower power cost and smaller volume, it possesses the equivalent image processing capability of a X86 computer. The outcome shows that the system referred in this paper can process images at 30 frames per second in VGA resolution.

9273-104, Session Post

Optical information processing, computer generated Fourier hologram, and 3D display

Zhaohui LI, Jianqi Zhang, Xiaorui Wang, Xidian Univ. (China)

A new method is proposed by incorporating virtual variable-focal-length lenses into computer generated Fourier hologram (CFGH) to make a viewing perspective cue emerging in reconstructed images. The proposed approach is based on a combination of monocular stereoscopic principle and digital hologram display, thus it owns properties coming from the two display modals simultaneously. Therefore, it can overcome the drawback of the unsatisfied visual depth perception of the reconstructed three-dimensional (3D) image in a holographic projection display. Firstly, an analysis on characteristics of conventional CFGH reconstruction is made, which indicates that a finite depth-of-focus and a non-adjustable lateral magnification are responsible for the depth information lack on a fixed image plane. Secondly, the principle of controlling lateral magnification in reconstructions by virtual lenses is demonstrated. And the relation model is deduced, which involves the depth of object, the parameters of virtual lenses, and the lateral magnification. Next, considering perspective distortion of human vision, the focal-lengths of virtual lenses are determined. After employing virtual lenses in the CFGH, the reconstructed image on focal-plane can deliver the same depth cues as that of the monocular stereoscopic image. Finally, the depth-of-focus enhancing produced by a virtual lens and the effect on the reconstruction quality from the virtual lens are described. Numerical simulation and electro-optical reconstruction experimental results show that the proposed algorithm can improve the depth perception of the reconstructed 3D image in holographic projection displays. The proposed method provides a possibility of uniting multiple display models to enhance 3D display performance and viewer experience.

9273-105, Session Post

Simultaneous cartoon-plus-texture image deconvolution by using variational image decomposition

Huasong Chen, Nanjing Univ. of Science and Technology (China); Keding Yan, Nanjing Univ. of Science and Technology (China) and Xi'an Technological Univ. (China); Jun Zhang, Zhenhua Li, Nanjing Univ. of Science and Technology (China)

Because of various factors, an acquired image often suffers from the blurring effect in the imaging process. How to recover the true image from a single blurred noisy image is a challenging problem in image processing. Up to now, many effective algorithms have been proposed to solve this kind of problems, such as PDE based methods, and wavelets based methods, statistics based methods. Among these, total variation based method is the most popular and effective one which can recover images with sharp edges. However, real images usually have two layers, namely, cartoons (the piece-wise smooth part of image) and textures (the oscillating pattern part of the image). How to simultaneously recover cartoons and textures of the image is a new problem in image deconvolution. Previous image deblurring methods either recover the texture while losing some structure, or recover the structure of image while losing some textures, few works consider simultaneously recovering both the parts of images. In this paper, we propose a image deconvolution algorithm which can simultaneously restore the cartoon and texture of the image based on variation based image decomposition method. We use the total variation norm and its dual norm to regularize the cartoon and texture, respectively. We recommend an efficient numerical algorithm based on the splitting versions of augmented Lagrangian method to solve this problem. In contrast to recently developed methods for deblurring images, the proposed algorithm not only gives the restored image with information of both parts, but also gives a decomposition of cartoon and texture parts. Numerical simulation examples are given to demonstrate the applicability and usefulness of our proposed algorithms in image deconvolution.

9273-106, Session Post

Applications of just-noticeable depth difference model in joint multiview video plus depth coding

Chao Liu, Ping An, Yifan Zuo, Zhaoyang Zhang, Shanghai Univ. (China)

A new multiview just-noticeable-depth-difference (MJNDD) Model is presented and applied to compress the joint multiview video plus depth. Many video coding algorithms remove spatial and temporal redundancies and statistical redundancies but they are not capable of removing the perceptual redundancies. Since the final receptor of video is the human eyes, we can remove the perception redundancy to gain higher compression efficiency according to the properties of human visual system (HVS). Traditional just-noticeable-distortion (JND) model in pixel domain contains luminance contrast and spatial-temporal masking effects, which describes the perception redundancy quantitatively. Whereas HVS is very sensitive to depth information, a new multiview-just-noticeable-depth-difference (MJNDD) model is proposed by combining traditional JND model with just-noticeable-depth-difference (JNDD) model. The texture video is divided into background and foreground areas using depth information. Then different JND threshold values are assigned to these two parts. Later the MJNDD model is utilized to encode the texture video on JMVC. When encoding the depth video, JNDD model is applied to remove the block

artifacts and protect the edges. Then we use VSR5.3.5 (View Synthesis Reference Software) to generate the intermediate views. Experimental results show that our model can endure more noise and the compression efficiency is improved by 18 percent compared to JMVC while maintaining the subject quality. Hence it can gain high compress ratio and low bit rate.

9273-107, Session Post

The application of dynamic phase-shift in light pulse sampling

Dezhen Lu, Wei Cui, Yan Zhou, Songtao Fan, Xinwei Wang, Yuliang Liu, Institute of Semiconductors (China)

The range-gated imaging technology can efficiently "gate out" the back-scattering noise and other background noise, which improves the signal to noise ratio of the laser imaging system. So it is widely used in underwater exploration, inclement weather (rain, snow, etc.) imaging detection, rescue and other fields. The key of range-gated system to achieve higher quality imaging is the synchronization between pulsed laser and gated ICCD. Compared to trigger synchronization control method, external trigger synchronization control overcome(s) knowing the real laser emitting moment. So the impact of laser itself is neglected, which causes higher precision detection. The key technology of external trigger synchronization control method is to sample the electric signal detected by the high-speed photo-detector. To sample the electric signal transformed from the laser pulse, the sampling system must work at very high frequency. High frequency circuit prevents the imaging system to stable imaging, and cause the imaging system bad anti-interference ability. We proposed the dynamic phase-shift to sample the electric signal transformed from the laser pulse. By changing the sampling system's global clock phase, we could get a series of clock which have arithmetic sequence phase. When using the clocks with arithmetic sequence phase to sample the electric signal simultaneously, the sampling frequency is determined by the equivalent clock generated by the arithmetic sequence phase clocks, which is much higher than the global clock frequency. Thus offers an efficient sampling method without increasing the global clock frequency of the system. In this paper, we studied the principle of dynamic phase-shift, and applied it to the sampling system in external trigger synchronization range-gated imaging system. The results showed that the dynamic phase-shift sampling could achieve 1GHz sampling rate and avoid the drawbacks of high frequency circuit.

9273-108, Session Post

Characteristic extraction and matching algorithms of ballistic missile in near-space by hyperspectral image analysis

Li Lu, Wen Sheng, Shihua Liu, Xianzhi Zhang, Air Force Early Warning Academy (China)

The realm of Near Space, which is subject to the category between the aviation and aerospace officially lies between 20km and 100km according to the International Aeronautical Federation. This area is of interest for military surveillance purposes because that the traditional assaults are difficult to search and track the targets. If a platform in the near-space carries a high sensitivity of imaging spectrometer so that the ballistic missile in the deep space can be detected easily by using of it. In this way, it can greatly reduce the technical difficulty and development costs and shows a relatively complete strategic early warning ability as soon as possible.

However, the high dimensionalities of hyperspectral data are obtained by the use of the imaging spectrometer will lead

to a large amount of computation in each dimensionality of subsequent target matching and identification. It is difficult to meet the real-time requirement of the ballistic missile target recognition, so the algorithm of characteristic and matching by hyperspectral image analysis should be studied to the aims of simple extraction and full dimension reduction.

In this paper, two different algorithms of characteristic and matching of the ballistic missile hyperspectral data are studied, which called the quantization coding and the transverse counting. The ballistic missile hyperspectral data of imaging spectrometer from the near-space platform are generated by numerical method. The simulation results show that two algorithms extract the characteristic of the ballistic missile adequately and accurately. The algorithm based on the transverse counting has the low complexity and can be implemented easily compared to the algorithm based on the quantization coding does. The transverse counting algorithm also shows the good immunity to the disturbance signals and speed up the matching and recognition of subsequent targets.

9273-109, Session Post

Ultrasonic televiewer image encoding based on block prediction

Zhengbing Zhang, Wei Zhang, Yangtze Univ. (China)

In recent years, image acquisition equipment has been widely adopted in the field of well logging. However, the data transfer rate of the logging system is limited by the transmission cables. Thus, data compression for well logging images has attracted many attentions of researchers. In this paper, an ultrasonic televiewer image encoding method based on block prediction is proposed. The original image is divided into non-overlapping blocks of 8-by-8 pixels. The pixel values of the current block to be encoded are predicted from previously encoded and decoded blocks. The pixels of the bottom rows of the blocks north and north east to the current block, and/or the pixels of the right column of the block west to the current block are used as prediction references. There are 9 prediction modes to be chosen to predict the current block. The prediction mode that minimizes the differences between the original and predicted block is chosen. The prediction difference block is called as a residual block that is transformed with Discrete Cosine Transform (DCT), and the DCT coefficients are quantized. After Zig-Zag scan, the quantized DC coefficients are encoded with prediction coding, while the quantized AC coefficients are encoded with run-length coding and Huffman coding. In addition to the codes of the residual block, the best prediction mode selected for each block is also encoded and sent to the decoder. The decoding process is the inversion of encoding. Experimental results show that the performance of the proposed method is much better than JPEG.

9273-110, Session Post

Seismic data compression based on wavelet transform

Zhengbing Zhang, Wei Zhang, Yangtze Univ. (China)

Seismic exploration is one of the most important ways for oil exploration. In recent years, some new technologies such as multi-dimension, multi-components and high precision methods have been adopted in seismic exploration. This makes seismic exploration data increase explosively. Large volume seismic data results in serious problems in transmission, storage and processing of the data. Therefore, seismic data compression has attracted great attentions of researchers. In this paper a seismic data compression method based on wavelet transform is proposed. As theoretical foundation for the compression, the statistical characteristics of the original data and the

corresponding wavelet coefficients are analyzed. It is discovered that the seismic data has much larger dynamic range and more plentiful mid- and low-frequency information than images. Since the seismic data is usually acquired with 2 ms sampling interval in 6 seconds time for each trace, there are 3000 samples per trace. The seismic data is divided into blocks of 3000 samples by 3000 traces. For each block, the original block is decomposed into 4 sub-bands at each decomposition level with 2-dimensional discrete wavelet transform. A three-level multi-resolution decomposition with bi-orthogonal wavelet filters results in 9 detail sub-bands and 1 low-resolution sub-band of wavelet coefficients. The wavelet coefficients in the 9 detail sub-bands are encoded with embedded zero-tree wavelet coding algorithm. The coefficients in the low-resolution sub-band are encoded with DCT based algorithm. Experimental results show that the proposed method is capable of efficient compression with little or no artifacts for a wide range of seismic data.

9273-111, Session Post

A design method of the distortionless catadioptric panoramic imaging based on freeform surface

Yisi Wu, Zhenrong Zheng, Yinxu Bian, Zhejiang Univ. (China)

In order to make a system that has a new system structure and innovative algorithm to realize infinite scene imaging, a design method of the distortionless catadioptric panoramic imaging model is proposed. The panoramic model mainly consists of two parts—a reflecting surface system and a CCD camera. A high-order rotary symmetry mirror based on spherical mirror is designed to reflect light onto a CCD image plane through a lens. The size and the high-order numerical solution of the surface is determined by the camera's parameters, which need to be calibrated first. A relatively much more simple and intuitional mapping relationship between the real image plane and the projection surface is established and consequently acquire low distorted imaging features. And the design of freeform surface is applied to the reflecting surface to correct distortion, making the image more suitable and convenient for observing. All these make the performance of distortionless and real-time imaging for a 360° cylindrical scene. Imaging features of infinite scene imaging was analyzed for the new system. The simulation results show that compared with traditional system consists of hyperboloidal or paraboloidal mirror, the new system has simple design, attaining higher performance and has the advantage of small scene distortion and keeping high resolution on the edge of the picture. It can be applied in robot navigation, monitoring and other places demanding wide field of view.

9273-112, Session Post

Compression of multispectral image using HEVC

Feiyu Gao, Xiangyang Ji, Qionghai Dai, Tsinghua Univ. (China)

Predictive Lossy Compression has been found to be an interesting alternative to conventional transform coding techniques in multispectral image compression. Recently, High Efficiency Video Coding (HEVC) standard has shown significant improvement over state of the art transformation based still-image coding standard. In this paper we study the properties of multispectral image and propose a predictive lossy compression

scheme based on HEVC. Empirical analysis shows that our proposed method is superior to the existing state of the art predictive lossy compression schemes.

9273-113, Session Post

Design of HD binocular stereo display system based on ARM11

Bin Zhuo, Junsheng Shi, Yonghang Tai, Yunnan Normal Univ. (China)

Based on the characteristics of 0.5' micro AM-OLED and the binocular parallax principle of human being, we designed a HD stereo display system used hardware platform of ARM11 and embedded Linux as the operating system. System used S3C6410 as the MCU, Side-by-Side or Top-and-Bottom 3D video source, which inputted from the HDMI or SD card, was converted to the Frame Timing Mode and Field Timing Mode video format which processed through the video coding algorithm. At the same time, the outputting 3D synchronous signal controlled the left and right AM-OLED to receive corresponding parallaxic images. HD stereo video sources achieved an improvement effect on the dual AM-OLED after the optical system amplified, which presented an image distance equivalent to the human eyes 2.5 meters, the diagonal dimension of 46 feet natural lifelike scene in front of the user. Combined synchronous signal with Frame Timing Mode and Field Timing Mode, the HD binocular stereo system displayed a preferable result for the customs.

9273-114, Session Post

A new metric to assess temporal coherence for video retargeting

Ke Li, Bo Yan, Binhang Yuan, Fudan Univ. (China)

In video retargeting, how to assess the performance in maintaining temporal coherence has become the prominent challenge. In this paper, we will present a new objective measurement to assess temporal coherence after video retargeting. It's a general metric to assess jittery artifact for both discrete and continuous video retargeting methods, the accuracy of which is verified by psycho-visual tests. As a result, our proposed assessment method possesses huge practical significance.

9273-115, Session Post

An effective guess for Gerchberg-Saxton-type algorithms

Kaiyun Wei, Xin Jin, Graduate School at Shenzhen, Tsinghua Univ. (China); Yifu Hu, Graduate School at Shenzhen, Tsinghua Univ. (China); Qionghai Dai, Graduate School at Shenzhen, Tsinghua Univ. (China)

Gerchberg-Saxton-type (GS-type) algorithms retrieve the phase information from light distributions, such as the magnitude of their spatial Fourier spectrum, to reconstruct the object structures. However, using random guesses as the initial inputs, the reconstruction quality of GS-type algorithms is unpredictable. And, it always leads to a large number of iterations to reach convergence. In this paper, a singular value decomposition (SVD) based method is proposed to generate an effective phase guess for GS-type algorithms using a low rank approximation. Images with different scattering intensities are captured by a new-built scattering imaging system. By testing on the images, the reconstruction performances of GS-type algorithms using

different ranks of approximations as the initial input, generated by different numbers of the largest singular values, are analyzed. It demonstrates that the proposed SVD based method can effectively reduce the number of iterations for GS-type algorithms under the same reconstruction error. Selecting the largest 14.05% to 20.7% singular values to generate the low rank approximation presents more than 97% of probability to reach the same reconstruction error with that of random guesses with an average of 50% reduction in the number of iterations. The proposed approach can also outperform random guesses both in terms of steady state error and iteration times. Compared with the average performance of random guesses, the proposed SVD based approach reduces the steady state error of recovered images by 70.77% on average and reduces the iteration times by 56.1% on average.

9273-116, Session Post

Improved gray world color correction method based on weighted gain coefficients

Bin Pan, Zhiguo Jiang, Junfeng Wu, BeiHang Univ. (China)

Gray world algorithm is a simple but widely used global white balance method for color cast images. However, this algorithm only assumes that the mean values of the R, G, and B components tend to be equal, which may lead to false alarms in some normal images with large areas of single color background, for example, images in ocean background. Another defect is that gray world algorithm may cause luminance variations in the channels having no cast. We note that though different in mean values, standard deviations of the three channels are supposed to converge in color cast images, which is not suitable for those false alarms. Based on this discrepancy, through a mathematical manipulation both on mean values and standard deviations of the three channels, a novel color correction model is proposed by weighting the gain coefficients in gray world model. All the three weighted gain coefficients in the proposed model tend to be 1 on images containing large single color regions so as to avoid false alarms. For the color cast images, the channel existing color cast is given a weighted gain coefficient much less than 1 to correct color cast, while the other two channels are distributed weighted gain coefficients approximately equal to 1 thus to ensure that the proposed model has little negative effects on channels with no color cast. Experiments show that our model presents better performance in color correction.

9273-117, Session Post

Misalignment-matching heterodyne detection using an array of detectors

Hongzhou Dong, Mingwu Ao, Ruofu Yang, Chunping Yang, Univ. of Electronic Science and Technology of China (China)

We point out that the amplitude of intermediate frequency current is just the spectrum value of quantum efficiency distribution function of detector, and the value is related to the misalignment angle. This conclusion indicates that a matching quantum efficiency distribution function will enhance the signal strength, which can be realized by an array detector in which the current gain of each detector can be adjusted by controller. A fast scanning detection can be achieved by using such array detector. The scheme has the merit of wide range target detection, which is verified by numerical simulations.

9273-118, Session Post

Double-channel multi-spectral video acquisition with complementary code patterns

Danhua Liu, Xidian Univ. (China); Huan Li, Beijing Institute of Space Mechanics and Electricity (China); Dahua Gao, Air Force Engineering Univ. (China); Guo Li, Guangming Shi, Xidian Univ. (China)

Temporal resolution is crucial for the multi-spectral imaging of dynamic scenes, such as, reconnaissance of moving target, observation of living cells under fluorescence microscope, etc. The traditional multi-spectral imaging methods need multiple exposures to capture a full frame spectral image, which leads to a low temporal resolution and thus lose their value for dynamic scenes. This paper proposes a novel double channel multi-spectral video acquisition method with the coded aperture snapshot spectral imager (CASSI). The method has two distinct advantages: (1) A high temporal resolution can be achieved, because our method samples the 3D spectral scene with 2D array sensor in only one snapshot. (2) A high recovery quality of multi-spectral video is obtained, due to the use of complementary coded patterns in two channels and the sparse regularity in the recovery process. Simulation results demonstrate the efficacy of the proposed method.

9273-119, Session Post

Aircraft detection based on probability model of structural elements

Long Chen, Zhiguo Jiang, BeiHang Univ. (China)

The detection of aircrafts is an important task in the field of remote sensing. In past decades, researchers used various approaches to detect aircrafts based on classifiers for overall aircrafts. However, with the development of high-resolution images, the internal structures of aircrafts should also be taken into consideration now. To address this issue, a novel aircrafts detection method for satellite images based on probabilistic topic model is presented. We model aircrafts as the connected structural elements rather than features. The proposed method contains two major steps: 1) Use Cascade-adaboost classifier to identify the structural elements of aircraft firstly. 2) Connect these structural elements to aircrafts, where the relationships between elements are estimated by hierarchical topic model. We use latent dirichlet allocation model to build the connection-rules and discover the relations between elements. In our method, images can denote documents, topics as the types of aircrafts, words as structural elements. From this, we can suppose that if structural elements in certain positions have large frequencies to appear in an image patch simultaneously, a unified topic label will be assigned to them. The model effectively encodes spatial structure by spatial relationships among aircraft structural elements. It places strict spatial constraints on structural elements which can identify differences between similar features. For comparison, classifiers such as Cascade-adaboost and SVM are trained and tested on the same dataset which includes 100 images from Google-Earth. Compared with other methods, the experimental results show that our method yields higher precision and lower false alarm rates.

9273-120, Session Post

Efficient stereo matching algorithm with edge-detecting

Jing Liu, Beijing Univ. of Posts and Telecommunications (China)

Stereo vision is a hot research topic in the field of computer vision and 3D video display. Disparity map figure is one of the most crucial steps. In order to obtain correct disparity maps for 3D reconstruction and computer vision, many algorithms have been developed for stereo disparity estimation in recent years. Actually, diversity of the algorithms mostly relies on the optimization approach which determines the main characteristics including complexity and precision of the methods. Balancing the accuracy and execution time is the fundamental constraints of stereo matching algorithms, especially in consumer electronics application.

Here, a novel constant computational complexity algorithm based on separable successive weight summation (SWS) among horizontal and vertical direction is presented. The cost aggregation is the most important processing step to achieve more accurate disparity maps than original algorithm. The proposed algorithm eliminates iteration and support area independently, which saves computation and memory space compared with the SWS aggregating cost values effectively along large regions by four passes. The weight area of four directions is determined by the intensity similarity of four neighborhood pixels. The computation includes six additions and four multi-applications per pixel for each candidate disparity value. The similar measure of gradient is also applied to improve the original algorithm. The edge of image is an important characteristic, which is discontinuous area including the useful information for stereo matching. Image segmentation and edge detection is applied to the stereo matching ideas to accelerate the speed and accuracy of matching algorithm. The image of edge is extracted to reduce search scope for the stereo matching algorithm. In the discontinuity region of the image edge, search scope is increased to acquire better matching effect. Dense disparity map was obtained through local optimization. To test the performance of the stereo matching algorithm, it is realized by C++. Experimental results show that the algorithm is fast and efficient, and the matching noise is well reduced and the matching precision is improved in depth discontinuities and low-texture regions

9273-121, Session Post

Multi-channel super-resolution with Fourier ptychographic microscopy

Weixin Jiang, Yongbing Zhang, Graduate School at Shenzhen, Tsinghua Univ. (China); Qionghai Dai, Tsinghua Univ. (China)

Fourier ptychographic microscopy (FPM) is a recently developed imaging method, which stitches together a sequence of low-resolution images in Fourier space in the iterative manner. However, current FPM algorithm mainly focuses on the problem of super-resolving single channel (grayscale) images, while treating the problem of multi-channel (color) images super-resolution as a simple linear combination of single channel images in RGB channels. The multi-channel image super-resolution only simply considers the luminance component of the image, but neglects the chrominance components. As a result, the high-resolution color image super-resolved by this method always has problems of dispersion when compared to the high-resolution image observed under high-magnification lens. In this paper, a new method is proposed for super-resolving multi-channel images, which considers the luminance components of the images as well as the chrominance components. Instead of

super-resolving the image in RGB color channels respectively, the proposed method decomposes the image into YUV channels. Then the super-resolving algorithm will be applied to the Y channel which contains the luminance components. Under the procedure of FPM algorithm, the amplitude of the selected region which is extracted from the input images will be replaced by the collected image following the concept of phase retrieval. After each replacement, the result image will be decomposed into HSI channels and the value of the channels will be adjusted to solve the problem of dispersion. The concept of iterative algorithm is adopted in the FPM algorithm to get a convergent result, and after each iterative we propose a method to correct the result, based on the relationship among the RGB channels. Experimental results demonstrate that the dispersion can be eliminated, compared with the super-resolving multi-channel image got from original FPM algorithm. Besides, the robustness of Fourier ptychographic imaging is improved and the running time of the super-resolution of color images is reduced.

9273-122, Session Post

Efficient mode decision algorithm for scalable high-efficiency video coding

Nandi Shi, Ran Ma, Panpan Li, Ping An, Qian Zhang, Shanghai Univ. (China)

Due to the demand diversification for high-definition video which is transmitted over networks, the heterogeneous needs of current networks and display devices (from low-resolution to HDTV) make scalable video coding (SVC) be necessary. SVC has been extensively studied and divided into three well-known scalabilities: spatial, temporal and quality.

In general, motion information is non-scalable, even though it is one of the main parameters in the codec. In fully scalable video codec, motion information scalability can further reduce the requirement of bit rate and collaborate with other scalabilities flawlessly. So motion information scalability is of great significance.

A scalable motion model (SMM) is proposed in this paper, which is based on the analysis of the requirements of motion information scalability in high-definition texture and depth video coding. The proposed SMM include two parts: motion precision scalability and variable block size (VBS) scalability that mainly is used for low bit rate. The main processing is as follows:

1. Motion precision scalability is realized by progressively coding based on motion information integer pixel precision, 1/2 pixel precision, 1/4 pixel precision and 1/8 pixel precision.
2. In high-definition video coding, VBS can be easily obtained through quad-tree coding structure. Some motion information nodes which are similar or identical with the parent node adopt the simplest direct copy in order to save the bit-rate.
3. Moreover, based on the correlation between texture and depth video data, the corresponding depth map information is introduced in SMM which can adaptively adjust the search range of motion.

9273-123, Session Post

Explore temporal-spatial relations: transient super-resolution with PMD sensors

Chaosheng Han, Xing Lin, Jingyu Lin, Yebin Liu, Qionghai Dai, Tsinghua Univ. (China)

Transient imaging gives us a direct view of how light travel in the scene, which leads to exciting applications such as looking around corners. Low-budget transient imagers, adapted from

Time-of-Fight (ToF) cameras, reduce the barrier of entry for performing research in this new imaging modality.

However, the image quality is far from satisfactory due to the limited pixel resolution of the adopted PMD sensors. In this paper, we explore the temporal information in transient video to improve its spatial resolution by illumination modulation.

Our key perspective is to formulate a theoretical model for the relationship between time-profile and the corresponding 3D details of each pixel. To be brief, the pulse width of time profile in each pixel is proportional to the cross product of the illuminating direction and the surface normal. In the implementation, we first acquire and reconstruct transient videos by Fourier analysis at multiple illumination positions; and then fuse the low-spatial resolution images to calculate the surface normal with modified coefficient, which is related to the reflectance ratio of different materials. Finally, an optimization procedure is employed to split the pixels and enhance the spatial resolutions of transient video.

Our experimental results demonstrate that our super-resolved transient video can not only reveal more details of object structure, but may also uncover materials property. We hope the idea of utilizing temporal-spatial relations will give new insights to the research and applications of transient imaging.

9273-124, Session Post

An auto-calibration approach for multi-projector 3D display

Shao Tang, Lei Zhang, Yongbing Zhang, Graduate School at Shenzhen, Tsinghua Univ. (China)

A typical multi-projector 3D display system is composed of a well-arranged projectors array and a screen. For such systems, precise calibration of projectors is extremely important for ensuring projected images/videos to coincide exactly in the same region of the screen, thus obtaining high quality 3D display experience. Conventional calibration is achieved by adjusting pose of projectors manually with the built-in keystone correction function, which is imprecise and time-consuming. In this paper, we propose an auto-calibration approach using feature detection and matching technique via an uncalibrated camera to improve both the calibration efficiency and precision. Auto-calibration is achieved in the following three steps: First, a well-designed typical picture with rich contents and patterns is displayed by all the projectors in sequence, which is captured by a camera fixed at a suitable position one by one. Second, one of these captured images is chosen as the reference image, and the feature detection (such as SURF) and matching technique is employed to obtain the homography transformation between each projectors' image and the reference image. And third, each projector's images/videos are pre-warped to the reference pose according to the corresponding homography matrix. All the projectors' image could coincide well after the calibration since each of them can coincide with the reference image.

The whole procedure can be finished in minutes, and the calibration error also hardly increase with the number of projectors. What's more, to the best of our knowledge, our approach is the first fast auto-calibration approach employed in the multi-projector 3d display systems.

9273-125, Session Post

A large-scale multi-projector glass-free 3D display system

Shao Tang, Lei Zhang, Yongbing Zhang, Graduate School at Shenzhen, Tsinghua Univ. (China)

3D movie experience with glasses has already been enjoyed in cinema for a long time, glass-free 3D experience is still a long-term goal for cinema movie display whose screen width can go beyond 10 meters. A large scale glass-free 3D display system which provides large-scale glass-free 3D experience is devised in this paper.

This system mainly consists of two parts, namely projector array and display screen. Multiple projectors are arranged to construct a projector array in a rear-projection or front-projection way. The distance between every two neighboring projectors is the same and the spacing distance can be adjusted to change the system's performance. The display screen made up of lenticular sheet and diffuser is used to differentiate light beams from multi-projector and display images of different views for users at different position. A prototype with 100-inch display screen and 8 projectors is built, which could provide 8-view glass-free 3D experience. In the prototype, the synchronization of different projectors and the calibration of projectors are also addressed. Furthermore, our system is free from the vertical stripe noise problem which is a big drawback for many projection-type 3D display systems. By adjusting the relative position of projectors and the display screen, the bright horizontal lines resulting from the reflection of projectors' light can be eliminated, and by adjusting the distance between neighboring projectors, nearly smooth motion parallax experience is supported.

Our proposed approach provides a feasible solution for glass-free 3D cinemas, which seems to be the only feasible approach before holographic cinemas become practical.

9273-126, Session Post

Motion-blurred image restoration based on joint transform correlator

Xueting Hong, Yixian Qian, Xiaowei Shi, Zhejiang Normal Univ. (China)

To restore the motion blurred image caused by various vibration and attitude variation in remote imaging, an approach is presented which is based on joint transform correlator (JTC). An auxiliary high-speed CCD is used to capture image sequences. When the prime CCD is imaging in exposure period, these image sequences are optically calculated by JTC system, and image motion vector can be effectively detected and point spread function (PSF) is accurately modeled instantaneously, it will alleviate greatly the complexity of image restoration algorithm. Finally, a simple restoration algorithm is proposed to restore the blurred image. We have also constructed an image restoration system based joint transform correlator. The experimental results show that the proposed method has improved image quality greatly.

9273-127, Session Post

Image reconstruction in Fizeau interferometry

Yuanyuan Ding, Xin-Yang Chen, Chaoyan Wang, Shanghai Astronomical Observatory (China)

Optical interferometry and optical aperture synthesis imaging technology is one of the significant technique utilized to measure astronomical objects with high angle resolution. It may be used to precisely measuring the shapes, sizes and position of astronomical objects and satellite, it also can realize to space exploration and space debris, satellite monitoring and survey. It is very important for Scientific research and military application. Fizeau-Type optical aperture synthesis telescopes originated from stellar interferometers with long baselines. It has the advantage of short baselines, common mount and multiple sub-apertures, so it is feasible for instantaneous direct imaging through focal plane combination.

Image reconstruction is the last step in the optical interference imaging, it is one of the most critical technologies. This paper is mainly concerned the structure of Y-type Fizeau interferometry, and the simulation of image restoration and image denoising. The research objects are binary stars and satellite, the Richardson-Lucy (RL) method and the Ordered Subsets Expectation Maximization (OS-EM) method are researched based on the Y-type Fizeau interferometry. It is proved that we can get the high resolution image of binary stars and satellites used RL and OS-EM.

We also developed a image reconstruction software based on Visual C++. As we know, image restoration needs to deal lots of images, and the high computational complexity brings a lot of problems. Modern GPUs are very efficient at manipulating computer graphics, and their highly parallel structure makes them more effective than CPUs. So in the future we also will propose a reconstruction software based on CUDA architecture, and We hope to be able to achieve quasi real time image processing.

9273-128, Session Post

Image reconstruction in speckle interferometry

Yuanyuan Ding, Shanghai Astronomical Observatory (China)

Speckle imaging technique is one of the several effective methods, which can overcome atmosphere turbulence effects and obtain diffraction-limited resolution of objects. It is achieved by the integration of a series of short-exposure images of the object.

This paper is the part of a series dedicated to the speckle imaging of binary stars carried out by the research team of Shanghai Astronomical Observatory. The observation experiments were carried out from 2010 to 2012 with 1.56-m telescope using a speckle camera, and the high resolution image were reconstructed successfully.

In this paper, we mainly concerned speckle interferometry and iterative shift-and-add. Speckle interferometry was proposed by Labeyrie in 1970, the information obtained in this manner is not easily interpreted because the final output after processing is the autocorrelation of the object. This technique has been widely used in the observational astronomy, especially in binary stars. Iterative Shift-and-Add is working in spatial domain, the complex Fourier phase recover is avoided in this method and the data processing become much easier.

As we know, speckle imaging algorithm needs to deal thousands of images, and the high computational complexity brings a lot

of problems. Modern GPUs are very efficient at manipulating computer graphics, and their highly parallel structure makes them more effective than general-purpose CPUs for algorithms where processing of large blocks of data is done in parallel. So we proposed a reconstruction software based on CUDA architecture, compared with C++ program based on CPU, the speed ratio can reach 10 times.

9273-129, Session Post

Remote three-dimensional video mobile display platform for naked eyes

Changxin Jia, Beijing Univ. of Posts and Telecommunications (China)

The traditional 2D video technology can not meet people's urgent desire for a better video quality, which leads to the rapid development of 3D video technology. Simultaneously people want to watch 3D video in portable devices at anytime and anywhere. For achieving the above purpose, a remote 3D video play platform is demonstrated. The platform includes a server and a client. The server is used for transmission of different formats of video and the client is responsible for receiving remote video for the next decoding and pixel restructuring. Here improved Live555 is used for the video transmission server. Live555 is a cross-platform open source project which provides solutions for streaming media such as RTSP protocol and supports transmission of multiple video formats. At the receiving end, a player developed in our laboratory is used. The player based on the Android system, which is with all the basic functions as the ordinary players and able to play normal 2D. Also RTSP is implemented into this structure for telecommunication. In order to achieve stereoscopic display, make pixel rearrangement is needed in the player's decoding part. The decoding part is the local code which JNI interface calls so that we can extract video frames more effectively. The video formats can be left and right, up and down and nine grids. In the design and development, a large number of key technologies from Android application development have been employed, including a variety of wireless transmission, pixel restructuring and JNI call. By employing these key technologies, the system has been finally completed. After some updates and optimizations, the video player can play remote 3D video well anytime and anywhere and meet people's need ideally.

9273-130, Session Post

Under partially-coherent phase recovery algorithm

Yanliu Liu, Anhui Univ. (China)

The goal of phase retrieval is to recover the phase information from intensity distribution which is an important topic in optics and image processing. The algorithms based on the transport of intensity equation only need to measure the spatial intensity of the center plane and adjacent light field plane, and reconstruct the phase object by solving second order differential equations. The algorithm is derived in the coherent light field. And the partially coherent light field is described more complex, the field at any point in the space experiences statistical fluctuations over time. Therefore, traditional TIE algorithms cannot be applied in calculating the phase of partially coherent light field. In this paper, a phase retrieval algorithm is proposed for partially coherent light field. First, the description and propagation equation of partially coherent light field is established. Then, the phase is retrieved by TIE Fourier transform. Experimental results with simulated uniform and non-uniform illumination demonstrate the effectiveness of the proposed method in phase recovery for partially coherent light field.

9273-131, Session Post

Application of time-resolved glucose concentration photoacoustic signals based on an improved wavelet denoising

Zhong Ren, Jiangxi Science and Technology Normal Univ. (China) and Nanchang Univ. (China); Guodong Liu, Zhen Huang, Jiangxi Science and Technology Normal Univ. (China)

Real-time monitoring of blood glucose concentration (BGC) is a great important procedure in controlling diabetes mellitus and preventing the complication for diabetic patients. Noninvasive measurement of BGC has already become a research hotspot because it can overcome the physical and psychological harm. Photoacoustic spectroscopy is a well-established, hybrid and alternative technique used to determine the BGC. According to the theory of photoacoustic technique, the blood is irradiated by pulsed laser with nano-second repetition time and micro-joule power, the photoacoustic signals contained the information of BGC are generated due to the thermal-elastic mechanism, then the BGC level can be interpreted from photoacoustic signal via the data analysis. But in practice, the time-resolved photoacoustic signals of BGC are polluted by the varieties of noises, e.g., the interference of background sounds and multi-component of blood. The quality of photoacoustic signal of BGC directly impacts the precision of BGC measurement. So, an improved wavelet denoising method was proposed to eliminate the noises contained in BGC photoacoustic signals. To overcome the shortcoming of traditional wavelet threshold denoising, an improved dual-threshold wavelet function was proposed in this paper. Simulation experimental results illustrated that the denoising result of this improved wavelet method was better than that of traditional soft and hard threshold function. To verify the feasibility of this improved function, the actual photoacoustic BGC signals were tested, the test results demonstrated that the signal-to-noise ratio (SNR) of the improved function increases about 40-80%, and its root-mean-square error (RMSE) decreases about 38.7-52.8%.

9273-132, Session Post

High-emulation mask recognition with high-resolution hyperspectral video capture system

Jiao Feng, Xiaojing Fang, Yongjin Wang, Nanjing Univ. of Posts and Telecommunications (China); Shoufeng Li, Grünberg Research Centre, Nanjing University of Posts and Telecommunications (China)

We present a method for distinguishing face from high-emulation mask. Nowadays a series of high-emulation masks have been applied to commit crime. High-emulation mask with soft texture, natural skin color, clear facial features and lifelike appearance, is difficult to be recognized when worn and it is used by criminals for activities such as card numbers and passwords being stolen on ATM increasingly. In this case, traditional face recognition which can just recognize external characteristics is of no effect. Multispectral imaging technologies have been widely used in many fields, for example, remote sensing, cell detection, culture heritage detection and so on. In this paper, we use the proposed high-resolution hyperspectral video capture system to detect high-emulation mask by capturing spectrum information. In this system, an RGB camera is used for normal face recognition by imaging the observed face directly. A prism and a gray scale camera is used for capturing spectral images of the observed face. In the experiment, we capture the spectral image of the true face as reference data in advance. When the image captured by

RGB camera indicates the correct identification, spectral images captured by the gray scale camera have to be compared with the reference data. If the two sets of data fit well, the observed face can be identified as true face, otherwise, it can be high-emulation mask. As multispectral imaging offers additional spectral information about physical characteristics, mask made of silica gel can be easily recognized via the analysis of multispectral images.

9273-133, Session Post

Image restoration based on wavelets and curvelets

Bo Chen, Peking Univ. (China); Yang Yang, Information Engineering Univ. (China)

The performance of high-resolution imaging with large optical instruments is severely limited by atmospheric turbulence. Without correction, the angular spatial resolution is limited to the ratio wavelength over Fried's parameter. In the past 30 years, various numerical post processing methods then permit the restoration of the observed object. Adaptive optics (AO) offers a real-time compensation for turbulence. One can therefore record long-exposure images without losing the object's high spatial frequencies that correspond to the fine details. However, the correction is often only partial, and image restoration is required for reaching or nearing to the diffraction limit. In this paper, a novel deconvolution algorithm, based on both the wavelet transform and the curvelet transform (NDbWC).

The NDbWC algorithm is applied to the restorations of point source images of astronomical star and images of expanded object. Experimental results prove that this algorithm works well not only for short exposure images of point source star, but also for long exposure images of expanded object. The PSNR of restored expanded object images are raised. The effect of adaptive optics images has been improved. The NDbWC algorithm works better than classical wavelet-regularization method in deconvolution of the turbulence-degraded image with low SNR.

9273-134, Session Post

Multi-phases and high frequency based accurate 3D reconstruction using ToF camera

Ding Liang, Yebin Liu, Wei Yan, Qionghai Dai, Tsinghua Univ. (China)

The depth quality of a time-of-flight (ToF) camera is influenced by many systematic and non-systematic errors. We present a simple method to correct and reduce these errors without additional changes of devices. The positions of light source and camera are usually considered to be the same, but in fact they are slightly different. A ToF camera captures the fly distance of light, which is not double of the depth if high accuracy is wanted. Compared to traditional calibration method, we take the position of light source into consideration, and calibrate the light source together with camera to reduce the depth distortion. Besides, a Look-up Table (LUT) is used to correct pixel-related errors, which are caused by the manufacture of ToF sensor. This LUT is obtained by directly lighting the camera. Using high frequency to reduce random noises further enhances the depth accuracy. Besides, we capture images with multiple phases and apply FFT to get the true distance. By the proposed approach, we are able to reconstruct an accurate 3D model, whose RMSE of measured depth is below 1.4mm.

9273-136, Session Post

Excitation of topological insulator plasmons by two-dimensional periodic structure

Xiaofeng Gu, Weibing Lu, Xiaobing Li, Jian Wang, Southeast Univ. (China); Jun Hu, Southeast University (China)

Plasmons induced by topological insulator (TI) Bi₂Se₃ micro-ribbon arrays have been experimentally observed recently (Nature nanotechnology 2013, 8, 556-560). In this letter, the surface plasmons excited by TI Bi₂Se₃ micro-disk arrays are investigated by the methods of full-wave numerical simulations, which are validated in comparison with the experimental results of micro-ribbon arrays. Numerical simulation results show that thin Bi₂Se₃ micro-disk arrays can support dipolar plasmon resonances in the terahertz (THz) regimes and the absorptions can be tuned by the structure parameters. In addition to the plasmon mode, two phonon-mode responses are also observed, which reconfirms the experimental results of micro-ribbon arrays. Our work further proves that TI can be a good candidate of plasmonic platform.

9273-137, Session Post

Improvement on the polynomial modeling of digital camera colorimetric characterization

Xiaoqiao Huang, Hongfei Yu, Junsheng Shi, Yonghang Tai, Yunnan Normal Univ. (China)

The digital camera has become a requisite for everyday life, also imaging applications, and it is important to get more accurate color with digital camera. The colorimetric characterization of digital camera is the basis of image copy and color management process. One of the traditional methods for deriving a colorimetric mapping between camera RGB signals and CIE XYZ tristimulus values uses polynomial modeling with 3rd polynomial transfer matrices. In this paper, an improved polynomial modeling is presented, which suggests to replace the camera RGB values with the normalized luminance in the traditional polynomial modeling. The improved modeling can be described by a two stage model. The first stage, the relationship of the camera RGB values and normalized luminance with six gray patches in the The X-rite ColorChecker 24-color card was described as "Gamma", camera RGB values were converted into normalized luminance using Gamma; the second stage, the traditional polynomial modeling was improved to the colorimetric mapping between normalized luminance and CIE XYZ tristimulus values. Meanwhile, this method was used under daylight lighting environment, the users can not measure the CIE XYZ tristimulus values of the color target char using professional instruments, but they can accomplish the task of the colorimetric characterization of digital camera. The experimental results show that: (1) the proposed method for the colorimetric characterization of digital camera performs better than traditional polynomial modeling; (2) it's a feasible approach to handle the color characteristics using this method under daylight environment without professional instruments, the result can satisfy for request of application.

9273-24, Session 6

Unsupervised abnormal crowd activity detection using interaction power model

Shengnan Lin, Hong Zhang, Feiyang Cheng, BeiHang Univ. (China); Mingui Sun, Univ. of Pittsburgh (United States); Ding Yuan, BeiHang Univ. (China)

Abnormal event detection in crowded scenes is one of the most challenging tasks in the video surveillance for the public security control. Different from previous work based on learning, we proposed an unsupervised Interaction Power model with an adaptive threshold strategy to detect abnormal group activity by analyzing the steady state of individuals' behaviors in the crowded scene. Firstly, the optical flow field of the potential pedestrians is only calculated within the extracted foreground to reduce the computational cost as calculating the optical flows within the whole image domain is a time-consuming task. Secondly, each pedestrian can be divided into patches of the same size, and the interaction power of the pedestrians will be represented by the motion particles which describe the motion status at the center pixels of the patches. The motion status of each patch is computed by using the optical flows of the pixels within the patch. For each motion particle, its interaction power, defined as its steady state of the current behavior, is computed among all its neighboring motion particles. Finally, the dense crowds' steady state can be represented as a collection of motion particles' interaction power, i.e., the larger the motion particles' interaction power is, the more instable the dense crowds is. Here, an adaptive threshold strategy is proposed to detect abnormal events by examining the frame power field which is a fixed-size random sampling of the interaction power of motion particles. Experimental results on the standard UMN dataset and online videos show that our method could detect the crowd anomalies and achieve a higher accuracy compared to the other competitive methods published recently.

9273-25, Session 6

A coarse to fine method to detect the salient region

Xiaodong Hu, Hong Zhang, Hao Chen, BeiHang Univ. (China); Helong Wang, China Aviation Optical-Electrical Technology Co., Ltd. (China); Mingui Sun, Univ. of Pittsburgh (United States)

The task of salient region detection aims at establishing the most important and informative regions of an image. In this work, we propose a novel method that tackles such task as a process from superpixel-level location to pixel-level refining. Firstly, we over-segment the image into superpixels and compute an affinity matrix to estimate the similarity between each two superpixels according to both color contrast and space distribution. The matrix is then applied to aggregate superpixels into several clusters by using affinity propagation. To measure the saliency of each cluster, three parameters are taken into account including color contrast, cluster compactness and proximity to the focus. We appoint the most salient one to three clusters as the coarse salient region.

For the refining step, we regard each selected superpixel as an influential center. Hence, the saliency value of a pixel is simultaneously determined by all the selected superpixels. Practically, several Gauss curves are constructed based on the selected superpixels. Pixel-wise saliency value is decided by the color distinction and spatial distance between one pixel and the curves' centers. We evaluate our algorithm on the publicly available dataset with human annotations, and experimental results show that our approach has competitive performance.

9273-26, Session 6

Tablet-based two-dimensional measurement for estimating the embryo area of brown rice

Yuttana Intaravanne, Sarun Sumriddetchkajorn, National Electronics and Computer Technology Ctr. (Thailand); Anchalee Prasertsak, International Rice Research Institute (Thailand)

The embryo or germ of a rice seed is growing to the shoot and the root parts of a seedling. In the early stage, the germinated embryo directly receives food from the endosperm. How healthy of the seedling can be predicted by physically measuring the areas of the embryo and endosperm. In this work, we show for the first time how the embryo and endosperm areas of a brown rice can be spatially measured. Our key design is based on the utilization of a tablet equipped with our lens module for capturing the rice seed image under white light illumination. Our Windows-based program is developed to analyze and separate the image of the whole brown rice into the embryo and endosperm parts within 2 seconds per seed. Our tablet-based system is just 32.5 x 20 x 6.5 cm³ with 4 kilograms, capable to easily carry to the field.

9273-27, Session 6

A vein display system based on three-dimensional reconstruction

Danting Wang, Beijing Institute of Technology (China)

Venipuncture is the most common way of all invasive medical procedures, but it can fail even operated by a skillful physician. Vein display system can help to locate subcutaneous veins by capturing NIR vein image and displaying a recalculated image on the skin surface. Traditional vein display device can only obtain the two-dimensional information of the vein which loses the depth information. It may cause inconvenience since users are required to recalibrate the system every time the imaging distance changes.

In this paper, we design a stereo-vision-based vein display system for venipuncture. The three-dimensional vein structure is reconstructed from image pair acquired from two near-infrared cameras and projected to the skin by a DLP projector.

The principal of stereo vision is used to reconstruct the three-dimensional vein structure. The algorithms applied in the process of three-dimensional reconstruction include image processing, camera and projector calibration, epipolar rectification, stereo correspondence and triangulation. To generate the projected image from three-dimensional vein structure, we incorporate various coordinate systems and perform coordinate transformation between them. The experiment result shows that it can acquire a good three-dimensional structure and display a correct vein image on the skin.

9273-28, Session 6

Detection for manipulation history of seam insertion and contrast enhancement

Jianwei Li, Yao Zhao, Rongrong Ni, Beijing Jiaotong Univ. (China)

With the widespread use of computer and the Internet, more and more techniques are available to manipulate digital images. Thus the authority of digital image content is becoming crucial. Compared with digital image watermark, forensic techniques

are more practical in identifying authority of pictures without embedding watermark formerly. However, existing forensic technologies always focus on detecting a single manipulation while the forger normally conducts more than one operation on digital images. In this case, it is imperative to determine the processing history of the image. In this paper, we propose an algorithm which is capable of detecting the processing history of contrast enhancement and seam insertion technology. We have a hypothesis that images are alternatively altered by either seam insertion or contrast enhancement, or both of them. However, neither seam insertion detection algorithms nor contrast enhancement detection algorithms can deal with both of them in the same time. Based on the analysis of these two operations, if contrast enhancement is followed by seam insertion, both of the features can be reserved. Whereas most features of seam insertion are covered in the situation of seam insertion followed by contrast enhancement. Furthermore, we analyze the inherent relevant between seam insertion and contrast enhancement. By means of detecting the amount and length of suspicious seams, we will find the trace of seam insertion under the operation of contrast enhancement. Therefore, both contrast enhancement followed by seam insertion and seam insertion followed by contrast enhancement can be detected correctly. A plenty of experiments verify the effectiveness of our algorithm.

9273-29, Session 7

Wide field-of-view microscopy based on focal spot grid scanning (*Invited Paper*)

Jigang Wu, Shanghai Jiao Tong Univ (China)

Conventional microscope often suffered from limited field of view because of lens aberration, especially when using high-magnification objective lens which implies high resolution. To overcome this limitation, we propose a wide field-of-view microscopic technique by using a two-dimensional focal spot grid to illuminate the sample while scanning the sample. In this way, the resolution and field of view will be determined by the focal spot size and the grid area, respectively, and the achieved field of view can be an order of magnitude larger than conventional microscope with similar resolution. Because of the scanning image reconstruction, the lens aberration has minor effect and won't impose a limitation of the field-of-view, in contrast to the case in conventional microscope.

In the focal spot grid based wide field-of-view microscopy, there are several issues worth careful studies: 1) generation of the focal spot grid; 2) focal spot size; and 3) focal depth and optimal focusing position. We performed experiments to successfully generate the focal spot grid by holographic recording and by using Talbot effect, and used it for wide field-of-view microscopic imaging. Experiments and numerical simulations show that the focal spot of the focal spot grid is usually different from Gaussian spot normally used in laser scanning microscope and need different criteria to evaluate resolution and focal depth. We show that the full-width-at-half-maximum size and the power concentration percentage of the spot center peak are reasonable criteria and consistent with existing foci searching techniques.

9273-30, Session 7

Joint optimization of scene reconstruction and segmentation from light field images

Lipeng Si, Qing Wang, Guoqing Zhou, Northwestern Polytechnical Univ. (China)

A plenoptic camera captures the 4D radiance from a scene containing implicit depth map in the light field data. Depth information helps many low-level vision tasks, like image segmentation, extending from 2D images to 3D scenes, that

makes plenoptic cameras outperform than traditional cameras in these areas. This paper proposes a novel method of depth recovery and scene segmentation simultaneously from the light field image of a plenoptic camera. Assuming that objects in a scene are visually and spatially coherent, we model the depth recovery and scene segmentation as object boundary estimation in 3D space. First, a rough segmentation and depth map are estimated respectively. Then we bridge them by assigning a set of 3D planes to each segment to approximate the object's depth distribution. The planes are tuned to make the depth estimation better fit the original light field data; in turn, depth discontinuity helps to refine the segmentation results. We address this joint optimization in a framework of energy minimization in an iterative way. We have evaluated the proposed algorithm on a camera array dataset and some benchmarks. Experimental results have shown that our approach can obtain accurate depth map with sketchy geometry information of a scene and meaningful objects segmentation results which can further be used in more semantic vision tasks.

9273-31, Session 7

Light-field-based phase imaging

Jingdan Liu, Tingfa Xu, Beijing Institute of Technology (China); Weirui Yue, Guohai Situ, Shanghai Institute of Optics and Fine Mechanics (China)

Phase contains important information about the diffraction or scattering property of an object, and therefore the imaging of phase is vital to many applications including biomedicine and metrology, just to name a few. However, due to the limited bandwidth of image sensors, it is not possible to directly detect the phase of an optical field. Many methods including the Transport of Intensity Equation (TIE) have been well demonstrated for quantitative and non-interferometric imaging of phase. The TIE offers a simple technique for computing the phase from two or more defocused intensity images. Usually, the defocused images were experimentally obtained by shifting the camera along the optical axis with slight intervals. Note that light field imaging has the capability of taking an image stack focused at different depths by digitally refocusing the captured light field. In this paper, we propose to combine light field microscopy and the TIE method for phase imaging, taking the digital-refocusing advantage of Light Field Microscopy. We demonstrate the propose technique by simulation and experimental results. Compare with the traditional camera-shifting technique, light-field imaging allows the acquisition of the defocused images without any mechanical instability and therefore demonstrate advantage in practical applications.

9273-32, Session 7

Light field creating and imaging with different order intensity derivatives

Yu Wang, Huan Jiang, Beijing Technology and Business Univ. (China)

Microscopic image restoration and reconstruction is a charming topic in the image processing and computer vision, which can be widely applied to life science, biology and medicine etc. A light field creating and imaging method is proposed for transparent or partially transparent microscopic samples, which is based on the transport of intensity equation (TIE) and Taylor expansion theorem. In traditional TIE technique, the first derivative of intensity at the focal plane is obtained using two defocus planes and finite difference (FD) methods. But when the distance between these two planes is large, the linearity assumption inherent to the FD approximation is invalid. On the contrary, when the distance between these two planes is small, the signal

to noise ratio of the derivative approximation will be reduced because the information change of these two planes is weak. For overcoming nonlinearity error and noise effect due to the above factors and obtaining the better results when the samples are thick, Taylor expansion of the axial intensity and multiple axial plane images can be used based on the fact that intensity curves are possessed of smooth property over multiple wavelengths of defocus when intensity paraxially propagates in a complex-field. Then different order derivatives of intensity are got by polynomial fitting. Finally these derivatives can be used to create and reconstruct the light field of the sample. The results show the effectiveness and feasibility of our method.

9273-34, Session 8

Light field imaging for fun and profit (Keynote Presentation)

Jingyi Yu, University of Delaware (United States)

A light field captures a dense set of rays as scene descriptions in place of 3D geometry. Applications are numerous, from both commercial and scientific perspectives. Recent advances on computational imaging have enabled novel and efficient light field acquisition devices. For example, the new Lytro and Raytrix cameras are able to capture light fields in a single shot but at a very low spatial and angular resolution. In this talk, I present a new class of image processing algorithms and camera designs that can significantly improve the spatial, angular, and temporal resolution in light field imaging.

Spatial Resolution: We develop a simple but effective technique by maneuvering the demosaicing process. We first show that traditional solutions that demosaic each individual microlense image and then blend them for refocusing is suboptimal. We instead propose to demosaic the synthesized view at the rendering stage by first mapping the rays onto the refocusing plane and then conduct resampling.

Angular Resolution: We introduce a light field triangulation scheme to improve the angular resolution. Our triangulation technique aims to fill in the ray space with continuous and non-overlapping simplices anchored at sampled points (rays). Such a triangulation provides a piecewise-linear interpolant useful for angular super-resolution. We develop a novel triangulation algorithm that uses the depths and structures of 3D lines as constraints for producing high quality triangulations. For robust depth estimation, we further present two light field stereo matching algorithms that greatly outperform the state-of-the-art.

Spatial-Angular Resolution: We further present a unified framework to simultaneously enhance the spatial and angular resolutions by stitching multiple light fields. We first estimate the warping function between two light fields and then stitch them by finding an optimal cut through the overlapping region. We further accelerate the graph-cut algorithm via a coarse-to-fine scheme. We demonstrate various stitching applications to improve the field-of-view as well as translational and rotational parallaxes of the light fields for 3D displays.

Temporal Resolution: Finally, we construct a hybrid-resolution stereo camera system for acquiring and rendering dynamic light fields. Our system couples a high-res/low-res camera pair to replace the bulky camera array system. From the input stereo pair, we recover a low-resolution disparity map and upsample it via fast cross bilateral filters. We subsequently use the recovered high-resolution disparity map and its corresponding video frame to synthesize a light field using GPU-based disparity warping. Our system can produce racking and tracking focus effects at a resolution of 640x480 at 15 fps.

9273-35, Session 8

Low-budget transient imaging using photonic mixer devices (Keynote Presentation)

Wolfgang Heidrich, The Univ. of British Columbia (Canada)

Transient imaging is a recent imaging modality in which short pulses of light are observed "in flight" as they propagate through a scene. Transient images are useful to help understand light propagation in complex environments and to analyze light transport for research and many practical applications. Two such examples are the reconstruction of occluded geometry, i.e. "looking around a corner", or measuring surface reflectance.

Unfortunately, advances in research and practical applications have so far been hindered by the high cost of the required instrumentation, as well as the fragility and difficulty to operate and calibrate devices such as femtosecond lasers and streak cameras.

9273-36, Session 9

Research on application of plan surveying technology in shot-put sports

Jian Zhang, Wuhan Institute of Physical Education (China);
Wanjuan Song, Hubei Univ. of Technology (China)

As there may be measuring errors caused by elasticity of measuring tools, uneven fields and man-made interface, thus impacting scientificity and fairness of contests when adopting manual measurement in shot contests, this article puts forward apply monocular vision measuring technique to achievement measure based on domestic and international research status of monocular vision measuring technique and combines characteristics of shot fields to propose an approach to measure throwing range with plane calibration. The experiments proved that this approach is feasible in throwing events.

9273-37, Session 9

A compression method of EIs in integral imaging

XueSong Li, Shigang Wang, Yuanzhi Lu, Xianglong Hui,
Xiaoyan Wang, Jilin Univ. (China)

Integral Imaging is a technique capable of reproducing a continuous parallax, full-color, continuous point of view, and real perspectives of the scene. When the difference between the depth of most objects in the scene is not great, this paper studies the element images (EIs) compression in this case. First calculate the best match displacement of pixels in EIs through stereo matching approach, and recode the number of pixels at a certain match displacement. If the number of pixels within a small depth is much greater than the number of pixels within the other regions, most objects in the scene can be considered similar depth of field. Otherwise, the method of this article does not apply. Since the resolution of each image is small, approximate that the match displacement of all pixels in one EI are the same. If most of the horizontal displacement of the best

match for most pixels is 2 pixels, the horizontal adjacent EIs can be regarded as shifted 2 pixels; if the resolution of each EI is 20×20 , every two EIs in horizontal direction at intervals of 9 can be approximated seen as seamless. If a total of 50 horizontal EIs, one EI will be extracted every 10 horizontal EIs, then the horizontal direction can be extracted 5 EIs, This 5 EIs can be seen as an approximation spliced into a complete image. While the remaining 45 horizontal images can be assembled into 9 complete images. Then video encoding method can be used for these 10 images.

9273-38, Session 9

Full-reference quality assessment of stereoscopic images by learning binocular receptive field properties

Kemeng Li, Feng Shao, Gangyi Jiang, Ningbo Univ. (China)

The quality assessment of 3D images encounters more new challenges than its 2D counterparts. Directly applying 2D image quality metrics cannot deal with these challenges. In this research, we propose a new full-reference quality assessment for stereoscopic images by learning binocular receptive field properties. We proposed a full-reference (FR) quality assessment method for stereoscopic images by learning binocular receptive field properties from stereoscopic images. The main contributions of this work are as follows: 1) In the training phase, we capture the latent structure of the reference images by learning multiple dictionaries on different scales; 2) In the quality estimation phase, we compute sparse feature similarity (SFC) index by considering phase difference and amplitude difference from sparse coefficient vectors, and compute global luminance similarity (GLS) index by considering luminance changes; 3) We calculate sparse energy and sparse complexity as the basis of binocular combination w.r.t. the previously learnt dictionaries and the estimated sparse coefficient vectors. Since our work only need limited sparse features for quality evaluation, this can bring new insights for the 3D video coding standardization and other 3D video applications.

9273-46, Session 9

Optical image encryption based on a modified radial shearing interferometer

Dajiang Lu, Wenqi He, Xiang Peng, Shenzhen Univ. (China)

A novel method for optical image encryption based on a modified radial shearing interferometer is presented. In this method, a plaintext image is first encoded into a phase-only mask, and then modulated by a random phase mask (secret key), the result is regarded as the input of the radial shearing interferometer and divided into two coherent lights, which interference with each other leading to an interferogram, i.e., ciphertext, which can be used to retrieve the original plaintext by using a recursive algorithm. The decryption result also depends on the shear ratio (auxiliary key), which largely improves the security level of the proposed cryptosystem. The aforementioned encryption procedure can be achieved digitally or optically while the decryption process can only be analytically accomplished. Numerical simulation is provided to demonstrate the validity of this method.

9273-40, Session 10

Computational imaging of light in flight (Invited Paper)

Matthias B. Hullin, Univ. Bonn (Germany)

One of the main challenges in computer vision stems from the fact that visual data is highly ambiguous: given any two-dimensional image, there are infinitely many possible hypotheses of real-world scenes that would explain what we see. In large part, this ambiguity can be traced back to the very mechanism of image capture: every pixel value of our camera is an integral of the so-called plenoptic function over space, angle, wavelength and time. It is only in the last 15 years that we have seen the development of novel imaging modalities that sample the temporal, angular and spectral dimensions to produce high-dimensional plenoptic images, facilitating many vision tasks that are considered to be very hard on monocular 2D image data.

The research direction of transient imaging operates on a time resolution fast enough to resolve non-stationary light distributions in real-world scenes. It enables the discrimination of light contributions by the optical path length from light source to receiver, a dimension unavailable in mainstream imaging to date. Until recently, such measurements used to require high-end optical equipment and could only be acquired under extremely restricted lab conditions. By introducing a computational imaging technique operating on standard time-of-flight image sensors, we for the first time were able to "film" light in flight in an affordable, practical and portable way. Just as impulse responses have proven a valuable tool in almost every branch of science and engineering, we expect light-in-flight analysis to impact a wide variety of applications in computer vision and beyond.

9273-41, Session 10

Partial scene reconstruction using Time-of-Flight imaging

Hongkai Xiong, Yuchen Zhang, Shanghai Jiao Tong Univ. (China)

This paper is devoted to generating the coordinates of partial 3D points in scene reconstruction via time of flight (ToF) images. Assuming the camera does not move, only the coordinates of the points in images are accessible. The exposure time is two trillionths of a second and the synthetic visualization shows that the light moves at half a trillion frames per second. In global light transport, direct components signify that the light is emitted from a light point and reflected from a scene point only once. Considering that the camera and source light point are supposed to be two focuses of an ellipsoid and have a constant distance at a time, we take into account both the constraints: (1) the distance is the sum of distances which light travels between the two focuses and the scene point; and (2) the focus of the camera, the scene point and the corresponding image point are in a line. It is worth mentioning that calibration is necessary to obtain the coordinates of the light point, and can be fulfilled in two steps: (1) choose a scene that contains some pairs of points in the same depth, of which positions are known; and (2) take the positions into the last two constraints and get the coordinates of the light point. After calculating the coordinates of scene points, MeshLab is used to build the partial scene model. The proposed approach is favorable to estimate the exact distance between two scene points.

9273-42, Session 10

Three-dimensional patterning in transparent materials with spatiotemporally-focused femtosecond laser pulses

Fei He, Bin Zeng, Jielei Ni, Wei Chu, Zhaohui Wang, Shanghai Institute of Optics and Fine Mechanics (China); Koji Sugioka, RIKEN (Japan); Ya Cheng, Shanghai Institute of Optics and Fine Mechanics (China)

According to specific configurations, three-dimensional (3D) patterning involves both 3D bioimaging and laser micromachining. Recent advances in bioimaging have witnessed strong interests in the exploration of novel microscopy methods capable of dynamic imaging of living organisms with high resolution, and large field of view (FOV). For most, applications of bioimaging should be limited by the tradeoff between the speed, resolution, and FOV in common techniques, e.g., confocal laser scanning microscopy and two-photon microscopy. However, a recently proposed temporal focusing (TF) technique, based on spatio/temporal shaping of femtosecond laser pulses, enables depth-resolved bioimaging in a wide-field illumination. This lecture firstly provides a glimpse into the state-of-the-art progress of temporal focusing for bioimaging applications. Then we reveal a bizarre point spread function (PSF) of the temporal focusing system, both experimentally and theoretically. Methods towards measuring the spatiotemporal characteristics as well as optimizing the PSF of this temporally focused laser beam are also investigated. Moreover, it is demonstrated that this technique can be implemented into the field of femtosecond laser processing, hastening a wide variety of intriguing applications such as suppression of out-of-focus nonlinear interaction, enhancement of the peak intensity of femtosecond filamentation, second-harmonic generation (SHG) in air, and so on. It can be expected that this newly emerged technique will exhibited new advances in not only 3D nonlinear bioimaging but also femtosecond laser micromachining in the future.

9273-43, Session 10

3D camera with 2.8M pixels based on TOF principle

Xiuda Zhang, Zhejiang Univ. (China)

A three-dimensional (3D) camera based on time of flight (TOF) principle is demonstrated. With a synchronized laser pulses, both intensity and depth images can be obtained. This detector is a commercial charged coupled device and the light source is a 8x8 pulse semiconductor laser diode array. The pixel array is up to true 5 million and the frame rate is up to 40 frames per second (fps). Both the work principle and the distance resolution of the camera are discussed. A scene between 3m to 5m is detected and a 3D scene is demonstrated with a 1932x1452 pixels array and a distance resolution of 2.5cm.

9273-44, Session 10

Depth map super-resolution and enhancement for time-of-flight cameras

Yangguang Li, Lei Zhang, Yongbing Zhang, Graduate School at Shenzhen, Tsinghua Univ. (China)

This paper proposes a novel approach aiming at conducting super-resolution and enhancement to the depth maps captured by 3D Time-of-Flight (ToF) cameras. The depth maps are of low-resolution with noisy and coupled with registered high-resolution color images captured by the RGB cameras. The proposed method is inspired by the image super-resolution model of sparse representation taking both registered color images and depth images into consideration. The fact of discontinuities in depth and coloring tend to co-align enables us to obtain high-resolution depth maps with sharp edge. Unfortunately, the texture-copying artifacts is always coming with edge sharp process as a side effect. To avoid the texture-copying problem, the high-resolution depth images were always made over smooth. Thus, we integrate the registered color images guide into the sparse-representation model to get more excellently high-resolution depth maps. The goal can be achieved in two steps: 1) Using the registered color images to guide the up-sampling process of depth maps. 2) Enhancing and rectifying the depth map obtained based on sparse signal representation. That is, we change the color images into intensity images, and train the intensity images to get two dictionaries of smoother images and original images. The sparse representation can be achieved through the over smooth depth maps and the smoother image dictionary by pursuit algorithms and applied with the original image dictionary to generate the enhanced and precise high-resolution depth maps. The experiment shows that our approach can obtain high-resolution depth maps in terms of both objective and subjective quality improvements.

Conference 9274: Advanced Sensor Systems and Applications VI

Thursday - Saturday 9 -11 October 2014

Part of Proceedings of SPIE Vol. 9274 Advanced Sensor Systems and Applications VI

9274-1, Session 1

Novel approach for simultaneous wireless transmission and evaluation of optical sensors (*Invited Paper*)

Niels Neumann, Tobias Schuster, Dirk Plettemeier,
Technische Univ. Dresden (Germany)

Optical sensors can be used to measure various quantities such as pressure, strain, temperature, refractive index, pH value and biochemical reactions. The interrogation of the sensor can be performed spectrally or using a simple power measurement.

However, the evaluation of the reflection or transmission sensor signal and the subsequent radio transmission of the results is complicated and costly. A sophisticated system setup comprising a huge number of electrooptical components as well as a complete radio module is required. This is not only expensive and unreliable but also impractical within harsh environment, in limited space and in inaccessible areas.

Radio-over-Fiber (RoF) technology implies signals modulated on an electrical carrier being transmitted over fiber by using optical carriers. Combining RoF techniques and optical sensors, a new class of measurement devices readable by a radio interface is introduced in this paper. These sensors use a modulated input signal generated by a RoF transmitter that - after being influenced by the optical sensor - is directly converted into a radio signal and transmitted. This approach enables remote read-outs of the sensor and its evaluation by radio transmission. Thus, costly and sensitive equipment in the vicinity of the measurement location is avoided. The equipment can be concentrated in a central location supporting existing radio transmission schemes (e.g. Wifi).

In the full paper, the concept will be discussed and analyzed in detail. First measurements of a demonstrator (temperature sensor with wireless readout at 2.4 GHz) will be presented underlining the potential of the system approach.

9274-2, Session 1

Magneto-optic sensor based on field-induced birefringence compensation

Changsheng Li, BeiHang Univ. (China)

Two novel magneto-optic sensors are proposed which are based on mutual compensation of external field-induced birefringence in sensing materials. As we know, external magnetic field can cause linear birefringence in some optical materials, such as nitrobenzene (C₆H₅NO₂) liquid, i.e. Cotton-Mouton effect. And magnetic field-induced linear birefringence is proportional to the square of external magnetic field. On the other hand, nitrobenzene also exhibit electrooptic Kerr effect, where electric field-induced linear birefringence is proportional to the square of external electric field. Thus, when linear birefringence in nitrobenzene increases with external magnetic field, we can control the applied electric field to decrease the linear birefringence until it reaches zero. Thus we can know the amplitude of magnetic field to be measured from the given compensating electric field. Another magneto-optic sensor is based on some optical materials exhibiting both Faraday magneto-optic effect and electrogyration effect, such as lead molybdate (PbMoO₄) crystal. For this kind of crystal, the magnetic field-induced Faraday rotation angle is proportional to external magnetic field. Meanwhile, for the same crystal, an external electric field can also cause the optical polarization rotation angle. Both polarization rotations are

circular birefringence. In principle, the magneto-optic Faraday rotation angle can be compensated by the electrogyration angle. Thus, external magnetic field can also be measured from the compensating electric field. The above two magneto-optic sensors can be used for closed-loop measurement of magnetic field.

9274-3, Session 1

A hybrid optical fiber sensor network with the function of self-diagnosis and self-healing

Shibo Xu, Tiegeng Liu, Chunfeng Ge, Cheng Chen, Hongxia Zhang, Tianjin Univ. (China)

We develop a hybrid wavelength division optical fiber network multiplexing distributed fiber-optic sensors and quasi-distributed FBG sensor arrays which detect vibrations, temperatures and strains at the same time. The network has the ability to locate the failure sites automatically designated as self-diagnosis and make protective switching to reestablish sensing service designated as self-healing by cooperative work of software and hardware. The processes above are accomplished by master-slave processors with the help of optical and wireless telemetry signals. All the sensing and optical telemetry signals transmit in the same fiber either working fiber or backup fiber. We discuss the robustness of the network in two different light source distributions: shared and dedicated protection. We take wavelength 1450nm as downstream signal and wavelength 1350nm as upstream signal to control the network in normal circumstances, both signals are sent by a light emitting node of the corresponding processor. There is also a continuous laser wavelength 1310nm sent by each node and received by next node on both working and backup fibers to monitor their healthy states, but it does not carry any message like telemetry signals do. When fibers of a sensor unit are completely damaged, the master processor will lose the communication with the damaged node and the nodes behind it. However we install RF module in each node to solve the possible problem. Finally, the whole network state is transmitted to host computer by master processor. Operator could know and control the network by human-machine interface if needed.

9274-4, Session 1

Effect of induced linear birefringence on Faraday current sensor using ultra low birefringence optical fiber

Bramhadeo A. Sawale, Central Power Research Institute (India)

The paper discusses change in behavior of current sensor using ultra low birefringence optical fiber under induced linear birefringence due to bending stress and other unintended external influencing parameters. There is a great deal of interest in studying induction of linear birefringence in ultra low birefringence optical fiber. In optical current sensor, due to bending stress, it is seen that the linear polarization of light in the fiber employed is not maintained and it changes to elliptical polarization. Once the ultra-low birefringence optical fiber is employed as a sensor, prevention or elimination of induced linear birefringence due to bending stress and external influencing parameters is very important because these induced linear birefringence alters or even quenches the desired results. Furthermore, it renders the device unstable as this induced

birefringence causes difference in phase velocities and distort polarization. Practical experience of behavior of Ultra-low-birefringence Optical Fiber for bending stress is presented. It was noticed that linearly polarized light through the fiber loses its property of linear polarization and again regains the polarization cyclically and thus the output of the sensor changes accordingly.

9274-5, Session 2

Advances of distributed optical sensor systems for applications in industries and biomedicine (*Invited Paper*)

Xiaotian Steve Yao, Tianjin Univ. (China) and Suzhou Optoring Technology Co., Ltd. (China) and General Photonics Corp. (United States); Zhihong Li, Tianjin Univ. (China) and Suzhou Optoring Technology Co., Ltd. (China); James Chen, Hongxin Chen, General Photonics Corp. (United States); Zhenyang Ding, Zhuo Meng, Longzhi Wang, Ya Su, Tiegeng Liu, Tianjin Univ. (China)

We describe the newest advancements of distributed optical sensor systems, including distributed polarization crosstalk analyzer (DPXA), Optical Frequency Domain Reflectometer (OFDR), and Optical Coherence Tomography (OCT), for a wide range of applications in fiber optic gyroscopes, PM fiber characterization, fiber and structural health monitoring, wafer inspection, dental examination, and blood glucose monitoring. The related works are conducted at the Polarization Center of Tianjin University, Suzhou Optoring Technologies, Ltd, and General Photonics Corporation.

9274-6, Session 2

Long-range high spatial resolution optical frequency-domain reflectometry based on optimized deskew filter method (*Invited Paper*)

Zhenyang Ding, Yang Du, Tiegeng Liu, Tianjin Univ. (China); Xiaotian Steve Yao, Tianjin Univ. (China) and General Photonics Corp. (United States); Bowen Feng, Kun Liu, Junfeng Jiang, Tianjin Univ. (China)

Optical frequency-domain reflectometry (OFDR) has been attracting considerable attention for a number of applications, including diagnosing optical fiber network, and distributed optical fiber sensing such as temperature, strain, vibration, gas and so on. Although sub-millimeter resolution is achievable, the measurement range is limited to a few tens of meters, because a nonlinearity effect or nonlinear phase in the beating signals of OFDR. To extend the measurement range further, we present a simple but effective method to achieve a long-range high spatial resolution OFDR by using an optimized deskew filter method, where the frequency tuning nonlinear phase obtained from an auxiliary interferometer is used to compensate the nonlinearity effect in the beating signals generated from a main OFDR interferometer. The method can be applied for the entire spatial domain of the OFDR signals at once with a high computational efficiency. In addition, we integrate two optimized method to the deskew filter method. One hand, we use a cepstrum method to estimate the time delay in the auxiliary interferometer with high accuracy. On the other hand, we use the higher orders of Taylor expansion to estimate the nonlinear phase, which can obtain more "specific information" of nonlinear phase and reduce the errors caused by the first order of Taylor expansion. With our proposed method we experimentally demonstrated a factor of 187 times improvement in the spatial resolution by comparing

the results of an OFDR system with and without nonlinearity compensation. In particular we achieved a measurement range of 80 km and a spatial resolution of 20 cm and 80 cm at distances of 10 km and 80 km.

9274-7, Session 2

Chaotic Brillouin optical coherent domain reflectometry

Zhe Ma, Taiyuan Univ. of Science and Technology (China); Mingjiang Zhang, Taiyuan Univ. of Technology (China)

A distributed-feedback laser diode (DFB-LD), subject to optical feedback via a fiber ring cavity, is used as the chaotic light source. The strength and polarization state of the feedback light are adjusted by a variable attenuator (VA) and polarization controller (PC). A narrow line-width tunable laser was used as a light source, and the light beams inject into an electro-optic modulator (EOM) modulated by the chaotic light source. A mini-MBC was used to control the EOM. The output chaotic light with narrow line-width was divided into two light beams by a coupler. One of the beams was directly used as the reference light of self-heterodyne detection, after passing a 16-km delay fiber and tunable delay line for controlling the correlation peaks. The other beam was injected into the sensing fiber (8km SMF) as the pump light, after being amplified by an Er-doped fiber amplifier (EDFA) to 15.98 dBm. An optical filter composed of fiber Bragg grating (FBG) with a 3-dB bandwidth of about 10 GHz was inserted in order to suppress the Rayleigh scattering and the Fresnel reflection in the sensing fiber. The optical beat signal of the reference light and the Stokes light was detected by balanced photo-diodes (BPD) and converted to an electrical signal. The relative polarization state of the two light beams was optimized by adjusting polarization controllers manually. The signal was monitored by an electrical spectrum analyzer (ESA) and an electrical oscilloscope (Osc). The measurement data were transferred to a personal computer (PC).

9274-9, Session 2

Brillouin optical correlation domain reflectometry based on random phase codes

Mingjiang Zhang, Jing Chai, Taiyuan Univ. of Technology (China)

A novel technology to measure the distribution of temperature along an optical fiber is proposed. The method relies on the phase modulation of two optical waves by a common pseudo-random bit sequence (PRBS). The PRBS symbol duration is much shorter than the acoustic lifetime, therefore, the spontaneous Brillouin scattering is effectively confined to narrow correlation peaks. The separation between neighboring peaks can be arbitrarily long, which is controlled by the PRBS length. Thus, compared with the traditional Brillouin optical time domain reflectometry (BOTDR), the technique can improve the spatial resolution. We detect the spontaneous Brillouin scattering with controlling the interference of the pump light and the reference light. By using the variable optical delay line in the branch of the reference light, we can make the spontaneous Brillouin scattering localized.

9274-10, Session 3

Tilted fiber Bragg gratings as mechanical and biochemical sensors (*Invited Paper*)

Tuan Guo, Bai Ou Guan, Jinan Univ. (China); Hwa-Yaw Tam,

The Hong Kong Polytechnic Univ. (Hong Kong, China);
Jacques Albert, Carleton Univ. (Canada)

The tilted fiber Bragg grating (TFBG) is a new kind of sensor that possesses all the advantages of well-established Bragg grating technology in addition to being able to excite cladding modes resonantly. This device opens up a multitude of opportunities for single-point sensing in hard-to-reach spaces. Over the past four years, our research group has been developing multimodal fiber grating sensors based on tilted FBGs in various shapes and forms, always keeping the device itself simple to fabricate and compatible with low-cost, standard FBG technology. In this talk, we reviewed our progresses in TFBG sensors for mechanical and biochemical applications, including temperature-independent TFBG vibration sensor and accelerometer, chirped TFBG micro-displacement sensor, two demonstration TFBG vector vibroscope, polarimetric multi-mode TFBG rotation sensor, reflective TFBG refractometer based on strong cladding to core recoupling, polarimetric TFBG biosensors for in-situ detection of density alteration in non-physiological cells.

9274-11, Session 3

Dual fiber Bragg grating configuration-based fiber acoustic sensor for low-frequency signal detection

Dong Yang, Shun Wang, Ping Lu, Deming Liu, Huazhong Univ. of Science and Technology (China)

We propose and fabricate a new type fiber acoustic sensor based on dual fiber Bragg gratings (FBG) configuration. The acoustic sensor head is constructed by putting the sensing cells enclosed in an aluminum cylinder space built by two C-band FBGs and a film of 50 μm thickness. One end of each FBG is longitudinally adhered to the film by UV glue. One of the two FBGs is employed for transmitting light, and the other for reflecting. The dual FBGs play roles not only as signal transmission line but also as sensing component, they demodulate each other's optical signal mutually during the measurement. The output optical power experiences fluctuation in a linear relationship along with a variation of axial strain and surrounding acoustic interference. So a precise approach to measure the frequency and sound pressure of the acoustic disturbance is achieved. Experiments are performed and results show that a relatively flat frequency response in a range from 100 Hz to 1 kHz with the average signal-to-noise ratio (SNR) above 22 dB is obtained. The maximum sound pressure sensitivity of 90 $\mu\text{W}/\text{Pa}$ was achieved with the R-squared value of 0.99284 and the sound pressure range of 100.3-118.5dB. It has potential applications of low frequency signal detection. Owing to its direct self-demodulation method, the sensing system reveals the advantages of easy to demodulate, good temperature stability and measurement reliability. Besides, performance of the proposed sensor could be improved by optimizing the parameters of the sensor, especially the films, or employing an anechoic chamber.

9274-12, Session 3

Analysis on intensity demodulated strain sensing based on multiple phase-shifted FBG

Xiaolei Zhang, Shandong Academy of Sciences (China)

An intensity demodulated strain sensing scheme based on a pair of multiple phase-shifted fiber Bragg grating (FBG) is investigated. The reflected spectrum of the sensing multiple phase-shifted FBG is slightly offset from the reference multiple phase-shifted FBG. Consequently simultaneous wavelength shifts of all subchannels are expected under uniform pressure.

By introducing a broadband source, any change of wavelength will result in various power change which can be received by the photodetector related to the external strain signal. The multiple phase-shifted FBGs are designed using the transfer matrix method to obtain uniform and high transmission, and fabricated by dithering phase mask method which provides the required apodization and phase shifts. A mathematical model is constructed to analyze the strain sensing scheme by relate the power change to reflectivity spectrum, thus help us optimize the design and fabrication of multiple phase-shifted FBG to achieve maximum sensitivity and signal-to-noise ratio (SNR). The multiple phase-shifted FBGs with different phase shift numbers are designed so as to make comparisons. The experimental results show that the strain sensitivity can be significantly enhanced by over 10dB using multiple phase-shifted FBG compared to a normal FBG.

9274-13, Session 3

Broadband-trimming band-rejection filters using chirped and tilted fiber gratings

Fu Liu, Tuan Guo, Chuang Wu, Bai Ou Guan, Jinan Univ. (China)

Broadband-trimming band-rejection filters based on chirped and tilted fiber Bragg gratings (CTFBG) are proposed and experimentally demonstrated. The flexible chirp-rate and wide tilt-angle provide the gratings with broadband filtering functions over a large range of bandwidth (from 10 nm to 150 nm), together with a low transmission loss (less than 1dB) and a negligible back-reflection (lower than 20 dB). The slope profile of CTFBG in transmission can be easily tailored by adjusting the tilt angle, grating irradiation time and chirp rate-grating factor, and it is insensitive to polarization of launch condition. Furthermore, by coating the CTFBG with a suitable polymer (whose refractive index is close to that of the cladding glass), the cladding modes no longer form weakly discrete resonances and leave a smoothly varying attenuation spectrum for high-quality band rejection filters, edge filters and gain equalizers.

9274-14, Session 3

Strain transfer error analysis of flexible armoring-wire packaged FBG sensor used for asphalt pavement monitoring

Huaping Wang, Wanqiu Liu, Zhi Zhou, Dalian Univ. of Technology (China)

Asphalt pavement is the most widely used in transportation field, which has been paid more and more attention for the high-frequency occurred damage leading to repeated maintenance and economic loss. Therefore, it is significant to capture the mechanical properties of asphalt pavement under vehicle loads and environmental effect. Optical fiber sensing technology has been expected as an efficient way to realize this function. Taking the local high-precision detection into account, FBG has been selected as the sensing element, flexible armoring wire has been chosen as the protective layer and FRP clamps have been employed to deliver the deformation of host material to fiber core. Strain transfer error analysis of this flexible armoring-wire packaged FBG sensor embedded in asphalt surface course under vertical area load has been investigated. Finite element analysis and lab tests of this asphalt mixture block embedded with the proposed FBG sensor has been conducted to check the availability of the deduced strain transfer error modification function. Results indicate that this FBG sensor could be used to detect strain of asphalt pavement and much higher-precision detection could be achieved after eliminating the strain transfer error with the derived function.

9274-15, Session 3

Packaged FBG sensor for real-time stress monitoring of the deep-water riser

Jian Xu, Dexing Yang, Yajun Jiang, Meirong Wang, Huailun Zhai, Yang Bai, Northwestern Polytechnical Univ. (China)

The stress monitoring for the under-water risers in drilling platform, especially in the semi-submersible drilling platform, is very important to prevent the risers from overload and damage. A packaged fiber Bragg gratings (FBGs) sensor for real-time stress monitoring is designed for the applications on oil drilling risers under 3000 meters deep water. A copper tube that is a main component of the sensor has a small hole with a diameter of about 1mm along its axes and a large groove at its each end face. The bare FBG is passed through the small hole and fixed to its two ends by epoxy resin. Then the copper tube is packaged by filling the large groove with structural adhesive. A gap between the two types of glues is left in order to avoid that the outer water-pressure is applied on the epoxy resin through the structural adhesive. The relationships between the stress of the riser and the strain, tension, pressure, temperature of the single sensor are discussed. The tension sensitivity of the sensor is 136.75 pm/KN in the range of 0 to 10KN while its R-square is better than 0.99997. Meanwhile, the maximum error between the actual values and fitted values in four repetitive tension tests is 5.4pm. The pressure and temperature characteristics of the sensor are also studied experimentally. The results show that there is a good linear response between water-pressure and the central wavelength from 0MPa to 30MPa, and the sensor can survive even under the pressure more than 30MPa. In addition, the central wavelength of the sensor shifts linearly with increasing the temperature from 0 to 40°C, so the pressure and temperature can be easily compensated when the sensor is used for stress monitoring of the under-water risers.

9274-16, Session 4

Graphene-coated microfiber Bragg grating for ammonia gas sensing

Anqi Zhang, Yu Wu, Baicheng Yao, Yuan Gong, Yunjiang Rao, Univ. of Electronic Science and Technology of China (China); Kin Seng Chiang, City Univ. of Hong Kong (China)

The excitation of surface field and evanescent enhancement in the graphene based optical waveguide have shown sensitive to the refractive index of surrounding media and potential applications in high-sensitivity biochemical sensing. In this paper, we investigate the graphene-coated microfiber Bragg gratings (GMFBGs) with different diameters for ammonia gas sensing. The maximum sensitivity with 6 pm/ppm is achieved experimentally when the microfiber's diameter is 10 μm. Moreover, by adjusting the diameter of the GMFBG, the sensing performance of the GMFBGs can be optimized. Experimental results indicate, when the diameter is range of 8-12 μm, the GMFBG shows the characteristics of high sensitivity, relative low attenuation, and large dynamic range.

9274-17, Session 4

Measurements of high frequency vibration using fiber Bragg grating sensors packaged on PZT plate

Qiaofeng Fang, Wentao Chen, Zhenyu Yin, Yunqi Liu, Shanghai Univ. (China)

Much attention has been paid for the real-time monitoring

of large building, construction, and bridge, et al. Different techniques have been adopted for the detection of the vibration. Thanks to the advantages of high sensitivity, good stability, anti-interference to electromagnetic, et al, fiber Bragg grating (FBG) sensors have been developed for the safety monitoring of the large buildings.

In this paper, we demonstrate the FBG vibration sensors working at a frequency up to 900 kHz. The FBGs were surface-mounted on the piezoelectric (PZT) ceramic, which is used as the vibration sensor head. A nonlinear response was measured with a periodically strong response at the frequencies of 1 kHz, 5 kHz, 12 kHz, 40 kHz, 70 kHz and 400 kHz. Four kind of polymer were used to package the FBG on the PZT plate. The gratings have similar pattern of vibration response with different deviation on the output voltage. The FBGs packaged with the polymer 705b and EPO-TEK 353ND were found to have a better response at lower frequency, while the FBGs packaged with the polymer T120-023-C2?TRA-BOND F112 have a better response at higher frequency. Especially the FBGs packaged with the polymer T120-023 - C2 can work at the frequency of 900 kHz. The strain transfer coefficients are higher for the FBGs glued with the polymer EPO-TEK 353ND and T120-023-C2. The sensors could be developed for the real-time monitoring of the large infrastructure.

9274-18, Session 4

Integrated Raman spectroscopic sensor based on silicon nanowire waveguides

Xianxin Jiang, Jian-Jun He, Zhejiang Univ. (China)

Raman spectroscopy is a powerful analytical and research tool which has found a variety of applications owing to its high specificity and rich information content. In this article we propose a novel Raman spectroscopic sensor which employs silicon nanowire waveguides for excitation and collection of Raman signal, and an integrated micro-ring resonator as a filter. A 1550nm tunable laser is coupled into the device, and along propagation in the sensing waveguide, analyte cladded directly on the core layer is excited, and the corresponding Raman signal is collected by the same waveguide through evanescent coupling. The Raman signal is filtered by the micro-ring resonator and then detected by a photodiode. Theoretical calculations indicate that power density in the evanescent field of the waveguides is extremely high due to the large index contrast of silicon-on-insulator, which will greatly enhance the Raman scattering process. Preliminary experimental results show that the extinction ratio of the micro-ring resonator filter is more than 40 dB and the Q value is about 15000. Simulation results show that this high stray light rejection of the ring filter allows Raman signal at wavenumber as low as 30 cm⁻¹ to be observed. The integration of the filter and potentially the detector and a tunable semiconductor laser can greatly reduce the system size and cost. In conclusion, by employing silicon waveguide as excitation and collection of Raman signal, along with an integrated micro-ring filter, a detector and a tunable laser, a miniaturized Raman spectroscopic sensor can be realized on SOI platform.

9274-19, Session 4

High signal-to-noise acoustic sensor using phase shift gratings interrogated by the Pound Drever Hall technique

Peter Kung, QPS Photonics Inc. (Canada)

Optical fiber is made of glass, an insulator, and thus it is immune to strong electromagnetic interference. Therefore, fiber optics is a technology ideally suitable for sensing of partial discharge (PD) in both transformers and generators. Extensive development efforts have been used to find a cost effective solution for

detecting partial discharge, which generates acoustic emission, with signals ranging from 30 kHz to 200 kHz. The requirement is similar to fiber optics Hydro Phone, but requires higher frequencies. There are several keys to success: there must be at least 60 dB signal-to-noise ratio (SNR) performance, which will ensure not only PD detection but later on provide diagnostics and also the ability to locate the origin of the events. Defects that are stationary would gradually degrade the insulation and result in total breakdown. Transformers currently need urgent attention: most of them are oil filled and are at least 30 to 50 years old, close to the end of life. In this context, an issue to be addressed is the safety of the personnel working close to the assets and collateral damage that could be caused by a tank explosion (with fire spilling over the whole facility). This paper will describe the latest achievement in fiber optics PD sensor technology: the use of phase shifted fiber gratings with a very high speed interrogation method that uses the Pound-Drever-Hall technique. More importantly, this is based on a technology that could be automated, easy to install, and, eventually, available at affordable prices

9274-37, Session Post

The approach of restraining Faraday effect of fiber optic gyroscope with reverse twist optical fiber

Xiao Cheng, Jun Liu, Jianling Yin, Jun Lu, Mechanical Engineering College (China)

Faraday magneto-optic effect of optical fiber gyro is the reciprocity error source that affects the performance of fiber-optic gyro, especially the precision of fiber optic gyroscope. The magnetic sensitive mechanism of fiber-optic gyroscope is introduced in this paper and the main source of radial and axial magnetic sensitivity error is analyzed. The circular birefringence of the fiber is improved by twisting. With coupled wave equations of twist optical fiber, an expression that can evaluate circular birefringence degree of optical fiber is obtained. Based on the above analysis, this paper puts forward an approach that a length of reverse twist optical fiber is spliced onto the original optical fiber ring of fiber optic gyro. This approach can produce high circular birefringence. The reciprocity phase of original optical fiber ring is compensated so that the purpose that restrains magnetic sensitivity error of optical fiber gyro is achieved. The feasibility of this method is discussed.

9274-38, Session Post

Simulation for optimal design of metal film on surface plasmon resonance sensor

Chen H. Bin, Jimei Univ. (China)

Based on the principle of surface plasmon resonance (SPR) sensor, the influence of metal film was illuminated. According to the MATLAB simulation, the performance of SPR sensor using Au and Ag film was compared. The optimal thickness was 52nm and 38nm, respectively. In view of the features of Au and Ag film, Ag+Au hybrid metal film was proposed. On the basis of simulated result, it could be concluded that the performance of SPR sensor with 50nm composite film (Ag film 20nm) was excellent.

9274-39, Session Post

Simulation on the particle flow in laser airborne particle counting sensor

Jiancheng Lai, Ting Zou, Chunyong Wang, Wei Yan,

Yunjing Ji, Zhenhua Li, Nanjing Univ. of Science and Technology (China)

Laser airborne particle counting sensor (LAPCS), based on light scattering of particle, is specially used in clean environment monitoring. LAPCS samples the air by a pump, and uses a laser illuminating the sampled air in the chamber, then counts the total number of scattering signal and its amplitude distribution, which can characterize the number of particles and size distribution. The structure of air-flow-path in LAPCS directly influences the flow of sampling air, the particle trajectories and velocity distribution in chamber that will influence the performance of LAPCS. In this paper, a finite element arithmetic based on Ansys Fluent14 software environment was developed to simulate the air flow and particle flow in LAPCS. Based on numerical calculations, velocity distribution of airflow and particle trajectories in chamber of LAPCS with different nozzles are presented intuitively. A few particles probably are disturbed outside the air-flow path and pass the photosensitive area many times, which can make the LAPCS iteration count. The results can provide a theoretical basis for optimizing design of the LAPCS.

9274-40, Session Post

Fiber-tip bubble-structure microcavity sensor

Daru Chen, Shujun Luo, Xiaowei Ma, Xiaogang Jiang, Zhejiang Normal Univ. (China); Gaofeng Feng, Junyong Yang, Hangzhou Futong Communication Technology Co., Ltd. (China)

A Fabry-Perot interferometer sensor based on a fiber-tip bubble-structure micro-cavity is proposed, fabricated, and demonstrated for hydrostatic pressure sensing and transverse load sensing. A segment of a well-cleaved multimode fiber with a core diameter of is processed with chemical etching based on a solution of HF 40% and the bubble-structure micro-cavity is fabricated by using arc discharge at the end of the processed multimode fiber. The sensor can be considered as a two-beam Fabry-Perot interferometer with one beam from the silica-air interface on the left side of the bubble and the other from the air-silica interface on the right side of the bubble. The broadband light is injected into the fiber-tip bubble-structure micro-cavity by splicing the multimode fiber with the bubble-structure micro-cavity to a 3-dB optical coupler and the reflective spectrum of the bubble-structure micro-cavity is measured by an optical spectrum analyzer. Both hydrostatic pressure sensing with a sensitivity of -0.1 nm/MPa and transverse load sensing with sensitivity of 3.64 nm/N are experimentally demonstrated based the proposed fiber-tip bubble-structure micro-cavity sensor. The proposed sensor is demonstrated with a relative low temperature sensitivity of about $2 \text{ pm/}^\circ\text{C}$. Properties of the fiber-tip bubble-structure micro-cavities with different sizes are investigated. The sensor has the advantages of low-cost, ease of fabrication and compact size, which make it a promising candidate for hydrostatic pressure sensing or transverse load sensing in harsh environments.

9274-41, Session Post

Tunable mode coupler in the microfluidic channel for the fiber optics refractive index sensor

Gao Ran, Jiang Yi, Beijing Institute of Technology (China); Gang Li, Ying Zhou, China Academy of Aerospace Aerodynamic (China)

We propose and demonstrate a highly sensitive optical fiber microfluidic refractometer. An in-line MI was carried out with

a conventional fusion splicer. A section of the photonic crystal fiber (PCF) was cleaved, and the free end face of the PCF was filmed with the gold film, of which the reflectivity was 98%. Then a section of the PCF with the length of 300 μm was fused to completely collapse holes by using an arc discharge technique. At the collapsed region, the propagation mode was divided into two beams due to the mode-field mismatch, and part of the fundamental core mode in the SMF coupled to the cladding modes in the PCF. The fundamental core mode and the cladding mode propagate along the PCF with different effective refractive index, which forms an in-line MI. A microhole is fabricated in the collapsed region by using femtosecond laser beam, which combines the tunable mode coupler and microfluidic channel. The mode field diameter of the guided light is changed with the refractive index (RI) in the microfluidic channel, which results in the tunable coupling ratio between the core and the cladding in the PCF. Therefore, the refractive index of the liquid in the microfluidic channel is detected by interrogating the fringe visibility of the reflection spectrum. These experiments results demonstrate that the sensor is insensitive with the temperature and strain, and a RI sensitivity of up to 150.7 dB/RIU is achieved, establishing the tunable mode coupler as a sensitive and versatile sensor.

9274-42, Session Post

Confocal ring cavity as micro-optical gyro element

Vladimir Y. Venediktov, Saint Petersburg Electrotechnical Univ. "LETI" (Russian Federation) and Saint Petersburg State Univ. (Russian Federation); Yuri V. Filatov, Egor V. Shalymov, Saint Petersburg Electrotechnical Univ. "LETI" (Russian Federation)

Passive ring cavities are now treated as the most promising sensitive elements for cheap and technologically simple microoptical gyro for mass production. Usually the single-mode planar waveguides are considered to be the only possible technology for such devices implementation. However, our analysis shows that in some cases the confocal ring cavity, characterized by degeneration of transverse modes, can be the better alternative for such a device technology. The paper considers possible advantages and disadvantages of such an approach, its limitations and technology prospects.

9274-43, Session Post

Simplified design of diaphragm-based fiber optic extrinsic Fabry-Perot accelerometer

Zhaogang Wang, Wentao Zhang, Jing Han, Hao Xia, Fang Li, Institute of Semiconductors (China)

Fiber optic Fabry-Perot sensor, compared with other fiber optic sensors, with its unique advantages such as simple structure, small in size, has received great attention. Common diaphragm based fiber optic Fabry-Perot accelerometer (FOFPA) consists of diaphragm as elastic element, mass as inertial element, fiber tip or fiber collimator, reflector such as a mirror, and columnar shell. Fiber tip is coaxially fixed on the top of the shell, a diaphragm-mass structure is at the middle. A reflector on the mass and the end face of fiber tip constitute a FP interferometer. It is a simple structure, but could be further simplified through some improvements.

A fiber optic Fabry-Perot accelerometer with diaphragm-mass-collimator gathered structure is presented. This design simplifies the manufacturing process and compacts the structure. The operation principle based on Fabry-Perot interference is

described. Several tests using intensity demodulation scheme which can control the working point of FOFPA were carried out. Experimental results show that: (1) axis sensitivity of the proposed FOFPA is 37.6 dB (re: 0 dB=1 V/g) with a fluctuation less than 2 dB in a frequency bandwidth of 20-200 Hz, and the calculated value is 39.6 dB, (2) the resonant frequency is about 350 Hz, and the calculated natural frequency is about 378 Hz, (3) the measurement range is about 74 dB@100 Hz, and the resolution is about 52 μg @100 Hz.

9274-44, Session Post

Differential check accelerometer based on double fiber 45 degrees Fabry-Perot interferometers

Jing Han, Shijiazhuang Tiedao Univ. (China) and Institute of Semiconductors (China); Wentao Zhang, Institute of Semiconductors (China); Baochen Sun, Shijiazhuang Tiedao Univ. (China); Zhaogang Wang, Institute of Semiconductors (China); Hongbin Xu, Shijiazhuang Tiedao Univ. (China) and Institute of Semiconductors (China); Fang Li, Institute of Semiconductors (China)

The paper describes a construction of differential check accelerometer based on double fiber 45 degrees Fabry-Perot (F-P) interferometers. The support beam consists of a mass block in the middle and can oscillate freely when the sensor is subject to the vibration. Two 45 degrees F-P cavity fixed to the mass up and down respectively can change the length of cavity by the sensor vibrating. The 45 degrees F-P cavity include two mirrors and a fixed 45 degrees mirror in the steel tube. The first mirror of F-P is the end face of G-lens placed in the support abutment, which joint with a 105/125 nm fiber, and the second mirror is a silver plated diaphragm placed in the steel tube, the light can change its direction at the 45 degrees mirror in the reflecting. In order to get more reflected light the two mirrors' reflectivity are 4 % and 90 % respectively. As a result the detected acceleration can be got through the light signal converting to electrical signal. Due to the process of sensor vibrating, one cavity's length increases and the other shortens which makes the two 45 degrees reflection light interference cavity have equivalent but opposite sign variable size. Thus, measurement sensitivity doubled, and the influences by temperature and other negative factors on the mass are offset as well. The theoretical sensitivity can reach 15.6 rad/g while the resonant frequency of the accelerometer is 300 Hz.

9274-45, Session Post

A novel porous silicon-based multilayer dielectric-grating structures for diffraction-based sensing

Jiaqing Mo, Xi'an Jiaotong Univ. (China); Yajun Liu, Changwu Lv, Xiaoyi Lv, Zhenhong Jia, Xinjiang Univ. (China)

Porous silicon material and device has attracted more attention for use as biochemical optical sensors due to its large surface area, total compatibility with standard microelectronic processing, and easy fabrication. In particular, various porous silicon-based photonic device structures have been successfully adopted for enhancing sensitivity, such as polybasic photonic crystals, waveguides, diffraction gratings, and grating-coupled porous silicon waveguides.

Ryckman et al. reported porous silicon diffraction grating biosensors for a cost-effective stamping technique. However, the diffraction efficiency of these porous silicon-grating sensors in previous works cited above is not high due to the loss of energy

radiated to the substrate. In order to solve the above problem, we have reported a novel simple porous silicon based on the grating optical sensor by adding high-reflectivity porous silicon stacks between the substrate and grating for improved diffraction efficiency of the top surface grating, which can improve detection sensitivity considerably. And, a 500 nm grating height was used.

After further studies with the optimization of the grating height design, we have found that it was about 30 nm of grating height showing higher sensitivity. Thus, in this paper, a novel porous silicon-based multilayer dielectric-grating structures by adding high-reflectivity porous silicon stacks between the substrate and grating was fabricated, and the porous silicon grating height was set to be about 30 nm, the grating period was 4 μm , the air filling factor was 50%. Aminopropyltriethoxysilane (APTES) was employed as a probing molecule, and the sensitivity increased up to about 10 times compared with that of previous work.

9274-46, Session Post

Intensity modulation photonic crystal fiber based refractometer in the visible wavelength range

Yun Liu, Shimeng Chen, Xinpu Zhang, Wei Peng, Dalian Univ. of Technology (China)

A novel evanescent field refractometer based on a two-core photonic crystal fiber (TWPCF) sandwiched between standard communications fibers and operating at visible wavelength is demonstrated. A short piece of TWPCF was inserted into two grade index MMFs(62.5/125 μm) which were used as lead in and lead out fibers. When light is injected from the leading MMF into the PCF, multiple high order modes of the TWPCF will be excited due to the core-diameter mismatch and propagate along the fiber. The TWPCF section functions as a tailorable bridge between the excited high order modes and the surrounding refractive index (SRI). With a light filter inserting in the front of white light, the transmission spectrum of the light through the sensing region occurs in a well-defined wavelength bands. As a result, the peak power of the transmission light is tailored with the SRI perturbation via the MMF-TWPCF-MMF structure. By simply monitoring the power variation of the transmission light at a given wavelength, the SRI can be measured. The experiment result shows a quadratic relation between the light intensity and samples within RI range of 1.33-1.41 while a linear response can be achieved from the 1.33-1.35 which is a most used RI range for biologically sensing. The advantages of this sensor are simple fabrication, compact size, and low-cost power detection at the well-defined wavelength bands. In addition, with specified coating materials, it is expected the proposed cost-effective RI sensor can be applied for various biological and chemical sensing.

9274-47, Session Post

Photonic crystal fiber refractive-index sensor based on multimode interferometry

Zhenfeng Gong, Xinpu Zhang, Yun Liu, Wei Peng, Dalian Univ. of Technology (China)

We report a type of multimode fiber interferometers (MMI) formed in photonic crystal fiber (PCF). To excite the cladding modes from the fundamental core mode of a PCF, a coupling point is formed. To form the coupling point, we used the method that is blowing compressed gas into the air-holes and discharging at one point, and the air-holes in this point will expand due to gas expansion in the discharge process. By placing two coupling points in series, a very simple all-fiber MMI can be implemented.

The detailed fabrication process is that the one end of the PCF is tightly sealed by a short section of single mode fiber (SMF) spliced to the PCF. The other end of the PCF is sealed into a gas chamber and the opened air holes are pressurized. The PCF is then heated locally by the fusion splicer and the holes with higher gas pressure will expand locally where two bubbles formed. We tested the RI responses of fabricated sensors at room temperature by immersing the sensor into solutions with different NaCl concentration. Experimental results show that as refractive-index (RI) increases, the resonance wavelength of the MMI moves toward longer wavelengths. The sensitivity coefficients are estimated by the linear fitting line, which is 46nm/RIU, 154nm/RIU with the interferometer lengths (IL) of 3mm and 6mm. The interferometer with larger IL has higher RI sensitivity. The temperature cross-sensitivity of the sensor is also tested. The temperature sensitivity can be as low as -16.0pm/ $^{\circ}\text{C}$.

9274-48, Session Post

A new refractive index sensor based on Mach-Zehnder interferometer fabricated by two cascaded single-mode fiber corners

Qingguo Shi, Zhejiang Normal Univ. (China)

The sensor in this article is mainly depend on Mach-Zehnder interference principle. So, we fabricate two cascaded single-mode fiber corners in a fiber. the two corners can form an MZI. assume that a beam of light entered from the left side of the optical fiber, at the first corner, because of the uneven structure, the input optical signal is split into two optical paths, along the core (core mode)and the cladding of the fiber(cladding mode), respectively, and then is recombined together at the second corner. Because of the phase difference between the core and cladding modes, we can find Interference spectrum by a spectrometer. The MZI could be used to measure many environmental parameters, such as refractive index. Since the refractive index of the fiber cladding is sensitive to the solution. So, if the refractive index changes, the refractive index of the cladding will change too, then, we can find the spectrum shift. According to this, by changing the refractive index of the liquids from 1.333 to 1.418, we find the dip(A) moved from 1606 to 1587.5nm approximately. This is a high refractive index sensitivity about 2350nm/RI unit (RIU). Compared with other similar sensors, it is very easy to make, and, the single-fiber fiber is easy to get, So, this device cost little. Besides, the structure of the sensor is compact and strong. Last but not least, the sensor is not sensitive to temperature, which is benefit to the measurement of refractive index. We believe it will find applications in chemical and physical sensing fields, and be large-scale product.

9274-49, Session Post

The tapered surface plasmon resonance fiber sensor based on separated input-output channels

Shimeng Chen, Yun Liu, Wei Peng, Dalian Univ. of Technology (China)

We present a wavelength-tunable tapered optics fiber surface Plasmon resonance (SPR) biochemical sensor by polishing the end faces of multimode fibers(MMF). Two hard plastic clad optical fibers joint closely and are used as the light input and output channels. Their end faces are polished to produce two oblique planes, which are coated with gold film to be the sensing surface and the front mirror. To enhance the light coupling between the input and output fibers, the profile-surfaces of the fibers are also polished slightly. The presence of the tapered

geometry formed by the two oblique planes in the orthogonal directions makes it possible to adjust incident angle through changing the tilt angles of the two end faces, so as to achieve tuning the SPR coupling wavelength-angle pair. Compared with previous researches based a tapered optic fiber probe, we report the approach theoretically increase the signal noise ratio (SNR) by separating incident and emergent light propagating in the different coordinate fiber. Since fabricating the sensing surface and the front mirror on the two fibers to replace one single fiber tip, there is more incident light can reach the sensing surface and satisfy SPR effective. In addition, this improvement in structure has advantages of large grinding and sensing area, which can lead to high sensitivity and simple manufacture process of the sensor. Experimental measurement demonstrates the sensor has a favorable SPR resonance absorption and the ability of measuring refractive index (RI) of aqueous solution. This novel tapered SPR sensor has the potential to be applied to the biological sensing field.

9274-50, Session Post

A new type of Hartmann-Shack wavefront sensor based on compressive sensing technique

Mingwu Ao, Univ. of Electronic Science and Technology of China (China)

This paper presents a new type of Hartmann-Shack wavefront sensor for adaptive optics field, the new sensor detect the focus position of micro lens by compressive sensing technique, then retrieve the wave front. The method makes full use of the sparse characteristics of the micro lens array focus, the wavefront information can be obtained by the time modulation and sparse matrix photosensitive device sampling. Because of the sparse matrix photosensitive device sampling, and it can be avoided by using large data array photosensitive sensor - such as CCD and CMOS image sensors, this new type of wavefront sensor is very beneficial to reduce the difficulty of high speed and light wavefront detection technology.

9274-51, Session Post

Fabrication and simulation of cascaded Fabry-Perot micro-cavities in fibers

Fan Gu, Xiaobei Zhang, Jiabao Xiong, Fufei Pang, Tingyun Wang, Shanghai Univ. (China)

Cascaded Fabry-Perot micro-cavities are fabricated in the single mode fiber by the femtosecond laser to inscribe the reflected index changed mirrors in the fiber totally covering the fiber core. The cascaded Fabry-Perot micro-cavities are made up of three reflected index changed mirrors, or to say of two Fabry-Perot cavities with two different lengths. The theoretical mode of Fabry-Perot micro-cavities considering the reflected mirror loss is established firstly, through the way of transfer matrix method. Simulations are performed to give a brief understanding on the Vernier effect of cascaded micro-cavities. The parallel inscription method of the femtosecond laser fabrication is studied to get the regular reflection spectrum whose fringe contrast is experimentally up to 10dB. It is a promising method to increase the contrast of interference fringe, and improve the resolution of the interference fringe to bring it to a better performance in temperature sensing fields.

9274-52, Session Post

Temperature measurement using second-order Stokes waves of multiwavelength Brillouin-erbium fiber laser

Yi Liu, Mingjiang Zhang, Peng Wang, Yun-Cai Wang, Taiyuan Univ. of Technology (China)

A novel temperature measurement using second-order Stokes waves of multiwavelength Brillouin-Erbium fiber laser (MW-BEFL) is proposed and investigated experimentally. 500 m single mode fiber (SMF) is used as both Brillouin gain media and fiber under test (FUT). Because frequency shift as temperature of the second-order Stokes wave is twice as more as that of the first-order Stokes wave, temperature measurement resolution is improved by twice. In the experiment, the first-order Stokes wave with 1.036 MHz/°C temperature elevation coefficient and 1.138 MHz/°C temperature reduction coefficient and second-order Stokes wave with 2.006 MHz/°C temperature elevation coefficient and 2.339 MHz/°C temperature reduction coefficient are obtained. The results are agreement with theoretical result. This configuration has a promising application for temperature sensing.

9274-53, Session Post

Long-period fiber grating sensor in hollow eccentric optical fiber

Xing Zhong, Chunying Guan, Harbin Engineering Univ. (China)

In addition to conventional single-mode fibers (SMFs), long period fiber gratings (LPFGs) have been written in various special fibers, such as polymer optical fibers, D-shaped cladding fibers, micro-structured optical fibers, eccentric core fibers, and some photonic crystal fibers. These LPFGs showed particularly strong dependence on the temperatures, refractive index. However, LPFGs for sensing are always sensitive to many kinds of parameters simultaneously. And in many practical applications, we often require that the LPFGs are only sensitive to one or two parameters to simplify the measurement equipment and data demodulation. Then we need some special sensors to satisfy the actual demands.

In this paper, the sensing characteristics of hollow eccentric optical fiber (HEOF) LPFG fabricated high-frequency CO₂ laser were investigated experimentally. The HEOF comprises a large central air hole, a quasi-elliptical core and an annular cladding. A thin cladding is between the air and core. We studied the influence of the different bending directions of the HEOF-LPFG on its bending characteristic. The resonant wavelength responses of the proposed LPFG to both the directions and curvatures are investigated respectively. The results indicated that the HEOF-LPFG had different sensitivities on different directions and it is insensitive to bending and the biggest sensitivity only is 1.3nm/m-1 in the range of 0-5m-1. More than that, the dependences of this grating on temperature and axial stress were also studied, obtaining the response rates of 56.7 pm/°? and 0.3 pm/?? respectively. Obviously, the HEOF-LPFG is more sensitive to temperature and immune to curvature and axial stress. HEOF-LPFG can be employed to measure the single parameter and simplify the measurement equipment and data demodulation in practical application.

9274-54, Session Post

Characteristics of all-solid photonic crystal fibers with radial linear arrays

Chunying Guan, Jing Yang, Harbin Engineering Univ. (China)

In 2003, the first all-solid holey fibers (SOHO) made of two types of multicomponent glass was drawn. The structure of the all-solid PCF remained unchanged during the fiber drawing. Therefore, it is useful to avoid structural deformations through using this method. All-solid PCFs can make fiber lasers as the core is doped with rare-earth ions.

In this paper, a simple structure of all-solid microstructured fiber, in which the core-modes are only guided by the photonic bandgap (PBG) effect, is proposed and numerically characterized. This fiber is composed of 8 linear arrays of high refractive index dielectric rods ($n=1.478$) radially symmetry arranged around the low refractive index substrate ($n=1.45$). The finite element method (FEM) is used to analyze the characteristics of proposed fiber. The calculated results show that the distance between the adjacent band gaps is very close, minimum loss of 0.35dB/km can be achieved. With increasing the space between high refractive index rods and the refractive index difference between high refractive index rods and core, the band gap will move to the long wavelength direction. The fundamental guided mode of this fiber is closed to the lower edge of the band gap and the effective refractive index is extremely close to 1.45. With decreasing the bending radius, the short wavelength edge of PBG is severely affected and shifts to the long wavelength, while long wavelength edge of PBG suffers relatively little impact. By adjusting the number of high refractive index dielectric layers, we can effectively change the effective mode area, resulting in the large mode area fiber.

9274-55, Session Post

Ion detection method based on laser-induced ions fluorescence for ion mobility spectrometer

Kaitai Guo, Kai Ni, Guangli Ou, Xiaoguo Zhang, Quan Yu, Xiang Qian, Xiaohao Wang, Graduate School at Shenzhen, Tsinghua Univ. (China)

Ion mobility spectrometry (IMS) is widely used in the field of chemical composition analysis. Faraday cup is the most classical method to detect ions for IMS in atmospheric condition. However, simply gathering ions may not have the ability to sense the precious few ions because the amplification of circuits is limited (10¹⁰-10¹¹). There are some ion collectors with the ability of pre-amplification (10⁵-10⁷), such as electron multiplier and multi-channel plate, but these devices only work in the vacuum environment.

In this paper, we introduced a novel way using photomultiplier in the atmospheric environment instead of faraday cup. Fluorescent ions which were selected by IMS get excited when they fly through the laser excitation area. The fluorescence emitted by the excited ions was captured exponentially and amplified through proper optoelectronic system.

Two pivotal knots of this method are investigated in this paper. The first one is the fluorochrome. Because the ions are detected in condition of gaseous phase, the property of fluorochrome may be changed. We compared many kinds of commonly used fluorescent dyes. An appropriate fluorescence dye was chosen as a fluorescence carrier. The other one is the detection means. There is a serious of reasonable light path and means was designed in the IMS to ensure the number of accepted photons. And the advantages and disadvantages of different optical receiver were discussed in the paper.

Compared with faraday cup, the laser-induced ions fluorescence method may find potential application in more system in the atmosphere condition.

9274-56, Session Post

Laser sensor for monitoring radioactive contamination

Alexsandr Grishkanich, National Research Univ. of Information Technologies, Mechanics and Optics (Russian Federation) and Saint Petersburg Electrotechnical Univ. "LETI" (Russian Federation); Victor Bespalov, Sergey Kascheev, Valentin Elizarov, Aleksandr Zhevnikov, National Research Univ. of Information Technologies, Mechanics and Optics (Russian Federation); Sergey Vasiev, The State Atomic Energy Corp. ROSATOM (Russian Federation)

The leading position occupied by the severity of the consequences of emergencies at nuclear facilities ("Lighthouse" 1957 Sarov, 1997; Fukushima, 2011). In such cases, the determining factor of radioactive isotopes are pollution inert gas, cesium, iodine, strontium, and others. The amount of radioactive isotopes in environment defines the level of radioactive air pollution. Current inspection methods are performed by the contact, because they are based on registration of α - β -types of radiation (distance not more 20 m). Other checking methods of the radioactivity in atmosphere are performed by the spectroscopic diagnostic of isotopes.

Radionuclides frequency spectra are characterized by isotope shifts, each structure is different isotopic mass numbers and the corresponding number of neutrons. For example, isotopes of strontium Sr86, Sr90 and Sr84 frequency shifts correspond to relatively stable Sr88, equal to $5.8 \cdot 10^{-3} \text{cm}^{-1}$, $11.4 \cdot 10^{-3} \text{cm}^{-1}$ and $12.4 \cdot 10^{-3} \text{cm}^{-1}$. Therefore, the identification can only radionuclides with measuring means having a ultra-spectral resolution ($\Delta \lambda / \lambda > 1000$).

Method was developed for the detection of radiation pollution from accidents at at radiation hazardous objects. Experiments were carried out using the method of fluorescence analysis and Raman spectroscopy. Preliminary results show the applicability of these methods in problems of remote monitoring. Preliminary results of experiments show the real possibility to register of leakage of a radionuclide with concentration U235O₂, U238O₂ at level of 10⁸-10⁹ cm⁻³ by Raman-scattering circuit, and concentration Sr90 and Cs137 at level of 10¹³-10¹⁵ on a safe distance (100 m) from the contaminated object.

9274-57, Session Post

Laser remote spectroscopy for geological exploration of hydrocarbons deposits

Alexsandr Grishkanich, Victor Bespalov, Valentin Elizarov, Aleksandr Zhevnikov, National Research Univ. of Information Technologies, Mechanics and Optics (Russian Federation); Aleksandr Il'inskiy, All Russian Petroleum Research Exploration Institute (Russian Federation); Sergey Kascheev, National Research Univ. of Information Technologies, Mechanics and Optics (Russian Federation)

The main geophysical method for underground oil and gas detection is the seismic survey. However, its predictive accuracy in favorable conditions is, at best, 30%. In addition, it has a particularly low efficiency in searching non-anticlinal traps and complex structures, which are typical in East Siberia. Therefore, oil exploration requires additional methods, based on different physical principles.

Laser sensing can serve as a highly effective method of exploration in the present context. Development and introduction of nonlinear optics may increase detection sensitivity.

To solve the problem of airborne pipeline monitoring, leak detection, and oil exploration, we have created an airborne lidar with ultraspectral resolution. The development of this apparatus aims at determining the most promising methods to obtain spectral information, to increase the sensitivity level of spatial and spectral resolutions, to increase the accuracy of referencing the wavelength scale while reducing the size dimension and weight, to introduce unified equipment modules. In their selective capability of determining the spectra, modern spectrometers are divided into multispectral, hyperspectral, and ultraspectral

Experiments were carried out using the method of CARS. Preliminary results show the applicability of these methods in problems of remote exploration. Minimal concentrations of 200 ppb of heavy hydrocarbon gas have been remotely measured in laboratory tests. As estimations have shown the reliability of heavy hydrocarbon gas detection by the integration method of seismic prospecting and remote laser sensing in CARS circuit can exceed 80%.

9274-58, Session Post

Development of a long-gauge vibration sensor

Peter Kung, QPS Photonics Inc. (Canada)

Recently, we found that by terminating a long length of fiber of up to several kilometers with an in-fiber cavity structure, the entire structure can detect vibrations over a frequency range from 5 Hz to 100 Hz. We want to determine whether the structure (including packaging) can be optimized to detect vibrations at even higher frequencies. The structure can be used as a distributed vibration sensor mounted on large motors and other rotating machines to capture the entire frequency spectrum of the associated vibration signals, and therefore, replace the many accelerometers, which add to the maintenance cost. This will replace the many accelerometers used for maintenance. Similarly, it will help detect in-slot vibrations inside an air cooled generator which causes intermittent contact leading to sparking under high voltages. However, that will require the sensor to detect frequencies associated with vibration sparking, ranging from 6 kHz to 15 kHz. Then, at even higher frequencies, the structure can be useful to detect acoustic vibrations (30 kHz to 150 kHz) associated with partial discharge (PD) in generators and transformers. Detecting lower frequencies in the range 2 Hz to 200 Hz makes the sensor suitable for seismic studies and falls well into the vibrations associated with rotating machines. Another application of interest is corrosion detection in large reinforced concrete structures by inserting the sensor along a long hole drilled around structures showing signs of corrosion. The frequency response for the proposed long gauge vibration sensor depends on packaging.

9274-60, Session Post

The effect of linear birefringence on fiber optic current sensor based on Faraday mirror

Rongxiang Zhang, Tianjin Univ. (China) and Hebei Univ. (China); Xiaotian Steve Yao, Tiegeng Liu, Lin Li, Tianjin Univ. (China)

Current sensors always play an important role in the electric power industry for measurement, fault diagnostics and relay protection. In recent years, with the increasing of current level, it is very difficult for traditional current sensors to meet the

demand. Fiber optic current sensors (FOCSs) have received considerable attention due to a number of interesting properties, such as good electrical insulation, immunity to electromagnetic interference, no magnetic saturation, small size, etc. FOCS based on the Faraday effect is limited by the small Verdet constant of silica, so in order to increase the sensitivity, lots of turns of fibers around the current conductor are needed, which will increase the linear birefringence (LB) in the fiber and add errors.

Faraday mirror can be employed to compensate the LB by exploiting the non-reciprocity of Faraday effect and the reciprocity of LB. In this paper, the structure and principle of the FOCS using Faraday mirror are addressed, and the simulated results showing the influence of LB on FOCS are presented. The results indicate that the influence of LB disappears when the current is null. However, when the current is not zero, the LB is not removed and the extent of effect is different with different current. Considering the LB is not easy to remove, a method to directly measure Faraday rotation in the presence of LB by time multiplexing of three different states of polarization is proposed. The Faraday rotation can be deduced directly from the detected signals and the LB need not be compensated physically by employing this technique.

9274-61, Session Post

Vehicle self-velocimeter for navigation system based on a linear image sensor

Xin He, Xiaoming Nie, Jian Zhou, Xingwu Long, National Univ. of Defense Technology (China)

The idea of using the method of spatial filtering velocimetry based on a linear CMOS image sensor is proposed to provide accurate velocity information for vehicle self-contained navigation system. A new method is proposed to determine the error source of the system. The image sensor is employed both as a detector and as a pair of differential spatial filters so that the system is simplified. The spatial filtering operation is fully performed in a field programmable gate array (FPGA). The approach of fast Fourier transform (FFT) is employed to obtain the power spectra of the filtered signals. Because of limited frequency resolution of FFT, a frequency spectrum correction algorithm, called energy centrobaric correction, is used to improve the frequency resolution. The velocities of the side surface of a high precision rotary table and the radiating frequencies of an LED are measured. The experimental results show that the measuring error of velocity of a rotary table is about 0.73% and the measurement uncertainty of 1000 times tests is 0.55%; the radiating frequency of an LED is measured under the condition of no imaging system, and the measurement uncertainty turns out to be within 10⁻⁵. Error sources of the system are analyzed and it is concluded that the main error source of the device is the imaging system. In a word, the velocimeter can satisfy the requirements of non-contact, real-time, high precision and high stability velocity measurement of moving surfaces and has the potential of application to vehicle self-contained navigation system.

9274-62, Session Post

Fiber-optic temperature sensor based on specialty triple-clad fiber

Xinghu Fu, Haiyang Xie, Chao Zhang, Peng Guo, Guangwei Fu, Weihong Bi, Yanshan Univ. (China)

As one of the most common physical quantity, the temperature is monitored strictly in industrial production, chemical experiment and biomedical sciences. The conventional electronic temperature sensor has some disadvantages including low sensitivity, vulnerable to outside magnetic interference, high

measurement error, etc. The optical fiber sensor with high sensitivity, anti-electronic magnetic fields, corrosion resistance is attracting more attention. Therefore, a fiber-optic temperature sensor based on specialty triple-clad fiber (STCF) is proposed. Based on coupling mode theory, the STCF can be equivalent to a rod waveguide and two tube waveguides. The different mode dispersion curves are calculated and a resonance wavelength is obtained. A straightforward experiment is performed to prove the temperature sensitivity. The fiber-optic temperature sensor is fabricated by two sections of SMF splicing at both the end of the 10-mm long STCF respectively. It works on mode-coupling between the core and fluorine-doped silica inner cladding of STCF at a particular wavelength, which can finally leak out from fluorine-doped silica inner cladding to air-holes. So a spectrum with band-stop filter characteristic can be obtained. An ASE optical power, a temperature control cabinet and an optical spectrum analyzer are used for temperature test. The relationship between the transmission spectra and temperature is analyzed, and the errors are also given. Experimental results shows that the temperature sensitivity can be achieve 97.2pm /? in 20-90? and there is a good repeatability. The resonance wavelength has a red shift and increase as increasing temperature. Thus, this sensor can be used for temperature monitoring in time.

9274-63, Session Post

Temperature characteristic of hollow-core photonic crystal fiber resonator

Lishuang Feng, Hongchen Jiao, Xiaoyuan Ren, Wenshui Song, BeiHang Univ. (China)

The change of birefringence difference of the fiber can be caused by the variation of ambient temperature, which will lead to the change of lightwave polarization state in the fiber. In the resonator fiber optic gyro systems, the variation of lightwave polarization state of the light transmission in the fiber can bring about the measurement error of the system. As the effect dues to ambient temperature variation cannot actually be avoided, the ambient temperature variation is an important factor affecting the performance of the gyro. The hollow-core photonic crystal fiber (HCPCF) resonator is designed to reduce the variation of refractive index difference caused by the temperature variation. The two resonators are place in a temperature controllable chamber in order. Resonance curves in different ambient temperatures of the two resonators are obtained by sweep laser frequency. As free spectral index (FSR) and interval between primary and secondary polarization states in a certain temperature can be achieved from the resonance curve, the temperature coefficients of the HCPCF refractive index difference and PMF refractive index difference can be figured out. The average temperature coefficient of the HCPCF refractive index difference is 3.4×10^{-10} , while that of the PMF refractive index difference is 1.48×10^{-8} . It is verified experimentally that the temperature coefficient of the HCPCF refractive index difference is decreased about two orders of magnitude lower than that of the normal polarization maintaining fiber (PMF). Applying the HCPCF to gyro system will relax the effect acted on gyro performance by temperature drift efficiently.

9274-64, Session Post

Polydimethylsiloxane-fabricated optical fiber sensor capable of measuring both large axial and shear strain

Yu Shen, Ziyuan Wang, Huaihai Wen, Zhou Zhi, Dalian Univ. of Technology (China)

Fiber optic sensor (FOS) has received much attention in the field of Structure Health Monitoring (SHM) due to its advantages of

low weight, small size, high sensitivity multiplexing ability, free of electromagnetic interference and long durability. However, in harsh environments, structures often undergo large strain where few traditional fiber optic sensors could survive. This paper report a novel material with features of light-transparent, chemically inert, thermally stable material Polydimethylsiloxane(PDMS) fabricated large axial/shearing strain sensor. The sensor was fabricated by directly coupling a conventional signal mode fiber into half cured PDMS material using a translation stage under the inspection of a microscope. Meanwhile, a laser diode and a photo detector were used in the fabrication process to make sure the sensor achieved minimum light loss. An experiment was conducted later to investigate the sensor's transmission characteristic in 1310nm infrared laser relating with the applied axial/shearing strain. The results show that the proposed sensor survived an axial strain of 7.79×10^{-6} micro-strain ; a shear of 6.49×10^{-4} micro-strain with a good linearity and repetition. The experiment indicates that the proposed sensor can potentially be used as strain sensing elements in Structure Health Monitoring systems under earthquake or explosion.

9274-65, Session Post

Application of pulse cavity ring-down spectroscopy technique for aerosol extinction measurement

Guo Jie, JinXiang Dong, Wang L. Ming, Shao Jie, Zhejiang Normal Univ. (China)

In recent years, there has been a rapid rise in the use of pulse cavity ring-down spectroscopy (CRDS) to determine the optical properties of atmospheric aerosols. In the present work ,we describes the design and performance of a CRDS system for measuring extinction coefficients of atmospheric aerosols. CRDS based methods can achieve impressive sensitivity owing to the long effective path lengths involved. More importantly, the method is not affected by laser intensity fluctuations since the rate of attenuation of light is the measured variable rather than absolute irradiance. The extinction coefficient is a function of the cavity ring-down time. Determining an accurate decay time is critical to precise measurements of the extinction coefficients. The average and standard deviation of the decay time (τ_0) is measured 6 hours ,cavity filled only with dry nitrogen) is about 42.21?s and 0.16?s, respectively. Moreover, a minimum detectable aerosol extinction coefficient of 0.41 Mm^{-1} is achieved. Allan deviation plots for the value of τ_0 measurements, close to a flicker noise. The minima ($\sim 5.8 \times 10^{-4}$ s) in the Allan plots indicate the optimum average time (~ 60 s) for optimum detection performance. To test the performance of the CRDS system, we monitored the optical properties of ambient aerosols on the campus of the Zhejiang Normal University from January 3rd to January 7th, 2014. During this period, the extinction coefficients of atmospheric aerosols exhibited high variability ranging from clear days such as January 6th to a heavy pollution episode from 18:00 p.m.in January 4th to 12:00 a.m.in January 5th.

9274-66, Session Post

Optical fiber vibration sensing system using distributed gain amplification method

Zhengxian Zhou, Univ. of Shanghai for Science and Technology (China) and Anhui Normal Univ. (China); Songlin Zhuang, Univ. of Shanghai for Science and Technology (China)

A distributed gain amplification method is proposed and demonstrated in optical fiber vibration sensing system based on

phase-sensitive optical time domain reflectometer. An acoustic optical modulator is adopted to generate narrow pulses, which injected to sensing fiber to generate Rayleigh backscattering light. The experimental results show that up to 45-km sensing range with 50-ns pulse width are achieved. And the amplitude of vibrations is equal in three positions including 804 m, 20154 m and 43855 m.

9274-67, Session Post

Depolarization characteristics of the cloud particle on interferometric particle imaging

Hongxia Zhang, Jing Liu, Mengran Zhai, Dagong Jia, Tiegeng Liu, Tianjin Univ. (China)

The cloud particle is usually divided into liquid particle and solid particle. The liquid droplet is spherical, while solid particle is non-spherical, such as ice crystal particles with complicated shape. Discrimination of cloud phase state plays an important role in detecting cloud microphysical parameter. Based on Mie scattering theory and the generalized Mie scattering theory, a new method using depolarization characteristics has been proposed to discriminate the phase state of cloud particle. The depolarization characteristics of scattered light between spherical particles and non-spherical particles are different. For non-spherical particles, the interference fringes on interferometric particle imaging before and after depolarization are also different, which differs from spherical particles. The light reflected from particle surface and the light refracted via particle would form defocused interferogram. A beam splitter prism has been used to divide scattering light into two parts and a depolarization device has been placed in one of the scattering light path. The two interference fringes before and after depolarization have been captured by two CCD cameras respectively, then compared. The results can be used to determine the shape and the phase state of cloud particle. Ice crystal particles which can be equivalent to spheroid particles have been studied. Studies have shown that depolarization degree is related to aspect ratios of spheroid and different orientations of spheroid with respect to the incident beam.

9274-68, Session Post

Numerical investigation of photonic crystal fiber sensor sensitivity based on evanescent wave absorption

Benchong Li, Jun Lou, Hongzhi Xu, Jie Huang, Ben Xu, Weimin Shen, China Jiliang Univ. (China)

Recently, many methods have been developed for simulation or analysis of the sensor sensitivity of photonic crystal fiber based on evanescent wave, either for gas sensing or for biological detection. Relative sensitivity is varies along with the fiber length. This characteristic is very difficult to simulate accurately by those methods. In this paper, it is shown RSOFT BeamPROP based on finite difference beam propagate method?FD-BPM?as a fairly robust and simple program, due to the existence of a graphical environment, to perform good accuracy simulations with the sensor relative sensitivity. Results are compared with reference experiments, focusing on evanescent wave sensor sensitivity of photonic band-gap crystal fiber (PBG-PCF), where the longer of the incident light wavelength and the greater of fill factor, the more energy in the air holes and the higher of sensor relative sensitivity.

9274-69, Session Post

Vectorial E-field sensing using pigtailed photonic probes for aperture-field mapping of antennas

Changlei Wang, Xinwei Chen, Shuai Wu, East China Research Institute of Electronic Engineering (China)

The aperture-field mapping is very important to diagnosing the amplitude and phase distribution of the antenna under test(AUT). Since such measurements need to be done without influence to the actual field distribution near the aperture, traditional metallic near-field probes, such as horn antennas, waveguide slots, et al, are irrespective. Miniature electro-optic E-field sensors offer good possibility for such near-field or very near-field measurements, because of its small size and little perturbation to the AUT. Moreover these devices have high resolution and reduced dimensions. In this paper, we have present a simple photonic microwave probe to measure the electric field vector distribution at a distance shorter than one wavelength from the aperture of a antenna. The photonic E-field probe is a type of pigtailed electro-optic sensor and consists of an electro-optic crystal supported by a quartz sleeve. The probe is all-dielectric, without any metallic materials. Those physical and electrical features make the photonic sensor attractive when used as a probe for near-field antenna measurements. A patch antenna with a resonant frequency at 6.5GHz was designed and fabricated. Both amplitude and phase distribution of the two tangential E-field components are mapped by using the present photonic probe. Simulation was carried out as well, and compared with the experimental measurements. The result shows great correspondence for amplitude distribution between simulations and experiments, as well as for the phase distribution except for some random tiny frustrations. The methods to improve the stability of measurement system are briefly discussed.

9274-70, Session Post

Influence of laser linewidth on spectral ripple in fold-type cavity ring-down measurement

Zhongqi Tan, Suyong Wu, Xingwu Long, Wenjian Wei, National Univ. of Defense Technology (China)

So-called spectral ripple a special phenomenon only existing in fold-type cavity ring-down spectrometer, and it is believed as deriving from the interference effect of different lights on the folded mirror. To investigate the influence of this phenomenon, on fold-type cavity ring-down measurement, some representative instances of laser linewidth are simulated and analyzed, and some experiments are carried on. It is found that the increasing of laser linewidth can make the amplitude of the spectral ripple decrease, more importantly, which can make the ring-down signal no longer decay as a single exponential but as the double exponential function.

9274-71, Session Post

Optical fiber voltage sensor based on Michelson interferometer using Fabry-Perot demodulation interferometer

Xinwei Chen, Shengnan He, Dandan Li, Kai Wang, Yanen N. Fan, Shuai Wu, East China Research Institute of Electronic Engineering (China)

We present an optical fiber voltage sensor by Michelson interferometer (MI) employing a Fabry-Perot (F-P) interferometer and the DC phase tracking signal processing method. By mounting a MI fabricated by an optical fiber coupler on a piezoelectric (PZT) transducer bar, a dynamic strain would be generated to change the optical path difference (OPD) of the interferometer when the measured voltage was applied on the PZT. Applying an F-P interferometer to demodulate the optical intensity variation output of the MI, the voltage can be obtained. The experiment results show that the relationship between the optical intensity variation and the voltage applied on the PZT is approximately linear. Furthermore, the phase generate carrier (PGC) algorithm was applied to demodulate the output of the sensor also.

9274-72, Session Post

A micro particle launching apparatus based on mode-division-multiplexing technology

Fangfang Cao, Zhihai Liu, Harbin Engineering Univ. (China)

We propose and demonstrate a trapped yeast cell being launched away from the fiber tip with a certain speed to a certain position without moving the optical fiber in a single fiber optical trapping system. We excite both LP01 mode and LP11 mode beams in a same normal communication fiber core to generate the optical scattering force and trapping force by molding the fiber tip into a special tapered-tip shape.

The LP11 mode beam, whose power mainly exists in the middle part of core radius while the LP01 mode beam, whose power mainly propagates in the center of core, therefore we need to mold the fiber tip into a special shape, which guide the LP11 mode beam focusing with a large convergence angle to generate the optical trapping force, and simultaneously, guide the LP01 mode beam not focusing and generating the scattering force to launch the micro particle, therefore a selective chemical etching procedure is developed for fabricating this special tapered fiber tip. A yeast cell of 6 μ m diameter is trapped and then being launched away.

Besides that, we also built a physical model to analyze the micro particle dynamic behavior characteristics during the launching moment. This micro particle directional launching function expanded new features of fiber optical tweezers based on the normal communication fiber, providing for the possibility of more practical applications in the biomedical research fields.

9274-73, Session Post

Birefringence characteristic research of 40 microns supersmall diameter elliptical cladding type polarization maintaining fiber

Tao Zhang, Harbin Engineering Univ. (China)

With the progress of study on fiber optic gyroscope (FOG), the higher demand for performance of polarization maintaining fiber (PMF), and miniaturization is one of the important development direction. Compared to other stress-induced PMF, the birefringence of elliptical cladding type PMF has small effect when we make stress area smaller, and it can meet the requirements of fiber optic gyroscope. Therefore, 40 microns supersmall diameter elliptical cladding type polarization maintaining fiber can be the preferred option of the FOG towards light, small, spiritual direction. In this paper, we use finite element method to analysis stress-induced birefringence of 40 microns supersmall diameter elliptical cladding type PMF, get the stress contours on cross-section of PMF, and calculate the

stress birefringence, the polarization mode field distribution and modal birefringence. Under the given simulation conditions, the magnitude of stress birefringence in core is about 10^{-4} , and the magnitude of modal birefringence is about 10^{-4} . The results show that 40 microns ultrafine diameter elliptical cladding type PMF has a uniform stress field distribution and a large birefringence. It is conducive to achieve miniaturization of PMF.

9274-74, Session Post

Sensing properties of metal-coated microcylinder

Zhuo Zhang, Jinyi Gu, Mi Li, Yuejiang Song, Nanjing Univ. (China)

Recently, metal-coated microcavity is gradually attracting researchers due to its specific mode characteristics. This microcavity can transfer electromagnetic waves on the surface of the metal by surface plasmon polariton (SPP) mode, and its SPP mode has a very high local interaction and enhancement effect. Meanwhile, hybrid whispering gallery mode (WGM) also exists in this kind of resonant cavity. In this paper, the sensing properties (Q factor, refractive sensitivity and limit of detection) of metal-coated microcylinder are calculated as a function of microcylinder radius and metal layer thickness from its analytical eigenequation. Compared with the numerical simulation, analytical solution method is more physically meaningful. The Q factor of asymmetrical SPP (SPPa) mode can be greater than the symmetric SPP (SPPs) mode which is opposite to one-dimensional metal-dielectric slab structure. That is a new discovery of two-dimensional structure metal-coated microcavity. And the Q factor of the TE polarization hybrid SPP-WGM is two orders of magnitude higher than TM polarization hybrid SPP-WGM and SPP mode. The refractive sensitivity of SPPs mode reaches 3500nm/RIU, which are two orders of magnitude higher than the traditional dielectric microcavity. If the thickness of the metal thin layer is further reduced, the refractive sensitivity of SPPs mode will be further improved. Meanwhile, the refractive sensitivity of SPPa mode is relatively stable and about 1000nm/RIU. In summary, the SPP modes in this kind of waveguide have a relatively high Q-factor (more than hundreds) and an ultra-high refractive sensitivity (as high as thousands of nm/RIU) which may have great potential applications in field of biological and chemical sensing.

9274-75, Session Post

Surface plasmon resonance sensor based on grapefruit-type photonic crystal fiber with silver nano-filling

Lei Zhang, Yibo Zheng, Shijiazhuang Univ. of Economics (China)

With the rapid development of fiber-optic SPR sensor and the improvement of PCF manufacture process, many scholars put forward photonic crystal fiber (PCF) based SPR sensors in recent years, and plenty of simulations and calculations have been made, showing great advantages and well application prospects. The sensing mechanism is through coupling the leaky core mode to the plasmon to achieve resonance sensing. The use of the photonic crystal fiber, with its flexible design, makes it easy to equate the effective index of the core mode to that of the material under test. Thus phase matching condition between the core mode and the plasmon can be easily achieved at the required wavelength and then resonance occurs.

In this article, surface plasmon resonance sensors based on grapefruit-type photonic crystal fiber (PCF) with different silver nano-filler structure have been analyzed and compared though

the finite element method (FEM) by using COMSOL Multiphysics software. The regularity of the resonant wavelength changing with refractive index of the sample has been numerically simulated. The surface plasmon resonance (SPR) sensing properties have been numerically simulated in both areas of resonant wavelength and intensity detection. Numerical results show that excellent sensing characteristics of the silver nanowires filling structure can be achieved as the radius of the nanowires is 150nm, with both spectral and intensity sensitivity in the range of 4×10^{-5} – 5×10^{-5} RIU. Comprehensive comparing of the three different proposed filling structure indicate that the 150 nm silver wire filling structure is suitable for spectrum detection and 30 nm silver film coating structure is suitable for the amplitude detection.

9274-76, Session Post

Temperature and pressure measurement based on tunable diode laser absorption spectroscopy with gas absorption linewidth detection

Yunxia Meng, Tiegeng Liu, Kun Liu, Junfeng Jiang, Tao Wang, Ranran Wang, Tianjin Univ. (China)

A gas temperature and pressure measurement method based on Tunable Diode Laser Absorption Spectroscopy (TDLAS) detecting linewidth of gas absorption line was proposed in this paper. Combined with Lambert-Beer Law and ideal gas law, the relationship between temperature, pressure and gas linewidth with Lorentzian line shape was investigated in theory. Taking carbon monoxide (CO) at 1567.32 nm for example, the linewidths of gas absorption line in different temperature and pressure were obtained by simulation. According to the simulation results and detected linewidth, the undefined temperature and pressure of CO gas were measured. The gas linewidth detection, avoiding the influence of laser intensity, is an effective temperature and pressure measurement method. The method also has the ability to detect other gases temperature and pressure with Lorentzian line shape.

9274-77, Session Post

Ground deformation monitoring of Fujian urban agglomeration in the western strait based on fusion of multi-source SARs

Jifeng Wu, Zhiqiang Yang, Kainan Zhang, Chang'an Univ. (China)

Fujian urban agglomeration in the western strait is located in southeast China. It is the base for promoting cooperation and peaceful reunification. According to the development plan, Fuzhou, Quanzhou, Zhangzhou coastal economic belt is one of the key development areas. The urban development is restricted by the geographical conditions, according to the survey, fuzhou basin, quanzhou basin and zhangzhou basin are located in the confluences of Changle-Nan'ao fault zone with the Min river downstream fault zone, Jin river downstream fault zone, the confluence of downstream of the Jiulong river estuary fault zone, and they are new organic characteristics of fault basin. Because the region has relatively good living conditions, it causes the densely populated. At the same time, in the process of natural sedimentation loose quaternary strata, groundwater is abundant, and easily over-exploited, which causes the occurrence of land subsidence accordingly. This paper is from the security of urban economic development, to reduce and avoid the impact of geological disasters perspective. It is focusing on the possible impact of land subsidence in the area of large city and major projects. Based on the analysis of regional geological

structure characteristics, we use the synthetic aperture radar interferometry technique, with the small baseline subset D-InSAR method, get different data sources, such as ASAR, PALSAR images with different polarizations. Then we process, research and analysis the data, in combination with various space measurement technology such as GPS and leveling, accurately grasp the rate of land subsidence situation and research area. And we preliminary estimate the impact of land subsidence to urban development, which provided the scientific basis for the development of the Fujian urban agglomeration construction and the sustainable utilization of marine resources.

9274-78, Session Post

The effect of near-infrared laser beam on the surface modification of metal complex based on 3D laser scanning system

Mali Zhao, Tiegeng Liu, Junfeng Jiang, Tianjin Univ. (China)

High-precision 3-dimensional metallization is difficult to realize in specific nonmetallic areas by using the traditional methods such as wet-chemical and mechanical methods because of the disadvantage that usually they cannot achieve selective modification. In this paper, 3-dimensional laser scanning system was applied to achieve the modification of specific regions of the sample surface. In 3-dimensional laser scanning system, the laser beam, after going through dynamic focusing system, was reflected by galvanometers and then focused by f-theta lens on the sample surface. The changes in surface characteristics of the blends of polycarbonate and acrylonitrile butadiene styrene copolymers (PC/ABS) mixed with Cu-Cr complex by the laser irradiation with the wavelength of 1064nm were investigated. Through analysis it was found that the smooth surface of the original samples was changed to a micropore structure accompanied by an increased surface roughness as well as an increased water contact angle. The chemical composition percentage had changed and the metal components of copper and chromium were detected after the laser irradiation. The irradiated areas were degraded into organic ligand fragments, volatile gas and reducing metal ions of Cu^{1+} and Cr^{3+} . Besides, the thickness of the deposited metal layer and the adhesive force between the metal layer and the substrate after electroless plating varied according to the laser parameters such as laser power density, frequency and scanning speed. As shown in the experiment, the thickness of deposited copper layer exceeded 11 μm and the deposited nickel layer exceeded 2 μm respectively.

9274-20, Session 5

Very high-resolution optical spectral analysis based on Brillouin dynamic gratings (*Invited Paper*)

Yongkang Dong, Taofei Jiang, Harbin Institute of Technology (China)

High resolution optical spectral analyzers (OSAs) play an important role for high-accuracy sensing. In this paper, a novel method for an ultrahigh resolution optical spectrometry based on Brillouin dynamic gratings (BDGs) is proposed and demonstrated. A coherent acoustic wave is generated in an optical fiber through stimulated Brillouin scattering, and the acoustic wave modulated the fiber refractive index forming a BDG. Operating in the weak grating condition, the BDG reflection bandwidth is inversely proportional to the grating length, so a narrow reflection spectrum can be achieved by creating a long BDG in an optical fiber. In our scheme, an ultra-narrow bandwidth optical filter is constructed by operating a BDG in a long single-mode fiber (SMF), and the optical spectrometry is performed by

sweeping the center wavelength of the BDG-based filter through a swept-tuned laser. A phase modulator is used to create a multi-peak spectrum with an interval of 1 MHz to verify the capability of the spectral resolution of the BDG-OSA. In the experiment, a 4-fm (0.5 MHz) spectral resolution is achieved by operating a BDG in a 400-m SMF, and the wavelength coverage can be readily extended to C+L bands with a commercial tunable laser. The BDG-OSA features ultrahigh resolution, large wavelength coverage and simple direction-detection scheme, and the reflectivity of the BDG can be flexible adjusted by changing the pump power to accommodate the power of the signal light and subsequently can extend the OSA dynamic range.

9274-21, Session 5

High Q silica microbubble resonators fabricated by heating a pressurized glass capillary

Zhe Yu, Tiegeng Liu, Junfeng Jiang, Kun Liu, Wenjie Chen, Xuezhi Zhang, Xujun Lin, Wenhui Liu, Tianjin Univ. (China)

Microbubble resonators combine the unique properties of whispering gallery mode resonators with the capability of integrated microfluidics. The microbubble resonator is fabricated by heating the tapered tip of a pressurized glass capillary with oxyhydrogen flame. Firstly, a microtube with a diameter of 250 μ m is stretched under heating of oxyhydrogen flame, the heating zone length is set to be 200 μ m and the length of stretch is set to be 7000 μ m. Then nitrogen will be pumped in to the tapered microtube with the pressure of 0.1Mpa, the tapered tip will be heated by the oxyhydrogen flame continuously until a microbubble forms. An optical fiber taper with a diameter of 2 μ m, fabricated by stretching a single-mode optical fiber under flame was brought in contact with the microbubble to couple the light from a 1550nm tunable diode laser into the whispering gallery mode. The microbubble resonator has a Q factors up to 1.5 \times 10⁷ around 1550nm. Different concentrations of ethanol solution (from 5% to 30%) are filled into it in order to test the refractive index sensing capabilities of such resonator, which shows a sensitivity of 82nm/RIU.

9274-22, Session 5

AGC technology in a digital optical fiber sensing system with PGC modulation and demodulation

Jianfeng Tang, Shuidong Xiong, National Univ. of Defense Technology (China)

When the interferential fiber optic sensor system is working, the amplitude of interference light intensity on the detector fluctuates all the time, because of the influence of various factors inside the system itself and from the external environment. In the process of photo-to-electric conversion, when the intensity becomes too large it will lead to circuit saturated distortion, while when the light intensity became too small, it will reduce the signal-to-noise ratio, as a result of the effect of quantization noise introduced by the AD conversion. However, if the amplitude of the signal is maintained in a reasonable range, even though there exists small fluctuations, the influence of fluctuations can be eliminated using PGC demodulation, which has been proved in the paper "Research on low frequency signal detection technique for interferometric fiber optic sensor", written by Ye Xin.

In this paper, we analyze the impact of fluctuations of different magnitudes on signal demodulation with the theoretical method and simulation. A reasonable control method is put forward and an auto gain control (AGC) module with a gain range of -10dB to 30dB is designed and produced based on the AD602 chip.

Through changing the gain of amplification circuit in terms of the amplitude of PGC signal, the signal fluctuation is kept in a reasonable range, thus the influence of fluctuations can be eliminated using PGC demodulation.

Finally, experiments are conducted to verify that this AGC method could effectively improve the accuracy of demodulating signal from interference light intensity with a magnitude fluctuation less than 40dB.

9274-23, Session 5

Coreless optical fiber-based surface plasma resonance sensor

Xiaotong Gao, Yun Liu, Xiuxin Liu, Shimeng Chen, Mengdi Lu, Wei Peng, Dalian Univ. of Technology (China)

In this work, a novel optical fiber surface plasmon resonance (SPR) sensor for biochemical analysis is presented. The basic sensor consists of a coreless optical fiber 125 μ m in diameter connected with a thin layer of gold, and a 62.5/125 μ m multimode fiber. The coreless optical fiber, the thin layer of gold, and the medium which is under test constitute a typical three-decker. First of all, we mainly focus on numerical simulation of fiber-optic SPR sensor's sensitivity which can be affected by technical parameters such as metal thickness, sensing area length. According to the basic principle of SPR, we apply Matlab programming to simulate transmission spectrum with fixed fiber core diameter and specific Angle. Besides, the length of the sensing area and the thickness of gold film are simulated respectively, so as to find the best theoretical sensing area length and thickness of the gold film. Second, we select the sensor with the best parameters to detect the salt solution of different concentrations, and verify the feasibility of this kind of sensing device by experiment. Finally, through the study of chemical modification of the sensor, we implement the specificity of detection of chemicals. The use of a multimode fiber which is small in diameter facilitates the production process and shortens the production time based on maintaining high sensitivity. Sensing sensitivities have been achieved to be 2270nm/RIU for 1.3288-1.3753 RIU range of tested salt solutions. The device is compact, achievable, and has functioned as a biochemical or immunological sensor.

9274-24, Session 5

Optofluidically-tunable Thulium-doped fiber laser based on multimode interference with a large claddingless fiber

Xiaowei Ma, Daru Chen, Zhejiang Normal Univ. (China)

A novel optofluidically tunable Thulium-doped fiber laser (TDFL) based on a multimode interference (MMI) fiber filter is experimentally demonstrated with a widely tuning range from 1813.52 nm to 1858.70 nm. The wavelength tuning of the TDFL is achieved by employing an MMI fiber filter which is formed by splicing a segment of a special claddingless fiber that is a pure silica fiber without fiber cladding to single mode fibers. The claddingless fiber with a diameter of 200 μ m is gradually vertically covered by refractive index matching liquid, which leads to a wavelength tuning of the transmission peak of the MMI fiber filter. Using a 12.80mm-length claddingless fiber, 10nm bandpass fiber filter with the center wavelength of 1812.74nm is achieved. The relationship between the refractive index of the refractive index matching liquid and the peak wavelength shift of the MMI fiber filter is also discussed. When the claddingless fiber gradually covered by the liquid with the refractive index of 1.402, 1.428, and 1.446, a tuning range of 15.20nm, 26.78nm, and 45.71nm is realized respectively. Using the tunable MMI fiber filter controlled by the refractive index matching liquid of 1.446, a ring-structure

Thulium-doped fiber laser with a tuning range of 45.18nm, a side-mode suppression ratio (SMSR) better than 40 dB, and a 3dB bandwidth less than 0.16nm is achieved. On the whole, The demonstrated TDFL had a wide tuning range, highly linear tuning response, and its tuning range could be chosen by using liquids with different refractive index.

9274-25, Session 5

Micro-bubble-based wavelength division multiplex optical fluidic sensing

Xuezhi Zhang, Tiegeng Liu, Junfeng Jiang, Kun Liu, Zhe Yu, Wenjie Chen, Wenhui Liu, Tianjin Univ. (China)

Single-molecule sensing in bio-chemistry have been demonstrated by utilizing Whisper-Gallery-Mode (WGM) based resonator with ultra-high quality factor. Recently, capillary has been brought forward to support the WGM based optofluidic sensing, which combines the path of light propagation and analyte chamber together, and simplifies the sensing system dramatically. To achieve high sensing precision, micro-bubble with ultrahigh quality factor can be realized by heating a capillary under a pressure of nitride. Besides, wavelength division multiplex technology can enhance the sensing capacity by detecting various samples simultaneously. WGM can be selected simulated in the micro-bubble by a contradirectional coupler made by polymer grating. Some grating parameters, including duty cycle, period, width, length, index modulation are numerically simulated by FDTD solution software to find their impacts on the WGM selected process. Grating with a particular period can simulated a WGM in micro-resonator on purpose. The interference of different bubble resonators is also discussed in this paper.

9274-26, Session 5

Reconfigurable single passband microwave photonic filter based on frequency comb and stimulated Brillouin scattering

Deng W. Zhou, Harbin Institute of Technology (China)

A widely tunable and reconfigurable single passband microwave photonic filter (MPF) is theoretically analyzed and experimentally demonstrated using the frequency comb technique and stimulated Brillouin scattering (SBS). The transfer function of Brillouin amplification with frequency comb is theoretically derived from the SBS coupled-wave equations. When one of the 1-order sideband of the phase modulated signal light matches with the broadband Brillouin gain region, the conversion from phase modulation to amplitude modulation is conducted, and the beat signal between carrier and amplified sideband is directly detected by photo-detector. The frequency of the beat signal is equal to that of the input microwave. The multi-frequency phase modulation is proposed to generate a frequency comb as the pump light and tailor the Brillouin gain profile. The experimental results show a sharp-edge and flattop passband response MPF with a maximum -3-dB bandwidth of 209 MHz and a -20-dB bandwidth of 294 MHz by using an 11-peaks comb. The -3-dB bandwidth of the MPF is also reconfigurable from 34 MHz to 307 MHz through changing the frequency number and the frequency interval of the combs. The best MPF shape factor (S) of 1.37 is gained adopting a 7-peaks comb with the frequency interval of 30MHz, which is defined as the ratio of -20-dB to -3-dB bandwidth. A larger continuously-tuned range from 3 GHz to 20 GHz with very low ripple is demonstrated by tuning the pump laser wavelength. Meanwhile the out-of-band rejection above 40 dB is easily obtained.

9274-27, Session 6

Measurement of high-intensity focused ultrasound fields using miniaturized all-silica fiber-optic Fabry-Perot hydrophones (Invited Paper)

Pinggang Jia, North Univ. of China (China); Lei Liu, Dai-Hua Wang, Chongqing Univ. (China)

In recent years, high-intensity focused ultrasounds (HIFUs), as a novel non-invasive surgery technology, have been used effectively for cancer therapy. In order to ensure the treatment safety, the acoustic pressure distributions and the size of the focal regions of HIFU fields need to be measured and characterized accurately. In our previous work, a lateral sensitive all-silica fiber-optic Fabry-Perot (TAFOFP) ultrasonic hydrophone and a tip-sensitive TAFOFP ultrasonic hydrophone for measuring HIFU fields were developed.

In this paper, the sensing models of lateral sensitive TAFOFP ultrasonic hydrophone and tip-sensitive TAFOFP ultrasonic hydrophone are respectively investigated by analyzing the interaction of the Fabry-Perot cavity with ultrasonic pressure and the optical interference of Fabry-Perot. The lateral sensitive and tip-sensitive TAFOFP ultrasonic hydrophone systems and the corresponding experimental setups are established to measure HIFU fields, respectively. The two TAFOFP ultrasonic hydrophones with different fiber-optic sensor holders are fixed on the three-dimensional positioning system through a connecting rod. The acoustic pressure distributions of the HIFU field along the X-axis, Y-axis, and Z-axis and the normalized acoustic pressure distribution of the HIFU field in the focal region are tested in the degassed water. The acoustic pressure measured by a calibrated piezoelectric ceramic needle hydrophone is used as a reference acoustic pressure. The acoustic pressures measured by lateral sensitive and tip-sensitive TAFOFP ultrasonic hydrophones are compared with reference acoustic pressure. Experimental results show that the tip-sensitive configuration can measure the acoustic pressure distribution in the focal plane with high spatial resolution.

9274-28, Session 6

Simultaneous measurement of acoustic pressure and temperature in the HIFU fields using all-silica fiber optic Fabry-Perot hydrophone

Dai-Hua Wang, Lu-Yu Zeng, Ping Gang Jia, Lei Liu, Xin-Ying Jiang, Chongqing Univ. (China)

In recent years, high-intensity focused ultrasounds (HIFUs), as a novel non-invasive surgery technology, have been used effectively for cancer therapy. The main principle of HIFU therapy is to accurately focus the acoustic energy on the in vivo tumour tissue through the skin. Tissue temperature within the focal region is instantly raised to 65-100 ° during HIFU exposure, which will immediately induce the coagulation necrosis in the tumour without destroying the normal tissue. To ensure the treatment safety, the acoustic pressure distributions and the size of the focal regions of HIFU fields need to be measured and characterized accurately. To assess therapeutic efficacy, the temperature measurement at focal regions also need to be measured.

In our previous work, a tip-sensitive all-silica fiber-optic Fabry-Perot (TAFOFP) ultrasonic hydrophone for measuring HIFU fields is developed. Considering the developed fiber-optic F-P sensor is slightly sensitive to the temperature, the phase bias point of the interference output will change with temperature variations. The active phase biased point scheme is used to

realize the simultaneous measurement of acoustic pressure and temperature. The laser wavelength is feedback controlled with proportional-integral-derivative (PID) algorithm to track the phase biased point. The experimental setups in the degassed water and tissue phantom are built for measuring the acoustic pressure and temperature. Experimental results show that the sensing system can simultaneously measure the acoustic pressure and temperature.

9274-29, Session 6

A positioning algorithm based on super-resolution time delay estimation in dual Mach-Zehnder interferometry vibration sensor

Qinnan Chen, Tiegeng Liu, Kun Liu, Junfeng Jiang, Zhenyang Ding, Liang Pan, Chunyu Ma, Tianjiao Chai, Chang He, Tianjin Univ. (China)

Dual Mach-Zehnder Interferometry (DMZI) vibration sensor can detect and locate the disturbance event along the sensing cable by applying the time delay estimation (TDE) technique. The precision of the TDE is affected by limited sampling rate and noise effect which limits the accuracy of location. We propose a positioning algorithm based on Super Resolution Time Delay Estimation in the dual Mach-Zehnder Interferometry (DMZI) vibration sensor. The algorithm on the basis of the correlation peak precise interpolation method, and use second order correlation and Hilbert difference to improve itself. The correlation peak precise interpolation method compute waveform of the main correlation peak only using the main segment of the cross power spectrum, the peak can be interpolated in any accuracy without increasing calculation. The fine spectrum is calculated with a modified Chirp z transform which can reduce a barrier affection caused by standard FFT. Second order correlation can effectively suppress noise and Hilbert difference can further sharpen the correlation function peaks. The proposed positioning algorithm fusing the above techniques will not only improves the resolution of correlation function but also has strong anti noise performance and peak detection ability. We experimentally demonstrate that the proposed positioning algorithm can greatly improve the positioning accuracy. Compared with the traditional positioning algorithm, the positioning error of the proposed algorithm has been reduced an order of magnitude.

9274-30, Session 6

Fiber optic pressure sensing method based on Sagnac interferometer

Yi Zhang, Zhi Zhuang, Ying Chen, China Academy of Engineering Physics (China); Yuanhong Yang, BeiHang Univ. (China)

Pressure method using polarization-maintaining photonic crystal fiber (PM-PCF) as sensing element based on Sagnac interferometer is proposed to monitor inter layer pressure in especial compact structure. Sensing model is analyzed and test system is set up by using Sagnac interferometer technique. When no disturbance is induced, the phase difference of the light propagating in the slow and fast axes of the PM-PCF in a Sagnac loop is fixed, but under transverse pressure loaded on PM-PCF, the refractive indices of the slow and fast axes will change due to the elastic-optical effect and the phase difference will also changes accordingly and finally induce the shift of the interferometric spectrum.

Pressure measurement is achieved by detecting the wavelength

shift from output of the Sagnac interferometer through the calibration experiment. A section of PM-PCF as sensing element is laid under a flexible polymer foil cushion, and the calibration pressure curve is achieved by experiment using pressure load tester with 0.05% precision to apply a load from 0 to 10KN, so the relation of pressure and wavelength shift can be determined by calibration.

It can be concluded from the experimental results that the output interference fringes are shifted linearly with pressure. The dynamic range of 10KN, sensing precision of 2.6%, and pressure sensitivity of 0.4414nm/KN are achieved, and the strain relaxation phenomenon of cushion can be observed obviously. The sensor has better capability to restrain interference brought up by fluctuation of environment temperature due to temperature sensitivity is only -11.8pm/°.

9274-31, Session 6

Health monitoring of electric power communication line using a distributed optical fiber sensor

Lidong Lu, China Electric Power Research Institute (China)

For maintenance of the optical fiber ground wire (OPGW) that is used as the electric power communication line, Brillouin optical time domain reflectometry (BOTDR) is employed as the distributed optical fiber sensor (DOFS) to sense some possible dangers such as lightning stroke and ice covering on the OPGW. In experiment, a positive electrode with high pulsed current and a negative electrode are adopted to form a lightning impulse system with duration time of 200ms for simulation of the lightning stroke process, and a tensile force loading apparatus is also constructed to simulate the strain influence of the ice covering on the OPGW. Experimental results demonstrate that the BOTDR can sensitively locate the lightning stroke incidents with the quantity of electric discharging larger than 100C and the strain component has little interference on temperature monitoring as the fiber contained in the OPGW is generally free of strain, and in the ice covering condition the strain feature appears only when the extra tensile force on the OPGW is over 30kN. Additionally, the vibration of OPGW does not disturb both the temperature and strain monitoring. As to further applications of DOFS for the OPGW health monitoring, it is important to enhance its spatial resolution.

9274-32, Session 6

The application of fiber optical sensor based on optical vortex to high-resolution strain measurement

Linxun Chen, Li Yang, Univ. of Science and Technology of China (China)

Using fiber sensor for the strain measurement in earthquake precursor has attracted increasing attention. Since it can not only overcome the difficulties in traditional electronic measuring system such as zero drift, poor stability, high sensitivity to the electromagnetic environment, but also benefit for networking and long distance measurement. However, earthquake precursor measurement requires the resolution to be 10^{-9} , which is hard to be reached for traditional fiber sensor without the device of sensitivity enhancement.

We propose a new method to solve this problem. As we know, if we superpose a vortex beam and the fundamental Gaussian beam together by a coupler, a pattern of interference spiral will be formed, and the spiral will rotate linearly depending on the phase difference between the two beams at the output. Based on the principle, we place the fiber generating Gaussian beam in

a changing environment. Then the change of longitudinal strain causes the linear change of phase difference, resulting in the rotation of the interference spiral. Subsequently, we use image processing based on mathematical morphology to extract feature points of sequential frame interference images, and obtain the dependence of the spiral rotation angle on the strain for our fiber optical sensor. We demonstrate theoretically that the strain resolution over 10^{-9} can be reached with an only 1 meter long fiber, wide linearity and small measurement error are achieved as well.

Optical vortex carrying different topological charges ($l=1,2,3$) are all considered. Comparative analyses are given including sensitivity, measurement error, minimum resolution and maximum allowed strain variation between adjacent frames. We conclude that optical vortex with single charge fits our sensing application best.

9274-33, Session 7

Time dynamic in electric-field-assisted surface plasmon resonance system

Waleed S. Mohammed, Bangkok Univ. (Thailand); Sakoolkan Boonruang, National Electronics and Computer Technology Ctr. (Thailand); Htet H. Kyaw, Joudeep Dutta, Sultan Qaboos Univ. (Oman)

Surface Plasmon Resonance (SPR) sensor has been widely used in several applications. The sensing approach is by exciting the electron oscillation on the metal surface, surface wave, with an optical wave. At resonance, where the incident beam phase matches to a surface wave, light is totally absorbed. Hence, an adsorption of a target molecule on the sensor surface changes the resonance conditions. In general system, ones detect the resonance shift in different manners such as resonance angle, resonance wavelength and intensity shift, for example. To detect heavy metal ion in water, it requires surface modification to bind the ion on the surface. This step can be minimized by combining anodic stripping voltammetry with SPR sensor.

This paper proposes an alternative technique to drive the ion in the solution located at the sensor surface by applying an external electric force to a flow channel. Doing so, surface modification can be as well neglected. The system is referred to as "Electric-Field assisted SPR system." The physics of ion deposition is demonstrated using ion mobility in water model focusing on time dynamics of ion deposition. With enough force, the ions can stack on the sensor depending on ion concentration, ion mass, and flow speed. The experimental results shows that it is possible to detect amount of Cadmium ion (Cd^{2+}) in water as low as 250 parts per billion (ppb). In addition, the time dynamic detection approach has high potential for selective ion detection system as will be shown in the analytical model.

9274-34, Session 7

Spectral multiplexing-guided mode resonance sensor array

Sakoolkan Boonruang, National Electronics and Computer Technology Ctr. (Thailand); Waleed S. Mohammed, Bangkok Univ. (Thailand)

In this paper, a Guided Mode Resonance (GMR) optical sensor is experimentally demonstrated for spectral multiplexing sensors' array. The sensing scheme utilizes resonance effect due to phase matching between first-order diffracted waves and waveguide modes. That causes total reflection at resonance. The resonance spectrum is highly sensitive to changes in the refractive index as well as any additional molecular adsorption on the sensor surface. That utilizes GMR sensor to be successfully applied as

a label-free biosensor. Implementation of multiplex detection readout system requires an imaging sensor array or spectrometer based detection scheme with an assistance of a modulating technique. Here, an alternative approach is presented where GMR sensor array is used to have resonances at shifted spectra. The collective multiline resonance spectrum produced by the array can be simultaneously detected using a single spectrometer. Multiline resonance array is achieved through a chirped grating, which is employed to minimize the crossed coupling between each array via higher-order diffraction. The resonance spectrum is linearly proportional to the grating period along the axis. Using laser interference lithography incorporating with nano-imprinting technique, the chirped grating with a period changing from 400 to 500 nm is fabricated on a Spin-On-Glass ($n=1.4$) film coated on a glass slide ($n=1.52$). Then, TiO_2 high refractive index ($n=2.4$) film with ~ 100 nm thickness is coated on the grating by a sputtering technique. The fabricated device is successfully demonstrated for a two-channel sensor array with sensitivity up to 120 nm/RIU.

9274-35, Session 7

Optical chemical pH sensors based on polymeric planar waveguides

Amit Garg, Acharya Narendra Dev College (India); Shivshankar Gaur, Shivaji College (India); Kailash N. Tripathi, K.R. Mangalam Univ. (India)

The polymers have come a long way and are extensively used in various photonic devices such as optical switches, modulators, LEDs, sensors etc. Various kinds of sensors like gas sensors, biosensors, chemical sensors and pH sensors have been fabricated. We report here a planar dye-doped optical chemical pH sensor. We have fabricated dye-doped planar waveguides and have studied the effect of different pH solutions on the output intensity and absorption spectra of the waveguides. Methyl Red (MR), Bromocresol Purple (BCP), Bromothymol blue and bromophenol blue were used for doping. They were separately doped in Polystyrene (PS) solution and in Styrene Acrylonitrile (SAN) solution respectively. The effect of pH solutions was observed on the absorption spectra and output intensity of the planar waveguides fabricated using spin coating. It was observed that for pH solutions to which the dye is sensitive output intensity decreased and the same was seen in the absorption spectra. The doped polymeric planar waveguides showed sensitivity for pH ranging from 4.5 to 9. These dye-doped polymer waveguides can be used as optical chemical pH sensors.

9274-36, Session 7

Sensing characteristics of clad-modified with nanocrystalline metal oxide fiber optic gas sensor

Dillibabu Sastikumar, National Institute of Technology, Tiruchirappalli (India); Renganathan B. Balusamy, Indian Institute of Technology Madras (India)

Fiber optic gas sensors clad-modified with nanocrystalline metal oxides are proposed for ambient temperature operation. Study shows optical properties of metal-oxides with air medium influence sensing. Absorption characteristics of nanocrystalline Ce-doped ZnO, Sm_2O_3 and ZnO with air and methanol, ethanol and ammonia and their effect on sensing are analysed.

For Ce-doped ZnO, absorbance was 1.9, 2.7 and 1.4 in air, methanol and ammonia, respectively. For Sm_2O_3 , it was 1.75, 1.1 and 1.5, in air, ammonia and ethanol.

Gas sensitivity could be related to gas concentration and difference of light absorption (ΔA) between gas and air. For Ce-doped ZnO, the ΔA between air and methanol is 0.8 and, air and

ammonia is 0.5. It exhibited sensitivity of 96 and 07 $\times 10^{-3}$ /kPa, for methanol and ammonia. For Sm_2O_3 , the ΔA between air and ethanol is 0.25 and, air and ammonia is 0.65. The sensitivity is 76 and 14 $\times 10^{-3}$ /kPa for ethanol and ammonia.

For Ce-doped ZnO, the ΔA between air & methanol (0.8) and between air & ammonia (0.5) is comparable, however, the gas sensitivity is very poor for ammonia (07 $\times 10^{-3}$ /kPa) compared to methanol (96 $\times 10^{-3}$ /kPa). For Sm_2O_3 , large sensitivity (76 $\times 10^{-3}$ /kPa) is observed though the ΔA is very less (0.25) compared to Ce-doped ZnO (0.8).

It appears that large gas sensitivity for Ce doped ZnO is primarily due to large absorption of light by gas molecules, however, interaction of gas molecules is lesser. For Sm_2O_3 , it is due to primarily more number of interacting gas molecules with lesser absorption.

Thursday - Friday 9 -10 October 2014

Part of Proceedings of SPIE Vol. 9275 Infrared, Millimeter-Wave, and Terahertz Technologies III

9275-1, Session 1

The Fano resonances in terahertz metamaterials (*Keynote Presentation*)

Wei Cao, Oklahoma State Univ. (United States); Ibraheem Al-Naib, Queen's Univ. (Canada); Ranjan Singh, Nanyang Technological Univ. (Singapore); Weili Zhang, Oklahoma State Univ. (United States) and Tianjin Univ. (China)

The spectral characteristic of a Fano resonance is a distinct and unique asymmetric line shape. It arises from the destructive interference between a bright continuum mode and a discrete dark mode. Metamaterials have facilitated the observation of Fano resonances in the realm of classical electrodynamics and have spurred intense interest to exploit their peculiarities due to low loss and very sharp resonance features. We present the excitation of terahertz Fano resonances in asymmetric metasurface building blocks. By introducing a weak asymmetry in a two gap split ring resonator, a Fano resonance evolves in the low-frequency flank of the symmetric fundamental dipole mode resonance. This Fano resonance has much higher quality factors than that known from single gap split ring resonators. However, the quality factor decreases exponentially with increasing degree of asymmetry. The highest quality factor that we have achieved in the terahertz Fano resonators is 227. We engineered a design where extremely sharp quadrupole as well as Fano resonances are excited at normal incidence for two different polarizations of the incident electric field. The manipulation of terahertz radiation by exploiting high quality factor Fano and quadrupole resonances in metamaterials could usher in next-generation terahertz photonic devices for delay, storage, filtering, sensing, and nonlinear applications.

9275-2, Session 1

Imaging of terahertz surface plasmon polaritons (*Invited Paper*)

Yan Zhang, Capital Normal Univ. (China)

Surface plasmon polaritons (SPPs) are collective electromagnetic excitations propagating along the metal/dielectric interfaces, evanescently confined in the perpendicular direction. With the ability of subwavelength scale manipulation, the SPPs are attractive for a variety of applications in areas such as near-field sensing, super-resolution imaging, and nanolithography. Fundamental devices for exciting, guiding, and focusing the SPPs have been extensively investigated. However, in the visible spectral range, the primary ways used to characterize the functionality of those devices can obtain only the intensity of the SPPs and the phase information is lost completely, which is unfavorable for the design and characterization of the SPPs devices. The SPPs field excited by the terahertz (THz), known as the Sommerfeld or Zenneck waves, are weakly confined in the dielectric side. The $1/e$ field extension of THz-SPPs from the metal surface can arrive several millimeters into the air. The weak confinement and the scale of the wavelength enable the detection of the THz-SPPs with techniques which are available in the THz spectral range. The THz time domain spectroscopy (TDS) system and THz balanced electro-optic holographic imaging system are primary techniques to detect the THz radiation. An obvious advantage of the above techniques is the ability to obtain the phase information of the THz radiation. The TDS system have already been successfully used to detect the THz-SPPs point by point. Even so, the amplitude and phase images of THz-SPPs have not obtained yet probably due to the complexity of synchronous movement of detection devices used in the TDS

system.

A THz-SPPs imaging system is proposed to obtain both the amplitude and phase images of the THz-SPPs. A CCD is used as the detector and the probe beam is expanded for achieving more information. Only the ZnTe crystal, which is used as the detector, is scanned along the propagating direction of THz-SPPs. The feasibility of this system is demonstrated by imaging a focusing THz-SPPs generated by a semicircular slit. The amplitude images of THz-SPPs for different frequency are presented and compared. The Gouy phase shift during the focusing has also been clearly seen from the phase information. The finite-difference-time-domain (FDTD) algorithm is adopted to replicate the THz-SPPs focusing images. The simulation results verify the reliability of the system.

9275-3, Session 1

Effect on influenza hemagglutinin protein binding with neutralizing antibody using terahertz spectroscopy technology

Yiwen Sun, JUNLAN ZHONG, Shenzhen Univ. (China); JIAN ZUO, CUNLIN ZHANG, Department of Physics, Capital Normal University (China)

Terahertz dielectric spectroscopy is sensitive to probe several aspects of biological systems. We have reported the dielectric spectra is able to identify the type of the charges in the hydrogen-bonded antibodies' networks in our previous work. Recently we demonstrate a highly sensitive terahertz time-domain spectroscopy method to monitor binding interaction of influenza hemagglutinin (HA) proteins against its primary target antibody F10. The detectable minimum concentration of the HA protein was down to 7.5ug/ml using the terahertz time-domain spectroscopy method. The terahertz dielectric properties of HA was strongly affected by the presence of a specific antibody. Molecular arrangement or even concentration can also affect the signal. For instance, we have demonstrated the remarkable frequency-dependent absorption for HA protein was 113ug/ml. As expected, this absorption property for HA has been maintained in the HA/irmAb mixtures solutions as no binding interaction between them. Additional absorption increase at 29ug/ml for H9/irmAb, which indicated the irmAb antibody has a patent absorption at this concentration probably. While the obvious absorption for HA has been shifted to 56ug/ml for H9-F10 complex solution. Moreover, we found that the corresponding absorption coefficient is significantly higher than the bulk HA protein after F10 was added in and also presents the prominent distribution signature in terahertz dielectric spectra. Furthermore, by increasing the concentration of the HA protein in antibody solution we can deduce the number of the effective recognize sites in the stalk region of HA which can be efficiently identified and targeted by the neutralizing antibody.

9275-4, Session 1

Terahertz isolator in metal plate waveguide

Fei Fan, Nankai Univ. (China); Sai Chen, Nankai University (China); Shengjiang Chang, Nankai Univ. (China)

One-way transmission devices, such as isolator and circulator, are widely used for forbidding back-reflected radiation, realizing impedance matching and decoupling in the transmission system, which can protect the radiation source and improve the system

stability. Until recently, some preliminary works for terahertz (THz) isolators have been reported. However, these devices still cannot meet practical applications due to the weak performances in isolation, insertion loss and operating bandwidth, so developing an easy-to-manufacture, high isolation, broadband, and low-loss THz isolator is an important issue in THz technology and application.

In this work, we present a terahertz (THz) isolator in metal parallel plate waveguide (PPWG). A magneto-optical film with 30 μ m thickness is coated on one side of the metal plate of PPWG with 100 μ m width, forming a metal- magneto- air- metal hybrid waveguide. Due to the non-reciprocity of magneto-optical medium and the asymmetry of the waveguide structure, this waveguide show a strong one-way transmission property. The numerical simulation shows that this THz isolator has a maximum isolation of 30dB and a 20dB operating bandwidth of 90GHz under a magnetic field of 0.3T, and its insertion loss is smaller than 0.5dB. Moreover, this operating frequency band can be widely tuned from 0.4THz to 1THz by changing the external magnetic field. The further investigation shows that the periodically structured magneto-optical film can greatly enhance the isolation of this isolator in PPWG to more than 40dB.

9275-5, Session 1

Tailoring structural parameters for enhancing the polarization properties of silver helical metamaterials in terahertz regime

Shuvan Prashant Turaga, Kwan Bum Choi, Yuanjun Yan, Andrew A. Bettiol, National Univ. of Singapore (Singapore)

Metallic helices have been extensively researched and demonstrated for their application as broadband circular polarizers in different frequency regimes. For making such 3D helices, two photon lithography (TPL) has been employed in conjunction with electroplating of metals. Recently, our group has demonstrated selective silver electroless plating of two photon fabricated polymer (SU-8) structures on silicon substrate. This procedure allows us to make metal-coated polymer helices. These helices, by virtue of their high chirality, induce circular polarization. TPL process parameters are responsible for the structural features of polymer helices. The helices have elliptical cross-sectional profile arising due to elliptical focal spot size (about 3:1) of the laser in the z-direction. This elliptical profile is an additional control parameter of chirality for these structures.

In this work, we examine how these fabrication process parameters could be tailored to obtain higher extinction ratios for circular polarizers in THz regime. Moreover, we analyse the role of aspect-ratio of helices in their polarizing action. We will present both simulation and experimental results to show the improved performance of the polarizers.

9275-6, Session 2

Highly-sensitive terahertz biosensor from flexible metamaterial (Keynote Presentation)

Biaobing Jin, Lanju Liang, Jian Chen, Liang Ding, YaYi Hou, Nanjing Univ. (China)

Bull's-eye-shaped metamaterial exhibits multiple electromagnetically-induced transparency (EIT)-like windows. These EIT windows exhibit low loss and high refractive-index sensitive characteristics, which highly desirable for sensing application. In this work, we report the simulation, fabrication, and the analysis of equivalent circuit model with flexible Bull's-

eye-shaped metamaterials used for terahertz sensing. The proposed metamaterial unit cell is composed of five concentric rings, and this metal structure based on the polyimide substrate with the permittivity constant 3.1 and loss tangent 0.05. First, the influences of the thickness with the coating layer and the substrate of the THz sensor have been investigated by above three ways, the shifting effect saturates at approximately 10 μ m and no further significant shift. Next, Streptavidin-agarose (SA) was fabricated based on THz metamaterial functionalized by octadecanethiols and biotins. At the first, second, third, fourth window of multiple EIT, frequency shifts of 10 GHz, 15 GHz, 30 GHz and 29 GHz were observed for the polyimide of thickness is 10 μ m. The frequency shifts are 22.63 GHz, 25.4 GHz, 28.3 GHz, 28.3 GHz respectively for simulation. Good agreement is obtained between the experimental results and simulation, which implies that our structure is a good sensor for bio-molecule detection.

9275-7, Session 2

THz spectra of 1D-grating metamaterials: from metallic SP resonances to all-dielectric trapped modes (Invited Paper)

Yuping Yang, Minzu Univ. of China (China); Chuwen Lan, Tsinghua Univ. (China); Bin Cui, Genxiang Chen, Minzu Univ. of China (China)

The high-resolution, resonant phenomena in all-dielectric, 1D-grating metamaterials are presented. Compared with the surface plasmon (SP) resonances in the 1D metallic grating, the all-dielectric structures exist a series of high-Q trapped mode resonances, and display strong frequency-selection and polarization sensitivity. In agreement with the experimental observation, the coupling effects of subwavelength high-permittivity ($\epsilon_r = 11.6$) arrayed silicon lines which exhibit magnetic and electric Mie resonances were investigated by finite element method (FEM) simulations.

9275-8, Session 2

Conductively coupled resonator scheme for dispersive transparency in metamaterials (Invited Paper)

Shuvan Prashant Turaga, Jianfeng Wu, Agnieszka Banas, Krzysztof Banas, Andrew A. Bettiol, National Univ. of Singapore (Singapore)

We present and demonstrate a novel planar metamaterial design possessing electromagnetically induced transparency (EIT)-like transmission behaviour. The single resonator design involves physically coupled split-ring resonator (SRR) and a dipolar ring as opposed to inductively coupled resonators investigated in the past. Both experiments and simulations reveal a dispersive transparency due to coupled resonances. We explain the underlying mechanism by visualizing the fields and the currents excited in the structure using numerical simulations. On comparing the conductive and inductive coupling scenarios, conductive coupling was found to coerce the direction of light induced currents and stronger in effect than inductive coupling. Resonance tuning is achieved by moving the bar coupling the SRR and the ring. Experiments have shown good conformity with simulations. Hence, we show that conductive coupling has potential in tailoring coupled resonances of desired quality factor and fabricating metamaterials for enhanced sensing.

9275-9, Session 2

Terahertz properties of metallic checkerboard patterns and related structures

Yoku Tanaka, Keisuke Takano, Osaka Univ. (Japan); Abdallah Chahadih, Abbas Ghaddar, Xiang-Lei Han, Francois Vaurette, Univ. des Sciences et Technologies de Lille (France); Willie Padilla, Boston College (United States); Tahsin Akalin, Univ. des Sciences et Technologies de Lille (France); Masanori Hangyo, Osaka Univ. (Japan)

According to the Babinet's principle, screens with self-complementary patterns are expected to show a frequency-independent transmittance below the diffraction frequency. An ideal metallic checkerboard pattern (MCP) is such an example. However, the ideal MCP cannot be realized because each metallic square is connected at one point, which makes the physical resistance at this point undefinable. In this study, we investigate the electromagnetic response of the MCPs made with the accuracy of several tens of nm very close to the self-complementary pattern in the terahertz region to reveal the critical nature of the MCP.

We fabricated the MCPs by electron-beam lithography. The structural differences among samples are about 100 nm, which is less than 0.1% of the wavelengths (about 600 μm at 0.5 THz). The MCPs are consisted of 450 nm thick gold on a high resistively silicon substrate.

It is revealed that the experimental spectra are singularly affected by the slight structural differences. In addition, it is shown that the spectra are affected by a finite resistance of the small metallic regions of the connection regions of squares and their structural randomness. The sample having the structure most close to the self-complementary MCP shows the least frequency dependent response.

We also investigate the MCPs which have additional slits in metallic squares. It is shown that the spectral and polarization response is drastically changed by the slits with very small area. These results show that slight structural differences and additional elements offer new degrees of freedom for controlling THz waves.

9275-10, Session 2

Terahertz gas sensing based on high Q one-dimensional photonic crystal cavity

Tao Chen, Hua Zhang Han, Jun Jian Liu, Zhi Hong, China Jiliang Univ. (China)

With the significant advances in generation and detection techniques of terahertz signals, terahertz technology has attracted considerable attention and has been extensively investigated during the past decades, due to its potential applications in many fields such as biochemical sensing, security screening, military detection, and high speed communication. Owing to the increasing demand for high sensitive biochemical sensors, it is valuable to investigate the design of terahertz gas sensor. Although refractive index sensor of gases has already been investigated in the optical regime, those facilities are extremely expensive and not accessible to many researchers. Considerably less work has concentrated on the gas refractive index sensing technology in terahertz regime. Here, we present a terahertz gas sensor based on a simple one-dimensional photonic crystal cavity. Although the manufacture process is quite easy, this cavity exhibits quite high quality factors for assisting the realization of very high sensitivity in the gas refractive index sensing and can be used for identifying different pure gases versus a change in concentration of one gas. Transmission

measurements of the one dimensional photonic crystal cavity under different gaseous environments showed that the resonant frequency depends linearly on the refractive index of the ambient gas, which can then be measured by monitoring the resonance shift. In our experiment, a change of the refractive index by 1.4×10^{-5} leads to a shift of the resonant frequency by 4 MHz, which corresponds to 6% of the change of hydrogen concentration in air. By using the former reported quality factor of 1.1×10^4 , a refractive index change as small as 7×10^{-6} can be expected. The experimental results also verified its applications in N₂, and CO₂ gas detections.

9275-11, Session 2

Low-frequency vibration study of amino acids using terahertz spectroscopy and solid-state density functional theory

Feng Zhang, Keisuke Tominaga, Kobe Univ. (Japan); Michitoshi Hayashi, Houg-Wei Wang, National Taiwan Univ. (Taiwan)

Understanding the low-frequency normal modes of amino acids, the building blocks of proteins, is crucial to reveal the vibration-function relationship in the macromolecular system. Recent advances in terahertz spectroscopy (THz) and solid-state density functional theory have ensured the accurate access to low-frequency modes of amino acids. A new knowledge people have learnt so far is that the inter- and intra-molecular vibrations are strongly coupled with each other in the THz region through the vibrational coordinate mixing. Rich information is believed embedded in this phenomenon [1,2].

We will introduce an analytical mode-decoupling method that allows for the accurate decomposition of a normal mode of interest into the three intermolecular translations, three principal librations and various intrinsic intramolecular vibrations. We will demonstrate a theoretical analysis by using the L-alanine system as an example. The mode-decoupling method helps reveal new intramolecular vibrational modes on the first hand, and more importantly, shed light on a new phenomenon of the intramolecular vibrational coordinate distribution (IVCD). IVCD describes the broad distributions of important intramolecular vibrations, e.g. NH₃⁺ torsion, COO⁻ torsion and CH₃ torsion, in the low-frequency normal modes.

The IVCD concept may imply solutions to a string of unsettled problems relevant to the low-frequency molecular vibrations, e.g. the formation mechanism of the peptide bonds, the explanation of the line shape of CH₃ tunneling in the small molecular system as well as the first onset of anharmonicity of CH₃ rotation in the protein system.

[1] F. Zhang, O. Kambara, K. Tominaga, J. Nishizawa, T. Sasaki, H.-W. Wang and M. Hayashi, RSC Adv., 4, 269-278, (2014)

[2] F. Zhang, M. Hayashi, H.-W. Wang, K. Tominaga, O. Kambara, J. Nishizawa, and T. Sasaki, J. Chem. Phys. 140, 174509 (2014).

9275-12, Session 3

THz wave generation from micro-plasma (Invited Paper)

Fabrizio Buccheri, Xi-Cheng Zhang, Institute of Optics, Univ. of Rochester (United States)

Laser-induced plasmas with longitudinal size smaller than 40 μm are investigated as a source of broadband terahertz (THz) radiation. We report the measurement of THz waveforms generated in ambient air with laser excitation energies as low as 0.66 μJ . The experimental results suggest the laser-induced micro-plasma as a promising approach to scale down the power

budget for broadband terahertz spectroscopy.

Gas plasmas induced by femtosecond laser pulses have been intensively studied as a source of THz wave radiation. Compared to solid-state THz emitters, i.e., nonlinear crystals or photoconductive antennas, ionized gases can produce broadband THz emission spanning multiple octaves of the electromagnetic spectrum. Moreover, the absence of a damage threshold allows scaling up the THz emission up to peak electric fields in the order of MV/cm by increasing the pulse energy of the pump laser without increasing the beam size.

However, the requirement for the gas to be ionized forbids reducing the pulse energy of the laser excitation below the ionization threshold of the species. Therefore, THz generation from laser-induced gas plasmas requires the use of amplified ultrafast laser, with pulse energies of hundreds of μJ .

We herein address the energy threshold issue by exploiting the ponderomotive force generated at the focus of an intense laser beam to drive the creation of a THz transient in the plasma. Our approach is to focus the laser excitation with a high numerical aperture (NA) objective providing a localized high electron density and a steep intensity gradient. Using a 0.85 NA air immersion objective we obtained plasmas with longitudinal and transverse size less than 40 μm .

We measured a THz waveform with estimated laser pulse energy as low as 0.66 μJ (Fig. 1a). This value consists in more than one order of magnitude improvement on laser threshold energy compared to elongated plasma, i.e., few mm to several cm, generation schemes. The emission is directional and oriented perpendicularly respect to the propagation direction of the pump laser (Fig. 1b and 1c). Due to the cylindrical symmetry of the problem, the THz emission can be visualized as an expanding ring lying on the plane normal to the laser propagation direction, similar to a spherical wave caused by dropping a bead into a body of water.

Further optimization of the source efficiency will allow the replacement of amplified lasers for performing broadband THz spectroscopy with low energy sources. Moreover, we envision the micro-plasma to find use in THz near-field applications, since it provides an unbreakable subwavelength THz source.

9275-13, Session 3

Electro-optic sampling of terahertz pulses based on non-collinear Cherenkov phase-matching (*Invited Paper*)

Masahiko Tani, Shinpei Ozawa, Shogo Azuma, Satoshi Tsuzuki, Takashi Furuya, Stefan Funkner, Gudrun Niehues, Univ. of Fukui (Japan); Elmer S. Estacio, Univ. of Philippines Diliman (Philippines); Kazuyoshi Kurihara, Kohji Yamamoto, Univ. of Fukui (Japan); Michael I. Bakunov, N.I. Lobachevsky State Univ. of Nizhni Novgorod (Russian Federation)

In this paper we report a non-collinear and non-ellipsometric electro-optic (EO) sampling technique, which is free from the velocity mismatch problem and the influence of the birefringence. The non-collinear Cherenkov phase-matching makes it possible to use nonlinear optical media with a large velocity mismatch between the optical and THz regions, such as LiNbO_3 as the EO crystal for detection of THz pulsed wave detection. By using a coupling prism made with Si, the influence of absorption in EO crystal can be much reduced. In addition, by using Cherenkov phase matching we can use any optical sampling wavelengths. With the non-collinear phase-matching it is also possible to use the "heterodyne EO sampling" scheme, which does not require any polarization optics. The heterodyne EO sampling is based on the intensity modulation of the sampling optical beam originating from the interference with the optical waves originating from

the sum frequency generation (SFG) or difference frequency generation (DFG) with the incident THz radiation. An interesting feature of the heterodyne EO sampling is the frequency resolved detection of THz waves. In the conference presentation, the properties of the non-collinear and non-ellipsometric electro-optic sampling for THz wave detection are reviewed.

9275-14, Session 3

Terahertz spectroscopy study of carrier dynamics and transient photoconductivity in CdSSe nanobelts (*Invited Paper*)

Xinhai Zhang, South Univ. of Science and Technology of China (China)

CdSSe nanowires (NWs) and nanobelts (NBs) have received much attention and are considered as promising materials for applications in the area of photonics, photodetectors, photovoltaics, and photocatalysis. To optimize the performance of these electronic and optoelectronic devices, a comprehensive understanding of the transient electrical and optical response, carrier relaxation and diffusion as well as the size- or surface-dependent effect on the carrier dynamics is essential. However, there are few investigations on the transient photoconductivity of 1-D CdSSe nanostructures or any other nanobelt materials. It is extremely challenging to measure the conductivity of semiconductor nanostructures due to the inherent difficulties with the fabrication of Ohmic contacts on nanostructures with the traditional techniques. However, the transient complex-valued and frequency-dependent photoconductivity of nanostructures can be easily probed by the THz spectroscopy. In this talk, I will present the THz spectroscopy study of carrier dynamics and transient photoconductivity of CdSSe NBs. In equilibrium condition (without photoexcitation), the carrier dynamics is mainly affected by the surface depletion region. However, upon photoexcitation, the surface effect is masked by the high photocarrier concentration. In this case, the carrier dynamics is mainly determined by the carrier localization due to composition disorder. The contributions to the carrier mobility from different types of scattering or interaction (surface depletion region scattering, alloy scattering, and optical phonon scattering) are also studied. Our results help to elucidate fundamental physical processes of electron transport in the ternary alloy nanobelts, and are useful for the device application of $\text{CdS}_x\text{Se}_{1-x}$ nanobelts.

9275-15, Session 3

Super-resolution terahertz imaging by femtosecond laser filament in air

Jiayu Zhao, Nankai Univ. (China); Wei Chu, Shanghai Institute of Optics and Fine Mechanics (China); Lanjun Guo, Zhi Wang, Jing Yang, Tao Zeng, Guoliang Yu, Bo Yang, Delong Zhao, Shan He, Haolin Tian, Dan Lu, Weiwei Liu, Nankai Univ. (China); Ya Cheng, Zhizhan Xu, Shanghai Institute of Optics and Fine Mechanics (China)

Resolution enhancement of terahertz (THz) imaging is one of central concerns in the THz science and technology research. Here, we report on a novel super-resolution THz imaging method via the femtosecond laser filament in air, which refers to the plasma channel created by a femtosecond laser pulse.

Super-resolution THz imaging was carried out by inserting a Printed-Circuit-Board plate with multiple through-holes in the middle of the filament. The diameter of each hole is about 600 micrometers. Comparing the image of the multiple holes under optical microscope (resolution: 5 micrometers) and the corresponding scanning THz image, no significant blurring effect

could be noticed. Reminding ourselves that the peak wavelength of the THz pulse generated in our experiment is about 750 micrometers, which is even larger than the size of the holes on the PCB plate. According to the optical image, three hole pitches have characterized widths of about 60, 80 and 75 micrometers, respectively. And they can be clearly resolved by the THz imaging. Hence, the resolution of the obtained THz image by our method is much smaller than the THz pulse wavelength.

The knife-edge method was applied to measure the THz beam diameter along the plasma column. The diameter of the THz beam, which propagates inside the filament, varies from 20 micrometers to 50 micrometers, which is significantly smaller than the wavelength of the THz wave. This phenomenon makes a novel super-resolution THz imaging technique feasible.

9275-16, Session 3

Grating-patterned sub-wavelength terahertz beam characterization via an all-optical knife-edge technique

Sze Phing Ho, Univ. du Quebec (Canada) and Univ. Teknologi Malaysia (Malaysia); Anna Mazhorova, Mostafa Shalaby, Institut National de la Recherche Scientifique (Canada); Marco Peccianti, Univ. of Sussex (United Kingdom); Matteo Clerici, Institut National de la Recherche Scientifique (Canada) and Heriot-Watt Univ. (United Kingdom); Alessia Pasquazi, Univ. of Sussex (United Kingdom); Yavuz Ozturk, Ege Univ. (Turkey); Jalil B. Ali, Univ. Teknologi Malaysia (Malaysia); Roberto Morandotti, Institut National de la Recherche Scientifique (Canada)

The knife-edge (KE) technique is a well known profiling method for laser beams and it is widely used in terahertz (THz) characterization. It has been demonstrated that the KE technique is applicable in the characterization of sub-wavelength THz sources in a near-field configuration using the temporal information to achieve the full profile retrieval [1]. Nevertheless, the KE is still a mechanical technique where the distance between the actual field generation plane and the blade plus its physical thickness introduce inherent inaccuracies in the determination of the sub-wavelength features of a source. A novel and non-contact technique is introduced here, where an all-optical, ultra-thin knife-edge is demonstrated relying on the electromagnetic shielding by photo-excited free carriers at the output facet of the THz generation crystal, thus eliminating the physical blade. Terahertz pulses are generated through optical rectification of femtosecond pulses from a ZnTe crystal. Counter propagating ultraviolet pulses (wavelength = 400nm) are exploited to induce a photo-carrier layer via single photon absorption in proximity of the output surface of the THz-emitting ZnTe crystal. A pump illumination pattern consisting of narrow bright fringes (fringes spacing around 30micron, achieving sub-wavelength scale in THz regime) is generated by a Fresnel biprism with the apex angle of 177degree, mounted prior to the ZnTe crystal. Our results demonstrate the possibility of a novel, all-optical, ultra-thin-thickness KE as an effective and promising profiling technique for sub-wavelength THz sources in different shapes.

References: [1] M. Peccianti et al., IEEE J. Sel. Topics Quantum Electron. 19, 1 (2013).

9275-17, Session 4

Processing sequence for non-destructive inspection based on 3D terahertz images (Invited Paper)

Hugo Balacey, Jean-Baptiste Perraud, Joyce Bou Sleiman, Lab. Ondes et Matière d'Aquitaine (France); Jean-Paul Guillet, Univ. Bordeaux 1 (France); Benoit Recur, The Australian National Univ. (Australia); Patrick Mounaix, Univ. Bordeaux 1 (France)

Terahertz (THz) tomography is a recent imaging technique allowing 3D contact-free inspection of soft materials since the low energy of THz waves provides a high contrast imaging of small-size and low-density samples. Thus a new processing sequence, dedicated to 3D THz image analysis, is proposed to demonstrate the efficiency of THz imaging as a complementary technique with respect to X-ray.

Tomographic acquisition of the sample is performed using a three-axes motorized stage: two translations (to acquire each 2D radiograph by a raster scanning) and one rotation (to acquire several radiographs at different viewing angles). This acquisition corresponds to the processing sequence input.

First, an optimized tomographic reconstruction algorithm is computed, considering the THz wave Gaussian propagation and denoted THz expectation maximization for transmission tomography (THz ML-TR), to provide a 3D volume imaging the acquired sample.

Second, an automated segmentation is performed using a K-mean algorithm to extract the different regions of interest (ROI), which are, at least, the background, the acquisition/reconstruction artifacts and the object of interest. Then the background (largest cluster) and the geometrical noise cluster are removed in order to provide a 3D rendering of the sample only.

Local analysis and measurements are finally performed from such a 3D rendering. For instance, surface or volume dimensions can be done to corroborate dimensional constraints of industrial samples. Another application consists of obtaining the set of topological cavities inside the object, estimating its porosity or highlighting hidden cracks.

This processing sequence will be validated by the analysis of several objects, such as historic pieces or industrial samples.

9275-18, Session 4

Fabrication of broadband antireflection coating at terahertz frequency using a hot emboss method (Invited Paper)

Yunzhou Li, Bin Cai, YiMing Zhu, Univ. of Shanghai for Science and Technology (China)

Because of the imperfection of Terahertz (THz) emitters, the power of THz radiation still stays in a relatively low (nW) lever. Therefore, how to reduce unnecessary transport losses of THz radiation becomes a vital problem for the purpose of increasing signal to noise ratio of THz systems. Recently, a gradient-index anti-reflection (AR) technology is developed very which can not only decrease reflections to an extremely low lever but also provide a broadband and omnidirectional AR effect. In THz region, many technologies, for example chemical etching etc., are utilized to realize such gradient-index structures, but the processes are toxic and complicated. Polymer materials are of excellent processibility, low cost merits, which have been widely used in optical elements fabrication.

In this study, we use polystyrene (PS) to fabricate a gradient-index AR coating by a simple hot-emboss method successfully.

First, a PS layer is spin-coated on a silicon substrate and heated higher than glass-transition temperature. Then, a needle-made mould is pressed on the PS layer and demoulded. The fabricated AR structure is shown in Fig. 1, each unit of the non-periodic sub-wavelength structure is an inverted coniform pinhole (Figure 1) which leads to a gradual refractivity. A THz-time domain spectroscopy is used to evaluate the effect of the AR layer, the results are shown in Fig.2. From the Fig.2 we can see that after the AR coating the transmittance of the high-resistance silicon can be greatly improved.

9275-19, Session 4

Terahertz polarization conversion of metallic microstructures on the different thickness of polyimide substrates

Chang Gu, RuiRui Huang, Kuan Kou, Guozhong Zhao, Capital Normal Univ. (China) and Beijing Key Lab. for Terahertz Spectroscopy and Imaging (China)

With the development of THz technology, the need of different functional terahertz devices is becoming more and more urgent. Manipulation of electromagnetic wave polarization states is one of the essential and challenging tasks in the terahertz band. In recent year, the metamaterial has been one of the rapid growing topics due to their unique properties in manipulation of electromagnetic waves. In particular, metamaterials can change the polarization of incident wave by designing an appropriate structure, such as double layer meanderline, which can achieve conversion from linear polarization to elliptic polarization. Meanderline structure was first used in the microwave field as quarter-wave plate. In this paper, we have investigated the dependence of the different thicknesses of substrate on the polarization of terahertz wave through the meanderline. The meanderline wave plates are designed by using software of CST Microwave Studio. The 200 nm thickness of gold film is used as metallic layer deposited on polyimide substrate with different thicknesses. The ellipticity η is obtained by the simulation including transmission and phase, $\eta=0$ corresponds to linearly polarized transmission, while $\eta=1$ and -1 corresponds to left-handed and right-handed polarization. The intermediate value of η indicates the elliptically polarization. The simulation results show that the absolute value of ellipticity reach maximum 0.999 at 0.505 THz, 0.479 THz and 0.391 THz when the substrate thickness $t=10\mu\text{m}$, $30\mu\text{m}$ and $60\mu\text{m}$, respectively. In addition, the metallic microstructure of meanderline displays a large bandwidth of THz operation. The ellipticity is over 99% in the THz band of 457 GHz to 532 GHz, 426 GHz to 508 GHz, 356 GHz to 486 GHz corresponding the above three kind of substrate thicknesses. The bandwidth become larger and occurs redshift with increasing of substrate thickness. These results provide a reference for the design and manufacture of THz polarization conversion device.

9275-20, Session 4

A new architecture of high dynamic range readout circuits for IR FPA

Dazhao Jiang, Qinghua Liang, Ruijun Ding, Shanghai Institute of Technical Physics (China)

The high-speed and high dynamic range readout circuits can realize a good performance that achieving intra-scene wide dynamic range?and the readout circuit could get more details of a target view that include very dark and very bright signal. A new architecture of readout circuit with high speed and high dynamic range is introduced. In order to achieve high dynamic range, we use a special architecture of readout circuit. The circuit allow

the very high signal to input, and output the signal without be damaged. The input stage use a CTIA architecture in the circuit, and connect a feedback circuit and a S/H circuit in the output of CTIA. The architecture of the feedback is a circuit to control the reset switch of CTIA, when a strong signal inputing, the feedback circuit judge the signal of output, if the signal over the threshold signal that have been set, the feedback circuit output a reset signal, the output of CTIA is reseted to the initial state. A counter records the reset signal, and get the total times of reset. At the last stage of integration period?the S/H circuit samples the signal and a integration period is over. As the circuit could realize multiple reset, the signal would never reach saturation state, and achieve a very high range in the output. We simulate the designed circuits with Cadence IC, and test the functions, and analyze the performance of the circuit from the results.

9275-28, Session Post

Data reconstructed method of LWIR interferometric hyperspectral imager based on CUDA

Zhixiong Yang, Kunming Institute of Physics (China)

With the development of LWIR interference imaging spectrometry,ground applications have posed higher requirements for higher processing rate and real time processing in spectrum reconstruction. In this paper,reconstruction methods and CUDA processing are especially discussed,a spectrum reconstruction technology based on the developing CUDA technology is presented. Experiments show that this method can significantly improve the processing rate of spectrum reconstruction and meet the demands of ground applications.

9275-29, Session Post

Research on the infrared image processing algorithm based on FPGA

Li Xin, BeiHang Univ. (China)

Because of the difference of the imaging cells of the infrared imaging system, the infrared images have the problem of nonuniformity. The infrared images only can be used after nonuniformity correction. This paper introduces an algorithm for infrared image nonuniformity correction based in FPGA. And it completes the design of an infrared image processing system which is component of one single chip of FPGA as core device. This paper details the algorithms of infrared image nonuniformity correction ,blind detection and compensation, and the image enhancement, which are suitable to implement on FPGA. Efficient addition and multiplication module is also designed in this paper. By using these algorithms and the application of pipeline technology and ping-pong operation of the memory, the system logic resource used in this system is effectively reduced and the efficiency of the system operation is obviously improved. Because infrared imaging are influenced by environmental temperature, this paper also proposes an infrared nonuniformity correction algorithm with the compensation if environment temperature based on FPGA. This algorithm is very effective to reduce the influence of the environment temperature on infrared imaging. The images with and without processing are both send to PC by Camera_link image acquisition card to calculate the uniformity of the images. The effect of the system is very good which is proved by contrasting the uniformity data before processing and after processing.This infrared image processing system for infrared imaging laid a foundation for the application of the infrared image in the field of military, industry and civilian.

9275-30, Session Post

Ratios of multi-harmonic for measuring line shape and concentration in TDLAS under low absorbance

Lijuan Lan, Yan-Jun Du, Zhimin Peng, Yufeng Liu, Yanjun Ding, Tsinghua Univ. (China)

Line shape is the key function of tunable diode laser absorption spectroscopy (TDLAS), which is determined by gas temperature, pressure, concentration, and spectroscopy constants. The advantage of traditional direct absorption spectroscopy (DAS) is that it can directly determine line shape, which can infer gas pressure and concentration. However, DAS is easily influenced by particles concentration, laser intensity fluctuations, and baseline-fitting errors that often hamper the accurate determination of absorbance shape. Wavelength modulation spectroscopy (WMS) has high sensitivity and signal-to-noise ratio (SNR), while the measurement of gas parameters are all based on the known line shape, and there is still no efficient and acceptable method to determine line shape in the recent. In the present paper, we propose a method that employs the ratios of the 2nd and 4th harmonics at the line center to measure line shape under low absorption. And combined with the "calibration-free 2f/1f" method, gas concentration can be computed. In validating the precision of this method, the transition of CO₂ at 6982.0678 cm⁻¹ is selected to measure line shape and concentration in laboratory conditions and under weak absorption. Experimental results coincide well with the expectations, thus confirming the accuracy of the proposed method with respect to gas monitoring.

9275-31, Session Post

Far-field beam-pattern of a twin-slot HEB mixer at 600GHz

Kangmin Zhou, Purple Mountain Observatory (China); Yan Delorme, Alexandre Feret, Roland Lefevre, Frederic Dauplay, Thibaut Vacelet, Observatoire de Paris (France); Zheng Lou, ShengCai Shi, Purple Mountain Observatory (China)

In this paper, we report on the measured and simulated far-field beam-patterns of a quasi-optical NbN superconducting hot electron bolometer (HEB) mixer at 600GHz. This superconducting HEB mixer consists of an extended hemispherical lens with a diameter of 12.7mm and an extension length of 2.45mm, a twin-slot planar antenna (two slots measuring 148.5 μ m x 10.4 μ m with a separation of 78.98 μ m) and a 5.5-nm thick NbN thin-film microbridge with an area of 2 μ m x 0.2 μ m. The far-field beam pattern of this mixer is measured by a direct-detection technique with a dynamic range of nearly 25dB, showing an FWHM beam angle of 2.7 $^\circ$ and -18dB level of the first side-lobe. The measured beam of the quasi-optical mixer is nearly collimated and has good Gaussian beam efficiency. In addition, the far-field beam-pattern is measured at different DC bias voltages of the superconducting HEB mixer and at different bath temperatures. The measured results are compared with the ones simulated by two different methods. Detailed measurement and simulation results will be presented.

9275-32, Session Post

2D reconstruction of terahertz Gabor inline digital holography

Yun-Da Li, Qi Li, Jia-Qi Hu, Yongpeng Zhao, Harbin Institute of Technology (China)

Terahertz imaging can make up the defect of imaging opaque samples in visible light domain. Digital holography is a new technology for extracting full information of the original object. In the paper, the improved angular spectrum AS algorithm is coupling the original AS algorithm with direct current (DC) suppression method, apodization and piecewise-nonlinear transformation. The reconstruction characteristics of the algorithm have been studied by numerical analysis and experimental researches. The experimental results validate the application value of the algorithms in improving 2D reconstructed image quality in terahertz Gabor inline digital holography.

9275-33, Session Post

Simulated annealing method for material parameter extraction with terahertz time-domain spectroscopy

Dongxiong Ling, Hongcheng Wang, Xiaoyuan Huang, Yonghe Guan, Dongguan Univ. of Technology (China)

So far, in the practical application, only a narrow time window of the sample waveform is considered to extract the material parameters, i.e., only the first pulse propagation through the sample is considered, however, the first pulse of THz wave can not isolated in the low refractive index and(or) a thin sample. Thus, by use of this simple extraction approach the studied material is constrained by a certain boundary condition, such as a higher refractive index and(or) thick samples; then a new improved method, the simulated annealing method, is introduced by canceling the restrictions in the common method. The simulated annealing method seeks the global minimum of the error function to obtain material constants where the characterized material is not constrained by a certain boundary condition. It is shown from the research results that more accurate material parameters can be acquired to meet the actual requirements of material analysis by use of the simulated annealing method.

9275-34, Session Post

Investigation on terahertz parametric oscillators using GaP crystal with a noncollinear phase-matching scheme

Zhongyang Li, North China Univ. of Water Conservancy and Electric Power (China)

Terahertz parametric oscillator (TPO) using GaP as gain medium with a noncollinear phase-matching scheme is investigated. Frequency tuning characteristics of the terahertz wave (THz-wave) by varying the phase-matching angle and pump wavelength are analyzed. The wide tuning THz-wave can be generated by varying the phase-matching angle and pump wavelength. Gain and absorption characteristics of the THz-wave are investigated. The maximum value of the gain coefficient in GaP is over three times than the gain coefficient in LN. The characteristics of GaP and LiNbO₃ (LN) are compared when the two crystals used as gain medium for the TPO. Compared with LN, the parametric process generating THz-wave from GaP exhibits larger interaction volume among mixing waves, higher parametric gain of the THz-wave and much lower absorption coefficient in the THz region. Based on the analyses above, GaP is more suitable than LN to be used as gain medium for TPO.

9275-35, Session Post

Remote sensing hazardous and toxic gases by passive open-path FTIR in public places

Bei Ma, Peng Rao, Xiao Zuo Dai, Shanghai Institute of Technical Physics (China)

In recent years open-path FTIR systems (active and passive) have demonstrated great potential and success for environment gas pollution remote detection as its higher spectrum resolution, a large range of spectrum and high spectral flux. However, there are few reports about FTIR used to detect hazardous and toxic gases in the case of terrorist acts and chemical accidents in those places, such as public stadium and subway or train station and highway or chemical plants. In those places, passive infrared is an emerging method for remote sensing of hazardous and toxic gases and FTIR is an ideal instrument to give an early warning and situation assessment, which is helpful for emergency response personnel at site to take appropriate measures to protect passengers, works and residents. Passive open-path FTIR remote sensing the target gases spectrum due to the temperature difference with background. Retrieving the measured spectrum, we can get potential target gas spectrum. By the Lamber-Beer Law we can calculate column concentration of the gases. spectrum interpolation and correlation algorithm give a good way to detect the gas species by contrast to the standard gas library.

9275-36, Session Post

A W-band subharmonic Schottky mixer for millimeter imaging

Jie Hu, Purple Mountain Observatory (China); Chengjiang Zhang, Qing Ding, China Academy of Aerospace Aerodynamics (China); Zheng Lou, ShengCai Shi, Purple Mountain Observatory (China)

A W-band subharmonic waveguide Schottky diode mixer based on quartz substrate is presented, which will be used as the detector for the millimeter imaging. The key issue for designing a high frequency Schottky mixer is to accurately model the Schottky diode and extract the imbedding impedance of the diode. Thus the modelling of the Schottky diode in the 3-D full wave simulator (HFSS) based on its physical dimensions is first discussed and the imbedding impedance is exactly extracted as well as the parasitic parameters of the diode. Then a combination simulation of field simulator(HFSS) and the circuit simulator(ADS) is conducted in order to optimized the performance of the subharmonic mixer. The RF probe, LO filter and the IF filter are simulated in HFSS, and then the S parameters of them are imported to ADS to do the standard harmonic balance simulation.

The designed working frequency of the mixer is centered at 100GHz and the LO is 49.5GHz. A standard measurement of single sideband mixer conversion(SSB) was carried out. The power of the RF is calibrated by the power meter. The measured conversion loss is better than 10dBm over 95-105GHz with 8dBm LO pump at 49.53GHz, which is good enough for the application. The measured result is also in excellent accordance with the simulated model.

9275-37, Session Post

Frequency spectrum of a THz QCL in pulse mode measured by an FTS system

Shaoliang Li, Purple Mountain Observatory (China) and Univ. of Chinese Academy of Sciences (China)

In this paper, we report on the spectrum measurement of a THz pulse signal using an FTS system. The THz pulse signal is a quantum cascade laser (QCL) at 3.7THz with changeable repeating frequency and duty cycle. With a fixed duty cycle, the repeating frequency is changed to investigate the minimum pulse time which can be measured with an FTS system. The relationship between the spectrum intensity and the pulse time is investigated through the variance of the duty cycle with a given repeating frequency. Detailed experimental results will be presented.

9275-38, Session Post

Power enhancement of a terahertz-integrated photomixer/antenna by using a resonant antenna

Han-Cheol Ryu, Sahmyook Univ. (Korea, Republic of)

Continuous-wave (CW) terahertz (THz) systems based on photomixing have received considerable attention owing to their wide range of application fields, such as spectroscopy, imaging, sensing, and wireless communications. They are superior to pulsed-wave systems in terms of frequency selectivity, frequency resolution, compactness, and cost. However, the low output power of a THz photomixer is not sufficient for real applications. The output power of a photomixer has been continuously improved by increasing the optical-to-terahertz conversion efficiency through developing photoconductive materials and optimizing the geometry of the photomixer. In this paper, a resonant folded dipole antenna is proposed to increase the output power of a terahertz integrated photomixer/antenna. The antenna was optimized using an electromagnetic simulator. The resistance of the optimized antenna was about 40 times as high as that of a self-complementary broadband antenna. The optimized antenna was fabricated on low-temperature-grown GaAs (LTG-GaAs) and measured using a liquid-helium-cooled silicon bolometer. Two distributed-feedback tunable diode lasers were scanned for photomixing and the two lasers were controlled by using a feedback loop system to constantly maintain the output optical power and to set the target frequencies exactly. The measured THz output power of the proposed folded dipole antenna integrated with a THz photomixer showed resonant characteristics at the resonant frequency bands. As expected, the THz output power increased at the resonant frequency bands, but it was limited by the laser power and bias voltage.

9275-39, Session Post

Personnel screening with terahertz optomechanical scanning imaging

Lantao Guo, Beijing Institute of Technology (China); Xin Liu, Science and Technology on Electro-Optical Information Security Control Lab. (China); Chao Deng, Beijing Institute of Technology (China); Yuan-Meng Zhao, Cunlin Zhang, Capital Normal Univ. (China)

Passive terahertz imaging can receive terahertz signal radiated by human body. So it's expected a better way for human body security check due to its safety. Also many materials have properties in the THz region help passive terahertz imaging detection be able to an important complementary method in

security research region. This attributes a practical aspect of THz application region

This paper presented a passive THz opto-mechanical scanning imaging method and corresponding imaging system using a single detector with a trihedral scanning mirror. This method overcame the disadvantage of image quality due to the movement of the focused mirror. The system improved the imaging speed through employing two frame scanning flapping mirrors. Also the trihedral scanning mirror and an ellipsoidal mirror were adopted for the system to streamline the structure and increase the scanning speed. The parameters were set as follows: the best imaging distance was 1.9m, the image height was 2m, the image width was 1m, the imaging time was 2s, and the resolution was 3cm. We imaged humans with different objects hidden under their clothes, such as belt buckle, mobile phone, bus cards, keys and other items. All the tested stuffs could be detected and recognized from the image.

9275-40, Session Post

Design of a ROIC with high dynamic range for LWIR FPAs

Yongcheng Zhai, Shanghai Institute of Technical Physics (China)

In this paper, a high performance readout integrated circuit (ROIC) designed for long wave infrared (LWIR) detectors is introduced, which has high dynamic range (HDR). To accommodate the wide scene dynamic range requirement, special circuit architecture is used to the input unit cell. A capacitive feedback transimpedance amplifier (CTIA) as input circuit is used to provide high injection efficiency, low input resistance, good linearity, precise voltage bias. Because of the restriction of the layout area, four unit cells will share an integration capacitor and each unit cell has a sample and hold capacitor, which allows the infrared focal plane arrays (IRFPA) to be operated in full frame snapshot mode and provides the maximum integration time available. The parasitic parameters are extracted when the layout is finished. According to the result of post-layout simulation, the design is improved, which leads to the great improvements of the majority of parameters. The simulation results confirm that the ROIC provides over a factor of 70dB dynamic range with the 5.0v power supply and the total power dissipation less than 150mW. The final chip is fabricated with HHNEC 0.35um 1P4M process technology, and the pixel occupies a 30um²30um area.

9275-41, Session Post

Design of high-efficiency conically taper coupler for terahertz waveguides

Tianji Chen, Ting He, Bo Zhang, Jingling Shen, Capital Normal Univ. (China)

A coupler is important in terahertz waveguide experiments, it can enhance terahertz beam intensity to increase detective signal. We simulated the coupler's S-parameter in the frequency range from 0.2THz to 4THz and electric field distribution. Based on the preliminary simulation results and the parameters of CW THz laser and radius of the anti-resonant waveguide in our laboratory we designed a terahertz coupler coupling terahertz radiation into anti-resonant waveguide, optimized geometric parameters and integrated terahertz emitting antenna holder with the coupler. The coupler is combination of a conically taper waveguide and a cylinder waveguide. The cylinder waveguide is used to connect anti-resonant waveguide, the conically taper waveguide is used to collect incident terahertz radiation and concentrate it. Incident

terahertz radiation goes into the big radius port of the conically taper waveguide, passes through the cylinder waveguide and couples into anti-resonant waveguide. We simulated the coupler used in collimated terahertz radiation and it placed just behind terahertz emitting antenna. Our optimizing result is that the cylinder waveguide's radius matching anti-resonant waveguide is 1mm, the length of it is 4mm; the conically taper waveguide's small radius is as the same as the cylinder waveguide, the big radius is 8mm, the length of it is 15mm. In simulation results the terahertz electric field is concentrated around the symmetric axis by the coupler, S-parameter is almost -5dB, which means the output power is almost 50% to the total input power.

9275-42, Session Post

Identification of polypeptides by using SOM neural networks

Jianwei Liu, Ting He, Bo Zhang, Jingling Shen, Capital Normal Univ. (China)

Sample with no characteristic absorption can be identified by refractive index features. In this work, qualitative and quantitative identification of THz spectra of polypeptides using self-organization feature map (SOM) artificial neural network has been demonstrated. The absorption and refractive index features of three polypeptides, including Argline Acetate, Alarelin Acetate and Bivalirudin Trifluoroacetate, were measured by using the terahertz time-domain spectroscopy technique in the range 0.2-2.2 THz. Our results show that the three measured polypeptides show high similarity in absorption spectra and difference in refractive index spectra with the value of 1.762, 1.647 and 1.682 at 1.0 THz, respectively. After the network training process, the collected spectra were identified by the well-trained SOM network at another time.

Analyzing the result, we can see that the refractive index spectra are clustered and identify more availability than the absorption, which can be an effective method in identification of THz spectra of polypeptides especially when there is no obvious difference in absorption spectra but significant differences in refractive index spectra.

9275-43, Session Post

Applications of Bruggeman effective medium theory in mixture using terahertz spectrum

Leiwei Zhang, Jian Zuo, Cunlin Zhang, Capital Normal Univ. (China)

Terahertz time-domain spectroscopy is used to research the intermolecular or intramolecular interactions and some optical properties, such as refractive index, dielectric constant and absorption coefficient. As the dopant in terahertz band, non-absorbing particles, such as polyethylene or others, are usually mixed with pure biological samples by compressing tablets. Due to inhomogeneity and different particle sizes in the tablets, the unobvious absorption from pure sample was affected by doped particle in mixtures. In order to extract the permittivity of pure sample from mixture, Bruggeman effective medium approximation (EMA) theory can be applied. The optical constants and the permittivity of the pure sample can be obtained by using EMA from a composite medium of biological sample and polyethylene. EMA is employed in this work and the relationships between the calculation results and particle sizes are to be explored. It shows that the practicability of Bruggeman effective medium theory in the identification of terahertz spectrum of mixture.

9275-44, Session Post

Electrical and optical properties of polyimide/carbon composites in the THz region

Guo-teng Duan, Lin Li, Beijing Institute of Technology (China)

Carbon nanotubes are the excellent absorber for the terahertz wave, making it an attractive candidate absorber for terahertz bolometric detector. But there is no easy way to get patterned Carbon nanotubes film, therefore, we have developed a method that polyimide/carbon nanotube composites film can easily be made by the ultrasonic dispersion reaction and patterned by the film spinning coating and patterning by lithographic process. The ultrasonic dispersion reaction at different time and different frequency were studied. The results show that with ultrasound frequency of 325Hz and ultra-sonication time of 90 min, the carbon nanotubes were well dispersed in the polyimide film. The solid content of the solid polyimide/carbon nanotube composites is 4%. And the film can easily be patterned by lithographic process. Terahertz properties of polyimide/carbon nanotube composites were explored with terahertz time-domain spectroscopy. It is showed that the absorption coefficient and refractive index all increased at the THz band due to the increase of the charge carrier density. The experimental data were analyzed with Cole-Cole formula of dipole relaxation under the assumption that conductive particles dispersed in the matrix behaved like dipole and contributed mainly to the dielectric loss in the THz frequency range.

9275-45, Session Post

Influence of incident wave polarization on the transmission properties of terahertz metamaterials

Lishuang Feng, Chenlong Li, Zhen Zhou, BeiHang Univ. (China)

Terahertz (THz) modulator is a critical component in terahertz communication system, and fabricating split-ring resonators (SRR) on semiconductor substrate is one of the most promising ways to achieve high modulation depth and high modulation speed. However, there is a limitation on the practical use since SRR unit is sensitive to the incident wave polarization. In order to design novel polarimetric THz devices for application expanding, we simulate and analyze the influence of incident wave polarization on the THz transmission spectrum of structures composed of SRR with different rotation symmetry.

The structure composed of double SRRs is studied first, and the results show that it displays different transmission properties when the incident wave polarization is rotated of 90 degrees. Then the structures consisted of triple, quadruple, sextuple and octuple SRRs are investigated, respectively, using the same simulation model. All the structures are patterned on intrinsic gallium arsenide (GaAs) with the same periodicity, line width, gap and almost the same element area. The EM responses of proposed structures under different polarization incidence THz wave are simulated with finite element method. The simulation results demonstrate that the polarization-sensitive characteristic is determined by the rotation symmetry of the SRR-metamaterials units. The structure with more rotation symmetry is beneficial to get the more polarization-independence. However, increase of symmetric SRR units may cause the decrease of the quality factor (Q), which results in the degradation of the modulation depth. It's interesting to check if there is a novel metamaterials structure to remove the tradeoff or prove it always exists. This work is in progress.

Our work can be a guide for the design of novel metamaterials

modulator and other polarimetric THz devices. The simulation results will be verified utilizing THz time-domain spectroscopy in the future.

9275-46, Session Post

Non-moving-mirror Fourier transformation spectroscopy based on optical frequency comb

Honglei Yang, Haoyun Wei, Hongyuan Zhang, Yan Li, Tsinghua Univ. (China)

Since the advent of optical frequency comb (OFC), many precise metrology have been prosperously growing, such as absolute ranging and high-resolution spectroscopy. In this paper, a new approach to gas absorption spectroscopy based on an improved Fourier-Transformation Spectroscopy (FTS) layout with an OFC source is proposed. In this system, the moving mirror that is common in Michelson Interferometer of conventional FTS does not exist, which avoids the error from scanning part. We adjust the repetition rate of OFC with equal step. Thus, the pulses along the short arm will march through and sample the pulses propagating via the long arm with equal step. The scanning step from changing the repetition rate is traced to microwave frequency standard because that OFC is stabilized to Rb clock, whose accuracy is about 4 orders of magnitude better than that of He-Ne laser in FTS. In addition, the replacement of thermal source by laser source results higher radiation and energy efficiency. According to theoretical analysis, there is an inverse relationship between the resolution and the optical path difference in the two arms. Assuming the number difference in two arms is N, the maximum of the repetition rate change is N times smaller than the case of N equaling to 1. The tuning step of the repetition rate has a same rule as the resolution.

9275-47, Session Post

Terametrics: A new tool for modelling and interpretation in terahertz time-domain spectroscopy

Zhuo-yong Zhang, Mingyu Ma, Yuhong Xiang, Zhenwei Zhang, Capital Normal Univ. (China)

Terahertz time-domain spectroscopy (THz-TDS) has been used in various fields for material recognition and detection. The THz-TDS spectral interpretation and modeling are a challenging work for most problem solvers, especially for complicated practical systems. A new software package called Terametrics, which imply mathematical and statistical methods used for data modeling and interpretation of terahertz frequency electromagnetic waves, was developed by our group for spectral interpretation and modeling in THz-TDS. This software can read THz-TDS spectral data and output the prediction results based on established models. This software includes several spectral pre-processing methods including smoothing, derivative, multiple scattering correction (MSC), and orthogonal signal correction (OSC). The software divides data set based on boot-strapped Latin-partition method. Optimal factors can be selected based on principal component analysis (PCA). The multiple linear regression (MLR), partial least squares (PLS) modeling establishment for qualitative and quantitative analyses. Several real examples of THz-TDS were given to show the effectiveness of the Terametrics.

9275-48, Session Post

Experimental methods of indoor millimeter-wave radiometric imaging for personnel concealed contraband detection

Taiyang Hu, China Academy of Space Technology (China); Zelong Xiao, Nanjing Univ. of Science and Technology (China); Hao Li, China Academy of Space Technology (China); Rongchuan Lv, China Academy of Space Technology (China); Xuan Lu, Nanjing Univ. of Science and Technology (China)

The increasingly emerging terrorism attacks and violence crimes around the world have posed severe threats to public security, so carrying out relevant research on advanced experimental methods of personnel concealed contraband detection is crucial and meaningful. All of the advantages of imaging covertly, avoidance of interference with other systems, the superior ability of imaging through natural or manmade obscurants, and the intrinsic property of being safe to persons under screening, have effectively combined to enable millimeter-wave (MMW) radiometric imaging to offer great potential in personnel concealed contraband detection. Based upon the current research status of MMW radiometric imaging and urgent demands of personnel security screening, this paper mainly focuses on the experimental methods of indoor MMW radiometric imaging. The reverse radiation noise resulting from super-heterodyne receivers will seriously affect the imaging experiments carried out at short range, so both the generation mechanism and eliminating methods of this noise are investigated. Then, the benefit of sky illumination no longer exists for the indoor radiometric imaging, and this phenomenon leads to the decrease in radiometric temperature contrast between target and background. In order to enhance the radiometric temperature contrast for improving indoor imaging performance, the noise illumination technique is adopted in the indoor imaging scenario. In addition, the speed and accuracy of concealed contraband detection from acquired MMW radiometric images are usually restricted to the deficiencies in traditional artificial interpretation by security inspectors, thus an automatic recognition and location algorithm by integrating improved Fuzzy C-means clustering with moment invariants is put forward. A series of original results are also presented to demonstrate the significance and validity of this method.

9275-49, Session Post

Test system of 100GHz photodetector impulse response at NIM

Jianwei Li, National Institute of Metrology (China)

Electrooptic sampling has been shown to be a very powerful technique for making time-domain measurements of fast electronic devices and circuits. In this paper, we review the principles of electrooptic sampling technique for electronic waveform probing with applications to characterizing 100GHz photodetector pulse response. The 100GHz photodetector impulse response data by Gaussian line shape fitting: 7.57ps. Once calibrated, this photodiode plays the role of an electrical waveform primary standard with known impulse response and can be used as a reference input pulse source for instruments like sampling oscilloscopes, power meters, pulse laser, etc..

9275-50, Session Post

Extracting accurate complex refractive index from solid pellets based on time-domain terahertz reflection spectroscopy

Ping Sun, Yu Zhang, Lin Zhang, Yingfeng He, Yun Zou, Qiongzhen Jia, Qinghua Yang, Beijing Normal Univ. (China)

As a novel spectral detection technology, terahertz time-domain spectroscopy (THz-TDS) is widely used in studying the optical properties of materials in the THz domain. The precise determination of the complex refractive index of the materials is important for analyzing the interaction between THz radiation and materials. In this paper, a complex filtering method for eliminating systematic and random noises of THz-TDS is proposed. This method is the combination of deconvolution and wavelet filtering algorithms. A self-reference method for extracting the complex refractive index of material accurately is proposed in order to avoid a phase error due to the misplacement between the surfaces of the reference and sample using the time-domain terahertz reflection spectroscopy. The basic idea of self-reference method is that the first and the second peaks of the reflection spectrum of solid pellets are regarded as the reference and sample signals, respectively. Thus more information of samples can be extracted because of a longer optical path, and meanwhile, phase error can be avoided by obtaining the reference and sample signals through a single measurement. According to the Fresnel formulas, we deduce the expression of complex refractive index and then design an iterative algorithm for solving it. We choose the glucose solid pellets as samples to test the self-reference method. After measuring the time-domain reflection spectrum, we adopted the complex filter method for filtering and utilized the self-reference method to extract the complex refractive index. Based on Density Functional Theory (DFT), the characteristic absorption spectrum of multiple glucose molecules in the THz absorption spectroscopy was obtained by the simulation analysis on the vibration of multiple glucose molecules. The results indicate that the absorption peaks appear in the absorption coefficient curves at the corresponding frequency positions which are consistent with the results of the simulation based on DFT. So the methods we proposed can help improve the retrieval accuracy of complex refractive index.

9275-51, Session Post

Spectroscopy of glycerol in THz range using microfluidic chip-integrated micropump

Bo Su, Xue Han, Ying Wu, Cunlin Zhang, Beijing Key Lab. for Terahertz Spectroscopy and Imaging (China) and Capital Normal Univ. (China)

Terahertz time-domain spectroscopy (THz-TDS) is a detection method of biological molecules with label-free, non-ionizing, non-intrusive, no pollution and real-time monitoring. But owing to the strong THz absorption by water, it is mainly used in the solid state detection of biological molecules. In this paper, we present a microfluidic chip technique for detecting biological liquid samples using the transmission type of THz-TDS system. The microfluidic channel of the microfluidic chip is fabricated in the quartz glass using Micro-Electro-Mechanical System (MEMS) technology and sealed with polydimethylsiloxane (PDMS) diaphragm. The length, width and depth of the microfluidic channel are 25mm, 100 μ m and 50 μ m, respectively. The diameter of THz detection zone in the microfluidic channel is 4mm. The thicknesses of quartz glass and PDMS diaphragm are 1mm and 300 μ m, individually. Another one of the same quartz glass is

used to bond with the PDMS for the rigidity and air tightness of the microfluidic chip. In order to realize the automation of sampling and improve the control precise of fluid, a micropump, which comprises PDMS diaphragm, pump chamber, diffuser and nozzle and flat vibration motor, is integrated on the microfluidic chip. The diffuser and nozzle are fabricated on both sides of the pump chamber, which is covered with PDMS diaphragm. The flat vibration motor is stuck on the PDMS diaphragm as the actuator. We study the terahertz absorption spectroscopy characteristics of glycerol with the concentration of 98% in the microfluidic chip by the aid of the THz-TDS system, and the feasibility of the microfluidic chip for the detection of liquid samples is proved.

9275-52, Session Post

Target recognition of passive terahertz human body image

Ran Zhao, Yuan-Meng Zhao, Chao Deng, Cunlin Zhang, Capital Normal Univ. (China)

No Abstract Available

9275-53, Session Post

Terahertz spectra of glycerol, water, and their mixture in a microfluidic chip

Xue Han, Bo Su, Ying Wu, Cunlin Zhang, Beijing Key Lab. for Terahertz Spectroscopy and Imaging (China) and Capital Normal Univ. (China)

A terahertz microfluidic chip which was fabricated out of quartz and polydimethylsiloxane (PDMS) was designed. The quartz acted as a substrate, on which a microfluidic channel with a height of 50 μm was etched by lithography technology. PDMS is a kind of easy fabricated and cheap polymer to cover the quartz substrate. It's widely used in microfluidic applications for its numerous characteristics such as good insulation, colorlessness and transparency, high-voltage endurance and excellent optical quality. The transmittance of the chip was measured first. Increasing the frequency from 0.2 THz to 1.4 THz decreases the transmittance of microfluidic chip rapidly, where reaches as high as 80% when the frequency is 0.2 THz. The chip shows a high transmittance of above 40% from the range from 0.2 THz to 0.8 THz. Then THz spectra of glycerol, water and their mixture in the microfluidic chip were measured, respectively. Not only the time domain spectra but frequency-dependent amplitude spectra present significant differences of different kinds of liquids and different concentrations of the same glycerol. The absorption spectra result shows a monotonic increase in the absorption coefficient of the glycerol, water and the mixture with increasing frequency, respectively. It matches the fact that different molecules or the same molecules of different concentrations present different absorption coefficients in the terahertz band. All of the above indicate that this microfluidic chip is available in measurement of the samples in liquid and it's able to realize real-time and label-free measurement for biochemistry samples in terahertz time-domain-spectroscopy (THz-TDS). Since the depth of the micro-channel is 50 μm , the detectable liquid in the chip only has an value of less than 10 μL , microfluidic chips offer a new platform for performing THz spectroscopy of small quantities of biomolecules using low-power THz sources.

9275-54, Session Post

Passive THz body-scan image processing for object detection

Yuan-Meng Zhao, Chao Deng, Cunlin Zhang, Ran Zhao, Yue Li, Capital Normal Univ. (China)

The THz region occupies the part of the electromagnetic spectrum between 30 μm and 3 mm. THz radiation, which is a form of low level energy naturally emitted from all materials such as rocks, animals and people, doesn't involve any of the harmful radiation like the traditional X-ray. In addition, it can be readily transmitted through most non-metallic and non-polar mediums. Due to these characteristics, since the last two decades, there has been an increased interest in THz imaging for security applications, to uncover concealed weapons, dangerous materials or illegal products on person. Two imaging approaches associated with this technology are active imaging method and passive imaging method. Passive imaging method, without the use of an external illuminator, has the advantage of achieving a good balance between security and civil liberties. We began to study the passive THz optical-mechanical scan imaging method many years ago. From our previous work, we have developed different types of passive THz security screening system and got some initial THz body-scan images, however, limited by the THz detector properties, the target recognition ability of the system still needs to be improved. Therefore, a series of image processing methods were developed to restore and enhance the originally captured THz images. The purpose of this paper is to introduce the image processing methods used in the systems for improving the system's object detection ability. The image processing methods mainly include the following steps. First, the vertical stripes and noises are filtered by using a variety of masks through methods such as smoothing filtering and median filtering, so that we improve the uniformity of the image. Second, we improve the contrast and resolution by performing image enhancement and restoration. Third, the person and objects are segmented from the image, and then we draw their contour outline by means of computing the gradient image. Finally, we optimize the display effect of the object areas by using pseudo-color transformation and image fusion which involves using a registered visible image, and describing the edges of person and targets through a virtual image. Both the simulation experiment results and the actual system performing results demonstrate the efficacy of our methods. The resulting images can clearly distinguish the human body's edge from the background and display the position of the possible concealed objects. We can draw a conclusion that the method introduced in this paper has the capability to help the checkpoint security staff easily detect the concealed targets on person remotely. In the end, we discuss the future research direction which will be to further improve the image resolution.

9275-55, Session Post

A single-frame terahertz image super-resolution reconstruction method based on sparse representation theory

Yue Li, Yuan-Meng Zhao, Chao Deng, Cunlin Zhang, Capital Normal Univ. (China)

In recent years, a lot of terrorist attacks occur frequently, and public safety is increasingly become focus of attention by many countries. In order to effectively prevent and combat the occurrence and expansion of these criminal activities, to improve the effectiveness and accuracy of security detection systems doesn't brook any delay. Nowadays the metal security doors, X-ray detectors and infrared detectors are commonly used in public safety testing, but there are still some disadvantages, while passive terahertz security instrument can compensate for their

shortcomings. Terahertz wave has a strong penetrating power, which can pass through the clothes, and cause no ionization damage to the human body and the objects being checked. After the security check simulation in the laboratory, we obtain the original terahertz body-scan image with hidden metal objects under the clothes. However, during the image transfer process, taking the impacts of THz detector performance and external environment into account, the quality and resolution of the output images are decreased. In order to improve the image quality, there are two methods: one is to improve the performance of the hardware, but the effect is not satisfactory and it will increase the production cost of the equipment; the other is to obtain high-resolution image by using digital image processing, which is a particularly important software technique. Therefore, how to obtain high-resolution images through image reconstruction based on current capture devices and observations has become a hot topic today. One way to solve this problem is using image super-resolution reconstruction which is based on the image degradation model and prior information. Image super-resolution reconstruction is an important image processing technology which is able to improve the visual effect and it prepares for image post-processing. With the development of machine learning and pattern recognition technology, learning-based image super-resolution reconstruction algorithm get more and more research attention and the image processing results are much better than traditional methods. Super-resolution reconstruction based on sparse representation is one of the emerging methods, and sparse representation of image has become a hot spot in recent years.

In this paper, we propose a single-frame terahertz image super-resolution reconstruction method based on the theory and methods of sparse representation, and apply the sparse dictionary method to THz images. We focus on analyzing the sparse representation in terahertz image super-resolution reconstruction. In order to process the images, we first do image preprocessing including de-noising and gray stretch. Because the noise of original image is mainly Gaussian noise, we select the median filter for de-noising and smoothing. In order to distinguish the background, human body and the hidden metal fields within the human body, we carried out contrast stretching to the de-noised image, namely gray stretch. After smoothing the image again, we reconstruct super-resolution image based on sparse dictionary and selected one of the common methods of learning dictionary, K-singular value decomposition (K-SVD), to construct the sparse dictionary. Finally, by super-resolution processing we analyze the image processing results and compared with the result of classic super-resolution image processing algorithms, such as bilinear interpolation, bi-cubic interpolation, iterative back-projection and convex projection algorithm. We evaluate all super-resolution image results with both subjective evaluation and objective evaluation. Subjective evaluation mainly relies on the effect of human visual perception and objective evaluation indexes include RMSE and PSNR. Through the evaluation results we can obviously see that the algorithm proposed in this article is able to get much better super-resolution images than conventional algorithms.

9275-56, Session Post

A polarization-independent terahertz modulator based on metamaterials with symmetric structure

Jingsuo He, Lei Jiao, Hailin Cui, Cunlin Zhang, Capital Normal Univ. (China)

This paper proposed a polarization independent terahertz modulator based on gold-Si metamaterials with symmetric structure, and aimed to modulate terahertz wave in communication systems. The transmission properties have been investigated in the 2 terahertz regime. We find that the resonance

frequency of this device can be actively controlled by pump laser. The numerical simulations and experiments with OPTP system show that this device acts as a modulator with intensity modulation depth of 70% by gold structure.

9275-59, Session Post

Terahertz imaging system based on Bessel beams via 3D printed axicons at 100GHz

Changming Liu, Xuli Wei, Zhongqi Zhang, Kejia Wang, Wuhan National Lab. for Optoelectronics (China); Zhenggang Yang, Huazhong Univ. of Science and Technology (China); Jinsong Liu, Wuhan National Lab. for Optoelectronics (China)

Terahertz (THz) imaging technology shows great advantage in nondestructive detection (NDT), since many optical opaque materials are transparent to THz waves. In this paper, we design and fabricate dielectric axicons to generate zeroth order-Bessel beams by 3D printing technology. We further present an all-electronic THz imaging system using the generated Bessel beams in 100GHz. Resolution targets made of printed circuit board are imaged, and the results clearly show the extended focal depth of Bessel beam, indicating the promise of Bessel beam for THz NDT.

9275-60, Session Post

Orbit angular momentum encoding at 0.3 THz via 3D printed spiral phase plates

Xuli Wei, Changming Liu, Zhongqi Zhang, Kejia Wang, Wuhan National Lab. for Optoelectronics (China); Zhenggang Yang, Huazhong Univ. of Science and Technology (China); Jinsong Liu, Wuhan National Lab. for Optoelectronics (China)

Terahertz wave carrying OAM would boost the capacity of free-space communication with a high carrier frequency and additional degrees of freedom. In this work, we present an experimental demonstration of THz orbital angular momentum (OAM) encoding via 3D printed spiral phase plates (SPPs). By using four "coding" SPPs with topological values -2, -1, +1, +2, we can encode OAM information onto THz waves and generate temporal varying OAM states with controlled sequences (i.e., 2-bit coding). By using interference between OAM beam and a reference Gaussian beam, the OAM information can be detected from the interference fork pattern.

9275-21, Session 5

Transport properties in narrow-gap semimetallic two-dimensional and far-infrared detector superlattice (Keynote Presentation)

Abdelhakim Nafidi, Driss Barkissy, Abderrazak Boutramane, Hassan Chaib, Univ. Ibn Zohr (Morocco); Bernabé Marí Soucase, Univ. Politècnica de València (Spain)

We report here transport properties and bands structure performed in the envelope function formalism in HgTe(40 nm)/CdTe(15 nm) superlattice (SL) grown by MBE. Calculations of the spectra of energy $E(d_2)$, $E(k_z)$ and $E(k_p)$, respectively, in the direction of growth and in plane of the superlattice; were performed in the envelope function formalism. The energy

$E(d_2, \gamma, 4.2 \text{ K})$, shown that when d_2 increase the gap E_g decrease to zero at the transition semiconductor to semimetal conductivity behaviour (at $d_2=10 \text{ nm}$) and become negative accusing a semimetallic conduction. The angular dependence of the transverse magnetoresistance follows the two-dimensional. A reversal of the sign of the Hall coefficient occurs at 3.2 T. The weak-field Hall coefficient present a small maximum at about 30 K attributed to the presence of an acceptor resonant state. At 4.2 K, the sample exhibits n type conductivity with a Hall mobility of $1500 \text{ cm}^2/\text{Vs}$. Whereas, the electrons mobility was $\mu_n=6700$ and $n=6.2 \cdot 10^{11} \text{ cm}^{-2}$ (with $\mu_n/\mu_p=15$ and $p/n=42$). In intrinsic regime, $R_H T^{3/2}$ indicates a gap $E_g = 5.3 \text{ meV}$ in agreement with calculated $E_g(?, 300 \text{ K}) = 6 \text{ meV}$. The calculated bands gap $E_g=E_1-HH_1$ goes to zero at $T=148\text{K}$ with a transition semimetal to semiconductor conductivity. The formalism used here predicts that the system is semimetallic for our $d_1/d_2 = 2.67$ and d_2 sup 11 nm. Here, $d_2=15 \text{ nm}$ and $E_g(\gamma, 4.2 \text{ K}) = -4.1 \text{ meV}$ so this sample is a narrow gap semimetallic, two-dimensional and far-infrared detector. Ref M. Braigue, A. Nafidi, et al, Journal of Low Temperature Physics, Volume 171, Issue 5-6, pp 808-817, (2013)

9275-22, Session 5

Detection of terahertz spectra of liquids by chirp-induced coherent Raman spectroscopy (Keynote Presentation)

Stefan Funkner, Katsuya Saito, Gudrun Niehues, Yoshiki Yazawa, Takashi Furuya, Kohji Yamamoto, Masahiko Tani, Univ. of Fukui (Japan)

Understanding intermolecular interactions is a key issue for the theoretical description and experimental investigation of liquids. Because intermolecular interactions are mediated by weak forces, the frequencies of the corresponding dynamics are often located in THz regime.

Here, we present a THz Raman spectrometer, which utilizes broadband-width laser pulses in order to investigate nonlinear THz spectra of liquids by means of the spectral focusing technique. In our experiment the laser pulses, which are provided by a regenerative amplifier, pass an optical stretcher where a linear chirp is imprinted to every pulse. Next, the pulse train is sent to an interferometer where every pulse is split into a pump and a probe pulse by a 50/50 beam splitter. With the delay stage of the interferometer, we are able to adjust the time delay of the pump and probe pulses. Finally, both pulses overlap at the sample position where coherent Raman scattering occurs.

With our experiment, we can investigate stimulated Raman gain scattering, inverse Raman scattering as well as the transition between both processes. The frequency of the scattering process is related to the beat frequency between the pump and probe beam and can be selected by adjusting the time delay between both beams using the delay stage of the interferometer part. Hence, by scanning with the delay stage we directly obtain the spectrum in the frequency domain. Our experiments with organic liquid samples show that we can investigate a frequency range from 100 GHz to 10 THz with the presented setup.

9275-23, Session 5

Detection and evaluation of oil and gas resources by terahertz spectroscopy (Invited Paper)

K. Zhao, China Univ. of Petroleum (China)

Oil and gas are significant strategic resources for sustainable development of both the economy and society in China. The difficulties and challenges facing the oil and gas industry place higher demands on the existing methods and technology.

As a rapidly developing tool for prospecting and evaluation, terahertz technology has progressed from initial detection of petrochemical products to upstream and midstream sectors of the oil and gas field, including oil prospecting and evaluation, exploitation and detection, and so on. The oil and gas industries have expressed great interest in the promising applications, and wider commercialization of terahertz technology is to be expected.

9275-24, Session 5

The optimization research of the very long wavelength QWIPs (Invited Paper)

Qian Li, ZhiFeng Li, Ning Li, Xiaoshuang Chen, PingPing Chen, XueChu Shen, Wei Lu, Shanghai Institute of Technical Physics (China)

Due to the GaAs-based material, which has mature material growth and device processing technology, GaAs/AlGaAs quantum well infrared photodetectors (QWIPs) are particularly suitable for high uniformity and large area applications of infrared focal plane array (FPA). By changing the parameters of the quantum well structure, it is relatively easy to shift the detecting band extending from 8 - 10 microns to long wavelength infrared of 12 microns, and even to very long wavelength infrared (VLWIR) of 15 microns, which is particularly suitable for lower temperature detecting of the target object. We optimize the very long wavelength GaAs/AlGaAs QWIPs in three parts: (1) By designing the structure of the quantum wells carefully, we can control the electronic states to form the effective bound-to-quasi-bound states, which is experimentally proved to be the best working mode in QWIPs at wavelength of 15 microns. The working mechanisms of the quasi-bound states, including the two processes of tunneling and thermionic emission, are also investigated in detail; (2) Using an optimized hybrid structure of grating metal-dielectric-metal plasmonic cavity and QWIPs, we can control the photonic mode for an efficient light coupling. The results show that more than 10 times of absolute enhancement of infrared photoresponses are obtained, compared with that of 45 degree edge facet light-coupling device; (3) We report our achievement of the 320×256 n-type QWIP FPA based on GaAs/AlGaAs with the peak wavelength of 14-15 microns. At the working temperature of 50 K, the response bandwidth is greater than 2 microns and peak detectivity of the FPA reaches $1.0 \times 10^{10} \text{ cm} \cdot \text{Hz}^{1/2}/\text{W}$.

9275-25, Session 5

A 20MHz 15 μm pitch 128x128 CTIA ROIC for InGaAs focal plane array

Zhangcheng Huang, Yu Chen, Songlei Huang, Jiaxiong Fang, Shanghai Institute of Technical Physics (China)

A 128x128 matrix readout integrated circuit (ROIC) for $15 \times 15 \mu\text{m}^2$ InGaAs focal plane array (FPA) is reported in this paper. Capacitive-feedback Trans-Impedance Amplifier (CTIA) and correlated double sampling (CDS) are both involved in ROIC pixel which dissipates 90nW and has a full-well-capacity (FWC) of about $78,000e^-$. Noises of ROIC pixel which operated in integration then read (ITR) and integration while read (IWR) modes are analyzed in detail. In column circuit, a new pre-charging technique is developed to realize readout rate of 20MHz and reduce power dissipation of 128 column circuit to 17mW. The ROIC is fabricated with 0.18- μm 3.3V mixed signal CMOS process. Test results show that the ROIC has an input referred read noise of about $150e^-$ and a readout rate of more than 20MHz.

9275-26, Session 5

Infrared image segmentation method based on spatial coherence histogram and maximum entropy

Songtao Liu, Dalian Naval Academy (China); Tongsheng Shen, China Defense Science and Technology Information Ctr. (China); Yao Dai, Dalian Naval Academy (China)

In the fields of image segmentation, such methods based on histogram and optimal objective functions?for example, Otsu method, maximum entropy method, maximum correlation method and maximum Renyi entropy method, are very important. However, when they are used for infrared image segmentation, they are weak in suppressing background noises. To overcome this deficiency, the one-dimensional (1D) histogram is developed into 2D histogram, then 2D Otsu method, 2D maximum entropy method, 2D maximum correlation method and 2D maximum Renyi entropy method are put forward. However, the 2D histogram suffers from the problem of high computational amount while it improves the ability of suppressing background noises. Therefore, many optimization methods are also presented, such as particle swarm optimization, genetic optimization, etc. In order to achieve both background noises suppression and fast computation, a novel infrared image segmentation method based on spatial coherence histogram and maximum entropy is proposed. First, spatial coherence histogram is presented by weighting the importance of the different position of these pixels with the same gray-pixel, which is obtained by computing their spatial variance. This histogram can not only represent the spatial connectedness better than 2D histogram, but also be implemented fast since it is still 1D histogram in essence. Then, maximum entropy method is used to segment the histogram and get image segmentation results. The main features of this proposed method is that it can not only get better segmentation results, but also have a faster computation than traditional 2d histogram segmentation methods, so it is suitable for fast infrared image segmentation.

9275-27, Session 5

Design of the small pixel pitch ROIC

Qinghua Liang, Dazhao Jiang, Yongcheng Zhai, Lei Gao, Shanghai Institute of Technical Physics (China) and Univ. of Chinese Academy of Sciences (China); Ruijun Ding, Shanghai Institute of Technical Physics (China)

Since the technology trend of the third generation IRFPA towards resolution enhancing has steadily progressed, the pixel pitch of IRFPA has been greatly reduced. A 640x512 readout integrated circuit (ROIC) of IRFPA with 15μm pixel pitch is presented in this paper. As we all know, the integrating capacitor is a key performance parameter when considering charge capacity, dynamic range and pixel area, so we adopt the effective method of 2 by 2 pixel sharing an integrating capacitor to increase charge capacity. The input unit cell architecture will contain two parallel sample and hold parts, which not only allow the FPA to be operated in full frame snapshot mode but also make the digital timing design easier. Different applications need more matching input unit circuits. Because the area of 2x2 pixel is 30μm², an input stage based on direct injection (DI) which has medium injection ratio and small layout area is proved to be suitable for middle wave (MW) while BDI with single stage cascode amplifier of 45.6dB for long wave (LW). By adopting the 0.35μm 2P4M mixed signal process, the circuit architecture can make the total effective charge capacity of 4Me⁻ per pixel with 2V output range. According to the simulation results, this circuit works well under 5V power supply and achieves less than 0.1% nonlinearity.

9275-57, Session 5

Terahertz vibrational spectroscopy of hydrogen bonds and higher-order conformation of macromolecules (*Invited Paper*)

Hiromichi Hoshina, Hal Suzuki, RIKEN (Japan); Shigeki Yamamoto, Osaka Univ. (Japan); Yukihiro Ozaki, Kansai Gakuin Univ. (Japan); Setsuko Yajima, Wakayama Univ. (Japan); Chiko Otani, RIKEN (Japan)

Spectroscopy in the terahertz (THz) frequency region has become easier with the recent development of the terahertz time-domain spectroscopy (THz-TDS) technique. Low frequency vibrational peaks observed in THz spectra show information about intermolecular structure rather than intramolecular structure. THz spectroscopy will become a powerful tool for monitoring higher order conformations of large molecules.

Recently, we have measured the THz spectra of poly(3-hydroxybutyrate) (PHB) and found clear differences between the spectrum of amorphous PHB and that of crystalline PHB. The THz polarization spectra are measured for a stretched PHB sample and the directions of the vibrational transition moments are determined. To investigate low frequency vibrational modes more thoroughly, low-frequency Raman spectra are also measured for crystalline PHB. The observed vibrational modes in both THz and Raman spectra were successfully assigned by a quantum mechanical simulation of spectra with the Cartesian coordinate tensor transfer method, which can provide realistic spectra of the PHB by considering the intermolecular interactions among polymer chains.

On the basis of these results, the structural change in PHB has been studied. The isothermal crystallization of PHB was monitored with the help of THz absorption spectra. The observed spectra clearly show the crystal growth, and the crystallization rate by Avrami's model. The isothermal crystallization spectra are analyzed using two-dimensional correlation spectroscopy. By using the synchronous and asynchronous data plots, the correlation between the absorption peaks and the temporal order of the changes in spectral intensity is determined.

We have also observed the THz absorption spectra of polyamides. Spectra of Nylon6, Nylon6/6, Nylon12, Nylon11 were measured and compared with the X-ray diffraction patterns. A peak at 3 THz was commonly observed in the spectra of all nylons and assigned as the characteristic vibrational mode of NH...OC hydrogen bonds. The other peak at 6.6 THz was observed only in the spectra of nylons in α crystal form. Using this peak, Brill transition of Nylon-6, in which α form changes into other crystal structure, was monitored in the temperature dependent spectra. The drastic change of the absorption intensity was observed at the Brill transition temperature.

THz absorption spectroscopy works powerfully not only for polymers but also for other soft materials. Spectra of organogels were measured and show vibrational peaks due to the N-H...O=C hydrogen bond of gel-network. Temperature-dependent spectroscopy showed a drastic spectral change at the sol-gel transition temperature. The change in THz vibrational frequency is indicative of the structural collapse of the hydrogen-bonded fibrous architecture in the sol phase.

- [1] Hiromichi Hoshina, et al. IEEE Transactions on Terahertz Science and Technology, 3(3), pp. 248-258 (2013)
- [2] Hal Suzuki, et al. Chemical Physics Letters, 575, pp. 36-39 (2013)
- [3] Shigeki Yamamoto, et al. The Journal of Physical Chemistry B, 117, pp.2180-2187 (2013)
- [4] Hiromichi Hoshina, et al. Chem. Phys. Lett., 608, 173 (2014)

9275-58, Session 5

Two-dimensional metamaterials made of TiO₂ spheres in the terahertz region

(Invited Paper)

Masanori Hangyo, Keisuke Takano, Osaka Univ. (Japan);
Fumiaki Miyamaru, Shinshu Univ. (Japan); Riad Yahiaoui,
XLIM, CNRS, Univ. de Limoges (France); Michael I.
Bakunov, N.I. Lobachevsky State Univ. of Nizhni Novgorod
(Russian Federation); Hiroshi Miyazaki, Tohoku Univ.
(Japan)

Recently, metamaterials made of dielectrics attract much attention from microwave to visible regions. Subwavelength particles of dielectrics show Mie resonances and negative permeability is realized at some resonance frequencies. For realizing negative permeability, very high permittivity and low loss are needed for dielectric materials. In the microwave region, it is easy, but in the THz region, it is rather difficult because the dielectric loss is high for most dielectric materials. We proposed to use TiO₂ to fabricate metamaterials in the terahertz region. The real and imaginary parts of the permittivity of ceramic TiO₂ is more than 100 and about 1, respectively, in the terahertz region. We fabricated a two-dimensional array of TiO₂ cube by ceramic process and demonstrated negative permittivity at around lowest Mie resonance frequency by the THz-TDS. To obtain negative refractive index (double negative), we combined the negative permittivity of metal mesh and the negative permeability of the TiO₂ sphere array. By a simple method, we fabricated two-dimensional composite metamaterial of the metal mesh and TiO₂ sphere array. The transmission spectra indicate the realization of the negative index band. Further, we demonstrated that a TiO₂ array on a silver substrate works as a nearly perfect absorber at around Mie resonance frequencies. Finally, we discuss the effect of the shape of the dielectric particle on Mie resonance characteristics.

Thursday - Saturday 9 -11 October 2014

Part of Proceedings of SPIE Vol. 9276 Optical Metrology and Inspection for Industrial Applications III

9276-1, Session 1

Phase retrieval for optical metrology (Invited Paper)

Giancarlo Pedrini, Ahmad Faridian, Wolfgang Osten, Institut für Technische Optik (Germany)

Digital holography is a technique which has proved to be convenient to retrieve the phase of a wave front. In the first part of the presentation, the principle of digital holography is explained and applications are shown. We will see how time resolved digital holography can be used for the measurement of deformation of microelectromechanical systems (MEMS) and discuss methods for improving the spatial resolution by illuminating the sample with structured light or using short wavelength. Furthermore, we will show how digital holography may be used for the reconstruction of objects obscured by a strong diffuser or a reflective opaque surface. Traditionally, the concept of holography is associated with the recording of the 3D information of objects illuminated by coherent light but holograms of incoherent illuminated or self-emitting objects may be recorded as well.

One possible drawback of digital holography is the use of the reference beam which entails additional optical elements and a tedious and sometimes cumbersome process of alignment optimization. Methods which do not use a reference offer a simple experimental setup and are an alternative to digital holography. In the second part of the presentation, we discuss methods to retrieve the phase of a wavefront without using a reference and their applications, in the investigation of microscopical objects.

9276-3, Session 1

Pixel correspondence calibration method of a 2CCD camera based on absolute phase calculation

Zonghua Zhang, Guoquan Zheng, Shujun Huang, Hebei Univ. of Technology (China)

In recent years, with the development of optical components, optical three-dimensional measurement technology continues to mature. Industrial inspection, real-time monitoring and many other applications put forward higher requirements for measurement speed and texture capturing [1-2]. Due to the advantages of fast, high precision, insensitive to ambient light and color texture [3], infrared structured light measurement method has been gradually paid more attention and opened up ideas of optical measurement techniques. The existing methods used two image sensors to capture information from infrared and visible light channels simultaneously [4], so coordinate transformation between the two cameras is needed to build 3D texturing representation. Most recently, we present a novel method to simultaneously obtain 3D shape and color texture of moving objects by using a 2CCD camera [5]. However, some initial experiments show that the pixels are not aligned between the IR CCD sensor and the visible CCD sensor.

This paper presents a novel calibration method to build up pixel correspondence between the IR CCD sensor and the visible CCD sensor of a 2CCD camera by using absolute phase calculation. Vertical and horizontal sinusoidal fringe patterns are projected onto an accurate white surface through the visible and infrared channels of a DLP projector. The visible and infrared fringe patterns are captured by the IR sensor and visible sensor respectively. Absolute phase of each pixel at IR and visible

channels is calculated by using the optimum three-fringe number selection method [6]. The precise pixel relationship between the two channels can be determined from the obtained absolute phase data. Experimental results show the effectiveness and validity of the proposed calibration method. Due to using continuous phase information, this method can accurately give pixel-to-pixel correspondence.

9276-4, Session 1

Matching method of the vision image captured by the Lunar Rover exploring on lunar surface

Lichun Li, Jianliang Zhou, Jun Sun, Desheng Shang, Wei Zhang, Cheng Yang, Beijing Aerospace Control Ctr. (China)

Facing the lunar surface survey of the Lunar Exploring Engineering, the paper summarizes the environment sensing technology based on vision image. For the image matching is the most important step in the process of the lunar exploring images, the accuracy and speed of the matching method is the key problem of the lunar exploring, which play an important role in the rover auto navigating and tele-operating. To conquer difficult problem that there are significant illumination variation of the imaging, lack of image texture, and non-uniform distribution of the image texture, the huge change of the disparity for the prominent target in the scene, in the image process Engineering, the image matching method is proposed which divided the whole image into $N \times N$ regions, and each region employs the Forstner algorithm to extract features by a special parameters? by which the semi-uniform distribution features of whole image and avoiding of the features gathering is achieved. According to the semi-uniform distribution features, the Sift and Least Square Matching method are used to realize accurate image matching. Guided by the matched features of the first step, the locale plane is detected and is used to restrict dense image registering. The matching experiments of simulating images and real images show that the method is effective to deal with the image captured by the lunar exploring rover, that has large variation of illumination and lacking of image texture. The robustness and high accuracy of the method is also proved. The method satisfied the request of the lunar surface exploring.

9276-5, Session 1

Analysis and comparison of angle measurement error compensation methods

Dabao Lao, WeiHu Zhou, Dong Shi, Academy of Opto-Electronics (China)

Angle measurement is a basic factor of coordinate measuring instruments such as laser tracker. There are two approaches to improve angle measuring accuracy. The first method is improving hardware performance, for example, enhancing grating resolution and axis precision, due to which, the size of angle measuring sensor will be bigger, and the cost more expensive. The second method is error compensation in software, by which complicated hardware and high cost are unnecessary to improve angle measuring accuracy. Various angle measuring error compensation methods are compared sufficiently, among which Polynomial Fitting, Cubic Spline and Harmonic Analysis are implemented. The issue of solving nonlinear equations in Harmonic Analysis

error compensation method is analyzed, Least Squares method and Genetic algorithm are adopted separately to solve the equations. In last, on the basis of turntable calibration by high precision autocollimator combined with polyhedron, angle measuring errors are obtained to practice the three methods. Before compensation, the angle error is ± 1.21 arcsecond. After compensation by the three methods of polynomial fitting, cubic spline and harmonic analysis, the error is reduced to ± 0.63 arcsecond, ± 0.59 arcsecond, ± 0.45 arcsecond, The results prove theoretical analysis and compare of the compensation methods.

9276-9, Session 1

Single-shot three-dimensional shape measurement of specular surfaces by orthogonal color fringe pattern reflection technique

Yuxiang Wu, Huimin Yue, Yong Liu, Univ. of Electronic Science and Technology of China (China)

A convenient method based on fringe reflection technique with a single color fringe pattern is presented in this paper for fast or dynamic measurements. A color screen and a color CCD camera are required in the system. The orthogonal color fringe pattern, which is composed with a horizontal fringe pattern in the red channel and a vertical fringe pattern in the blue channel, is displayed by the screen. The CCD camera captures the distorted color fringe pattern via the tested specular surface. The horizontal and vertical fringe patterns will be distinguished directly once the composite color fringe pattern is read by the software like MATLAB. After we get the phase of the horizontal and vertical fringe patterns by Fourier transform profilometry, the two directions slope distributions of the tested specular surface can be acquired by the slope-phase relation of fringe reflection technique, and the shape can be reconstructed by the intergral of the slope. Therefore, the whole shape measurement can be completed by a single fringe pattern. Complexity and accuracy comparasions of the proposed method and the existed method are given. The presented method is proved to have a good performance by simulations and experiments.

9276-6, Session 2

Development of linear LED projector for high-speed and wide-range 3D shape measurement (*Invited Paper*)

Motoharu Fujigaki, Toshimasa Sakaguchi, Yorinobu Murata, Wakayama Univ. (Japan)

Non-contact shape measurement method is important for various fields. Compact 3D shape measurement equipment is also required. A shape measurement by a phase shifting method can measure the shape with high spatial resolution because the coordinates can be obtained pixel by pixel.

A key-device to develop compact equipment is a grating projector. Authors developed a linear LED projector and proposed a light source stepping method (LSSM) using the linear LED projector. The shape measurement equipment can be produced with low-cost and compact without any phase-shifting mechanical systems by using this method. Also it enables us to measure 3D shape in very short time by switching the light sources quickly. A phase unwrapping method is necessary to widen the measurement range. A general phase unwrapping method with difference grating pitches is often used. It is one of a simple phase unwrapping method.

In this paper, a grating projector for high-speed 3D shape measurement with phase unwrapping is developed. This

projector can switch two pitches electrically. Therefore, it can be applied to high-speed and wide-range 3D shape measurement. The structure of the projector and the experimental result of the wide-range shape measurement using the projector are shown.

9276-7, Session 2

A high-reflective surface measurement method based on conoscopic holography technology

Xu Cheng, ZhongWei Li, Yusheng Shi, HengShuang Zhao, Huazhong Univ. of Science and Technology (China)

Measuring high-reflective surfaces using optical method is always a big challenging problem. This paper presents a high-reflective surface measurement method based on conoscopic holography technology using a 4D motion platform equipped with a conoscopic holography optical probe. There are two key problems needed to solve before the automate scan of the complex shape surface: the coordinate calibration and the path planning. To improve the calibration efficiency and accuracy, the coordinate calibration is divided into two parts: the rough calibration based on the SVD-based transformation estimation algorithm and the accurate calibration based on the iterative closest point algorithm. For the path planning, we take use of the fast scanning speed of the optical probe to ensure the density of the measured point cloud. Hence the path planning consists of two aspects including: the path points generation based on the local curvature, the path points verification taking account of the lens depth of the filed to ensure that the measured surface is in the scope right. In addition, by scanning the objects having high-reflective surface, such as the metal blades, coins and other work-pieces, the effectiveness of the measurement method has been verificated.

9276-8, Session 2

Three-dimensional reconstruction of specular reflecting technical surfaces using structured light microscopy

Johannes Kettel, Claas Müller, Univ. of Freiburg (Germany); Holger Reinecke, University of Freiburg, Department of Microsystems Engineering (IMTEK) (Germany)

In computer assisted quality control the three-dimensional reconstruction of technical surfaces is playing an ever more important role. Due to the demand on high measurement accuracy and data acquisition rates, structured light optical microscopy has become a valuable solution for the three-dimensional measurement of technical surfaces with high vertical and lateral resolution. However, the three-dimensional reconstruction of specular reflecting technical surfaces with very low surface-roughness and local slopes still remains a challenge to optical measurement principles. Furthermore the high data acquisition rates of current optical measurement systems depend on highly complex and expensive scanning-techniques making them impractical for inline quality control.

In this paper we present a novel measurement principle based on a multi-pinhole structured light solution without moving parts which enables the three-dimensional reconstruction of specular and diffuse reflecting technical surfaces. This measurement principle is based on multiple and parallel processed point-measurements. These point measurements are realized by spatially locating and analyzing the resulting Point Spread Function (PSF) in parallel for each point measurement. Analysis of the PSF is realized by pattern recognition and model-fitting algorithms accelerated by current Graphics-Processing-Unit (GPU) hardware to reach suitable measurement rates. Using the

example of optical surfaces with very low surface-roughness we demonstrate the three-dimensional reconstruction of these surfaces by applying our measurement principle. Thereby we show that the resulting high measurement accuracy extends the current state of the art towards cost-efficient three-dimensional surface reconstruction suitable for inline quality control.

9276-10, Session 2

Optimized design of a TOF laser range finder based on time-correlated single-photon counting

Huanqin Wang, Yixin Yang, Zhe Huang, YangYang Cao, Institute of Intelligent Machines (China); Huaqiao Gui, Anhui Institute of Optics and Fine Mechanics (China)

A time-of-flight (TOF) laser range finder based on time-correlated single photon counting (TCSPC) has been developed. By using a Geiger-mode avalanche photodiode (G-APD) with the ability of detecting single-photon events and Time-to-Digital Converter (TDC) with picosecond resolution, a good linearity with 4.5 cm range resolution can be achieved in the range of 1-10 m. This paper highlights a significant advance in improving the key parameters of this system, including the range resolution and measurement dynamic range. In our experiments, it was found that both of the range resolution and the measurement dynamic range were limited by the signal to noise rate (SNR) and the inherent jitter of system. For the long-range distance measurement, the range resolution of system is mainly limited by the SNR of system. However, the range resolution of system cannot be improved infinitely by increasing the SNR of system, since the main influence factor of the range resolution has been turned into the inherent jitter of system when the SNR of system is high enough, especially for short-range distance measurement. Taking all of these factors into account, some optimized designs have been proposed to improve the range resolution and measurement dynamic range simultaneously. By contrast experiments, we found that the main inherent jitter of system derived from the system clock source and at least 200 ps jitter, while the total jitter of system is about 800 ps, can be reduced by using a high-steady crystal oscillating sources with low jitter instead of the conventional DDS based signal source. For the analysis means of echo signal, though the Cross-Correlation algorithm is a popular proposed analysis method for TCSPC based TOF range finder, we found that, for the short range measurement with high SNR, the Gaussian fitting algorithm has been demonstrated to be more effective than Cross-Correlation algorithm in improving the range resolution, since the inherent jitter of system obeys Gaussian distribution. Besides, some other optimized designs, including adopting a telephoto lens with small view angle before detector, choosing some proper filters with narrow FWHM in receiver, etc, have also been adopted to improve the range resolution of system by improving the SNR of system. The final experiment results show that, after all of these optimization designs, the range resolution of system is better than 3 cm and the measurement dynamic range is enlarged to 40 m when the sampling time is as short as 10 ms, which is sufficient for many applications of 3D object recognition, computer vision, reverse engineering and virtual reality.

9276-11, Session 2

Development of inner profile measurement probe for pipes, tubes, and holes: case examples and additional topics (Invited Paper)

Toru Yoshizawa, NPO 3D Associates (Japan); Toshitaka

Wakayama, Saitama Medical Univ. (Japan); Masayuki Yamamoto, NPO 3D Associates (Japan); Kizuku Machi, Saitama Medical Univ. (Japan)

We have been involved in developing probes for inner profile measurement of pipes, tubes and holes which may be large or small. Request for inner profile and/or diameter measurement of pipes and pipe-like objects with holes are becoming more and more strong, and especially necessity for measuring smaller inner diameter is intensely strong, that is, probes with smaller outer diameter are required to meet requirement from various fields such as mechanical engineering, automobile and aircraft industry and civil engineering. We have proposed measurement method that incorporates a ring beam device with a laser diode (LD) and a cone mirror inside. Disk-like beam from the ring beam device gives an inner cross-section of the objective. However, recent request for measuring smaller and smaller inner diameter is very large, and a conventional probe consisting of glass or plastic tube with such devices as a CCD camera, a cone mirror and LD built-in proved too large to realize such smaller diameter as smaller than 5mm. Hence we tried to utilize optical fibers. Up to now, a probe with the size of 5mm in diameter is under trial. As far as we checked the inner surfaces of smaller holes under 5mm in diameter, endoscopes and/or borescopes have been mainly used. However these are not available for capturing inner profiles numerically. At this stage of development, we are applying the fiber ring beam device in combination with a rigid borescope to attain 5mm-size probe. In addition, we are aiming to realize such a small size probe as 3mm in diameter.

9276-12, Session 3

Optimizing binary dithering patterns to improve phase quality (Invited Paper)

Junfei Dai, Zhejiang Univ. (China); Chen Gong, Song Zhang, Iowa State Univ. (United States)

Our recently research demonstrated that the binary defocusing technique with dithered patterns has numerous merits over squared binary defocusing method or pulse width modulation method. However, because the dithering methods developed printing field are generic to arbitrary images, they usually did not consider the unique structures of the images (e.g., sinusoidal structures for our case). Therefore, directly applying those dithering algorithms may not generate the highest possible phase quality. In our research, we have developed several different optimization algorithms that successfully improved phase quality. In general, the optimization are either occur in the phase domain or the intensity domain. Our prior research found that the optimization in intensity domain seems provide better results than that in the phase domain if a three-step phase-shifting algorithm is used; whilst they tends to produce similar quality of phase if a four step phase-shifting algorithm. However, our prior research was performed under different context, and there is no direct comparison. This research will thoroughly compare the influences of phase-shifting algorithms on the resultant phase quality. Specifically, we perform the same number of iterations for optimization, the same size of optimization patches, and start with the same patterns. The variables are optimization domain (i.e., phase versus intensity); and the step number for a phase-shifting algorithm (e.g. three step, four step, and six step). We will firstly perform all comparisons through simulation, then verify the simulation results with experiments, and finally provide some guidelines on the selection of optimization strategies.

9276-13, Session 3

A hand-held high-resolution 3D shape measurement system using structured and unstructured illumination

Kai Zhong, Huazhong Univ of Science and Technology (China); ZhongWei Li, Huazhong Univ. of Science and Technology (China); Xiaohui Zhou, Wuhan Univ. (China); Yusheng Shi, Congjun Wang, Huazhong Univ. of Science and Technology (China)

Structured light illumination has been extensively used in stereo vision systems due to its achievement in high-accuracy. Among the codification strategies of structured light, sinusoidal fringe pattern for codification permits pixel-level spatial resolution 3D shape measurement by phase-shifting technology. However, in order to measure arbitrary shape surfaces, many more images should be captured to allow wrapping the phase pixel by pixel, which is undesirable for fast 3D measurement. At present, the hand-held measurement systems are in great demand due to their high-efficiency. Besides the lightweight design of hardware, the key to realize hand-held 3D scanning is finishing the measurement in a very short time. To address on this issue, this paper presents a fast 3D shape acquisition method by projecting structured and unstructured pattern. The structured patterns consist of three-step phase-shifting, sinusoidal fringe patterns, and the phase can be determined reliably by phase-shifting algorithm. Multi-view constraint constructed by one projector and two cameras is used to build the correspondence of stereo views of cameras. In order to remove the correspondence ambiguity caused by multiple fringe number, an unstructured pattern using random monochrome speckle is employed to reject wrong candidates and promises a correct 3D result. So only four images per camera can be used to reconstruct 3D result, which is very suitable for hand-held 3D shape measurement. Moreover, parallel computing technology can be used to speed up the proposed method to achieve real-time processing. Finally the experiments using developed hand-held 3D measurement system verify the performance of the proposed method.

9276-14, Session 3

Rapid three-dimensional optical metrology with single-color structured light coding map

Haihua Cui, Ning Dai, Xiaosheng Cheng, Jiangqiang Che, Nanjing Univ. of Aeronautics and Astronautics (China)

This paper presents a novel stereo-code-based color three-dimensional(3D) shape measurement that only require one colorful phase coding map. Phase fringe pattern is encoded based on RGB model and color visual grade. There are 8 types of colors used for encoding the sinusoidal fringe image. There is a big visual grade between each two adjacent stripes for easy distinguish. After the elimination of the background color of object surface with Caspi's color calibration method, the fringe boundary is recognized with adaptive color threshold algorithm, the adjacent different color stripes are encoded for initial coarse stereo matching. The coarse matching provides a fast correspondence between images. The wrapped phase map is retrieved through Fourier transform method and used for accurate sub-pixel stereo matching. The local phase matching has a robust resistance to noise, even if the acquired wrapped phase has a poor quality with the Fourier transform. Experiments are performed to demonstrate that the proposed method could achieve high-quality 3D measurement even with extremely low-quality fringe patterns caused by bright color. This proposed method has three characteristics: (1) acquire good measurement result of colorful objects with color calibration; (2) obtain a

robust stereo-code based on recognition of colorful boundary; and (3) finish superfast 3D measurement with only one coding map captured. Experiments demonstrated that the proposed method is suitable for generating high-speed measurement of moving objects with a single stripe pattern.

9276-15, Session 3

Polarization scattering methods applied in particle analyzing

Li Da, Nan Zeng, Hui Ma, Graduate School at Shenzhen, Tsinghua Univ. (China)

The efficient particle measurement methods are very important for the assessment of ambient air quality. Compared with other methods, the light scattering method has the advantages of non-destructive and real time detection, and has been used in the detection and analysis of particle composition and concentration. Different from non-polarized light scattering detection, polarized light scattering is suitable for the measurement of fine particles, such as PM1 and PM2.5. In this paper, we establish a three-component model to describe three typical particle elements in atmospheric suspended matters, and also set several pollution state changes according to some reported real measured data. By our primary polarization simulation under weak scattering approximation, we analyze Mueller matrix elements fluctuation with the different changes of particle concentration and distribution, and then extract two characteristic elements to follow the status particle composition. The results imply the potential of the backscattered polarization characterization to distinguish and evaluate the parameter variation in an atmospheric particulate model, and also show the possible sensitivity higher than the non-polarization characteristic.

9276-16, Session 3

Compact camera for 3D position registration of cancer in radiation treatment

Toshitaka Wakayama, Saitama Medical Univ. (Japan); Yoshihisa Kamakura, NPO 3D Associates (Japan); Kazumasa Nakamura, Kyushu Univ. (Japan); Toru Yoshizawa, NPO 3D Associates (Japan)

Radiation treatments have been attracted many interests as one of revolutionary cancer therapies. Today, it is possible to treat cancers without any surgical operations. In fact, the radiation treatments technology is now available to radical cure cancers inside the brain, lungs and so on. In the fields of the radiation treatments, it is important to registrate the 3D position of the cancer inside the body precisely and instantaneously. Until now, the x-ray stereographic projections and the infrared guided systems have been employed for the registrations. However, these registration techniques have some problems such as the exposure due to x-ray and the lowness of the 3D registrations for the infrared. To overcome this drawback, we aim at developing a compact camera for 3D position registrations. In this trial, we have applied three-dimensional shape measurement technology based on the fringe pattern projection. In 2008, our group developed a high-speed pattern projector for three-dimensional shape measurement using a laser diode and a single MEMS mirror. The spatiotemporal conversion technique was introduced to our projection system. The point beam from the laser diode is transformed into a line beam after passing through a cylindrical lens. Then, the line beam is two-dimensionally scanned on the sample surface. When the output of laser beam is sinusoidally controlled, sinusoidal fringe patterns are formed on the sample. If the initial phase of the input signals applied to the laser diode

is adjusted, it can achieve phase shifting technique. In our experiment, we employed a projector we proposed and a CCD camera, and we show some experimental results for the 3D registrations.

9276-17, Session 3

Dynamic measurement of Stokes parameters and birefringence mapping by full-Stokes polarization camera (Invited Paper)

Yukitoshi Otani, Shuhei Shibata, Utsunomiya Univ. (Japan)

Polarization science and technology have become an important area in the field of optomechatronics, especially in display technology, optical data storage, semiconductor technology, nano-material research, and biomedical technology. Until now, a two-dimensional birefringence measurement have been proposed by a polarization camera whose adjacent 4 pixels are aligned to 0, 45, 90 and 135° of azimuthal direction of linear micro-polarizer. Although it works as some as rotating linear polarizer, a snap shot image for 4-step phase shifting is possible to provide technique after divided pixels up same azimuthal direction of linear micro-polarizer. However, it is impossible to measure s3 term of Stokes parameters. In this paper, a real-time full-Stokes polarimeter by a polarization camera and a birefringence mapping are proposed by a polarization camera. It is not only a real-time measurement of Stokes parameters but also a real-time birefringence mapping with retarder calibration simultaneously.

9276-18, Session 4

Real-time scanner error correction in white-light interferometer (Invited Paper)

Dong Chen, Bruker Nano Inc. (United States); Joanna Schmit, Matthew J. Novak, Bruker AXS, Inc. (United States)

White light interferometers (WLI) have been widely used in many areas of surface measurements and characterizations for decades. It provides non-contact, fast, and full-field surface 3D measurements with vertical resolution in sub-nanometer range. Its applications include measurements of step height, surface roughness, films thickness, narrow trench and via and so on. However, the accuracy of the measurement is sensitive to scanner linearity where uniform constant steps over the scan range are required. Any scanner nonlinearity will result in measurement errors. This paper describes a real-time correction method for correcting scanner error in WLI measurement. It uses a reference position measurement device (PMD) to measure the actual scanner positions at each scan step. These measured scanner positions are then used to correct the measurement errors caused by the scanner nonlinearity in real-time. The correction is applied in both the phase-shift and coherent envelope signals simultaneously, and random scanner position errors can also be effectively suppressed

9276-19, Session 4

A robust automatic registration method for hand-held structured light 3D scanner

Guomin Zhan, Mengqi Wu, Kai Zhong, ZhongWei Li, Yusheng Shi, Huazhong Univ. of Science and Technology (China)

Current hand-held 3D(three-dimensional) scanners has become the development direction of 3D measurement. In case of the single measurement range size, the sensor-tracking devices or surface markers are need to realize multiple view alignment, thus limiting their functionality. For this, we propose an efficient fast registration methods based on both texture and geometry which can bring in additional information and compensate for ambiguities in the other cues. Together, we can use rotation-invariant geometric or photometric feature descriptors to extract faithful corresponding points for matching without sensor-tracking devices or surface markers. Meanwhile, range data alignment based on photometric properties is performed better using a RANSAC algorithm to rule out mismatching. Experimental results with real objects indicate the effectiveness of the proposed approach. We have applied this method to hand-held structured light 3D scanner.It realizes a single view 3D measurement within 0.12S and Real-time global registration.

9276-20, Session 4

System implementation of self-mixing interferometry technique-based measurement on Young's modulus

Ke Lin, Yanguang Yu, Zhenghao Liu, Jiangtao Xi, Huijun Li, Univ. of Wollongong (Australia); Cuiling Liu, Beijing Technology and Business Univ. (China)

Young's modulus (denoted by E) is an intrinsic and valuable quantity for appropriate estimation of material performance. E can be obtained from the resonant frequency from the vibration of the tested material sample excited by the external forces. In this paper, we present a system design for determining the parameter by using an optical feedback self-mixing interferometry (OFSMI) system. An OFSMI system consists of a laser diode (LD), a micro-lens and an external target. The material sample to be tested is used as the external target. The vibration of the sample causes the variation of the length of the external cavity, and then causes a modulated laser power of the LD. The modulation contains the vibration information of the tested samples. The OFSMI system can achieve high measurement accuracy with an extremely simple and inexpensive set-up, thus can be thought as a good candidate for the evaluation of material properties. The system design in this work includes the mechanical part for holding and exciting the tested samples, the optical part for picking up the vibration information from the samples and the system modeling for retrieving the two parameters. In order to accurately determinate E, the exclusive supporting system is used for holding the material sample of specific dimension. The complex waveform of the LD output power is studied and simulated by using our proposed system model. The proposed method is verified by simulation and experiments, and satisfied accuracy of the experiments is achieved.

9276-21, Session 4

Research on high-accuracy two-dimensional digital image correlation hardware measurement systems used in the engineering practice

Chen Guang, Ding Ke Qin, China Special Equipment Inspection and Research Institute (China); Qibo Feng, Beijing Jiaotong Univ. (China)

Digital image correlation (DIC) method is a rapid development of photomechanics technology. The basic principle of the method is calculated the correlation between before and after deformation

of the specimen surface speckle images, which is used to determine displacement and deformation. DIC measurement system includes hardware and software system. The former is the speckle image acquisition system, the latter are speckle image analysis algorithm and implementation procedures. Because the software analysis algorithm can achieve sub-pixel accuracy or even more, most of scholars have focused on the speckle image analysis algorithms. The system performance caused by the composition of hardware system has been less introduced. The hardware system mainly included the camera, lenses, lighting and other components. If hardware system is not perfect and stable, it will bring hundreds or even thousands of micro strain measurement error. These unfavorable factors make 2D-DIC inaccurate in small deformation tests. To some extent, it limits the application of 2D-DIC in the engineering practice. This paper analyzed that the various components of DIC hardware system impacted on the system performance. It was given that how to reasonably select the various components in the typical cases, as well as involved that the selection of 2D-DIC measurement system is applied to the actual engineering measurements in high temperature environment. These can provide support that 2D-DIC measurement system is better applied to the engineering practice.

9276-22, Session 4

The art of specifying surface quality (Invited Paper)

John Stover, The Scatter Works Inc. (United States);
Sen Han, Univ. of Shanghai for Science and Technology
(China)

If you open a catalog to buy an optic its surface quality will likely be given by a scratch/dig specification. This is useful information and low scratch/dig numbers usually mean a lower rms roughness and lower scatter, but you cannot find the rms roughness or make estimates of scatter levels from scratch/dig. If you measure a surface with a profilometer you can get bandwidth limited values of the rms roughness and the surface power spectral density function, but this information is often limited to spatial frequencies below about $0.1/\mu\text{m}$ and this is not high enough to even estimate visible scatter beyond about 5 degrees from specular. Scatter can be measured in BRDF or BTDF units, but instrumentation and measurements are expensive and change with incident angle, wavelength and polarization and cannot always be directly related to roughness statistics. This paper reviews what we know about the relationship between these various parameters and offers suggestions on how to approach application specific issues by defining and specifying surface quality.

9276-2, Session Post

A registration method based on profile matching for vegetation canopy measurement

Xudong Li, Yang Liu, Yunjiang Liao, Hongzhi Jiang, Huijie Zhao, BeiHang Univ. (China)

Measuring the three-dimensional structure of vegetation canopy is of great significance for the validation of remote sensing data and the study of vegetation radiative transfer modeling. When using laser triangulation as a measuring method, the structure of the whole vegetation canopy cannot be obtained by using only single-view measurement because of the limitation of the field of view of the measuring system. So multi-view measurement followed by a registration of the results (that is, point cloud) obtained from different views becomes an effective way for the

measuring task. Most of the existing registration methods cannot be directly applied to the vegetation canopy point cloud for different reasons: Marker-based registration may lead to leaves damage because of the need of sticking and tearing markers. Feature-based registration may not work because it is hard to extract the traditional line-features or plane-features from the vegetation canopy point cloud. This paper presents a registration method by using leaf profile matching. Firstly, segment the point cloud by using a clustering algorithm. The point cloud is divided into subsets that are corresponding to the single leaf. Then the leaf profile of every single leaf is extracted from the point cloud and fitted with splines. Finally, by calculating and matching the parameters of the splines such as curvature and torsion, the profile features of the same leaf in different views are registered, thus the registration of multi-view point cloud is achieved. The experiments on measured leaves point cloud are presented to show the feasibility of the proposed method. The registration method proposed can be applied not only to the vegetation canopy point cloud registration; it can also be applied to other kinds of point cloud registration.

9276-45, Session Post

An updated equation for the refractive index of air

Wenchen Li, Xiao Zuo Dai, Ning Dai, Shanghai Institute of
Technical Physics (China)

Laser has been widely applied in spectroscopic and metrological measurement. High-precision laser measurement is affected by the refractive index of air. In order to apply the algorithm in some situations which need a low calculation complexity and high-precision algorithm, the algorithm of the refractive index of Ruedger was updated. As the error of Ruedger's algorithm mainly comes from the concentration of carbon dioxide, wavelength of laser, temperature, humidity, here we will do some revision about these factors in the algorithm. In the most recent decades, the definition of standard air is redefined in this paper because of the average concentration of carbon dioxide in the atmosphere has been changed. And the concentration of carbon dioxide in the air is not constant, so the effect of carbon dioxide on the refractive index of air is taken into the updated algorithm. So the updated algorithm adapts to the real atmosphere well. The effects of dry air and humid air on the algorithm are also corrected, so the value of updated algorithm is much closer to that of the reference algorithm. At last, the performance of the updated algorithm is analyzed. The performance of the updated algorithm is compared to that of the reference algorithm and the real measured data, the results of the comparison shows that the performance of the algorithm has been improved after correction. Comparing to the reference algorithm, the performance of the updated algorithm is relatively poorer, but the target of little changed calculation complexity and greatly improved performance of the updated algorithm is achieved. The updated algorithm can be well applied in some specific occasions.

9276-46, Session Post

Correction of refraction index based on adjacent pulse repetition interval lengths

Dong Wei, Masato Aketagawa, Nagaoka Univ. of
Technology (Japan)

Length measurement is the infrastructure for both scientific and industrial uses. In July 2009, the national standard tool for measuring length in Japan changed from an iodine-stabilized helium-neon (He-Ne) laser to a femtosecond optical frequency comb (FOFC). How to practically perform a distant measurement that is directly linked to an FOFC length standard is the most

urgent and meaningful challenge.

Basic problems of this challenge are which parameter should be used as a ruler and how to perform length measurement. This paper is intended to give a description to the concept, the principle, and a demonstration of a new technique, called adjacent pulse repetition interval length based (APRIL-based) two-color method, which was developed for a high-accuracy length evaluation. The basic idea of this new technique was based on the analogy between the wavelength and the adjacent pulse repetition interval length. Since the wavelength-based two-color method can eliminate the inhomogeneous disturbance of effects caused by the phase refractive index, therefore the APRIL-based two-color method can eliminate the air turbulence of errors induced by the group refractive index.

In this paper, we answer three questions. The first one is why harmonic generation from an optical frequency comb has the same repetition frequency as the original frequency comb. The second one is why two-color method can eliminate the inhomogeneous disturbance of effects caused by the refractive index. The third one is how to perform APRIL-based two-color method for correction of refraction index.

A demonstration of the proposed method is presented. From the result of the preliminary experiment, it has been show the feasibility of the proposed method.

9276-47, Session Post

Accurate and automatic extrinsic calibration method for blade measurement system integrated by different optical sensors

Wantao He, Huazhong Univ. of Science and Technology (China)

Fast and precise 3D inspection system is in great demand in modern manufacturing processes. At present, the available sensors have their own pros and cons, and hardly exist an omnipotent sensor to handle the complex inspection task in an accurate and effective way. The prevailing solution is integrating multiple sensors and taking advantages of their strengths. For obtaining a holistic 3D profile, the data from different sensors should be registered into a coherent coordinate system. However, some complex shape objects own thin wall feather such as blades, the ICP registration method would become unstable. Therefore, it is very important to calibrate the extrinsic parameters of each sensor in the integrated measurement system. This paper proposed an accurate and automatic extrinsic parameter calibration method for blade measurement system integrated by different optical sensors. In this system, fringe projection sensor (FPS) and conoscopic holography sensor (CHS) is integrated into a multi-axis motion platform, and the sensors can be optimally move to any desired position at the object's surface. In order to simple the calibration process, a special calibration artifact is designed according to the characteristics of the two sensors. An automatic registration procedure based on correlation and segmentation is used to realize the artifact datasets obtaining by FPS and CHS rough alignment without any manual operation and data pro-processing, and then the Generalized Gauss-Markoff model is used to estimates the optimization transformation parameters. The experiments show the measurement result of a blade, where several sampled patches are merged into one point cloud, and it verifies the performance of the proposed method.

9276-48, Session Post

Multiple-neighborhood filtering method for building 3D information recovering

Longjia Zhang, Ye Zhang, Harbin Institute of Technology (China)

In this paper, a multiple-neighborhood filtering (MNF) method is proposed for building 3D-information recovering. Optimization of digital surface models (DSM) is the most necessary part in 3D building reconstruction. Points could not be determined in all areas mainly owing to matching failure. When correlation coefficient of a matched point is below a threshold value, this point is rejected and its height is not computed, so meaning outliers and reducing completeness of 3D-information. When we remove the outliers, 'holes' of 3D-information are appeared and lie over.

MNF mainly focuses on building rather than whole scene by other methods. Building has fewer points than whole scene and its edge is harder to recover. We need to tile the domain of a building grid into smaller chunks of different sizes. To smooth out any outliers at the edges of each chunk, MNF allows the chunks some fractional overlap, interpolating between them in the overlapped region. Then MNF composes each chunk into the whole surface. As MNF is not an interpolation, it smoothly extrapolates to recover edge of building. The resulting holes are filled with the nearest remaining measurements. We can build a gridded surface with the values at a set of nodes.

Experiments show MNF could greatly improve completeness of 3D-information. Threshold value of matching correlation coefficient will influence completeness. But no matter what the threshold is defined, completeness after optimization is stabilization around 85%. As threshold is normally set to 0.5, completeness can improve from 70.25% to 86.09%. MNF has a good robustness.

9276-49, Session Post

3D measurement for industrial from digital design and manufacturing laboratory

Changye Guo, Nanjing Univ. of Aeronautics and Astronautics (China)

No Abstract Available.

9276-50, Session Post

Analysis on how spectrum affects the test of solar cell electrical property

Dingpu Liu, Chengying Shi, China Academy of Telecommunication Research (China); Haifeng Meng, Yingwei He, National Institute of Metrology (China); Haipeng Li, Liang Xu, Fan Zhou, China Academy of Telecommunication Research (China)

Nowadays, more attentions may be paid to irradiance and temperature during the electrical performance tests of solar cell and module. But the light spectrum will also largely determine test results. During the electrical performance test, irradiance is generally traced by standard solar cell. Considering that the short circuit current (I_{sc}) is generally used in the testing process as a basis for the irradiance calibration, and the I_{sc} of reference cell consists of spectral distribution of light source and the spectral response of the cell together. So spectral mismatch should be analyzed from this two aspects. Natural light spectrum will be affected by atmospheric conditions and seasons, and artificial

solar simulator's spectrum is different in thousands of ways. Also because of the response wave band of the spectrum range is different, when using standard solar cell or pyranometer as the basis of the irradiance calibration, there should be respectively different results. Beyond that, two cells made of polycrystalline silicon with different spectral response may also lead to different results. We analyzed the deviation based on the above factors, and discussed how to reduce the spectral mismatch deviation, then increase the accuracy of the solar cell electrical performance test methods.

9276-51, Session Post

A new technique of recognition for coded targets in optical 3D measurement

Changye Guo, Xiaosheng Cheng, Haihua Cui, Ning Dai, Jinping Weng, Nanjing Univ. of Aeronautics and Astronautics (China)

A new technique for coded targets recognition in optical 3D-measurement application is proposed in this paper. Traditionally, point cloud match is based on homologous features, which is time-consuming and not reliable. For this, we paste some coded targets onto the surface of the object to be measured to improve the optimum target location and accurate correspondence among multi-source images. Circular coded targets are used, and an algorithm to automatically detect them is proposed. This algorithm extracts targets with intensive bimodal histogram features from complex background, and filters noise according to their size, shape and intensity. In addition, targets' identification is conducted out by their ring codes. We affine them around the circle inversely, set foreground and background respectively as 1 and 0 to constitute a binary number, and finally shift one bit every time to calculate a decimal one of the binary number to determine a minimum decimal number as its code. In this 3D-measurement application, we build a mutual relationship between different views containing three or more coded targets with different codes. Experiments show that it is of efficiency to obtain global surface data of an object to be measured and is robust to the projection angles and noise.

9276-52, Session Post

Binocular videogrammetric system for three-dimensional measurement in low-speed wind tunnel

Ye Zhu, Yonggang Gu, Chao Zhai, Univ. of Science and Technology of China (China)

In order to avoid the defects of contact measurement, such as limited range, complex construction and disability of 3-D parameter acquisition, we built a binocular videogrammetric system for measuring 3-D geometry parameters of wind tunnel test models, for instance, displacement, rotation angle and vibration, in low-speed wind tunnel. The system is based on the principles of close-range digital photogrammetry. As a non-contact system, it acquires parameters without interference in the experiments, and it has adjustable range and simple structure. It is worth mentioning that this is a real-time measurement system, so that it can greatly compress the experiment period, furthermore, it is also able to provide some specific experiments with parameters for online adjustment. In this system, images are acquired through two industrial digital cameras and a PCI-E image acquisition card, and they are processed in a PC. The two cameras are triggered by signals from a function signal generator, so that images of different cameras will have good temporal synchronization to ensure the accuracy of 3-D reconstruction. A two-step stereo calibration technique

using planar pattern developed by Zhengyou Zhang is used to calibrate these cameras. Results of wind tunnel test indicate that the system can provide displacement accuracy less than 0.1% and rotation angle accuracy less than 0.1 degree, besides, the vibration frequency accuracy is superior to 0.1Hz in the low-frequency range.

9276-53, Session Post

An improved bundle adjustment model and algorithm with novel block matrix partition method

Ze Min Xia, Zhongwei Li, Kai Zhong, Huazhong Univ. of Science and Technology (China)

Sparse bundle adjustment is widely applied in computer vision and photogrammetry. However, existing implementation is based on the model of n 3D points projecting onto m different camera imaging planes at m positions; the implementation can't be applied to commonly monocular, binocular or trinocular imaging systems. Because the current calibration target circle center pixel coordinates extraction methods can not achieve the desired accuracy, we will get m different intrinsic camera parameters, even if we use only one camera. To avoid the above phenomenon, a novel design and implementation of bundle adjustment algorithm is proposed in this paper. The improved bundle adjustment model presented in this paper is based on n 3D points projecting onto the same camera imaging plane at m positions, with this model we can get better optimizing result. To improve the performance of the improved algorithm, a novel sparse block matrix partition method is proposed, with which we can do less order of sparse matrix inverse and get higher computing speed. Subsequently, the effectiveness and robustness of the improved bundle adjustment algorithm is verified through both simulation and practical experiment, that we got lower reprojection error and higher reconstruction precision with the optimized calibration result of the improved bundle adjustment compared to the result of existing method. Finally, this paper analyzes the influence of calibration target circle center pixel coordinates extraction accuracy on the bundle adjustment algorithm presented in this paper and existing method with a simulation experiment, as a result, the bundle adjustment algorithm presented in this paper has a better tolerance to pixel coordinates error.

9276-54, Session Post

High-speed three-dimensional shape measurement using spatial frequency encoding and DLP projector

Yanshuai Tu, Yong Li, Hongzhen Jin, Jian Wang, Zhejiang Normal Univ. (China)

Generally, a high-speed camera is needed in high-speed three-dimensional shape measurement system based on fringe projection. High resolution and high-speed camera is expensive and requires large bandwidth for data transmission. On the other hand, high-speed projector becomes cheaper and cheaper these days. A method based on Fourier transform profilometry (FTP) is proposed. The spatial frequency encoding fringes are projected with high frame rate and deformed fringes are captured with low frame rate. Several fringes are integrated in one captured image. The directions and/or frequencies of these fringes are different. It means that the deformed fringes are encoded with different spatial frequency. These fringes are separate in spatial frequency domain. So, the phase of different fringe can be obtained by filtering the image with different filter. Then several 3D shapes are obtained from one captured image. The process of measurement

is as following. Firstly, N fringes in a loop are projected with a DLP projector. Secondly, an image is captured with a camera exposed in the loop. Thirdly, repeat step one and two to record the deformed fringes. Finally, FTP method is adopted for shape reconstruction. The experiments are carried out under the condition of N=3 to verify proposed method. During experiments, a DLP projector works at 360fps, every loop is captured by a camera running at 120fps. A motion pendulum and facial expressions are measured. The proposed method improves the speed of 3D shape measurement and reduces the cost of measurement system as well.

9276-55, Session Post

Verification and analysis of stray light in high-power laser system

PingXian Huang, Zhaofeng Cen, Xiaotong Li, Zhejiang Univ. (China)

In high-power laser system, the optical transmission element surface's residual reflection and diffraction element multistage diffraction of stray light, will increase the local temperature of the system and cause the optical element deformation, damage and wavefront distortion. They can also change the beam divergence angle, thus seriously influencing the beam quality and propagation properties and bringing damage to the components in the system. Thus using the relevant analysis software for rigorous analysis of stray light is very important work. Software reliability and the precision is the important guarantee of reliable analysis results. Although we can use the actual system operating to verify the accuracy of the results of the analysis software, it's very complicated, highly costly, also not intuitive. There is a risk of damage system, so it is necessary to establish specialized experiment system and validate the analysis result more conveniently and directly.

This article is based on the simulation and experiment by using ASAP and our software of stray light analysis to build models and analyse the focusing lens, diffractive element, combined lens, etc. Determining the ghost image's order, number, location and relative strength after the light pass through the components with the surface's reflection and Fresnel diffraction. Then the simulation is verified on the specialized experimental device. Through comparison of software simulation and actual measurement, we find out the ghost image's position and the distribution of stray light. Through continuously experiments, we find out the major source and dense area of stray light so that we can make appropriate adjustments to improve the performance of stray light. Then the reliability and precision of the model can be verified indirectly.

9276-56, Session Post

Cost-effective and full-field method for measuring vibration of loudspeaker membrane using fringe projection

Jian Wang, Yong Li, Zhiliang Zhang, Peng Gao, Zhejiang Normal Univ. (China)

The quality of reproduced sound of loudspeaker highly depends on the vibration and radiation properties of the membrane. Usually, the vibration of loudspeaker membrane is measured with scanning vibrometry, Laser Doppler Vibrometry etc. The full-field vibration can not be measured simultaneously. We proposed a cost-effective and full-field method for measuring vibration of loudspeaker using general industrial camera and fringe projection. The loudspeaker is excited by a sinusoidal signal. The fringe pattern is projected on the measured loudspeaker membrane that is dynamically deformed. Then the deformed

fringes are grabbed by a camera. A trigger generation circuit is designed to control the camera. The trigger signal sweeps in the period of the sinusoidal signal. The image acquisition process is as follows. First, calculate the sampling time interval of two images and get the first image at a point of the first cycle of the excitation signals. Second, the image is grabbed after N complete incentive periods and additional sampling time interval (N can be adjusted according to the frequency of the excitation signal). Third, repeat step 2 till get a complete cycle of loudspeaker membrane deformation. The Fourier Transform Profilometry (FTP) is adopted for shape reconstruction. The proposed method is validated with experiments. The experimental results are same as which obtained by high-speed camera. The cost of proposed measurement system is dramatically lower than that using high-speed camera.

9276-57, Session Post

Optical image encryption in phase space

Jun Liu, Quanying Wu, Univ. of Science and Technology of Suzhou (China); Guohai Situ, Shanghai Institute of Optics and Fine Mechanics (China)

The double random phase encoding system is linear, and the dependencies between plaintext and ciphertext is not complicated, with leaving a great hidden danger to the security of the encryption system. This paper is aimed at the disadvantages of the linear characteristics of classical optical encryption and implemented the optical image in phase space which based on the theory of phase space. Then, it has researched the bilinear properties of Wigner distribution function and its ambiguity function. The dimensions of the encrypted image have been increased and the key space has been expanded. By means of the computer simulation of one-dimensional signal encryption and the security analysis selected known-plaintext attack approach, the encoding technology in phase space offers higher level of security the classical scheme. It is important to the research in the field of information security.

9276-58, Session Post

Influence of both angle and position error of pentaprism on accuracy of pentaprism scanning system

Kun Xu, Univ. of Science and Technology of Suzhou (China); Sen Han, Univ. of Shanghai for Science and Technology (China); Quanying Wu, Univ. of Science and Technology of Suzhou (China); Qiyuan Zhang, Suzhou H&L Instruments LLC (China)

Pentaprism scanning system has been widely used in the surface and wavefront measurement of large aperture optical system, based on its property of beam turning of 90 degrees. But due to the manufacturing and position errors of pentaprism, the optical axis will deflect and bring error to measurement results. A good error analysis method is indispensable. In this paper, we develop a mathematical model of pentaprism containing errors of itself. For manufacturing errors, we just consider angle errors and size errors. 11 angle parameters are selected to determine angles of pentaprism, four angles in the bottom pentagon, five angles between bottom and side, two angles to determine the top face. 2 size parameters are selected to determine the size. For Position error, it can be divided into two parts: translation errors and rotation errors. 6 parameters are selected to determine position error. All these parameters are put into the model and the Monte Carlo method is used to set the random values of parameters within their tolerance range, then exact ray tracing is doing on the finished model and the optical axis deflection angle value

is calculated. After multiple ray tracings, a scatter diagram is formed statistically. By changing the value range of parameters, we get different scatter diagrams, through which we get the maximum angle of optical axis tilt, analyze the influence of each error parameter and the synergy of multiple error parameters. This work proposes an accurate and thorough approach to simulate and analyze the influence of pentaprism error on the Pentaprism scanning system, which is beneficial to the further improvement of measuring precision.

9276-59, Session Post

Optimal design of optical length in low turbidity measurement system with wavelength 1310 nm and 1550 nm

Huibin Cao, Jianguo Liu, Huaqiao Gui, Jie Wang, Anhui Institute of Optics and Fine Mechanics (China); Huanqin Wang, Institute of Intelligent Machines (China)

To meet the need of long distance transmission in low turbidity measurement system for low-loss, a new optical structure with wavelength 1310nm and 1550nm as the incident light is employed. In this research, experiments have been done for different optical length of the two wavelength light sources. The results show that: first, the transmitted light intensity has big difference under the circumstance of same concentration and optical length, though the loss has no remarkable difference transmitted in optical fiber between 1310nm and 1550nm. Second, the optimized optical length for better absorbance has been determined for 1310nm and 1550nm and it is irrelevant to the incident intensity. Third, the intensity of the two transmitted light decreases exponentially with the increase of optical length. For example, when the range of the optical length of 1310nm is 0.5mm-2mm, the transmitted intensity is about 60%-79% and the absorbance is 0.12-0.42. The transmitted intensity is about 5%-44%. When the range of the optical length of 1550nm is 0.5mm-2mm and the absorbance is still 0.12-0.42. Our experimental data provides the basis both for the optical length selection of these two light sources in water and the near-infrared spectral wavelength selection.

9276-60, Session Post

The research of filtering on images with noises of the three-mirror aperture optical system

Jun Wang, Youqing Wang, Quanying Wu, Junliu Fan, Univ. of Science and Technology of Suzhou (China)

Noise is inevitable in the imaging process of sparse aperture optical system, such as Gaussian noise, speckle noise and salt & pepper noise. The influence of above noises on the three-mirror aperture system is analyzed and compared by simulations. Median filter and mean filter are applied to deal with the images which are polluted by the above three noises. Images interfered by Gaussian noise can be distinguished to 40 lp/mm by median filter compared with 32 lp/mm by mean filter. Images polluted by speckle noise can not be handled by median filter and mean filter, because there are still large amounts of noise remaining in images after filtering. Median filter can largely eliminate the influence of salt & pepper noise on the image: images can be distinguished to 36 lp/mm in horizontal direction, and 40 lp/mm in vertical direction. Otherwise, mean filtering can remove the white salt & pepper noise easily, but do nothing for the black pepper noise. As a result, median filter is suitable for the images of the three-mirror aperture system with Gaussian noise and salt & pepper noise, while the mean filter has a quite limited applicable range.

9276-61, Session Post

Measuring the displacement of the movable guard electrode in the new vertical calculable capacitor at NIM

Jianbo Wang, Tongji Univ. (China) and National Institute of Metrology (China); Jin Qian, Zhongyou Liu, Xiuying Liu, Zhuliang Lu, Lu Huang, Cong Yin, National Institute of Metrology (China); Tongbao Li, Tongji Univ. (China)

A new type vertical calculable capacitor has been built at National Institute of Metrology (NIM) cooperated with National Measurement Institute of Australia (NMIA). The calculable capacitor is the highest accuracy equipment apparatus except the quantum voltage and the quantum resistance in the electromagnetic metrological field. In order to precisely measure the capacitance, the accurate displacement measurement of the two guard electrodes in the calculable capacitor is the key point. This paper describes the method of measuring the displacement of the Fabry-Perot cavity, which is constructed by the two guard electrodes in the calculable capacitor at NIM. One concave reflective mirror, with 5 m radius and 70% reflectivity, is on the top of the bottom fixed guards electrodes. The other planar mirror is assembled at the end of the moveable guard electrodes. This F-P interferometer employs a self-made lamb-dip stabilized He-Ne 633 nm laser to measure the displacement of the moveable guard electrodes. The internal modulation, which is used for laser stabilization, is also employed for locking the F-P interferometer. The displacement of the moveable guard electrodes is integer multiples half of the laser wavelength, when the F-P cavity is locked to the stabilized lamb-dip laser. An iodine stabilization He-Ne 633 nm laser is employed to simultaneously calibrate the wavelength of lamb-dip laser. In present phase, the uncertainty can reach 10⁻⁹ level with the displacement of 205 mm, which is estimated by the experimental results of calculable capacitor.

9276-62, Session Post

Cramer-Rao analysis of three-channel phase diverse wave-front sensing for Golay3 aperture

Junliu Fan, Jun Wang, Mengmeng Hu, Quanying Wu, Univ. of Science and Technology of Suzhou (China)

The phase diversity wavefront sensing (PDWFS) technique is a posteriori image-based wavefront sensing technique which was first presented for optical imaging by Gonsalves. As a byproduct, the aberrations of the optical system can also be derived using two images collected simultaneously whose pupil phase differs from each other in a known manner, which has been successfully implemented to the Hubble Space Telescope. Here, with the use of previous work by other authors, the Cramer-Rao lower bound (CRLB) expression for three-channel phase diversity aberration estimation problem is developed for the Golay3 sparse aperture, which is mainly aberrated by piston and tilt errors. Monte Carlo analysis of the PDWFS CRLB is used due to the dependence of CRLB on the true values of piston and tilt errors being estimated. The ensemble average of the piston and tilt errors is used to evaluate the performance of different beam splitting ratio schemes. The numerical simulation shows that compared with the traditional diverse scheme, an in-focus image plus a image with 2 rad defocus, adding the third image can result in lower MSE of piston and tilt errors which is determined by different beam splitting ratio. The results also reveal that for extended target object, the MSE value of piston and tilt errors can be orders of magnitude higher than that from a point source target.

9276-63, Session Post

Dual-frequency laser displacement and angle interferometer

Shijie Zhao, Pei Huang, Minhao Zhu, Haoyun Wei, Yan Li, Tsinghua Univ. (China)

Traditional method of laser angular interferometers based on a Michelson Interferometer or its modifications have the same principle: changing the angle displacement to an optical path difference. However, measuring the angular error of a stage travels is a dynamic process. The main trouble is lack of displacement information and need to be solved urgently. A traditional method is using two dual-frequency interferometers to get the displacement and angular. In this paper, a new kind of displacement and angle interferometer is introduced. In this interferometer, displacement and angular are measured simultaneously by special optical path. The interferometer consists of a stabilized orthogonal polarization dual-frequency laser, a monolithic prism and additional optical and electronic components. The dual-frequency laser is divided into reference light and measurement light by a beam-splitting prism. The measurement light spatially separated into horizontal polarized light and vertical polarized light by the polarization splitting prism. Changing by a fixed 45°-tilted reflector, the vertical polarized light is parallel to the horizontal polarized light. These parallel lights reflected by two cube-corner prisms at a moving target. Compared with the reference light, the displacement and angular are measured. Different from the traditional method, there is only one reference cube-corner prism in this system. Thus, the angular measurement accuracy is better. The angular accuracy of this displacement and angular interferometer is better than ± 0.25 arc sec in comparison with an autocollimator.

9276-64, Session Post

Ellipsometer for surface topography measurement of ultrathin films

Fangfang Meng, Yan Li, Xuejian Wu, Tsinghua Univ. (China)

The 2-D topography ellipsometer is a new rapid full-field imaging technique for high spatial resolution studies of thin films, which is proposed to provide reliable, real-time measurement of thickness in a manufacturing environment. This paper studied the relationship between the configurations of the ellipsometer such as (1) three/four/five-intensity-measurement techniques and (2) the azimuth angles of polarizer and compensator, with its performance in our ultra-thin films (0 to 30 nm) measurement application. The concept is based on polarizer, compensator, specimen, and analyzer combined with image capturing and processing systems. The ellipsometer illuminates the sample with light of fixed polarization and uses a rotating analyzer to measure the polarization of the reflected light. Fourier analysis of the light transmitted by the analyzer is used to obtain full-field distributions of the ellipsometric parameters, sequentially is able to calculate the thickness of a thin film in two dimensions. The number of images and an optimizing input configuration are particularly useful for measuring very thin films on silicon (0 to 30 nm). The three/four/five-intensity-measurement techniques are used and compared. The three-intensity-measurement method showed the best measurement speed, and highest experiment accuracy due to the movement of the CCD pixels with the rotation of the analyzer. The best azimuth angles of polarizer and compensator are calculated as 1° and 172° respectively, and verified by the experiment. The effect of this set of azimuth values is to make light reflected from films to be nearly circularly polarized with the thickness of a film within 0 to 30 nm, which reduced noise and enhanced measurement precision. The experimental results verified the ability and performance of

our 2-D topography ellipsometer. The errors regarding the ellipsometric parameters measurements are discussed.

9276-65, Session Post

Virtual image distance measurement for long sighting distance pilot lamp

Hui Huang, Xiangning Li, Yuqing Wang, Feng Sui, Univ. of Shanghai for Science and Technology (China)

A high requirement about the light source visual position whose measurement accuracy is greatly affected by the precision of the optical system is needed for long sighting distance pilot lamp. The structural precision of the emergent beam is low because of using light-emitting diode (LED) array as light source in addition to the big structure of pilot lamp, resulting in difficulty to position virtual image. In order to measure virtual image distance of LED array, a method is proposed based on the principle of optical measurement system for the optic that is inconvenient to inspect directly. Long focal lens is used to receive the edge rays from the optical system export. The virtual image distance is calculated on the basis of the edge-ray principle and the geometrical optics formulas. Firstly, a black board with two narrow slits is put on the surface of the lens to receive the edge rays and filter stray light. Then two symmetrical bright stripes can be seen on an observation screen located on the other side of the lens by moving the LED source and the screen. Finally, the virtual image distance could be analyzed according to two symmetrical phenomena on the observation screen. Comparing the image distance formed by the real source with the virtual source, the accuracy of the method is verified. Experimental results indicate that the measuring accuracy is within ± 1 m to LED light source whose ideal virtual image distance is about 60m. The quality of the black board and the system errors should be taken into account during the actual experiments. This method can basically meet the measuring accuracy requirement of long-range LED virtual image distance.

9276-66, Session Post

Precision judgment criteria and supplement data processing method in high-precision ranging with dual-comb lasers

Qian Zhou, Yang Li, Kai Ni, Mingfei Xu, Hao Dong, Graduate School at Shenzhen, Tsinghua Univ. (China); Guanhao Wu, Tsinghua Univ. (China)

Traditional laser ranging contains the incoherent method (time-of-flight method) and the coherent method. The time-of-flight method can realize rapid measuring but with low precision, while the incoherent method can achieve high precision but has the problem of long ranging period. The dual-comb lasers ranging method combines time-of-flight and coherent method proposed by Ian Coddington in 2009 can balance the measuring speed and precision. This method uses a pair of femtosecond frequency combs, and it can complete 5000 ranging per second at the precision of 1 μ m.

In simulation of this measuring principle based on Matlab/Simulink, it is found that the selection of repetition frequencies has great impact on the result precision, that is, only certain laser repetition frequencies can achieve the good results. This paper analyzed the reason of this phenomenon, and proposed judgment criteria in laser frequency selection based on analysis results. The sampled signals are classified into three types according to their frequencies, which are decided by the laser source repetition frequencies. When the frequency components of sampled signal are appropriate in the range of Nyquist

frequency, the error can be less than 0.1 μ m, otherwise the error can be several micrometers or larger. Two supplementary methods in actual measuring are also proposed to enhance the ranging performance to a certain degree. One is adopting low-pass filter at Nyquist frequency before sampling, and the other is remaining only proper curve part in data processing stage.

9276-67, Session Post

Novel high-speed method using gray level vector modulation for 3D shape measurement

Guiwen Lin, Shenzhen Univ. (China)

In order to satisfy the high speed characteristic of real-time measurement, a novel method using gray level vector modulation is introduced. Combining gray code with linear coding principle, new coding patterns using gray level vector method is designed and projected onto the object surface. Each pixel corresponds to the designed sequence of gray values as a feature vector. The unique gray level vector is dimensionally reduced to a resulting value which could be used as characteristic information for binocular matching. Experimental results further demonstrated the correctness and feasibility of the proposed method with fewer component patterns and less computational time.

9276-68, Session Post

A new usage of ASIFT for the range image registration

Chunyang Liu, Dong Li, Jindong Tian, Shenzhen Univ. (China)

This paper addresses the range image registration problem for views having overlapping area and which may include substantial noise. The current state of the art in range image registration is best represented by the well-known iterative closest point (ICP) algorithm and numerous variations on it. Although this method is effective in many domains, it nevertheless suffers from two key limitations:

It requires prealignment of the range surfaces to a reasonable starting point and it is not robust to outliers arising either from noise or low surface overlap. This paper proposes a new approach that avoids these problems for precision range image registration, by using a new, robust method based on ASIFT followed by ICP. Up to now, this approach has been evaluated by experiment. We define the fitness function to calculate the time for the convergence stage of ICP, because the time required is very important. ASIFT are capable of image matching even when there is fully affine variant. The novel ICP search algorithm we present following ASIFT offers much faster convergence than prior ICP methods, and ensures more precise alignments, even in the presence of significant noise, than mean squared error or other well-known robust cost functions. The paper presents thorough experimental results to show the improvements realized by this method.

9276-69, Session Post

A new geometrical model and mathematical method for three-dimensional surface reconstruction based on phase-shifting structured light technique

Suzhi Xiao, Wei Tao, Hao Yan, Hui Zhao, Shanghai Jiao

Tong Univ. (China)

A new geometrical model and mathematical method for three-dimensional surface reconstruction with phase-shifting structured light technique is proposed. First, there will be no restriction to camera and projector's relative alignment on parallelism and perpendicularity with the proposed method. In the new geometrical model, the camera and the projector are all described by a pinhole model. In order to establish the transformation relationship of the phase to (x,y,z)-coordinates, an imaginary reference plane is set up which is parallel with the projector plane. Based on the triangular relations and geometric similarity, a one-to-one mapping between the depth information and the absolute phase value at each pixel is established. The x and y coordinates are inferred from the depth z coordinate. Thus, the 3-D coordinates are expressed by three equations which include system intrinsic and extrinsic parameters. The 3-D surface is reconstructed by resolving the equations. Second, a simple two-step plane-based calibration procedure with printed checkerboard is adopted to acquire the system parameters. By this means, no calibration gauge block is needed and no precise control and alignment of the calibration plane are required. Third, a look-up-table compensation method is presented to avoid the accumulation of errors introduced in the structured light system. The experimental results demonstrate the effectiveness and accuracy of the proposed methods. The depth measurement error is less than rms 0.61mm when a flat plane moves from 410mm to 470mm away from the projector. Experiments on a gypsum ball and a head statue are performed to verify the system's capabilities of measuring complex 3-D objects.

9276-70, Session Post

An optimized FBG-based fatigue monitoring strategy on deepwater risers

Xuan Li, Peng Ren, Zhi Zhou, Jinping Ou, Dalian Univ. of Technology (China)

For the sake of the increasing demands of oil and gas essential for industrial developments, scientists as well as engineers have exerted great efforts in obtaining such natural resources deposited in the deep water. Consequently, a great number of deepwater systems have been created and put into service. Risers, which function as the channel between platform and wellhead, play a key role in oil and gas transportation. Subjected to coarse environmental conditions and uncertain loading patterns, risers would display complex dynamic behaviors which could result in severe fatigue damages. Recently, riser response is commonly measured using passive and durable Fiber Bragg Grating (FBG) strain sensors in industry safety, especially for Integrity Management (IM). However, for technique difficulties as well as economical consideration, it is impossible to execute distributed fatigue monitoring on the whole riser, which makes it essential to find out an optimized method utilizing the least number of sensors to reconstruct the global response of risers. This paper propose a method which combines H2 norms and Kalman filter to give optimal state estimation of risers based on limited FBG-based dynamic strain information. The H2 norms are used to give guideline for optimized sensor placement. Meanwhile, Kalman filter realizes the global response reconstruction of risers as well as minimize the environmental disturbance. The accuracy and efficiency of the method has been verified by a numerical case. This study provides an FBG-based early warning technique for industry application of deepwater risers in future.

9276-72, Session Post

Effects of fiber position and morphology on the far-field mode field diameter testing

Meng Ting Hu, Jinrong Tian, Yanrong Song, Li Wang, Beijing Univ. of Technology (China)

Mode field diameter is one of the most important parameters for single mode fiber, closely linked to many features of it. In experiment, we measured mode field diameter in the far-field scanning system by preparing some different fiber end morphology using the fiber cutting knife, scissors, HF acid and controlling fiber measurement position. The source is diode laser in the system with center wavelength at 1550 nm. Comparing the measurement results, we discussed the effects of fiber morphology and position on the mode field diameter testing, and presented the solution to improve the experimental precision.

9276-73, Session Post

Hyperspectral visible-near infrared imaging for the detection of waxed rice

Mantong Zhao, Univ. of Shanghai for Science and Technology (China)

Presently, unscrupulous traders in the market use the industrial wax to wax the rice, and their aim is to make the rice in the good color and luster. The industrial wax is a particularly hazardous substance. That is to say, the odorless, colorless substance is deadly when consumed over a long period of time. Visible-near infrared hyperspectral images (400-1,000 nm) can be used for the detection of the waxed rice and the non-waxed rice. This study was carried out to find effective testing methods based on the visible-near infrared imaging spectrometry to detect whether the rice was waxed or not. An imaging spectroscopy system was assembled to acquire catering images from 80 grains of waxed rice and 80 grains of non-waxed rice over visible and near infrared spectral region. Spectra of 160 grains of rice were analyzed by principal component analysis (PCA) to extract the information of hyperspectral images. PCA provides an effective compressed representation of the spectral signal of each pixel in the spectral domain. We used PCA to acquire the effective wavelengths from the spectra. Based on the effective wavelengths, the predict models were set up by using partial least squares (PLS) analysis and Fisher linear discriminant analysis (LDA). Also, compared with the PLS of 91.75% for waxed rice and 92.7% for non-waxed rice detection rate, Fisher LDA gives 100% and 96.7% detection rate. The result demonstrated that the Fisher LDA could detect the waxed rice better, while illustrating the hyperspectral imaging technique with the visible-near infrared region could be a reliable method for the waxed rice detection.

9276-74, Session Post

Soluble solids content and firmness non-destructive inspection and varieties discrimination of apples based on visible near-infrared hyperspectral imaging

Yao Zhou, Univ. of Shanghai for Science and Technology (China)

For apples, soluble solids content (SSC) and firmness are two very important internal quality attributes, which play key roles in postharvest quality classification. Visible-near infrared

imaging techniques (Vis-NIR) have effective potentials for non-detection of apples' internal qualities. In this study, Vis-NIR hyper spectral imaging will be used for the non-destructive variety discrimination and the prediction of soluble solids content (SSC) and firmness of apples. Spectral of 396 apple samples from four varieties were extracted. There were 264 samples of apples used for calibration and the left 132 samples for prediction. After collecting hyper spectral images of calibration samples, we used sugar meter and firmness tester combining with the national standard method to measure SSC and firmness reference values of each calibration samples. Then the principal component analysis (PCA) was used to extract the effective wavelengths of reflectance. The reference values of apples and effective wavelengths of reflectance can be used to set linear regression models based on partial least squares regression (PLS). Once the prediction model is established, in order to get the predicted values of apples, we only need achieve the effective wavelengths of reflectance of prediction samples combining with the program of MATLAB. Then we can save the predicted values as independent variables of the Linear Discriminant Analysis (LDA) to realize varieties discrimination. The accuracy of varieties discrimination was 96.97%. The correlation coefficients are 0.9608 for SSC and 0.9127 for firmness values in the prediction set. The results indicated that the methods to soluble solids content and firmness non-destructive inspection and varieties discrimination of apples based on Vis-NIR hyper spectral imaging was reliable and feasible.

9276-75, Session Post

Sensing driver awareness by combining fisheye camera and Kinect

Wuhe Zou, Lei Zhang, Ning Dai, Shanghai Institute of Technical Physics (China)

In this paper, we propose a Driver's Awareness Catching System to sense the driver's awareness. The system consists of a fisheye camera and a Kinect. The Kinect mounted inside vehicle is used to recognize and locate the 3D face of the driver. The fisheye camera mounted outside vehicle is used to monitor the road. The relative pose between two cameras is calibrated via a state-of-the-art method for calibrating cameras with non-overlapping field of view. The camera system works in this way: First, the SDK of Kinect released by Microsoft is used to track driver's face and capture eye's location together with sight direction. Secondly, the eye's location and sight direction are transformed to coordinate system of fisheye camera. Thirdly, corresponding view field is extracted from fisheye image.

As there is a small displacement between driver's eyes and the optical center of fisheye camera, it will lead to a view angle deviation. Finally, we did a systematic analysis of the error distribution by numerical simulation and proved the feasibility of our camera system. On the other hand, we realized this camera system and achieved desired effect in real-world experiment.

9276-76, Session Post

High-frequency deformation grating fabrication techniques and applications

Xianglu Dai, Tsinghua Univ. (China); Yanjie Li, Univ. of Jinan (China); Huimin Xie, Tsinghua Univ. (China)

The rapid development of micro-electronics and micro-nano material engineering makes it an urgent task to characterize the mechanical properties of micro-device and micro-nano material accurately. From the available literatures, the grating-based optical methods have been successfully applied to the deformation measurement in the above fields. These methods include the scanning moiré method, geometric phase analysis

and grid method which can realize the micro/nano-deformation measurement under different high-resolution microscopes. In addition, in order to realize an effective and high accuracy measurement, the high-quality grating is necessary and crucial in the application of the above-mentioned methods. In this report, some new grating fabrication methods were proposed which includes focused ion beam (FIB), nanoimprint lithography (NIL) and soft lithography.

This report mainly focuses on the recent development of our research group in the following aspects: (1) grating fabrication technique by using the FIB; (2) grating fabrication technique with the NIL; (3) grating fabrication technique based on the soft lithography; (4) microscopic deformation measurement of metal material by SEM moiré technique; (5) the residual stress measurement of MEMS using the SEM moiré technique.

From our study, we can conclude that the FIB, NIL and soft lithography are suitable to fabricate the micro/nano grating, and show a good potential for the further application; the scanning moiré technique based on the micro/nano gratings shows the advantages of large area measurement, high precision, no requirement for preparing reference grating and real-time measurement.

9276-77, Session Post

Precision issues in angle measurements by means of autocollimator

Yuri V. Filatov, R. A. Larichev, Saint Petersburg
Electrotechnical Univ. "LETI" (Russian Federation)

In the past few years in high-precision angle metrology has been set a problem. During the comparison measurements of angle polygon held by several national metrology laboratories there was found a significant disagreement in results, that exceeded accuracy declared by each laboratory. The most trustworthy hypothesis explaining this was influence of non-flatness of angle polygon reflecting faces. In fact deviation of reflecting surface topography from plane doesn't affect accuracy of measurements – it brings ambiguity in definition of measurand. Thus true value being measured becomes a matter of reflecting surfaces topography and chosen method for definition of normal to these surfaces. Regarding angle measurements with aid of autocollimator the uncertainty of result will be determined by multiple factors such as reflecting face topography, autocollimator lenses aberrations, measuring information processing, device and reflecting surface alignment etc.

Point of this work is to investigate mechanics and to give an estimate to the influence of different parameters on angle measurement uncertainty. These investigations are carried out in order to generate sufficient parameter set that could be used to bring into agreement measurements performed with different autocollimators, angle standards and measuring setups.

All conclusions are theoretical and estimates are obtained by mathematical modeling. Fourier optics methods and Zernike polynomials are implemented.

9276-23, Session 5

Dynamic 3D shape measurement based on grating projection and Fourier fringe analysis (Invited Paper)

Qican Zhang, Zhiling Hou, Xiaoahui Wang, Xue Li, Sichuan Univ. (China)

Three-dimensional (3D) shape measurement for a dynamic object or scene, whose height distributions is varying with the time, has been a hot topic in recent years due to its wide field

of application. A technique of dynamic 3D shape measurement, using a combination of gray or color grating projection and a most frequently used mathematical tool--Fourier fringe analysis, has been developed and widely used over past ten years in our research group, due to its particularly merits of requesting a easy-to-use equipment and requiring only one frame of the deformed fringe pattern to reconstruct the full-field height distribution with fast data processing. This technique is based on the idea of projecting and superposing a carrier fringe pattern onto the surface of the tested dynamic object, then recoding a sequence deformed fringe patterns with a commercial or high-speed camera from other view direction and reconstructing its corresponding 3D shape with Fourier fringe analysis. In this paper, the basic principles of this method, including the 2D gray or color-encoded grating projection and 2D (or 3D) Fourier fringe analysis are introduced, and some typical applications such as the vibration analysis of the cone of a loudspeaker, the shape reconstruction of a dynamic and spatially isolated object, and the flapping motion of a Flapping-wing Micro Air Vehicle (FMAV) are also demonstrated.

9276-24, Session 5

Extraction of surface morphological features of optical elements by contourlet transform

Linfu Li, Xiangchao Zhang, Hao Zhang, Xiaoying He, Min Xu, Fudan Univ. (China)

With the development of precision optical engineering, higher manufacturing qualities are demanded for advanced optical systems. Accurate analysis and evaluation of the surface topographies are important to improve the machining qualities of optical elements. Many functional optical components contain specific structures and features. While the conventional characterization methods in surface metrology deal with stochastic textures only, as a consequence they cannot be utilized for micro-optics.

The contourlet expansion, composed of bases oriented at various directions in multiple scales with smaller redundancy rate, has good performance in the representation of borderlines. It is good at detecting the smoothness of optical structured surfaces along the sharp edges. Moreover, it can capture sufficient directional information and achieve sparse representation of the salient features. Thus it is adopted as a powerful tool for characterizing the surface topographies of optical elements. In this paper, we will investigate the performance of contourlet transform for the extraction of different feature components from structured surfaces. A brief introduction is presented to the contourlet transform first. A concrete analysis of sparse representation and de-noising performance about contourlet transform was presented. Some effective technologies are developed for noise removal, tool mark identification and sharp edge detection, i.e. to characterize surface features of different scales and directions on the non-smooth micro-structured surfaces.

Also the validity of the proposed characterization methods is demonstrated by numerical experiments. The results indicate that the proposed method shows remarkable superiority over the conventional Fourier transform and general wavelet based methods.

9276-25, Session 5

Evaluation of surface roughness, homogeneity, and defects using light scattering techniques

Sven Schröder, Marcus Trost, Tobias Herffurth, Angela

Duparré, Fraunhofer-Institut für Angewandte Optik und Feinmechanik (Germany)

Light scattering techniques are an extremely interesting approach to characterizing optical and non-optical surfaces with respect to roughness and defects. The method is fast, non-contact, extremely robust with respect to vibrations, and at the same time very sensitive down to sub-nanometer roughness levels. Several tools will be presented that enable measurements to be performed even on very large (diameter > 600 mm) and curved surfaces with a 100% coverage of the surface. Examples are discussed ranging from smooth mirrors to structured surfaces. Surface power spectral densities and surface roughness are determined from the scattering results and compared to results obtained by white light interferometry and atomic force microscopy.

9276-26, Session 5

Comparing digital-light-processing (DLP) and liquid-crystal-on-silicon (LCD) technologies for high-quality 3D shape measurement *(Invited Paper)*

Song Zhang, Iowa State Univ. (United States)

This paper presents a thorough comparison between the projector using the digital-light-processing (DLP) technology and liquid-crystal-display (LCD) technology for high-quality 3D shape measurement. Our prior experience indicated that there are significant differences between these two technologies depending upon the employed fringe generation method (i.e., focused sinusoidal or binary defocusing). Namely, the DLP technology performs better using the binary defocusing technique since the resultant fringe contrast is higher; and the LCD technologies is better when the focus sinusoidal method is used because the LCD has less stringent timing requirement for the systems. However, no thorough comparisons have been carried out. This study will utilize the latest commercially available DLP and LCD projectors and thoroughly compare their differences on high-quality 3D shape measurement. Specifically, we will not only study each individual color, we will also study the combinations of different colors. The binary defocusing and focused sinusoidal fringe projection methods will be evaluated under all these scenarios. Experimental data will be presented and hopefully conclusions will be drawn on choosing one of the two technologies once the fringe generation method is determined for a particular application.

9276-27, Session 6

Ghost imaging and its potential application to dimensional measurement for the weak signal field *(Invited Paper)*

Yasuhiro Mizutani, Kyuki Shibuya, Tetsuo Iwata, Univ. of Tokushima (Japan)

Over the last decade, ghost imaging (GI) has become a remarkable optical technique, based on the correlation measurements of light intensity between a reference and an object field. For this technique, an object information is obtained by using a point detector. Notably, GI allows us to reconstruct the image of an object from non-spatial resolution information using the intensity correlation. Additionally, GI is expected to be the preferred imaging technique for weak intensity because it uses correlation measurements. However, GI has the disadvantage that it needs a number of measurements to reconstruct a high-visibility image. In other words, the visibility of the reconstructed image is dependent on the accumulated

number of measurements. This problem is attributed to the use of a speckle pattern with a random intensity distribution in time and space for illumination light. Furthermore, in the configuration of GI, the visibility of the reconstructed image is dependent on the spatial resolution of a dimensional detector for identifying the speckle pattern in the reference field. To overcome this problem, computational GI (CGI) is proposed as an improved method of configuration for GI using known illumination patterns. Because of a recent attempt, CGI has become available for stereoscopic three-dimensional measurement using several point detectors.

In this paper, we propose the reduction theory of the accumulated number of measurements by applying a circulatory pattern that uses the Hadamard matrix and provide an application for dimensional measurements.

9276-28, Session 6

Solutions on micro lens applied in multiple configuration systems

Hua Liu, Quanxin Ding, Luoyang Institute of Electro-Optical Equipment (China); Liwei Zhou, Beijing Institute of Technology (China)

On the development of modern optics, the zoom system is becoming more and more widely, but the zoom system design method and the structure of existing has limited its application in some micro systems, such as that and are easy to solve, the short service life. Some novel optical elements, it without using any moving components, have certain ability of independent zoom. The element is applied to the zoom system, can complete the traditional optical elements in some kind of difficult situation, such as to complete the function, to avoid the traditional zoom system is complicated in structure, and easy to solve shortcomings, to promote the miniaturization, in smart zoom system. The research to the advanced lens technology and its application in micro zoom system mainly completed the following work: firstly, the geometrical optics and optical aberration theory, imaging model, analyze the aberration theory, discusses on aberration changes in focal length variation situation. To determine the optical power required for ordinary elements, will no longer have to freedom of aberration correction, and without changing the lens weight, size and structure stability, while increasing the degree of freedom in design, and the imaging properties were discussed. Results solved the wide spectrum, and MTF matching problem, research and evaluate of system optimization in system Modulation Transfer Function (Modulation Transfer Function, the MTF), Energy concentration (Radial Energy Analysis, REA), diffusion (Spot Diagram, RMS) and other aspects and so on as qualitative criterion to achieve application requirements; Compared with the traditional conventional design, system sensors on the system efficiency, volume and weight have increased.

9276-29, Session 6

The assessment of industrial CT probing error

Yushu Shi, Sitian Gao, Xu Song, National Institute of Metrology (China); Dongsheng Li, China Jiliang Univ. (China); Wei Li, Qi Li, Shi Li, National Institute of Metrology (China)

In recent years, industrial CT are becoming more and more popular not only in the nondestructive testing (NDT), but also in the geometric coordinate measurement, benefit from its excellent three dimensional imaging and inner geometry measurement. There are many specifications about the acceptance and reverification test of traditional coordinate measuring machine

(CMM), like tactile CMM. However, the assessment method of industrial CT's dimensional measurement ability still can't reach an agreement now, due to its complicated working principle and appeared relative late.

Similar to traditional CMM, probing error of industrial CT is used for assessing the 3D measurement error of the machine in a very small measurement volume. Referring to the specifications about the CMM, and some standards or drafts about industrial CT, a research on the assessment of probing error of industrial CT is conducted here. Lots of assessment tests are carried out on the industrial CT Metrohm1500 in the National institute of metrology, using standard balls with different size and materials. The test results demonstrate that probing error of industrial CT can be affected seriously by the measurement strategy and standard balls. According to some further analysis about the test results, the assessment strategy of industrial CT' probing error is concluded preliminary, which can ensure the comparability of the assessment results in different industrial CT system.

9276-30, Session 6

A driving step auto-access method for single-wavelength microscopic interference

Xin Guan, Hubei Univ. of Technology (China) and Hubei Univ. of Technology (China); Xuanze Wang, Zhongsheng Zhai, Liangen Yang, Hubei Univ. of Technology (China)

Single wavelength microscopic interferometry, driven by the Piezoelectric Transducer (PZT), is a common surface topography measurement method. Its measurement accuracy is directly determined by the original phase acquisition precision of each pixel in area array CCD. Traditional phase identification methods adopt 3 points or 4 points algorithm to obtain the phase. However, they require the displacement step, actuated by the PZT, to strictly keep the same to satisfy the 90° phase condition. Therefore, these methods are only suitable for the strict anti-seismic experimental environment or conditions with high precise closed-loop PZT actuator and strict calibration of interferometric wavelength as well.

An auto-acquisition driving step method for the single wavelength microscopic interferometry is presented in this paper. To begin with, interference sequence diagrams, containing the surface topography information, were gathered by the CCD under open-loop PZT actuating. Next, two pixels whose phase difference is approximate 90° were selected as the calculating center to obtain smoothed gray values with regional gray average algorithm, which can reduce the influence of random noise. In the third place, an optimal fitting algorithm for the ellipse, formed by the average gray values, was proposed to obtain the amplitudes and offsets of the two gray values array. According these fitting parameters and gray values, the drive step can be calculated by elliptic equations. Experiments show that, this method can reduce the requirement conditions of measurement conditions and improve the measurement accuracy.

9276-31, Session 6

Long-range active retroreflector to measure the rotational orientation in conjunction with a laser tracker

Oliver Hofherr, Univ. of Freiburg (Germany); Christian Wachten, PI miCos GmbH (Germany); Claas Müller, Holger Reinecke, Univ. of Freiburg (Germany)

High precision optical non-contact position measurement is a key technology in modern engineering. Laser trackers (LT) can

determine accurately x-y-z coordinates of passive retroreflectors. Next-generation systems answer the additional need to measure an object's rotational orientation. To date, these devices are based either on photogrammetry or on enhanced retroreflectors.

In the past we have presented a new method to measure all six degrees of freedom in conjunction with a LT. The basic principle is to analyze the orientation to the LT's beam path by coupling-out laser radiation on detectors. The optical design is inspired by a cat's eye retroreflector equipped with an integrated beam splitter layer where the laser beam is partially reflected two times. This results in two laser beams for further analysis.

Now we optimized the method and designed a prototype which is optimized for long-range measurements. The spherical aberration is compensated and the optical dimensions and refractive indices are chosen to minimize the divergence angle.

The prototype is designed with a specified measuring range of 360° for roll angle measurements and ± 12° for pitch and yaw angle respectively. The new design reduces the divergence angle for the reflected beam by one order of magnitude. The wavefront distortion could be reduced to < 0.1 λ (633 nm) for beam diameters up to 8 mm. The repeatability for measuring the pitch and yaw angle is < 0.0005°. Our research now focuses on the measurement of the roll angle and these results will be included within this publication, too.

9276-32, Session 6

Experimental studies of the influence on object surface characteristics on the fringe patterns (*Invited Paper*)

Jiangtao Xi, Yifan Wei, Yanguang Yu, Qinghua Guo, Univ. of Wollongong (Australia)

Fringe pattern profilometry (FPP) based on digital fringe projection has been widely used to measure the 3-D shape of object. The denoising of the fringe patterns is one of the key tasks to improve the accuracy of measurement.

There are already some existing methods for denoising the fringe patterns. One widely used method is based on partial differential equations, which is flexible and has stable results. Another method is based on Windowed Fourier Filtering and an Adaptive Windowed Fourier filtering method enables lossless reconstructed fringe patterns. There are also some other methods with different advantages. Although all of these researches have provided the algorithms to reduce noise from fringe pattern, there is not enough work focusing on the influence of object surface characteristics on the fringe patterns.

This paper presents a comparative study which focuses on the influence caused by the characteristics of object with different material. In order to obtain comprehensive data, we did the experiments in different object surface characteristics in terms of colour, shape and reflectivity. From the experiments, we can obtain not only the characteristics of the noise resulting from different material, but also the data of same material in different colour and shape. Then the data which is obtained from the experiment will be analysed. 5-step-PSP is used to reconstruct the object for different material of object. The noise properties obtained are employed for the development of effective denoising algorithms to improve the measurement accuracy.

9276-33, Session 7

3D multi-modal optical metrology for industrial applications (*Invited Paper*)

Malgorzata Kujawińska, Marcin Malesa, Krzysztof Malowany, Warsaw Univ. of Technology (Poland)

Recently most of the measurement tasks in industry refer to characterization and monitoring of 3D objects and structures and their performance under changing conditions. This may require full-field determination of many physical quantities including: their shape, displacements, strains, dynamic parameters (e.g. resonance frequencies), temperature distribution or internal structure. In the paper we describe the hierarchical and multimodal measurement concept which enables to deliver results with requested sensitivity and accuracy and perform automatically measurements in difficult industrial conditions. The reported measurement systems provide vital information to improve security and efficiency of technological process and/or improve a product. The example measurement systems, based on enhanced optical methods, fulfilling different tasks during production processes are presented including:

- 3D digital image correlation method supported by thermovision, structured light and method is applied for structural integrity analysis in heat-and-power generating industry, building industry and testing of highly responsible composite structures;
- interferometric methods incl. two-beam and white light interferometry are used for parallel on-wafer quality control system for M(O)EMS;
- digital holography, photoelasticity and diffraction tomography are applied for technology optimization for microelements with functional 3D distribution of refractive index.

Finally the perspectives of implementation of full-field optical measurement methods in wide range of industrial applications and the importance of their formal acceptance in the standard industrial procedures are discussed.

9276-34, Session 7

New method of optical flat flatness verification system

Hao Sun, Univ. of Shanghai for Science and Technology (China) and Suzhou H&L Instruments LLC (China); Xueyuan Li, Suzhou H&L Instruments LLC (China); Sen Han, Univ. of Shanghai for Science and Technology (China) and Suzhou H&L Instruments LLC (China); Jianrong Zhu, Zhenglai Guo, Suzhou Institute of Measurement and Testing Technology (China); Yuegang Fu, Changchun Univ. of Science and Technology (China)

Optical flat is commonly used in optical testing instruments, flatness is the most important parameter of forming errors. As a measure, optical flat flatness index to have good precision. Current measurement in our country is heavily dependent on the artificial visual interpretation, through aperture tolerance (N) and local aperture tolerance (ΔN , $\Delta 2N$) to characterize the flatness. The efficiency and accuracy of this method cannot meet the demand of industrial development.

In order to improve the testing efficiency and accuracy of measurement, it is necessary to develop an optical flat verification system, which can obtain all surface information rapidly and efficiently, at the same time, in accordance with current national metrological verification procedures. This paper reviews current optical flat verification method and solves the problems existing in previous test, by using new method and its supporting software. Final results show that the new system can

improve verification efficiency and accuracy, by comparing with JJG 28-2000 metrological verification procedures method.

9276-35, Session 7

Mode-disturbing effect of laser speckle in optical fibers

Weimin Sun, Yunxiang Yan, Yu Jiang, Jianchao Zheng, Harbin Engineering Univ. (China)

Laser is a usual light source in many measurement applications, because it has good coherence. To measure the light transmission of a large-core fiber, we designed and setup a testing system using a He-Ne laser. The light from the laser could be focused to an ideal point to incident the fiber. On other hand, the output spot from the fiber suffers serious coherent noise, which is called as speckle. Even using multi-image average or removing mask filter, we can't reduce the influence of the speckle remarkably. So we made a mode-disturbing device to vibrate the fiber at a certain frequency and amplitude. To check the effectiveness of the fiber vibrating method and to find the best parameters for our fiber mode-disturbing device, we set different working frequencies from 1 to 80 Hz. And we set the CCD exposure time at 100ms, 500ms and 800ms. According to the experimental results, the speckle is much more sensitive to the working frequency of vibrating the fiber than the expose time. After comparing different frequencies, 60Hz is chosen as the optimized frequency to effectively suppress the speckle, decrease the speckle contrast. The output of the large-core fiber could fit to a 2-D Gaussian function. So we can measure the diameter of the spot based on the fitting result. Using this mode-disturbing system, we measured the focal ration degradation of a large-core fiber and studied on the bend effect of the fiber.

9276-36, Session 7

The model about the package structure of LED and the light intensity distribution

Haojie Sun, Shanghai Publishing and Printing College (China); Mengyuan Li, Jie Zhuang, Dawei Zhang, Univ. of Shanghai for Science and Technology (China)

Base on the principles of the LED package structure and the LED optical model, we use Tracepro to do the simulation of LED devices. By changing the parameters of LED model, such as the package structure, the size of reflective cup, the height of chip and the angle of the reflective bowl, etc, we simulate the light intensity distribution curve of LED in different structures and find different results. That is a big height, a lager angle and a smaller curvature will make a better condenser effect. Compare with measurement data which shows that intensity distribution abide by some laws. Those conclusions can use in guiding the package structure design of LEDs.

9276-37, Session 7

Diagnostics of temperature measurement errors for in-situ LED epitaxial growth

Dong Yan, Institute of Microelectronics, Chinese Academy of Science (China) and Key Lab. of Microelectronics Devices & Integrated Technology (China); Shing Lee, Institute of Microelectronics (China) and Key Lab. of Microelectronics Devices & Integrated Technology (China); Jianpeng Liu, Institute of Microelectronics (China)

Epitaxial growth of light emitter structure on sapphire as well as silicon substrates by Metal-organic chemical vapor deposition (MOCVD) is studied. In this paper, a wafer-selective reflectance, temperature and curvature in-situ sensor is developed for real time characterization of growing films. Temperature is critical for wavelength uniformity across the epitaxial wafer. With in-situ emissivity corrected pyrometry measurements via an optical window, the possibility and degree of temperature measurement errors is demonstrated. Not only systematic errors such as electronic artifacts and detector spectral response were examined, but random sources like unintentionally deposition on the optical window, beam drift from wafer tilting and stray light effects are expected to be compensated. Then, a correction scheme for the in-situ optical system is explored. A dynamic correction factor in the emissivity calculation equations is introduced to eliminate the deposition induced errors. Beam drift from wafer tilting is eliminated by a design margin of optical head and stray light effect is corrected using a single fitting parameter in the thermal radiance equations. In this paper, the technical realization steps of the correction scheme in industrial applications are also described. Finally, the measurement experiments of several LED epitaxial process run in the MOCVD were carried out to further verify the applicability of this improved in-situ sensor. The result shows the improved scheme not only provides an effective way of improving the system, but also may help us to better understand the influences of temperature and reaction conditions for epitaxial growth of light emitters.

9276-38, Session 7

Deformation evaluation methods under high-temperature and relative applications (Invited Paper)

Zhanwei Liu, Beijing Institute of Technology (China);
Huimin Xie, Tsinghua Univ. (China)

The need for accurate characterization of the mechanical behavior of materials at high temperatures has led to the development of numerous measurement techniques. In this study, some novel high temperature deformation carrier manufacturing techniques, such as fabricating high temperature resistant gratings and speckles using micro-machined technology, are developed. The novel high temperature moiré and DIC methods based on the developed deformation carrier are also introduced. The developed high temperature DIC method can be used to deformation measurement at a high temperature of up to 1100 °C by combination of the high temperature blackbody radiation suppression technique and simple white light illumination. The strain distribution regularity near-interface regions of Thermal Barrier Coatings (TBCs) during a thermal shock of 1100 °C was investigated using the developed method. During heating stage of the thermal shock, tensile and shear strain concentrations were found along the interface direction in the ceramic coat near the ceramic coat/bond-coat interface, indicating that the inner regions of the ceramic coat near the interface are a weak link. However, large residual tensile strain/stress concentration perpendicular to the interface direction in the ceramic layer are generated during cooling stage of the thermal shock, and after lots of thermal shock cycles, deboning cracks parallel to the interface could be formed in the position of the strain concentration. Experimental results show that this method can be applied to real time mechanical performance investigation of TBCs' near-interface regions under thermal shock environment.

9276-39, Session 8

Effects of lens aberrations in phase space (Invited Paper)

Guohai Situ, Guohai Li, Shanghai Institute of Optics and Fine Mechanics (China)

Phase space distributions such as the Wigner Distribution Function and Ambiguity function are very powerful tools to characterize the behavior of optical beams propagating in various optical systems. For instance, it is well known that when a beam passes through an ideal thin lens, the associated Wigner distribution function experiences a shear along the frequency axes. However, practical optical systems are not ideal. One must take the lens aberrations into account when analyzing and designing an optical system, in particular for imaging and metrology applications. In this paper, we present a theoretical and numerical study of how the Wigner Distribution Function evolves when a beam passes through a thin lens with aberrations characterized by the Zernike polynomials. The result shows that a deformation effect occurs in Wigner distribution function when aberrations present. Thus the design of optical imaging and metrology systems is to reduce or eliminate the deformation from phase space optics point of view.

9276-40, Session 8

Analysis of fiber similarity metric for fiber tract clustering in white matter of human brain

Xufeng Yao, Songlin Zhuang, Univ. of Shanghai for Science and Technology (China)

MR diffusion tensor imaging fiber tracking (DTI-FT) could lead to false propagation because of image noise and low resolution of DTI. A variety of fiber clustering (FC) approaches have been used to refine the tract configuration. One most aspect of FC algorithms is the measure of fiber similarity metric. In this paper, the fiber similarity metric are compared by varying the two parameters of distance factor and length factor. For evaluating our results, the corticospinal tract (CST) of a healthy human data in vivo was chosen. Based on the selected fiber similarity metric, each curved fiber of the CST was mapped to a point by kernel principal component analysis (KPCA), and then the point clouds of CST was clustered by hierarchical clustering which could distinguished false fiber points from true fiber points. Through our experiment, the optimum fiber similarity metric was deduced and showed more reliable capability in decreasing the false fiber points. In conclusion, the optimization of fiber similarity metric is vital in FC algorithms and it could effectively optimize the visualization of fiber bundles and would help a lot in the visualization of fiber bundles.

9276-41, Session 8

Optical fiber power measurement using different transfer standards

Nan Xu, National Institute of Metrology (China)

A comparison of power response with different transfer standard optical fiber power detectors is present. Traceable to cryogenic radiometer, these planar, focus-planar and trap detectors have different characteristics during the optical fiber power values transfer because of the different input angles or fiber connectors. The power response of planar InGaAs detectors are determined by a free space light from a 1546nm DFB laser source, and transferred by an optical fiber light input. For different types

of fibers and fiber connectors, a new trap detector is suitable for the optical fiber power measurement, which has very little sensitivity for a variety of input conditions. Power response of the trap detector is also determined and transferred under the same condition. With a great improvement of light absorbance, the trap detector can be used as a good optical fiber power transfer standard. The combined uncertainty for the fiber power measurement is less than 0.6%.

9276-42, Session 8

The interferometric method for measuring the generatrix of high-precision cone

Yanhui Kang, Heng Zhang, National Institute of Metrology (China)

Cone parts are widely used in advanced manufacturing and precision mechanics, providing air proof, torque transmission and so on. The linearity of generatrix is one of the important parameters, and the required accuracy can be up to sub-micrometers. In order to realize the rapid and high precision generatrix measurement of smooth surface cone, a laser interferometric method is proposed based on the structure of typical Fizeau interferometer. The high precision optical flat is used for reference standard, and the surface of cone is the measurand. Two cylinder lens with different focal length realize unidirectional extension of parallel beam, solving the problem of CCD camera fringe resolution. The interference fringes are curved because of the cone angle and the linearity, and the peak is the basis for accurate determination of the generatrix. Two fringe processing techniques are described in detail, which are single-frame and phase-shifting methods. Single-frame method includes two steps, i.e. the calculation of integer part and fractional part. The advantage of this method is the simple measurement structure. Phase-shifting method needs Piezoelectric Transducer (PZT) to generate several steps for phase calculation, with the advantage of high accuracy and the disadvantage of complex structure. The experimental result shows that the linearity measurement accuracy can be better than 0.2 μ m.

9276-43, Session 8

A high-accuracy subaperture stitching system for nonflatness measurement of wafer stage mirror

Yunjun Lu, Shanghai Institute of Optics and Fine Mechanics (China); Feng Tang, Shanghai Institute of Optics and Fine Mechanics (Japan); Xiangzhao Wang, Yong Li, Xiulong Wan, Fudong Guo, Fengzhao Dai, Shanghai Institute of Optics and Fine Mechanics (China)

In the stepper and scanner, the position accuracy of the wafer stage is influenced by the flatness of the stage mirror. The fabrication and testing of stage mirror is increasingly important as the development of lithography technology. Generally, the stage mirror has large aperture and high local flatness. In some cases, the nonflatness is less than 20nm PV in 30mm area, and the clear aperture is larger than 400mm in one direction. Precise surface flatness measurement is necessary for the computer controlled polishing of stage mirror. The measurement accuracy in local area should be higher than $\lambda/100 = 632.8\text{nm}/100 = 6.328\text{nm}$ PV, and the testing aperture should be extended to 400mm or even larger. So far, there is no commercial interferometer which can meet both of the special needs.

A subaperture stitching system, including a commercial 4-inch Fizeau interferometer, was presented in this paper. Absolute test was used to calibrate the surface figure of the reference mirror with the accuracy better than $\lambda/100$ PV. Subaperture stitching

was used to extend the measurement aperture larger than 450 \times 50mm. High stitching accuracy was realized by optimizing system design and stitching algorithm. Experimental data were presented both before and after the optimization. Stitching measurements were carried out for stage mirrors during surface polishing. Comparison tests were also made with a 24-inch interferometer. The results show that the stitching system has the advantages of larger dynamic range, higher spatial resolution, and better measurement accuracy in local area.

9276-44, Session 8

Future and advantages of membrane optical elements (Invited Paper)

Xing Zhong, Guang Jin, Changchun Institute of Optics, Fine Mechanics and Physics (China)

Membrane optical elements are ultra-light, folding and easy to be very large, so they have significant advantages in many fields, especially in space optics. The research current of membrane optical elements is introduced. The different types of them using for reflection, refraction and diffraction are summarized. Progress on membrane optics in CIOMP these years are presented. Some practical pictures and experiment are shown, containing the simulation, surface shape optimization and testing of electrostatic stretching membrane mirror. The structural design and surface accuracy testing of cable-net mirror and its sunlight focusing application. The influence of stitching error of membrane photon sieves on wavefront.

9276-71, Session 8

A high-speed camera with auto adjustable ROI for product outline dimension measurement

Qian Wang, Wei Ping, Beijing Institute of Technology (China)

Currently most domestic factories still manually detect machine arbors to decide if they meet industry standards. This method is costly, low efficient, and easy to misjudge the qualified arbors or miss the unqualified ones, thus seriously affects a factories' efficiency and credibility. In this paper, we design a specific high-speed camera system with auto adjustable ROI for machine arbor's outline dimension measurement. The entire system includes an illumination part, a camera, a mechanical structure part, and a signal processing part based on FPGA. The system will help factories to realize automatic arbor measurement, and improve their efficiency and reduce their cost.

The illumination part is a 8 x 28 LED pulse illumination array for a 200mm x 100mm detection area. The challenges for this part are the cooling and power driving issues. The central component of the camera part is a 2048 x 1088 high-resolution CMOS. The CMOS uses a ROI (Region of Interest readout) function, which automatically adjusts the CMOS exposure area as an arbor rolls on a tilted conveyor belt. With this function, the CMOS frame rate can reach 2873 f/s and above. The mechanical part was designed to service the whole system. An arbor rolls along a mechanical track. The detection and classification of an arbor is finished when it roll off the track. The detection speed is one arbor per second with accuracy 0.1mm. When the arbor is in the system illumination area, it blocks LED light, and forms a sharp shadow on the CMOS imaging. In this paper, we use FPGA for real-time signal processing. The FPGA calculates the minimum diameter of each cross-section of an arbor, restores its three-dimensional contour in real time using the CMOS image, and then determines if it is qualified.

Conference 9277: Nanophotonics and Micro/Nano Optics II

Thursday - Saturday 9 -11 October 2014

Part of Proceedings of SPIE Vol. 9277 Nanophotonics and Micro/Nano Optics II

9277-1, Session 1

Silicon hybrid nanoplasmonics devices and integration (*Invited Paper*)

Daoxin Dai, Zhejiang Univ. (China)

Recently silicon hybrid nanoplasmonic waveguides are becoming very attractive as a promising candidate to realize next-generation ultra-dense photonic integrated circuits because of the ability to achieve nano-scale confinement of light and relatively long propagation distance, as well as the compatibility with the CMOS process used for silicon photonics. Silicon hybrid nanoplasmonic waveguides also offer a way to transfer and process both photonic and electronic signals along the same nanoplasmonic circuit, which is desirable in order to combine the advantage of both photonics and electronics for high-speed signal processing and an easy realization of active components. In this way, the hybrid nanoplasmonic waveguide can be utilized locally where it is needed. In this paper, we give a review for our recent work on silicon hybrid nanoplasmonic waveguides and devices. First, the structures and properties of some typical silicon hybrid nanoplasmonic waveguides are compared. Second, some typical functionality elements for nanophotonic integration circuits are presented. In particular, some devices combining pure silicon nanowires and hybrid nanoplasmonic waveguides are demonstrated so that the hybrid nanoplasmonic waveguide is used locally and pure silicon nanowires are used globally. Thirdly, we give a review some ultrasmall on-chip polarization handling devices based on silicon hybrid nanoplasmonic waveguides by utilizing the huge birefringence and the significant polarization-dependence of the modal field profile. Finally the application (e.g., photodetection) of silicon hybrid plasmonics waveguides for the mid-infrared range is also discussed.

9277-2, Session 1

Silicon-based optoelectronic devices in 300mm platform (*Invited Paper*)

Eric Cassan, Delphine Marris-Morini, Institut d'Électronique Fondamentale (France); Jean-Marc Fédéli, CEA-LETI (France); Charles Baudot, STMicroelectronics (France); Jean-Michel Hartmann, CEA-LETI (France); Frédéric Boeuf, STMicroelectronics (France); Laurent Vivien, Institut d'Électronique Fondamentale (France)

We present experimental results of silicon modulators based on carrier depletion and Ge photodetectors fabricated on 300mm-SOI wafers available in large-scale microelectronic foundries. Mach Zehnder modulators based on 950 μm -long phase shifters using both lateral pn or interleaved diodes have been characterized. A 3 dB optical bandwidth of 20 GHz was obtained for the interdigitated phase shifter while 26 GHz was obtained for the lateral pn phase shifter. Both devices have worked at 40 Gbit/s with extinction ratio as high as 8 dB and on-chip losses of 4.9 dB. 40Gbit/s Ge detectors integrated in Si waveguide were also characterized. Both optoelectronic devices have been link to form 40Gbit/s optical communication.

9277-3, Session 1

Silicon Photonics for the near infrared and the mid infrared (*Invited Paper*)

Graham T Reed, Youfang Hu, Goran Z Mashanovich, Frederic Y Gardes, David J Thomson, Jordi Soler-Penades, Milos Nedeljkovic, Ali Z Khokhar, Paul M Thomas, Callum Littlejohns, Arifa Nazir-Ahmed, Scott Reynolds, Robert Topley, Colin J Mitchell, Stevan Stankovic, Thalia Dominguez-Bucio, Peter R Wilson, Ke Li, Taha M Ben Masaud, Antulio Tarazona, Harold M H Chong, David J Richardson, Periklis Petropoulos, Univ of Southampton (United Kingdom)

This paper summarises our recent work on Silicon Photonics. We target a range of applications utilising both active and passive devices. The following work is discussed: modulators and drivers, integration, waveguides for multi-layer photonics, multiplexers, and mid IR silicon photonics.

When we consider device fabrication, we consider both performance and manufacturability. Consequently we aim for simplicity of processing, repeatability and low cost. Where possible, self-aligned processes are used, and device designs target specific applications. For example, our modulator designs use self-aligned fabrication to ensure that the junction of a depletion modulator is always in the same position within a waveguide. Similarly we utilise a simple single etch process for an angled MMI based multiplexing structure for a reliable mux/demux device for up to 8 channels. For multi layer photonics, we are utilising Hot-wire CVD, as a low temperature material deposition method, to enable back end processing and photonic complexity scale-up. Using this approach we have implemented 50Gb/s modulators with integrated drivers, an integrated 10Gb/s short reach communications link, and a series of novel device designs for both near infra-red and mid infra-red applications (e.g. 1-6).

For the emerging mid infra-red field, we have developed a series of building blocks, ranging from alternative waveguide structures, to passive device and modulators, to facilitate the fabrication of increasingly complex circuits and systems at longer wavelengths.

9277-5, Session 1

Design, fabrication, and optimization of silicon slot photonic ring resonators

Weiwei Zhang, Samuel Serna, Xavier Le Roux, Laurent Vivien, Eric Cassan, Institut d'Électronique Fondamentale (France)

Silicon slot waveguides, as high index contrast hollow core guiding structures, are able to significantly diminish the detrimental effect of free carriers due to Two-Photon-Absorption in the telecommunication window and bring potential hybrid optical applications considering the enhancement of the electric field in the slot region.

Here, we report the design, fabrication, and the theoretical/experimental optimization of slot ring resonators infiltrated by a linear liquid as an experimental demonstration towards hybrid silicon photonic devices. All pass ring resonator (APR), add-drop ring resonator (ADR) and ring enhanced Mach-Zehnder interferometer (REMZI) based in slot rings with 50 μm radii and loaded by slot buses are fabricated and characterized. Different strip-slot mode convertors are investigated in order to quantitatively determine the influences on the transmission

efficiency and the quality factors of the resonance peaks. Several methods are used to properly extract the coupling loss from bus to ring structures and the propagation/bend losses inside the ring resonators. Those methods include fitting the through-port spectrum of APR, analyzing FSR/FWHM/ER based on ADR and analyzing ER based on APR and REMZI. The resonances ER slightly decrease and the peaks become shaper after oxidation/deoxidation processes because of smoothing silicon side wall roughness. It leads to Q-factors above 65,000 and total losses (coupling/propagation/bends) reduced to the order of 7dB/cm (initially of 20dB/cm). These results evidence very promising possibilities to enhance the ring resonator properties with the hybrid slot configuration.

9277-58, Session 1

Large-scale silicon photonic circuit design

Xu Wang, James Pond, Lumerical Solutions, Inc. (Canada); Chris Cone, Mentor Graphics Corp. (United States); Lukas Chrostowski, The Univ. of British Columbia (Canada); Jackson Klein, Lumerical Solutions, Inc. (Canada); Jonas Flueckiger, The Univ. of British Columbia (Canada); Amy Liu, Dylan McGuire, Lumerical Solutions, Inc. (Canada)

Silicon photonics has become a promising technology for photonic integrated circuits. Recently, there has been a dramatic increase in the scale and complexity of silicon photonic circuits, which introduces many new design challenges and creates a need for efficient and standardized design flows.

The behavior of a large-scale circuit, whether electrical or photonic, is not trivially related to the individual component performance. Indeed, in silicon photonic circuits such as WDM transmitters and optical switches, optical routing, signal crosstalk and reflection can affect the overall circuit performance. Moreover, the high sensitivity of components to manufacturing variations has dramatic circuit-level consequences that must be predicted by circuit simulations. Such simulations require compact models that can accurately represent the behavior of each component, and the compact model parameters must be extracted from physical level simulation and experimental results.

We present a complete design flow for large-scale silicon photonic circuits, from schematic design to tapeout, using component-level and circuit-level simulation tools combined with standard EDA tools. We show how circuits can be simulated in both the time and frequency domains, including the effects of bidirectional and, where appropriate, multimode and multichannel waveguides. We also show how individual components such as grating couplers, waveguides, splitters, filters, electro-optical modulators and detectors can be simulated, and good agreement with experimental results can be obtained. We then show how the compact model parameters, with inclusion of fabrication process variations, can be extracted for use in circuit-level simulations. Finally, we show an example of the full design flow.

9277-6, Session 2

Hybrid III-V/silicon SOA for photonic integrated circuits *(Invited Paper)*

Peter Kaspar, Romain Brenot, Alban Le Liepvre, Alain Accard, Dalila Make, Guillaume Levaufre, Nils Girard, François Lelarge, Guang-Hua Duan, III-V Lab. (France); Ségolène Olivier, Christophe Jany, Christophe Kopp, Sylvie Menez, MINATEC (France)

Silicon photonics has reached a considerable level of maturity, and the complexity of photonic integrated circuits (PIC) is steadily increasing. As the number of components in a PIC grows, loss management becomes more and more important. Integrated semiconductor optical amplifiers (SOA) will be crucial components in future photonic systems for loss compensation. In addition, there are specific applications, where SOAs can play a key role, such as optical gates in packet switching or modulated reflective SOAs in carrier distributed passive optical networks (PON). It is, therefore, highly desirable to find an integration platform that allows the integration of SOAs on silicon.

Various methods are currently being developed to integrate light emitters on silicon-on-insulator (SOI) waveguide circuits. Many of them use III-V materials for the hybrid integration on SOI. Various types of lasers have been demonstrated by several groups around the globe. In some of the integration approaches, SOAs can be implemented using essentially the same technology as for lasers. In this paper we will focus on SOA devices based on a hybrid integration approach where III-V material is bonded on SOI and a vertical optical mode transfer is used to couple light between SOI waveguides and guides formed in bonded III-V semiconductor layers. In contrast to evanescent coupling schemes, this mode transfer guarantees a good confinement factor in the gain material and allows for efficient light amplification. We will outline the fabrication process of our hybrid components and present some of the most interesting results from a fabricated hybrid SOA.

9277-7, Session 2

All optical control of silicon photonic resonators based on photothermal effects *(Invited Paper)*

Min Qiu, Zhejiang Univ. (China)

Silicon-on-insulator (SOI) technology is an excellent platform for integrated photonic circuits, due to its good light confinement and low propagation loss. We have numerically and experimentally investigated the effect of photothermal tuning of Si waveguides integrated with a plasmonic nanoheater, i.e. optical absorber. For a Si micro disk resonator, an optical absorber can be integrated directly on its top, and the temporal response of the proposed structure is relatively fast with rise/fall time around 2.0 ns. The performance of our all-optically pumped photonic devices is close to the state-of-the-art values in thermal-optical switches based on an electrode-driven heater. Comparatively, plasmonic light absorbers have advantages such as compact size, low heat capacity, high efficient light-to-heat conversion and elementary fabrication process. Photothermal optical switching via this approach can be important for applications, where contactless light switching or routing is needed.

9277-8, Session 2

A new Si photonics platform for DWDM implementation

Ziyi Zhang, Kazumi Wada, Motoki Yako, Ju Kan, Naoyuki J. Kawai, The Univ. of Tokyo (Japan); Koji Yamada, Tai Tsuchizawa, Hiroshi Fukuda, Nippon Telegraph and Telephone Corp. (Japan)

We have proposed a mid-index-contrast (MiDex) platform with silicon nitride (SiN_x) allows 100GHz spacing dense wavelength division multiplexing (DWDM) without any a thermalize operation, such as reported counter heat compensation or optical index counter compensation by micro scale heater or specific polymer cladding. Channel wavelength dependence on temperature within 100GHz was demonstrated at chip

temperature varies to 80 °C from room temperature. Both chemical vapor deposition (CVD) and physical vapor deposition (PVD) process was employed as SiNx film deposition process. Thermo-optic coefficients (dn/dT) were estimated from peak shifts of thermally controlled ring resonators, where PVD and CVD was found to have comparable dn/dT 1.9×10^{-5} [RIU/K] (peak shift of 1.25[GHz/K]) at C-band, 20-80 °C PVD-SiNx was demonstrated to be more preferred material because no process related N-H bond was introduced to SiNx film whereas N-H absorption was clearly appeared in SiNx waveguides by chemical vapor deposition (CVD). Also, room temperature PVD deposition realized back-end process compatibility. The results indicate that SiNx, especially PVD-SiNx, is such a fascinating material for DWDM application considering narrow wavelength spacing with temperature instability.

9277-9, Session 2

Ultra-compact broadband nanowire-to-slot waveguide mode converter based on SOI

Ying Qi, Junming An, Yue Wang, Xiaoguang Zhang, Institute of Semiconductors (China)

Novel ultra-compact high-efficiency broadband mode converter between silicon (Si) nanowire and silicon slot waveguide based on Silicon-on-Insulator (SOI) is proposed in this paper. By introducing a gradual-width S-band structure between Si nanowire and slot waveguide, the favorable transition between nanowire mode (Gaussian-like mode) and slot mode (non-Gaussian-like mode) can be obtained and then the coupling efficiency is improved. The structure is simulated and optimized by using the three-dimension Finite-Difference Time-Domain Method (3D-FDTD). Through the parameters optimization of the structure, the coupling efficiency η (the single coupling efficiency is defined as: $\eta = P_{out}/P_{in} \times 100\%$) can be over 90% by only 200nm-length converter over 600 nm wavelength range (1250 to 1850 nm) for a quasi-TE mode, that is the smallest size to our knowledge. When the length of the mode converter is increased to 2 μ m, the coupling efficiency can reach 99%. There is a tradeoff between the footprint and the coupling efficiency. We also find that the mode converter has good performance with different claddings, including silica (the index of silica is $n_s=1.445$) and organic materials (the index is $n_s=1.6-1.7$), which is important to its use in nonlinear processes such as ultrafast all-optical switching, optical modulation and detection based on slot waveguide. The design process is given in details and theoretical analysis can give explanations to the simulation results. We get the mode converter fabricated by using technology processes of Electron-beam-lithography (EBL) and inductively-coupled-plasma (ICP) etching. This presented mode converter can meet the demand of ultra-compact, wavelength-insensitive of monolithic integration.

9277-10, Session 2

High-contrast grating hollow-core waveguide splitter applied to optical phased array

Che Zhao, Ping Xue, Hanxing Zhang, Chao Peng, Weiwei Hu, Peking Univ. (China)

The 1x2 high contrast grating hollow-core waveguide splitter applied to optical phased array is designed and fabricated on SOI for the first time. The experimental results indicate its good performance on beam splitting and wide bandwidth.

9277-11, Session 2

Polarization independent propagation and polarization rotation in plasmonic waveguides

Qin Chen, Lin Jin, Suzhou Institute of Nano-tech and Nano-bionics (China)

Plasmonic devices are very attractive for ultracompact silicon photonics. However, surface plasmon wave can only be excited by TM polarization. This polarization dependence similar to that caused by high index contrast in SOI material induces considerable polarization-dependent dispersion and loss in optical fibers communication and is not desired for polarization division multiplexing system. Polarization rotator can be a solution, but the current techniques all depend on accurate alignment in lithography on subwavelength waveguides. In this paper, we first propose a polarization independent plasmonic waveguide consisting of dielectric and metal films cladded silicon waveguide, where the polarized guided modes are confined in the low-index dielectric layers on either top surface or sidewalls of the silicon waveguide. The structure can also be applied to realize the polarization insensitive plasmonic active devices like modulators. Alternatively, we investigate the polarization rotation effect in such a waveguide when the dielectric and metal claddings on one sidewall of the silicon waveguide are removed. The asymmetric cross section induces a hybridization of the polarization modes and a large mode index difference. As a result, a polarization conversion efficiency of 99.7% with an insertion loss of 2.2 dB is obtained at a waveguide length of 9.7 μ m. Most importantly, the device can be easily fabricated by oblique deposition of asymmetric metal and dielectric claddings without accurate alignment in photolithography. In a word, the proposed plasmonic devices have great potential to manipulate the polarization in silicon photonics.

9277-12, Session 2

GeSi photonics for telecommunication applications

Papichaya Chaisakul, The Univ. of Tokyo (Japan) and Institut d'Électronique Fondamentale (France); Vladyslav Vakarin, Univ. Paris-Sud 11 (France); Delphine Marris-Morini, Institut d'Électronique Fondamentale (France); Jacopo Frigerio, Giovanni Isella, Politecnico di Milano (Italy); Kazumi Wada, The Univ. of Tokyo (Japan); Laurent Vivien, Institut d'Électronique Fondamentale (France)

We discuss a mid-refractive index contrast (MiDex) GeSi-based photonics for future dense wavelength division multiplexing (WDM) systems. We show that MiDex Ge-rich Si $_1$ -xGe $_x$ can be used as both a passive low loss waveguide and a virtual substrate to facilitate epitaxial growth of Ge-based active devices. Refractive index contrast between the Ge-rich Si $_1$ -xGe $_x$ waveguide and the Si $_1$ -yGe $_y$ ($y < x$) lower cladding layer is small enough to overcome polarization dependent losses and detrimental fabrication tolerances of WDM system based on the widely-investigated high refractive index contrast optics (HiDex) of Si on SiO $_2$ waveguide. Moreover, simulations and experiments indicate that the index contrast between Ge-rich Si $_1$ -xGe $_x$ waveguide and the Si $_1$ -yGe $_y$ lower cladding layer is still high enough to ensure compactness of important on-chip photonic components including passive waveguide and GeSi-based array waveguide grating (AWG). Last but not least, we experimentally prove that Ge-rich Si $_1$ -xGe $_x$ layers can act as a virtual substrates to facilitate a low temperature high quality epitaxial growth of Ge-based active components. Our studies show that MiDex GeSi-based photonics could uniquely provide both passive and active functionalities necessary for future dense WDM systems, which

potentially could not be obtained using the widely-developed HiDex systems.

9277-13, Session 3

Photonic spin Hall effect in plasmonics and metamaterials (*Invited Paper*)

Anatoly V. Zayats, King's College London (United Kingdom)

The ability to manipulate the polarization state of light is one of the basic photonic functionalities. Polarization control is usually achieved using retardation effects in natural birefringent crystals. Metallic nanostructures allow unprecedented flexibility in light polarisation manipulation, since plasmonic excitations have distinct polarisation properties. In turn, the use of polarization (spin) of light interacting with plasmonic nanostructures and metamaterials opens up new horizons for signal manipulation in conventional and quantum domain using solid-state analogies, such as, photonic spin Hall effect. The controlled interaction of light with plasmonic nanostructures using spin of light allows one to manipulate sub-wavelength optical signals with high precision. In this talk we will discuss approaches and application nanoplasmonic devices for light spin manipulation as well as new approaches using spin of light to control optical signals. The role active functionalities in light polarization control, such as nonlinearities and gain/loss manipulation will also be discussed. Polarisation effects in plasmonic metamaterials with hyperbolic dispersion and non-Hermitian metamaterials with loss-coupled polarisation states will be considered. In different realisation, plasmonic metamaterials allow one to achieve very strong circular birefringence and circular and linear dichroism, and can be used for designing subwavelength-thin polarization components. We will also discuss the possibility of all-optical ultrafast control of reflected or transmitted light polarisation state by employing intrinsic metal nonlinearities.

9277-14, Session 3

Plasmonic graphene-antenna photodetector and transistor (*Invited Paper*)

Zheyu Fang, Peking Univ. (China)

Nanoscale antennas sandwiched between two graphene monolayers yield a photodetector that efficiently converts visible and near-infrared photons into electrons with an 800% enhancement of the photocurrent relative to the antennaless graphene device. The antenna contributes to the photocurrent in two ways: by the transfer of hot electrons generated in the antenna structure upon plasmon decay, as well as by direct plasmon-enhanced excitation of intrinsic graphene electrons due to the antenna near field. This results in a graphene-based photodetector achieving up to 20% internal quantum efficiency in the visible and near-infrared regions of the spectrum. This device can serve as a model for merging the light-harvesting characteristics of optical frequency antennas with the highly attractive transport properties of graphene in new optoelectronic devices.

9277-15, Session 3

Controlling the resonance fluorescence of a two-level atom in the near-field of a plasmonic prolate nanospheroid

Eugene Chubchev, Yulia V. Vladimirova, Victor N. Zadkov, Lomonosov Moscow State Univ. (Russian Federation)

We analyze theoretically modification of the resonance fluorescence spectrum of a two-level atom driven by a linearly polarized monochromatic field near the plasmonic nanostructure (a metallic nanospheroid) as a function of the geometric parameters of the nanospheroid and the atom's location around the nanospheroid.

The influence of the plasmonic nanoparticle was taken into account by using effective values (modified by the nanoparticle) for the Rabi frequency and the linewidths in the expression for the resonance fluorescence spectrum. It is shown that one can control this spectrum varying the aspect ratio of the nanospheroid and the atom's location around the nanospheroid, as well as by the polarization of the incident laser field. These parameters affect the local field enhancement and the modification of the total decay rate of the atom interacting with the nanospheroid, which leads to modification of the resonance fluorescence spectrum of the atom (frequency shift of the satellite lines in the Mollow-type triplet, widths of the lines and the spectrum intensity) by contrast with that one in free space.

It is shown that by varying the aspect ratio of the spheroid one can vary the radiative decay rate in the range of 10^{-2} to 10^6 of the decay rate in free space. Distribution of the near-field in the vicinity of the nanospheroid and atomic decay rates have complicated structures and drastically depend on the aspect ratio. The correct selection of the aspect ratio of the nanospheroid allows controlling the intensity of the fluorescence signal.

9277-16, Session 3

Making metallic micro-/nanostructures interactive to TE-polarized light

Zhijun Sun, Xiamen Univ. (China)

Metallic nanostructures can be used to manipulate light in the subwavelength scale due to excitation of surface plasmons (SPs). This opens an avenue to developing plasmonic devices for various applications. But SPs are transverse-magnetic (TM) waves, and can be optically excited in metallic nanostructures with only TM-polarization component of the incidence light. Thus transverse-electrically (TE) polarization component of the light is usually excluded from mesoscopic optical interactions in metallic nanostructures. Generally, a surface mode with evanescent distribution of its field in the transverse direction is essential for a wave to be confined in a subwavelength scale to propagate and oscillate.

Here we propose to modify the surface of metal structures such that TE-polarized incidence light can excite SP-like quasi surface waves (SWs) to propagate at metal surfaces, thus TE-polarized light become capable to interact with metallic nanostructures. In this report, we will first present principles and basic properties of the quasi surface waves. And then we demonstrate interactions of TE-polarization light with various modified metallic micro-/nano-structures that have interesting optical properties, novel or similar to those of SP-induced effects by TM-polarization light. These include enhanced transmission through metallic nanoslit arrays, localized quasi TE surface wave resonances, perfect absorption of TE-polarization light at metal surfaces and their field enhancement, etc.. Interaction of metallic micro-/nano-structures with TE-polarized light is expected to improve performances of various plasmonic devices and have potentials

in developing new functional metallic mesoscopic structures and devices.

9277-17, Session 3

Recent developments in graphene-based active and passive optical devices

Ran Hao, Zhejiang Univ. (China)

Graphene has shown promising perspectives in optical active components due to the large active-control of its permittivity-function. We will review our recent progress in graphene-based active and passive optical devices, including graphene-based slow light waveguide, graphene-based optical modulators and graphene-based logic gates. We proposed and numerically analyzed an extremely wideband slow light in a graphene-based grating waveguide. The strongly delayed wave ($120 < n_g < 167$) with extremely large bandwidth ($2.7\text{Thz} > \Delta \omega > 0.7\text{Thz}$) can be dynamically controlled via the gate-voltage dependent optical properties of graphene. Additionally, multi-layer graphene-based modulator, few-layer graphene-based modulator, four kinds of graphene-based logic gates, and the corresponding figure-of-merits are reviewed. The results show that graphene is an excellent material for enhancing the modulation effect in silicon, and has great potentials for CMOS compatible high efficiency optical devices, showing significant influence for optical interconnects in future integrated optoelectronic circuits. Both of the graphene-based active and passive optical devices can be dynamically tuned by utilizing the gate-voltage dependent optical property of graphene.

9277-18, Session 3

Constructing of special light-intensity distributions by means of axicons

Sergey A. Degtyarev, Svetlana N. Khonina, Image Processing Systems Institute (Russian Federation) and Samara State Aerospace Univ. (Russian Federation)

We considered laser beams focusing with different types of axicons including metalized axicons. We ran numerical simulations with Comsol and received 3D-area-distributed electric fields amplitude. Helmholtz equation was solved in Comsol with finite elements method to simulate the process. Incident laser beams impinges on axicons and diffract on the ones. We studied an intensity distribution in a near-field. Special types of intensity distributions were obtained like photon spirals and sharp focused light. 3D-structures of axicons were taken into consideration. Refractive and diffractive axicons and spiral axicons were observed. Also we conducted full-scale experiments for verifying numerical simulations. Using a scanning near-field optical microscope we measured beams which were focused by axicons. We scanned a 3D volume nearby an axicon. It was made by scanning of few planes which is laid beyond an axicon at different distances. In considered cases near-field measurements demonstrated good qualitative agreement between experiments and simulation. Particularly spiral field-intensity distribution was obtained in a near-field. We named this distribution the photon spiral. Also we analyzed different methods of creation of a longitudinal-polarized optical far-field. We considered Especial-polarized laser beams focusing with spherical lenses and diffractive and refractive axicons. It has been shown that diffractive axicon is the most advantageous considered element for longitudinal polarized beam forming.

9277-19, Session 4

Nonlinear optics in photonic crystal nanocavity quantum dot lasers (*Invited Paper*)

Yasutomo Ota, Katsuyuki Watanabe, Satoshi Iwamoto, Yasuhiko Arakawa, The Univ. of Tokyo (Japan)

Nonlinear optical effects are enhanced when photons are confined both in time and space. This is proven to be prominent when using micro/nanocavities with high Q-factors and small mode volumes, such as microdisk, plasmonic cavities and photonic crystal nanocavities. A way to further enrich such nanoscale nonlinear optical systems is putting semiconductor-based active emitters inside. This would ultimately lead to efficient frequency-converted nanolasers that may enable one to synthesize arbitrary wavelengths of coherent light on a microscale chip under electrical carrier injection, together with the capability of dense integration.

Here, we study in-situ intra-cavity frequency conversion of light generated inside photonic crystal nanocavity lasers under optical carrier injection. We used GaAs-based nanocavities containing InAs quantum dots as laser gain media. The system shows high nonlinear frequency doubling efficiencies over 10 %/W and enables the observation of second harmonic generation even when the average intracavity photon number is below 0.1. On crossing the near-infrared lasing threshold, we observed a change in the frequency doubling efficiency induced by a change in the photon statistics of the intracavity laser field from thermal to coherent. We also show that the combined broadband InAs quantum dot gain, small cavity footprint and the lack of a restrictive phase matching requirement enabled the micro-integration of 26-different-color nanolasers covering almost the entire visible range. We believe that these frequency conversion nanolasers could be useful for studying few photon nonlinear optics, as well as for on-chip synthesis of arbitrary wavelengths of light.

9277-20, Session 4

Raman silicon laser using photonic crystal nanocavity (*Invited Paper*)

Yasushi Takahashi, Osaka Prefecture Univ. (Japan)

Raman scattering has been a useful phenomenon for examining the static stress of various silicon devices since the 1970's. From the early 2000's, the Raman effect has also attracted attention due to its potential to add active functionality to pure silicon devices. Raman silicon lasers using rib waveguide resonators have been an important advance in silicon photonics. However, these lasers need the assistance of reverse-biased p-i-n diodes in order to remove the free carriers generated by two-photon absorption and they have thresholds as high as 20 mW, even when a high-Q ring-cavity structure on the cm-scale is used. Very recently, we have reported a micrometer-scale continuous-wave Raman Si laser with an ultralow threshold of 1 microwatt, using a photonic crystal heterostructure nanocavity without any p-i-n diode. This device utilizes an unusual pair of high-Q resonant modes in the heterostructure nanocavity. The pair is superior in terms of all of the aspects that are important for enhancing the Raman gain when the device is fabricated along the [100] crystalline direction on a (001) silicon-on-insulator substrate. We believe that this breakthrough will stimulate silicon photonics research in a number of areas.

9277-21, Session 4

Nonlinear Fano resonance in photonic crystal waveguide and cavity system: physical properties and applications

Yi Xu, Jinan Univ. (China); Andrey E. Miroshnichenko, The Australian National Univ. (Australia)

During last decade, the Fano resonances in nanoscale structures have gained numerous attentions due to their capability of building sensors, switches, filters in a very compact scale[1]. The Fano resonances manifest themselves as asymmetric profiles in transmission or scattering line shape, which originates from the resonant constructive and destructive interference phenomena in waves scattering [2]. Photonic crystal waveguide and side-coupled cavity system provides a superior platform for observing and manipulating Fano resonance[3-5]. Utilizing the Kerr nonlinearity in the photonic crystal cavity, we can obtain tunable response of such system which manifests as the nonlinear Fano resonance. We will discuss the physical properties of nonlinear Fano resonance found in different photonic crystal waveguide and side-coupled cavity systems[6-11]. Applications including enhancement of nonlinear response, manipulating optical flow, tunable optical diode and optical biosensor based on these properties are proposed based on the modified Fano-Anderson model and numerically demonstrated via the finite difference time domain method.

Y. Xu acknowledges the support from NNSF (Grant No.11304047), Foundation for Distinguished Young Talents in Higher Education of Guangdong Province (Grant No. 2013LYM0067). The work of A. E. Miroshnichenko was supported by the Australian Research Council through Future Fellowship program (FT110100037).

References

1. A. E. Miroshnichenko, S. Flach, and Yu. S. Kivshar, *Rev. Mod. Phys.* 82, 2257 (2010).
2. U. Fano, *Phys. Rev.* 124, 1866 (1961).
3. S. Fan, *Appl. Phys. Lett.* 80, 908-910 (2002).
4. A. E. Miroshnichenko, S. F. Mingaleev, S. Flach, and Yu. S. Kivshar, *Phys. Rev. E* 71, 036626 (2005).
5. A. E. Miroshnichenko, Yu. Kivshar, C. Etrich, T. Pertsch, R. Iliw, and F. Lederer, *Phys. Rev. A* 79, 013809 (2009).
6. Y. Xu and A. E. Miroshnichenko, *Phys. Rev. A*, 84, 033828 (2011).
7. Y. Xu and A. E. Miroshnichenko, *Europhysics Lett.*, 97, 44007 (2012).
8. Y. Xu, and A. E. Miroshnichenko and Anton S. Desyatnikov, *Opt. Lett.* 37, 4985-4987 (2012).
9. S. Weimann, Y. Xu, R. Keil, A. E. Miroshnichenko, S. Nolte, A. A. Sukhorukov, A. Szameit, and Y. S. Kivshar, *Phys. Rev. Lett.* 111, 240403 (2013).
10. X. Q. Li and Yi Xu, *Opt. Commun.* 301, 7-11 (2013).
11. Y. Xu and A. E. Miroshnichenko, *Phys. Rev. B* 89 134306, (2014).

9277-22, Session 4

Traveling plasmon interaction with light

Yugao Deng, Kazumi Wada, The Univ. of Tokyo (Japan)

While electronics consist mainly of two devices, i.e., transistors and interconnects, quite a few devices have to be implemented to construct circuits in photonics, such as light emitter, modulator, multiplexer/demultiplexer, photodetector, isolator and interconnect. This is one of the fundamental challenges in photonics in integration.

Based on coupling the Maxwell's equations with electron motions, it has been predicted that a light mode in conductive waveguides should strongly interact with the traveling plasmons

and should show amplification.

With this amplifying mode, multifunctional optical devices compacting the function of light emitter, modulator, and amplifier are feasible. Thus, this could be an important cornerstone for silicon photonics. By analytically solving the Maxwell's equations, a secular equation showing the entangling of light mode and electron mode is obtained. We briefed a couple of key interactions of light with electrons according to the electron density and its relative velocity to light from the equation. With a current flowing parallel to the light, the amplifying mode shall appear in waveguide of IV group semiconductors such as Si and Ge, if only the waveguide has a proper electron density, controlled light velocity and strong light confinement. The operation wavelength are optimized at 1.55 μ m or 10.6 μ m, which corresponds to our communication band and the CO₂ laser light relatively. Silicon photonics provides a fundamental test bed to understand the predictions experimentally.

9277-23, Session 4

Manipulation of photonic spin Hall effect with space-variant Pancharatnam-Berry phase

Xiaohui Ling, Hengyang Normal Univ. (China) and Shenzhen Univ. (China); Xunong Yi, Shenzhen Univ. (China); Zhaoming Luo, Yachao Liu, Hunan Univ. (China); Hailu Luo, Hunan Univ. (China) and Shenzhen Univ. (China); Shuangchun Wen, Shenzhen Univ. (China) and Hunan Univ. (China)

Photonic spin Hall effect (PSHE) manifests as spin-dependent splitting of photons. It is generally believed to be a result of the spin-orbit interaction which describes the mutual influence of the spin (polarization) and the trajectory of the light beam. This spin-orbit interaction can lead to a kind of geometric phase, Pancharatnam-Berry phase. Here, we report an experimental observation of the PSHE in a dielectric-based birefringent metasurface. By suitably designing the metasurface with homogeneous phase retardation but space-variant optical axis directions, we govern the PSHE via space-variant Pancharatnam-Berry (PB) phase originated from the local polarization manipulation of the metasurface, essentially, the topological spin-orbit interaction between the light and the metasurface. Unlike the previously reported PSHE with the spin-dependent splitting occurred in coordinate space, the splitting caused by the space-variant PB phase occurs in momentum space. Actually, this PB phase can be contributed by the inhomogeneous metasurface as well as the incident polarization distribution. Hence, modulating the polarization distribution of the incident light and/or the structure geometry of the metasurface, we can manipulate the PB phase, and thereby the PSHE. Our results may offer an effective way to manipulate the photon spins and a route for spin-controlled nanophotonic applications.

9277-46, Session Post

Broadband polarizer or band-pass filter based on a dielectric grating with top and bottom metallic coverings

Jing Nie, Hu-Quan Li, Huazhong Univ. of Science and Technology (China); Wen Liu, Huazhong Univ. of Science and Technology (China) and Univ. of Science and Technology of China (China)

In this paper we evidenced a broadband transparency from middle infrared to radio spectrum and a band-pass transmission in far infrared based on a sandwich-like grating structure

consisting a dielectric grating layer and two metallic covering layers on the top and bottom side of it. It indicates that broadband polarizer or band-pass filter can be inspired from the structure. As a polarizer, the extinction ratio is about 50dB in middle infrared which increases as the wavelength grows larger; over 90% transmittance for TM polarized light can be maintained from middle infrared to radio spectrum, which doesn't degrade for incident angle from 0° to 90° . As a band-pass filter working in far infrared region, the resonant transmission peak can be tuned by either varying the thicknesses of the dielectric grating layer or of the metallic coverings. When the resonant transmission peak is tuned from shorter to longer wavelength by increasing the thickness of dielectric grating, the peak transmittance is increased from 61% to 93%, with full width at half maximum (FWHM) bandwidth increases from 13% to 20%. Besides, in order to achieve high peak transmission, the thickness of metallic coverings should be optimized. In consideration of physical mechanism, the step-boosted characteristic of broadband transmission is contributed by the first-order Fabry-Perot (FP)-like cavity resonance supported in the dielectric grating layer along the horizontal direction, while the band-pass transmission is a hybridization resonant mode between the first order FP-like cavity resonance along the horizontal direction and the first-order FP-like cavity resonance along the vertical direction supported in the dielectric grating layer.

9277-47, Session Post

Visible light stealth based on 2D holographic antireflection coatings

Ying Liu, Guozheng Yao, Academy of Armored Force Engineering (China)

Research on visible light stealth began in World War II. The objects covered with thermal electrochromic, photochromic and electrochromic intelligent chromic materials can be concealed by external environment. Another way to make an object invisible is using "meta-material" to guide the light round the object and then propagate along the original direction. No matter which method mentioned above, they all need to introduce light from air into stealth materials. Therefore, it has important implications for research on anti-reflective materials.

The early anti-reflective film is $1/4$ wavelength film and multilayer dielectric film based on the destructive interference principle. In 1967, Bernhard found that the moth eye has a typical micro structure, and this structure can effectively reduce the reflection of surface. In 1973, Clapham et al imitated the moth-eye structure and fabricated antireflection film. It's superior anti reflection performance captured the attention of scientists. Nowadays, various methods have been proposed to fabricate antireflection film with sub-wavelength structures. Unfortunately, most of the fabrication technologies have the shortcomings of high cost, small size, and long production cycle. Holographic lithography is a low-cost method for fabricating large area periodic structures.

Theory suggests that when the period is less than $3\lambda/2$ there are only 0 order and 1 order diffractions. When the period is less than $\lambda/2$, there will be only 0 order diffraction. Therefore, the period of anti-reflection film for visible light is usually smaller than 260nm. As we know, the smaller the structure is, the more difficult the film to be fabricated. So, in this paper, we use holography method to produce two-dimensional sub-micron periodic structures. In this size, optical diffraction effects can not be ignored.

The two-dimensional periodic structure with 300nm and 350nm were fabricated, and the transmission, reflection and diffraction efficiency of oblique incident visible light were tested. Theoretical analysis and experimental results show, as long as the design is reasonable, sub micron structure light will have obvious anti reflection effect on visible light.

9277-48, Session Post

Femtosecond laser pulse-induced periodic surface structures on MgZnO thin films

Hongying Wang, Zhen Cheng, Xi'an Univ. of Arts and Science (China); Hua Guang Cheng, Xi'an Institute of Optics and Precision Mechanics (China); Yuanyuan Li, Xi'an Univ. of Arts and Science (China)

Intensively increasing research activities in the field of laser-induced periodic surface structures (LIPSS) have been studied for past several decades and observed on many types of materials. These structures, also termed as ripples, are usually divided into Low Spatial Frequency LIPSS (LSFL) and High Spatial Frequency LIPSS (HSFL). LSFL are observed with a period λ_{LSFL} close to or somewhat smaller than the irradiation wavelength λ and an orientation perpendicular to the laser beam polarization. These LSFL ripple formation is attributed to surface and bulk plasma wave interference as the key mechanisms underlying the nanostructuring process. HSFL spatial periods significantly is smaller than the irradiation wavelength ($\lambda_{HSFL} < \lambda/2$). These HSFL are always predominantly for transparent materials and their orientations often perpendicular and sometimes parallel to the polarization. The main different mechanisms are mainly involved in interference effects along with transient changes in the optical properties during laser irradiation, second harmonic generation (SHG), excitation of surface plasmon polaritons, or self-organization.

Magnesium oxide (MgO) is a promising material for controlling the optical band gap engineering of the ZnO crystal system. Mg-doped ZnO (MZO) thin films formed by alloying ZnO with MgO showed that the band gap energy varies with the Mg concentration. In this work, high repetition rate femtosecond (fs) laser pulses were employed to produce various nanostructures on MZO thin film with Mg concentration of 1.3 at%, 4.51 at%, respectively. These MZO films were fabricated by radio-frequency magnetron sputtering. By using different laser parameters and irradiation conditions, it is possible to manipulate the shapes and sizes of the nanostructures. The results show that surface ripples structure has been influenced by Mg concentration. Different laser fluence threshold and pulse number were obtained for different Mg concentration of MZO film. The average edge ripple period is in the range at a period of approximately 250 nm-570 nm oriented perpendicular to the laser polarization as well as ripples at a period of about $2.2\lambda_m - 2.5\lambda_m$ running parallel to the polarization are observed. Morphological ripple features measured by scanning electron microscope (SEM) demonstrate that these structures originate from melting and rapid resolidification.

9277-49, Session Post

Compact and high-performance silicon-on-insulator polarization beam splitter based on microring resonator

Junbo Yang, Jingjing Zhang, Suzhi Xu, National Univ. of Defense Technology (China)

A compact polarization beam splitter (PBS) based on a microring resonator is proposed and demonstrated numerically by utilizing the full vectorial mode-matching (FVMM) theory and the coupled mode theory (CMT), which are introduced in the aspects of the width of waveguide, the height of waveguide, the radius of microring, and coupling coefficient, etc. Simultaneously, the finite difference time-domain (FDTD) method, a powerful and accurate method for finite size structure, is chosen to simulate and design this PBS. When TE and TM polarized light at $1.55\mu m$ are launched into the input port simultaneously, the resonator will drop TM polarized light to the drop port and transmit TE

polarized light to the though port. In this way, two orthogonal polarization states are split and transferred to different output ports. The extinction ratio in the order of 10dB is achieved initially based on our recent work. The initial experimental results are also given, which includes three microring resonator with the radius of 15 μ m, 10 μ m, and 5 μ m, respectively. The proposed PBS structure could be utilized to develop ultracompact optical polarization modulating device for large-scale photonic integration and optical information processing.

9277-50, Session Post

Tunable optical properties of gold semi-shell nanoparticles

Xingfang Zhang, Zaozhuang Univ. (China)

The optical properties of gold semi-shell nanoparticles with different shell thicknesses, physical parameters and inter-particle separations are theoretically studied by discrete dipole approximation method. The numerical results show that the extinction resonance wavelength of semi-shell nanoparticle is first blue-shifted and then red-shifted as the shell thickness increases, the shell thickness corresponding to resonance wavelength shifting to opposite direction increases with the increase of dielectric constants of the inner core material and the embedding medium, and with the increase of inter-particle separation between two semi-shell nanoparticles. The shift of the resonance wavelength is ascribed to the mutual interactions between plasmon hybridization and phase retardation. The plasmon hybridization plays an important role as the shell thickness is thin, as the shell thickness get thicker, phase retardation effect will become significant.

9277-51, Session Post

Analysis on polarization characteristics in SiGe/Si optical waveguide gyroscope

Xu Yang, Dongsheng Yang, Guangchen Liu, Hailiang Zhang, Zhongqi Tan, National Univ. of Defense Technology (China)

In this paper, the influence of the polarization characteristics of the SiGe/Si optical waveguide gyroscope on signal detection accuracy is analyzed. The relationship between the polarization, the structural parameters of the ring resonator and the systematic zero drift caused by polarized fluctuation in the resonant waveguide gyroscope was studied. Under certain structural parameters of the system, the system structure parameters are simulated using finite-difference time-domain (FDTD) method, and a matrix method is adopted to derive the relationship between the finesse of cavity, the system parameters such as zero drift and polarization fluctuation noise. Obtain the requirements of high-precision signal detection system for polarization-dependent parameter, which provides a theoretical basis for the decrease of polarization fluctuation noise and the actual build of the system.

9277-52, Session Post

Extraordinary optical transmission in the symmetry-reduced double layer metallic grating structure

Yuzhang Liang, Rui Hu, Mengdi Lu, Wei Peng, Dalian Univ. of Technology (China)

In this paper, a metal-dielectric dual-wavelength spectral filtering

structure based on symmetry-reduced double layer metallic gratings is presented by using FDTD method. The structure symmetry is reduced by alternatively shifting metal nanowires of the top layer metallic grating, rather than changing relative position between the top and down layer metallic gratings. Our proposed structure shows two remarkable narrow band transmission dips at normal incidence, which is distinct different from symmetric one with one dip. The appearance of the two narrowband resonance dips is attributed to different guided mode resonances in the dielectric layer, one corresponding to a symmetric mode, the other corresponding to an antisymmetric one usually not be excited; and thanks to the symmetry breaking, both of these mode can be excited. The influence of different structure parameters on two resonance dips is also investigated. Moreover, the effect of the thickness of the top and down layer metallic grating on two transmission dips is investigated in detail. We find that the thickness of the top layer and down layer metallic gratings have a different role in adjusting the wavelength position of two dip, respectively. The down layer thickness only can tune one of two dips, and the wavelength position of the other dip keep constant with the change of the thickness. Surprisingly, when the down layer thickness achieves certain value, transmission dip can be transformed from two to only one dip even if the existence of symmetry breaking. The physical mechanism of the phenomenon is investigated. The angular tolerance of two transmission dips in this structure with different thickness of the top layer and down layer metallic gratings is also further studied. It is more feasible and convenient to tune the position of transmission dip by modifying the thickness than by changing the period and width of the metal nanowires in the fabrication of some filters device. This work can be used to develop subwavelength metallic-grating-based multi-wavelength and narrow-band spectral filters.

9277-53, Session Post

Tunable dual-band infrared polarization filter based on a metal-dielectric-metal compound rectangle strips array

Biao Chen, Fujian Normal Univ. (China); Xiahui Zeng, Xiyao Chen, Minjiang Univ. (China); Yuanyuan Lin, Yishen Qiu, Hui Li, Fujian Normal Univ. (China)

A tunable dual-band infrared polarization filter has been proposed and investigated in this paper. Based on the perfect absorption characteristic of the metal-dielectric-metal sandwich structure, the reflection spectrum shows filter performance. This filter consists of three layers. The top layer is a compound metal nano-structure array composing of an asymmetrical cross resonator and a rectangle strip. The middle and bottom layer are dielectric spacer and metal film, respectively. The calculated results show that the filter property is closely related to the polarization of incident light. When the light polarization parallels to the long direction of the rectangle strip, two resonant wavelengths (1310nm and 2000nm) are filtered, and in contrast only one resonant wavelength (1516nm) is filtered when light polarization vertical to it. Moreover, we found that the resonant wavelength is strongly depended on the length of the rectangle strip which caused the resonant effect. Therefore, the filter wavelength can be tuned freely for different light polarization by adjusting the length of the corresponding rectangle strip. We can change one or two filter wavelengths at a time or change the three filter wavelengths at the same time. In addition, the calculated results show all the intensities at the filter wavelengths are closed to zero, which implies the filter can exhibit good filtering performance.

9277-54, Session Post

Optical fiber surface plasmon resonance sensor with surface modified gold nanorods for biochemical detection

Lixia Li, Yuzhang Liang, Lingxiao Xie, Mengdi Lu, Wei Peng, Dalian Univ. of Technology (China)

A novel gold nanorods (GNRs) modified optical fiber localized surface plasmon resonance (LSPR) sensor is demonstrated for refractive index sensing. The gold nanorods (GNRs) assembled film as the sensing layer was built on the polyelectrolyte (PE) multilayer modified sidewall of an unclad optical fiber. The sensing strategy relies on the interrogation of the transmission intensity change due to the evanescent field absorption of immobilized gold nanorods on the fiber surface. Under the electrostatic interactions, Poly(allylamine hydrochloride) (PAH)/poly(sodium 4-styrenesulfonate) (PSS) films were formed through layer-by-layer (LbL) assembly by alternately soaking the charged surface of the optical fiber in the aqueous solutions of PAH and PSS. The optical properties and surface analysis of nanorods layer fiber were characterized through transmission measurements and field emission scanning electron microscopy (FESEM). The influence of the thickness of polyelectrolyte films prepared by the LbL technology was investigated. Simultaneously, the feasibility of the proposed film coupled nanorods optical fiber LSPR sensor in monitoring a series of concentration sucrose solutions with different refractive index is examined. The preparation procedure for this LSPR sensor is simple and have outstanding reproducibility. Compared with the traditional optical fiber SPR structure with continuous gold film, the proposed optical fiber LSPR sensor has higher sensitivity. Results suggest that the compact sensor can perform qualitative and quantitative detection in real-time biomolecular sensing.

9277-55, Session Post

Properties of single wall carbon nanotubes array antennas in the optical regime

Xiaofang Wu, Yuesong Jiang, Houqiang Hua, BeiHang Univ. (China)

Single wall carbon nanotubes(SWCNTs) can be metallic, depending on their chirality. For their nanoscale geometric dimension, SWCNTs can be used as antennas to convert high-frequency electromagnetic radiation such as optical radiation into localized energy and vice versa. However, at optical frequencies, traditional antenna design theory fails for metals behave as strongly coupled plasmas. As a matter of fact, an optical antenna responds to a shorter effective wavelength which depends on the material properties and geometric parameters. In this letter, we derived the relationship of effective wavelength with the wavelength of incident radiation for SWCNTs optical antenna, assuming that the SWCNTs can be described by a free electron gas according to the Drude model. Furthermore, the properties of SWCNTs optical antenna are analysed and discussed. SWCNTs optical antenna hold great promise for increasing solar energy conversion efficiency.

9277-56, Session Post

In-line graphene-covered-microfiber polarizer

Xiaoying He, Min Xu, Xiangchao Zhang, Hao Zhang, Fudan Univ. (China)

Graphene has attracted enormous research interest because of

its extraordinary electronic and optical properties. It is a single atomic-layer, and two-dimensional structure with honeycomb crystal lattices. Graphene is a zero band-gap semiconductor, thus giving rise to unique electronic properties such as a high Fermi velocity ($\sim 1/300$ of the speed of light), a vanishing effective mass, a huge electrical mobility, and so on. Such electronic properties make it have particularly interesting applications in electronic devices. Moreover, it has remarkable optical properties, making it become an ideal optical material for realizing multiple functions of signal transmitting, modulating, polarizing, and detecting. Its saturable absorption due to Pauli blocking enables graphene to be used as a saturable absorber in broadband, ultrafast mode-locked lasers in telecommunications. In this paper, a graphene-covered-microfiber polarizer based on the saturable absorption of graphene has been demonstrated. It is found that the broadband polarization extinction ratio is related with the radius-scale of the microfiber. When the radius size of the microfiber is down to $0.8 \mu\text{m}$, its polarization extinction ratio is up to -27dB . Furthermore, the broadband polarization properties has also been presented at the different microfiber radius varied from 0.6 to $0.9 \mu\text{m}$. Numerical calculations reveal its polarization mechanism originates from the differential attenuation of the p-polarized and s-polarized modes, which comes from asymmetric structure of the graphene-covered-microfiber waveguide. Unlike the graphene polarizers based on D-shape fiber, the graphene-covered-microfiber polarizer can support transverse-magnetic-mode surface wave propagation due to asymmetric saturable absorption.

9277-57, Session Post

Dual band filter based on subwavelength metal grating with groove caved in and waveguide layer below

Rui Hu, Yuzhang Liang, Lingxiao Xie, Mengdi Lu, Wei Peng, Dalian Univ. of Technology (China)

Interactions between different resonance modes in optoelectronic structures may introduce coupled modes that can be utilized to explore special optical functions that cannot be realized by conventional methods. A novel dual band filter based on sub-wavelength metal grating with groove caved in and waveguide layer below is proposed in this paper. The metal grating is caved with a groove in the middle of every metal trip, and a waveguide layer with higher refractive index is placed between the metal grating and glass substrate. Using the finite-difference time-domain (FDTD) method, we research the implied physical mechanism by investigating the transmission spectrum with the changing of the structural parameters and the electromagnetic field distributions at some specific wavelengths, such as peaks and valleys in the transmittance. In our simulation, we chose Ag as the grating material and Drude-Lorentz model is employ to describe the dielectric constant. It is found that the two resonance bands are determined by different structural parameters, which due to different mechanism, FP resonance and waveguide resonance, and we also take the groove cavity mode into account when the standing wave oscillates in the groove and result in the dips between two peaks. Besides, the most notable of these features is that the increase of the grating height doesn't shift these two resonance wavelength at all, and groove parameters only move the first peak wavelength regularly, which could be an excellent candidate for dual band filter in the telecom wavelengths. Our proposed structure with subwavelength may provide potential applications in optoelectronic devices.

9277-59, Session Post

Quantum dots with a fluorescence quantum yield close to 100% obtained by modeling the epitaxial shell structure and controlling the shell growth

Pavel Linkov, National Research Nuclear Univ. MEPhI (Russian Federation)

Modern nanotechnological applications in biosensing and optoelectronics demand high-quality fluorescent semiconductor nanocrystals (quantum dots, QDs). Formation of a highly uniform, stable inorganic shell is necessary for synthesizing core/shell QDs with the maximal quantum yield. Current methods of QD shell formation include layer-by-layer precursor deposition, with an intermediate step of its adsorption followed by annealing (successive ionic layer adsorption and reaction, SILAR). This method ensures control over the epitaxial shell thickness and, hence, the optical and energy transfer properties of the QDs. However, the structural model used in SILAR assumes that nanocrystals are spherical, which contradicts experimental data. QDs observed in TEM are nonspherical and vary in shape and crystal lattice type[1]. This is why the SILAR model yields very approximate results.

We suggest an alternative method for depositing epitaxial shells onto wurtzite CdSe QD cores. It is based on mechanistic modeling of CdSe nanocrystal growth using crystallographic data and layer-by-layer addition of CdSe monomers to the growing QD, starting from the stage of an individual CdSe 'molecule' or a more complex nanocluster. We have developed models of layer-by-layer nanocrystal coating that more correctly reflect the QD geometry seen in TEM micrographs and used them for precise calculation of the shell precursor quantities necessary for obtaining QDs with highly uniform epitaxial shells. This allowed us to synthesize QDs with photoluminescence quantum yields close to 100% in a wide spectral range.

[1] Linkov, P., Artemyev, M., Efimov, A., Nabiev, I. (2013) *Nanoscale*, 5, 8781-8798.

9277-60, Session Post

Stimulated emission from polymer distributed feedback waveguide using interference ablation

Bo Zhang, Capital Normal Univ. (China)

A polymer distributed feedback (DFB) laser was fabricated by two-beam interference from MEH-PPV film on clear glass substrate. A direct-writing technique was reported that achieves large-area 1D DFB polymer lasers. The polymer thin film was exposed to a single-shot illumination of the interference pattern of one UV laser pulse at 355 nm. The direct-writing and the lasing character of 1D DFB polymer lasers were demonstrated. The results show the lower threshold and full width at half maximum (FWHM) from DFB polymer laser than slab waveguide. The peak position is tuned by changing the period from 330 nm to 350 nm. The results show that the simple and low-cost technique that enables highly reproducible mass fabrication is required for the easy realization and more profound investigation of the polymer lasers based on the DFB configuration.

9277-61, Session Post

Mid-infrared photonic crystals in silicon and porous silicon

Zhiya Dang, Mark Breese, Agnieszka Banas, Shuvan

Prashant Turaga, Sara Azimi, Dongqing Liu, National Univ. of Singapore (Singapore)

Ion beam irradiation combined with electrochemical etching of p-type Si is a true 3D Si micromachining method. In direct nanobeam writing, a finely focused beam of MeV ions is scanned over the Si wafer surface and as it penetrates the semiconductor, the ion stopping process damages the Si crystal by producing additional vacancies in the semiconductor. By controlling the dosage of the focused beam at different locations, any pattern of localized damage can be built up. The irradiated wafer is then electrochemically anodized in HF electrolyte in which an electric current is passed through the wafer, and p-Si is formed selectively. After removal of p-Si, Si structures are obtained. When the fluence is low enough, the highly damaged region forms high porosity porous silicon instead, and by removing high porosity regions, Porous silicon structures are obtained.

The structures fabricated using this process has been used for mid infrared photonic crystals, the simulation and characterization results show partial or complete photonic band gap in mid infrared range. One advantage of this method is its ability to integrate multiple levels of photonic crystals in one single chip, while the other is the tunability enabled by infiltration of variety of medium into porous silicon and this opens up a potential application in sensors.

9277-62, Session Post

Efficient manipulation of energy flow utilizing graphene plasmonic self-focusing lens

Guoxi Wang, Xueming Liu, Chao Zeng, Xi'an Institute of Optics and Precision Mechanics (China)

The ability to manipulate the optical fields and energy flow of light is at the heart of modern information and communication technologies, as well as quantum information processing schemes. However, because photons are uncharged, it is still elusive to effectively control them by electrical means. In recent years, many metal-based plasmonic devices for subwavelength light management have been proposed theoretically and demonstrated. For example, plasmonic Luneburg lens and Eaton lens are experimentally demonstrated by tailoring the topology of a dielectric layer adjacent to the metal surface.

Different from the metal-based plasmonic lenses, we propose a graphene-based self-focus (Selfoc) lens for manipulating the energy flow of graphene plasmonic (GP) waves in infrared regime. The proposed Selfoc lens can be used to focus and collimate GP waves that propagate along the graphene by appropriately tuning the external gate voltage. In addition, we investigate the dispersion of the proposed Selfoc lens. It is found that such a lens is dispersionless over a wide frequency range. To illustrate the application of the proposed lens, we demonstrate that the image transfer of two point sources separated by a distance of $\lambda_0/30$ (λ_0 is the incident wavelength in vacuum) can be realized on the graphene. The proposed graphene-based Selfoc lens can be flexibly tuned by controlling the external bias voltage and possesses high confinement of SPPs, which paves the way for effectively manipulating energy flow of light at nanoscale.

9277-63, Session Post

Slab-modulated uniform and sampled Bragg gratings in SOI ridge waveguides

Huiye Qiu, Longyan Univ. (China); Ping Yu, Zhejiang Univ. (China); Yuxia Su, Longyan University (China); Xiaoqing Jang, Zhejiang Univ. (China)

We demonstrate uniform and sampled Bragg gratings in silicon-on-insulator ridge waveguides. The sidewall corrugations are designed in the sides of silicon slab of ridge waveguides. Based on this structure, the coupling coefficient κ and the bandwidth $\Delta\lambda$ can be controlled by varying the distance d between the corrugations and the ridge with high fabrication tolerance. The relationships of κ , $\Delta\lambda$ and d are calculated by using coupled-mode theory. Calculated results show that weakly coupling strength can be achieved by choosing a larger d , therefore, larger grating depth can be adapted for small bandwidth. The slab-modulated gratings are fabricated by electron-beam lithography. The thicknesses of the silicon ridge and the slab are 70 nm and 150 nm, respectively. The ridge width is 500 nm and the total width is 1100 nm. The length of the uniform gratings is 500 μm with a period of 294 nm. A bandwidth of 3 nm at the center wavelength of 1550 nm for uniform gratings is measured for our 100 nm slab-sidewall corrugation. The center resonant wavelength shifts 5 nm when the ridge width varies from 490 nm to 530 nm. The sampled grating includes 20 sampling periods, with a burst length of 5.88 μm and a duty cycle of 0.2. The measured transmission spectra of the sampled gratings show five 0.4 nm-bandwidth notches. The measured spacing is about 10.5 nm, which means a group index of about 3.9. The measured results show good agreement with theoretical analyses.

9277-64, Session Post

Analysis of sharpness Fano resonance curve based on eye-like resonator

Xiaowei Lou, wang fan Sr., cui jinjiang II, dong ningning III, xu jiangen IV, tan huiming V, Suzhou Institute of Biomedical Engineering and Technology (China)

For a single ring resonator sensor, this exists the maximum sharpness, appearing at the extinction ratio of -6dB. However, the maximum sharpness of single ring resonator sensor is sensitive for the coupling coefficient. In order to obtain the maximum sharpness, the coupling region of single ring must have a higher precision of manufacture. To solve this problem, this paper propose eye-like resonator which is formed by a ring resonator (named inner loop) embedding in the dual-bus-coupled ring resonator (named outer loop). Eye-like resonators can generate asymmetric Fano-resonance spectrum on the drop port, numerical calculation of spectrum on the drop port is utilized by the transfer matrix method. As the round trip loss varies, the maximum value of sharpness and the corresponding transmission at the resonant point are obtained by tuning the phase ratio of the outer loop to the inner loop, the maximum value of sharpness increases with the round trip loss, as the outer loop and inner loop coupling coefficient changing, the maximum value of sharpness of Fano-resonance change slowly in a wide range. As the round trip loss and the outer loop and inner loop coupling coefficients varies, the corresponding transmission at the resonant point remains almost unchanged, about -6dB. The sharpness of Fano resonant peak is insensitive for the coupling coefficients, which can reduce the requirements of manufacture of coupling region.

9277-65, Session Post

Fabrication of nano-pillar with sub-100nm resolution based on thiol-ene

Man Zhang, Qiling Deng, Lifang Shi, Hui Pang, Axiu Cao, Song Hu, Institute of Optics and Electronics (China)

This paper demonstrates an approach to fabricate nano-pillar based on thiol-ene via soft-lithography. The template is porous alumina membrane with ordered nano-holes with the diameter of 40-70nm. The nano-pillar consists of rigid thiol-ene features on

an elastic poly(dimethylsiloxane) (PDMS) support. It is capable of patterning both flat and curved substrate. The thiol-ene is a new green UV-curable polymer material, including a number of advantages such as rapid UV-curing in the natural environment, low-viscosity, low-cost, high resolution, and high Yong's modulus. First of all, low-viscosity thiol-ene was spinning onto a silicon wafer. Then, an elastic PDMS was placed on the resist-covered silicon wafer and a part of thiol-ene was ahered off the PDMS, which was subsequently placed against the template and cured under UV-radiation. Finally, the template was removed and we obtained nano-pillar on PDMS substrate. Here, we fabricated a two-layer structure using this technique, which included rigid thiol-ene nano-pillar with sub-100nm resolution and soft PDMS substrate. The experiment results show that this approach can be used to fabricate high-resolution features and the thiol-ene is an excellent imprint resist. The fabrication technique in this paper is simple, low-cost, high-resolution and easy to high throughput, which has broad application prospects in the preparation of nanostructures.

9277-66, Session Post

Fabrication of two-dimensional periodic nanocale arrays with tunable absorption bands

Haibin Ni, Ming Wang, Long Li, Tianyi Shen, Nanjing Normal Univ. (China)

We propose a method to fabricate two dimensional periodic nano-arrays in large area with high quality. Sol-Gel co-assembly method was employed to assembly monolayer of highly ordered Polystyrene (PS) microsphere/silica gel arrays. Silica gel was formed in interstitials of ordered PS spheres through sol-gel process during the assembly period. Then PS spheres was partially removed to change the morphology of the nano-array, and followed by sputtering a layer of Ag film on the two dimensional array to complete the fabrication process. SEM image of the fabricated structure was shown in Figure.1(a).

Reflection spectrum of the two dimensional periodic nano-array was measured, and two reflection minima in visual and near infrared range were observed, as shown in Figure. 1(b) and (c). By adjust the morphology of the nano-array and the thickness of Ag film, the two reflection minima wavelength can be continuously tuned in a wide range. For example, covers 400nm-1500nm when periodicity of the array is 690nm. For most wavelength in this range, minima relative reflectivity is less than 5%. Moreover, Figure of merit of the absorption band is about 5, depending both on the morphology of the nano array and Ag film thickness.

Figure. 1 (a) SEM image of fabricated periodic nano-array, (b) and (c) reflection spectra of the nano-array, t is etch time and d is Ag film thickness.

9277-67, Session Post

Kinetic study of self-assembly of multilayer films using a wavelength-interrogation surface plasmon resonance sensor

Zhe Zhang, Jie Liu, Beijing Jiaotong University (China); Zhi mei Qi, Dan feng Lu, Institute of Electronics, Chinese Academy of Sciences (China)

Layer-by-layer self-assembly ultrathin films continue to be of significant interest among researchers for its broad application in diverse areas. Based on electrostatic attraction between materials with opposite charges, multilayer films of (PSS/Cyt c) 6, (GNPs/

Cyt c) 5 and (PDDA/DNA) 6 had been successfully fabricated on the surface of gold chip, respectively. The adsorption processes have been followed by in situ spectral surface plasmon resonance (SPR) technique in real time. The experimental results demonstrate that adsorption of materials onto the gold chip can induce a red shift of resonance wavelength and the amount of adsorption can be determined by the change of resonance wavelength. Kinetics studies suggest that adsorption of cytochrome c (Cyt c) or deoxy ribonucleic acid (DNA) obeys Langmuir-isotherm theory, while adsorption of gold nanoparticles (GNPs) obey diffusion-controlled model. These results also indicate that GNPs need more time to reach adsorption equilibrium than Cyt c and DNA, due to a small value of diffusion coefficient. The resonance wavelength of (PSS/Cyt c)6 shows a good linear increasing with the layer. However, (PDDA/DNA)6 and (GNPs/Cyt c)5 present exponentially increase. Moreover, through controlling the number of assembled layer, the thickness of multilayer films can be designed precisely.

9277-68, Session Post

Electrowetting actuation of a dye-doped fluorescent droplet

Raphael A. Guerrero, Rea Divina C. Mero, Ateneo de Manila Univ. (Philippines)

We report tunable color output from a fluorescent dye-doped droplet actuated by electrowetting. The system design is compact and straightforward, with minimal voltage requirements for effective actuation. Our planar electrowetting set-up employs a bottom electrode prepared by depositing Cu on a glass slide via thermal vapor deposition at a base pressure of 2.6×10^{-5} Torr. A film thickness of 13 nm is achieved with a deposition time of 180 s. The substrate is exposed to the atmosphere at room temperature for 48 h to allow the formation of a thin surface layer of copper oxide. Thickness of the resulting dielectric layer is estimated at 2 μ m. Fluorescent droplets are sourced from a 1 mM solution of rhodamine 6G in distilled water. DC voltage for electrowetting actuation is applied through a Pt wire electrode. Images of the droplet are analyzed for contact angle measurements. Initial contact angle for a dye-doped droplet is 72.1 degrees. At a maximum applied voltage of 20 V, the contact angle decreases to 56.5 degrees. Emission spectra are collected as the droplet fluoresces under UV illumination. The light source for fluorescence experiments is a 25 mW laser with an output wavelength of 355 nm. Over an electrowetting voltage range of 0 to 20 V, the peak fluorescence wavelength shifts from 568 to 546 nm. The tunable fluorescence output from yellow to green, in addition to the variable surface wetting capability, of the droplet has promising implications for display technologies.

9277-24, Session 5

Exciton-polariton laser diodes (*Invited Paper*)

Sven Höfling, Univ. of St. Andrews (United Kingdom) and Julius-Maximilians-Univ. Würzburg (Germany); Christian Schneider, Arash Rahimi-Iman, Julian Fischer, Matthias Amthor, Julius-Maximilians-Univ. Würzburg (Germany); Ivan Savenko, Ivan A. Shelykh, Univ. of Iceland (Iceland); Vladimir D. Kulakovskii, Institute of Solid State Physics (Russian Federation); Stephan Reitzenstein, Technische Univ. Berlin (Germany); Na Young Kim, Martin Kamp, Stanford Univ. (United States); Alfred Forchel, Julius-Maximilians-Univ. Würzburg (Germany)

Polariton lasers do not rely on stimulated emission of cavity

photons, which sets stringent conditions on the threshold current in a conventional laser. Indeed, it has been demonstrated in optically pumped systems, that bosonic polariton lasers can outperform standard lasers in terms of their threshold power. The polaritons, which are part light and part matter quasiparticles, can undergo a condensation process into a common energy state. The radiated light from such a system shares many similarities with the light emitted from a conventional photon laser, even though the decay of the polaritons is a spontaneous process.

We discuss properties of polariton lasers and condensates in GaAs based microcavities. Special emphasis is given to the system's response to an applied magnetic field. We introduce the magnetic field interactions as a reliable tool to distinguish a polariton laser from a conventional photon laser device. In particular, we will discuss the first successful realization of an electrically pumped polariton laser, which marks a promising step towards the exploitation of polaritonic devices in the real world.

9277-26, Session 5

Quantum computing and quantum networking with solid-state single spins and single photons

Chaoyang Lu, Univ. of Science and Technology of China (China)

Single-photon sources based on semiconductor quantum dots offer distinct advantages for quantum information, including a scalable solid-state platform, ultrabrightness and interconnectivity with matter qubits. A key prerequisite for their use in optical quantum computing [1] and solid-state networks is a high level of efficiency and indistinguishability. Pulsed resonance fluorescence has been anticipated as the optimum condition for the deterministic generation of high-quality photons with vanishing effects of dephasing. In this talk, I will describe our recent experiments on generating pulsed single photons from single quantum dots under true s-shell excitation [2]. Pi pulse-excited resonance fluorescence photons show a vanishing (~1%) two-photon emission probability and a Hong-Ou-Mandel interference visibility of ~97%, which were used to demonstrate high-fidelity quantum controlled-NOT gate. Then I will describe methods to generate bandwidth-tunable single photons from spin-flip Raman transitions, and high-visibility quantum interference between single photons from two coherently pulsed driven quantum dots at a distance [3]. Finally, I will discuss our recent results of generating Greenberger-Horne-Zeilinger-type spin-photon entanglement and quantum state transfer between single photons and single spins. Reference: [1] Pan et al. Rev. Mod. Phys. 84, 777 (2012); Cai et al. Phys. Rev. Lett. 110, 230501 (2013). [2] He et al. Nature Nanotechnology 8, 213 (2013). [3] He et al. Phys. Rev. Lett. (2013).

9277-27, Session 5

Inter-triplet spin-spin interaction effects on singlet fission rate

Xianfeng Qiao, Huazhong Univ. of Science and Technology (China)

Singlet fission is a bimolecular process in organic photovoltaic and light-emitting materials maintaining both energy and spin quantum conservations. This process undergoes a spin-correlative intermediate triplet-triplet pair with nine sub-states. Inter-conversion between these sub-state, as a consequence of the competition between spin-exchange and spin-spin interactions within intermediate triplet-triplet pair states, essentially determines the singlet fission rate. An external

magnetic field can modulate the inter-conversion and thus the fission rate, allowing us to reveal the fission process by monitoring the change in fluorescence intensity upon external magnetic field. In this report, we discussed the influences of inter-triplet spin-spin interaction on singlet fission rate by using magnetic field effects of photoluminescence (MFE_PL) based on tetracene.

9277-25, Session 6

A novel structure for electro-absorption modulator based on Ge/SiGe-coupled quantum wells

Yusi Chen, Xiaochi Chen, Yijie Huo, Ching-Ying Lu, Edward T. Fei, Kai Zang, Yangsen Kang, Theodore I. Kamins, James S. Harris, Stanford Univ. (United States)

On-chip optical interconnects are promising candidates for future low-power and high-speed CMOS integrated circuits. A high performance CMOS-compatible modulator is one of the most important components for optical interconnects. In this abstract, a novel electro-absorption modulation mechanism based on coupled-quantum-wells (CQW) is proposed. Compared to a quantum-confined-stark-effect (QCSE) modulator with multiple non-interacting, single-QWs, the newly designed CQW modulator has two sub-quantum wells partially decoupled by a small barrier between them. The modulation mechanism is based on the decoupling of electron and hole wave-functions in the CQWs. State "0" corresponds to the case without any bias voltage, where a large wave-function density overlap results in strong absorption. On the other hand, state "1" corresponds to the case with a small applied electrical field (~1-5kV/cm), where the tremendous decoupling of electron and hole wave-functions due to the center barrier leads to sharp decrease of absorption. In comparison, the operation of a typical QCSE modulator requires an applied electrical field higher than 50kV/cm due to the partial overlap of electron and hole wave-functions at the applied electrical field. The power consumption for this new CQW modulator can be lower than 20fJ/bit, and the calculated speed can be higher than 10Gbps, which outperforms the best Ge/SiGe QCSE modulator to date. A proof-of-concept Ge/SiGe CQW modulator based on this novel modulation mechanism was designed and fabricated. The experimental results are in agreement with simulation. From simulation and experiment, we demonstrate the working principle and modulation effect of such a CQW modulator, which shows great potential as a key component for future on-chip optical interconnects.

9277-28, Session 6

Substrate-blind photonic integration based on high-index glass materials (Invited Paper)

Juejun Hu, Univ. of Delaware (United States)

Traditional photonic integration technologies are inevitably substrate-dependent, as different substrate platforms stipulate vastly different device fabrication methods and processing compatibility requirements. Here we capitalize on the unique monolithic integration capacity of composition-engineered non-silicate glass materials to enable multifunctional, multi-layer photonic integration on virtually any technically important substrate platforms. We show that high-index glass film deposition and device fabrication can be performed at low temperatures (< 200 °C) without compromising their low loss characteristics, and is thus fully compatible with monolithic integration on a broad range of substrates including semiconductors, plastics, textiles, and metals. Application of the

technology is highlighted through two examples: demonstration of high-performance mid-IR photonic sensors on fluoride crystals, and 3-D photonic integration on flexible and stretchable plastic substrates.

9277-29, Session 6

Functional optical devices based on manipulating phoXon by nanostructure (Invited Paper)

Yidong Huang, Kaiyu Cui, Xue Feng, Zhilei Huang, Tsinghua Univ. (China)

Nanostructure can manipulate not only electrons and photons but also phonons, which provides an approach to develop new functional devices.

Phonons can be manipulated by nanostructure to couple with photons. In this work, an optomechanical cavity is proposed based on optomechanical crystals in a nanobeam. Only by adjusting the radius of air holes, an optomechanical coupling rate as high as 1.24 MHz is obtained. Moreover, the nanobeam cavity exhibits a high mechanical frequency of 4.58 GHz with a small effective mass of 96 fg. The typical transmission spectrum of a nanobeam cavity demonstrates a single optical resonance at 1502 nm and a quality factor over 20000.

To further enhance the optomechanical coupling, a hetero optomechanical crystal nanobeam cavity is proposed. This structure confines the optical and mechanical mode with two periodic structures and possesses resonant optical and mechanical mode of 194 THz (corresponding to wavelength of 1.55 μm) and 5.88 GHz with Q-factor of 20000 and 490000, respectively. By concentrating and enhancing overlap of optical field and strain field, the simulated optomechanical coupling rate of the cavity is as high as 1.31 MHz, which, as far as we know, is the highest optomechanical coupling rate reported.

9277-31, Session 6

Floating AC-DEP (dielectrophoretic) manipulations of fluorescent nanoparticle at metal nanostructure for plasmonic applications

Jinsik Kim, Hyun-Joon Shin, Kyo Seon Hwang, Korea Institute of Science and Technology (Korea, Republic of); Jung Ho Park, Korea Univ. (Korea, Republic of)

We proposed the fluorescent nanoparticle manipulations with non-contacted electrodes for plasmonic applications. The floating AC-DEP force was applied to manipulate the fluorescent nanoparticles at the formed metal nano-structures in electrode gap.

The electrode gap was optimized to induce enough floating DEP force around the nano-structure to manipulate the nano particles. 10μm wide gap of electrode was acquired to apply the DEP force at various designed manipulation location of metal nano-structure in the gap of electrodes which is not connected with metal nano-structures.

25 nm zinc sulfide capped cadmium selenide (CdSe/ZnS) QDs (0.8 nM, emission wave-length: 605 nm) and 100nm polystyrene nano bead (1 nM, emission wave-length: 610nm) were used. 100 nm wide gold nano-structures were fabricated with e-beam lithography and lift-off process. Before the formation of metal nanostructure, micro electrodes was fabricated to apply the electric field around the metal nano-structures with photolithography and lift-off process. In the both lift-off processes for nanostructure and micro electrode, 50 nm thick

gold layer with a 10 nm thick chrome layer was deposited using e-beam evaporator at low deposit rate of 0.1 nm/sec to acquire smooth surface.

We applied the 8 Vpp, 3 MHz sine wave to accomplish the positive DEP force and it occur 108 V/m electric field and electric field gradient around gold nanowire with floating AC. The fluorescent nanoparticle's attachment on the nanowire is confirmed by fluorescent optical analysis. The fluorescent nanoparticles are located at designed metal nano-structures for plasmonic applications.

9277-32, Session 6

Characteristics of extinction efficiency factor for PM2.5 particles based on Mie scattering theory

Yan Ni Guo, Liang Chao Li, Xidian Univ. (China)

In recent years, haze has become a new type of environmental disaster, it is also one of the most disturbance factors in remote sensing image. Now, to study the influence of haze on electromagnetic waves has got more and more attention. In this paper, the definition of haze and composition of PM2.5 particles were introduced. And based on Mie scattering theory, the extinction characteristics of single and mixture of PM2.5 particles with different size and refractive index were analyzed. The calculation shows that the extinction efficiency factor of single PM2.5 particle changes with the different particle size and refractive index, the oscillation of extinction curves become obvious with different particle size in the case of weak absorption, when it is strong absorption, this phenomenon will disappear. At the same time, based on the study of extinction efficiency factor for single particle and the equivalent method, it is found that the extinction efficiency factor of a lot of particles increase rapidly with the change of particle sizes, then, it will decrease and tend to a constant. The factor is also associated with the change of the width of particle size distribution and refractive index, usually not monotonous. For external mixture of particles, the extinction curve also relates to the mixing ration for the mixing particles. Because there are many mixture of particles in reality, the study of characteristics of extinction efficiency factor in this paper is significant for the research on the optical characteristics of PM2.5 particles in practice.

9277-33, Session 6

Continuing research on the classical spiraling photon model

Hongrui Li, Shandong Normal Univ. (China)

Based on the classical spiraling photon model proposed by Hongrui Li, the laws of reflection, refraction of a single photon can be derived, the polarization, total reflection, evanescent wave and Goos-Hanchen shift of a single photon can be explained. But it is a unfinished photon model. The spiraling diameter of a photon is not definite. In this paper, we will continue the research work on this new theory. According to the fact that the diffraction limit of light and the smallest diameter of the focal spot of lenses are all equal to the wavelength λ of the light. We can get that the spiraling diameter of a photon equals to the wavelength λ , so we have that the angle between the linear velocity of the spiraling photon θ and the component of the linear velocity in the forward direction θ_b is 45° . And then θ^2 is equal to θ_b^2 plus θ_a^2 (θ_a is the other component of the linear velocity θ . It is perpendicular to θ_b). That is $\theta^2 = \theta_a^2 + \theta_b^2 = 2C^2$ (C is the velocity of light in vacuum and θ_b equals to C). So the energy of a classical spiraling photon $E = (1/2)m\theta^2 = (1/2)m2C^2 = mC^2$. It is coincide with Einstein's mass-energy relation. And also it is obtained that the velocity of the evanescent wave in the vacuum is slower than the

velocity of light in glass in straight line. In this way, the optical fiber can slow the light down.

9277-4, Session 7

Fabrication and characterization of Er silicate compound nanowire light source

Xingjun Wang, Chao Xu, Zhewei Zhang, Zhiping Zhou, Peking Univ. (China)

In recent years, Erbium (Er) silicates and Yttrium (Y) and Ytterbium (Yb) co-doped Er silicates have attracted intensive investigations due to their efficient luminescence at 1.53 μ m. The potential applications are monolithic integrated light emitters or optical waveguide amplifiers for silicon photonics. However, it turned out that its large Er silicate waveguide transmission loss and high pumping power required inhibited the possibility of achieving high gain with device size scaled down. In order to solve the problems, we use single crystal Er-Yb/Y silicate compound nanowires as the waveguide material to reduce the transmission loss due to fewer defects in single crystal nanowire.

We fabricated the Er silicate compound nanowire by a Au catalyzed chemical vapor deposition (CVD) at O₂ atmosphere with ErCl₃ power, silicon powder, and Au catalyzed Si substrate. Various tools are used to analyze the morphology, chemical composition and crystal structure of nanowires, including SEM, EDX, TEM and XRD. SEM shows a relative uniform morphology of these nanowires with diameters of several tens to hundred of nanometers, and length from several to more than ten micrometers. The peaks in the XRD spectrum of pure Er silicate matched with data erbium chloride silicate (Er₃Cl(SiO₄)₂). High-resolution TEM and EDX analysis on shell and core reveals that the nanowires are SiO₂-Er₃Cl(SiO₄)₂ core-shell heterostructures. The 1.53 μ m peak was observed. This property of Er silicate nanowires indicate that it is a promising material for achieving high gain nanowire optical waveguide amplifier and laser.

This work is partially supported by National Natural Science Foundation of China Grant Nos. 61377056, 61036011 and Program for New Century Excellent Talents in University.

9277-30, Session 7

Fabrication of 2 inches nano patterned sapphire substrate with high uniform by two beams laser interference lithography

LongGui Dai, Fan Yang, Mingdong Xuan, Yang Jiang, Hong Chen, Haiqiang Jia, Wenxin Wang, Institute of Physics (China)

Many techniques have been introduced for improving internal quantum efficiency and light extraction efficiency of the GaN-based LEDs, such as epitaxial lateral overgrowth (ELOG), surface roughening, metal mirror reflect layer and patterned sapphire substrate (PSS). Among them, the PSS technique has attracted much more attention, because it can improve both crystalline quality and light extraction efficiency of LEDs. Compared with micro-scale patterned sapphire substrate (MPSS), nano-scale patterned sapphire substrate (NPSS) has better performance in improving the light extraction efficiency of LEDs. Laser interference lithography (LIL) has been adopted to prepare nano-patterns over a large area in recent years. LIL is very flexible to change the period and line width of the nano-patterns. Furthermore, it meets the large area, high efficiency and economy requirements of the industrial NPSS production. In our work, uniform triangle truncated pyramid arrays with period of 480 nm are successfully fabricated on 2 inches sapphire substrate by two beams LIL system using a 325 nm He-Cd continuous wave laser as a light source. Dry etching and wet

etching techniques are ingeniously combined to ensure patterns are transferred precisely without damaging or contaminating the sapphire substrate. The process parameters, pattern morphology and feature sizes are systematically investigated. The deviation is $\pm 5\%$ for the bottom width of the triangle truncated pyramid arrays on the whole sapphire substrate, that is suitable for the application in the NPSS industrial production.

9277-36, Session 7

Developing colloidal I-III-VI semiconductor nanocrystals for light-emitting and display applications

Haizheng Zhong, Beijing Institute of Technology (China)

Currently, lighting consumes 22% of all electricity produced in the world. Phosphor-converted white light-emitting diodes (pc-WLEDs) are excellent candidates to replace incandescent lamps due to the merits of high luminous efficiency, longer lifetime as well as polarized emissions. Colloidal CuInS₂ based nanocrystals exhibit tunable spectroscopic properties with particular properties such as a wide tunable spectral window covering the NIR region (500-750nm), larger Stokes shifts (> 200 meV), broader emissions spectra with full width at half maximum (FWHM), and a longer photoluminescence (PL) lifetime, as well as possible low toxicity and low cost. All of these features might provide ways to enhance the performance of WLEDs and create "smart" lighting systems. Recently, we developed the synthetic techniques to produce high quality CuInS₂ based nanocrystals at tens grams and reported the fabrication of high color rendering (up to ~ 95) and high efficiency (up to ~ 70 lm/W) pc-WLEDs using CuInS₂ based NCs. The thermal degradation effect is a great challenge to achieve the commercialization of NCs based WLEDs. To overcome this challenge, we recently turned to the remote WLEDs encapsulation configuration through integrating CuInS₂ based NCs into composite films. Based on the NCs based color conversion composite films, we successfully designed and fabricated two prototype intelligent remote lighting systems for living room and agriculture lighting using the remote LED configuration. The results show that CuInS₂ based NCs meet the requirements of general illumination and agricultural fill light applications. We believe that current success in materials synthesis and application explorations will pave the way to commercial products.

9277-37, Session 7

High-quality GaAs nanowires epitaxy on patterned Si substrates

Shiyan Li, Xuliang Zhou, Xiangting Kong, Jiaoqing Pan, Institute of Semiconductors (China)

Epitaxial growth of III-V compound semiconductors on Si has attracted significant attention for many years due to the potential for monolithic integration of III-V based optoelectronic devices with Si integrated circuits. There are three major problems for GaAs monolithic epitaxy on Si, respectively the large lattice mismatch, the difference in thermal expansion coefficient, and growth of a polar material on a nonpolar substrate. Various dislocation reduction techniques have been proposed, such as graded SiGe buffer layers, thermal cycles annealing (TCA), and strained-layer superlattices (SLs) as dislocation filters. Unfortunately, these methods generally require relatively thick epitaxial layers and/or complex epitaxial process. This study relates to the heteroepitaxy of GaAs on nanopatterned Si substrates using the selective aspect ratio trapping method. The dislocations originally generated at the GaAs/Si interface are mostly isolated by the SiO₂ side wall. High-quality GaAs nanowires have been grown on Si(001) substrates by metal-

organic chemical vapor deposition. A method of two-step epitaxy of GaAs is performed to achieve a high-quality GaAs layer with a narrow FWHM of HRXRD. Material quality was confirmed by Scanning electron microscope (SEM) and photoluminescence (PL) measurements. We also simulated the distribution of the light field on the nanoscale GaAs layer used the FDTD method. The light field confined well in the 250nm width GaAs nanowire. It can be used in the Nanolasers on Silicon as light sources.

9277-38, Session 7

Measurement of quantum efficiency and doping concentration in InP nanowires

Fan Wang, The Australian National Univ. (Australia); Leigh M. Smith, Univ. of Cincinnati (United States); Qiang Gao, Kun Peng, Yanan Guo, Lan Fu, Hark Hoe Tan, Qiang Gao, Chennupati Jagadish, The Australian National Univ. (Australia)

Semiconductor nanowires are of great interests because of their unique properties that can be exploited for a range of electronic and optoelectronic device applications. However, measurement of the doping levels in nanowires is not trivial and requires complicated and time consuming device fabrication techniques. Internal quantum efficiency (IQE) is one of the most important parameters for characterizing optoelectronic devices. In semiconductor nanowire laser, the lasing threshold depends on IQE. Here we introduce a simple and efficient analysis method, which provides a rapid optical way to simultaneously measure the IQE and doping concentration for semiconductor material.

Power dependent photoluminescence (PL) mapping and lifetime mapping are conducted on Si-doped WZ InP nanowires grown by selective area epitaxy. By analyzing and fitting the integrated PL curves for different excitation power levels, the internal quantum efficiency (IQE) for the section of nanowire illuminated by the laser spot can be evaluated. From the PL intensity decay curve, the non-radiative lifetime and doping concentration can be calculated. This method enables a simple and efficient way to quantify the IQE, non-radiative lifetime and doping concentration distribution along the nanowire, which are directly related to emission brightness, crystal quality and doping efficiency, respectively.

9277-39, Session 7

Ex-situ preparation of high-conductive polymer/SWNTs nanocomposites for structure fabrication

Qingchuan Guo, Reza Ghadiri, Thomas Weigel, Andreas Aumann, Evgeny L. Gurevich, Cemal Esen, Ruhr-Univ. Bochum (Germany); Yan Li, Peking Univ. (China); Wei Cheng, Boris Chichkov, Laser Zentrum Hannover e.V. (Germany); Andreas Ostendorf, Ruhr-Univ. Bochum (Germany)

In this article we present 2PP method to fabricate structures on the basis of conductive photosensitive nanocomposites. For this, we have pursued two different steps. The first step was to develop a homogeneous dispersion of nanocomposites by directly mixing in the polymer and high conductive SWNTs with different concentrations; The second step was using the 2PP effect induced by femtosecond laser pulses to write novel conductive micro- and nanostructures containing SWNTs. The SWNTs can be effectively dispersed directly into the polymer by sonication methods. The conductivity of the nanocomposites was tuned by increasing the concentration of SWNTs. The prepared samples exhibit excellent optical transparency at 2PP processing

wavelength, and can be used by means of 2PP to write structures. Structures with conductivity have been produced based on 2PP processing of polymer/SWNTs nanocomposites.

9277-40, Session 8

Nanostructures for photovoltaic devices (Invited Paper)

Ching-Fuh Lin, Hong-Jhang Syu, Subramani Thiyagu, Chen-Chih Hsueh, National Taiwan Univ. (Taiwan)

The fossil burning had led to the concerns of global warming, dramatic change of weather, and so the increasing attention of alternative renewable energy. Solar energy makes it one of the good choices due to its abundance. Nonetheless, the limited solar intensity makes the deployment of solar panels need a huge area to provide sufficient energy. Thus low cost and high productivity are very important for photovoltaics. Here we report the low-cost approaches to fabricate nanostructures for photovoltaic devices. First, we use organic materials for light absorption and infiltrate them into ZnO nanorods that are grown using solution process. This platform with ZnO nanorods can lead to PCE of more than 7% for several organic polymers. The best one is over 8%. Second, Si nanowires are combined with the organic materials to form p-n junction. The fabrication can also be fabricated using solution process of very low cost. The device so far demonstrated PCE of above 12%. The Si nanowires could significantly reduce the reflection due to the light trapping effect. We also developed a technique based on chemical etching nano-structures to form very thin films of single-crystal Si. The film thickness could be from around 5 μm to 20 μm . The film has very good crystal orientation, almost identical to Si wafer. The rest of the Si wafer can be reused to form more single crystalline Si thin films, so the material cost can be reduced to only 1/10 or less. Details will be discussed.

9277-41, Session 8

ZnO nanorods on optical compact disk for high-efficiency photodegradation of organic compound (Invited Paper)

Din Ping Tsai, Academia Sinica (Taiwan); Yu Lim Chen, I-Da Chiang, Wen Ting Hsieh, Li-Chung Kuo, Min Lun Tseng, Hao Ming Chen, Chih-Kai Chen, National Taiwan Univ. (Taiwan); Hung Ji Huang, Instrument Technology Research Ctr. (Taiwan); Ru-Shi Liu, National Taiwan Univ. (Taiwan)

Environmental protection is one of the most important issues for the better life of mankind in the 21st century. Since 1972, researchers have been working on using semiconductor photocatalyst for chemical deposition reaction. Among the photocatalytic materials, zinc oxide (ZnO) has attracted much attention due to its high photosensitivity, stability, low cost, and wide band gap. For environmental treatment, we have developed a simple process for growing large-area upright ZnO nanorods on the polycarbonate optical disk substrate, while a correspondingly designed photocatalytic spinning disk reactor was fabricated. The photocatalytic activity was evaluated by the degradation of methyl orange dye (MO) as a model compound in aqueous solution. More than 40% of methyl orange can be decomposed within 40 minutes. Less than 8% of the methyl orange remained in the aqueous solution after a 160-minute treatment. The chemical-catalytic durability of ZnO nanorods on the optical disk was also tested. After five repeated and continuous photocatalytic reactions, the efficiency of chemical processing can still maintain more than 90% in 500 minutes and the reaction curves are also unchanged for these assigned

reactions. We believe that this work is very promising for the industrial photocatalytic environmental treatment since optical disks are cheap, readily available and very commonly used in our daily life and the annual production capacity of optical storage disk is nearly 20 billion disks in recent years in Taiwan.

9277-42, Session 8

Ultra-thin film nanostructured gallium arsenide solar cells

Yangsen Kang, Yusi Chen, Yijie Huo, Li Zhao, Jieyang Jia, Huiyang Deng, James S. Harris, Stanford Univ. (United States)

Although the state-of-the-art III-V multi-junction cells have achieved the highest energy conversion efficiency among all types of solar cells, these cells are only applicable to high concentration systems due to high costs of substrates and epitaxial growth. To utilize widespread terrestrial applications, the cost of III-V solar cells has to be driven down. Thus, ultra-thin film absorbers with advanced light management are desired. Here we demonstrate an ultra-thin film nano-structured GaAs solar cell with only 300 nm thick absorber. To enhance the absorption in this thin absorber, this cell consists a nano-textured $\text{Al}_0.8\text{Ga}_{0.2}\text{As}$ window layer on the front side reducing the reflection and trapping the light, as well as a metal reflector on the back side further increasing the light path. The optimized structure demonstrates a spectral averaged absorption of 94% at normal incidence, which is equivalent to 1 μm thick planar film with a perfect anti-reflection coating on the front side and a perfect reflector on back side. Moreover, this cell can achieve over 85% spectral averaged absorption up to 70 degree off normal incidence. All these photon managements result in a 15% increase of short circuit current compared to the control device without nano-structured window. This kind of nano-structured cells requires much thinner absorber, thus reduces epitaxial growth cost and increases yield significantly. On the other side, this ultra-thin cell fabricated via flip-chip bond and epitaxial lift-off can be transferred to cheap flexible substrate, therefore leading to low $\$/\text{W}$ and high kW/kg solar cells.

9277-43, Session 8

Chemical exfoliation and optical characterization of threading-dislocation-free gallium-nitride ultrathin nanomembranes

Rami T. ElAfandy, Mohammed A. Majed, Tien Khee Ng, Boon S. Ooi, Lan Zhao, Dongkyu Cha, King Abdullah Univ. of Science and Technology (Saudi Arabia)

Semiconductor nanostructures, with feature sizes comparable to the length scale of nanoscale physical processes, have generated tremendous scientific interests as well as practical applications stemming from the engineering of low dimensional physics phenomena. Due to the manifestation of quantum effects and the increased surface to volume ratio, these nanostructures acquire unique properties that are, to a great extent, different from their bulk or micron-sized counterparts. Unlike 0D and 1D nanostructures, such as quantum dots and nanowires, respectively, 2D structures, such as nanomembranes, are unrivalled in their scalability for high yield manufacture and are less challenging in the handling with current transfer techniques. Furthermore, due to their planar geometry, nanomembranes are compatible with the CMOS technology. Due to these superior characteristics, there are currently different techniques in exfoliating nanomembranes with different crystallinities, thicknesses and compositions. In this work we

demonstrate a new facile technique of exfoliating gallium nitride (GaN) nanomembranes with novel features, namely with the non-radiative cores of their threading-dislocations being etched away. The exfoliation process is based on engineering the gallium vacancy density during the GaN epitaxial growth with subsequent preferential etching. Based on scanning and transmission electron microscopies, as well as micro-photoluminescence measurements, a model is proposed to uncover the physical processes underlying the formation of the nanomembranes. Raman measurements are also performed to reveal the internal strain within the nanomembranes. After transferring these freely suspended GaN nanomembranes to other substrates, we demonstrate the temperature dependence of their bandgap by photoluminescence technique, in order to shed light on the internal carrier dynamics within the 25 nm thin nanomembrane.

9277-44, Session 8

Remote fluorescence correlation spectroscopy using silver nanowires

Liang Su, Haifeng Yuan, Gang Lu, Katholieke Univ. Leuven (Belgium); Johan Hofkens, Katholieke Univ. Leuven (Belgium) and Univ. of Copenhagen (Denmark); Hiroshi Uji-i, Katholieke Univ. Leuven (Belgium)

Fluorescence correlation spectroscopy (FCS), a powerful tool to resolve local properties, dynamical process of molecules, rotational and translational diffusion motions, relies on the fluctuations of fluorescence observables in the observation volume. In the case of rare transition events or small dynamical fluctuations, FCS requires few molecules or even single molecules in the observation volume at a time to minimize the background signals. Metal nanoparticle which possess unique surface plasmon resonance (SPR) have been used to reduce the observation volume down to sub-diffraction limited scale while maintain at high analyt concentration up to tens of micromolar. Nevertheless, the applications of functionalized nanoparticles in living cell are limited due to the continuous diffusion after cell uptake, which makes it difficult to target the region of interests in the cell. In this work, we demonstrate the use of silver nanowires for remote excitation FCS on fluorescent molecules in solution. By using propagation surface plasmon resonance which supported by the silver nanowire to excite the fluorescence, both illumination and observation volume can be reduced simultaneously. In such a way, less perturbation is induced to the target region, and this will broaden the application of single-cell endoscopy based on plasmonic waveguides.

9277-69, Session 8

ZnTe:O highly-mismatched alloys synthesized by ion implantation for intermediate band solar-cell application

JianDong Ye, Nanjing Univ. (China) and The Australian National Univ. (Australia); Kang Zhen, Shulin Gu, Nanjing Univ. (China); Fan Wang, Hark Hoe Tan, Chennupati Jagadish, The Australian National Univ. (Australia)

The concept of intermediate band solar cell (IBSC) has recently attracted renewed attention to achieve high power conversion efficiency. Highly mismatched alloys (HMAs) such as GaAs:N and ZnTe:O have been employed as an active absorption layer to demonstrate the concept of IBSCs. In this work, ZnTe:O highly mismatched alloys have been produced by isoelectric oxygen implantation into ZnTe and the microstructural and optical properties of ZnTe:O materials have been investigated in detail. The proper dose of oxygen ions led to the formation of

intermediate band located at the energy level of -0.45eV below the conduction band, which is well consistent to that of the presently reported ZnTe:O IBSCs and also in good agreement with the energy level calculated by band anticrossing (BAC) model. High dose of oxygen ions caused ZnTe surface layer amorphous and enhanced the deep level emission around 1.6eV . Time-resolved photoluminescence has shown the carrier dynamics in the extended states of conduction band and the localized states of intermediate band. The lifetime of carriers in IB (?) is 129ps , higher than the lifetime of carriers in conduction band, indicative of localized characteristics of electronic states in the intermediate band. It is resulted from the fluctuations in the local oxygen concentration which produces both energetic and topological disorder in ZnTe. This study demonstrates that the implantation may provide an effective and straightforward way to produce HMAs alloys for IBSCs, and the reduction of lattice disorder is needed to convert localized states of intermediate band into extended states, which is crucial to realize high efficiency ZnTe:O based intermediate band solar cells.

9278-1, Session 1

Artificial magnetic meta-molecules: from three dimensional ring resonators to toroidal metamaterials (*Invited Paper*)

Din Ping Tsai, National Taiwan Univ. (Taiwan) and Academia Sinica (Taiwan); Wei Ting Chen, Pin Chieh Wu, Yao-Wei Huang, Chun Yen Liao, Wei-Lun Hsu, National Taiwan Univ. (Taiwan); Vassili A. Fedotov, Vassili Savinov, Nikolay I. Zheludev, Optoelectronics Research Ctr. (United Kingdom); Ai Qun Liu, Nanyang Technological Univ. (Singapore)

Metamaterials composed of artificial structures in subwavelength scale with extraordinary properties which may not be found in nature, such as negative refractive index and light cloaking. In particular, the negative magnetic permeability arises from the magnetic resonance in metamaterials is attractive to a wide attention due to the innovative optical properties and practical applications. So far, the split-ring resonators (SRRs) have been commonly treated as magnetic meta-molecule for generating artificial magnetism and magnetic interaction between them. Here, we report the three-dimensional SRRs that accompanied with magnetic response excited via normal illumination. By integrating a couple of upright SRRs, the plasmon induced transparency (PIT) as well as toroidal dipolar response is able to be excited and observed. The toroidal resonance is a kind of fundamental resonance mode that differs from electric or magnetic multi-dipole expansion and showing a higher quality factor in its spectral response due to the non-radiating configuration. As a result, we also show a promising way based on the toroidal resonance to approach the lasing spaser application, a coherent light source in a spatial region much smaller than the wavelength. Furthermore, we proposed a three-dimensional toroidal structure that supported toroidal resonance under normal incidence with large incident angle tolerance for more efficient electromagnetic energy harvesting. These properties have promising applications in the field of plasmonics, such as integrated 3D plasmonic metamaterials, plasmonic biosensor and lasing spaser.

9278-3, Session 1

Spatial control of surface plasmon polariton excitation at planar metal surface

Zhichao Ruan, Zhejiang Univ. (China)

Since a flat metal surface is the simplest geometry sustaining surface plasmons, it is of fundamental importance in plasmonics to efficiently excite the SPP field on the surface. The established excitation techniques, including the prism coupling method, have practical significance for applications including surface-enhanced sensing and spectroscopy, plasmonic nonlinear optics, and plasmon optical tweezers.

Here we propose that the SPP excitation on a flat metal surface can be dramatically enhanced by phase modulation of each wave-vector component of an incident light. We show that under a conventional illumination the spatial components of the incident light have destructive interference on the SPP excitation, and it strongly limits the SPP excitation and lowers the field intensity. We demonstrate that the destructive interference can be canceled out by shaping illumination beam with a tailored relative phase for the different wave-vector components. As a consequence, the excited SPP field under the phase-shaped beam illumination is concentrated to a hot energy spot, and the

electric field intensity is enhanced about three folds at the peak in comparison with the conventional Gaussian beam illumination. The proposed phase-shaped beam approach provides a new degree of freedom to fundamentally control the SPP excitation and benefits the development of surface-enhanced applications.

9278-4, Session 1

Plasmonic trapping and manipulation of metallic particles and nanowires and its applications

Changjun Min, Yuquan Zhang, Junfeng Shen, Wei Shi, Nankai Univ. (China); Xiaocong Yuan, Shenzhen Univ. (China)

We propose a novel dynamic plasmonic tweezers for trapping and manipulating metallic particles and nanowires and demonstrate its application on Surface-enhanced Raman scattering (SERS). In the first part, we discuss the interaction mechanism between metallic particles and the sharp peak of surface plasmons (SPs) in the plasmonic tweezers excited by a highly focused radially polarized beam. We show that metallic particles of nanometer to micrometer sizes can be attracted and trapped in such plasmonic tweezers instead of being repulsed by a conventional optical tweezers due to high scattering force. Through numerical analysis, we find that the resultant total force in the plasmonic tweezers is the result not of a stronger gradient force dominating an opposing scattering force, but instead of a dominant gradient force assisted by a weak scattering force acting in the same direction. Next we consider manipulating metallic particles and nanowires by modifying the properties of incident beam in the plasmonic tweezers. We show that metallic particles in plasmonic vortices can be trapped and rotated in a certain radius depending on orbital angular momentum (OAM), and metallic nanowires' position and orientation can be controlled by polarized direction of light. Finally, we introduce the application of the plasmonic tweezers in SERS. By trapping and dragging a single gold nanoparticle with the plasmonic tweezers, we demonstrated a dynamic single-particle-film SERS system, which produces a high SERS enhancement factor of $\sim 10^9$, and therefore provides a promising approach to controllable SERS detection and imaging.

9278-5, Session 1

Manipulating light propagation with geometric metasurfaces: fundamentals and applications

Lingling Huang, Benfeng Bai, Qiao Feng Tan, Guo Fan Jin, Tsinghua Univ. (China); Thomas Zentgraf, Univ. Paderborn (Germany); Shuang Zhang, The Univ. of Birmingham (United Kingdom)

Metasurfaces have shown promising properties for achieving full control of light. Various applications based on metasurfaces have been demonstrated in recent years, such as ultrathin metalens, background-free quarter-wave plates, spin-hall effect of light, and spin controlled photonics. Here, we propose and investigate the principle and applications of a novel class of metasurface with interfacial phase discontinuities under the illumination of circularly polarized light [1-4]. The emitted phase can be continuously controlled in local subwavelength unit cells simply by arranging orientation angles of nanorods. Such metasurfaces show special advantages such as the dispersionless phase modulation, the helicity-switchable property, and the independent control of light phase and amplitude. Several

applications based on such metasurface were experimentally studied and demonstrated, including the generalized law of refraction [1], the generation of broadband vortex beam [1], a dual-polarity metalens [2], a helicity-switchable unidirectional SPP launcher [3], and 3D optical holography [4], as shown in Fig. 1. All these applications show intriguing and superior properties of the metasurface and work in the visible and near-IR range. The ultra-thin metasurface may pave the way towards beam shaping, large capacity data storage, optical information processing, holography-based techniques and so on.

References:

1. Huang L, Chen X, Mühlenbernd H, Li G, Bai B, Tan Q, Jin G, Zentgraf T, Zhang S. *Nano Letters*, 2012, 12:5750-5755.
2. Chen X, Huang L, Mühlenbernd H, Li G, Bai B, Tan Q, Jin G, Qiu C-W, Zentgraf T, Zhang S. *Nature Communications*, 2012, 3:1198.
3. Huang L, Chen X, Bai B, Tan Q, Jin G, Zentgraf T, Zhang S. *Light-Science & Applications*, 2013, 2:e70.
4. Huang L, Chen X, Mühlenbernd H, Zhang H, Chen S, Bai B, Tan Q, Jin G, Cheah K-W, Qiu C-W, Li J, Zentgraf T, Zhang S. *Nature Communications*, 2013, 4:2808.

9278-49, Session 1

Thermal instability in plasmonics (*Invited Paper*)

Ilya A. Fedorov, Moscow Institute of Physics and Technology (Russian Federation); Alexei L. Bogdanov, Western Digital Corp. (United States); Gennady Tartakovskiy, Del Mar Photonics (United States); Sergey Vergeles, L.D. Landau Institute for Theoretical Physics (Russian Federation); Vladimir Parfenyev, Moscow Institute of Physics and Technology (Russian Federation); Andrey Karlovich Sarychev, Institute for Theoretical and Applied Electrodynamics (Russian Federation)

Plasmon nanolasers, also known as SPASERs, were suggested by Bergman and Stockman in 2003. Quantum plasmonics attract much attention in recent years due to the numerous potential applications in the plasmonics. We consider thermal effects in the metal nanoresonator immersed in the active, laser medium. The size of the resonator is much less than the wavelength. The plasmon field inside the nanoresonator operates as a quantum object. Due to the nanosize of the resonator, the internal plasmon electric field is about the atomic field even for few plasmon quanta. The coupling between the plasmon field and plasmon resonator is anomalous strong. We develop the quantum dynamics of the plasmon field and show that the SPASER may be the subject of thermal instability. When number of the plasmon is maintained at the stationary level the loss increases with increasing the temperature of the SPASER. Therefore, the heat generation increases with the increasing the temperature. We have positive feedback and corresponding thermal instability. When the energy, accumulated in the plasmon nanoresonator, exceeds the instability threshold the temperature increases exponentially. We find the increment of the temperature growth and lifetime as function of the loss in metal and the structure of the plasmon resonator. We consider how the thermal instability influence the luminescence and find how the lasing threshold is changed. The coherence of the light emitted by the plasmon laser is also considered. The thermal stability of the nanolaser is important for many applications, such as transmitting and processing optical signals on a scale much smaller than the wavelength.

9278-6, Session 2

Plasmons in atomically thin materials (*Invited Paper*)

Francisco Javier García de Abajo, ICFO - Institut de Ciències Fotòniques (Spain); Alejandro Manjavacas, Rice Univ. (United States)

The recent observation and extensive theoretical understanding of plasmons in graphene has triggered the search for similar phenomena in other atomically thin materials, such as noble-metal monolayers⁸ and molecular versions of graphene.⁹ The single-atom carbon layer features several advantages with respect to more conventional materials, including a large electro-optical tunability and extreme optical-field enhancement, which are suitable building blocks to produce complete optical absorption, extreme light modulation, and ultra sensitive response down to the single-molecule level. Interestingly, these phenomena can be electrically modulated at microelectronic speeds through the use of gating technology. However, plasmons in graphene have only been observed at mid-infrared and lower frequencies, and therefore, small molecular structures⁹ and atomically thin metals⁹ constitute attractive alternatives to achieve fast electro-optical modulation in the visible and near-infrared (vis-NIR) parts of the spectrum. Here, we will discuss the challenges and opportunities introduced by these types of materials, including their application to quantum optics, electro-optical devices, and sensing.

9278-7, Session 2

Manipulation of second harmonic generation from metasurfaces (*Invited Paper*)

Tal Ellenbogen, Nadav Segal, Shay Keren-Zur, Netta Hendler, Tel Aviv Univ. (Israel)

It is well known by now that plasmonic metamaterials (MM) and metasurfaces (MS) can be engineered to have new forms of linear optical response that cannot be achieved with natural bulk materials. In recent years it was shown that MM and MS can also be engineered to have large second order optical nonlinearities. Naturally it was investigated as a new means to generate active nonlinear optical devices, including all-optical switches, efficient frequency converters, etc. However, despite these efforts, not many active devices were demonstrated to date. In addition, the nonlinear generation efficiency of the studied MMs is still not comparable to conventional nonlinear optical materials, which makes it unattractive for applications.

In this work we employ concepts from the fields of phased array antenna theory and nonlinear photonic crystals to shape the second harmonic generation (SHG) near-field and far-field radiation properties from arrays of split ring resonators (SRRs). We show by numerical models and experimentally that the emission can be directed and that the emission direction can be controlled by changing the properties of the arrays or by changing the wavelength of the exciting beam at the first harmonic. This can be used as a new form of all-optical nonlinear scanner based on extremely thin metasurface. In addition, the ability to direct the nonlinear emission is used by us to demonstrate experimentally focusing of the SH from the metasurface without the need of an additional lens. Using this structure, we achieved almost two orders of magnitude intensity enhancement at the focal point. These methods open the door for development of new integrated nonlinear active devices based on MS and provides a major step forward towards the development of efficient nonlinear metamaterials.

9278-8, Session 2

Free-standing chiral plasmonics

Eunice Sok Ping Leong, Jie Deng, Siji Wu, A*STAR Institute of Materials Research and Engineering (Singapore); Eng Huat Khoo, A*STAR Institute of High Performance Computing (Singapore); Yanjun Liu, A*STAR Institute of Materials Research and Engineering (Singapore)

Chiral plasmonic nanostructures offer the ability to achieve strong optical circular dichroism (CD) activity over a broad spectral range, which has been challenging for chiral molecules. Chiral plasmonic nanostructures have been extensively studied based on top-down and bottom-up fabrication techniques. Particularly, in the top-down electron-beam lithography, 3D plasmonic nanostructure fabrication involves layer-by-layer patterning and complex alignment, which is time-consuming and causes many defects in the structures. Here, we present a free-standing 3D chiral plasmonic nanostructures using the electron-beam lithography technique with much simplified fabrication processes. The 3D chiral plasmonic nanostructures consist of a free-standing ultrathin silicon nitride membrane with well-aligned L-shape metal nanostructures on one side and disk-shape ones on the other side. The free-standing membrane provides an ultra-smooth metal/dielectric interface and uniformly defines the gap between the upper and lower layers in an array of chiral nanostructures. Such free-standing chiral plasmonic nanostructures exhibit strong CD at optical frequencies, which can be engineered by simply changing the disk size on one side of the membrane. Experimental results are in good agreement with the finite-difference time-domain simulations. Such free-standing chiral plasmonics holds great potential for chirality analysis of biomolecules, drugs, and chemicals.

9278-9, Session 2

Nonlinear graphene plasmonics

Andrey Gorbach, Univ. of Bath (United Kingdom)

Graphene is a purely two-dimensional form of carbon, where atoms are arranged in a honeycomb lattice. Recent studies of graphene reveal its great potential for applications in photonics and optoelectronics. In particular, graphene supports surface plasmons in mid-infrared and terahertz range, where metals have no significant plasmonic response. Also, recent experimental and theoretical studies of graphene report that it could have the highest optical nonlinearity among known materials.

In this work, theoretical approach is developed for analysis of nonlinear wave phenomena in plasmonic guiding structures with graphene. The approach is based on asymptotical expansion of Maxwell equations with nonlinear boundary conditions. Self-focusing of TE and TM surface plasmons is considered in a dielectric-graphene-dielectric structure. The nonlinearity due to graphene was found to be dominant for highly localized TM plasmons. The corresponding nonlinear coefficient reflects the unique surface-only structure of nonlinear polarization in graphene. On the contrary, relative contribution of dielectric substrate/cladding to the overall nonlinearity becomes comparable to and even dominant over graphene nonlinearity for weakly localized TE plasmons. The nonlinear coefficients due to dielectric substrate and graphene have similar structure in this case. Based on this analysis, the general expression for the effective χ -3 tensor for graphene is derived. It is demonstrated, that when considering nonlinear response of graphene, the effective thickness is much larger than the actual thickness of the graphene sheet.

9278-10, Session 2

Coherent perfect absorber based on metamaterials

Guangyu Nie, Quanchao Shi, Zheng Zhu, Harbin Engineering Univ. (China); Jinhui Shi, Harbin Engineering Univ. (China) and Southeast Univ. (China)

Recently, metamaterial has attracted much attention due to its unique electromagnetic properties that do not occur in natural materials. In this work we achieve a selective perfect absorption in ultra-thin metamaterials as a result of coherently controlled electromagnetic responses by placing metamaterials at a node or anti-node of the standing wave interference pattern. The standing wave is formed by two coherent counterpropagating beams, the signal and control beams. Here we will mainly investigate the coupling mechanism of bilayered metamaterials with a standing wave and the selective coherent perfect absorption in bilayered metamaterials by the two coherent beams. The metamaterials consist of bilayered asymmetrically split rings (ASR) with different twist angles 0° and 180° , spatially separated by a very thin dielectric substrate. Electric and magnetic dipolar excitations can be selectively enhanced or eliminated when the ASR is placed at the antinode and the node of the standing waves, meaning that the phase difference of the signal and control beams is 0° and 180° . The simulated results show that coherent perfect absorption can be realized at three different frequencies and in particular each one can be switched on/off depending on the phase difference between the signal and control beams. In comparison with 50% absorption in the single-layer ASR metamaterial, the coherent perfect absorption occurs with larger than 90% absorption. In summary, we realize an ultra-thin subwavelength coherent perfect absorber that holds much more flexibility operating at any frequency ranging from microwave to optical regimes. The response of metamaterials can be coherently tailored by easily changing their position in the standing wave.

9278-11, Session 2

The focusing properties of the spiral plasmonic lens

Jiaming Li, Jie Li, Shan Huang, Feng Lin, Peking Univ. (China); Xing Zhu, Peking Univ. (China) and National Ctr. for Nanoscience and Technology of China (China)

We systematically investigate the focusing properties of the spiral plasmonic lens fabricated on gold film with different parameters, such as the chirality of the incident light, the pitch of the spiral and the incident light wavelength. The surface plasmon polaritons distribution on the film is analytically calculated as vortex field of the Bessel beam. The three-dimensional finite-difference time-domain (FDTD) simulation demonstrates that when the chirality of the incident light and the spiral is opposite, not only when the ratio between the pitch of the spiral and the SPPs wavelength equals to 1, the plasmonic lens can focus the incident light into a focal spot at the surface, But when the ratio is the close to 1 (about 0.5--1.5), there will be a focal spot near the center of the spiral, and the focal spot will shift with the ratio along a fixed direction in nanoscale. Also, we found that when the ratio between the pitch of the spiral and the SPPs wavelength is an integer (except for 1), there will be a doughnut shape with a dark center corresponding to a first-order, or a higher-order evanescent Bessel beam at the center. And we provided a theoretical formula for the topological change of the vortex field. The focusing properties are verified experimentally using a scanning near-field optical microscopy (SNOM) for different structural parameters. The experimental result agree with the theoretical result very well. Our studies are useful to understand the physical mechanism of the plasmonic focusing and have many potential applications for the nano-scale plasmonic devices.

Work supported by National Science Foundation of China (Grant nos. 61176120, 61378059, 11374023)

9278-12, Session 3

Light produces a nano-forest of trees as metamaterials (*Invited Paper*)

Satoshi Kawata, Osaka Univ. (Japan) and RIKEN (Japan)

There have been a variety of methods proposed for the fabrication of metamaterials. Among them we have proposed and reported three-dimensional laser drawing of micro/nano structures based on two-photon photo-polymerization [1] and the selective metal coating on the fabricated polymer structures [2]. We also invented direct two-photon photo-reduction of metal structures in three dimensions [3]. The resolution of the structure is less than a hundred nanometers. In this presentation, after the review of such drawing methods I will discuss about the laser-beam induced self-growing of structures [4], and show our latest results of self-grown three-dimensional metamaterials [5]. Three-dimensional nano-structures made of silver as dendrite have been grown under the light illumination. The structures are fractals of different orders and kinds. We discuss about the fractal dimensions of the structures and show the applications of them to surface enhanced Raman scattering analysis with many of pictures of nano-forests.

References

- [1] S. Kawata, H.-B. Sun, T. Tanaka, K. Takada, Finer features for functional microdevices-Micromachines can be created with higher resolution using two-photon absorption, *Nature* 412, 697-698, 2001.
- [2] F. Formanek, N. Takeyasu, T. Tanaka, K. Chiyoda, A. Ishikawa, S. Kawata, Selective electroless plating to fabricate complex three-dimensional metallic micro nanostructures, *Appl. Phys. Lett.* 88, 083110, 2006.
- [3] Y.-Y. Cao, N. Takeyasu, T. Tanaka, X.-M. Duan, S. Kawata, 3D Metallic Nanostructure Fabrication by Surfactant-Assisted Multiphoton-Induced Reduction, *Small* 5, 1144-1148, 2009
- [4] S. Shoji, S. Kawata, Optically-induced growth of fiber patterns into a photopolymerizable resin, *Appl. Phys. Lett.* 75, 737-739, 1999.
- [5] N. Takeyasu, N. Nishimura, S. Kawata, submitted.

9278-13, Session 3

Coupling between silver nanowire and single quantum dots (*Invited Paper*)

Hongxing Xu, Institute of Physics (China)

Surface plasmons provide the ability to enhance the weak interaction between individual quantum emitters and photons for quantum information applications. The generation of single plasmons by coupling Ag NW with single quantum emitters opens the prospects of using quantum optical techniques to control single SPs and designing novel quantum plasmonic devices. Here we study the coupling between a Ag NW and individual quantum dots (QDs). By controlling the QD-NW separation distance, the coupling strength can be controlled. By using an atomic force microscope to manipulate a silver nanoparticle to create a nanogap between a Ag NW and a Ag nanoparticle, the efficient coupling of the QD in the nanogap with the Ag NW is demonstrated by the enhanced emission intensity and the reduced fluorescence lifetime. We also experimentally realize resolving single plasmons generated by two QDs on a silver nanowire. The accurate positions of the two QDs with separation ranging from microns to 200 nm within the diffraction limit are determined by using super-resolution imaging method.

The efficiency of plasmon generation due to the exciton-plasmon coupling is obtained for each QD.

9278-14, Session 3

An infrared biosensor based on graphene plasmonic for integrated nanofluidic analysis

Wei Wei, Jinpeng Nong, Zhu Yong, Guiwen Zhang, Chongqing Univ. (China)

We propose an infrared biosensor for nanofluidic analysis based on graphene plasmonics, which consists of an inverted trapezoidal nanochannel etching on a silicon substrate and a graphene sheet covered on the top of the structure. The change of refractive index due to the absorption of biomolecules in the nanochannel can be detected by measuring the wavelength shifts of resonant dips. An optical model based on finite element method is built. The sensitivity and the accuracy of the sensor are evaluated in detail and the factors that affect these performances, including the apex angle, the height, the opening width of the nanochannel and the Fermi energy level of graphene, are also investigated. Numerical simulation results shown that an increasing of the apex angle and the opening width or decreasing of the height and Fermi energy level can give rise to the red-shift of the operating wavelength and the increasing of the sensitivity. However, the transmission curves broaden, resulting in a lower accuracy. In addition, a high sensitivity value of up to 2500nm/RIU can be achieved in an optimized structure. Such a biosensor combining the merits of graphene plasmons and the adsorption of biomolecules may provide a brand new idea for designing infrared sensor in future nanofluidic analyzing applications.

9278-15, Session 3

Silicon-based extraordinary transmission through nanohole array with gain media

Mehdi Afshari, Zhiping Zhou, Peking Univ. (China)

After discovery of extraordinary transmission subwavelength hole arrays structures patterned on a metal film have generated wide interest as they offer high optical transmission and strong localized electric near-field intensities. However, the large ohmic losses exhibited by SPs in the optical regime represent a fundamental limitation that reduces drastically the practical applicability of EOT properties. Furthermore, not compatible with CMOS platform make it difficult for application purposes. As a possible solution to this fundamental problem, gain medium have been introduced to compensate the loss created by metallic film. But the most important yet challenging requirements for gain material are to be CMOS compatible and working at telecommunication regime.

The aim of this paper is to theoretically study optical amplification of EOT properties in periodic hole arrays incorporating optically pumped gain media. The gain media was selected Erbium/Ytterbium(Er/Yb) silicate that is CMOS compatible with photoluminescence peak at telecommunication regime. Use of Er³⁺ ions has the advantages of proven, stable, and low-noise operation at the technologically important 1.54 μ m region. To excite the active material a laser with a maximum power of 372 mW at the wavelength of 1480 nm is applied.

Geometrical parameters was obtained by solving the surface plasmon dispersion relation on periodic hole arrays. The condition for lossless propagation was obtained analytically. Simulation results shows that for lossless propagation we will need higher gain value. By considering higher gain values the absorption was approached to zero and 5.5 dB transmission enhancements was observed at telecommunication wavelength.

9278-16, Session 3

Effective model for plasmonic coupling: theory and experiment

Meng Qiu, Bin Xi, Shiyi Xiao, Hao Xu, Lei Zhou, Fudan Univ. (China)

Plasmonic couplings between nanoparticles generate fascinating physical phenomena, which can be utilized to realize certain applications. However, theoretical understandings on such problems are relatively behind experimental developments. Most theoretical efforts are based full wave simulations, which are not only computational complicated but also physically less transparent. A complete effective model accounting for both electric and magnetic dipole terms in plasmonic nanoparticles, derived from a rigorous ground, is highly desired and is the key motivation of present work.

Based on the generalized tight-binding method for dispersive photonic media and a multiple-expansion technique, we derived an analytical model for plasmonic coupling coefficient between two NPs, which includes all interacting terms between electric and magnetic dipoles of the NPs, such as the standard dipolar interactions between electric and magnetic dipoles in different NPs, the electric dipolar interaction contributed from radiation effect, and the interaction between electric and magnetic dipoles.

We performed full-wave simulations and microwave experiments on particular plasmonic coupled systems to verify the effective model, which show that our effective model can well describe the plasmonic coupling behaviors in general cases. In particular, when the NP is large enough so that a quasi-static approximation is no longer valid, one has to take the radiation correction term into account to reasonably describe the plasmonic coupling behaviors, and the EM cross-interaction term is crucial to explain an intriguing mode-sequence reversal effect discovered in particular coupled NP systems. In addition, we found that the coupling strength between certain plasmonic nanoparticles can be tuned through varying the orientations of NPs, leading to interesting phenomena such as ultra-slow-wave plasmon propagation.

9278-17, Session 4

Unusual optical force and torque acting on plasmonic objects (Invited Paper)

Che Ting Chan, Hong Kong Univ. of Science and Technology (Hong Kong, China)

Light can exert optical force and torque on any object it encounters. It is commonly assumed that light should move a particle forward. We found that under some special circumstances, light can pull instead of push. For example, non-diffracting beams can pull particles with simultaneous electric and magnetic responses. Chirality can also facilitate optical pulling force. The optical force acting on a chiral particle is different from an achiral particle due to chirality dependent terms which couple mechanical linear momentum and optical spin angular momentum and such coupling can serve as a mechanism to achieve the optical pulling. We also demonstrate chirality can facilitate light to push sideways. We found that an anomalous lateral force can be induced in a direction perpendicular to that of the incident photon momentum if a chiral particle is placed above a substrate that does not break any left-right symmetry. Analytical theory shows that the lateral force emerges from the coupling between structural chirality (the handedness of the chiral particle) and the light reflected from the substrate surface. Such coupling induces a sideways force that pushes chiral particles with opposite handedness in opposite directions. We will also address the phenomenon of "negative optical torque", meaning that incoming photons carrying angular momentum rotate an object in the opposite sense. Surprisingly this can

be realized quite straightforwardly in simple structures. Field retardation is a necessary condition and discrete rotational symmetry of material object plays an important role. The optimal conditions are explored and explained.

9278-18, Session 4

Plasmon and compositional mapping of plasmonic nanostructures in two and three dimensions (Invited Paper)

Emilie Ringe, Rice Univ. (United States)

Recently, co-reduction of Au and Pd has allowed the synthesis of complex Au core/AuPd shell nanoparticles with elongated tips and cubic-like symmetry. Optical studies have shown strong plasmonic behavior and high refractive index sensitivities. In this paper, we describe the composition and the near-field plasmonic behavior of those complex structures. Electron tomography, coupled with monochromated STEM-EELS, Cathodoluminescence, and EDS mapping reveals the different resonant modes in these particles, and shows that Pd, a poor plasmonic metal, does not prevent strong resonances and could actually be extremely helpful for plasmon-enhanced catalysis.

9278-20, Session 4

Multi-coloring and light harvesting in transparent organic solar cells

Qin Chen, Long Wen, Suzhou Institute of Nano-tech and Nano-bionics (China)

Organic solar cells (OSCs) incorporated with multi-coloring capabilities and high efficiencies open a route to the integration into building decorations and electronic display equipment, which dramatically extends solar energy applications. However, the transmission spectra of transparent OSCs are currently dominated by the active layer properties, suffering from not only low efficiencies due to light transmission or reflection loss but also the poor color purities. In this paper, we proposed a multi-colored transparent OSC based on PCPDTBT-PCBM containing a metallic nanodiscs-patterned dielectric/metal/dielectric transparent conductive electrode. The short-circuit current densities under AM1.5G illumination are 38-58% higher than the reference semi-transparent cells and up to 87-100% that of their opaque counterparts. The high efficiencies are due to the marked suppression of transmission loss at the off-resonance wavelengths and the increased light harvesting in the photoactive layer, i.e. light guiding in photoactive layer and broadband backward scattering from the metallic nanostructures. Simultaneously, the luminosities are at the same level as the reference semi-transparent cells and the color purities have been significantly improved due to the resonant transmission induced by the metallic nanodiscs. Full-gamut coloring and luminosity adjusting for the transmission light can be achieved by simply tuning the period and the filling factor of the metallic nanodiscs. The results show promising potential in the building integrated photovoltaics and self-powered colorful electronic display devices.

9278-39, Session Post

Research on the plasma Yagi-Uda nanoantenna with backfire

Jie Wang, Yumin Liu, Zhongyuan Yu, Hongbo Lv, Changgan Shu, Chunwei Ye, Beijing Univ. of Posts and Telecommunications (China)

Plasmonic antenna has been a hot topic over the past years. Plasmonic antenna is a device that can effectively collect light energy and control optical radiation at sub-wavelength scale. The backfire antenna is one of the plasmonic antennas which have been applied into the radio frequency field for a long time. However, it is seldom taken into consideration in the nanophotonic field until recently. The backfire technique is applied from the design of Yagi-Uda antenna. The geometric model of Yagi-Uda is composed of four parts: director, reflector, feed and electric dipole. The backfire antenna adds a large reflector in front of directors. The electric dipole is resonated to near metal particle and generates localized surface plasmon (SPP) that causes high location electric field enhancement. The cavity between larger and small reflector sustains a propagating SPP that bounces back and forth. In the end, the wave propagates toward to the small reflector. In this paper, we make a study on the directive gain, one of the most important parameters of backfire antenna, compared with Yagi-Uda antenna. The results indicate that the backfire antenna improves the directive gain evidently. Then, in order to better understand the possibility of antenna performance, we investigate how the directive gain is affected by tuning the parameters such as the size of reflector, feed, and directors. The model is numerical simulated by using the finite element method. The antenna structure is optimized further and the maximum directive gain increases up to 2.6 times. In the end, the Yagi-Uda antenna with tapering directors and backfire is also studied. To the fixed number directors of Yagi-Uda antenna with backfire, it has an optimized tapering angle to get the maximum directive gain.

9278-41, Session Post

Tunable terahertz switching based on chiral metamaterial

Tingting Lv, Harbin Engineering Univ. (China); Jinhui Shi, Harbin Engineering Univ. (China) and Southeast Univ. (China); Guangyu Nie, Quanchao Shi, Zheng Zhu, Harbin Engineering Univ. (China)

We present the first demonstration background-free THz switch in a photoactive chiral metamaterial based on polarization conversion. Here, we create an ultrathin switchable THz metamaterial constructed of an array of 90°-twisted asymmetrically split ring apertures (ASRAs) with incorporated photo-conductive silicon. The orthogonal arrangement of two stacked resonators makes the metamaterial chiral due to the cross coupling between the magnetic and electric responses. The hybridized metamaterial allows us to effectively tune the cross-polarization transmission by controlling the conductivity of the active material using external optical stimuli. The THz metamaterial exhibits a photoexcited mode-switching effect and a tunability of the resonant frequency is about 11%. The transmitted wave in our proposed metamaterial exhibits relatively high purity of polarization that is different from input signal and optical background. The underlying mechanism of the observed polarization effect and the photoexcited mode-switching effect can be well understood by Born-Kuhn model and surface current distributions at resonant modes of the cross-polarization transmission peaks. Current driven around ASRAs by the incident wave is electromagnetically coupled to the current around the ASRA of the second layer. The induced current in the second layer is then reemitted into the transmitted wave with a

different polarization state. For the two cases of no pump and strong pump, resonant modes of the metamaterial at the cross-polarization transmission peaks further investigate the physical origin of the photoexcited mode-switching effect. The proposed THz metamaterials provide a new mechanism of mode switching to control THz wave propagation and are beneficial in designing polarization devices.

9278-42, Session Post

Substrate-mediated charge transfer plasmons in simple and complex nanoparticle clusters

Ziwei Li, Zheyu Fang, Peking Univ. (China)

A conductive substrate can provide a simple and straightforward way to induce charge-transfer plasmon modes in Au nanoparticle clusters. For a simple dimer structure, a remarkably narrow charge transfer plasmon, which differs dramatically from the dipolar plasmon mode of the electrically isolated nanostructure, is clearly observed. For a more complex nonamer cluster that supports a strong Fano resonance on an insulating substrate, a mixed charge transfer-dipole mode is observed, where charge transfer is induced on the outer nanoparticles, establishing an opposing dipole on the intervening central particles, resulting in a strongly damped far field response.

9278-43, Session Post

Gold nanoparticles extraction from dielectric scattering background

Xin Hong, Jingxin Wang, Zheng Jin, Dalian Univ. of Technology (China)

The ability visualize, track and quantify molecules and events directly inside living cells with high temporal and spatial resolution is essential for understanding biological systems. The most commonly used approaches to do this are based on the detection of the fluorescently labeled molecules. The major drawback of fluorescent markers is that after a finite number of photocycles they will convert to a non-fluorescent state there by limiting the available observation time. The unique advantages such as brightness, non-photobleaching, good bio-compatibility make gold nanoparticles desirable labels and play important roles in biotech and related research and applications. Gold nanoparticles provide superior alternatives to fluorescent markers. A method have detected individual nanoparticles down to 5 nm in diameter. Then the challenge in extracting these nanoparticles is however the small amplitude of the expected signal and they submerge in the dielectric scattering background. Here we propose a dual-wavelength detection method by employing a high sensitive cross-polarization microscopy. We conduct a scanning imaging experiment in the same optical system with a couple of wavelengths, one of them is 633nm which can excite localized surface plasmon resonance phenomenon, and another is 532nm. We can distinguish gold nanoparticles from other dielectric scattering particles after dealing with the images and comparing them. The attraction of this new method lies in the fact that it can extract individual nanoparticles from the dielectric scattering background effectively and it will have wide application in biomedical field.

9278-44, Session Post

Beam manipulation in bilayered gradient metamaterials

Quanchao Shi, Guangyu Nie, Zheng Zhu, Harbin Engineering Univ. (China); Jinhui Shi, Harbin Engineering Univ. (China) and Southeast Univ. (China)

We demonstrate beam manipulation in an ultrathin chiral metamaterial- so called metasurface, based on a gradient phase change along the metamaterial surface. The metamaterial is composed of a dielectric spacer layers and two metallic layers that are perforated with asymmetrical split ring apertures. The geometries of two metallic layers are identical but arranged by a twist angle of 90°. The orthogonal arrangement of two asymmetrical split ring apertures(ASRAs) give the metasurface a chiral characteristics that promises highly efficient polarization conversion and suppresses copolarization transmission. In this work, the beam manipulation phenomenon requires a metamaterial with phase discontinuities, i.e. a constant phase shift along the metamaterial surface. To control beam steering, a key aspect is to achieve a phase changes within a range of 0-360°. The proposed metasurface relies on eight ASRAs in a super cell to modulate the phase of transmitted waves. Our proposed metasurface is capable of partially scattering the incident wave into an orthogonally polarized wave. By tuning the geometry parameters of eight ASRAs, phase gradient of 0-360° can be realized for the cross-polarization transmitted waves in a super cell so that the transmitted waves can be refracted toward a prescribed direction. Numerical simulation results indicate that varied phase discontinuities on the metasurface modify the wavefront of the transmitted beam and the linearly polarized incident wave can be deflect in a designated direction after passing through the metasurface having a subwavelength scale. The metamaterials with phase discontinuity provide many opportunities to developing beam shaping or beam steering devices.

9278-45, Session Post

Chiroptical activity of planar plasmonic nanostructures

Huang Tao, Jiaming Li, Feng Lin, Peking Univ. (China); Xing Zhu, Peking Univ. (China) and National Ctr. for Nanoscience and Technology of China (China)

In order to improve the detection sensitivity of molecular conformation by chiroptical spectroscopic techniques, it is important to study the interaction between chiral molecules and surface plasmons. Planar nanoarrays can excite surface plasmons, but they usually cause a very large circular dichroism contribution in the circular dichroism spectroscopy, which is far greater than that of chiral molecules and makes reliable circular dichroism measurements difficult. We will present our new nanostructure to overcome this difficulty.

In this work, a new chiral planar periodic plasmonic nanostructure with special arrangement of achiral nanoholes has been designed. We arranged four nanoholes as a unit of parallelogram and then arrayed these units periodically. Even though the individual nanohole is achiral, the effect of each unit is chiral, resulting in the chirality of the whole structure. The circular dichroism of this plasmonic nanostructure is simulated by Finite Different Time Domain method. The results show that this kind of chiral structure can have a circular dichroism contribution about 10-100mDeg, which is in the level of chiral molecules. Then we have prepared this kind of planar periodic plasmonic nanostructure by electron beam lithography and will measure its circular dichroism by circular dichroism spectroscopy to prove our simulation results. This kind of nanostructure would lay the

foundation for reliable circular dichroism measurement when chiral molecules and surface plasmons interact.

Work supported by National Science Foundation of China (Grant nos. 61176120, 61378059, 11374023)

9278-46, Session Post

Plasmonic focusing in spiral nanostructures under linearly polarized illumination

Jie Li, Jiaming Li, Feng Lin, Xing Zhu, Peking Univ. (China)

In this work, a simple way was given to realize surface plasmon focusing with Archimedes spiral nanostructure, which can break through the limitation of just using circular polarization light. We first experimentally validated that a spiral plasmonic lens can focus circular polarization light with a given handedness while simultaneously defocus the circular polarization of the opposite chirality. Then we used scanning near-field optical microscope(SNOM) and finite difference time domain(FDTD)simulation to study the relations between pitch of the spiral lens and the interference pattern. It's found that when pitch $d \neq \lambda$, there will be a ring with a dark center spot in the middle of the structure, and with the increase of the pitch the diameter of the ring will become larger and larger. Further, instead of circular polarized light, we tried to use linearly polarized light to realize surface plasmon focusing. It's demonstrated that spiral plasmonic lens with certain pitch can focus surface plasmon by using linearly polarized illumination regardless its polarization directions. In FDTD simulation the full width at half maximum of the focal spot is around 200nm, while it is about 250nm in SNOM detection under 671nm incident light. For a better physical insight into this problem, FDTD simulations were used to investigate the influence of the structure parameters of the spiral lens such as the size, the number of turns, and the width of the spiral slot. The focal spot intensity at the center of structure can be modulated by these parameters and then we gave the cause analysis.

This work is supported by National Science Foundation of China Grant nos. 61176120, 61378059, 11374023?

9278-47, Session Post

Film-coupled log-periodic optical antennas for near-infrared light absorption

Yuzhou Tian, Ding Zhao, Qiang Li, Min Qiu, Zhejiang Univ. (China)

In nanostructure, localized surface plasmon resonance promotes the research of plasmonic absorber, leading to various kinds of the absorbance structures and promising applications. Absorption properties of film-coupled log-periodic optical antennas with three-layered metal-insulator-metal (MIM) architecture nanostructure in the near-infrared region are numerically investigated. The parameter of the structure unit decreases to 0.5 μ m, several times smaller than the previous studies. After optimizing the relevant parameters, the maximum absorption for TE and TM polarizations at normal incidence reach to 95% and 93%, respectively, and the optimal absorption of around 90% can be simultaneously obtained for both cases. It is shown that the main absorption peak is independent to light polarizations at normal incidence. Moreover, the log-periodic antenna-assisted absorption represents distinct polarization selectivity at high-order resonances, leading to potential applications in spectrum filtering and polarization detecting. 35% and 40% of the absorption difference can be achieved with different parameters, respectively. For oblique incidence, only the incident light of specific wavelengths within a narrow incidence

angle can be almost entirely trapped inside the absorber, indicating special direction and wavelength selectivity of the absorber. Additionally, to further explain the superiority of this log-periodic morphology, we have also studied the nanostructure of the same sizes without any trapezoidal configuration, i.e., regular triangle antennas. The grooves in the structure play a decisive role in high absorption properties, contributed by much higher charge density and stronger resonance. Proposed nanostructured absorber would offer a great potential to biosensing, photovoltaic technology, integrated device, nonlinear optics, etc.

9278-48, Session Post

High-efficiency reflective metasurface-based broadband meta-hologram

Wei-Yi Tsai, Wei Ting Chen, Kuang-Yu Yang, National Taiwan Univ. (Taiwan); Chih-Ming Wang, National Dong Hwa Univ. (Taiwan); Yao-Wei Huang, Pin Chieh Wu, National Taiwan Univ. (Taiwan); Greg Sun, Univ. of Massachusetts Boston (United States); Shulin Sun, Lei Zhou, Fudan Univ. (China); Ai Qun Liu, Nanyang Technological Univ. (Singapore); Din Ping Tsai, Academia Sinica (Taiwan) and National Taiwan Univ. (Taiwan)

Holograms are the optical devices to reconstruct pre-designed images, which have been advanced dramatically with the development of today's nanotechnology. However, applications of hologram are still limited by the constituent materials, and their working range is narrow relatively. Over the past decade, plasmonic metamaterials have attracted many attentions, they perform strong variations in their reflectance and/or transmittance spectra accompanied with dramatic optical phase modulation due to surface plasmon resonances. In this paper, we reported the high-efficiency meta-surface and meta-hologram with broadband working frequencies. By using plasmonic metamaterials, the application of holographic devices can be expanded into arbitrary frequency regions, and much functionality is allowed. We utilized the phase modulation at plasmonic resonance of gold cross-nanoantennas to record two polarization-controlled images on a meta-hologram. Our meta-hologram is reflective type with significantly higher efficiencies than what have been designed and achieved so far using metamaterials. Our reflective hologram also has many advantages such as simple fabrication process, low metal absorption, broad working spectral range, and greater tolerance to variation of incident angle and light incoherence. Finally, the meta-hologram can potentially be used to realize active hologram at arbitrary frequency by combining with the techniques of tunable metamaterials.

9278-21, Session 5

Aluminum plasmonics (*Invited Paper*)

Naomi J. Halas, Rice Univ. (United States)

The field of plasmonics has been built almost exclusively around the properties and applications of noble and coinage metals. For large-area and commercial applications, however, new plasmonic media are needed to satisfy the large demand and cost constraints of the marketplace. Aluminum, the third most abundant element in the earth's crust, is a highly attractive metal suitable for plasmonics, with the additional advantage of CMOS compatibility, allowing for its seamless integration into electronics manufacturing technology. We examine the properties of Al plasmonic nanostructures unique to this metal in several contexts. The plasmon resonances of Al plasmonic nanostructures primarily span the UV and visible regions of

the spectrum[1], supporting plasmon modes whose resonant energies are extremely sensitive to the bulk oxide content of the metallic nanostructure[2]. Applications of Al plasmonics in active devices such as photodetectors can provide a new route to spectral filtering and selectivity in such devices. Exploiting the chromaticity of Al plasmonics for color displays has its unique challenges due to the dielectric properties of Al, however, mechanisms for inducing narrowband resonances resulting in a vivid color response are possible using multiple approaches. A variety of synthesis/fabrication routes to Al nanostructures have recently emerged, creating new opportunities for the use of this metal in new and unanticipated plasmonics applications.

1. M. W. Knight et al., Nano Letters 12, 6000-4 (2012).
2. Nicholas S. King et al., ACS Nano 8, 834-840 (2014).

9278-22, Session 5

High-aspect-ratio SiNW arrays with AgNPs decoration for SERS applications (*Invited Paper*)

Minghui Hong, Jing Yang, National Univ. of Singapore (Singapore); Jinghua Teng, A*STAR Institute of Materials Research and Engineering (Singapore)

This research work aims to address the critical issues of sensitivity and reproducibility in SERS applications by optimizing the aspect ratio of SERS substrates based on SiNWs. Laser interference lithography is applied to fabricate highly periodical nanostructures, which contributes to more uniform signals over a laser patterned substrate. By controlling the reaction time of metal assisted chemical etching,[1] various aspect ratios of 3D SiNWs are obtained. Ag nanoparticles are decorated on the SiNWs to make SERS active substrates. The high SERS sensitivity is demonstrated by the measurement of Raman spectra of analyte molecules adsorbed on the 3D plasmonic SERS structures. As the height of the SiNWs increases, the higher aspect ratio is obtained. The light scattering inside the structures is more intense. Meanwhile, there are more analyte molecules located within the detection volume.[2] These two effects contribute to higher chances for light-matter interaction and thus lead to better SERS performance. However, the light trapping effect is also enhanced for higher SiNWs, which prevents the collection of the SERS signals. An optimized height of SiNWs needs to be obtained on this tradeoff.

9278-23, Session 5

Colloidal silver nanoparticle films as uniform SERS substrates for quantitative detection

Hung-Ying Chen, Meng-Hsien Lin, Chun-Yuan Wang, National Tsing Hua Univ. (Taiwan); Yu-Jena Chang, National Taiwan Univ. (Taiwan); Gwo Shangjr, National Tsing Hua Univ. (Taiwan)

Surface enhanced Raman spectroscopy (SERS) has received much attention due to its great potential for ultrasensitive detection even at the single molecular level. However, quantitative SERS measurements are still restricted by the poor uniformity of available SERS substrates. Here, we demonstrate that colloidal Ag nanoparticle films can be utilized as uniform SERS substrates. The close-packed Ag nanoparticles in these films allow the formation of regular dense arrays of "hot-spots", which can dramatically enhance the Raman signal in "hot-areas". We find that this bottom-up method for fabricating tunable SERS substrates is quite simple, robust, and scalable. Therefore, it can become an attractive approach for quantitative SERS

applications.

9278-24, Session 5

Green-synthesized plasmon-tuned silver nanoparticles for fiber optic ethanol sensing

Balasubramanian Karthikeyan, National Institute of Technology, Tiruchirappalli (India); Renganathan B. Balusamy, Indian Institute of Technology Madras (India); Dillibabu Sastikumar, National Institute of Technology, Tiruchirappalli (India)

We report chemical free and eco-friendly synthetic route using herbal plant *A.indica*, which functioned as an effective reducing and capping agent for the synthesis of silver nanoparticles (Ag NP's). Silver nanoparticles formation is confirmed through surface Plasmon absorption which is identified from its optical absorption studies. Strong band situated around 420 nm is attributed to SPR. With increase of the concentration of Ag salt, the full width at half maxima (FWHM) of the SPR band is reduced and correspondingly the peak intensity is increased. Functional groups present in the crude neem extract are analyzed by using FTIR studies. These particles are coated on a partially clad removed fiber and used for ethanol sensing. This particular sensing is based on the intensity based fiber optic sensing one. It is found that the particles responded well for the ethanol. We analyzed completely, concentration dependent sensing properties also.

9278-25, Session 6

Bimetallic nanostructures and their plasmonic properties (*Invited Paper*)

Jianfang Wang, The Chinese Univ. of Hong Kong (Hong Kong, China)

Plasmonic metal nanocrystals have received much attention owing to their attractive plasmonic properties. Their plasmon resonance wavelengths can be synthetically varied. Their absorption/scattering cross-sections normalized against their physical sizes are larger than those of atoms, ions, molecules, and semiconductor nanocrystals. Upon resonant excitation, they can concentrate light into near-field regions close to the metal surface. Moreover, the local density of photonic states around metal nanocrystals are largely enhanced around their plasmon wavelengths. These plasmonic features have enabled a number of applications with metal nanocrystals in a wide range of areas, such as imaging, sensing, nanomedicine, enhancement of linear and nonlinear optical signals, optics and optoelectronics. Bimetallic nanostructures combine together two different metals. They can provide properties and functions that are impossible from monometallic nanocrystals. In this presentation, I will focus on our recent studies of bimetallic nanostructures, including their preparation, plasmonic properties, and applications on sensing and plasmon-enhanced catalytic reactions.

9278-26, Session 6

Design and sensing applications of 2D plasmonic nanosheets (*Invited Paper*)

Wenlong Cheng, Monash Univ. (Australia)

Over the past two decades, substantial progress has been made in the controlled synthesis of plasmonic nanoparticles with controlled sizes and shapes by wet chemistry approaches.

As such, I have proposed for the first time "plasmonic periodic table" to draw analogy to atoms. However, unlike atoms for which chemists can manipulate almost at will, it remains a grand challenge how to manipulate artificial "plasmonic atoms" into highly-ordered arrays (superlattices). Using soft ligands including DNA, polymer surfactants, we have recently obtained free-standing, monolayered superlattice sheets in their ultimate thickness limit.

Here, I will discuss our recent research activities in interfacing hard plasmonic nanoparticles with soft ligands including DNA, polymer and alkyl molecules, particularly, focus on building the thinnest possible plasmonic nanoparticle superlattice sheets using plasmonic atoms from the artificial periodic table. Firstly, I will describe synthesis of high-quality "hard" plasmonic nanoparticles (including nanospheres, nanorods, nanocages, nanocubes, and nanowires). Secondly, I will cover the conjugation of "soft ligands" to "hard" particles as well as controlled assembly into free-standing thinnest possible superlattice nanosheets by virtue of DNA, polymer, and small molecule. Thirdly, I will describe our experimental and theoretical studies on plasmonic and mechanical properties of 2D superlattices.

9278-27, Session 6

Extreme light absorption architectures for solar-to-fuel conversion (*Invited Paper*)

Isabell Thomann, Shah M. Bahauddin, Hossein Robotjazi, Chloe Doiron, Rice Univ. (United States)

Concepts from metamaterials, plasmonics and nanophotonics are expected to be highly beneficial for the design of future solar energy conversion devices. Here, I will describe how we use these concepts to design advanced photoelectrode architectures for two challenging photocatalytic reactions: water splitting and CO₂ reduction. We focus on the light management aspect in extremely thin absorber structures to achieve broadband omnidirectional solar absorption while carefully choosing materials systems that allow for efficient charge separation and catalytic activity.

I will discuss the benefits of employing thin-film absorber photoelectrodes, which include the potential for enhanced charge carrier extraction, increased photovoltages and the possibility to exploit hot carriers for purposes of driving chemical reactions. I will also discuss our analytical models and three-dimensional electromagnetic simulations that we employ to meticulously engineer light absorption in two-dimensional materials and plasmonic metal nanostructures. Complementing these materials and device design efforts, we are developing an experimental characterization toolbox, including photoelectrochemical techniques and ultrafast spectroscopic techniques that will allow us to analyze the influence of distinct plasmon-induced effects (e.g., near-field concentration, hot charge carriers, heat generation) and non-plasmonic effects (e.g., sample morphology, catalytic and electronic effects, charge separation and recombination) on photocatalysis.

9278-28, Session 6

Polyaniline-modulated plasmonic modes in single gold nanorods and coupled gold nanospheres

Qifeng Ruan, Nina Jiang, Lei Shao, Jianfang Wang, The Chinese Univ. of Hong Kong (Hong Kong, China)

Active plasmonic structures with controllable plasmonic resonance properties open up a new dimension for plasmonics in both fundamental research and practical applications. The integration of plasmonic nanostructures with active materials

contributes to the fabrication of plasmonic circuits, chemical/biological sensors, smart windows, and information displays. Herein, we describe the uniform coating of polyaniline (PANI) on colloidal Au nanocrystals at varying thicknesses through surfactant-assisted chemical oxidative polymerization. By tuning the proton-doping level of the PANI shell, we can modulate the plasmonic properties of Au nanocrystals resulting from the remarkable change in the dielectric function of the surrounding PANI layer. The longitudinal plasmon resonance of single Au nanorods exhibits up to 10-dB scattering intensity modulation depth and 100-nm scattering spectral shift when the PANI shell is switched between the proton-doped and undoped states. We also prepared PANI-coated Au nanosphere homodimers with a series of interparticle distances and shell thicknesses. The transmutation of plasmon hybridization in the homodimers with varied interparticle distances under both states was observed by dark-field scattering measurements in conjunction with TEM imaging. With the assistance of finite-difference time-domain simulations, we clarified the evolution of the bonding dipolar mode and the emergence of the bonding quadrupolar mode. The peak wavelength difference between the bonding dipolar modes under the doped and undoped states was found to be negative-exponentially dependent on the interparticle distance. Our (Au nanocrystal core)/(PANI shell) nanostructures will facilitate the design and fabrication of high-performance plasmonic switches for programmable chromic materials, sensitive pH sensors, and reversible active plasmonic devices.

9278-29, Session 6

Double-layer gold gratings as refractive index sensors and unidirectional couplers for surface plasmon polariton

Chongjun Jin, Yang Shen, Sun Yat-Sen Univ. (China)

Double-layer gold gratings have been widely investigated for their application in metamaterials. Here we show that double-layer gold gratings can be served as localized surface plasmon resonance based refractive index sensors with ultimate figure of merit (FoM), and unidirectional couplers for surface plasmon polaritons (SPP) under normal incidence. We propose and demonstrate two-dimensional double-layer gold gratings (plasmonic gold mushroom array) as refractive index sensors with a FoM value of 108[1]. This plasmonic gold mushroom array is used to detect alpha-fetoprotein with a detection limit down to 15 ng/ml. We also experimentally demonstrate a simple structure (dislocated double-layer gold grating) as an high efficiency unidirectional coupler for SPP. The dislocated double-layer gold grating consists of a slanted dielectric grating sandwiched between two gold gratings. The upper gold grating has a non-zero lateral relative displacement with respect to the lower one. Numerical simulations show that a grating structure with 7 periods can convert 49% of normally incident light into surface plasmons, with a contrast ratio of 78 between the powers of the surface plasmons launched in two opposite directions. We explain the unidirectional coupling phenomenon by the dislocation-induced interference of the diffracted waves from the upper and lower gold gratings. Furthermore, we developed a simple and cost-effective technique to fabricate the structure via tilted two-beam interference lithography and subsequent shadow deposition of gold. The experimental results demonstrate a coupling efficiency of 36% and a contrast ratio of 43[2]. The relatively simple periodic nature of our structure lends itself to large-scale low-cost fabrication and simple theoretical analysis.

[1] Yang Shen, et al., Plasmonic gold mushroom arrays with refractive index sensing figures of merit approaching the theoretical limit, *Nature Communications*, 4, 2381(2013). DOI: 10.1038/ncomms3381.

[2] Tianran Liu, Yang Shen, Wonseok Shin, Qiangzhong Zhu, Shanhu Fan, Chongjun Jin, Dislocated double-layer metal gratings: an efficient unidirectional coupler, submitted to *Nano*

letters.

9278-30, Session 7

Nonlinear plasmonic metamaterials (Invited Paper)

Anatoly V. Zayats, King's College London (United Kingdom)

The enhanced nonlinear optical response can be facilitated using metals as active media. From this point of view, plasmonic structures are very promising for ultrafast all-optical applications at low light intensities providing both ultrafast nonlinear response and its enhancement. Hyperbolic metamaterials, in particular those based on plasmonic nanorod arrays, provide wealth of exciting applications providing designed linear and nonlinear properties, polarization control, spontaneous emission control and many others. Experiments and modeling have already demonstrated very strong Kerr-nonlinear response and its ultrafast recovery due to the nonlocal nature of the plasmonic mode of the metamaterial, so that small changes in the permittivity of the metallic component under the excitation modify the nonlocal response that in turn leads to strong changes of the metamaterial transmission. Such nonlinearities can be specifically engineered for a required wavelength range by changing the nanostructure parameters. Coupled plasmonic nanoparticles have also been proposed as a means to propagate energy through linear chains of closely coupled nanoparticle chains, while still maintaining sub-wavelength lateral widths. In this talk, we will discuss recent progress in experimental studies and numerical modelling of second- and third-order nonlinear optical processes in plasmonic metamaterials. Such nonlinear metamaterials provide a new class of optical media for ultrafast strongly-nonlinear processes, with numerous applications in optical communications, extraordinarily sensitive optical spectroscopies and sub-wavelength imaging technologies.

9278-31, Session 7

Nanoscale optical investigation of electronic properties of carbon nanotubes (Invited Paper)

Prabhat Verma, Osaka Univ. (Japan)

Single-walled carbon nanotube (SWNT) can show either semiconducting or metallic character, depending upon its configuration. Interestingly, Raman spectroscopy can distinguish between the two through the presence of Fano-interaction between the phonons and the free charge carriers, which is a signature of the metallic character. It is known that the electronic properties of SWNTs can change with deformation, which can be very interesting for devices where one would like to play around with the electronic properties. However, usual Raman microscopy cannot reveal the localization of such changes. In fact, the semiconducting SWNTs can locally show metallic characteristics even with a slight deformation, such as the one caused by the pressure of one SWNT crossing over the other in "X" shape. The effect, however, is extremely localized. We present TERS investigation of extremely localized semiconductor-to-metal transition of SWNTs in such a situation, where we can see how the Fano-interaction grows towards the junction and is localized within a few nanometers of its vicinity. At the same time, we have also discovered that new Raman modes appear in the same area near the junction, confirming extremely localized physical distortion of the nanotubes due to the pressure applied on one nanotube by the other. After exploring the deconvoluted components of the G-band Raman mode, we were able to reveal the change in electronic properties of a SWNT at extremely high spatial resolution of 15 nm along its length.

9278-32, Session 7

Toward active control of THz waves using graphene-based metasurfaces (*Invited Paper*)

Lei Zhou, Fudan Univ. (China)

Metasurfaces are ultra-thin metamaterials composed by artificial planar meta-atoms arranged in some specific macroscopic orders, and were found to exhibit extraordinary capabilities to control electromagnetic (EM) waves. However, so far the realized systems are all passive devices. Here, we combine graphene with meta-surfaces to achieve active control of EM waves in THz domain. We experimentally demonstrate that a maximum reflection phase change of 360 degrees can be achieved with such a device via changing external gate voltage. Our discovery paves the road for many applications in THz domain, some of which will be discussed with more details in the conference.

9278-33, Session 7

Highly-efficient photonic spin-hall effect and SPP couplers based on gradient metasurfaces

Shulin Sun, Qiong He, Shiyi Xiao, Weijie Luo, Wujiong Sun, Lei Zhou, Fudan Univ. (China)

Manipulating light in a controllable manner is highly desired in photonics research. To achieve this aim, recently researchers began to work on inhomogeneous metamaterials (MTMs) with complex macroscopic orders, particularly a class of planar metasurfaces (ultra-thin MTM layers) with tailored EM responses. Such meta-surfaces were found to exhibit strong abilities to control light propagations, leading to amazing physical effects such as anomalous refraction/reflection [1-4], propagating-wave to surface-plasmon-polariton (SPP) conversion [3], and flat-lens focusing [5]. In this talk, we will introduce our recent progresses along this direction. In particular, we will show how to realize highly efficient photonic spin-hall effect and high-efficiency SPP couplers based on metasurfaces. Both concepts and experimental realizations will be introduced.

References:

- [1] N. Yu, P. Genevet, M. A. Kats, et al.. *Science* 334, 333 (2011).
- [2] X. Ni, N. K. Emani, A. Kildishev, et al. *Science* 335, 427 (2012).
- [3] Shulin Sun, Qiong He, Shiyi Xiao, et al. *Nature Materials* 11, 426 (2012).
- [4] Shulin Sun, Kuang-Yu Yang, Chih-Ming Wang, et al. *Nano Letters* 12, 6223 (2012).
- [5] X. Li, S. Xiao, B. Cai, et al. *Optics Letters* 37, 4940 (2012).

9278-34, Session 7

Enhanced anti-Stokes one-photon luminescence from a single plasmon resonant nanoparticle

Guowei Lu, Yingbo He, Peking Univ. (China); Keyu Xia, Macquarie Univ. (Australia); Hongming Shen, Yuqing Cheng, Kebin Shi, Yun-Feng Xiao, Qihuang Gong, Peking Univ. (China)

Surface enhanced anti-Stokes one-photon luminescence is observed from a single gold nanorod, which is interestingly comparable to that of the Stokes. The anti-Stokes emission is found to be strongly related to both the state density of free

electrons and the localized surface plasmon resonances. The experimental results demonstrate that the plasmon resonances contribute to both excitation and emission in the photoemission. To explain the feature of light emission process, an analytical model is proposed by treating a single gold nanorod as a plasmonic resonator with quantized field, and it shows a good agreement with the experimental observations. Further experiments confirm the model by tuning the resonance frequency of the same particle, through either photo-thermal re-shaping or environmental index changing. Our experimental observation and the theoretical model provide a new view angle to understand the plasmon photoemission process.

9278-35, Session 8

Quantum plasmonics and plexcitonics (*Invited Paper*)

Peter Nordlander, Rice Univ. (United States)

In the talk, I will discuss various quantum mechanical effects in plasmonic and plexcitonic systems and how they can be exploited in applications: such as nonlinear optical devices; to induce chemical reactions in molecules physisorbed on a nanoparticle surface; to inject electrons directly into the conduction band of a nearby substrate; and to dramatically enhance the light harvesting efficiency of photonic devices.

9278-36, Session 8

Quantum description of coupled plasmonic systems (*Invited Paper*)

Xiaoguang Li, Shenzhen Institute of Advanced Technology (China); Ququan Wang, Wuhan Univ. (China); Zhenyu Zhang, Univ. of Science and Technology of China (China)

We carry out a combined experimental and theoretical study of the nonlinear optical responses of strongly coupled hybrid Fano systems consisting of gold nanorods decorated with near-infrared dye molecules. We show that, in the weak external field regime, the absorption rate of the hybrids at the Fano dip decreases as the concentration of the dye molecules increases, signifying effective suppression of the linear absorption around the dip. In the strong field regime, the severely suppressed linear absorption around the Fano dip in turn allows one-photon nonlinear responses to be readily revealed and drastically tuned by the photon energy, laser power, and dye concentration. These striking observations are interpreted within a microscopic model stressing on two competing processes: saturated plasmonic absorption of the nanorods and weakened destructive Fano interference from the bleached excitonic absorption of the molecules. Our findings offer new insights into the underlying physical principles of such strongly coupled plexcitonic systems and provide a promising strategy to the fabrication of plasmonic nanodevices with both pronounced nonlinearities and good figures of merit.

9278-37, Session 8

Plasmonic crystals from 1D to 3D fabricated by focused ion beam milling

Guangyuan Si, Northeastern Univ. (China); Jiangtao Lv, Northeastern Univ. (China); Fengwen Wang, Northeastern Univ. (China)

We show the fabrication of plasmonic crystals from 1D to 3D using focused ion beam milling. As typical examples, 1D gratings

with large aspect ratios, 2D nanoholes and nanorings with tunable profiles and 3D nanostructures with complex geometries are demonstrated, respectively. The fabricated devices are both theoretically and experimentally characterized and good agreement is achieved. Our approach may find extensive applications for plasmon related nanophotonics and optics.

9278-38, Session 8

Directional and enhanced spontaneous emission with corrugated metal probe

Hongming Shen, Guowei Lu, Yingbo He, Yuqing Cheng, Peking Univ. (China); Haitao Liu, Nankai Univ. (China); Qihuang Gong, Peking Univ. (China)

The topic of controlling emission direction has been investigated for various nanostructures, such as Yagi-Uda antenna, nanowire, compact nanodisk dimer, or even single nanoparticles. Yet, a critical problem for dipolar optical emitters placed on a dielectric substrate is that the main beam directed into the substrate is largely confined around the critical angle, leading to poor directivity. Here a 3D tapered metallic probe corrugated with several concentric gratings is proposed and exploited systematically. We calculate the angular radiation pattern, local field distribution, and quantum efficiency to quantify the excitation and emission gain to the overall spontaneous emission enhancement. The corrugated probe provides a powerful platform to tailor the single-molecule emission intensity and far-field emission direction for high collection efficiency, simultaneously. The simulation results show that the emission from a single oriented dipole coupled to the corrugated probe is highly directed into a cone with a narrow emission angle, which overcomes the limit of critical angle, and present significant fluorescence enhancement factor. The enhancement factor is nearly 55 times higher than that of a bare tip due to high directivity and contribution from the local excitation gain. Another remarkable point is the wavelength and separation dependence of the angular distribution pattern of the spontaneous emission, which provides a way for directional sorting of fluorescence and increasing of signal-to-noise ratio. These findings make a promising route to the development of corrugated antenna based spontaneous emission manipulation for a wide range of novel applications, such as in analytical chemistry, light emission devices, and tip enhanced fluorescence and Raman spectroscopy techniques.

Thursday - Saturday 9 -11 October 2014

Part of Proceedings of SPIE Vol. 9279 Real-time Photonic Measurements, Data Management, and Processing

9279-1, Session 1

Signal processing for linearized analog photonic transmission (*Invited Paper*)

Lianshan Yan, Zhiyu Chen, Southwest Jiaotong Univ. (China)

Transmitting analog signals over photonic links has been considered to be a promising technique for many applications, such as avionics, modern electronic warfare, and wireless communication systems. However, polarization effect, fiber Kerr effect, chromatic dispersion (CD) and RF nonlinearity are four major challenges for high-performance analog photonic links (APLs). The first two impairments will lead to the signal degradation, while the third one may induce the periodic power fading and the last one could produce serious third-order intermodulation distortions (IMD3). Therefore, APL needs to be optimized according to different requirements in various applications. In this paper, we firstly have established a propagation model based on coupled-mode theory and the small-signal analysis, and provided the general expressions for signal evolution along the standard single-mode fiber (SMF) links. Such model could describe the interaction of polarization effect, CD and nonlinearity. Afterwards, we have investigated different compensation schemes to enhance the linearity of the APL by using optical signal processing and digital signal processing, such as nonlinearity compensation based on a phase modulator (PM) combined with an optical filter, simultaneous compensation for CD and nonlinearity by using mixed polarizations, and linearized microwave downconversion link based on cascaded PMs or using post-processing technique. The results show that the spurious-free dynamic range (SFDR) of the APL could be improved significantly after compensations.

9279-2, Session 1

Coherent optical frequency-comb-based wideband signal channelization and analog-to-digital conversion (*Invited Paper*)

Feifei Yin, Yitang Dai, Jianqiang Li, Kun Xu, Jintong Lin, Beijing Univ. of Posts and Telecommunications (China)

The commercial and military radio frequency (RF) receivers are desired strongly to provide threat information more accurately and more rapidly. The traditional analog-component-based RF receiver is gradually replaced by digital receiver, which is with high flexibility and precision. However, nowadays applications drive the RF receiver towards higher frequencies and larger bandwidths, which poses a significant challenge to digital RF receiver due to the limited sampling ratio of ADC.

Though the photonics-assisted ADC has been studied for many years, in this presentation we will demonstrate a novel photonic ADC scheme. In the new scheme, the broadband RF signal spectrum is channelized into many frequency channels whose bandwidths are compatible with available digital electronics. Compared with the traditional scheme which is essentially a time-division de-multiplexed one, our proposal achieves the demultiplication in frequency domain, and is believed to benefit applications with multiple RF carriers. The division is obtained by two coherent optical frequency combs whose intervals are slightly different. The advantages, performance, and key issues will be discussed.

9279-3, Session 1

Instantaneous broadband RF signal acquisition based on optical serial coherent analyser (OSCAR) (*Invited Paper*)

Cheng Lei, Hongwei Chen, Ruiyue Li, Minghua Chen, Sigang Yang, Shizhong Xie, Tsinghua Univ. (China)

Broadband instantaneous RF measurement has always been a hot research topic for its critical application in radar and electronic warfare. Considering the wide frequency range of the broadband instantaneous RF signal and the limited processing capacity of the available electrical devices, the proposed optical serial coherent analyzer of radio-frequency (OSCAR) is to serially channelize the signal by the frequency shifting effect of the RFS loop, and then detect each channel with coherent receiver.

Alternatively, there are two system configurations for the different characteristics of the incoming RF signal. To capture the RF signal with relatively stable frequency components and high temporal continuity, a frequency scanning LO, which is produced by the RFS loop, is applied to mix with the upconverted RF signal. So the RF signal will be temporally serially partitioned and analyzed without loss. To capture all the frequency component within a temporally varying and sparse signal, the RFS loop is used to store the upconverted RF signal, and a coherent receiver is utilized to downconvert and analyze the signal piece by piece. And at the receiver, a balanced photodetector (BPD) guarantees the accuracy of measurement and gets rid of interferences of RF's self-beating.

With the proposed OSCAR, not only instantaneous frequency information, but also the detailed phase information of RF signals can be obtained. In the experimental demonstration, a RF measurement ranging from baseband to 40GHz with MHz resolution is successfully realized within several micro-seconds. Furthermore, OSCAR also provides a promising solution for various RF vector measuring applications.

9279-4, Session 2

Recent progress in on-chip signaling with ultra-compact integrated photonic devices (*Invited Paper*)

Jian Wang, Huazhong Univ. of Science and Technology (China)

In this paper, we review our recent research works in on-chip signaling with digital and analog modulation signals through ultra-compact integrated photonic devices. Using our designed and fabricated silicon photonic devices, 1) we experimentally demonstrate on-chip signaling of advanced multi-carrier multi-level modulation signals (e.g. OFDM m-QAM) in silicon microring resonators and silicon vertical slot waveguides; 2) we experimentally evaluate the on-chip analog signaling performance in silicon strip waveguides, silicon microring resonators and silicon photonic crystal cavities. On-chip terabit-scale digital signal transmission, i.e. 161 wavelength-division multiplexed (WDM) channels each carrying 11.2-Gbit/s OFDM 16-QAM signal (1.8-Tbit/s transmission capacity), and low-distortion analog signal transmission are achieved in the experiment with favorable performance using silicon photonic devices.

9279-5, Session 2

Narrowband rectangular optical filter design based on stimulated Brillouin scattering in optical fiber *(Invited Paper)*

Lilin Yi, Wei Wei, Weisheng Hu, Shanghai Jiao Tong Univ. (China)

Optical narrowband filtering ranging from MHz to several GHz plays an important role in high-resolution optical signal processing, especially in the context of the booming development of the high speed optical transmission systems. For some applications such as sub-band switching, the requirements for flexible filtering are also in great need of the tunability of the filter bandwidth and wavelength. An ideal tunable passband filter has a rectangular response consisting of an ultra-flat passband and very steep edges. The flat passband will not distort the signal at all thus keeping high signal fidelity. The steep edges can suppress interference from adjacent bands at the extreme. And the tunability makes it more flexible and reusable to meet different requirements.

In this paper, we present a narrowband rectangular SBS filter with tunable bandwidth from 50 MHz to 4 GHz at 15-MHz tuning resolution. We use external intensity modulation by an electrical comb whose amplitude and initial phase can be digitally controlled precisely. A feedback compensation process is proposed to revise the pump shape precisely. On the foundation of the feedback process, we further propose the nonlinearity management to mitigate the four-wave mixing effect and utilize a more suitable fiber with a single Brillouin gain peak to increase the filter flatness. As a result, the in-band ripple is decreased to -1 dB for all bandwidth cases while the unwanted out-of-band gain is further suppressed. Based on this filter, we demonstrate a sub-band extraction of a multi-band orthogonal frequency division multiplexing (OFDM) signal and prove the flexibility and validity of the filter.

9279-6, Session 2

Theoretical analysis on the sampling criteria for time-interleaved photonic analog-to-digital converters *(Invited Paper)*

Jianping Chen, Feiran Su, Guiling Wu, Shanghai Jiao Tong Univ. (China)

Time-interleaved photonic analog-to-digital converter (TIPADC) is emerging as a promising candidate to process ultra-wideband signals, whereas quantization is electrical in order to obtain large effective number of bits. In this paper, we study the issues on the signal sampling and reconstruction in the TIPADC from the systematic point of view. The sampling output and frequency response of the system are derived using a model that includes the photonic sampling, demultiplexing, photo detecting, electronic quantizing and digital processing. The signal sampling and reconstruction mechanism of TIPADC with a uniform system sampling rate and matched channels are illuminated with the spectrum of signal in each processing step. The effect of the sampling pulse and back-end electronics on the system frequency response is analyzed in detail. The feasible regions of the system for alias-free sampling in terms of system frequency response, and a set of sampling criteria on bandwidth of the sampling pulse and back-end electronics are presented for the TIPADC. The proposed model and sampling criteria are validated by simulations under different parameter configurations.

9279-7, Session 2

Real-time photonic differential equation solver with constant-coefficient tunable *(Invited Paper)*

Jianji Dong, Huazhong Univ. of Science and Technology (China)

Photonic integrated circuits for photonic computing open up the possibility for the realization of ultrahigh-speed and ultra wide-band signal processing with compact size and low power consumption. Differential equations model and govern fundamental physical phenomena and engineering systems in virtually any field of science and engineering, such as temperature diffusion processes, physical problems of motion subject to acceleration inputs and frictional forces, and the response of different resistor-capacitor circuits, etc. In this talk, we will review recent progresses on real-time photonic differential equation solver based on photonic integrated circuits. First, we demonstrate a solution to second order differential equation system based on cascaded microring resonators (MRRs). The MRRs are designed with different radii and quality factors (Q), corresponding to solving first-order linear ODE with different constant coefficients. Employing single and cascaded MRRs, respectively, first- and second-order linear ODEs are solved by the cascaded MRR unit. Second, we experimentally demonstrate a feasible integrated scheme to solve first-order linear ordinary differential equation with constant-coefficient tunable continuously. Besides, we analyze the impact of the chirp and pulse-width of input signals on the computing deviation. This device can be compatible with the electronic technology (typically complementary metal-oxide semiconductor technology), which may motivate the development of integrated photonic circuits for optical computing.

9279-8, Session 2

160 GSa/s all-optical pulsed sampling with a single semiconductor optical amplifier *(Invited Paper)*

Shangjian Zhang, Heng Wang, Xinhai Zou, Yali Zhang, Heping Li, Yong Liu, Univ. of Electronic Science and Technology of China (China)

All-optical sampling attracts considerable attention due to its crucial applications in high-speed optical analog-to-digital conversion. Several fiber-based optical sampling schemes have been demonstrated, such as self-phase modulation, cross-phase modulation, four wave mixing and Raman soliton self-frequency shifting. These schemes can provide ultra-fast sampling speed, but suffer the high operating power and performance instability. Semiconductor-based signal processing is promising because of low power consumption, high nonlinear efficiency and potential large-scale integration. We propose and demonstrate an all-optical sampling scheme using a single semiconductor optical amplifier, in which the analog optical signal is sampled through the nonlinear polarization rotation arising in the semiconductor optical amplifier. In the experiment, 40 GSa/s all-optical sampling for 2.5 GHz analog signal and 160 GSa/s all-optical sampling for 10 GHz analog signal are successfully demonstrated with commercially available fiber-pigtailed components. The 40 GSa/s all-optical sampling shows a fundamental conversion efficiency of 1.35 and a total harmonic distortion of 2.01% at the operating power of 5 mW. Our scheme requires only one semiconductor optical amplifier and has low power consumption, which shows much potential for the high-speed optical analog-to-digital conversion.

9279-9, Session 3

Energy-efficient optical pulse multiplication and shaping based on triply-sampled spectral filter utilizing fiber Bragg grating (*Invited Paper*)

Hongpu Li, Xuxing Chen, Shizuoka Univ. (Japan)

In the past few decades, all-optical technique for the multiplication of optical pulses has attracted a great interest due to its current or potential applications to the fields, such as the ultrahigh-speed optical communications, all-optical information processing, microwave photonics, optical computing, and quantum optics etc. To date, various techniques to generate optical pulse trains with an ultrahigh-repetition-rate from a low-repetition-rate one have been developed. Of them, the linear method based on the utilization of a spectrally filter, e.g. fiber Bragg grating (FBG), has been more well-established. On the other hand, the generation of flat-top temporal intensity profiles is highly desired for optical switching and frequency conversion applications that are very important in ultrahigh speed optical communication systems. A lot of efforts have also been made to realize this purpose. However, most of the proposed techniques before exhibit very poor energy-efficiency due to the utilization of the spectral filter with a high energy-loss.

In this paper, a novel triply-sampled spectral filter is firstly proposed for simultaneous pulse multiplication and arbitrary waveform shaping, to the best of our knowledge. The proposed method is based on the utilization of three spectral filters simultaneously with high energy efficiency, which can be realized by only one strong fiber Bragg grating with a reflection larger than 90%. With this method, pulse train with a repetition rate of 225-GHz and flat-top intensity profile is numerically demonstrated, which is generated from 1-GHz transform-limited Gaussian pulse train with pulse width of 0.4 ps.

9279-10, Session 3

CMOS-compatible source of heralded single photons for multiplexed quantum cryptography (*Invited Paper*)

Lucia Caspani, Christian Reimer, Institut National de la Recherche Scientifique (Canada); Matteo Clerici, Marcello Ferrera, Institut National de la Recherche Scientifique (Canada) and Heriot-Watt Univ. (United Kingdom); Michael Kues, Institut National de la Recherche Scientifique (Canada); Marco Peccianti, Alessia Pasquazi, Institut National de la Recherche Scientifique (Canada) and Univ. of Sussex (United Kingdom); Luca Razzari, Institut National de la Recherche Scientifique (Canada); Brent E. Little, Xi'an Institute of Optics and Precision Mechanics (China); Sai T. Chu, City Univ. of Hong Kong (China); David J. Moss, RMIT Univ. (Australia); Roberto Morandotti, Institut National de la Recherche Scientifique (Canada)

Integrated sources of single and entangled photons are currently one of the main research areas in quantum optics. Microring resonators are among the preferred solutions because of the increased generation probability provided by the field enhancement inside the cavity. In addition, high Q-factor microcavities can generate narrowband biphotons (~100 MHz), eventually compatible with atomic quantum memories.

However, in standard configurations the microcavities are pumped by external continuous wave (CW) lasers, which in turn require active stabilization methods to lock the pump

wavelength to the microcavity resonance. This solution is even less effective when microcavities with very high Q-factor (narrow linewidth) are considered. We demonstrated an integrated photon pair source based on an innovative pumping scheme that does not require an external pump laser. In this scheme the microresonator itself contributes to the generation of the CW pump, which in turns is automatically self-locked to the cavity resonance, providing stable operation without the need of active stabilization. The device is based on a CMOS-compatible high-index glass microring resonator and generates, via spontaneous four-wave mixing, multiplexed photon pairs distributed in a frequency comb compatible with the channel spacing of optical fiber communication networks (ITU grid, 200 GHz channel separation). We observed coincidence peaks (coincidence-to-accidental ratio > 10) on five different signal/idler wavelength pairs in the telecom range, symmetrically distributed around the pump, with a bandwidth of ~110MHz. We also measured a heralded auto-correlation dip as low as 0.144, thus demonstrating the suitability of this device as multiplexed source of heralded single photons.

9279-11, Session 3

Recent progress in nanophotonics (*Invited Paper*)

Marcello Ferrera, Heriot-Watt Univ. (United Kingdom); Nathaniel Kinsey, Mikhail Y. Shalaginov, Purdue Univ. (United States); Gururaj V. Naik, Stanford Univ. (United States); Viktoriia E. Babicheva, Technical Univ. of Denmark (Denmark); Clayton T. DeVault, Alexander V. Kildishev, Alexandra Boltasseva, Vladimir M. Shalaev, Purdue Univ. (United States)

Electronics, the most successful technology of our time, is going to reach its limit in terms of bandwidth and maximum affordable power density. Photonics has recently emerged as the most promising candidate in order to move forward and satisfy the constantly growing demand for bandwidth of our modern society. However, in order to repeat the unprecedented success of electronics we must enable the capability of design fabricate and link multifunctional photonic/opto-electronic devices on the same integrated chip. This is typically not achievable by using standard photonic components because of the diffractive nature of light which limits the typical size of the devices to abruptly half the operative wavelength. In order to solve this fundamental issue, the scientific community is focusing its attention on exploiting the coupling between photonic modes and the oscillation of the electronic plasma of metals (plasmonics). Doing so, it is possible to take advantage of the electromagnetic waves propagating at the metal dielectric interface (surface plasmon polaritons-SPP) or the localized surface plasmon resonances (LSPR) in order to gain an unprecedented control over light. These plasmonic modes are characterized by a very high k-vector, which corresponds to a deep sub-wavelength mode confinement.

This peculiar property of plasmonic modes may in principle allow for effective integration of photonics components. Here we report our most recent achievements in the development of plasmonic technologies mostly focused on; low loss interconnects, ultra compact modulator, CMOS compatible alternative materials (e.g. transition metal nitrides and transparent conductive oxides), and enhancement of quantum sources.

9279-12, Session 4

Recent progress in chip-based nonlinear optics for all-optical signal processing *(Invited Paper)*

Benjamin J. Eggleton, Blair Morrison, The Univ. of Sydney (Australia)

My talk reviews our recent progress in developing photonic circuits that exploit nanophotonics and optical nonlinearity to generate and manipulated photons at the single photon level for classical and quantum information processing. I will review our recent progress in developing silicon and chalcogenide based dispersion engineered photonic crystal circuits that offer exquisite control of light with a particular emphasis on slow-light enhancements. Highlights of this work include the first demonstration of optical solitons in silicon, integrate spatial multiplexing of heralded photons and ultra- compact optical switches and microwave photonic filters.

9279-13, Session 4

All-optical signal processing technologies based on space-time duality *(Invited Paper)*

Xinliang Zhang, Huazhong Univ. of Science and Technology (China)

Several all-optical signal processing functionalities on the basis of the space-time duality are performed and presented. Specifically, the temporal imaging using a time pinhole, triangular-shaped pulse generation based on self-convolution of a rectangular pulse, and flat-top pulse generation based on the convolution of rectangular pulses are experimentally demonstrated.

Firstly, the temporal pinhole-based imaging system consists of two sections of dispersive fibers connected by a temporal shutter, which is experimentally realized by a logic AND-gate with a short pulse. Theoretical analysis and experimental results show that the output waveform is reversed if the signs of the dispersion on both sides of the time-gate are identical, otherwise it is non-reversed if the signs of the dispersion are opposite. This is in accordance with the spatial pinhole imaging counterpart.

Secondly, the triangular-shaped pulse generator is built by two sections of dispersive fibers with opposite signs connected by a parametric mixing process, which corresponds to a temporal reduced 4-f system in addition with a pattern square operation at the Fourier plane. The achieved triangular-shaped pulse is the self-convolution of the input rectangular pulse, and its pulse width is half of that of the input. The triangular pulses with different pulse widths are successfully generated.

Lastly, the flat-top pulse generator is composed of three sections of dispersive fibers connected by a parametric mixing process, forming a temporal Y-branch reduced 4-f system in addition with a pattern multiply operation at the Fourier plane. The obtained flat-top pulse is the convolution of the rectangular pulses with different scales. It is isosceles-shaped characterized by the flat top as well as the linear raising-up and falling down edges. Furthermore, the top-width of the flat-top pulse can be tuned by simply setting proper dispersions of the system.

9279-14, Session 4

Ultrafast optical signal generation and processing based on fiber long period gratings *(Invited Paper)*

Reza Ashrafi, McGill Univ. (Canada) and Institut National de la Recherche Scientifique (Canada); Ming Li, Institute of Semiconductors (China); José Azaña, Institut National de la Recherche Scientifique (Canada)

Optical signal generation and processing are becoming increasingly important for a wide range of scientific and engineering applications, including high-speed optical telecommunications, optical computing circuits, optical biomedical imaging, advanced sensors and material/device characterization techniques. Optical approaches offer the possibility to overcome the severe speed limitations of present electronic circuits, which are practically limited to generation/processing speeds below a few tens of GHz. All-optical circuits would easily enable generation/processing speeds covering frequency bandwidths from 10s of GHz to several THz. As for conventional waveform generation/processing circuits in electronics, fundamental devices in the optical domain, such as basic processing functions and customized waveform generation schemes need to be realized and developed. Among all-optical implementation approaches, all-fiber technologies, e.g. fiber long period grating (LPG) and Bragg grating (BG), are attractive due to their simplicity, potential for low cost and full compatibility with fiber-optics and integrated-waveguide systems.

The spatial resolution limitation of presently available fiber grating fabrication technologies has limited the fiber-based waveform generation/processing schemes to temporal resolutions of at least several picoseconds, i.e. corresponding to a few 100s of GHz in terms of the bandwidth of waveform generation/processing. In this work, we present our recent research results demonstrating that arbitrary optical waveforms with bandwidths well in the THz regime can be generated/processed using fiber LPG devices [1-6]. The proposed LPG solutions enable one to synthesize/process optical waveforms with temporal resolutions down to the femtosecond range, i.e. far faster operation bandwidths than conventional BG-based optical waveform generation/processing schemes.

References

- [1] Ashrafi, R., Li, M., LaRochelle, S., and Azaña, J., "Superluminal space-to-time mapping in grating-assisted co-directional couplers," *Optics Express* 21(5), 6249-6256 (2013).
- [2] Ashrafi, R., and Azaña, J., "Terahertz bandwidth all-optical Hilbert transformers based on long-period gratings," *Optics Letters* 37(13), 2604-2606 (2012).
- [3] Ashrafi, R., Li, M., Belhadj, N., Dastmalchi, M., LaRochelle, S., and Azaña, J., "Experimental demonstration of superluminal space-to-time mapping in long period gratings," *Optics Letters* 38(9), 1419-1421 (2013).
- [4] Ashrafi, R., Li, M., and Azaña, J., "Coupling-strength-independent long-period grating designs for THz-bandwidth optical differentiators," *IEEE Photonics Journal* 5(2), 7100311 (2013).
- [5] Ashrafi, R., Li, M., and Azaña, J., "Tsymbol/s optical coding based on long period gratings," *IEEE Photonics Technology Letters* 25(10), 910-913 (2013).
- [6] Ashrafi, R., Asghari, M. H., and Azaña, J., "Ultrafast optical arbitrary-order differentiators based on apodized long-period gratings," *IEEE Photonics Journal* 3(3), 353-364 (2011).

9279-22, Session Post

Theory research on performance of high-speed random bitstream ranging system based on single-photon counting

Shanshan Shen, Qian Chen, Nanjing Univ. of Science and Technology (China); Weiji He, Nanjing university of science and technology (China); Hui dong Dai, Nanjing university of science and technology, (China)

This paper researches on random bitstream ranging model and propose a new output SNR model from photon statistics model. We introduce the arm probability of steady response model to SNR model forming new SNR model. In order to gain high output Signal-to-noise ratio, low bit error, firstly we study the relationship of SNR and the fraction of 1 in bitstream with different dead time. Monte carlo algorithms were developed to corroborate the theoretical results. The theory model is almost consistent with Monte Carlo simulation.

The results show that with the fraction of randomly distributed 1-bits in transmitted pattern increased, the system SNR is getting better first and then getting worse. Best pattern of transmitted bit stream according to different dead time leads to the best SNR and shorter dead time improves system SNR. In the case of 80ns dead time, fraction of 0.084 of one bit random distributed in the transmitted pattern achieves the best SNR. We also prove that system SNR can't increase infinitely with the growing signal photon energy, for higher signal levels, SNR degrades, due to a decreased arm probability which is involved in the new output SNR model.

Then we investigate the effect of bit rate on error probability. The theory is established by Gaussian jitter distribution disregarding the photon distribution. Monte carlo algorithms are first used to corroborate the theoretical results of the single arriving time error probability. Then 1000 times simulation is conducted to investigate the final range error probability. Gaussian distribution timing jitter of 440ps FWHM is introduced to reconstruct received bitstream pattern formed from the arrival times of returning single photon. We find that higher rate of bitstream brings higher possibility error of range. Suitable bit rate is restricted to 1 GHz according to jitter of 440ps FWHM.

9279-26, Session Post

Timing design and image processing of CMOS sensor LUPA-4000 based on FPGA

Li Xin, BeiHang Univ. (China)

This article describes a method of the timing sequence design for CMOS image sensor LUPA-4000. A FPGA based imaging system with the function of adjustable integration time, multiple-slope integration, parallel integration and reading, windowing readout has been designed. This design can satisfy the frequency of 66M limit frequency of LUPA-4000 and 20 frames of a second. As the fixed noise of LUPA-4000 is aloud and the image is not clear, an efficient real-time image processing algorithm is also described in this paper. First a black image should be acquired as the fixed noise image. The real-time images can be send out after subtracting the noise image. This method can effectively eliminate the fixed noise of the image, as the same time, the original image information has been maintained in the maximum degree. The test experiments on FPGA shows this design can drive LUPA-4000 working properly. Also this design takes full advantage of the accessibility features of the device, which provides a wider dynamic range and more flexible application of the device. The image sensor driven by this design improves imaging quality, which can be used for space exploration, especially for small space dynamic target tracking.

9279-33, Session Post

Synthetic transmit aperture technique in medical ultrasound imaging implemented on a GPU

Chuang Zhang, Xiaodong Chen, Yi Wang, Ying Li, Zhihai Jiao, Dao Yin Yu, Tianjin Univ. (China)

In the medical ultrasound imaging, the synthetic transmit aperture (STA) technique is very promising and has been a hot research topic. It is dynamically focused in both transmit and receive yielding an improvement in resolution. But this imaging technique sets high demands on processing capabilities and makes implementation of a full STA system very challenging and costly. Many attempts have been made to reduce the demands on the system making it a more realistic task to implement. In this paper we don't consider how to reduce the demands, but consider how to accelerate the processing speed of the system. The recent introduction of general-purpose graphic processing units (GPU) seems to be quite promising in this view, especially for the affordable programming complexity. In this paper we explain the main computational features of STA processing unit, trying to disclose the degree of parallelism in the operations. On the basis of the compute unified device architecture (CUDA) programming model and the extremely flexible structure of the Single Instruction Multiple Threads (SIMT) model, we show that the optimization of STA processing unit can be performed more efficiently. The input data is read from Matlab, the post-processing and display also use Matlab. Performance shows that, using a single NVIDIA GTX-650 GPU board, this amount to a speed up of more than a factor of 30 compared to a highly optimized beamformer running on our test workstation with a 3.20-GHz Intel Core-i5 processor.

9279-36, Session Post

Accurate time-of-flight measurement of particulate matter based on ECL-TTL counters

Deping Li, Jianguo Liu, Huaqiao Gui, Shuhua Huang, Yin Cheng, Yihuai Lu, Jie Wang, Anhui Institute of Optics and Fine Mechanics (China)

Because of its aerodynamic diameter of the aerosol particles are stranded in different parts of different human respiratory system, thus affecting human health. Therefore, how to continue to effectively monitor the aerosol particles become increasingly concerned about. Use flight time of aerosol particle beam spectroscopy spectrum of atmospheric aerosol particle size distribution is the typical method for monitoring atmospheric aerosol particle size and particle concentration measurement, and it is the key point to accurate measurement of aerosol particle size spectra that measurement of aerosol particle flight time. In order to achieve accurate measurements of aerosol particles in flight time, this paper design a ECL_TTL high-speed counter with ECL counter and TTL counter. The high-speed counter includes a clock generation, high-speed counter and the control module. Clock Generation Module using a crystal plus multiplier design ideas, take advantage of the stability of the crystal to provide a stable 500MHz clock signal is high counter. High count module design using ECL and TTL counter mix design, timing accuracy while effectively maintaining, expanding the timing range, and simplifies circuit design. High-speed counter control module controls high-speed counter start, stop and reset timely based on aerosol particles flight time, is a key part of the high-speed counting. The high-speed counting resolution of 4ns, the full scale of 4096ns, has been successfully applied aerodynamic particle spectrometer, to meet the precise measurement of aerosol particles flying time.

9279-37, Session Post

Random laser scattering pulse signal analysis in laser particle counter with lognormal distribution

Zhen Gang Yan, Weiping Sun, Xi'an Modern Control Technology Research Institute (China); Keding Yan, Nanjing Univ. of Science and Technology (China); Jie Li, Hongpeng Lv, Xijing Zhang, Xi'an Modern Control Technology Research Institute (China); Liang Xue, Shanghai Univ. of Electric Power (China); Shouyu Wang, Nanjing Univ. of Science and Technology (China)

The statistical distribution of natural phenomena is of great significance in studying the laws of nature. Here, in this paper, based on laser scattering particle counter, a simple random pulse signal generation and testing system is designed for studying the counting distributions of three typical objects including particles suspended in the air, standard particles, and background noise. Moreover, in order to have a deep understanding of the experimental results from laser scattering particle counter, a random process model is also proposed theoretically to study the random law of measured results. Both normal and lognormal distribution fittings are applied to analyze the experimental results, and we have proved that statistical amplitude and width distributions of particles suspended in the air, standard particles, and background noise match well with lognormal distribution when natural numbers are used as the variables using a two-parameter model testified by chi-square and correlation coefficient. This study is an important reference for statistical data processing for laser scattering particle counter, moreover, it will also be a useful guide for designing laser scattering particle counter with high accuracy and processing speed.

9279-38, Session Post

The applications of optical computerized tomography (OCT) in cold and hot complex flow fields

Yun-Yun Chen, Nanjing Univ. of Science and Technology (China); Li-zhu Chen, Fang Gu, Nanjing Univ. of Information Science and Technology (China)

Optical computerized tomography (OCT), as a branch of computerized tomography (CT) techniques, has been widely used to display and diagnose a variety of complex flow fields, due to its characteristics of real-time, stable, non-contact and can supply 3-D distributions. In practical applications, we found some different phenomenon when they are adopted in cold and hot complex flow fields. In this paper, the cold and hot flow field's optical computerized tomography diagnosis is analyzed and compared. In other words, the similarities and differences are discussed. The results show that 1) optical computerized tomography can directly reflect spatial distribution of the measured field's refractive index, for both the cold and the heat complex flow fields; 2) optical computerized tomography can reflect the true boundaries or structure of the cold flow fields, but can not well done for the heat flow fields. The involved results will help us to make better use of optical computerized tomography to diagnose various cold or hot complex flow fields.

9279-39, Session Post

Microwave photonic down-conversion based on phase modulation and Brillouin-assisted notch-filtering

Di Zheng, Southwest Jiaotong Univ. (China)

A photonic microwave downconverter that features simple structure and wide frequency tunable range is experimentally demonstrated. In order to obtain higher conversion efficiency, SBS-assisted notch filter is used to suppress the carrier of phase modulated signal. Due to the SBS-assisted notch-filtering is generated by the phase modulated signal itself, which simplify the system structure effectively. Furthermore, the effective suppression of the carrier of phase modulated signal and the diminishment of the second-order Stokes wave could be achieved simultaneously by optimizing the attenuation of the variable optical attenuator, which guarantee our scheme can operate over a wide frequency range.

9279-40, Session Post

The application of air-jet based optical coherence tomography to corneal biomechanical properties differentiation

Jiaying Zhang M.D., Chinese PLA General Hospital (China); Li-ke Wang, The Hong Kong Polytechnic Univ. (China); Wei-lun M. Ko, The Hong Kong Polytechnic Univ. (China); Tianjie Li, The Hong Kong Polytechnic Univ. (China); Lei Tian, Ying Gu, Chinese PLA General Hospital (China); Yongping Zheng, The Hong Kong Polytechnic Univ. (China)

Objectives: The corneal biomechanical properties are crucial for both the true intraocular pressure (IOP) measurement and the effect of LASIK surgery. Unfortunately, the corneal biomechanical properties can still not be evaluated exactly in vivo now.

Methods: The air-jet based spectral-domain optical coherence tomography (OCT) system was established for the application of corneal biomechanical properties measurement in this research. To mimic the different corneal elasticity, silicon phantoms in corneal shape with different silicon-oil ratios ranged from 1:0.4 to 1:4 were casted into the mould with the aspherical corneal posterior surface. The same elastic silicon in the matrix was for the tensile-strain test as calibration.

Results: Different elasticities among phantoms can be differentiated by the system and Young's Modulus was deduced to be coincident with the results of traditional tensile-strain tests. The relationships between IOP and Young's Modulus were linear. The creep was extracted from the difference between the position of the corneal surface post-puff and the initial position pre-puff. The linear relationship existed between creep and IOP. Linear relationships were also found between the air-puff pressure and corneal displacement regardless IOP inside the model.

Conclusions: Corneal model phantoms with different elasticities can be distinguished from one another by the air-jet based OCT system with the equivalent value with traditional methods. The system and method introduced here were potentially qualified for in vivo corneal biomechanical properties assessment in clinic, with which both the exact IOP and the avoidable keratoconus pre- / post-LASIK surgery are optimistically expected.

9279-41, Session Post

2?80Gbit/s multi-channel add-drop multiplexing in a single fiber

Jian Sun, Beijing Jiaotong Univ. (China)

All optical add-drop multiplexing have the capability of signal processing at ultra-high speeds. And, as most transmission today is based on multi-channels systems, it would be beneficial if such high speed add-drop multiplexing could deal with multi-channel signals, but it will be very difficult, because of detrimental inter-channel cross-talk due to effects as cross-phase-modulation (XPM) and four-wave mixing (FWM). Bidirectional propagation is applied to relieve the inter-channel cross-phase-modulation (IXPM) and inter-channel four-wave mixing (IFWM) by rapid walk-through between the signals traveling in opposite directions. Based on cross-phase-modulation (XPM)-induced frequency shifting, we propose a structure for optical time division multiplexing (OTDM) add-drop multiplexing operation. Simultaneous add-drop multiplexing of two 80Gbit/s OTDM signals in a single highly nonlinear fiber (HNLF) is demonstrated experimentally. In this add-drop multiplexer, data 1 and data 2 travel in opposite directions at the same wavelength. Any two tributary channels of OTDM signal can be added and dropped simultaneously by using the proposed add-drop multiplexing structure. The add-drop multiplexing performance is validated by bit-error-rate (BER) measurements. The experimental results show that the power penalty of dropped channel is less than 1.5 dB, and there is no distinct BER degradation for the added channel.

9279-42, Session Post

Aluminium alloy aerospace structure aperture measurement based on 3D digital speckle correlation method

Lu Bai, Beijing Institute of Strength and Environmental Engineering (China); Hongbo Wang, Jiangfan Zhou, Rong Yang, Hui Zhang, Beijing Institute of Strength and Environment Engineering (China)

In this paper, the aperture change of the aluminium alloy aerospace structure under real load is researched. Static experiments are carried out which is simulated the load environment of flight course. Compared with the traditional methods, through experiments results, it's proved that 3D digital speckle correlation method has good adaptability and precision on testing aperture change, and it can satisfy measurement on non-contact, real-time 3D deformation or stress concentration. It can be widely used in the aperture test in the area of aircraft load experiment.

9279-43, Session Post

Spectroscopic pump probe measurement for multilayer structured hydrogenated nano-crystalline silicon

Wei He, Andrey Kaplan, Ammar Zakar, The Univ. of Birmingham (United Kingdom); Igor V. Yurkevich, The Univ. of Birmingham (United Kingdom) and Aston Univ. (United Kingdom)

A femtosecond pump probe setup was built to do the spectroscopic pump probe reflection measurement for multilayer structured hydrogenated nano-crystalline silicon (nc-Si:H) sample. The optical property of multilayer nc-Si:H sample is characterised by the spectroscopic ellipsometry measurement

and multilayer optical model simulation firstly. Then, the interference of reflectance, transmittance and absorbance of sample with increasing wavelength can be figured out through the optical model calculation. Finally, we measured the pump probe reflection at around 300fs time delay and 0.6mJ/cm² pump fluence with spanning pump beam spectra from 570nm to 820nm. From the measurement data $\Delta R/R_0$, we can see there is Fabry-Perot fringe in the red side of the detecting probe spectra between 800nm and 810nm due to the pump induced dielectric constant variation of nc-Si:H material. Applying Drude model to fit the data, we obtained the excited carriers concentration and scattering rate for different pumping spectra. Moreover, when the pumping spectra is in the interference absorbance peak regions, such as 590nm, 660nm and 800nm, the excitation strength is much higher than the other pumping spectra. We realise that the multilayer structure can lead to the interference effect enhances the excited carriers plasma generation when the pumping spectra is in the around absorbance peaks region.

9279-44, Session Post

Image super-resolution via block sparse Bayesian model

Jiaquan Dong, Hong Zhang, Hao Chen, Ding Yuan, Beihang Univ. (China); Mingui Sun, Univ. of Pittsburgh (United States)

Image super-resolution is still a challenging task due to its ill-posed nature. Recently, super-resolution via sparse coding (ScSR) has attracted lots of attention. However, block sparse coding has been proved to be easier to get the actual sparse solution than simple sparse coding especially in noisy environment. In this paper, we propose a novel Block Sparse Bayesian Model (BSBM) to improve its performance. As other learning-based SR methods, our method is performed in a patch-wise manner due to the high dimensionality of image. We firstly construct a pair of dictionaries which jointly learned in corresponding low-resolution (LR) and high-resolution (HR) patch database, then find out the most approximant sparse representations of source LR patches in the LR dictionary, and finally recover the corresponding HR patches from the HR dictionary using the same sparse representation coefficients. Different from previous sparsity-based work based on the sparsity constraint easily, we additionally exploit intra-block correlation, even when block partition is not known, based on the BSBM model we proposed. Firstly, sparsity representation coefficients can be splitted into many blocks which can be overlapped each other and only some of them are nonzero. Secondly, to exploit intra-block correlation we assume that the sparsity representation coefficients of nonzero blocks satisfy multivariate Gaussian distribution. Then via MAP, we can model the intra-block correlation relationship to improve sparsity-based image super-resolution. Experiments show that our method has state-of-the-art performance compared to other standard methods.

9279-45, Session Post

Signal processing of fluorescent optical fiber temperature measurement based on Hilbert-Huang transform

Yajuan Yang, Zhiyong Wang, Xiaoping Yang, Tianjin Univ. of Technology (China)

In this work, we introduce a novel approach for data analysis, and we put forward the structure diagram of temperature measuring system. The fluorescent thermal probe is the ruby that has the advantages of compact structure and high temperature. Using the square wave signal of 70% duty cycle as the super bright

LED's modulation signal of 575 nm wavelength, compared to the square wave of 50% duty ratio, the sine wave can carry more excitation light power and improve the input signal-to-noise ratio, meanwhile it is easier to implement the sine signal modulation. Currently, the signal processing methods mainly have fast Fourier transform, short-time Fourier transform, wavelet transform, etc. But all of them have their own defects. The Hilbert-Huang transform (HHT) is composed of ensemble empirical mode decomposition (EEMD) and Hilbert transform. According to the difference of signal and noise characteristics, HHT can generate adaptive modal functions and decrease the noise out of signal effectively, so that the signal-to-noise ratio can be improved, and their shortcomings can be overcome. Therefore, the paper has shown that HHT is an effective and practical processing method for fluorescent signal. Meanwhile, the experiments can be proved that the structure design of fluorescent optical fiber temperature measuring system is reasonable, the scheme is feasible, and it is of strong practical value.

9279-15, Session 5

Broadband terahertz detection in solid-state media (*Invited Paper*)

Matteo Clerici, Institut National de la Recherche Scientifique (Canada) and Heriot-Watt Univ. (United Kingdom); Sze Phing Ho, Institut National de la Recherche Scientifique (Canada) and Univ. Teknologi Malaysia (Malaysia); Anna Mazhorova, Institut National de la Recherche Scientifique (Canada); Marco Peccianti, Alessia Pasquazi, Univ. of Sussex (United Kingdom) and Institut National de la Recherche Scientifique (Canada); Luca Razzari, Institut National de la Recherche Scientifique (Canada); Daniele Faccio, Heriot-Watt Univ. (United Kingdom); Jalil B. Ali, Univ. Teknologi Malaysia (Malaysia); Roberto Morandotti, Institut National de la Recherche Scientifique (Canada)

At Terahertz (THz) frequencies one of the most diffused technique for spectroscopic measurements is based on recording the investigated electric field in the time domain, and subsequently performing Fourier analysis. To measure the time-resolved electric field the most diffused techniques rely on optical rectification in second order nonlinear crystals or on photoconductive antennas. In both cases however, long free-carriers lifetime and optical absorptions limit the detection bandwidth to typically few THz. Recently, a broadband detection scheme relying on wave mixing in air between a short optical probe and the investigated THz pulse has been demonstrated and named Air Biased Coherent Detection (ABCD). In ABCD, the information on the THz electric field is retrieved through a modulating external DC field applied to the region where the optical probe and the THz pulse interact. Yet this technique requires high energy probes (around 50 pJ at 100fs probe pulse duration) high DC potentials and free space propagation. Furthermore the finite breakdown field in air limits the signal strength.

We have investigated a novel implementation of the ABCD technique relying on electric field induced second harmonic generation effect in few micron thick Silica (SiO₂) samples that can be easily operated with 100 V DC potentials. Exploiting the large breakdown voltage and the high nonlinearity of the glass we achieve high signal to noise ratio with < 1 pJ probe at moderate bias fields. THz field enhancement in sub-micrometers slits will be exploited as a possible route for improvement.

9279-16, Session 5

High-sensitive optical sensors based on in-fiber interferometers (*Invited Paper*)

Yiping Wang, Changrui Liao, Shen Liu, Jiangtao Zhou, Zhengyong Li, Shenzhen Univ. (China)

We reported a few high-sensitive optical sensors based on different types of in-fiber air bubbles those were fabricated by use of a commercial fusion splicer. A high-sensitivity strain sensor based on an in-fiber Fabry-Perot interferometer (FPI) with an air cavity was demonstrated by means of splicing together two sections of standard single-mode fibers. The sensitivity of this strain sensor was enhanced to 6.0 pm/μm by improving the cavity length of the FPI by means of repeating arc discharges for reshaping the air cavity. Moreover, such a strain sensor has a very low temperature sensitivity of 1.1 pm/°C, which reduces the cross sensitivity between tensile strain and temperature.

We also demonstrated a nanoscale silica diaphragm based fiber-tip Fabry-Perot interferometer for pressure sensing applications. The thinnest silica diaphragm with a thickness of ~320 nm has been achieved by use of an improved electrical-arc-discharge technique. Such a nanoscale silica diaphragm breaks the sensitivity limitation imposed by traditional all-silica Fabry-Perot interferometric pressure sensors. As a result, a high pressure sensitivity of ~1036 pm/MPa at 1550nm and a low temperature cross-sensitivity of ~960Pa/°C are achieved when a silica diaphragm with a thickness of ~500 nm is employed. Moreover, the all-silica spherical structure enhanced the mechanical strength of the micro-cavity sensor, making it suitable for high sensitive pressure sensing in harsh environment.

Moreover, we presented a type of phase-shifted fiber Bragg gratings based on an in-grating air bubble to develop a promising temperature, strain, and refractive index sensor and/or tunable optical filter. A microchannel vertically crossing the bubble is drilled by use of a femtosecond laser to allow liquid to flow in or out the air bubble. By filling different refractive index (RI) liquid into the bubble, the phase-shift peak is found to experience a linear red shift with the increase of RI, while little contribution to the change of phase shift comes from the temperature and axial strain.

This work was supported by the National Natural Science Foundation of China (grants no. 11174064, 61308027, and 61377090), the Science & Technology Innovation Commission of Shenzhen (grants no. KQCX20120815161 444632, and JCYJ20130329140017262), and the Distinguished Professors Funding from Shenzhen University and Guangdong Province Pearl River Scholars.

9279-17, Session 5

Fiber optical distributed vibration sensing with wide frequency response (*Invited Paper*)

Tao Zhu, Qian He, Chongqing Univ. (China)

High-frequency vibration incidents always refer to material damages in infrastructures, e. g. leakage of high-pressure gas pipeline and crack of material. Our research mainly focused on distributed vibration detection with high frequency response and spatial resolution based on phase-sensitive optical time domain reflectometry (OTDR).

Firstly, we applied a new signal processing method, moving averaging and moving differential method, in OTDR. Experimental results show that higher SNR can be achieved with less average number compared with conventional method. In that case, the frequency response was enhanced. Based on the moving averaging and moving differential method, we recently propose a novel system. The frequency information of vibration is

acquired by monitoring the backscattering light intensity, which can be treated as a discrete sampling process. According to the Shannon sampling theorem, the maximum frequency response of the sampling system can be enhanced by increasing sampling rate. In experiments, a frequency-difference probe pulse pair with a short time delay is used, and the experimental results agree well with the theory. This method allows the maximum detectable frequency response no longer restricted by the sensing fiber length.

Another configuration is based on the merge of μ -OTDR and interferometers. A distributed optical fiber sensing system merged μ -OTDR for vibration measurement with high-frequency response and high spatial resolution is demonstrated, where modulated pulses are proposed to be used as sensing source. Frequency response and location information are obtained by Mach-Zehnder interferometer and μ -OTDR technology, respectively. Spatial resolution of 5 m and the maximum frequency response of ~ 3 MHz are achieved in 1064 m fiber link when the narrow pulse width is 50 ns.

9279-18, Session 5

Ultraprecise measurement of resonance shift for sensing applications *(Invited Paper)*

Ciyuan Qiu, Shanghai Jiao Tong Univ. (China)

Resonator-based optical sensors detect the change of refractive index in the environment by measuring the resonance shift. The sensitivity of such sensors is determined by how precise one can locate the resonant wavelength, which is thought to be limited by the bandwidth and the quality factor of the resonator. Here we show that, with a tunable resonator, one can determine the resonant wavelength with ultrahigh precision. Using a silicon microring resonator with an embedded p-i-n junction for electro-optic tuning, whose quality factor is only 14,000, we measured the resonant wavelength with a resolution of 0.06 pm, which corresponds to an index sensitivity of 10^{-7} . This resonance measurement for sensing purposes can be done using a fixed-wavelength laser.

9279-19, Session 5

Modulation instability induced by low amplitude incoherent seed in optical fiber

Shanti Toenger, Duc Minh Nguyen, Thomas Godin, Yves Combes, Benjamin Wetzels, Thibaut Sylvestre, FEMTO-ST (France); Goëry Genty, Tampere Univ. of Technology (Finland); Frédéric Dias, Univ. College Dublin (Ireland); John M. Dudley, Univ. de Franche-Comté (France) and FEMTO-ST (France)

We investigate numerically and experimentally the influence of a low amplitude partially coherent amplified spontaneous emission (ASE) seed on the bandwidth and noise properties of picosecond modulation instability (MI) in a highly nonlinear fiber. By sweeping the ASE seed wavelength across the MI gain spectrum, significant resonant enhancement of the spectral bandwidth is observed with maximum broadening observed when the seed coincides with the maximum of the MI gain. Real-time measurements performed using dispersive time stretching reveal a corresponding improvement in the noise properties, where the spectral shot-to-shot fluctuations are stabilized. Degree of coherence cannot be used as a parameter of the noise properties due to the partially coherent nature of the ASE. Instead, the coefficient of variation C_v at a specific wavelength is used to measure the noise to signal ratio. Experiments varying the ASE bandwidth further show that the influence of the ASE seed is

only observed when its associated coherence time exceeds or is of the same order of magnitude as the pump pulses' duration, highlighting the importance of a stable amplitude modulation in effectively seeding MI dynamics. Generalized stochastic nonlinear Schrödinger equation simulations of spectral and noise properties is shown here to be in excellent agreement with experiment. Our results suggest that resonant ASE seeding can provide an important tool in controlling the spectral properties of MI, and this may impact studies related to fiber source development where high-power pump sources are used to generate broadband supercontinuum (SC) light. In such cases, spectral filtering of any ASE pump could provide a complementary technique to modify the SC properties.

9279-20, Session 5

Optical up-conversion of single sideband signal using low-cost radio-over-fiber system

Yiyang Gu, Jingjing Hu, Zijian Kang, Nuannuan Shi, Zhenlin Wu, Xiuyou Han, Mingshan Zhao, Dalian Univ. of Technology (China)

A novel optical single-sideband (OSSB) signal generation with simultaneous IF signal up conversion technique is proposed to overcome the fiber dispersion problem. With this up-conversion technique, a 26GHz OSSB signal is generated by using two low bandwidth intensity modulators in combination with fiber gratings. The intermediate frequency (IF) signal is 4GHz and a 5.5GHz or 11GHz low frequency local oscillator (LO) signal is modulated by employing frequency quadrupling technique or frequency doubling technique respectively. The 26 GHz OSSB radio frequency (RF) signal generated by mixing the intermediate frequency (IF) signal and low frequency local oscillator (LO) signal, is transmitted over 45 km standard single-mode fiber successfully. The received signal error vector magnitude (EVM) is 5.8% rms and 13% rms, with eye diagram widely open.

9279-21, Session 5

Simplified photonic approach for high-coding-efficiency digitalized microwave frequency measurement using multiple optical filter arrays with different FSRs

Bing Lu, Wei Pan, Xihua Zou, Peixuan Li, Xinkai Liu, Lianshan Yan, Bin Luo, Southwest Jiaotong Univ. (China)

A simplified photonic approach to microwave frequency measurement with digital outputs based on multiple parallel optical filter arrays, is proposed and experimentally demonstrated. In the proposed approach, multiple optical phase-shifted filter arrays in parallel with different free spectral ranges (FSRs) are designed to perform the frequency-to-amplitude conversion and the analog-to-digital conversion simultaneously. After power detection and decision operation, a digitalized result in the form of binary code with high-coding efficiency and high resolution is obtained. In particular, the high coding efficiency and the fine measurement resolution can be achieved with relaxed accuracy requirement on phase shifts of optical filters, by properly increasing the number of the optical filters. Therefore, the proposed system is easy to be implemented and robust to noise, due to the relaxed accuracy on phase shifts. A proof-of-concept experiment is performed. 8-bit binary digitalized results with a 5-bit effective number and a 2-GHz measurement resolution are obtained in the range from 10 to 40GHz, when two optical filter arrays are used.

9279-23, Session 5

Measurement of fiber's length using passively mode-locked fiber laser with a semiconductor saturable absorber mirror

Qiang Liu, Ming Wang, Hui Hao, Nanjing Normal Univ. (China)

A passively mode-locked fiber ring laser based on the semiconductor saturable absorption mirror (SESAM) and a new method for measuring the length of the optical fiber using it was presented and experimentally realized. The spectrogram of output pulses with different pump power is observed. The mechanisms of the fiber length's measurement which uses the cycle of stable mode-locked laser pulse proportional to the cavity's length to measure the length of optical fiber are discussed. And the length of optical fiber with hundreds of kilometers can be measured. The experimental results show a good agreement with the theory. And the whole experimental system is compact and stable for a long time, which has great meaning to develop new practical technology for measurement of the optical fiber's length.

9279-24, Session 5

Recognition technology research based on 3D fingerprint

Xiaoqian Tian, Zonghua Zhang, Hebei Univ. of Technology (China)

With the development of information technology, biometrics has been widely used for identity recognition in daily life. Physiological characteristics refer to data directly measured from the human body parts. Fingerprint, as one of the most important biometrics, has been widely studied and applied to personal recognition in both forensics and civilian. The current widespread use of fingerprint is identified by 2D (two-dimensional) fingerprint image. However, fingerprint is a 3D biological characteristic. The mapping from 3D to 2D loses 1D information and causes nonlinear distortion of the captured fingerprint. This leads to low accurate and even wrong recognition. With the development of 3D measurement techniques, it is increasingly important and necessary to apply 3D fingerprint to recognize person.

This paper presents a 3D fingerprint recognition method based on fringe projection technique. A series of fringe patterns generated by software are projected onto a finger surface through a projecting system. From another viewpoint, the fringe patterns are deformed by the finger surface and captured by a CCD camera. 3D shape data of the finger can be obtained from the deformed fringe pattern images. 3D fingerprint features can be extracted from the obtained 3D shape data. In order to reduce the capturing time, the projector and the camera are synchronized by trigger mechanism. The synchronization not only reduces the impact of the finger jitter but improves the stability and accuracy of the capturing system. Experimental results on measuring some 3D fingerprints and recognizing them show the accuracy and availability of the developed 3D fingerprint system.

9279-25, Session 5

3D palmprint data fast acquisition and recognition

Xiaoxu Wang, Zonghua Zhang, Hebei Univ. of Technology (China)

Information security has become a critical issue and receives

extensive attention in many application fields. As an important biometric characteristic, palmprint has wide application prospects in human identity recognition because it is highly accurate and incurs low cost [1]. Most of the existing research has focused on two dimensional (2D) palmprint recognition in the past decade. 2D palmprint loses 1D information when capturing palmprint images. As a 3D biometrics, 3D shape data can give undistorted palmprint information. Although some researchers have studied 3D palmprint data acquisition and recognition [2,3], the capturing time is long and the accuracy of recognition is low.

This paper presents a fast 3D palmprint capturing system and develops an efficient 3D palmprint feature extraction and recognition method. In order to fast acquire accurate 3D shape and color texture of palmprint, a DLP projector triggers a CCD camera to realize synchronization. By generating and projecting composite RGB fringe pattern images onto the measured palm surface, 3D palmprint data can be calculated from the fringe pattern images. In the meanwhile, color texture information can be directly captured or demodulated from the fringe pattern images. The periodic feature vector can be derived from the obtained 3D palmprint data and the corresponding color texture image, so undistorted multiple-dimensional biometrics is obtained. Using the obtained multiple-dimensional palmprint data, some feature matching test have been carried out. Experimental results on capturing 3D palmprint show that the proposed acquisition method can fast get 3D shape and color texture information of palmprint. The recognition results by using 3D palmprint are more accurate than 2D palmprint data.

9279-27, Session 6

Computational multi-dimensional imaging based on compound-eye optics (*Invited Paper*)

Ryoichi Horisaki, Tomoya Nakamura, Jun Tanida, Osaka Univ. (Japan)

Artificial compound-eye optics has been used for three-dimensional information acquisition and display. It also enables us to realize a diversity of coded imaging process in each elemental optics.

In this talk, we introduce our single-shot compound-eye imaging system to observe multi-dimensional information including depth, spectrum, and polarization. It is also applicable to increase the dynamic range and field-of-view. To realize the single-shot acquisition of the full-resolution multi-dimensional object, this system employs a method in compressive sensing, which is a powerful framework to reduce the number of required measurements compared with conventional ones based on the sampling theorem. Each elemental optics of our compound-eye camera encodes and multiplexes optically the multi-dimensional object with different processes. A single image captured by this camera is decoded and multi-dimensional information is retrieved by using a numerical algorithm based on compressive sensing.

We also demonstrate an extended depth-of-field (DOF) camera based on compound-eye optics. Three-dimensional objects cause a defocus phenomenon, which restricts the space-bandwidth product of cameras. Compound-eye optics provides a flexible framework to modulate computationally light rays, or the light field, from the objects. This framework virtually implements a phase plate in a computational process to realize such as an axially space-invariant point spread function. The virtual intermediate image, in which the DOF is extended but the object signal is blurred, is deconvolved to generate a sharp and extended DOF image.

9279-28, Session 6

Fast blur removal via optical computing (Invited Paper)

Jinli Suo, Tsinghua Univ. (China)

Non-uniform image blur caused by either camera shake or lens aberration is a common degradation in practical image and video acquisition. Different from the uniform blur, non-uniform blur is hard to deal with for its extremely high computation complexity since the blur model computation needs to be calculated pixel by pixel in spatial domain while cannot be accelerated by Fast Fourier Transform (FFT). Different from conventional deblur approaches using deconvolution algorithms by software, we propose to compute the most computational consuming operation, i.e. blur model calculation, by an optical computing system to realize fast and accurate non-uniform image deblur. Specifically, the blur model is calculated by one or several "projection and shooting" actions that can be easily conducted by a projector-camera system together with some task specific auxiliary elements. A setup composed by a projector-camera system as well as a high dimensional motion platform (for motion blur) or original camera lens (for optics aberrations) is implemented. The optical computing approach for restoring blurry imaged deteriorated by motion or defocusing can be reduce the computing time strikingly with respect to software computing. The method is applied on a series of experiments, either on synthetic or real captured images, to verify its effectiveness and efficiency.

9279-29, Session 6

Coherent Raman dual-comb spectroscopy and imaging (Invited Paper)

Takuro Ideguchi, The Univ. of Tokyo (Japan) and Max-Planck-Institut für Quantenoptik (Germany); Simon Holzner, Max-Planck-Institut für Quantenoptik (Germany); Birgitta Bernhardt, Max-Planck-Institut für Quantenoptik (Germany) and Ludwig-Maximilians-Univ. München (Germany); Guy Guelachvili, Institut des Sciences Moléculaires d'Orsay (France); Nathalie Picqué, Max-Planck-Institut für Quantenoptik (Germany) and Ludwig-Maximilians-Univ. München (Germany) and Institut des Sciences Moléculaires d'Orsay (France); Theodor W. Hänsch, Max-Planck-Institut für Quantenoptik (Germany) and Ludwig-Maximilians-Univ. München (Germany)

The invention of optical frequency comb made a huge impact in the field of precision spectroscopy because it provided a way to measure optical frequency with unprecedented accuracy. Since then, the precisely controlled laser has been used as a standard tool for precision measurements. In the last decade, other applications of the optical frequency comb have been demonstrated beyond the original purpose. Broadband direct molecular spectroscopy is one of those, which utilizes precision nature of the frequency comb. Among direct molecular frequency comb spectroscopy, dual-comb Fourier transform spectroscopy provides unprecedented measurement speed. Two laser frequency combs, which repetition frequencies are slightly detuned, generate pulse pairs with its time-delay scanned automatically, so that the system works as a fast scanning interferometer without mechanical moving part. The measurement speed is typically million times faster than the conventional one based on a Michelson interferometer. Such rapidness and precision opened up new opportunities in the field of broadband molecular spectroscopy.

Recently, the concept of dual-comb spectroscopy has been applied to nonlinear spectroscopy by the authors. A successful

demonstration of coherent Raman dual-comb spectroscopy showed a broadband Raman spectrum in the molecular fingerprint region (200-1400 cm⁻¹) within tens of microseconds. The authors also demonstrated a hyper-spectral imaging with this scheme. The label-free molecular vibrational spectroscopy and imaging could provide new diagnostic methods in a variety of scientific and industrial fields.

In this talk, we introduce the basics of dual-comb spectroscopy and discuss the potential of coherent Raman dual-comb spectroscopy.

9279-30, Session 7

Real-time multicolor stain-free imaging of tissue with stimulated Raman scattering microscopy

Yasuyuki Ozeki, Osaka Univ. (Japan)

Medical imaging of tissue has relied on time-consuming staining process, and there is a demand for rapid diagnosis of tissue. Stimulated Raman scattering (SRS) microscopy is attracting much attention because SRS allows high-speed imaging with chemical contrast. To discriminate spectral differences among different constituents, we have recently developed a SRS spectral microscopy system. This system can conduct video-rate Raman imaging, while the wavenumber can be controlled in frame-by-frame manner. As light sources, we employed a picosecond Ti:sapphire laser and a wavelength-tunable Yb-fiber laser system. The latter consists of a broadband oscillator, a spectral filter, and Yb-doped fiber amplifiers. The transmission wavelength of the spectral filter can be quickly controlled by changing the direction of the galvoscan mirror in 4-f arrangement. By using the SRS spectral microscopy system, real-time, multicolor imaging of unstained tissue samples is accomplished. I'll also show that the group-delay dispersion of the wavelength-tunable pulse source can be compensated for by introducing slight misalignment of the optics inside the wavelength filter. As a result, the repeatability of spectral data is much improved, allowing us to distinguish different types of lipids from the degree of saturation.

9279-31, Session 7

Image compression in fluorescence imaging using radiofrequency-multiplexed excitation by compressed sensing

Antony C. S. Chan, Edmund Y. Lam, Kevin K. Tsia, The Univ. of Hong Kong (Hong Kong, China)

FIRE has emerged to enable an order-of-magnitude faster than the current technologies. Similar to all high-speed real-time imaging modalities, FIRE inherently generates massive image data continuously. This technology imposed stringent requirement on data processing and storage in real-time. For example, an 8-bit, 250MSa/s digitizer fills up a 32GB RAM in only 128 seconds. At this data rate, the computer would not have time to transfer raw-data to secondary storage (e.g. hard disk) in real time. On-the-fly data compression is thus useful to delay such memory overflow, albeit the increased computer load in image reconstruction as the raw data have to be decompressed, decoded and then encoded to the desired image format.

Compressed sensing (CS) offers a solution here for FIRE. The reason is three-fold. First, the recorded image signal is highly redundant as each line scan in FIRE multiplexes (by radio-frequency) the pixel information in each line. Second, the fluorescence image of the biological cells are usually compressible, which implies sparsity. Third, the frequency-tagging scheme employed in FIRE is incoherent to the structure of the image. By exploiting above three properties in FIRE, the

digital data rate can be reduced significantly (as high as 95%) without modifying the FIRE system with the use of CS. That is, most of the line-scan measurements can be selectively/randomly discarded on the fly without degradation of image quality. The speed improvement is also reflected on the reconstruction step, as the traditional decompression-decode-encode sequence becomes a one-off CS decompression process.

9279-32, Session 7

Estimation of vibration frequency of loudspeaker diaphragm by parallel phase-shifting digital holography

Takashi Kakue, Yutaka Endo, Tomoyoshi Shimobaba, Tomoyoshi Ito, Chiba Univ. (Japan)

We report frequency estimation of loudspeaker diaphragm vibrating at high speed by parallel phase-shifting digital holography which is a technique of single-shot phase-shifting interferometry. This technique records multiple phase-shifted holograms required for phase-shifting interferometry by using space-division multiplexing. We constructed a parallel phase-shifting digital holography system consisting of a high-speed polarization-imaging camera. This camera has a micro-polarizer array which selects four linear polarization axes for 2×2 pixels. We set a loudspeaker as an object, and recorded vibration of diaphragm of the loudspeaker by the constructed system. By the constructed system, we demonstrated observation of vibration displacement of loudspeaker diaphragm. In this paper, we aim to estimate vibration frequency of the loudspeaker diaphragm by applying the experimental results to frequency analysis. Holograms consisting of 128×128 pixels were recorded at a frame rate of 262,500 frames per second by the camera. A sinusoidal wave was input to the loudspeaker via a phone connector. We observed displacement of the loudspeaker diaphragm vibrating at up to 20 kHz by the system. We also succeeded in estimating vibration frequency of the loudspeaker diaphragm by applying frequency analysis to the experimental results.

9279-34, Session 7

Multiwavelength digital holography utilizing the space-bandwidth capacity-enhance

Tatsuki Tahara, Toru Kaku, Yasuhiko Arai, Kansai Univ. (Japan)

Digital holography for recording multiwavelength and three-dimensional (3-D) information simultaneously by a single-shot exposure of a monochromatic image sensor without the crosstalk between the wavelengths is presented. Spatial frequency-division multiplexing of wavelengths using a single reference beam, which was proposed by a MIT research group (N. Lue, et al., Appl. Phys. Lett. 101, 084101, 2012), is used to record multiwavelength information. In this multiplexing technique, however, most of the space bandwidth cannot be utilized for recording object waves and then the crosstalk occurs easily. Therefore not detailed structures but only a whole image of a cell was observed. Our approach uses the space-bandwidth capacity-enhance (SPACE) (T. Tahara, et al., Appl. Phys. Express 6, 022502, 2013) to extend the space bandwidth available for recording object waves. A theoretical analysis clarified that the space bandwidth without the crosstalk is more than nine times in square extended in comparison to that obtained by the MIT's method when the wavelengths used to record a hologram are 532 and 640 nm. Simultaneous recording of dualwavelength and 3-D image with a single-shot exposure is experimentally demonstrated without the crosstalk while the crosstalk noise was severely shown in

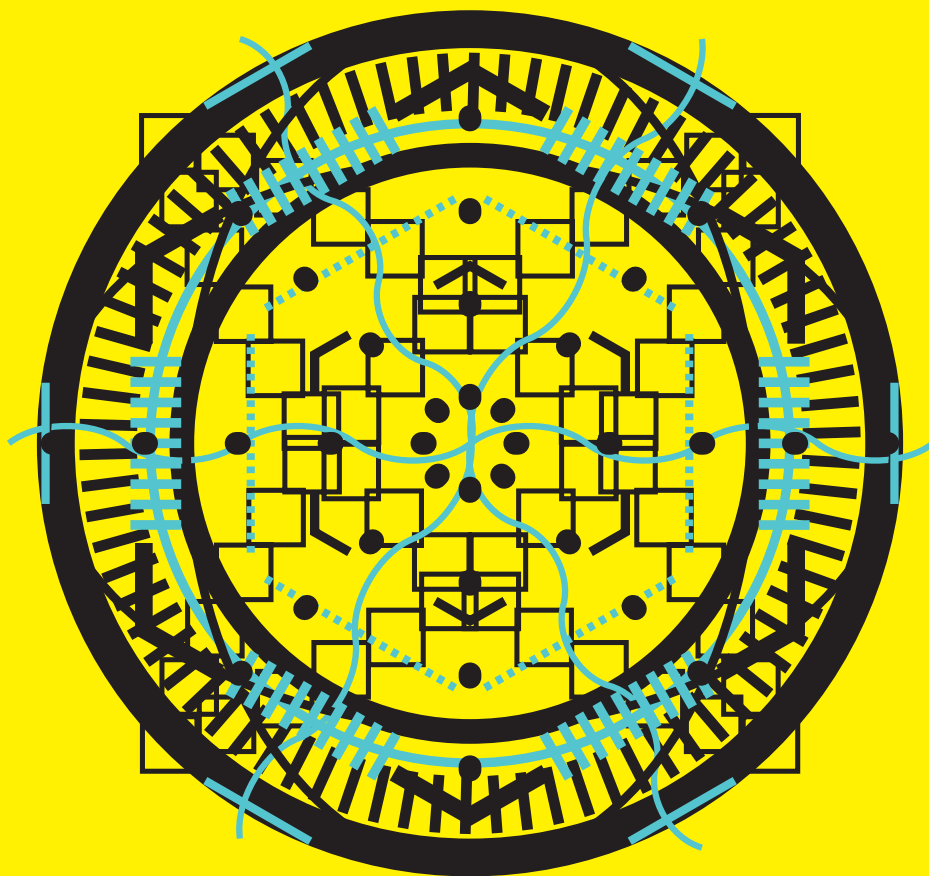
the image reconstructed by the conventional method. In the presentation, not only phase imaging using multiwavelength information but also the application to color imaging and a correction method using a developed digital signal processing to compensate the color shift will be presented.

9279-35, Session 7

Self-synchronized fast reflectance acquisition

Dongsheng An, Tsinghua Univ. (China) and Graduate School at Shenzhen, Tsinghua Univ. (China); Jinli Suo, Tsinghua Univ. (China); Haoqian Wang, Graduate School at Shenzhen, Tsinghua Univ. (China); Qionghai Dai, Tsinghua Univ. (China)

The hyper-spectrum data exhibits the structure, materials, and semantic meaning of a nature scene and its fast acquisition is of great importance due to its potential for parse these properties of dynamic scenes. Targeting for high speed hyper-spectrum imaging of a nature scene, this paper proposes to capture the coded hyper-spectrum reflectance of a nature scene using low cost hardware and reconstruct the latent data using a corresponding decoding algorithm. Except for a wide spectrum light source, the imaging system includes mainly a commercially available projector color wheel and a high speed camera, which both work at constant periods and are self-synchronized by our algorithm. The introduced light source and color wheel cost less than 50 dollars and makes the proposed approach widely available. The results on the data captured by our prototype system show that the proposed approach can reconstruct the high precision hyper-spectrum data at real time.



Helping engineers and
scientists stay current
and competitive



Optics &
Astronomy



Biomedical
Optics



Optoelectronics &
Communications



Defense
& Security



Energy



Lasers



Nano/Micro
Technologies



Sensors

SPIE. DIGITAL
LIBRARY

Find the answer
SPIEDigitalLibrary.org